The importance of sustainability ethics, toxicity and ecotoxicity in chemical education and research

Terry Collins,† Associate Editor for the Americas of *Green Chemistry*, strongly emphasises the important role of green chemistry in ensuring our sustainable future

Our modern high-technology civilization is not sustainable. This statement, since the publication of the Brundtland Report, has come to encompass two ideas presented here from the negative perspective. Firstly, many essential activities that, individually and collectively, are carried out each day to make our civilization work cannot be carried on into the indefinite future in anything approximating their current form. Secondly, we are operating our civilization in such a way that significant substance underpins the judgment that the welfare of future generations will not be comparably advantageous to our own. These ideas, now broadly accepted in a growing consensus, imply that someone is responsible for fixing things. If unsustainable technologies are part of the problem, the technical leadership has clear responsibility, and chemists are important members of that technical leadership. We must first ask, for each chemical problem identified, whether solutions are conceivable. If the answer is yes, our responsibility translates into a duty to engage fervently in finding solutions. If the answer is no, our responsibility translates into a duty to alert civilization to move away from the dependence that is undermining it.

Many technologies are part of our sustainability dilemma because their operation is incompatible with the long-term wellbeing of living things. Most of the known offenders are fundamentally chemical in nature and have developed since the First World War. We have been experiencing their benefits and discovering their damage for only a brief moment in human history and so it is not surprising that their novel sustainability challenges are difficult for us to deal with. The twentieth century growth in new technologies brought a dramatic increase in the quantity and complexity of the matter that flows daily from the ecosphere into the economy as its nourishment and, after the economic value has been extracted, back to the ecosphere from the economy as its waste. Some of the waste is toxic or ecotoxic, a portion of this exceptionally so, almost invariably in ways that were not perceived when the source technologies were developed. And undoubtedly, we will find other grim downsides of anthropogenic environmental pollutants to add to endocrine disruption, cancer causation, and stratospheric ozone depletion. Chemists are the master manipulators of matter and therefore, in principle, have the ability to design against toxicity and ecotoxicity.

†Lord Professor of Chemistry and Director of the Institute for Green Oxidation Chemistry, Carnegie Mellon University, Pittsburgh, Pennsylvania, USA.

During the twentieth century, chemists essentially mastered synthetic chemistry. Of course, there is much more to learn but our synthetic organic colleagues can now make virtually any organic chemical found in nature. This is a dazzling historical accomplishment for human beings from a starting point in a little over a century ago. But also during the twentieth century and on rare occasions much earlier, we realised that certain chemicals exhibit potent toxicity and ecotoxicity. How is it that we chemists have become incredibly powerful at making molecules and materials while hardly informing our students of anything in the subject areas of toxicity and ecotoxicity? Is this not a major breakdown in common sense? Does this not leave our students incompetent to practice chemistry while simultaneously ensuring that known harmful consequences are avoided for themselves, other people and the environment? These errors of the twentieth century, still rampant in the United States but being set right in a growing number of universities elsewhere, cannot be allowed to persist into the twenty-first century. The case for action is strengthened as the sustainability dilemma dawns on us all, bringing into focus the until-now obscure subject of sustainability ethics, which must be taught as an integral component of chemical education. The most important book in the field was written by Hans Jonas—'The Imperative of Responsibility: Finding an Ethics for the Technological Age'.

How should education change to better promote a sustainable future? In most universities the requirements of understanding for new chemists in the fundamentals of sustainability ethics, toxicity and ecotoxicity asymptotically approach zero. When, where, and how will this knowledge that is pivotal for producing chemists who can competently advance towards a sustainable future through their work be introduced into the curriculum? Those portions of endocrine disruption, cancer causation and ozone depletion that result from human activity arise because of the chemical properties of the economy–ecosphere matter flows. Toxicity and ecotoxicity arise because certain chemicals, having functional groups or regions that are, for example, electrophilic, nucleophilic or lipophilic, interact through these philicities with biochemicals or environmental chemicals to produce reactions that negatively impact the natural order. The philicities are unifying concepts of chemical reactivity. It would not be a huge departure from the current mechanistically oriented pedagogical approach to integrate reactions that have toxic and ecotoxic consequences as illustrations of the reactivity concepts. Bernd Jastorff, Reinhold Störmann and Uwe Wölcke from the University of Bremen do precisely this in their highly creative German textbook entitled, 'Struktur-Wirkungs-Denken in der

DOI: 10.1039/b307694f

Chemie—eine Chance für mehr Nachhaltigkeit'. Hopefully, this landmark work will soon be translated into many other languages. Chemists must quickly gain knowledge of toxicity and ecotoxicity to allow the design ethos of green chemistry to work properly.

The challenge is not simply one of educating future chemists, but also one of informing existing faculty of the ability they have to contribute to sustainability through green chemistry research. The incentives for academic faculty to embrace sustainability research early in the history of green chemistry are considerable. Just as sustainability presents us with the most troubling and complex technical challenges we face, it also highlights the most important technological opportunities crying out to be cracked by today's chemists. Finding the solutions will result in major economic progress. The new green processes can benefit the inventors and their universities if the intellectual property is properly protected. While green chemistry funding in the United States is currently inadequate, as Joan Brennecke and Mary Kirchhoff pointed out in a recent editorial (*Green.Chem*, 2003, **5**(2), 614), the arguments for expanded support are overwhelmingly strong and eventually will prevail. It is the saving grace of human beings that young people are idealistic. Through sustainability-related research, young chemists can advance the human journey in an entirely positive manner. Therefore, senior chemists who embrace sustainability problems will have access to the rapidly growing number of first class graduate students who wish to pursue a career in green chemistry.

How will green chemists and others interested in the educational change brave the veto from those academic and industrial colleagues who reject the call for change? We must find ways because so much is at stake. Achieving a sustainable civilization is foremost among our goals, but treasured possessions are also on the block. For example, currently there is widespread debate and concern in the chemical community about the low quality of our public reputation with particular concern that this might be driving brilliant young people away from chemistry. Correcting the above educational deficiencies is a required foundation of any honest attempt to improve our image. The public relations efforts, which have become so popular within certain sectors of industry and which so often amount to little more than stabs at hoodwinking the public into believing that black is white, will likely drag us all deeper into the deceiver's quagmire. The fact that any particular sector of the chemical industry has done and may still be doing much good for humanity does not provide it with an adequate defense for wilfully distorting or suppressing information concerning the dangers of any of its processes or products. Yet this shallow defense, coupled with a commandeering of credit for outstanding contributions from other sectors, is too often the chosen camouflage when the deceit becomes public. This behaviour, wherever it arises, will continue to hurt the chemistry community as a whole.

There is no defense whatsoever for the chemistry community not to move on and address the educational and research challenges of sustainability. Those who worry that scientific depth may be at stake simply do not know enough about what is going on right now in the infant field of green chemistry. We would all do well to let go of our anxieties over imagined consequences for our academic and industrial systems and open our minds to green chemistry's boundless potential to advance the human condition. The chemical enterprise as a whole will get stronger, not weaker, in the exercise. Only by becoming competent at designing chemical reactions and processes that are consistent with a sustainable future can chemistry achieve the honorable state in the public arena that we all desire for it. Couple such a state with a reasonably staged movement away from existing polluting products and processes and the general public will begin to picture chemistry accurately as a vital, exciting, and noble life-promoting profession.

How should research change to better promote a sustainable future? There are two limits for strategic planning linked by a continuum. At one limit, we could simply wait and do little that is ambitious or remarkable, abiding by the conviction that the best approach for enabling the required genius and breakthroughs to manifest themselves will be to operate the current panoply of research support programs along traditional lines. However, we must succeed in moving expeditiously toward a sustainable future. It is completely unacceptable that the over-consumption of nonrenewable natural resources and toxicity and ecotoxicity should lead to the gradual or precipitous collapse of our civilization while we all stand by and watch. So if we choose to collectively function at or near this strategic boundary, then we must ensure that brilliant young scientists will find their own ways to launch sustainability-oriented research careers. If nothing more happens than the committed continue to talk, write, and otherwise promote chemical sustainability problems—that is all that will happen.

At the second extreme, we could establish significant funding programs in green chemistry and other areas of sustainability-related education and research. If we choose to collectively function at or near this strategic boundary, then we owe it to society to have confidence among ourselves that the resources will lead to genuine sustainability-promoting research. The chemical community will be well equipped to serve the public in this mode when it has developed generally-held convictions of what important green chemistry is and, equally important, of what it is not. This will require expanded debate and consensus within the community and this journal, *Green Chemistry*, can help by providing an appropriate forum.

In my opinion, it will be obvious when chemists have fulfilled their singular historic obligation to promote sustainability through education and research. Every newly graduated chemist will have a thorough understanding of the fundamentals of sustainability ethics, toxicity and ecotoxicity and will know how to avoid pollution when designing chemicals and chemical processes. Chemists will have developed nonpolluting affordable technologies suitable for mass distribution that can convert solar to electrical and chemical energy with high efficiency. Through the properly informed design of chemicals and chemical processes, an economically vibrant, safe technology base will have been invented that is attractive to industry while being neither toxic nor ecotoxic. Scientists will have expanded the use of renewable organic materials, obtained from recently dead as opposed to fossilized organic matter, and will have optimized their balance in the global composition of chemical feedstocks—green chemists are already major participants in this important work.

Green chemistry has the potential to provide modern man with his most potent technical rudder for changing the quantity and constitution of the ecosphere–economy–ecosphere matter flows to steer our civilization toward a sustainable course. Therefore, the development of this journal by the Royal Society of Chemistry represents a timely positive tug at the helm, as it will do much to propel green chemistry forward.

Chemicals in the environment

The UK's Royal Commission on Environmental Pollution recently launched their report *Chemicals in Products: Safeguarding the Environment and Human Health* following some 2 years' study, interviews and visits to several countries (http://www.rcep.org.uk/chemicals/ch25-sum.pdf). The launch took the form of a press release which attracted several TV stations, as well as the press. The recognition of the importance of green chemistry in this context was indicated by the presence of an invited exhibition from the Green Chemistry Network (http://www.chemsoc.org/networks/gcn/). The report examines scientific understanding of the fate and effects of chemicals in the environment and the degree of uncertainty associated with that report. It also investigates the way that regulatory systems across the world attempt to manage the risk from chemicals, how they deal with the uncertainty and how they address public concerns about the process. This leads to a number of the recommendations being linked to best practice in countries around the world. The study deals with synthetic chemicals manufactured by industry and covers up to 100,000 chemicals currently on the market in greater than laboratory scale quantities. It is pointed out that less than 5% fall into categories that are currently approved for specific uses such as food additives and pharmaceuticals and that the rest can be used unless specifically regulated against.

The lack of information on chemicals is also the subject of attention in this report, which argues that the long and often complicated supply chain between manufacturer and the public end-user makes the flow of information along that chain less than satisfactory. This is made worse by what is described as a 'distinct lack of reliable data for the vast majority of (these) chemicals'. The report notes the various national and international initiatives to increase chemical testing including the new European White paper ("REACH") (see article on REACH by Michael Warhurst in this issue of *Green Chemistry*), but it adds its concerns to those of others over the costs of the testing proposed (in terms of money and animals used for the testing) and the practicality and adequacy of the proposed solutions. It considers much of the new legislation under consideration to be 'more of the same'.

The new approach that the report recommends is based on Listing, Sorting, Evaluation and Action. In order to rapidly screen the many chemicals in the marketplace it is suggested that we should first bring together the data that is available on persistence, bioaccumulation and toxicity and that this should be augmented by a system based on advanced computational techniques to identify molecules with particular physiological properties (here the practice of the US EPA on the pre-manufacture of new chemicals is noted). It aims to carry out at least preliminary evaluation of all relevant chemicals on a much shorter time-scale than many other proposals under consideration. This system if effective, would also reduce the need for animal testing.

Any such evaluation process will inevitably lead to a number of chemicals being banned, restricted or made prohibitively expensive. The design and development of new more-environmentally-benign and non-toxic chemicals will become critical if we are to achieve the very wide range of chemical effects that are made use of in modern society. The report recommends that in order to find better alternatives to existing chemicals the government should adopt substitution as a core goal of chemicals policy. This is accompanied by recommendations about improved information about chemicals on the market and their hazards, the use of assessment and monitoring programmes to inform substitution decisions, and a much improved flow of hazard information along the supply chain underpinned by legislation (the legislation currently being prepared in the Netherlands is highlighted as being appropriate) and by a government testing programme (here the government-sponsored programme in Sweden is noted as an example of good practice).

Green chemistry features prominently in the report and is seen as the way forward. Many of the green chemistry initiatives around the world are identified, as are the various activities including educational and awards programmes. However, the report strongly encourages a shift from more process-focused activities to those which better address product issues. We have made similar arguments in this journal. The need for new low-hazard chemicals represents a need for consumers and distributors, a challenge for the manufacturing industries and an opportunity for research. By making sure that the principles of green chemistry are applied throughout the supply chain from manufacturer to consumer we can help ensure that we do indeed move towards a better and more sustainable society.

James Clark, York, July 2003

DOI: 10.1039/b307692j

Denny Hjeresen

A profile of Denny Hjeresen, Director of the Green Chemistry Institute, outlining his viewpoints on various aspects of green chemistry

Timeline

1974: BS in Physiological Psychology, University of Washington, Seattle

1981: MS in Physiological Psychology minor in Ecology, University of Washington, Seattle

1984: Ph.D. in Physiological Psychology (Neuroscience Program), University of Washington, Seattle

Denny Hjeresen was born in Great Falls, Montana, in 1950 as the fifth child of Danish immigrants. He moved to the Pacific Northwest as a teenager and attended high school and college in the Seattle area. He currently lives at 2300 m in the mountains of Northern New Mexico with his wife of 28 years and three children (Ashley 20, Amanda 16 and Dane 11). In addition to serving as Director of the Green Chemistry Institute, Denny is completing 18 years at Los Alamos National Laboratory where he serves as Pollution Prevention and Sustainability Program Manager.

Denny is a serious extreme ski junkie and can usually be found knee to chest deep in powder somewhere in North America during the winter. When not skiing he can usually be found in the gym playing basketball with kids half his age and twice his talent. He is also a gourmet cook and wine—what is the right term—user. He has truly enjoyed building international alliances and has traveled to over 40 countries to date.

He became interested in green chemistry by following waste management and control issues to their logical source—design and synthesis.

What is your educational background?

Not chemistry, but biology. I began in physiological psychology at the University of Washington in Seattle and focused on the neurophysiological effects of environmental factors. I've been interested in waste minimization issues for over 20 years and have kept working my way upstream.

Who are/were your role model(s)

I have a few that have been highly influential on my thinking over time. First, my undergraduate and graduate advisor Steven Woods (now at the University of Cincinnati) taught me to view my scientific training as a tool rather than an endpoint. His view was that the problems change every day, but the skills to address them are permanent. Second, my mentor at Battelle PNNL, Richard Phillips, who taught me the value of the written word. If you can't explain it, you don't get to do it, was his motto. Finally, the tandem of Paul Anastas and Joe Breen taught me that there are principles that must be pursued with fierce dedication.

Why and how did you first get interested in green chemistry?

I was actually working on transferring supercritical fluid technology for cleaning from Los Alamos to the private sector when I discovered an intersection between EPA pollution prevention interests and those of the private sector. I helped to organize a cooperative effort between government, industry and the private sector interests in supercritical fluids—the Joint Association for the Advancement of Supercritical Fluid Technology (JAAST). Paul Anastas was one of the founding board members. Over a several-year period, JAAST evolved into what became the Green Chemistry Institute.

What are your current responsibilities and how do they relate to green chemistry?

I have two jobs: as Pollution Prevention Program Manager at Los Alamos National Laboratory in New Mexico I have many opportunities to incorporate upstream green chemistry principles into an enormously complicated environmental cleanup and nuclear/hazardous materials management problem. As Director of the Green Chemistry Institute there isn't an issue associated with green chemistry anywhere in the world that doesn't interest me. GCI has programs and projects in education, information dissemination, R&D, government and international outreach. In this situation, it helps to be hyperactive.

Do you think there are legislative barriers to the implementation of green chemistry?

Not really, but nor are there many legislative incentives. Much of our regulatory system in the U.S. is based on the stick end of the carrot/stick motivational spectrum. Green chemistry has always been intended to be a non-regulatory alternative to regulatory command-and-control mechanisms but much more could be done to enhance the incentives of the voluntary approach.

Are there other barriers to the implementation of green chemistry?

There are many, but the one that annoys me most is the recalcitrance of the chemistry education profession. Green chemistry in many university chemistry departments is treated as a threat, an imposition or an abandonment of 'science'. This during a period when creative students are avoiding chemistry careers like the plague. I think the answer lies in integration of green chemistry principles into current teaching rather than replacement of traditional chemical curricula, but attitudinal adjustment is definitely a problem. I believe another interesting problem is an underestimation of the scope of green chemistry. We often limit our discussions to technical disciplines (*e.g.*, catalysis, alternative reaction conditions or even ionic liquids) and don't talk about the impact of the technology alternatives on major global environmental issues (water quality,

DOI: 10.1039/b305716j

carbon emissions, or food production). Said another way, discussions often focus on the *how* of green chemistry rather than the *why*. This often limits the external perception of the field and its impacts.

Do you perceive any general funding problems for green chemistry, either in the USA or anywhere else?

Government funding of green chemistry in the U.S. is either static or declining. Part of the problem is the fragmented missions of different government agencies: the National Science Foundation sticks to basic research and avoids areas with industrial applications; the Department of Energy focuses only on the energy aspects of chemistry; and EPA is usually interested in remedial or monitoring methods and other agencies have even more divergent missions. Chemistry science funding is dropping across the board. This is another reason to focus attention on the larger impacts of green chemistry rather than the individual technical issues. However, this is only the government funding perspective. I believe, but can't document, that industry funding for green chemistry is on the rise. While motivated by both environmental and economic issues, such funding is likely to have significant impact and influence the behaviour of both other companies and academic researchers.

Do you have a view on the educational/teaching aspects of green chemistry?

What strikes me first is the need for educational materials with increasing depth. For green chemistry to be taught, teachers must have materials to teach from. Ingraining green chemistry into mainline texts is an unmet task. There are a lot of materials available thanks to Oxford University Press, the Royal Society of Chemistry and the American Chemical Society but they are typically supplemental materials rather than the sole text for a chemistry or engineering class. My measure of success in this area will be the publication of a mainline organic chemistry text built on green chemistry principles. The other issue with education is the need for materials on an international basis. There is a huge unmet demand for teaching materials in developing countries.

You must speak to a lot of people on your travels. Do you get an impression that many people face similar problems with respect to green chemistry? If so, what are these problems?

First, the fun of green chemistry is the first thing that people share. People get the point often more readily in developing countries than in more developed parts of the world. It is the students that really drive things. The problems of funding, crowded curricula and fossilized senior colleagues seem to be universal.

Should green chemistry really be a separate subject area of research endeavour? If so, why?

I think not. Green chemistry is an approach to environmental and economic problem solving that can be applied to a huge range of processes. I believe that integrating green chemistry into a variety of disciplines will ultimately be more successful than expecting those disciplines to come to green chemistry. I have actively pursued this philosophy in the merger of the Green Chemistry Institute into the American Chemical Society. There are green chemistry efforts going on with education, international meetings and publications. Green chemistry programming cuts across divisions as divergent as agriculture, pharmaceutical, industrial and engineering → chemistry, nuclear and many others.

Which are the main green chemistry journals you contribute to and why?

I like writing technical materials for *Environmental Science and Technology* when the subject is the broad impact of green chemistry on a global problem (agricultural production, water, *etc.*). My intent is to reach across disciplines to a non-green chemistry audience. When the subject is specific to green chemistry then I put it in *Green Chemistry*. When the subject relates to environmental processes beyond the scope of green chemistry (*e.g.*, treatment or recycling) I send them to the *Clean Processes and Environmental Policy*. Being on advisory boards for all three makes it a complicated choice sometimes.

What is your impression of the journal Green Chemistry*?*

The journal is making significant progress and attracting better-quality papers, which is critical to long-term success.

Highlights

Duncan Macquarrie reviews some of the recent literature in green chemistry

Pigments

Pigments are one of the most widespread class of products used by consumers. Recently, organic pigments have begun to appear which have lower toxicity than some of the older inorganic systems, often based on, for example, Cd, Cr and Pb. Such organic pigments, while being less toxic, often suffer from thermal and photochemical instability compared to the

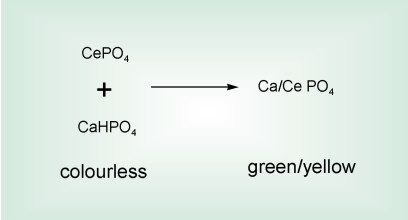

all-inorganic systems. Nobuhito Imanaka and colleagues from Osaka University have now produced a coloured inorganic system of low toxicity and with excellent colour properties (*Chem. Lett.*, 2003, 400). They achieved this by preparing a green/yellow Ca/Ce phosphate at high temperature from the corresponding pure phosphates (both of which are colourless). They foresee that this material may replace the current Cr-based green pigments.

Co-polymers

Control over polymer structure is a critical factor in the development of better performing materials. Copolymers are one such class of materials where a key

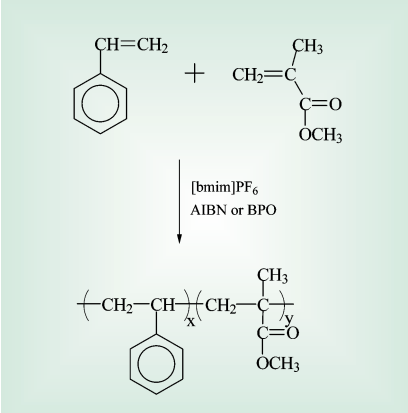

parameter is the reactivity ratio of the monomers. Jimmy Mays and his team at the Universities of Tennessee and Alabama have now shown that this parameter can be significantly different in an ionic liquid compared to a conventional solvent (*Chem. Commun.*, 2003, 1356). In [bmim]PF_6 the reactivity ratios in the styrene methyl methacrylate system are $r_{MMA} > r_{ST}$, a situation which is the opposite of the usual situation. This discovery may open the way for a different series of copolymers which may have improved performance.

Carbonylations

Carbonylation reactions represent a class of reactions which have wide utility. The replacement of phosgene with other reagents such as dimethyl carbonate or CO itself is of great interest, and a recent contribution from Fabio Ragaini and his team at the University of Milan is of

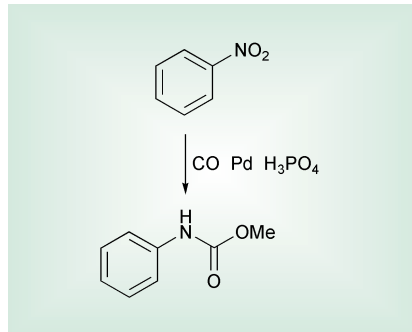

interest (*Angew. Chem., Int. Ed.*, 2003, **42**, 2886). They have investigated the Pd-catalysed carbonylation of nitrobenzene to methyl phenyl carbamate with CO in order to discover more about the mechanism. Their conclusions have led to improvements in the synthesis. The use of 85% phosphoric acid (probably the cheapest and simplest of the promoters they looked at) led to enhanced catalytic activity and lifetimes, approaching those required for a commercial application. The authors also hint that the dinitrotoluenes could also be transformed using these conditions, leading to the commercially extremely significant toluene diisocyanate derivatives.

Oxidations

The oxidation of alcohols to aldehydes using air is a tricky yet important transformation. Ivan Kozhevnikov and his group at the Leverhulme Centre for Innovative Catalysis at Liverpool University have developed a mixed metal oxide which is very good at such transformations (*Chem. Commun.*, 2003, 1414). Of a series of transition metals

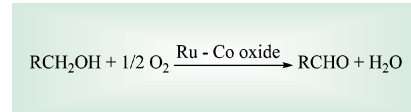

investigated, Co was found to be the most effective in combination with Ru. This combination, simply prepared by co-precipitation, was able to oxidise cinnamyl alcohol to cinnamaldehyde in toluene at reflux. Complete conversion was achieved in *ca*. 30 min, significantly faster than with pure RuO_2. Where necessary, the addition of a radical scavenger (a substituted phenol) suppressed the over-oxidation to acid.

Oxidation of hydrocarbons such as ethylbenzene to ketones using air has also been explored by the group led by Ben Feringa at the University of Groningen (*Tetrahedron Lett.*, 2003, **44**, 2003). They screened a series of Fe complexes based

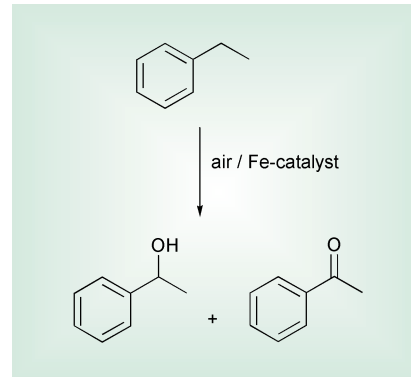

on tetradentate and pentadentate N ligands. The most active complexes were found to be derived from dimeric 2-pyridylimine ligands. With these around 10–13% oxidation to the alcohol and ketone was achieved at 80 °C, a relatively low temperature for such reactions. Use

DOI: 10.1039/b307626c

of hydrogen peroxide as oxidant was also possible, with the alcohol being favoured in this case, compared to the preferred ketone formed with air.

Reductions

Reduction of alkenes using palladium nanoparticles in ionic liquids has been carried out by Buxing Han and colleagues at the Chinese Academy of Sciences in Beijing (*Chem.. Commun.*, 2003, 1654). The nanoparticles were prepared directly in the ionic liquid, stabilised by

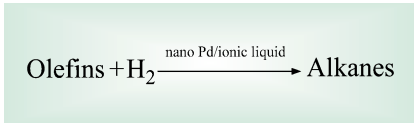

phenanthroline ligands and used without isolation as a hydrogenation catalyst. Hydrogenation of alkenes proceeded rapidly and with excellent yields. Hydrogenation of cyclohexadiene proceeded stepwise, giving the alkene in excellent yield, and later the alkane was formed quantitatively. The catalytic system could be reused several times without loss in activity or selectivity.

Heterogeneous catalysis

Enantioselective heterogeneous catalysis is gradually becoming more effective, mainly due to a better ability to control the binding of the catalytic species to the solid support. Now, John Meurig Thomas and Brian Johnson and their groups at

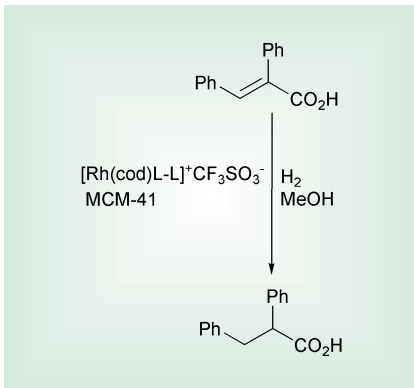

Cambridge University and the Royal Institute have published work relating to the simple heterogenisation of triflate salts of various metal complexes and their performance in enentioselective catalysis (*Helv. Chim. Acta*, 2003, **86**, 1753). They find that four different kinds of complex (with diamines, N,O complexes and N,P bidentate ligands), when adsorbed onto the highly regular MCM-41 silica, outperformed their homogeneous counterparts in terms of enantioselectivity, when they were tethered using the triflate route. It would appear that, given the correct mode of construction of the catalyst, that the additional constraints of the support pore system can enhance enantioselectivity rather than reduce it.

Similar results have been obtained by Thomas Maschmeyer and colleagues from Delft University (*J. Catal.*, 2003, **217**, 264, 275). They utilised two rhodium dimer species attached to a non-porous silica and to a MCM-41 system, in both cases using a surface bound carboxylic acid as linker. Hydrosilylation was made

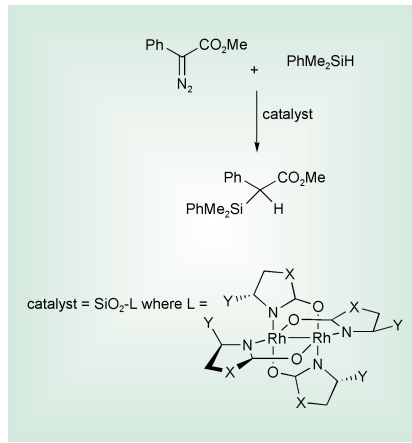

considerably more enantioselective (2% ee to 28% ee) by attachment of one of the two catalysts, while little change was noted with the other. This indicates that confinement can be beneficial in some cases. Cyclopropanation of styrene showed little change in selectivity, although *cis*:*trans* ratios were strongly affected by confinement.

Supported catalysts

A novel twist to supported catalysts has been provided by Mark Bradley and his groups at the University of Southampton (*Tetrahedron Lett.*, 2003, **44**, 4779). They have developed plugs of catalytically active polymers by sintering Merrifield resins with polyethylene. The plugs contain Pd-phosphine complexes, and

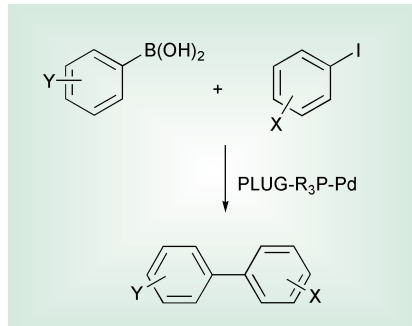

were shown to be effective catalysts for the Suzuki reaction, with high yields being achieved in all cases reported. The plug can be removed by tweezers and reused successfully.

Mannich reactions

The Mannich reaction is an atom economic route to combine three components in a single step, and generate highly functional products simply and directly. Shu Kobayashi and his co-workers from the University of Tokyo have utilised a hydrophobic polystyrene sulfonic acid in water to carry out these reactions efficiently under mild conditions (*Chem. Commun.*, 2003, 1644). While

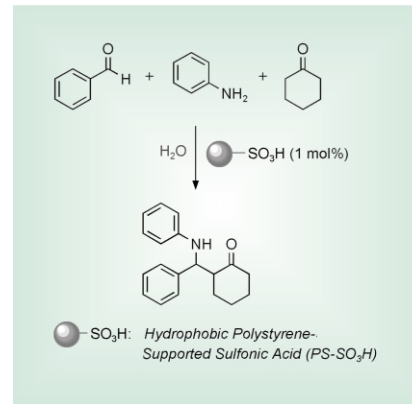

toluene sulfonic acid, Dowex resin (a polymeric sulfonic acid) and dodecylbenzenesulfonic acid were only moderately active, the polystyrenesulfonic acid was very active and led to high yields of the coupled products. The coupling of benzaldehyde, aniline and a series of carbonyl compounds proceeded smoothly and in very good yields. Phosphites could be used as a third component, yielding aminophosphonates.

Electrosynthesis

Electrosynthesis is a promising route to many organics. Rachid Bahrdadi and his team at the CNRS-University of Paris have now combined electrochemical synthesis with ionic liquids as electrolytes in some C–C bond-forming reactions (*Chem. Commun.*, 2003, 1434). They can carry out the formation of biaryls from ArX (or R–R from R–X) by reductive

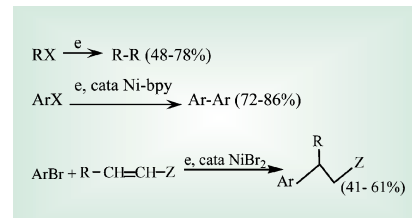

coupling in an ionic liquid in good yields. One drawback is the low ionic mobility in the viscous liquids, but this can be overcome by warming the system, or less attractively, by addition of a co-solvent. Coupling of ArX with alkenes was also possible, with good yields being achieved.

Fuel cells

The generation of electricity using fuel cells represents a potentially clean source of renewable energy. Uwe Schröder and his group from the Ernst Moritz Arndt University in Greifswald, Germany, have

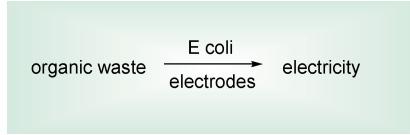

published details of a novel set-up which allows for novel microbial fuel cells with unusually high outputs (*Angew. Chem., Int. Ed*, 2003, **42**, 2880). Microbial fuel cells generate electricity by the decomposition of organic matter and thus can be seen as generating electricity from waste, while biodegrading it at the same time. Unfortunately, various difficulties have limited the current density. The work reported here resolves many of these difficulties, and the result is a >10-fold increase in current density. The key improvements are a multi-layered anode and a potential program which is designed to continually regenerate the electrodes, maintaining long-term activity. With these improvements current density can be improved from a maximum of 120 μA cm^{-2} to 1.5 mA cm^{-2}. Such improvements make the promise of power from waste a step closer.

Award for leading environmental engineer

Professor Roland Clift OBE, FREng, Distinguished Professor of Environmental Technology and Director, Centre for Environmental Strategy at the University of Surrey (UK) has been awarded the Royal Academy of Engineering's Sir Frank Whittle Medal for 2003. This medal is awarded for 'outstanding and sustained achievement by an engineer who has contributed to the well-being of the nation'.

Professor Roland Clift was selected for the award in recognition of his leading role in developing the holistic life cycle assessment of products—'cradle to grave' analysis—and its use as a systematic way of incorporating environmental and social issues in engineering decisions.

Professor Clift is one of the outstanding chemical engineers of his generation. He has a worldwide reputation for the application of sound engineering methods to the evaluation of environmental impact. He was an early advocate of the use of Life Cycle Assessment to develop an understanding of the environmental impact of processes and products from their inception to their final disposal. He has made major contributions to the development of analytical methods in convincing industry, government and commerce of the value of this approach.

Professor Clift pursued an early career in the field of particle-fluid systems and co-authored a seminal work on the subject. From 1981 and over the next decade, in Surrey, he built up one of the best research departments in the UK for work in particle technology.

From 1992, however, he established something completely new to a British university. His work has always been concerned with minimising the impact of technology on the environment, but he had come to realise that we can not hope to develop lasting solutions to long-term environmental problems without combining engineering with understanding provided by other disciplines: the new agenda represented by the concept of sustainable development requires the combination of academic disciplines, which are usually distinct. He therefore established the Centre for Environmental Strategy (CES) at the University of Surrey, a vibrant multidisciplinary group of engineers, scientists and social scientists. He was able to engage all of them to recognise the value of rigorous quantitative techniques combined with sensitivity to social concerns and priorities. CES is now recognised as a world centre of excellence in the environmental field and is widely consulted by industry and government.

Professor Clift led an initiative which generated research programmes in clean technology by three of the then UK Research Councils: Science and Engineering Research (SERC), Agriculture and Food Research (AFRC), and Economic and Social Research (ESRC). For this work he was awarded the OBE in 1994. The idea of clean technology has now been incorporated into all the programmes of these research councils, leading to the current Sustainable Technologies Initiative.

In 1996, partly because of his work in reconciling scientific and social criteria in environmental management, Professor Clift was appointed to the Royal Commission of Environmental Pollution and has played a leading part in studies which have already had a major influence on the policies of the UK government.

The real test of the value of Professor Clift's work is in its adoption by industry and in government policy. It has been used by mining and mineral processing companies in Australia and South Africa; by Companies like ICI and Unilever to understand and reduce their environmental impacts; in the consumer electronics sector to design products for minimum environmental impact over the whole product cycle; and even to resolve a dispute on self-chilling beverages between the EU and a US canning company.

Professor Clift is widely recognised for his work by invitations to participate in international meetings and committees and by his editorial positions. He is Visiting Professor in Environmental Systems Analysis at Chalmers University, Sweden. Professor Clift is a passionate advocate of the sound economic sense of sustainable development through minimising environmental impact, and of the role of engineers in sustainable development.

In view of the increasing awareness of the importance of an LCA approach to green chemistry it seems very appropriate that we congratulate Roland in this journal.

DOI: 10.1039/b307624p

REACH begins to see the light of day

Michael Warhurst, Senior EU Toxics Programme Officer at the WWF European Policy Office in Brussels, describes "REACH"—the most important legislation on chemistry to be introduced in the European Union

Introduction

On the 7th May 2003 the European Commission published a draft text of the new **R**EACH (**R**egistration, **E**valuation and **A**uthorisation of **CH**emicals) chemicals regulation. The text, amounting to around 1200 pages, was published on the internet for an 8-week consultation on workability, which ends on the 10th July: http://europa.eu.int/comm/environment/chemicals/whitepaper.htm

This consultation is the next stage of the European Union's (EU) long journey towards reforming the way chemicals are regulated in Europe. In the words of the Commission: *'The aims of the proposed new Regulation, which will replace 40 different pieces of current legislation, are to increase the protection of human health and the environment from exposure to chemicals while at the same time to maintain and enhance the competitiveness and innovative capability of the EU chemicals industry.'*

Most of the 1200 pages of the draft regulation are annexes, particularly a large annex on test methods and a smaller annex ensuring that substances that are already subject to marketing and use restrictions continue to be subject to the same restrictions—both of these annexes are very similar to current legislation. The heart of the new proposal is the Regulation itself, which is 66 pages long, with 117 articles. The intention is that the REACH regulation will lead to the repeal of a large amount of current legislation—the Regulation itself repeals 39 Directives and 2 Regulations!

The EU passes two types of law—directives and regulations. A Directive is not directly binding in the Member States, so Member State governments must write their own legislation to implement it. In contrast, a Regulation is binding in all Member States—it's proposed that the REACH legislation will be a regulation, therefore it will be binding on all 25 Member States of the enlarged European Union.

The Commission will gather the comments from the consultation, assess and agree any changes, then publish the regulation as a legislative proposal—it is predicted this publication could occur during October 2003. Once the legislative proposal is published, it will pass to Member State governments and the elected European Parliament, who will jointly finalise the legislation over a period of around 2 years, including two parliamentary readings. Parliament and Governments will have equal power over the final result, which will probably have to be finalised using a procedure called conciliation, a time-limited process that forces compromise.

The key elements of REACH

REACH is designed to be an integrated approach to the control of the production, import and use of chemicals in Europe. It intends to create a system which is based on information about chemicals, rather than ignorance, and which ensures that useful safety information flows down to those using chemicals. As mentioned in my earlier article,[1] the current regulatory system does not adequately fulfil these or many other requirements.

REACH can be thought of as fulfilling two key elements:

- it lays out the regulatory system that will be in place when it is fully implemented, when all chemicals on the market produced or imported at >1 tonne per annum are registered with safety data, and there is no longer a backlog of chemicals for which there is insufficient safety information.
- it describes the phased process to overcome the backlog of a lack of safety data on chemicals—including an 11-year period for registering safety information on chemicals.

REACH is complex, so this is only a brief description—the Commission has produced an explanatory note on the system which provides more details.[2]

Registration

One of the primary aims of the REACH system is to ensure there is sufficient information available on chemicals to enable their adequate control. The current regulatory system has required the notification of safety data on chemicals put on the market since 1981, as soon as more than 10 kg/y (per manufacturer—all tonnage thresholds are per importer or manufacturer, rather than cumulative totals for the substance) are produced. At the same time, those chemicals on the market since prior to 1981 (around 30,000 marketed at over 1 tonne per annum) have not had to have mandatory safety data. REACH proposes to change this:

- The threshold for registering new chemicals is increased from 10 kg to 1 tonne, with no animal testing required until 10 tonnes per annum are produced. This is a considerable deregulation over the current system.
- Substances used in process orientated research and development can be exempt from registration for 5 years, extendable for another 5 years in exceptional circumstances—this is a considerable deregulation from the current system.
- The existing—or 'phase in'—substances will have to be registered over an 11-year period following the entering into force of the regulation. If the regulation enters force in 2005 (2006 may be more likely), then this will lead a deadline of 2008 for chemicals produced or imported at over 1000 tonnes per annum per producer, whilst those produced or imported at 1–10 tonnes per annum would not need to be registered until 2016 (by which time these chemicals will have been on the market for more than 35 years). The exception to the later deadlines are lower tonnage chemicals

DOI: 10.1039/b307627j

that have carcinogenic, mutagenic or reproductive toxin classifications 1 or 2, which should all be registered by 2008.
• The registration information required varies with the tonnage, with chemicals produced at 1–10 tonnes per annum requiring information that can be produced by non-animal testing ('annex V')—this is predicted to cover 20,000 of the 30,000 existing chemicals.
• Traded intermediates are treated in the same way as other chemicals, whilst non-isolated intermediates are exempt, and isolated intermediates and isolated intermediates transported to one or two other sites (*e.g.* contract production) need to be registered, but only with available data, except in the case of those transported at >1000 tonnes per annum which require annex V. The situation regarding registration of polymers is too complex to describe in this article.
• The legislation incorporates mechanisms to assist (and in some cases force) data sharing and consortium formation, in order to avoid duplication of animal testing. In addition, there is an annex which lists the justifications that companies can use to avoid new testing, for example by claiming that the chemical they are registering is similar to another for which data exists.
• The registration package must include a chemicals safety report, in which the producer/importer should describe how 'adequate control' of risks can be achieved for those uses (or exposure scenarios) that the producer is supporting—which should cover 90% of uses of the substance.
• A number of groups of substances are exempt from registration including pharmaceuticals, vetinary medicines and food additives. Pesticides and biocides will be considered as having been registered for these uses if they have gone through the relevant EU system.

The registration itself will be sent, probably electronically, to a new chemicals agency. The registration will then be subjected to a basic, automated completeness check, to ensure that all parts are filled in. This completeness check won't look at the dossier in more detail (this is left to the optional Evaluation stage). The quality of the Agency's registration database will depend on the quality of the industry dossiers—but there will be market mechanisms to encourage quality as, for example, companies will have to send the chemicals safety report to their downstream customers—they also have an overarching Duty of Care.

Evaluation

Evaluation is carried out by Member States Competent Authorities—the authorities that operate chemicals policy in individual countries. In the UK this is Department for Environment, Food and Rural Affairs in association with the Environment Agency and the Health and Safety Executive.

There are two forms of evaluation proposed:

Normal evaluation. Companies registering chemicals produced at over 100 tonnes per year will also have to submit test plans to outline their justification for doing—or not doing—the extra tests required for these chemicals. Every test plan must be evaluated by a Competent Authority through normal evaluation.

Priority evaluation. Priority evaluation gives competent authorities the chance to review registration dossiers, to check them for accuracy, to look at cumulative releases and a range of other options. Such evaluations are voluntary for the Competent Authorities—the number of registration dossiers that are checked in this way will depend on how much resources individual Member States decide to put into priority evaluation.

Authorisation

Authorisation is a new regulatory mechanism, designed to deal with the chemicals of very high concern. It has two components—the identification of such chemicals, and the process by which authorisations are given to carry on using them. The intention of authorisation is to phase out the use of the worst chemicals—or at least to make it more expensive to carry on using them, as there will be a charge for an application for authorisation.

Criteria. Chemicals of very high concern are defined as:
• Chemicals that are classified as carcinogenic, mutagenic or reproductive toxins, categories 1 or 2.
• Chemicals that are persistent, bioaccumulative and toxic (PBT), defined with clear criteria, for example half life in fresh water greater than 40 days, bioconcentration factor over 2000 and long-term no-observed effect concentration for marine and freshwater organisations is less than 0.01 mg/l. There is a provision for other evidence to be used to identify chemicals as PBT.
• Chemicals that are very persistent and very bioaccumulative (vPvB), defined with clear criteria, for example half life in fresh water greater than 60 days and bioconcentration factor of over 5000. There is a provision for other evidence to be used to identify chemicals as vPvB.
• Chemicals, such as those having endocrine disrupting properties, which are shown to give rise to an equivalent level of concern as other substances subject to authorisation.

Identification of chemicals subject to authorisation will be the responsibility of the Agency and Competent Authorities, who will also prioritise which should be dealt with first.

Process. Once a chemical has been prioritised for authorisation, a date will be set beyond which no unauthorised use of the chemical will be permitted, along with a date at least 18 months earlier when companies must have applied for an authorisation for any use they wish to continue. There is also a provision for the exemption of uses or categories of use from authorisation.

There are two routes by which authorisation may be obtained:
• If the company can show that the risk to human health or the environment is adequately controlled. There is currently no provision for the regulator (generally the Agency and Commission) to refuse such an authorisation request if adequate control is justified. It is not currently clear what adequate control means for vPvB and PBT chemicals, nor for no-threshhold effects such as carcinogenicity and potentially endocrine disruption.
• If the company cannot show adequate control, then they must also submit a socio-economic analysis of the use, and the regulator may also consider the existence of safer alternatives, though 'the existence of alternatives is in itself insufficient grounds to refuse an authorisation'.

Authorisations may be time-limited, and may be reviewed if circumstances have changed.

Restrictions

The draft regulation includes a restrictions process, which is basically a modification of the current marketing and use restrictions process, redesigned to make it more rapid (hopefully). It also introduces the new option of restricting the manufacturing of a chemicals, rather than just its marketing and use—this provision will be used for the control of UNEP POPs for example.

The restrictions process is designed to deal with all unacceptable risks to human health and the environment from the manufacture, marketing or use of a substance. It complements authorisation,

providing a method of dealing with problems that authorisation doesn't address, for example neurotoxic effects or sensitisers.

Chemicals Agency, decision making and the public database

The draft regulation proposes the setting up of a new chemicals agency, which will have the role of administering the whole system. The Agency will also host a number of committees of representatives from Member States, which will create a decision making process, for example for authorisation. In most cases though the decisions will have to be enacted by the Commission, as only it has the legal competence, and REACH will have to be enforced by the Member States, as only they have competence in this area.

One of the Agency's roles will be the creation of a database of information on all registered substances, incorporating a short profile of hazardous properties, labelling requirements and any authorisations or restrictions—all non-confidential information from this database will be available over the internet to anyone in the world. It is clearly intended that most of the information transfer in the new system will be electronic, so it will be vital that an effective IT solution is constructed—fortunately work has already started on developing the 'REACH IT' system.

The relevance of REACH to green chemistry

REACH has the potential to change the landscape for the development of green chemistry, as long as the eventual legislation retains its current nature (and, in the view of the environmental NGOs, is slightly extended). For example:

- The authorisation system will have clear criteria for identification of the worst chemicals, signalling that they should be moved away from. Once chemicals enter authorisation itself, it will become more difficult to continue using them, therefore providing pressure to develop and adopt alternatives (though the environmental NGOs would like to see a stronger push for substitution within authorisation).
- The development of new chemicals is encouraged by a deregulation of the thresholds for registration, and research and development exemptions are extended.
- There will be a substantial expansion in both the information available about chemicals on the market—through the requirement to register—and in the accessibility of this information, through the creation of the internet registration database. There is also an obligation for chemical safety reports to pass down the supply chain, to ensure that downstream users know what they are using. These improvements in information will make it clearer where problems are, and encourage innovation to solve those problems. The current text will, however, leave one part of the supply chain in the dark—those companies that buy articles (*e.g.* fabric, components) will not receive any additional information about the chemical composition of the articles.

Next steps

The draft regulation is proving to be very controversial, with many and varied claims of costs and benefits being made.[3] It is clear that there is a huge debate ahead. After the consultation finishes (July 10th), the Commission will debate the results, and may revise its proposals. It is currently predicted that the Commission will then publish a legislative proposal in around October 2003, and then it will be up to Member State governments and the European Parliament to debate and finalise the legislation—a process that could take at least 2 years.

REACH has a real potential to substantially increase the drivers towards green chemistry. However, much remains in the balance and will depend on the outcome of the political debate over the next couple of years.

For further information contact: A. M. Warhurst, WWF European Policy Office, 36 Avenue de Tervuren, Box 12, 1040 Brussels, Belgium. Tel: +32 2 740 0926; Fax: +32 2 743 8819; e-mail: MWarhurst@wwfepo.org; http://www.panda.org/epo/toxics

References

1 A. M. Warhurst, *Green Chem.*, 2002, **4**(2), G20–G24.
2 European Commission, Explanatory note on the REACH system. 2003: Brussels, Belgium. European Commission, http://europa.eu.int/comm/enterprise/chemicals/chempol/reach/explanatory_note.pdf.
3 WWF and EEB, *A new chemicals policy in Europe—New opportunities for industry*, 2003, Brussels, Belgium. http://www.panda.org/downloads/europe/wwfeebreachnewopforindustry.pdf.

Communication

Ionic liquids are not always green: hydrolysis of 1-butyl-3-methylimidazolium hexafluorophosphate

Richard P. Swatloski, John D. Holbrey and Robin D. Rogers

Center for Green Manufacturing and Department of Chemistry, The University of Alabama, Tuscaloosa, AL 35487, USA. E-mail: rdrogers@bama.ua.edu; Fax: +1 205 348 0823; Tel: +1 205 348 4323

Received 22nd April 2003
First published as an Advance Article on the web 9th July 2003

1-Butyl-3-methylimidazolium fluoride hydrate has been identified crystallographically as a decomposition product created during purification of the hydrophobic ionic liquid 1-butyl-3-methylimidazolium hexafluorophosphate. This highlights the need to treat ionic liquids much as one would any other research chemical with potentially hazardous properties, unknown toxicity and/or stability, particularly when searching for 'green solvents'.

The perception that all Ionic Liquids (ILs) are green solvents may lead to inappropriate experimental design and utilization of these chemicals. ILs are advanced, technological solvents that can be designed to fit a particular application. Their uses as solvents for chemical synthesis have recently been extensively reviewed.[1,2] They offer new and interesting chemical and physical properties, but it is the very low to negligible vapor pressure exhibited by some ILs that has primarily attracted the attention of many researchers. This interest has been driven by perceived opportunities to effect improvements in the overall efficiencies of processes by using the principles of green chemistry.[3] Both industrial and academic research teams are trying to redesign chemical processes to reduce, or eliminate, losses of solvents, particularly volatile organic compounds (VOCs).

Although replacement of a VOC solvent in a process with a non-volatile solvent will, necessarily, reduce losses of VOCs through emissions, process efficiency, as determined by the *E*-factor,[4,5] or other 'green metrics'[6] depends on consideration of the overall process, not just the solvent used. In particular, it is important to emphasize that, although ILs are chemicals that can be applied as solvents and catalysts in green chemistry processes, they can not necessarily be considered, or described as green solvents.

It is important to note that although many IL-like organic salts have important industrial and commercial applications (*i.e.*, as surfactants, phase transfer catalysts, and electrolytes), the environmental fate and any potential toxicity issues for most ionic liquids are not known, particularly with respect to alkylimidazolium systems, initial data is only now being determined.[7] Without this information, *ILs should be treated with some caution, much as one would any other research chemical of unknown toxicity and/or stability*.[8]

We would like to illustrate this with what has become the 'ubiquitous' IL, 1-butyl-3-methylimidazolium hexafluorophosphate, [C_4mim][PF_6]. This IL has been used by many researchers for a combination of reasons, including ease of preparation (see cited references in Ref. 1 and 2), hydrophobicity (forming a biphase with water), and lack of vapor pressure, which present several obvious advantages as a potential replacement for VOCs in developing green processes. However, the wide spread interest in this IL is despite the well established instability of the $[PF_6]^-$ anion towards hydrolysis in contact with moisture,[9] forming volatiles, including HF, POF_3, *etc.*, which can dissolve glassware and damage steel autoclaves and reactors. The instability of hexafluorophosphate containing ionic liquids has been noted in a number of papers,[10] however the discussion is usually made in passing, and with no regard to the significant potential impact of IL decomposition or degradation.

Many novice researchers, preparing these ILs, may not be aware of the white fumes rising from the IL. This white fume may contain HF, among other species, which is very toxic and corrosive. *It is important to emphasize again that considerable care should be taken when handling possible HF-containing compounds.*

In common with many other researchers, we have frequently noted the evolution of acidic HF fumes, and formation of colorless solid around the opening to reaction vessels containing [C_4mim][PF_6]. Our initial assumption was that these were silicon fluorides formed from etching of glass by acid fumes. We report here, the identification by single crystal X-ray diffraction of 1-butyl-3-methylimidazolium fluoride monohydrate, [C_4mim]F·H_2O, as a crystalline decomposition product from hydrolytic degradation of [C_4mim][PF_6] during preparation and drying, using established synthesis.

[C_4mim][PF_6] was prepared following standard procedures by metathesis of [C_4mim]Cl with aqueous HPF_6, followed by washing with water, and drying with heating under reduced pressure, and finally under high vacuum in a glass flask. At this point etching of the glass, and formation of a white solid was observed on the surfaces of the flask at the interface with the ionic liquid. Samples of the solid were isolated from the IL by filtration and, upon inspection, crystals suitable for single crystal X-ray diffraction were identified and were air dried.†

Green Context

The assumption that ionic liquids are highly stable and robust materials is challenged in this article. The authors show that [C_4mim][PF_6], one of the most widely used of the ionic liquids, can decompose under the conditions used for its preparation, to give the fluoride hydrate. The decomposition reaction is thus likely to lead to the toxic product HF, as well as to the potential for release of HF during acidic reactions. ***DJM***

Fig. 1 shows the asymmetric unit and numbering scheme. The cations associate as dimers *via* overlapping alkyl tails. The

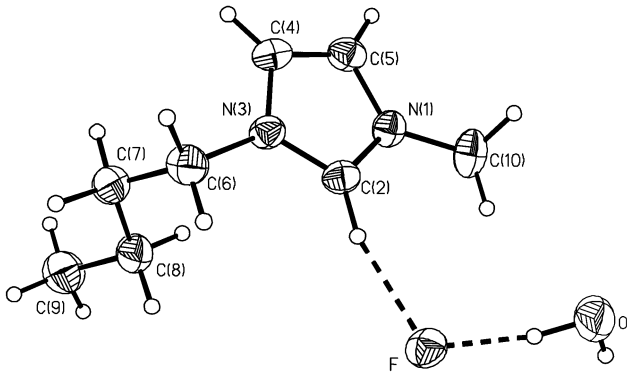

Fig. 1 Asymmetric unit in the single crystal X-ray structure of 1-butyl-3-methylimidazolium fluoride monohydrate.

dimers also make up the parallel sides of a box. The head, or H2A end, of the imidazolium ring is directed toward the tail, or H4A/H5A end, of its orthogonal neighbor. This pattern is maintained throughout the structure (Fig. 2; the alkyl chains

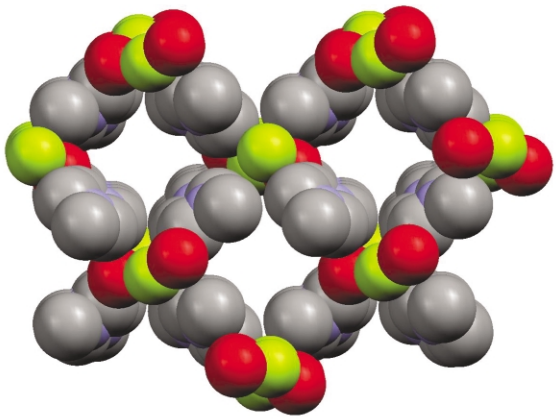

Fig. 2 Two dimensional boxes held together with perpendicular polymeric fluoride water chains. The alkyl-substituents of the imidazolium cations have been removed for clarity, and occupy the internal volume of the cavity.

have been omitted for clarity). The cationic boxes are held together in a three dimensional array *via* polymeric chains composed of water and fluoride ions (Fig. 3). These chains run

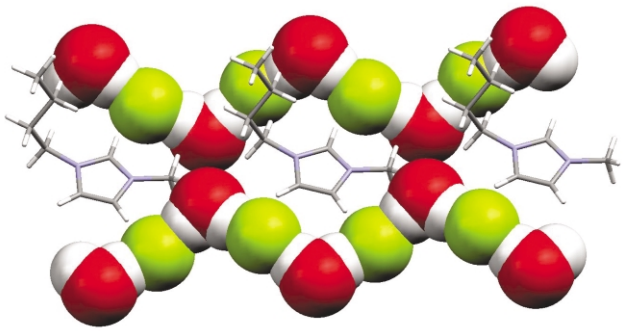

Fig. 3 Polymeric hydrogen-bonded chains F···H–O–H formed along the vertices of the boxes shown in Fig. 2.

orthogonal to the plane of the boxes and form the vertices of the boxes. As to be expected, it is the most acidic protons (H2A, H4A, and H5A) that are directed toward the vertices. Table 1 lists the hydrogen bonding interactions in the crystal. The shortest cation–anion hydrogen bond is from F to the acidic C(2)–H of the imidazolium ring (1.96(2) Å, compared to 1.82 Å for tri-coordinated fluoride ion in the structure of a tripodal imidazolium fluoride receptor.[11]

Table 1 Summary of hydrogen bonding interactions

Donor—H···Acceptor	D—H/Å	H···A/Å	D···A/Å	D—H···A/deg
C(2)—H(2A) ···F	0.95(2)	1.96(2)	2.879(2)	160(2)
C(4)—H(4A) ···F^{a}	0.95(2)	2.31(2)	3.089(2)	139(2)
C(5)—H(5A) ···F^{b}	0.96(2)	2.07(2)	3.027(2)	175(1)
C(6)—H(6B) ···F^{c}	1.00(2)	2.44(2)	3.359(2)	153(2)
C(10)–H(10A)···O	0.96(3)	2.56(3)	3.349(3)	139(2)
C(10)–H(10C)···O^{d}	0.95(3)	2.34(3)	3.262(3)	162(2)
O—H(1OA) ···F^{e}	0.89(3)	1.77(3)	2.656(2)	176(2)
O—H(1OB) ···F	0.95(3)	1.68(3)	2.625(2)	171(2)

Symmetry codes: $a = -1-x, -0.5+y, -0.5-z$; $b = -0.5-x, -1-y, -0.5+z$; $c = -0.5+x, -0.5-y, +z$; $d = -x, -0.5+y, -0.5-z$; $e = 0.5+x, -0.5-y, -z$.

The observation of IL degradation, and the isolation and characterization of one of the decomposition products, $[C_4mim]F{\cdot}H_2O$, indicates that, in many situations, $[PF_6]^-$-containing ILs may not be suitable or desirable. The synthetic procedures used to prepare hexafluorophosphate-containing ILs may have a significant influence on overall stability; hydrolytic decomposition of $[PF_6]^-$ anions is acid catalyzed, and consequently preparation by metathesis from a salt rather than acid may prove to be advantageous. However total removal of protic impurities is problematic, and decomposition through reaction with glass vessels or acidic reagents or products may also be major factors in real applications. Indeed, Cohen and co-workers[12] have reported that ILs with phosphate anions can be prepared from the corresponding $[PF_6]^-$ systems, presumably by hydrolysis, but no recognition is made that this will result in the production of up to 6 mole-equivalents of hydrofluoric acid, leading to serious safety concerns. In addition, as potential full-scale commercial applications of ILs come to fruition, end-of-life factors such as ultimate disposal have to be considered. From this perspective, environmentally acceptable disposal of ILs requires that the ILs contain only elements and functionalities that are amenable to either biodegradation or incineration; in both cases fluorous materials are undesirable.

Interestingly, imidazolium fluoride:HF adducts are being studied as ionic liquids.[13] Here again, it appears that the novel utility of these compounds is of more interest than any application as a 'green' solvent.

We would suggest that the concepts of *non-toxic pharmaceutically acceptable ions* and *GRAS* (generally regarded as safe) materials (taken from the pharmaceutical and food-additives industries) should be used to provide guidelines for the development of new ILs for which the toxicological and environmental hazards of the individual ions are established and can be considered to be acceptably low. The list of *non-toxic pharmaceutically acceptable anions* includes inorganic anions such as Cl^-, Br^-, SO_4^{2-}, PO_4^{3-}, NO_3^-, and organic anions such as acetate, succinate, glycolate, lactate, malate, tartrate, citrate, ascorbate, glutamate, benzoate, salicylate, and methanesulfonate. It will immediately be recognized that many of the anions from this (incomplete) list have been shown to support the formation of ILs. But it may also be obvious that many of these anions also are used for preparation of *crystalline* organic salts. Consideration of both structural and chemical properties of both the anion and cation must be made in order to (i) prepare ionic liquids and (ii) obtain desirable solvent properties for the IL. Thus, there are plenty of opportunities still available for fundamental development of new IL types, based on environmentally-responsible design practices, for which fluorine-containing ILs are unacceptable.

Acknowledgments

This research was supported by the U. S. Environmental Protection Agency's STAR program through grant number R-

82825701-0 and additional support to the Center for Green Manufacturing from the National Science Foundation Grant EPS-9977239.

Notes and references

† Data were collected on a Siemens CCD area detector-equipped diffractometer with Mo–Kα (λ = 0.71073 Å) radiation and solved using the SHELXTL software package. All non-hydrogen atoms were anisotropically refined and all hydrogen atoms were isotropically refined. Crystal data: formula $C_8H_{17}N_2OF$, M = 176.24, orthorhombic, a = 8.432(2), b = 10.439(2), c = 11.313(2) Å, V = 995.7(3) Å^3, T = 173 K, space group $P2_12_12_1$, Z = 4, μ(Mo–Kα) = 0.091 mm^{-1}, $R1$ = 0.0253, $wR2$ = 0.0631 ($I > 2\sigma(I)$). CCDC reference number 210400. See http://www.rsc.org/suppdata/gc/b3/b304400a/ for crystallographic data in .cif or other electronic format.

1 T. Welton, *Chem. Rev.*, 1999, **99**, 2071; J. D. Holbrey and K. R. Seddon, *Clean Prod. Processes*, 1999, **1**, 223; P. Wasserscheid and W. Keim, *Angew. Chem., Int. Ed.*, 2000, **39**, 3772; R. Sheldon, *Chem. Commun.*, 2001, 2399; C. M. Gordon, *Appl. Catal., A*, 2001, **222**, 101; H. Olivier-Bourbigou and L. Magna, *J. Mol. Catal. A: Chem.*, 2002, **182–183**, 419; J. Dupont, R. F. de Souza and P. A. Z. Suarez, *Chem. Rev.*, 2002, **102**, 3667.

2 *Ionic Liquids in Synthesis*, ed. P. Wasserscheid and T. Welton, VCH-Wiley, Weinheim, 2002; *Ionic Liquids; Industrial Applications for Green Chemistry*, ed. R. D. Rogers and K. R. Seddon, ACS Symposium Series 818, American Chemical Society, Washington DC, 2002.

3 *Green Chemistry: Theory and Practice*, ed. P. T. Anastas and J. C. Warner, Oxford University Press, Inc., New York, 1998.

4 R. A. Sheldon in *Precision process technology: perspectives for pollution prevention*, ed. M. P. C. Weijnen and A. A. H. Drinkenburg, Kluwer, Dordrecht, 1993, p. 125.

5 R. A. Sheldon, *J. Chem. Technol. Biotechnol.*, 1997, **68**, 405.

6 D. J. C. Constable, A. D. Curzons and V. L. Cunningham, *Green Chem.*, 2002, **4**, 521.

7 J. Ranke, K. Moelter, F. Stock, U. Bottin-Weber, J. Poczobutt, J. Hoffmann, B. Ondruschka, J. Filser and B. Jastorff, Chemical Preprint Server, CPS: biochem/0303001; E. A. Hassoun, M Abraham, V. Kini, M. Al-Ghafri and A. Abushaban, *Res. Commun. Pharmacol. Toxicol.*, 2002, **7**, 23.

8 Almost without exception, current commercially available ionic liquids have no supporting toxicological data available within MSDS information. For example, in the case of $[C_4mim][PF_6]$ most pertinent to this study, most suppliers indicate that the hazards have not been fully investigated. CHEMADA Fine Chemicals (HaNegrev, Israel) report LD_{50} data as 300–500 mg Kg^{-1} (rat/oral) and > 2000 mg Kg^{-1} (rat/dermal) but indicate that the ionic liquid is stable under normal conditions and that there is no available data on hazardous decomposition products.

9 J. R. Van Wazer, *Phosphorous and its Compounds*, Wiley, New York, vol. 1, 1958.

10 A. E. Visser, R. P. Swatloski, W. M. Reichert, S. T. Griffin and R. D. Rogers, *Ind. Eng. Chem. Res.*, 2000, **39**, 3596; S. I. Lall, D. Mancheno, S. Castro, V. Behaj, J. I. Cohen and R. Engel, *Chem. Commun.*, 2000, 2413; L. Gubicza, N. Nemestóthy, T. Fráter and J. Bélafi-Bakó, *Green Chem.*, 2003, **5**, 236.

11 S. Yun, H. Ihm, H. G. Kim, C.-W. Lee, B. Indrajit, K. S. Oh, Y. J. Gong, J. W. Lee, J. Yoon, H. C. Lee and K. S. Kim, *J. Org. Chem.*, 2003, **68**, 2467.

12 S. Lall, V. Behaj, D. Mancheno, R. Casiano, M. Thomas, A. Rikin, J. Gaillard, R. Raju, A. Scumpia, S. Castro, R. Engel and J. I. Cohen, *Synthesis*, 2002, **11**, 1530.

13 K. Matsunoto, R. Hagiwara, Y. Ito, S. Kohara and K. Suzuya, *Nucl. Instrum. Methods Phys. Res., Sect. B*, 2003, **199**, 29; K. Matsumoto, T. Tsuda, R. Hagiwara, Y. Ito and O. Tamada, *Solid State Sci.*, 2002, **4**, 23; R. Hagiwara, K. Matsumoto, T. Tsuda, Y. Ito, S. Kohara, K. Suzuya, H. Matsumoto and Y. Miyazaki, *J. Non-Cryst. Solids*, 2002, **312–314**, 414.

Communication

Solar light induced photocatalytic oxidation of benzyl alcohol using heteropolyoxometalate catalysts of the type $[S_2M_{18}O_{62}]^{4-}$

Thomas Rüther,*[a] Alan M. Bond*[b] and W. Roy Jackson[c]

[a] *Centre for Green Chemistry, Monash University, P. O. Box 23, Victoria 3800, Australia. E-mail: nathom@ozemail.com.au; Fax: +61 3 9905 4597; Tel: +61 3 9905 4532*
[b] *School of Chemistry, Monash University, P. O. Box 23, Victoria 3800, Australia. E-mail: a.bond@sci.monash.edu.au; Fax: +61 3 9905 4597; Tel: +61 3 9905 1338*
[c] *Centre for Green Chemistry, Monash University, P. O. Box 23, Victoria 3800, Australia. E-mail: William.roy.Jackson@sci.monash.edu.au; Fax: +61 3 9905 4597; Tel: +61 3 9905 4552*

Received 9th June 2003
First published as an Advance Article on the web 24th July 2003

A solar light induced photocatalytic cycle is described for the selective oxidation of benzyl alcohol in presence of a polyoxometalate catalyst and under very simple reaction conditions.

The oxidation of alcohols into the corresponding carbonyl compounds is one of the most important organic transformations in laboratory reactions[1] and chemical manufacturing.[2] Traditional methods involve the use of stoichiometric amounts of inorganic oxidants, such as manganese[3] and chromium[4] compounds, or organic systems,[5] thereby generating equimolar amounts of undesired and sometimes toxic wastes, which can be an obstacle in product isolation as well as their disposal.

These economically and environmentally questionable processes have been challenged recently by new catalytic processes,[6] many of them involving polyoxometalates.[7]

Heteropolyoxometalates,[8] like semiconducting materials to which they have been compared (Fig. 1) can harvest light energy and convert it into chemical energy.[9] Thus, polyoxometalates have been studied in photocatalytic processes, such as oxidation of alcohols and decomposition of halocarbons, with an emphasis on their physico chemical properties.[7c–e,9a,10]

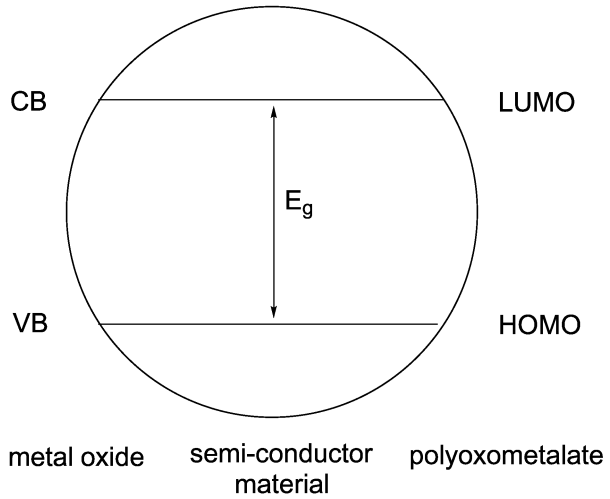

Fig. 1 Comparison between semi-conductors and polyoxometalates. E_g: energy gap, CB: conduction band, VB: valence band, LUMO: lowest unoccupied orbital, HOMO: highest occupied orbital.

In this communication we wish to report for the first time the solar light induced homogeneous photocatalytic oxidation of benzyl alcohol (BzOH or $PhCH_2OH$ in eqn. 1) to benzaldehyde (PhCHO in eqn. 1) under very simple reaction conditions, using the Wells–Dawson anions $[R_4N]_4[S_2M_{18}O_{62}]$ (M = W, Mo) as catalysts, eqn. 1. Extensive studies on the physico chemical properties of these anions have been reported earlier by Himeno[11] and ourselves.[12] The selective catalytic oxidation of BzOH has been described recently in several papers.[7h,13]

Acetonitrile solutions (5 ml) of BzOH (100 mM) and the polyoxometalate anion (2–4 mM) were exposed to solar light (outdoors) without stirring and in the presence of a layer of air-oxygen in stoppered 10 ml Pyrex flasks ($\lambda_{cutoff} \geq 280$ nm). After irradiation for 25 days, the solutions were analysed for products by GC and GC-MS. The results are given in Table 1.† In the presence of $[Bu_4N]_4[S_2W_{18}O_{62}]$ (2 mol%) a conversion of 29% BzOH was achieved, yielding 25.6% benzaldehyde and 3.4% benzoic acid (88% selectivity, estimated from GC analysis). In contrast, the same reaction performed in presence of $[Hex_4N]_4[S_2Mo_{18}O_{62}]$ (4 mol%) did not proceed beyond the stoichiometric amount of this anion.

Colour changes, observed during the photochemical oxidation experiments, help provide an explanation of the difference in the catalytic activity of the two anions. Reaction solutions involving $[Hex_4N]_4[S_2Mo_{18}O_{62}]$ changed from orange to dark green/blue, and those involving $[Bu_4N]_4[S_2W_{18}O_{62}]$ changed from almost colourless to blue, both characteristic of polyoxometalates being reduced.[8] However, as the reaction progressed, subsequent decolorisation was observed after some time in the solution containing the tungsten compound, indicating oxidation of reduced $[Bu_4N]_4[S_2W_{18}O_{62}]$ by protons (generated in eqn. 1a) and air-oxygen, eqn. 1b.

Green Context

Selective oxidation of primary alcohols is a difficult challenge if over-oxidation is to be avoided. Here, sunlight and heteropolymetallates have been shown to be a promising combination, with potential for being very green. While the initial results require further work to provide an effective synthetic method, the potential of the process warrants further investigations. ***DJM***

 DOI: 10.1039/b306521a

Table 1 Irradiation of acetonitrile solutions of BzOH (100 mM)[a] in presence of catalytic concentrations of the anions $[S_2M_{18}O_{62}]^{4-}$ (M = W, Mo)[a]

Complex [mol%]	Light source (irrad. time)	% conv. BzOH[c]	% yield aldehyde[c]	% yield acid[c]
$[S_2W_{18}O_{62}]^{4-}$ [2]	Solar light (25 d)	29	25.6	3.4
$[S_2Mo_{18}O_{62}]^{4-}$ [4]	Solar light (25 d)	4.5	3.5	[d]
$[S_2W_{18}O_{62}]^{4-}$ [1.9]	12.5 W[b] (48 h)	24	21	3

[a] Concentrations in last entry were 79 mM BzOH and 1.52 mM $[S_2W_{18}O_{62}]^{4-}$ respectively. [b] Artificial light, λ = 312–700 nm. [c] Determined by GC, using anisole as an internal standard. [d] Below accurate detection limit.

$$PhCH_2OH + [S_2M_{18}O_{62}]^{4-} \xrightarrow{\text{solar light}} PhCHO + [S_2M_{18}O_{62}]^{6-} + 2H^+ \quad (1a)$$

$$2[S_2M_{18}O_{62}]^{6-} + 4H^+ + O_2 \rightarrow 2[S_2M_{18}O_{62}]^{4-} + 2H_2O \quad (1b)$$

Ultimately, this led to an oscillating process in presence of $[Bu_4N]_4[S_2W_{18}O_{62}]$ (frequency: 12–24 h). In contrast no colour change was observed for reduced $[Hex_4N]_4[S_2Mo_{18}O_{62}]$, which does not undergo reaction 1b at an appreciable rate. Therefore $[Bu_4N]_4[S_2W_{18}O_{62}]$ acts as a catalyst in the photocatalytic cycle shown in Scheme 1. Previous studies revealed that oxidation of

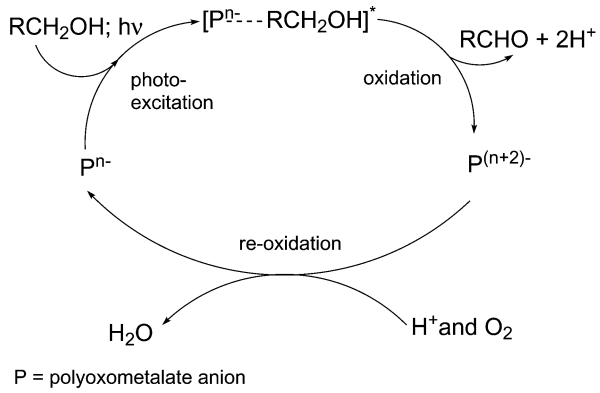

Scheme 1 Photocatalytic cycle.

reduced heteropolyoxometalates with protons and oxygen is sometimes feasible, but that the reaction rates are highly dependent on the nature of the polyoxometalate involved. Thus, oxidation of reduced polyoxomolybdates by H^+ and O_2 is frequently reported to be thermodynamically and/or kinetically unfavourable.[10a,b,e,14]

Very recently, we have demonstrated in quantitative photoelectrochemical experiments that reduced $[Bu_4N]_6[S_2W_{18}O_{62}]$ is oxidised in the presence of H^+ and O_2, whereas these reactions are not viable for reduced $[Hex_4N]_6[S_2Mo_{18}O_{62}]$. Importantly, it emerged from these studies that the polyoxometalate catalyst remained intact during the photocatalytic cycle.[15]

In order to enhance the reaction rate of the photoreaction, acetonitrile solutions (7 ml) of BzOH (79 mM) and $[Bu_4N]_4[S_2W_{18}O_{62}]$ (1.52 mM) were also exposed to a 12.4 W artificial light source in the visible region (λ = 312–700) whilst air-oxygen was continuously bubbled through the stirred solution. Under these conditions, a conversion of BzOH (24%) similar to that of the solar light reaction (25 days) was achieved within 48 h, yielding 21% benzaldehyde.

In summary a photocatalytic cycle, using solar light and the polyoxometalate catalyst $[Bu_4N]_4[S_2W_{18}O_{62}]$, has been established for the selective oxidation of benzylalcohol to benzaldehyde under very simple reaction conditions. It was shown that the efficiency of this process may be enhanced by improving the technical conditions, *e.g.* mirror arrangement for light focusing and harvesting, stirring, oxygen concentration in the solution. We believe that this initial essay into solar light induced catalytic oxidation of alcohols provides a useful platform for the development of an efficient process in terms of energy resources and practicability.

Notes and references

† Pyrex volumetric flasks used in these experiments had been thoroughly cleaned prior to the experiments by (i) soaking in dilute nitric acid, (ii) soaking in and rinsing with distilled water, followed by rinsing with acetone, (iii) drying in an oven. Reagents: acetonitrile not deairated (Merck OmniSolv® spectrograde 99.9%), BzOH (BDH GPR™ 99%), were used as supplied by the manufacturer. $[Bu_4N]_4[S_2W_{18}O_{62}]$[11c,12e] and $[Hex_4N]_4[S_2Mo_{18}O_{62}]$[12b] were prepared according to literature procedures. We thank A. G. Wedd (University of Melbourne) for helpful advice on their preparation. Solar light photochemical experiments were carried out on acetonitrile solutions prepared in pyrex flasks in parallel runs in the same location in Melbourne/Australia between 14/09/02 and 8/10/02. In artificial light photochemical experiments, the light beam was focused onto the acetonitrile solution by means of two lenses. Light source: Polilight PL6 (Rofin); prvided by courtesy of Ron Beckett, Water Studies Centre, Monash University. Product analysis: anisole was added as an internal standard; fused silica capillary column 30 QC 5BP/X5 (GC), HP 5 MS crosslinked 5% PH ME siloxane (GC-MS); the identity of products was further confirmed by comparison with authentic samples. Appropriate blank experiments confirmed that (i) the solvent is not photooxidised and (ii) reactions do not occur in the dark.

1 (*a*) R. C. Larock, *Comprehensive Organic Transformations*, VCH, New York, 1989, pp. 604 and 834; (*b*) M. Hudlicky, *Oxidations in Organic Chemistry*, ACS Monograph Ser. 186, American Chemical Society, Washington DC, 1990, p. 114; (*c*) *Comprehensive Organic Functional Group Transformations*, eds. A. R. Katritzky, O. Meth-Cohn, C. W. Rees, G. Pattenden and C. J. Moody, Elsevier Science, Oxford, 1995, vols. 3 and 5.

2 (*a*) G. Franz and R. A. Sheldon, in *Ullmann's Encyclopedia of Industrial Chemistry*, eds. B. Elvers, S. Hawkins and G. Schulz, VCH, Weinheim, vol. A18, p. 261; (*b*) *Kirk-Othmer Encyclopedia of Chemical Technology*, eds. J. I. Kroschwitz and M. Howe-Grant, Wiley, New York, 1991.

3 (*a*) Review of permanganate oxidation: R. Stewart, in *Oxidation in Organic Chemistry*, ed. K. Wiberg, Academic Press, New York, 1965, vol. 5A, p. 1; (*b*) D. Arndt, *Manganese Compounds as Oxidising Agents in Organic Chemistry*, Open Court, LaSalle, IL, 1981; (*c*) D. G. Lee, in *Oxidation in Organic Chemistry* Part D, ed. W. S. Trahanovsky, Academic Press, New York, 1982, ch. 2; (*d*) N. Singh and D. G. Lee, *Org. Process Res. Dev.*, 2001, **5**, 599.

4 (*a*) H. O. House, *Modern Synthetic Reactions*, Benjamin, Menlo Park, 1972, 257; (*b*) G. Cainelli and G. Cardillo, *Chromium Oxidations in Organic Chemistry*, Springer Verlag, Berlin, 1984; (*c*) S. V. Lee and A. Madin, in *Comprehensive Organic Synthesis*, eds. B. M. Trost, I. Flemming and S. V. Ley, Pergamon, Oxford, 1991, vol. 7, p. 251.

5 (*a*) Review on alcohol oxidation by activated DMSO method: T. V. Lee, in *Comprehensive Organic Synthesis*, eds. B. M. Trost, I. Flemming and S. V. Ley, Pergamon, Oxford, 1991, vol. 7, p. 291; (*b*) Review on the Swern oxidation: A. J. Mancuso and D. Swern, *Synthesis*, 1981, 165; (*c*) Use of hypervalent iodine compounds: D. B. Dess and J. C. Martin, *J. Org. Chem.*, 1983, **48**, 4155; (*d*) Review on the use of nitroxylradicals for alcohol oxidation: A. E. J. de Nooy, A. C. Besemer and H. van Bekkum, *Synthesis*, 1996, 1153.

6 (*a*) R. A. Sheldon and J. K. Kochi, *Meta-Catalysed Oxidations of Organic Compounds*, Academic Press, New York, 1981; (*b*) R. A. Sheldon, *Chemtech*, 1991, 566; (*c*) R. A. Sheldon, *Top. Curr. Chem.*, 1993, **164**, 23; (*d*) K. Sato, M. Aoki, J. Takagi, K. Zimmermann and R. Noyori, *Bull. Chem. Soc. Jpn.*, 1999, **72**, 2287 and literature cited therein (*e*) R. A. Sheldon, I. W. C. E. Arends and A. Dijksman, *Catalysis Today*, 2000, **57**, 157 and literature cited therein.

7 (*a*) Y. Ishii, K. Yamawaki, T. Ura, H. Yamada, T. Yoshida and M. Ogawa, *J. Org. Chem.*, 1988, **53**, 3587; (*b*) I. V. Kozhevnikov, *Russ. Chem. Rev.*, 1993, **62**, 473; (*c*) C. L. Hill and C. M. Prosser-McCartha, *Coord. Chem. Rev.*, 1995, **143**, 407; (*d*) M. Fournier and H. Mourad, in *Polyoxometalates in Catalysis*, ed. C. L. Hill, *J. Mol. Catal. A*, 1996, **114**, 53; (*e*) N. J. Crano, R. C. Chambers, V. M. Lynch and M. A. Fox in *Polyoxometalates in Catalysis*, ed. C. L. Hill, *J. Mol. Catal. A*, **114**, 65; (*f*) C. L. Hill (Guest ed.), *Chem. Rev.*, 1998, **98**, 1;

(*g*) R. Neumann, in *Transition Metals for Organic Synthesis*, eds. M. Beller and C. Bolm , Wiley-VCH, Weinheim, 1998, vol. 2, p. 331; W. R. Sanderson, *Pure Appl. Chem.*, 2000, **72**, 1289; (*h*) A. Haimov and R. Neumann, *Chem. Commun.*, 2002, 876; (*i*) P. Desrosiers, A. Guram, A. Hagemeyer, B. Jandeleit, D. M. Poojary, H. Turner and H. Weinberg, *Catal. Today*, 2001, **67**, 397; (*j*) T. Rüther, A. M. Bond and W. R. Jackson, *Aust. J. Chem*, 2002, **55**, 691 and literature cited in these references.

8 For a general account on polyoxometalates see: (*a*) *Polyoxometallate Chemistry*, eds. M. T. Pope and A. Müller, Kluwer Academic Publishers, Dordrecht, 2001; (*b*) M. T. Pope and A. Müller, *Angew. Chem., Int. Ed. Engl.*, 1991, **30**, 34.

9 (*a*) A. Hiskia, A. Mylonas and E. Papaconstantinou, *Chem. Soc. Rev.*, 2001, **30**, 62; (*b*) C. M. Prosser-McCartha, in *Photosensitization and Photocatalysis Using Inorganic and Organometallic Complexes*, eds. K. Kalyanasundaram and M. Gräzel, Kluwer Academic Publishers, Dordrecht, 1993, ch. 13, p. 307.

10 (*a*) C. L. Hill and D. A. Buchard, *J. Am. Chem. Soc.*, 1985, **107**, 5148; (*b*) E. Papaconstantinou, *Chem. Soc. Rev.*, 1989, **18**, 1; (*c*) R. F. Renneke, M. Pasquali and C. L. Hill, *J. Am. Chem. Soc.*, 1990, **112**, 6585; (*d*) D. Sattari and C. L. Hill, *J. Chem. Soc., Chem. Commun.*, 1990, 634; (*e*) A. Hiskia and E. Papaconstantinou, *Inorg. Chem.*, 1992, **31**, 163.

11 (*a*) S. Himeno, T. Osakai, A. Saito, K. Maeda and T. Hori, *J. Electroanal. Chem. Interfacial Electrochem.*, 1992, **337**, 371; (*b*) S. Himeno, K. Maeda, T. Osakai, A. Saito and T. Hori, *Bull. Chem. Soc. Jpn.*, 1993, **66**, 109; (*c*) S. Himeno, H. Tatewaki and M. Hashimoto, *Bull. Chem. Soc. Jpn.*, 2001, **74**, 1623 and literature cited in these references.

12 (*a*) A. M. Bond, D. M. Way, A. G. Wedd, R. G. Compton, J. Booth and J. C. Eklund, *Inorg. Chem.*, 1995, **34**, 3378; (*b*) D. M. Way, A. M. Bond and A. G. Wedd, *Inorg. Chem.*, 1997, **36**, 2826; (*c*) A. M. Bond, J. C. Eklund, V. Tedesco, T. Vu and A. G. Wedd, *Inorg. Chem.*, 1998, **37**, 2366; (*d*) J. C. Eklund, A. M. Bond, D. G. Humphrey, G. Lazarev, T. Vu, A. G. Wedd and G. Wolfbauer, *J. Chem. Soc., Dalton Trans.*, 1999, 4373; (*e*) P. J. S. Richardt, R. W. Gable, A. M. Bond and A. G. Wedd, *Inorg. Chem.*, 2001, **40**, 703; (*f*) P. J. S. Richardt, J. M. White, P. A. Tregloan, A. M. Bond and A. G. Wedd, *Can. J. Chem.*, 2001, **79**, 613 and literature cited in these references.

13 (*a*) A. Neumann and M. Levin, *J. Org. Chem.*, 1991, **56**, 5707; (*b*) D. W. Hall, G. Grigoropoulou, J. H. Clark, K. Scott and R. J. J. Jachuck, *Green Chem.*, 2002, **4**, 459; (*c*) V. R. Choudhary, P. A. Chaudhari and V. S. Narkhede, *Catal. Commun.*, 2003, **4**, 171.

14 D. C. Duncan and C. L. Hill, *J. Am. Chem. Soc.*, 1997, **119**, 243.

15 T. Rüther, V. M. Hultgren, B. P. Timko, A. M. Bond, W. R. Jackson and A. G. Wedd, *J. Am. Chem. Soc.*, in press.

Communication

Environmentally benign, sequential synthesis of 3,4-dihydro-2*H*-1,4-benzoxazines under phase transfer catalysis conditions†

Domenico Albanese,*[a] Andrea Donghi,[a] Dario Landini,[a] Vittoria Lupi[a] and Michele Penso[b]

[a] *Dipartimento di Chimica Organica e Industriale, Università degli Studi di Milano, via Venezian 21, 20133 Milano, Italy. E-mail: domenico.albanese@unimi.it; Fax: 390250314159; Tel: 390250314165*

[b] *Istituto CNR-ISTM, via Golgi 19, 20133 Milano, Italy*

Received 11th April 2003
First published as an Advance Article on the web 30th May 2003

An environmentally friendly synthesis of 2-substituted 3,4-dihydro-2*H*-1,4-benzoxazines has been carried out in a sequential fashion through the $R_4N^+F^-$ catalyzed ring opening of epoxides with arylsulfonamides, followed by *in situ* cyclization of the hydroxysulfonamides thus obtained with NaOH aq. and *n*-$C_{14}H_{29}N^+Me_3Cl^-$.

2-Substituted 3,4-dihydro-2*H*-1,4-benzoxazines have attracted considerable interest due to their potential therapeutic properties as intracellular calcium antagonists, serotonin receptors antagonists and antibacterial agents.[1] We recently reported a novel two-step synthesis of 2-substituted-3,4-dihydro-2*H*-1,4-benzoxazines **6** through the ring opening of epoxides **1** with (*o*-fluorophenyl)toluene-*p*-sulfonamide (**2**), followed by intramolecular nucleophilic displacement of the fluoride anion.[2] The ring opening step proceeds without solvent under phase transfer catalysis (PTC) conditions using K_2CO_3 as base, whereas the cyclization was also carried out under PTC conditions in water by using aqueous solutions of NaOH[3] or solid NaOH[4] in the presence of THF as solvent (Scheme 1).[5]

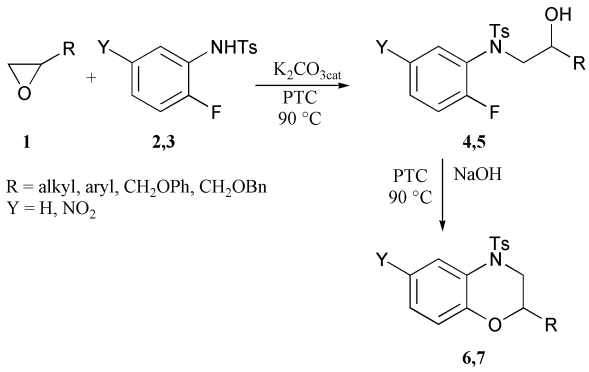

Scheme 1

In order to achieve an even more efficient and environmentally friendly process, we planned to develop a sequential procedure enabling the synthesis of benzoxazines **6,7** without isolation of intermediate hydroxysulfonamides **4, 5**, possibly without use of any organic solvent throughout the whole process. In fact, organic solvent removal is of paramount importance to minimize economic cost and environmental impact of chemical processes. In this context organic reactions in water have recently been the object of growing efforts since water is cheap, safe and a clean solvent.[6]

† Electronic supplementary information (ESI) available: experimental details. See http://www.rsc.org/suppdata/gc/b3/b304095j/

Here we report that the task could be efficiently achieved by using a very low amount of a quaternary ammonium fluoride, behaving as a base as well as PT catalyst, to generate the hydroxysulfonamides. The latter are then rapidly ring closed to benzoxazines by adding aqueous NaOH and a PTC catalyst to the reaction mixture.

The use of quaternary ammonium fluorides $R_4N^+F^-$ as bases in organic synthesis has been well known for many years.[7] In particular, they form with protic species hydrogen bond complexes $[Nu–H–F]^-Q^+$ that are useful reagents for nucleophilic substitutions.[8] For example we reported on the use of $Bu_4N^+F^-$ (TBAF) as catalyst to promote the ring opening of epoxides with thiols to generate the corresponding thioethers with excellent yields.[9]

When 50% aq NaOH was added to the reaction mixture after complete conversion of the epoxide **1a** to the hydroxysulfonamide **4a**, in the presence of catalytic amounts of $BnEt_3N^+Cl^-$ (TEBA) and solid K_2CO_3, 62% only of benzoxazine **6a** was obtained after 20 h (Table 1, entry 1). The sequential synthesis of benzoxazine **6a**, chosen as a model compound, was thus performed by stirring a mixture of TBAF·$3H_2O$ (0.1 equiv) and **2** (1 equiv) for 10 minutes to form the H-bond complex, and then the epoxide **1a** (1 equiv) was added‡ and the mixture heated at 90 °C for 1 h to ensure complete conversion to **4a** (Scheme 2). Solid NaOH was then added along with dioxane and heating was prolonged for 2 h

Green Context

Quaternary ammonium compounds have many uses as catalysts (including phase transfer catalysis) and reagents in organic chemistry. One of the most active types is the quaternary ammonium fluorides which are powerful nucleophiles, bases and desilylating agents. Unfortunately, these fluorides are also extremely hygroscopic and are easily decomposed. Here an *in situ* method for generating such an active onium fluoride is used in the context of a F^- catalysed ring opening of epoxides with arylsulfonamides *en route* to benzoxazines. This is a practical, high yielding route which is atom efficient and entirely organic solvent free. ***JHC***

Table 1 Optimization of the sequential synthesis of **6a** at 90 °C

Entry	Cat_1[a] (equiv.)	t_1[a]/h	Cat_2[a] (equiv.)	NaOH (equiv.)	t_2[a]/h	Yield[b] (%)
1	TEBA (0.1)[c]	1	—	50% (10)	20	62
2	TBAF (0.1)	1	—	$NaOH_{sol}$ (2)[d]	2	89
3	TBAF (0.1)	1	—	20% (2)	22	85
4	TBAF (0.02)	3	**8** (0.2)	50% (10)	1.5	93
5	TBAF (0.02)	3	**9** (0.2)	50% (10)	1.5	86
6	TEBA[f] (0.1)	1	**8** (0.2)	50% (10)	1.5	91
7	$TBAHSO_4$[f] (0.02)	4	**8** (0.2)	50% (10)	2	84
8	TEBA[f] (0.02)	4	**8** (0.2)	50% (10)	2	89
9	TEBA[f] (0.1)	1	—	50% (10)	24	55[g]
10	TEBA[e] (0.1)	1	**8** (0.1)	50% (10)	3.5	89
11	TEBA[e] (0.1)	1	**8** (0.05)	50% (10)	7	91

[a] Subscripts refer to the ring opening (1) and the ring closing (2) steps. [b] Overall yield. [c] With K_2CO_3 (0.1 equiv). [d] With dioxane 5 M. [e] With KF (0.2 equiv). [f] With KF (0.04 equiv) [g] Isolated by column chromatography along with 41% of **4a**.

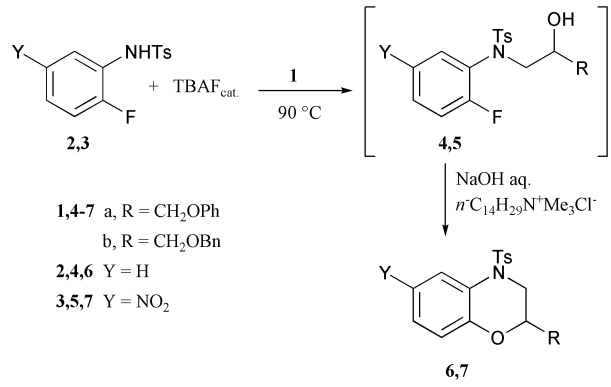

Scheme 2

generating 89% yield of **6a** (Table 1, entry 2). After this encouraging experiment we focused on the solvent free approach by using an excess of aqueous NaOH as the cyclization reagent and reaction medium.

Good yields of **6a** were obtained by using 20% aq NaOH, although in a significantly longer time (Table 1, entry 3). The ring opening step goes to completion in a short time even in the presence of only 2% of TBAF, however in this case the rate of the cyclization is strongly reduced and a second PT catalyst is needed to speed up the cyclization. The best result of the sequential process was obtained by using 2% of TBAF only in the ring opening step, followed by addition of 50% aq NaOH and n-$C_{14}H_{29}Me_3N^+Cl^-$ (**8**) to generate 93% overall yield of **6a** (Table 1, entry 4). The choice of **8** as the cyclization catalyst is of paramount importance for the process optimization since **6a** can be isolated by filtration of the reaction mixture after dilution with water. The same procedure is efficient with n-$C_{14}H_{29}BnMe_2N^+Cl^-$ (**9**) even though a slightly lower yield was obtained. The strong influence of the onium fluorides hydration state on their basicity and nucleophilicity is well known,[10] however comparable results, both in terms of yield and reaction rate, were obtained in this case when partially dehydrated TBAF was used.[11]

Although good yields of benzoxazines **6** were obtained, the use of alternatives to TBAF, which is a quite expensive and hygroscopic compound, would be desirable in order to develop a practical and economical procedure. The quaternary ammonium fluoride was thus generated *in situ* from a cheaper onium salt, *i.e.* TEBA and an excess of potassium fluoride. A mixture of TEBA, KF and **2** was therefore stirred for 10 min before epoxide addition. After heating for 1 h at 90 °C, 50% aq NaOH was added along with **8** and 91% of **6a** was isolated after 1.5 h (Table 1, entry 6). When $Bu_4N^+HSO_4^-$ ($TBAHSO_4$) was used to generate *in situ* TBAF, 84% of **6a** was isolated (Table 1, entry 7). A good result was also obtained by using 2% only of TEBA, although 4 h were needed to complete the ring opening step (Table 1, entry 8). It is worth noting that excellent overall yields of **6a**, although with longer reaction times, were obtained by reducing the amount of the cyclization catalyst **8** (Table 1, entries 10 and 11).

(2-Fluoro-5-nitrophenyl)toluene-*p*-sulfonamide (**3**) was also used as a nucleophile since a nitro group in position 6 of a 2-substituted benzoxazine was found to be an important tool to enhance its bioactivity.[12] The sequential procedure described above provides benzoxazine **7a** in 92% yield (Table 2, entry 3).

Table 2 Synthesis of benzoxazines **6, 7**[a]

Entry	Product	t_1[b]/h	t_2[b]/h	Yield (%)
1	**6a**	3	1.5	93
2	(*R*)-**6b**	4	3	91
3	**7a**	5	0.33	92

[a] a) TBAF (0.02 eq), 90 °C; b) NaOH 50% (10 eq), **8** (0.2 eq), 90 °C. [b] Subscripts refer to the ring opening (1) and the ring closing (2) steps.

As expected for an aromatic nucleophilic substitution, the additional nitro group facilitates the ring closure which goes to completion in only 20 min. It is also worth noting that enantiomerically pure 2-substituted benzoxazines can be isolated by using non racemic epoxides, as confirmed in the case of (2*S*)-[(benzyloxy)methyl]oxirane (**1b**) that generated (2*R*)-*N*-tosyl-2-benzyloxymethyl-3,4-dihydro-2*H*-1,4-benzoxazine (**6b**) in 91% yield (Scheme 3).

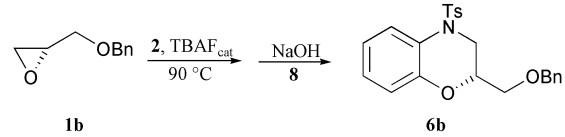

1b **6b**

Scheme 3

In summary, the use of catalytic amounts of a quaternary ammonium fluoride, generated *in situ*, provides a practical, high yielding method for the sequential synthesis of 2-substituted 3,4-dihydro-2*H*-1,4-benzoxazines, valuable intermediates for the synthesis of bioactive compounds.[1] This new protocol is atomically efficient and environmentally friendly since no organic solvent is required throughout the whole procedure and pure products can be isolated in short reaction times by filtration of the reaction mixture after water dilution.

Acknowledgements

The authors thank MIUR (National Project "Stereoselezione in Sintesi Organica, Metodologie e Applicazioni" and FIRB) and CNR for financial support.

Notes and references

‡ It is worth noting that epoxide **1a** is completely destroyed after heating at 90 °C for 1 h in the presence of 0.1 equiv. of TBAF only.

1 (*a*) A.-S. Bourlot, I. Sánchez, G. Dureng, G. Guillaumet, R. Massingham, A. Monteil, E. Winslow, M. D. Pujol and J.-Y. Mérour, *J. Med. Chem.*, 1998, **41**, 3142; (*b*) D. W. Combs, M. S. Rampulla, S. C. Bell, D. H. Klaubert, A. J. Tobia, R. Falotico, B. Haertlein, C. Lakas-Weiss and J. B. Moore, *J. Med. Chem.*, 1990, **33**, 380; (*c*) E. T. D'Ambra, G. K. Estep, R. M. Bell, A. M. Eissenstat, A. K. Josef, J. S. Ward, A. D. Haycock, R. E. Baizman, M. F. Casiano, C. N. Beblin, M. S. Chippari, D. J. Greo, K. R. Kullnig and T. G. Daley, *J. Med.*

Chem., 1992, **35**, 124; (*d*) M. Largeron, H. Dupuy and M. B. Fleury, *Tetrahedron*, 1995, **51**, 4953.
2 D. Albanese, D. Landini and M. Penso, *Chem. Commun.*, 1999, 2095.
3 D. Albanese, D. Landini, V. Lupi and M. Penso, *Adv. Synth. Catal.*, 2002, **344**, 299.
4 D. Albanese, D. Landini, V. Lupi and M. Penso, *Ind. Eng. Chem. Res.*, 2003, **42**(4), 680.
5 The ring opening step occurs in a regioselective fashion. A noticeable amount of the regioisomer, deriving from the nucleophilic attack on the substituted side of the epoxide, was detected in the case of styrene oxide only (see ref. 4).
6 (*a*) *Organic Synthesis in Water*, ed. P. A. Grieco, Blackie Academic and Professional, London, 1998; (*b*) C. J. Li and T. H. Chang, in *Organic Reactions in Aqueous Media*, Wiley, New York, 1997.
7 J. H. Clark, *Chem. Rev.*, 1980, **80**, 429.
8 I. Huertas, I. Gallardo and J. Marquet, *Tetrahedron Lett.*, 2001, **42**, 3439.
9 D. Albanese, D. Landini and M. Penso, *Synthesis*, 1994, 34.
10 D. Landini, A. Maia and A. Rampoldi, *J. Org. Chem.*, 1989, **54**, 328.
11 D. Albanese, D. Landini and M. Penso, *J. Org. Chem.*, 1998, **63**, 9587.
12 Y. Matsumoto, R. Tsuzuki, A. Matsuhisa, K. Takayama, W. Uchida, M. Asano, I. Yanagisawa and T. Yoden, *US Patent* 5 420 126, 1995.

Communication

Application of ionic liquid 1-methoxyethyl-3-methyl imidazolium methanesulfonate in nucleoside chemistry

Matthew C. Uzagare,[a] Yogesh S. Sanghvi[b] and Manikrao M. Salunkhe*[a]

[a] *Department of Chemistry, The Institute of Science, 15, Madam Cama Road, Mumbai-400 032, India. E-mail: mmsalunkhe@hotmail.com; Fax: +91 22 22816750; Tel: +91 22 22816750*

[b] *Manufacturing Process Department, Isis Pharmaceuticals, Inc., 2292 Faraday Avenue, Carlsbad, California 92008, USA. E-mail: Ysanghvi@isisph.com*

Received 13th May 2003
First published as an Advance Article on the web 30th June 2003

The ionic liquid 1-methoxyethyl-3-methyl imidazolium methanesulfonate (MOEMIM.OMs) is employed as a 'green' alternative to the conventional organic solvents used as a reaction medium in nucleoside chemistry.

Introduction

Nucleoside chemistry represents an important area of research for drug discovery. Nucleoside derivatives have found widespread application in cancer and viral chemotherapy.[1] Protected nucleosides also serve as building blocks for the synthetic oligonucleotides extensively used as probes for diagnostic purposes[2] and in antisense therapeutics.[3] As a result, nucleoside chemistry is an active area of research in industry as well as academia. However, insolubility of nucleosides in many organic solvents is a major obstacle to development of new methodologies. Further, solvents traditionally used in nucleoside chemistry such as pyridine, *N*,*N*-dimethylformamide (DMF), *N*-methyl pyrrolidone (NMP) are on 'environmental blacklists'. Hence, there is a need for development of new methods using environmentally benign media that could replace the conventional solvents and provide sufficient solubilization of 2′-deoxynucleosides.

Ionic liquids (ILs)[4] are now known to be 'green' alternatives for conventional organic solvents with negligible vapor pressure, unprecedented ability to dissolve a broad range compounds of organic and inorganic nature, and recyclability. In order to develop green processes in nucleoside chemistry, we have investigated the use of ionic liquids as a reaction medium in the reactions of nucleosides.

Results and discussion

In order to employ ILs as reaction media in the nucleoside chemistry, solubility is an important criterion. The solubility of thymidine (T) has been studied in different neutral ILs. Its solubility is found to be fairly good in 1-butyl-3-methyl imidazolium chloride (BMIM.Cl), but it is a solid or highly viscous liquid at ambient temperature and therefore cannot be employed in reactions of nucleosides. Solubility is found to be poor in ILs with tetrafluoroborate anions, namely 1-butyl-3-methyl imidazolium tetrafluoroborate (BMIM.BF_4), *N*-butyl pyridinium tetrafluoroborate and hexafluorophosphate anions, namely 1-butyl-3-methyl imidazolium hexafluorophosphate (BMIM.PF_6), however very high solubility of T was observed in 1-butyl-3-methyl methanesulfonate. The solubility of T was further studied in methanesulfonate ILs,† namely *N*-butyl pyridinium methanesulfonate (BPy.OMs), 1-ethyl-3-methyl imidazolium methanesulfonate (EMIM.OMs), *N*-ethyl pyridinium methanesulfonate (Epy.OMs) (Fig. 1). Solubility was found to be very high as compared to ionic liquids containing

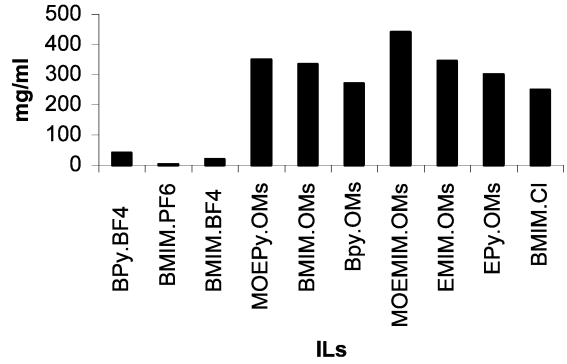

Fig. 1 Solubility of thymidine in different ILs expressed in mg ml^{-1}.

tetrafluoroborate or hexafluorophosphate anions. This may be due to the methanesulfonate anion, as the anion has major effects on the physical properties of ILs including miscibility.[5] There are recent reports of 'sugar philic' ionic liquids containing ether side chains that can dissolve glycolipids.[6] In another report MOEMIM.BF_4, which has a methoxyethyl side chain, is used for acylation of sugars.[7] In order to enhance the solubility of 2′-deoxynucleosides in methanesulfonate we studied the solubility of T in methanesulfonates having a methoxyethyl side chain in the cation *viz.* *N*-methoxyethyl pyridinium methanesulfonate (MOEPy.OMs), and 1-methox-

Green Context

Nucleoside chemistry is an important area of research, but one in which solvent choice is severely compromised by poor solubility. Most organic solvents are not suitable, the exceptions are undesirable from an environmental point of view. It is shown here that ionic liquids are suitable, since the solubility of nucleosides is very good, especially in a series of methanesulfonate salts. This paper illustrates the benefits of solubility and recoverability, as well as efficient reaction conditions, which can be provided by ionic liquids in this area of chemistry ***DJM***

 DOI: 10.1039/b305386e

yethyl-3-methyl imidazolium methanesulfonate (MOEMIM.OMs). The comparison of solubility can be seen in Fig. 1. The enhancement in solubility in these ionic liquids could be attributed to the ability of the oxygenated anion to hydrogen bond with 2′-deoxynucleoside. However, this effect is marginal as compared to that of the anion methanesulfonate.

The solubility of different nucleosides was studied in three methanesulfonate ionic liquids namely BMIM.OMs, EMIM.OMs and MOEMIM.OMs. As seen in Fig. 2, the solubility of

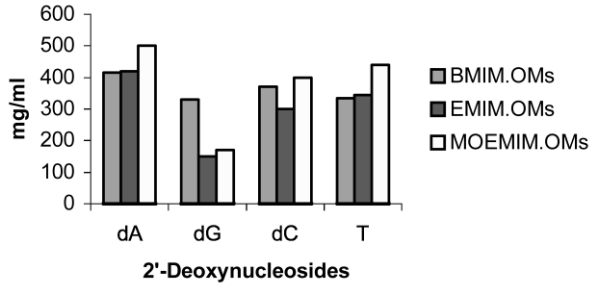

Fig. 2 Comparison of solubility of 2′-deoxyribonucleosides in three different methanesulfonate ILs.

thymidine and other 2′-deoxynucleosides is found to be better (except for 2′-deoxyguanosine in BMIM.OMs which precipitates on standing for about one hour) in MOEMIM.OMs as compared to other methanesulfonate ILs.

The solubility of different 2′-deoxynucleosides and *N*-protected 2′-deoxynucleosides was studied in MOEMIM.OMs. Solubility is observed to be comparable with conventional solvents and even greater in the case of some 2′-deoxynucleosides (Fig. 3). As can be seen from Fig. 3, comparing the

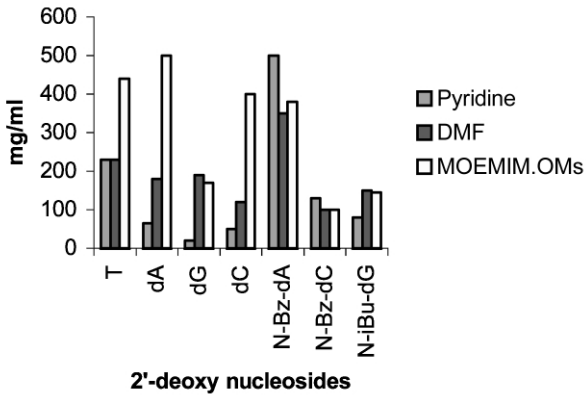

Fig. 3 Comparison of the solubility of 2′-deoxynucleosides in pyridine, DMF and MOEMIM.OMs expressed in mg ml^{-1}.

solubility of partially protected nucleosides with unprotected in MOEMIM.OMs, unprotected nucleosides are more soluble than their protected derivatives.

After identification of MOEMIM.OMs as an apparently ideal ionic liquid for nucleoside chemistry, we studied acylation and peracylation of 2′-deoxynucleosides (Scheme 1).

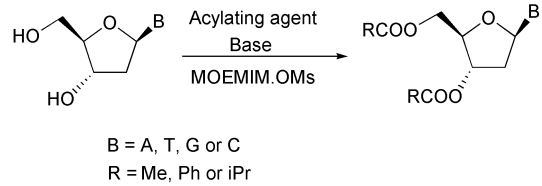

B = A, T, G or C
R = Me, Ph or iPr

Scheme 1 Acylation of 2′-deoxyribonucleosides in MOEMIM.OMs.

The acylation of 3′- and 5′-OH functional groups of sugar and NH_2 of base of 2′-deoxynucleosides was carried out with different acylating agents including acetic anhydride (Ac_2O), benzoyl chloride and isobutyryl chloride which are commonly used in peracylation of nucleosides in the presence of 1-methylimidazole (NMI) as base and 4-(dimethylamino)pyridine (DMAP) as catalyst. The products were easily isolated from the reaction media simply by extracting with ethyl acetate.

The acylation of T (1 mmol) was carried out by stirring 4 equivalents of Ac_2O in 1 ml MOEMIM.OMs. The reaction takes longer and does not give complete conversion of T to 3′,5′-diacetyl T even after extended time (Entry 1, Table 1). However, on addition of NMI (4 equiv.) and a catalytic amount of DMAP (0.2 equiv.), we could achieve complete conversion in a short time (Entry 2, Table 1). The acylation of 2′-deoxyadenosine (dA), 2′-deoxycytidine (dC) and 2′-deoxyguanosine (dG) was carried out in the same manner using 6 equiv. of Ac_2O, NMI (6 equiv.) and a catalytic amount of DMAP (0.2 equiv.) to give 3′,5′- and *N*-acylated derivatives of the corresponding 2′-deoxynucleosides (Entries 3, 4, and 5 in Table 1). The products formed in this reaction are easily isolated by extraction with ethyl acetate (2 × 20 ml) followed by washing with water, drying over sodium sulfate and distilling the solvent to yield products which are further purified by column chromatography and characterised by NMR and IR spectroscopy.

In order to study the selective acylation of amine functions of nucleoside relative to 3′- and 5′- hydroxy functional groups, acylation was carried out using 1 equiv. of Ac_2O with 1 equiv. of NMI and a catalytic amount of DMAP. However no selectivity was observed and the reaction yields a mixture of products. Peracylation of nucleosides is an important strategy used for the selective *N*-acylation of nucleosides in which, after complete acylation, the product is subjected to controlled hydrolysis to give *N*-acylated product. Complete benzoylation of 1 mmol of T, dA, and dC using 10 equiv. of benzoyl chloride and 10 equiv. of NMI as a base in 1 ml MOEMIM.OMs was accomplished in excellent yield (Entries 6, 7 and 8 in Table 1). The isobutyrylation of dG was carried out in a similar way using 10 equiv. of isobutyryl chloride and 10 equiv. of base NMI (Entry 9, Table 1). The products can be easily isolated by extraction with ethyl acetate (2 × 20 ml; 3 × 20 ml in the case

Table 1 Acylation of 2′-deoxynucleosides in MOEMIM.OMs IL

Entry	Nucleoside	Acylating agent (equiv.)	Base/Catalyst (equiv.)	Time/h	Yield (%)
1	T	$(CH_3CO)_2O$ (4)	—	27	89
2	T	$(CH_3CO)_2O$ (4)	NMI (4) DMAP (0.2)	1	92
3	dA	$(CH_3CO)_2O$ (6)	NMI (6) DMAP (0.2)	1.2	91
4	dC	$(CH_3CO)_2O$ (6)	NMI (6) DMAP (0.2)	1.3	92
5	dG	$(CH_3CO)_2O$ (6)	NMI (6) DMAP (0.2)	1.2	87
6	T	PhCOCl (10)	NMI (10)	1.3	95
7	dA	PhCOCl (10)	NMI (10)	1.5	94
8	dC	PhCOCl (10)	NMI (10)	1.5	93
9	dG	$(CH_3)_2COCl$ (10)	NMI (10)	1.8	85

of isobutyryl guanosine) followed by washing with sodium bicarbonate and drying over sodium sulfate. Distilling out the ethyl acetate yielded products that were further purified by column chromatography. In the case of dA (Entry 7, Table 1), *N*,*N*-dibenzoyl product was obtained. Controlled hydrolysis of products formed in these reactions (Entries 7, 8 and 9, Table 1) can give *N*-acylated deoxyribonucleosides.[8]

In order to compare acylation in MOEMIM.OMs to that in pyridine, acylation of T (1 mmol) using Ac_2O (4 equiv.) and DMAP (0.2 equiv.) in pyridine was carried out. The longer reaction time (~2.5 h) and tedious work-up in pyridine (which involves co-evaporation of pyridine with toluene followed by dissolving the mixture in ethyl acetate and washing the organic layer with water to ensure complete removal of pyridine) illustrate the usefulness of MOEMIM.OMs IL compared to traditional solvents. This is especially evident when considering the solvent-related 'green' benefits of the reusable IL. To confirm the latter possibility, MOEMIM.OMs from reaction of acylation of T (Entry 2, Table 1) was thoroughly washed with EtOAc (20 ml × 2) followed by drying under vacuum and reused in acylation of T; a similar reaction time was required for complete acylation with no loss in yield or purity of the product (Table 2). However, about 3 to 5% loss of IL was observed in each cycle due to handling.

Table 2 Recycling of MOEMIM.OMs

No. of cycles	% Yield
1	92
2	91
3	90

In conclusion, the environmentally benign ionic liquid MOEMIM.OMs is found to be a suitable solvent for the reactions of nucleosides. The solubility study shows better solubility of nucleosides in MOEMIM.OMs as compared to other ionic liquids investigated and the conventional solvents. Acylation and peracylations of the nucleosides are carried out in this IL with the advantage of ease of isolation of the product from the reaction medium by simply extracting with ethyl acetate and recycling of the ionic liquid. Thus, MOEMIM.OMs is a potential 'green alternative'[9] to the environmentally hazardous conventional solvents employed in the nucleoside chemistry. We continue our study towards the reuse of this ionic liquid in the reactions using acid chlorides and development of different reactions of nucleosides in this ionic liquid.

Experimental

The acylation of thymidine (T) was carried out by stirring thymidine (242 mg, 1 mmol), acetic anhydride (378 µl, 4 mmol) 1-methyl imidazole (220 µl, 4 mmol) and 4-dimethyl aminopyridine (25 mg, 0.2 mmol) in 1 ml ionic liquid MOEMIM.OMs for 1 h. On completion of the reaction (tlc, ethyl acetate), the product was extracted in ethyl acetate (10 ml × 2). The ethyl acetate layer was washed with water and dried over anhydrous sodium sulfate. Ethyl acetate was distilled out under vacuum to get the product, which was further purified by column chromatography (yield, 300 mg, 92%). **^{1}H NMR** (300 MHz, $CDCl_3$): δ 1.93 (s, 5-CH_3); δ 2.1(s, $COCH_3$); δ 2.44 (m, 2′-CH_2); δ 4.24 (s, 3′-H); δ 4.35 (s, 2′-CH_2); δ 5.2 (s, 4′-H); δ 6.32 (t, 1′-H); δ 7.28 (s, 6-H), δ 9.87 (bs, 3-NH).

Acknowledgements

This project was funded by Isis Pharmaceuticals, CA, USA. We are also thankful to Dr. P. P. Wadgaonkar, NCL, Pune, India for valuable suggestions and Dr. Douglas Cole (Isis) for his continued support.

Notes and references

† The methanesulfonate salts were prepared by single step reactions of methanesulfonate esters of alcohols with 1-methyl imidazole or pyridine in toluene to give respective salts. These salts were characterised by ^{1}H and ^{13}C NMR spectroscopy. In the typical procedure for preparation of the ionic liquid MOEMIM.OMs a mixture of 10 mmol of 1-methyl imidazole and 2-methoxyethyl methanesulfonate[10] (1.1 equiv.) was refluxed in 20 ml dry toluene in an inert atmosphere for 24 h to give the ionic liquid which formed a distinct immiscible layer at the bottom of the reaction mixture. The top layer of toluene was separated by decantation, the ionic liquid was washed with toluene followed by ethyl acetate and dried *in vacuo* to yield MOEMIM.OMs (yield 88%). **^{1}H NMR** (500 MHz, DMSO-d_6) δ 2.4 (3H, s), δ 3.24 (3H, s), δ 3.68 (2H, t, J = 4.5 Hz), δ 3.9 (3H, s), δ 4.95 (2H, t, J = 4.5 Hz), δ 7.79 (1H, s), δ 7.83 (1H, s), δ 9.29 (1H, s); **^{13}C NMR** δ 38.69, δ 51.55, δ 61.01, δ 72.73, δ 131.27, δ 131.94, δ 140.33, signal due to $CH_3SO_3^-$ is not observed. LCMS: *m*/*z* 141 (100%, MOEMIM$^+$); Purity (LCMS) 99.64%; water: 0.02%.

1 (*a*) M. MacCross and M. J. Robins, in *Chemistry of Antitumor Agents*, ed. D. E. V. Wilman, Blackie and Son, Glasgow, UK, 1990, p. 261; (*b*) R. K. Robins and G. D. Kini, in *Chemistry of Antitumor Agents*, ed. D. E. V. Wilman, Blackie and Son, Glasgow, UK, 1988, p. 11; (*c*) R. K. Robins and G. R. Revankar, in *Antiviral Drug Development*, ed. E. De Clercq and R. T. Walker, Plenum, New York, 1998, p. 11; (*d*) Y. S. Sanghvi and P. D. Cook, in *Nucleosides and Nucleotides as Antitumor and Antiviral Agents* ed. C. K. Chu and D. C. Baker, Plenum, New York, 1993, p. 311.

2 L. Lerman, *DNA probes: Applications in Genetic and Infectious Diseases and Cancer*, Cold Spring Harbor Laboratory, Cold Spring Harbor, USA, 1986.

3 S. T. Crooke and B. Lebleu, in *Antisense Research and Application*, CRC Press, Boca Raton, FL, 1993, p. 311.

4 (*a*) T. Welton, *Chem. Rev.*, 1999, **99**, 2071–2084; (*b*) P. Wasserchield and K. Wilhelm, *Angew. Chem., Int. Ed.*, 2000, **39**, 3772–3789; (*c*) R. Sheldon, *Chem. Commun.*, 2001, 2399–2407.

5 S. V. Dzyuba and R. A. Bartsch, *Tetrahedron Lett.*, 2002, **43**, 4657–4659.

6 N. Kimizuka and T. Nakashima, *Langmuir*, 2001, **17**, 6759–6761.

7 S. Park and R. J. Kazlauskas, *J. Org. Chem.*, 2001, **66**, 8395–8401.

8 N. S. Rao, P. Kumar, V. K. Chauhan, B. S. Garg and K. C. Gupta, *Nucleosides Nucleotides Nucleic Acids*, 2002, **21**, 393–400.

9 M. J. Earle and K. R. Seddon, in *ACS Symposium Series 819: Clean Solvents*, ed. M. A. Abraham and L. Moens, ACS, Washington, DC, 2002, p. 10.

10 2-Methoxyethyl methanesulfonate and MOEMIM.OMs are available from Sai Dru Syn Laboratories Ltd., Hyderabad, India. (www.saiintgroup.com).

Communication

A green method of adipic acid synthesis: organic solvent- and halide-free oxidation of cycloalkanones with 30% hydrogen peroxide

Yoko Usui and Kazuhiko Sato*

National Institute of Advanced Industrial Science and Technology (AIST), Tsukuba Central 5, Tsukuba 305-8565, Japan. E-mail: k.sato@aist.go.jp; Fax: +81-29-861-4852; Tel: +81-29-861-4852

Received 23rd May 2003
First published as an Advance Article on the web 11th July 2003

Cyclohexanone and cyclohexanol are oxidized to adipic acid in high yield with aqueous 30% H_2O_2 in the presence of H_2WO_4 as a catalyst under organic solvent- and halide-free conditions. It is important that no solvent is used in order to achieve high reactivity in this heterogeneous reaction. The use of *t*-butyl alcohol or dioxane as a solvent (homogeneous conditions) significantly decreases the yield of adipic acid from cyclohexanone. This ketone-to-dicarboxylic acid conversion is applicable to five- to eight-membered cyclic ketones. No operational problems are foreseen for a large-scale version of this green process.

Adipic acid is an important bulk chemical for the production of nylon-6,6.[1] Currently most industrial processes utilize the nitric acid oxidation of cyclohexanone and/or cyclohexanol.[2] This processing is cost-effective, however, it inevitably leads to nitrous oxide (N_2O) as a stoichiometric waste product.[3] N_2O is commonly thought to cause global warming and ozone depletion.[4] Thus, an environmentally friendly, yet practical procedure for the production of adipic acid from cyclohexanone and/or cyclohexanol is very desirable.[5]

Various oxidants including $KMnO_4$,[6,7] CrO_3,[8] and KO_2[9] have been elaborated for the synthesis of adipic acid from cyclohexanone and cyclohexanol. However, they are hazardous and expensive, and they form equimolar amounts of the deoxygenated compounds as waste products, preventing their use for large-scale reactions. Although air (molecular oxygen) is a clean oxidant, and the catalytic oxidation of cyclohexanone to adipic acid with O_2 has been reported, the reaction requires HMPA or acetic acid as a solvent.[10]

Hydrogen peroxide is an ideal oxidant because it has a high oxygen content, and water is the sole theoretical co-product.[11] This oxidant has become very inexpensive,[12] and in fact is produced in quantities of *ca.* 2.4 million metric tons year^{-1} for use, mainly as a bleach.[13] H_2O_2 can be a clean oxidant only if it is used in a controlled manner without organic solvents and other toxic compounds.[14,15]

We recently developed methods of performing practical epoxidation, the oxidation of alcohols, and other oxidation reactions with aqueous 30% H_2O_2 under organic solvent- and halide-free conditions.[5a,16] These methods give high-yields and are clean, safe, operationally simple, and cost-effective; they therefore meet the primary requirements of contemporary organic synthesis. Although the oxidation of cyclohexanone with H_2O_2 under homogeneous conditions using acetic acid or *t*-butyl alcohol as a solvent has been reported, the highest yield of adipic acid was *ca.* 50%, and the selectivity was relatively low.[17] Here, we report the practical procedures for adipic acid synthesis from the oxidation of cyclohexanone and cyclohexanol with aqueous 30% H_2O_2. These synthetic procedures satisfy the following conditions: (1) they are organic solvent- and halide-free systems; (2) they give a high yield; and (3) they are simple and involve safe manipulation. We also present a green and efficient method for C_5 to C_8 dicarboxylic acid synthesis.

The operation is very simple, even at a hectogram-scale synthesis, as shown in Scheme 1. Cyclohexanone (100 g), 30% H_2O_2 (382 g), and H_2WO_4 (2.50 g) were stirred in open air at 90 °C for 20 h to form adipic acid in > 99% yield (GC analysis). The collection of the crystalline product by filtration followed by drying in air produced a colorless, analytically pure adipic acid in 91% yield (135 g). The aqueous phase of the reaction mixture can be reused with 60% H_2O_2 to give adipic acid in 71% yield.† The oxidation of 100 g of cyclohexanol also produced crystalline adipic acid in 87% yield (127 g).

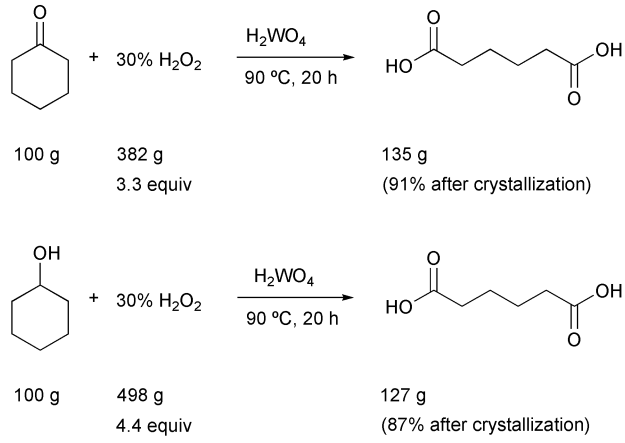

Scheme 1

A minimum pathway from cyclohexanone or cyclohexanol to adipic acid is shown in Scheme 2. The transformation is

Green Context

Clean oxidations are difficult to achieve, but this paper deals with a very efficient route to adipic acid (and other diacids). Aqueous hydrogen peroxide is used with cyclic ketones and a small amount of tungstic acid to directly provide the diacid, which solidifies upon cooling to give the product directly, without the use of promotors or solvents. ***DJM***

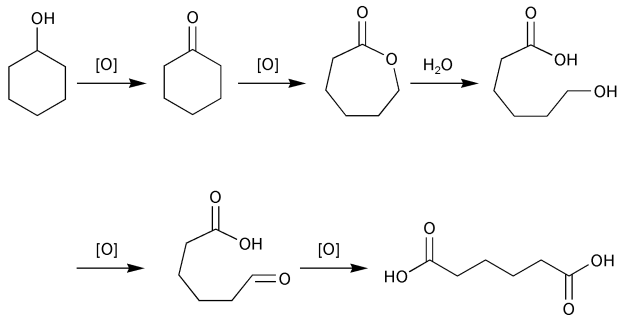

Scheme 2

achieved through multiple steps involving 4 types of oxidative reactions (two alcohol oxidations, Baeyer–Villiger oxidation, and aldehyde oxidation) and hydrolysis. Since the unproductive decomposition of H_2O_2 does not occur in this catalytic system, only a 3.3 molar amount of H_2O_2 per mol of cyclohexanone (3.0 mol in theory) is necessary for the three oxidation steps (a 4.4 molar amount of H_2O_2 in the case of cyclohexanol). In the course of the oxidation of cyclohexanone (43% conversion), adipic acid was solely formed in 43% yield at 90 °C for 10 h (GC and ^{1}H NMR analysis). None of the intermediates were observed. The oxidation of ε-caprolactone proceeded faster than that of cyclohexanone, to give 83% yield of adipic acid and 17% yield of 6-hydroxyhexanoic acid at 90 °C within 10 h. These results suggest that both Baeyer–Villiger oxidation and the oxidation of 6-hydroxyhexanoic acid in Scheme 2 are slow, but the former is probably the rate-determining step.

Although the reaction utilizes H_2WO_4 as the precatalyst, it is readily oxidized with H_2O_2 to form $H_2[WO(O_2)_2(OH)_2]$,[18] which is soluble in water [eqn. (1)]. The pK_a value is known to be 0.1. When Na_2WO_4 was used instead of H_2WO_4, the oxidation of cyclohexanone and cyclohexanol did not proceed. Since Na_2WO_4 is also readily oxidized with H_2O_2 to form $Na_2[WO(O_2)_2(OH)_2]$, the acidic nature of the catalyst is crucial for the reaction.

$$H_2WO_4 + H_2O_2 \xrightarrow{H_2O} H_2[WO(O_2)_2(OH)_2] \quad (1)$$

It is important that no solvent is used in order to achieve high reactivity in this heterogeneous reaction. The use of *t*-butyl alcohol or dioxane as a solvent (homogeneous conditions) significantly decreases the yield of adipic acid from cyclohexanone (31% with *t*-butyl alcohol, 52% with dioxane). Several peroxoketals (adducts of H_2O_2 to cyclohexanone) are spontaneously formed from cyclohexanone and H_2O_2 under the homogeneous conditions,[19] whereas such compounds were not observed under our heterogeneous conditions without organic solvent. In our reaction, Baeyer–Villiger oxidation would occur by the reaction of cyclohexanone and $H_2[WO(O_2)_2(OH)_2]$. The reason why the heterogeneous conditions show high reactivity remains unclear; nonetheless, it is likely that Baeyer–Villiger oxidation of cyclohexanone with $H_2[WO(O_2)_2(OH)_2]$ could be faster than that of peroxoketals.[20]

Table 1 shows the oxidation of five- to eight-membered cycloalkanones and cycloalkanols. A temperature of 90 °C was used as the optimum reaction condition. Lower temperatures decreased the yield of adipic acid from cyclohexanone to < 5% at 60 °C for 20 h. Higher temperatures are not desirable for safety reasons. When 0.05 molar amount of H_2WO_4 was used, adipic acid was obtained in 85% yield within 10 h. Under identical conditions to those used for cyclohexanone, cyclopentanone was converted to glutaric acid in 98% yield. The larger the ring size of the cycloalkanone, the lower was its reactivity. The seven- and eight-membered cycloalkanones need a 0.05 molar amount of the catalyst for completion of the oxidation. This is in accordance with the relative rate of Baeyer–Villiger oxidation with perbenzoic acid, which is known to be

Table 1 Oxidation of cycloalkanones and cycloalkanols with H_2O_2[a]

Entry	Substrate: Structure	Substrate: mmol	Product	Yield (%)[b]
1		10	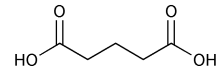	98
2	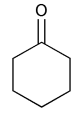	1019	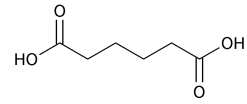	91[c]
3		10		99
4[de]		10		85
5[d]	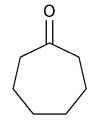	10	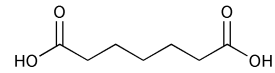	81
6[d]	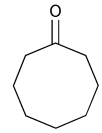	10	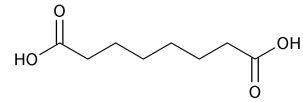	85
7[f]		10	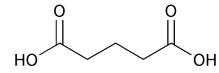	91
8[f]	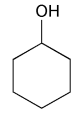	998	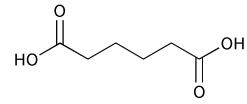	87[c]
9[f]		10		89

[a] Unless otherwise stated, reaction was run using 30% H_2O_2, substrate, and H_2WO_4 in a 330 : 100 : 1 molar ratio at 90 °C for 20 h. [b] Determined by GC analysis. Based on substrate charged. [c] Isolated yield after crystallization. [d] H_2O_2 : substrate : H_2WO_4 = 330 : 100 : 5. [e] Reaction for 10 h. [f] H_2O_2 : substrate : H_2WO_4 = 440 : 100 : 1.

cyclohexanone : cycloheptanone : cyclooctanone = 1.0 : 0.04 : 0.03.[21] In contrast to cycloalkanones, linear ketones resist this oxidation. Thus, 2-hexanone does not convert to the corresponding carboxylic acid.

This organic solvent- and halide-free synthesis of adipic acid from cyclohexanone and cyclohexanol is clean and safe under mild conditions that are less corrosive than those required for nitric acid oxidation. This ketone-to-dicarboxylic acid conversion is applicable for five- to eight-membered cyclic ketones. No operational problems are foreseen for a large-scale version of this green process.

Acknowledgement

We would like to thank Prof. R. Noyori for helpful comments and suggestions.

Notes and references

† *Typical procedure* (hectogram-scale oxidation of cyclohexanone with H_2O_2 and reuse of the water phase containing the tungsten catalyst): in the first run, a 1-liter, round-bottomed flask equipped with a magnetic stirring bar and a reflux condenser was charged with 2.50 g (0.01 mol) of H_2WO_4, water (50 mL), and 50 g (0.44 mol) of aqueous 30% H_2O_2. The mixture was heated to 55 °C until a clear solution was obtained, then 100 g (1.02 mol) of cyclohexanone and 332 g (2.93 mol) of aqueous 30% H_2O_2 were added. The mixture was heated at 90 °C for 20 h, and then cooled to room temperature. The homogeneous solution was allowed to stand at 0 °C for 12 h, and the resulting colorless precipitate was separated by filtration and washed with 20 mL of cold water. The product was dried in a vacuum to give 135 g (91% yield) of adipic acid as a colorless solid. Mp 151.0–152.0 °C; ^{1}H NMR (500

MHz, CD_3OD): δ 1.72 (m, 4H), 2.40 (m, 4H), 5.31 (brs, 2H); ^{13}C NMR (125 MHz, CD_3OD): δ 177.30, 34.57, 25.53; elemental analysis (%) calcd for $C_6H_{10}O_4$: C 49.31, H 6.90; found: C 49.40, H 6.71. In the second run, a 1-liter round-bottomed flask was charged with the water phase of the first run, which contained the tungsten catalyst, 100 g (1.02 mol) of cyclohexanone, and 191 g (3.37 mol) of aqueous 60% H_2O_2 were added. This mixture was heated at 90 °C for 20 h, and the homogeneous solution was allowed to stand at 0 °C for 12 h. The resulting colorless precipitate was separated, washed, and dried in a vacuum to give 106 g (71% yield) of adipic acid.

1 D. D. Davis and D. R. Kemp, in *Kirk–Othmer Encyclopedia of Chemical Technology*, ed, J. I. Kroscwitz and M. Howe-Grant, John Wiley & Sons, Inc., New York, 4th edn., 1991, vol. 1, pp. 466–493.

2 (*a*) D. D. Davis, in *Ullmann's Encyclopedia of Industrial Chemistry*, ed. W. Gerhartz, S. Y. Yamamoto, T. F. Campbell, R. Pfefferkorn and J. F. Rounsaville, VCH Publishers, Weinheim, 5th edn., 1985, vol. A1, pp. 269–278; (*b*) K. Weissermel and H.-J. Arpe, *Industrial Organic Chemistry*, VCH Publishers, Inc., New York, 3rd edn., 1997, pp. 239–242.

3 M. H. Thiemens and W. C. Trogler, *Science*, 1991, **251**, 932–934.

4 R. E. Dickinson and R. J. Cicerone, *Nature*, 1986, **319**, 109–115.

5 For a green route to adipic acid from cyclohexene and H_2O_2, see: (*a*) K. Sato, M. Aoki and R. Noyori, *Science*, 1998, **281**, 1646–1647; For synthesis from D-glucose, see (*b*) K. M. Draths and J. W. Frost, *J. Am. Chem. Soc.*, 1994, **116**, 399–400.

6 The $KMnO_4$ oxidation of cyclohexanone to adipic acid has been used in a textbook of organic experiments because this transformation is of educational value. For example, see: L. F. Fieser and K. L. Williamson, *Organic Experiments*, Houghton Mifflin Company, Boston, MA, 8th edn., 1998, pp. 254–264.

7 (*a*) E. Rosenlew, *Chem. Ber.*, 1906, **39**, 2202; (*b*) R. M. Acheson, *J. Chem. Soc.*, 1956, 4232–4237.

8 (*a*) L. Ruzicka, C. F. Seisel, H. Schinz and M. Pfeiffer, *Helv. Chim. Acta*, 1948, **31**, 422–426; (*b*) J. Rocek and A. Riehl, Jr., *J. Am. Chem. Soc.*, 1967, **89**, 6691–6695.

9 M. Lissel and E. V. Dehmlow, *Tetrahedron Lett.*, 1978, 3689–3690.

10 (*a*) T. J. Wallace, H. Pobiner and A. Schriesheim, *J. Org. Chem.*, 1965, **30**, 3768–3771; (*b*) S. Ito and M. Matsumoto, *J. Org. Chem.*, 1983, **48**, 1133–1135; (*c*) A. Atlamsani and J. Brégeault, *J. Org. Chem.*, 1993, **58**, 5663–5665; (*d*) W. Flemming and W. Speer, US Patent, 1935, 2 005 183; (*e*) W. J. Amend, US Patent, 1943, 2 316 543; (*f*) K. Tanaka and Y. Matsuoka, JP Patent, 2001, 213 841; (*g*) For oxidation of cyclohexane with O_2 in acetic acid, see: Y. Ishii, T. Iwahama, S. Sakaguchi, K. Nakayama and Y. Nishiyama, *J. Org. Chem.*, 1996, **61**, 4520–4526.

11 (*a*) C. W. Jones, *Applications of Hydrogen Peroxide and Derivatives*, Royal Society of Chemistry, Cambridge, 1999; (*b*) *Catalytic Oxidations with Hydrogen Peroxide as Oxidant*, ed. G. Strukul, Kluwer Academic, Dordrecht, 1992.

12 The current price is < 0.7 dollar kg^{-1} (100% H_2O_2 basis).

13 W. T. Hess in *Kirk–Othmer Encyclopedia of Chemical Technology*, ed. J. I. Kroscwitz and M. Howe-Grant, John Wiley & Sons, Inc., New York, 4th edn., 1995, vol. 13, pp. 961–995.

14 J. O. Metzger, *Angew. Chem., Int. Ed.*, 1998, **37**, 2975–2978.

15 There is a trend to use H_2O_2 as an oxidant for large-volume processes such as caprolactam synthesis (Sumitomo Chemical Co.) and propylene oxidation (BASF and Dow Chemical Co.). See: (*a*) *Sumitomo Chemical News Release*, 2000, Oct. 11; (*b*) *Dow Products and Businesses News*, 2002, Aug. 1.

16 (*a*) K. Sato, M. Aoki, M. Ogawa, T. Hashimoto and R. Noyori, *J. Org. Chem.*, 1996, **61**, 8310–8311; (*b*) K. Sato, M. Aoki, J. Takagi and R. Noyori, *J. Am. Chem. Soc.*, 1997, **119**, 12386–12387; (*c*) K. Sato, M. Aoki, M. Ogawa, T. Hashimoto, D. Penyella and R. Noyori, *Bull. Chem. Soc. Jpn.*, 1997, **70**, 905–915; (*d*) K. Sato, J. Takagi, M. Aoki and R. Noyori, *Tetrahedron Lett.*, 1998, **39**, 7549–7552; (*e*) K. Sato, M. Aoki, J. Takagi, K. Zimmermann and R. Noyori, *Bull. Chem. Soc. Jpn.*, 1999, **72**, 2287–2306; (*f*) K. Sato, M. Hyodo, J. Takagi, M. Aoki and R. Noyori, *Tetrahedron Lett.*, 2000, **41**, 1439–1442; (*g*) K. Sato, M. Hyodo, M. Aoki, X.-Q. Zheng and R. Noyori, *Tetrahedron*, 2001, **57**, 2469–2476.

17 (*a*) G. Payne and C. W. Smith, *J. Org. Chem.*, 1957, **22**, 1680–1682; (*b*) Y. Ishii, A. Adachi, R. Imai and M. Ogawa, *Chem. Lett.*, 1978, 611–614; (*c*) Y. Ishii, JP Patent, 1979, 135 720. For the oxidation of cyclopentanone with H_2O_2 and solid acid catalysts, see (*d*) J. Fischer and W. F. Hölderich, *Appl. Catal., A: Gen.*, 1999, **180**, 435–443.

18 A. F. Ghiron and R. C. Thompson, *Inorg. Chem.*, 1988, **27**, 4766–4771.

19 (*a*) M. S. Kharasch and G. Sosnovsky, *J. Org. Chem.*, 1958, **23**, 1322–1326; (*b*) P. R. Story, B. Lee, C. E. Bishop, D. D. Denson and P. Busch, *J. Org. Chem.*, 1970, **35**, 3059–3062.

20 A. Berkessel, M. R. M. Andreae, H. Schmickler and J. Lex, *Angew. Chem., Int. Ed.*, 2002, **41**, 4481–4484.

21 S. L. Friess and P. E. Frankenburg, *J. Am. Chem. Soc.*, 1952, **74**, 2679–2680.

Critical Review

Development of a non-toxic electrolyte for soft gold electrodeposition: an overview of work at University of Newcastle upon Tyne

M. J. Liew,* S. Roy and K. Scott

School of Chemical Engineering and Advanced Materials, Merz Court, University of Newcastle upon Tyne, Newcastle upon Tyne, UK NE1 7RU

Received 29th January 2003
First published as an Advance Article on the web 11th June 2003

Electroplated soft gold is widely used in the growing fields of micro- and opto-electronics as a conducting material for interconnects and devices. Due to problems related to resist compatibility, safety and disposal concerns, cyanide-free plating baths are now strongly in demand. The interest in developing non-toxic gold electrolytes, such as those based on sulfite complexes, has grown rapidly in recent years. The most common non-cyanide gold electrolyte is based on a gold-sulfite complex, which has problems related to stability and resist compatibility. Recently, a novel electrolyte that can be used for soft gold deposition, and is suitable for the formation of microbumps on wafers for electronic applications has been proposed. This bath, containing both thiosulfate and sulfite as complexing agents, is non-toxic, stable on storage and operation, and does not contain any chemical additives or stabilisers. At Newcastle University, we have tested this electrolyte for long term stability, suitability for large scale production, and recyclability (by electrowinning). We have reported the performance of this electrolyte here in this review.

1 Introduction

Electrodeposition of gold is not a new process, but has been widely used in the automotive industries, biomedical processes and electronics industries such as in computers, telecommunications, aerospace applications, *etc*.[1–10] The combination of excellent electrical conductivity with high corrosion resistance has led to the widespread adoption of gold as a standard material for interconnects such as contacts, bonds, and high reliability performance conductor applications. In the electronics industry, electrodeposited gold is used due to its remarkable characteristics in terms of electrical, chemical and optical properties, such as high purity combined with wear resistance of the deposits.

Due to the high intrinsic cost of gold, it is important and advantageous to identify the type of plating baths which can offer the best gold deposits for a deposition process. Therefore, microelectronics, optoelectronics and micro systems enterprises continue to search for electrolytes which are economical to use, whilst fulfilling the desired requirements of micro-devices.

Electroplated gold can be classified as either soft gold or hard gold. Hard gold is used as a contact material for electrical connectors and printed circuit boards (PCBs), relays and switches, which should be resistant to mechanical wear whilst having a low electrical contact resistance.[5,6,11] Hard gold alloys are particularly employed in those sections of the industry where the contact is subjected to wear by the making and breaking of connections. In general, hard gold is obtained by co-depositing gold with metals such as nickel, cobalt and iron as hardening agents.[11,12] Inclusion of these materials considerably alters the properties of the deposit, giving a significant rise in hardness and wear resistance.[13–15] The presence of impurities also reduces the tendency of the gold layer to weld by friction, which makes this material very attractive for connectors and contact applications.

Soft gold, on the other hand, is used for electronic packaging, such as fabrication of interconnects in integrated circuits (ICs), or forming connections to external devices, using tape automated bumping (TAB) or chip-on-glass (COG) and chip-on-flex (COF) techniques.[1–9] The key process in all these technologies is gold wafer bumping. In addition to its use in connecting driver ICs to flat panel displays, gold bumping is also used for high density of I/O (input/output) connections and many packaging applications.[4] Soft gold deposits have also been used to fabricate X-ray masks and three-dimensional microstructures by the LIGA process, which are useful in micro-electro-mechanical systems (MEMS).[7,8] In the opto-electronics industry, gold is used to fabricate interconnects and transmission lines.[10]

The above-mentioned technologies utilise a through-mask plating technique, which is illustrated in Fig. 1. The process involves the deposition of a conductive seed layer on a wafer, followed by photolithography.[16] After development, resist residue is removed by ashing with a plasma containing oxygen. Gold is then electroplated on the exposed areas of the wafer. Upon completion of plating, the remaining resist is removed, followed by seed layer etching.

Although the requirement for each device varies slightly, usually deposits require high purity, low stress and good adhesion to the substrate. Moreover, they should be sufficiently ductile and soft to prevent cracking, which may lead to bond

Green Context

The electroplating of gold is important in many areas including the rapidly growing fields of micro- and opto-electronics where the gold acts as a conducting material. Traditional cyanide-based plating baths are now strongly disfavoured for obvious toxicity concerns but also because of the ability of excess cyanide to attack the interface between the resist film and substrate. The article is an overview of the current status of gold plating in the micro- and opto-electronics industry. It is suggested that thiosulfate and sulfite complexes provide the best electrolyte for 'soft' gold deposition. ***JHC***

 DOI: 10.1039/b301176n

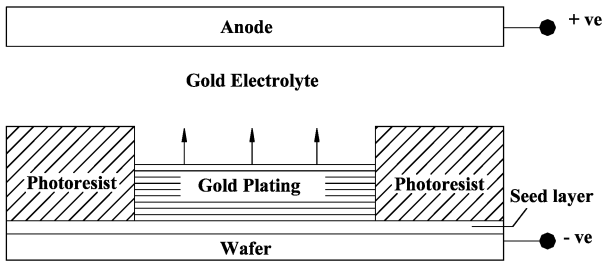

Fig. 1 Illustration of gold bump plating by through-mask plating.

failure. In order to achieve these properties, pure soft gold has to be electrodeposited from electrolytes because inclusion of any other material induces hardness and reduces ductility.

In conjunction with fabrication and packaging of semiconductor devices, soft gold is used as a finish for bonding gold or aluminium wire. Here, gold bumps are plated on the chip and circuit board which are wire bonded. Since the bonding of a large number of bumps is involved for each chip, uniformity in the bump geometry is important. Hence, the electrodeposited gold must be sufficiently soft so that the bumps are easily deformable to accommodate small variations in thickness.

2 Electrodeposition of soft gold

2.1 The process

Fig. 2 illustrates the process of electrodeposition using an electrolyte containing a metal ion. Within the *Helmholtz* double layer, the co-ordinated positive metal ion in its ligand field is attracted towards the cathode surface. The distribution of ligands around the metal is distorted in this region. The negatively charged complex ion becomes polarised in the electric field of the cathode, thus the ligand ions are freed and the metal is then deposited onto the cathode.[17]

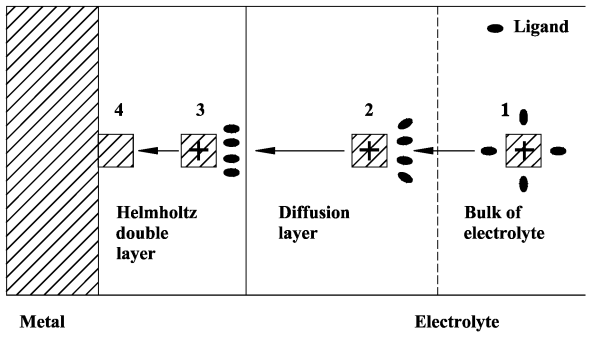

Fig. 2 Schematic diagram of gold deposition process.[17]

In general, the principal reaction for gold electrodeposition[17] from a plating bath containing either cyanide, sulfite or thiosulfate as the complexant is

$$\text{Au (I)-complex} + e \leftrightarrow \text{Au} + \text{complex} \quad (1)$$

For a homogeneous reversible reaction, the law of mass action dictates that

$$\frac{[\text{Au(I)} - \text{complex}]}{[\text{Au}][\text{complex}]} = \beta \quad (2)$$

where [Au], [complex] and [Au(I)-complex] are the concentrations of gold ion, complex ion and gold complex in the solution. The constant, β, known as the stability constant, is a measure of the strength of the complexant. Since the disproportionation of gold in solution is controlled by the concentration of gold complex, knowledge of the stability constant of the complex is essential for the determination of the bath stability.

2.2 Gold cyanide electrolyte

The conventional cyanide electrolyte for electroplating gold has been extensively studied in the past and a considerable amount of information on the process, as well as deposit properties and microstructure is available in the literature.[3,11,14,17–19] In general, acid cyanide baths at pH ≈ 5.0 are used to produce soft gold, and alkaline or neutral baths are used to produce hard gold.[17,18,20]

A common cyanide-based gold plating electrolyte compositions is shown in Table 1. Electrodeposition of soft gold on electronic devices and components is generally performed using a bath containing cyanoaurate(I) ions because gold cyanide complexes have the highest stability constant. The value of β for $Au(CN)_2^-$ is 10^{38}.[17] The main reasons for the popularity of cyanide-based electrolytes are that this bath is very stable and yields fine-grained gold deposits.[19] In addition, the deposits obtained are bright, adherent and have good corrosion resistance.

Table 1 Chemical composition of a common cyanide-based electrolyte used for soft gold deposition[17,20]

Chemical	Composition
$KAu(CN)_2$	0.05 M
KH_2PO_4	0.40 M
$K_3C_6H_5O_7$	0.25 M
$Na_2S_2O_3$	0.04 M

The primary disadvantage of using acid cyanide complexes is the presence of cyanide in solution, which makes waste disposal difficult. In addition, when the electrolyte is used under acid conditions, the gold cyanide complex can decompose, thus leading to the formation of undissociated HCN.[17]

$$HCN \leftrightarrow CN^- + H^+ \quad (3)$$

Free cyanide ions generated as a result of the gold deposition process are chemically active. The excess cyanide ions attack the interface between the resist film and substrate, lifting the resist and depositing extraneous gold underneath the resist in the process,[3,10] which is highly undesirable in most applications.[20] This results in the shape changes of the micro-devices, and thereby causes the loss of performance which is referred to as 'underplating'.

Since cyanide electrolytes are unstable in acidic conditions, most conventional cyanide baths are set to operate at pH 10.0, or above, due to safety considerations. However, cyanide-based electrodeposition processes at high pH value cannot be used for micro-device manufacture, mainly because photoresists are unstable at pH > 8.0. Since cyanide can also delaminate the resist at a low pH, its toxicity and poor compatibility with photoresists does not lend itself to the deposition of soft gold. In view of this, a lot of work has been carried out to develop non-cyanide baths which offer better resist compatibility.

2.3 Gold sulfite electrolyte

Sulfite is the most commonly used complex for gold deposition as an alternative to the cyanide electrolyte. It is non-toxic and suitable for plating soft gold in the microelectronics industry. Gold sulfite baths produce fine, smooth, bright and ductile gold deposits.[1,2,20–23] Moreover, the bath exhibits better compatibility with the resists and underplating of gold is less of a problem.[10,20]

In the sulfite-based bath, gold exists in the form of $[Au(SO_3)_2]^{3-}$. The stability constant, β, of the sulfite complex is approximately 10^{10}, which is several orders of magnitude smaller than that of the cyanide complex. On standing, the excess sulfite in solution tends to decompose spontaneously to form a precipitate of metallic gold and sulfite ions by the following disproportionation reaction:

$$Au(SO_3)_2^{3-} \leftrightarrow Au^+ + 2SO_3^{2-} \quad (4)$$

$$3Au^+ \rightarrow Au^{3+} + 2Au^0 \quad (5)$$

The sulfite ion itself can also decompose according to reaction 6, which forms hydroxyl ions. This equilibrium is pH-dependent.

$$SO_3^{2-} + H_2O \leftrightarrow SO_2 + 2OH^- \quad (6)$$

At a pH of 7.0, the equilibrium of sulfurous acid in reaction 7 starts to shift to the right, thereby releasing SO_2.

A second reaction is the cathodic reduction of sulfite to dithionite, $S_2O_4^{2-}$, the electrolysis of which can lead to a chemical reduction of gold ions to metallic gold.[24]

$$SO_2^- \leftrightarrow + SO_2\ S_2O_4^- \quad (7)$$

To counteract these stability problems, many Au (I) sulfite baths described in the literature are operated at pH ≥ 8.0.[1,2,7,8,10,20] This means that problems can still arise when photoresists, which are soluble in alkaline solutions are used. While the dissolution of these resists is slower, under milder alkaline conditions (as compared to cyanide electrolytes), significant organic contamination of the plating bath can occur as the plating process continues. This can affect deposit hardness, stress and morphology as well as make the process control difficult. Since conventional positive photoresists are unstable in alkaline pHs, it is desirable to use an electrolyte that can be operated at a neutral or acidic pH to minimise the interaction between the resist and the plating bath, whilst having better stability.

Commercially available sulfite baths have addressed this problem by incorporating proprietary stabilising additives. For example, the addition of organic amines, such as ethylenediamine, is known to stabilise the electrolyte and enables operation within a pH range of 5.0 to 8.0.[20] It has been found that the addition of 2,2′-dipyridine suppresses the disproportionation reaction to a large extent, presumably through the formation of its complex with Au^+.[25] No adverse effect was observed on hardness or surface morphology of the deposited gold. Furthermore, simultaneous addition of both a polyamine, such as ethyldiamine, and an aromatic nitro compound such as nitrobenzene has also been found to stabilise the Au (I)-sulfite complex to such a great extent that the bath can be operated at an even lower pH of 4.0 to 6.5.[21] However, from the environmental context, using such organic additives can cause waste disposal problems. Reuse of electrolytes, thereby, compromise the long term sustainability of the process.

As a second course of action, ammonium sulfite baths, which operate in the pH range 6.0 to 8.0, have also been developed. These baths are useful alternatives to the commonly used sodium sulfite electrolyte.[26] The ammonium sulfite electrolyte appears to be stable without additives and was found to be compatible with positive photoresists. However, As^{3+} is added as a grain refiner to improve the brightness of the gold deposits, which increases hardness.[23] Again, As^{3+} is a toxic material which poses waste disposal concerns.

Watanabe *et al.*[1] tested sulfite electrolytes containing cerium ions to improve the smoothness and softness of the gold films for the formation of microbumps. They also investigated whether the inclusion of conductive salts such as sulfuric acid and boric acids improved deposit smoothness. They reported that the addition of heavy metal ions such as thallium and arsenic were effective in improving the topology of deposited gold, but these additives are highly toxic which makes them unsustainable in the long term.

2.4 Gold thiosulfate electrolyte

Gold thiosulfate complex, $[Au(S_2O_3)_2]^{3-}$ offers better electrolyte stability because the value of β is 10^{26},[5] which is substantially greater than that of the sulfite complex. Thus, the thiosulfate complex might be expected to be a viable alternative to the sulfite complex. Gold electrolytes containing the Au (I)-thiosulfate complex have been known since 1913,[27] but never been used for making a practical plating bath for gold deposition. Extensive work has been carried out to study the electrochemical reduction of the thiosulfate system to determine the stability and also to explore the usage of the thiosulfate bath.[28,29] However, no publication of the usefulness of the thiosulfate bath for gold deposition has appeared, though there have been two reports of gold thiosulfate used as a source of gold for electroless plating.[30,31]

Although thiosulfate complexes of Au (I) are stable as solid salts, they have never formed the basis for an electrodeposition process, mainly due to the instability of excess thiosulfate ions, which disproportionate to form colloidal sulfur according to the following reaction,

$$S_2O_3^{2-} \leftrightarrow S^0 + SO_3^{2-} \quad (8)$$

At neutral or mildly acidic conditions, pH ≈ 6.0, protonation of excess $S_2O_3^{2-}$ forms HSO_3^- and colloidal sulfur, which hinders its industrial exploitation,

$$H^+ + S_2O_3^{2-} \leftrightarrow S^0 + HSO_3^- \quad (9)$$

At still lower pH values, the HSO_3^- ion combines with a second proton and yields H_2SO_3 which eventually leads to the evolution of sulfur dioxide. It is clear that reactions described in 8 and 9 impede the use of thiosulfate-based electrolytes for gold deposition.

2.5 Thiosulfate-sulfite mixed ligand bath

The possibility of electroplating soft gold specifically for the formation of microbumps on silicon wafers from a non-cyanide bath containing both thiosulfate and sulfite as complexing agents was proposed by Osaka and co-workers.[32] The bath, the composition of which is shown in Table 2, was reported to be

Table 2 Comparison of composition of gold thiosulfate-sulfite electrolyte used by Osaka and Newcastle group

	Composition	
Chemical	Osaka	Newcastle
$NaAuCl_4$	0.06 M	—
$HAuCl_4$	—	0.05 M
Na_2SO_3	0.42 M	0.42 M
$Na_2S_2O_3$	0.42 M	0.42 M
Na_2HPO_4	0.30 M	—
Tl_2SO_4	5–30 ppm	—

stable, which was attributed to the formation of a mixed thiosulfate-sulfite complex from the reaction shown below,

$$Au^+ + SO_3^{2-} + S_2O_3^{2-} \leftrightarrow [Au(SO_3)(S_2O_3^{2-})]^{3-} \quad (10)$$

The bath was operated at a slightly acidic pH of 6.0 and there was no need to add a stabiliser to suppress spontaneous decomposition. Gold deposition was carried out at a mildly elevated temperature of 60 °C. The best process conditions yielded a Vickers hardness of approximately 80 kg mm^{-2} (0.8 GPa). The addition of thallium ions, in the form of Tl_2SO_4, as a grain refiner was found to decrease hardness and improve surface morphology of the gold deposit. The improved bath offered soft gold deposits under safe, neutral, low temperature and stable plating conditions. However, there are some

problems with this electrolyte. Toxicity of thallium (human poison; lethal dose approximately 0.1 mg m^{-3}) is of concern.[33] The inclusion of Tl^+ affects adversely the bonding of gold wires to the plated structure.[34] Finally, the thallium content in the electrolyte needs close monitoring during process operation.

2.6 Thiosulfate-sulfite electrolyte studies at Newcastle

Based on the mixed ligand electrolyte of Osaka, Newcastle has developed an electrolyte for soft gold electrodeposition which has attempted to eliminate Na_2HPO_4 and Tl^+. Table 2 shows the formulation of gold electrolytes used by Osaka and Newcastle. As a first step, a method for formulating the gold electrolyte was developed at Newcastle.

The solution was prepared by first dissolving both the complexes together (0.42 M Na_2SO_3 and 0.42 M $Na_2S_2O_3$) with deionised water. It was found that Na_2SO_3 acted as a buffer and maintained the pH of the solution — if it were not added at the same time as $Na_2S_2O_3$, the solution pH decreased rapidly leading to sulfur precipitation. Thereafter, 0.05 M $HAuCl_4$ was added slowly to the solution containing the mixed ligand by means of a burette in order to avoid any rapid changes in pH. It was necessary to stir the solution as well as monitor the pH throughout the preparation process. If this method was not followed, the pH of the solution decreased rapidly, precipitating S^o and releasing SO_2.

UV-visible spectroscopy analysis was carried out to determine the gold complex in solution. The experiments revealed that Au(I) was complexed with thiosulfate — no evidence of a mixed complex was found.[35] Based on our results, we propose an alternative view of the system. We believe that the monovalent gold ion (Au (I)) is complexed by thiosulfate which has a relatively high stability constant.

$$2[Au(S_2O_3)_2]^{3-} \leftrightarrow Au_2S_2O_3 + 3S_2O_3^{2-} \quad (11)$$

The sulfite ligand, on the other hand, simply maintains a high level of bisulfite ions in the solution under neutral or mildly acidic conditions, which shifts the equilibrium between the thiosulfate, sulfur and bisulfite ions in eqn. 12 towards the left, making the formation of sulfur less favourable.

$$H^+ + (S_2O_3)^{2-} \leftrightarrow (HSO_3)^- \quad (12)$$

This means that gold is stabilised by the formation of $Au(S_2O_3)_2^{3-}$ ions and precipitation of sulfur is avoided by excess HSO_3^-. In this regard, the electrolyte constituents work in 'synergy'.

The use of this electrolyte was tested at the site of an industrial partner, where degradation in a sulfite electrolyte was observed typically after plating 20–25 wafers. Stability of the bath was monitored by depositing a total of 30 wafers in a flow cell over 2 weeks.[35] In these experiments, there was no apparent degradation or physical change in the electrolyte.

Table 3 summaries the performance of the electrolyte during tests at our industrial partner. In these experiments the process conditions for both the thiosulfate-sulfite and sulfite electrolyte were the same. The electrolyte pH remained near-neutral (pH 7.4) throughout the two weeks and the process remained stable during the entire period. The plating solution remained colourless and clear, showing no signs of precipitation.

After plating, each wafer was inspected for signs of dissolution, cracking or delamination of the photoresist. Fig. 3 shows no observable physical change of the resist on the wafer after electrodeposition from the thiosulfate-sulfite bath, which suggests that there was no significant interaction between the resist and the bath. Current efficiency of the gold deposition was determined gravimetrically from a series of plating experiments and the average current efficiency obtained was 98.9%,[35] which was slightly higher than the sulfite electrolyte.

Hardness measurements of the gold deposits were performed using a nano-indenter (Hysitron Triboindenter, Hysitron Inc.),

Table 3 Summary of sulfite and thiosulfate-sulfite electrolyte performance during tests carried out at industrial

	Sulfite	Thiosulfate-sulfite (Newcastle)
pH	9.5 ± 0.1/stable	7.4 ± 0.1/stable
Current efficiency	98.2%	98.9%
Cell potential	1.3 V	0.7 V
Resist compatibility	Poor Speckled pits found on resist surface	Good No changes in physical appearance of resist
Electrolyte stability	Average Signs of bath decomposition as colour changed to purple	Good No apparent degradation or precipitation
Hardness	Soft	Soft
Uniformity	Average	Average
Roughness	Smooth	Rougher

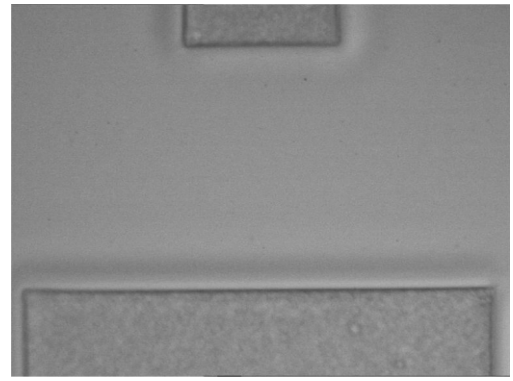

Fig. 3 SEM image of resist after deposition from modified gold thiosulfate-sulfite solution, pH 7.4 at 3.5 mA cm^{-2} (× 200 mag).

in which indentations were made on the specimen surface by a sharp indenter for a given dwell time under a given load range. Indentation loads applied in the experiments were in the range of 0.1 to 2.5 mN. The hardness of gold deposited from the thiosulfate-sulfite bath at three different current densities was compared to that of samples plated from the sulfite bath, shown in Fig. 4. Deposits obtained had hardness values in the range of 0.7 to 0.9 GPa, which are softer than the sulfite deposits (*ca.* 0.95 to 1.20 GPa).

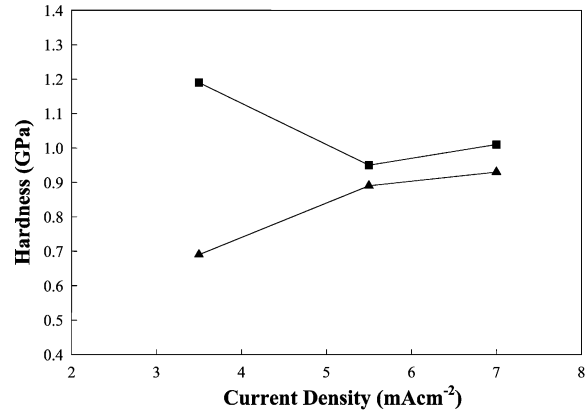

Fig. 4 Hardness of gold deposited from sulfite (■) and thiosulfate-sulfite (▲) electrolyte at different current densities.

Gold deposits from the plating electrolyte were bright and adherent. The plated structures, examined by scanning electron microscopy showed good reproduction of the photoresists mould. The gold structures achieved had straight side-walls

with top planar surface, shown in Fig. 5, and exhibits a columnar microstructure, similar to the deposits obtained from the electrolyte by Osaka and the sulfite bath.

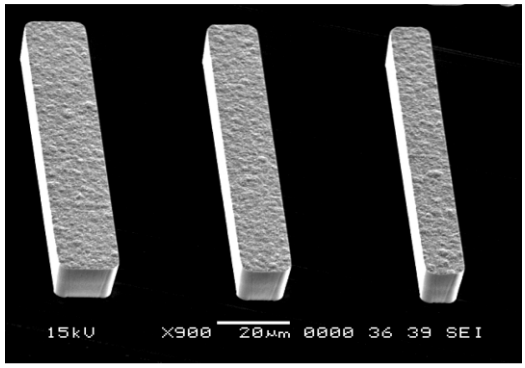

Fig. 5 SEM micrograph of gold test structure plated from the thiosulfate-sulfite electrolyte at 5.5 mA cm^{-2}.

The adhesion of the plated gold to the wafer surface was determined using a simple tape test. Although the test is qualitative and only gives an approximate assessment of adhesion, all wafers passed the test, indicating reasonably good adhesion of the gold bumps to the substrate. In addition, wire bonding tests also showed that there was no failure at the bump-wire junction. Roughness of gold deposited was found to be in the range of 2000–2500 Å, which is higher than the average deposits obtained from sulfite electrolytes.[36] It should also be noted that the electrolyte was not optimised to minimise surface roughness. In any case, the roughness values obtained is still adequate for majority of applications, and in certain instances, such as wire bonding, deposits require a rough surface.

Other properties such as thickness uniformity and stress of the plated structure were also investigated and were found to be compatible within the requirements for a wide range of micro and opto-electronic applications.[35] Comparison in thickness uniformity as a function of applied current density for both the sulfite and thiosulfate-sulfite electrolyte is shown in Fig. 6. Note that the thickness uniformity is expressed as a percentage of the ratio of the standard deviation to the mean and the value at each current density is the mean variation of three separate wafers. The figure shows that the uniformity of gold deposited from thiosulfate-sulfite electrolyte is superior to the sulfite for all current densities. The uniformity was found to be better when the applied current density was low, *i.e.* 3.5 mA cm^{-2}, where thickness uniformity was obtained with less than 3% variation. Future work is expected to focus on using pulse-plating techniques to further reduce surface roughness, and to modify plating and bath conditions to improve adhesion.

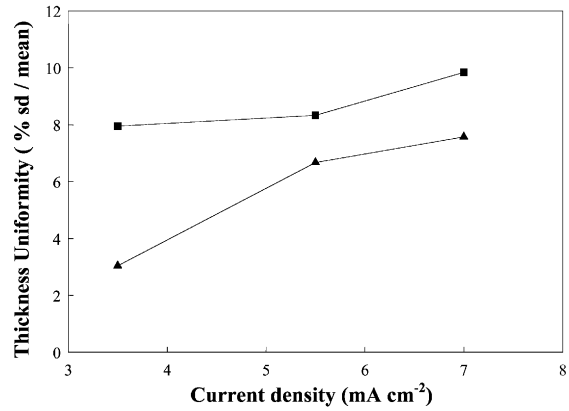

Fig. 6 The dependence of thickness uniformity on applied current density at solution flow rate 220 m^3 s^{-1} for sulfite (■) and thiosulfate-sulfite (▲) gold electrolyte. Uniformity is expressed as percentage of the ratio (% standard deviation/mean).

The mixed thiosulfate-sulfite electrolyte also has advantage over the acid-cyanide solution. Comparison of the chemical and physical properties is listed in Table 4. It is clear that for soft gold deposition purposes, the thiosulfate-sulfite electrolyte is a better alternative from hardness and resist-compatibility point of view, and offers a competitive process chemistry.

Conclusion

This article provides an overview of the electrolytes used for soft gold electrodeposition in the micro and opto-electronics industry. The development of a sustainable electrolyte based on the thiosulfate and sulfite complex has been compared with the traditional ones. In this electrolyte, Au (I) is complexed by thiosulfate, and the formation of colloidal gold is avoided. Sulfite, on the other hand prevents the formation of sulfur by maintaining a high level of bisulfite in the solution.

The feasibility of the thiosulfate-sulfite based electrolyte, developed in Newcastle University, to deposit soft gold onto wafers for device applications has been carried out on a large scale under industrial conditions. Solution pH remains relatively constant (± 0.1) and the bath remains clear and colourless with no apparent signs of degradation or precipitation. The electrolyte showed good compatibility with the resists used in the process.

Table 4 Comparison of acid cyanide and thiosulfate-sulfite gold plating electrolytes for soft gold deposition

	Acid cyanide	Thiosulfate-sulfite (Newcastle)
Chemical properties of plating bath		
Toxicity	Potentially toxic	Non-toxic
Operating bath pH	pH 5.0 (acidic)	pH 7.4 (near-neutral)
Bath stability	Best stability	Stable
Waste disposal	Gold recovery possible and CN^- is converted to CO_3^{2-}	Possibility of gold recovery by electrowinning
Resist compatibility	Penetrates and delaminates organic photoresist, which leads to 'underplating'	No significant attack on photoresists
Ease of bath preparation	Fairly difficult	Fairly difficult
Relative electrolyte cost	Controlled by the price of gold	Controlled by the price of gold
Physical properties of deposited gold		
Microstructure	Underplating may lead to shape change of gold bumps, causing loss of device performance	Straight side-walled gold bumps formed and good reproduction of photoresist mould
Brightness	Bright	Bright
Hardness	1.0 GPa (65 °C) 1.7 GPa (25 °C)	0.7–0.9 GPa (55 °C)
Roughness	Fine-grained	Slightly rough ~2000 Å
Anode products	Carbonate (non-toxic)	Sulfate (easily rendered non-toxic)

Gold wafers deposited were bright and adherent. Gold bumps had straight side-walls and were largely defect-free, making them suitable for wafer bumping applications. Hardness measurements obtained showed that a thiosulfate-sulfite bath yielded soft gold deposits which are softer compared to deposits from the sulfite bath. Under identical experimental conditions, gold thickness uniformity of thiosulfate-sulfite is more superior to sulfite, especially deposited at a current density of 3.5 mA cm^{-2}.

Acknowledgements

The work was performed in research facilities provided through an EPSRC/HEFCE Joint Infrastructure Fund award no JIF-4NESCEQ and was funded by EPSRC GR/M64314.

References

1 H. Watanabe, S. Hayashi and H. Honma, Microbump Formation by Noncyanide Gold Electroplating, *J. Electrochem. Soc.*, 1999, **146**(2), 574.
2 A. Gemmler, W. Keller, H. Ritcher and K. Ruess, High-Performance Gold Plating for Microdevices, *Plat. Surf. Finish.*, 1994, **81**, 52.
3 J. Traut, J. Wright and J. Williams, Gold Plating Optimization for Tape Automated Bonding, *Plat. Surf. Finish.*, 1990, **77**(9), 49.
4 J. Jasper and D. Shiels, Gold Bumps off the Danger List, *European Semiconductor*, 2000, **22**(7), 86.
5 Y. Okinaka and M. Hoshino, Some Recent Topics in Gold Plating for Electronics Applications, *Gold Bull.*, 1998, **31**(1), 3.
6 I. R. Christie and B. P. Cameron, Gold Electrodeposition Within the Electronics Industry, *Gold Bull.*, 1994, **27**(1), 12.
7 W. J. Daukler, D. J. Resnick, W. A. Johnson and A. W. Yanof, New Operating Regime for Electroplating the Gold Absorber on X-ray Masks, *Microelectron. Eng.*, 1994, **23**, 235.
8 W. Chu, M. L. Schattenburg and H. I. Smith, Low-Stress Gold Electroplating for X-ray Masks, *Microelectron. Eng.*, 1992, **17**, 223.
9 A. Maner, S. Harsch and W. Ehrfeld, Mass-Production of Micro-devices with Extreme Aspect Ratios by Electroforming, *Plat. Surf. Finish.*, 1998, **75**, 60.
10 K. Kosaki, M. Matsuoka, Y. Seiwa, S. Orisaka, K. Nishitani and M. Otsubo Stabilization of Gold Sulfite Bath for Microscale Plating in GaAs ICs, *Proceedings of the First Symposium on Electrochemical Microfabrication*, Eds. M. Datta, K. Sheppard and D. Synder, **PV 92–93**, pp. 317, The Electrochemical Society Proceedings Series, Pennington, NJ 1992.
11 Y. Okinaka, Significance of Inclusions in Electroplated Gold Films for Electronics Applications, *Gold. Bull.*, 2000, **33**(4), 117.
12 W. Sun and D. G. Ivey, Development of an Electroplating Solution for Codepositing Au-Sn Alloys, *Materials Science and Engineering*, 1999, **B65**, 111.
13 Y. Okinaka and S. Nakahara, Structure of Electroplated Hard Gold Observed by Transmission Electron Microscopy, *J. Electrochem. Soc.*, 1976, **123**(9), 1284.
14 T. E. Dinan and H. Y. Cheh, The Effect of Arsenic upon the Hardness of Electrodeposited Gold, *J. Electrochem. Soc.*, 1992, **139**(2), 410.
15 H. Y. Cheh and R. Sard, Electrochemical and Structural Aspects of Gold Electrodeposition from Dilute Solutions by Direct Current, *J. Electrochem. Soc.*, 1971, **118**(11), 1737.
16 L. T. Romankiw and E. J. M. O'Sullivan Handbook of Micro-lithography, Micromachining and Microfabrication, **Vol. 2**, Ed. P. Rai-Choudhury, pp. 197, SPIE Press, Bellingham 1997.
17 P. Wilkinson, Understanding Gold Plating, *Gold Bull.*, 1986, **19**(3), 75.
18 D. R. Gabe, Use of Cyanides in Surface Finishing: Environmental Considerations, *Trans. Inst. Met. Fin.*, 1997, **75**, B131.
19 D. R. Turner, *Proceedings of Symposium on Electrodeposition Technology, Theory and Practice*, Eds. L. T. Romankiw and D. R. Turner, **PV 87–17**, pp. 417, The Electrochemical Society Proceedings Series, Pennington, NJ 1987.
20 H. Honma and K. Hagiwara, Fabrication of Gold Bumps Using Gold Sulfite Plaing, *J. Electrochem. Soc.*, 1995, **142**(1), 81.
21 R. J. Morrisey, A Versatile Non-cyanide Gold Plating System, *Plat. Surf. Finish.*, 1993, **80**, 75.
22 J. Simon, Development of High Speed Gold Bumping Process Using a Sulfite Electrolyte, *Proceedings of the 9th Microelectronics Conf. Tokyo, Japan*, 1996, 265.
23 J. Horkans and T. Romankiw, Pulsed Potentiostatic Deposition of Gold from Solutions of the Au (I) Sulfite Complex, *J. Electrochem. Soc.*, 1977, **124**(10), 1499.
24 D. Mason, Time for Gold Sulfite: Part 2, *Plat. Surf. Finish.*, 1986, **73**(5), 20.
25 H. Honma and Y. Kagaya, Gold Plating Using Disulfiteaurate Complex, *J. Electrochem. Soc.*, 1993, **140**(9), L135.
26 J. Simon, W. Zilske and F. Simon, Development of a High Speed Gold Sulfite Electrolyte for Bumping, *Proceedings 1995 International Flip Chip, Ball Grid Array, TAB and Advanced Packaging Symposium*, 1995, 275.
27 W. S. Rapson and T. Groenewald, *Gold Usage*, Academic Press, Inc., New York 1978.
28 A. M. Sullivan and P. A. Kohl, Electrochemical Study of the Gold Thiosulfate Reduction, *J. Electrochem. Soc.*, 1997, **144**(5), 1686.
29 X. Wang, N. Issaev and J. G. Osteryoung, A Novel Gold Electroplating System: Gold (I)-Iodide-Thiosulfate, *J. Electrochem. Soc.*, 1998, **145**(3), 974.
30 T. Inoue, S. Ando, H. Okudaira, J. Ushio, A. Tomizawa, H. Takehara, T. Shimazaki, H. Yamamoto and H. Yokono, Stable Non-cyanide Electroless Gold Plating which is Applicable to Manufacturing of Fine Pattern Printed Wiring Boards, *Proceedings of the 45th IEEE Electronic Components Technology Conference*, 1999, 1059.
31 S. Ando, T. Inoue, H. Okudaira and H. Takehara, Super Stable Non-cyanide Electroless Gold Plating Bath which has been Applied to Advanced Wiring Board Manufacture, *Proceedings of the 20th IEEE Intl. Electronic Manufacturing Tech. Symp.*, 1997, 220.
32 T. Osaka, A. Kodera, T. Misato, T. Homma and Y. Okinaka, Electrodeposition of Soft Gold from a Thiosulfate-Sulfite Bath for Electronics Applications, *J. Electrochem. Soc.*, 1997, **144**(10), 3462.
33 R. J. Lewis Sr., *Rapid Guide to Hazardous Chemicals in the Workplace*, 4th Ed., John Wiley & Sons, Inc., USA 2000.
34 D. W. Endicott, H. K. James and F. Nobel, Effects of Additives in Gold Deposits on Semiconductor Wire Bonding, *Plat. Surf. Finish.*, 1981, **69**(8), 58.
35 M. J. Liew, Novel Gold Electrodeposition Process for Micro and Opto Electronics, PhD Thesis, University of Newcastle upon Tyne, 2002.
36 T. A. Green, S. Roy and M. J. Liew, Electrodeposition of Gold from a Thiosulfate-Sulfite Bath for Microelectronic and Optoelectronic Applications, *J. Electrochem. Soc.*, 2003, in press.

Packed-bed bioreactor synthesis of feruloylated monoacyl- and diacylglycerols: clean production of a "green" sunscreen†‡

Joseph A. Laszlo,* David L. Compton, Fred J. Eller, Scott L. Taylor and Terry A. Isbell

New Crops and Processing Technology Research USDA-ARS, National Center for Agricultural Utilization Research, 1815 N. University St., Peoria, IL 61604, USA. E-mail: laszloja@ncaur.usda.gov; Fax: +1-309-681-6524; Tel: +1-309-681-6322

Received 4th March 2003
First published as an Advance Article on the web 19th June 2003

A biocatalytic process for covalent incorporation of ferulic acid onto the glycerol backbone of vegetable oil proceeds efficiently, although rather slowly, with *Candida antarctica* lipase B in a packed-bed reactor. The bioreactor shows considerable long-term stability. Product yield is influenced by the water content of the fluid phase and enzyme support. The enzyme support modulates substrate concentrations through adsorption and subsequent release of reactants over the course of the reaction. The resulting product has excellent UVA/UVB absorbing properties, making it a potential substitute for conventional petroleum-based sunscreen active agents.

Introduction

Heightened awareness of the skin damaging effects of ultraviolet (UV) radiation by the public has lead to robust growth in sun and skin care personal product markets. While UV-B (290–320 nm) radiation is principally responsible for sunburn (erythemogenic effect), UV-A (320–400 nm) radiation promotes photo-damage and aging of the skin. A preponderance of sunscreens (80%) in U.S. and Western Europe markets rely on organic chemicals to provide UV protection.[1] The active ingredients most commonly employed in the U.S. are octyl methoxycinnamate (OMC), padimate-O (*N*,*N*-dimethyl-*p*-aminobenzoic acid octyl ester), and oxybenzone (2-hydroxy-3-methoxybenzophenone). In Western Europe, 4-methylbenzyldiene camphor (4-MBC) is also a prevalent sunscreen active ingredient. Use of these chemicals is quite high, as an active ingredient may constitute up to 25% by weight or volume of the sunscreen formulation.[2]

Recently, concerns have been raised about the potential adverse health and ecological effects of the commonly used sunscreen active ingredients.[3,4] The estrogenic activity of OMC and 4-MBC have been documented *in vitro* and *in vivo* with mice.[5] Although the ability of these chemicals to disrupt endocrine activity in humans has yet to be established, these findings serve to legitimize in the public's mind a desire to avoid "synthetic" chemicals and to prefer "natural" ingredients in their personal care products.[6] Current sunscreen active ingredients may also pose an ecological threat. As with other pharmaceuticals, these chemicals tend to be bioaccumulative and biopersistent.[7] Lakes frequented by sunbathers may have aquatic life impacted from the presence of relatively high levels of sunscreen active ingredients. These concerns indicate that a benign alternative to conventional UV active ingredients would be well accepted in the marketplace.

A sunscreen active ingredient can be derived from two natural plant components, ferulic acid and triglycerides.[8] Ferulic acid is a phenolic compound (a member of the cinnamic acid family) found in most higher plants. It is generally present in nature as esters with other plant components, such as the hemicelluloses and lignin fractions of the plant cell wall, as well as in suberin and cutin waxy surfaces of leaves and other plant parts. Ferulic acid is also found esterified to phytosterols present in grain products such as rice bran. As such, ferulic acid is a common component of the human diet. It is thus not expected to pose a threat to human health nor to the environment.

Transesterification of ferulic acid ethyl ester with vegetable oil produces a mixture of feruloylated monoacyl- and diacylglycerols that have a strong UVA/B absorbance as well as water resistance characteristics.[8,9] The reaction is catalyzed by immobilized *Candida antarctica* lipase B. Previous studies have shown the reaction to proceed efficiently, albeit rather slowly (144 h to reach equilibrium), in stirred batches of the enzyme.[9] While it was demonstrated that the immobilized enzyme could be used several times, it is likely that on a commercial production scale degradation and loss of the enzyme from its support would be severe with stirred batch reactors. In the present work, the use of the immobilized enzyme in packed beds is examined, anticipating that the mild operating conditions would greatly extend the service life of the catalyst. The value of using packed-bed bioreactors for the transformation of vegetable oils has been recently demonstrated.[10–13] Packed-bed processing should also allow a readily scalable approach to producing commercial quantities of the product. In addition, issues related to the pre- and post-production of product are addressed, demonstrating a synthesis

Green Context

The increasing awareness of the dangers of exposure to the sun is making worse the impact of sunscreens on the environment, especially aquatic systems. This paper reports on a clean alternative, based on the combination of naturally occurring phenolic compounds onto glycerol. The synthesis of the product is analysed in terms of the principles of green chemistry, and is seen to have a high degree of atom economy, as well as being (probably) very biodegradable.

DJM

† Electronic supplementary information (ESI) available: schematics of the packed-bed reactor and the CO_2 fractionation system, HPLC chromatographic analysis of SoyScreen™. See http://www.rsc.org/suppdata/gc/b3/b302384b/

‡ Names are necessary to report factually on available data; however, the USDA neither guarantees nor warrants the standard of the product, and the use of the name by the USDA implies no approval of the product to the exclusion of others that may also be suitable.

 DOI: 10.1039/b302384b

of a plant-derived, environmentally benign sunscreen that closely adheres to the tenets of green chemistry.

Results and discussion

Reaction analysis

Transesterification of soybean oil (SBO) with ethyl ferulate (EF) by immobilized lipase *Candida antarctica* lipase B (Novozym 435) produces a multitude of long-UV-absorbing feruloylated monoacylglycerols (FMG) and feruloylated diacylglycerols (FDG), collectively referred to as SoyScreen™ (Scheme 1). Equal proportions of the FMG and FDG are

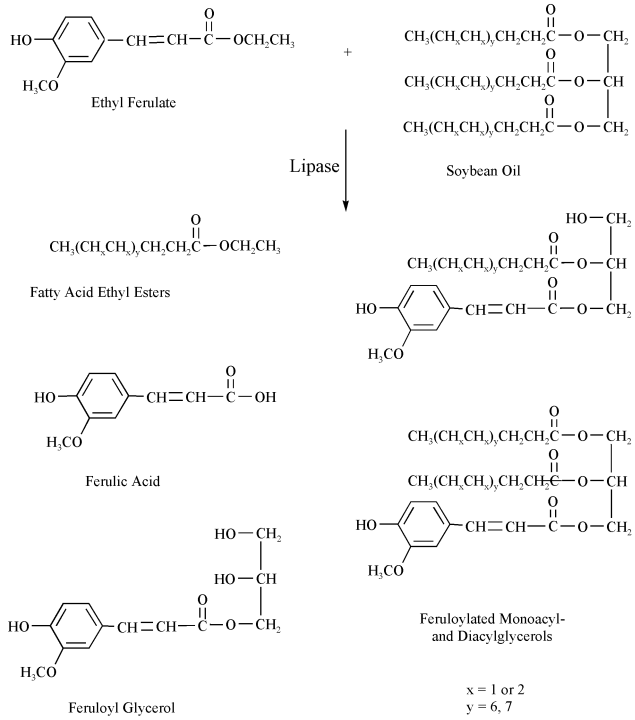

Scheme 1 Lipase reaction substrates and principal products. Feruloyl group substitution at the glycerol *sn*-3 position is shown for simplicity as the regioselectivity of the reaction is unknown.

produced. Additional UV-absorbing products formed in relatively small quantities are ferulic acid (FA), resulting from EF hydrolysis, and feruloyl glycerol (FG). The principal by-products from the reaction are fatty acid ethyl esters (FAEE). With an initial 1 : 1 molar ratio of EF to triglyceride, approximately 50% of the starting materials should convert to products at equilibrium, at which point the concentration of unreacted EF will equal that of the FAEE, so no further productive reaction will ensue. Generation of FA in this reaction is essentially irreversible as the enzyme is unable to appreciably esterify this substrate.[9] FG remains a reactive species and for the purposes of this study is considered a constituent of the SoyScreen™ product. Diferuloyl-substituted species have not been detected.[9]

The extent of conversion of EF and SBO to SoyScreen™ was determined most accurately by measuring residual EF and FA by high performance liquid chromatography (HPLC) rather than following the appearance of FMG and FDG. The latter approach overestimates the progress of the reaction. An additional correction was applied to the measurement of EF and FA in a sample by adjusting for small variations in the total ferulates (TF) concentration (*i.e.*, all feruloyl species, including EF and FA, monitored by UV spectroscopy at 325 nm), due to adsorption and desorption of EF to the enzyme support over the course of the reaction (see below). Thus the extent of SoyScreen™ production (θ) was calculated as

$$\theta = (1 - \frac{[EF] + [FA]}{[TF]})$$

Bioreactor kinetics

The performance of a packed bed of Novozym 435 in the conversion of EF and SBO to SoyScreen™ was examined for the time required for the reaction to reach completion (Fig. 1).

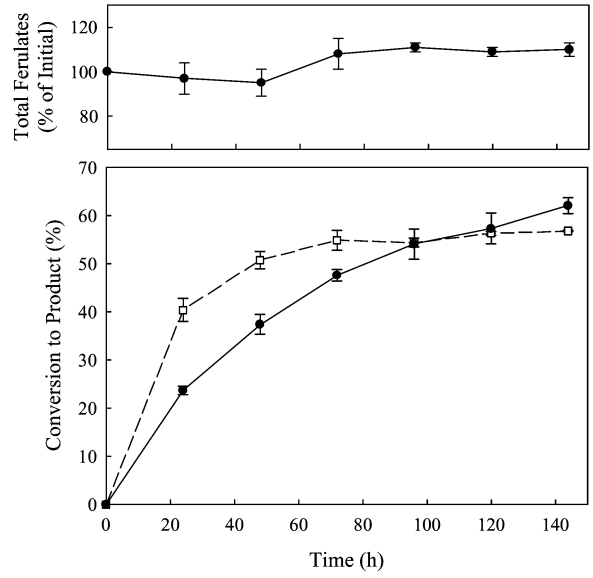

Fig. 1 Influence of bioreactor residence time on the conversion of EF to SoyScreen™ (lower panel) and the total ferulate concentration (upper panel). Data for the conversion to SoyScreen™ are the average of three trials made with fresh enzyme in the packed-bed bioreactor (●, solid line). Reaction results with immobilized enzyme (150 mg mL^{-1} of reactants) in stirred vials are the average of three separate trials (□, dashed line). Total ferulate concentration data are the average of four consecutive runs made with the same enzyme bed in the bioreactor.

For a freshly packed reactor the extent of reaction approached completion after approximately 144 h of operation. In contrast, the transesterification of triolein with caprylic acid ethyl ester by Novozym 435 reached equilibrium after 24 h at 45 °C.[14] Thus the kinetics of transesterification by the enzyme of SBO with EF are slow in comparison to those with more preferred acyl donors (long-chain fatty acid esters rather than cinnamic acid esters). The highest yield of SoyScreen™ observed after 144 h was 64%, which is somewhat greater than expected based on a simple equilibrium model of transesterification. This observation may indicate that the feruloyl substituted acylglycerols are slightly more thermodynamically stable than their corresponding diacyl- and triacylglycerols.

Stirred batches of immobilized enzyme and the SBO–EF reactants produced results similar to that of the packed-bed bioreactor (Fig. 1). Product yield was higher initially for stirred batches, but ultimately lower than with the packed-bed approach. Fracture of the enzyme support was evident in the stirred-batch reactions. The rapid initial kinetics of the reaction in stirred batches, followed by a relatively slower progression compared to the packed-bed reactor, may arise from greater surface reaction from the pulverized enzyme support and accompanying attrition of active enzyme by abrasion.

Continuous operation of the bioreactor over extended periods showed that multiple batches of SoyScreen™ could be prepared from a single charge of enzyme. Product yield dropped below 60% after the first two weeks of operation, then fluctuated

between 52 and 58% for the subsequent four weeks (data not shown). The apparent minor loss of enzyme activity after the first few batches cannot be attributed to occlusion of the support beads or channeling within the reactor because the measured included volume of the reactor bed did not change over this period of operation. Therefore, the small change in reactor performance with time most likely was due to thermal denaturation of the enzyme or changes in water activity (see below).

Influence of water

The amount of FA produced in the reaction was dependent on the water content of the reaction medium. Without a drying column, the FA content of the reaction medium slowly rose to represent 5–7% of the total ferulates by 144 h, while with a drying column the FA concentration was less than 2% (Fig. 2).

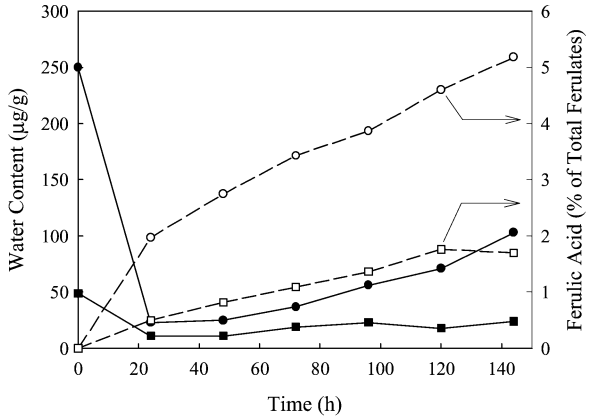

Fig. 2 Changes in the water content (solid lines; left axis) and ferulic acid concentration (dashed lines; right axis) of the fluid phase of the bioreactor during SoyScreen™ synthesis. The initial water content of the SBO was either left high (○, ●) or was lowered by drying with molecular sieves (□, ■), in which case a pre-column of molecular sieves was included in the flow stream of the reactor.

Without a drying column in line before the bioreactor, the water concentration in the reactor effluent still dropped dramatically to less than 10% of its initial concentration within the first 24 h of circulation, indicating that the enzyme support was adsorbing water. The pattern of water concentration in the SoyScreen™ over the course of the reaction suggests that the support acts as both a sink and source for water as the water solubility characteristics of the fluid phase change with time (*i.e.*, from a mixture of SBO and EF initially to the complex mixture of components comprising SoyScreen™ after 144 h of reaction). The partitioning of water between the enzyme support and fluid phase in packed-bed reactors has been noted by others.[15]

Water is not a product of the transesterification process and thus does not originate from the reaction itself. The enzyme support as supplied contains 1% (w/w) water according to the manufacturer, thus providing approximately 340 mg of water to the system. Each charge of reactants (EF and SBO) at the start of a transesterification run provides another 60 mg of water (240 mL containing 0.25 mg mL^{-1} of water), with the rinse SBO used to displace the product from the column after the completion of the reaction providing an additional 30 mg. With this protocol, sufficient water was introduced with each charge and discharge of the reactor to account for the ferulic acid produced. Use of an external column with molecular sieves helped minimize ferulic acid production by limiting the available water to that which came with the enzyme and its support.

Most enzymes need a critical amount of water to retain enzymatic activity in non-aqueous media, typically displaying a "bell-shaped" response to water activity.[16,17] This rule applies to lipases as well, with the apparent exception of *Candida antarctica* lipase B. It is generally observed that this lipase expresses its highest catalytic rates at very low water activities.[18–22] Thus it was surprising to see in our reaction lower product yield at very low water content in the medium (Fig. 3).

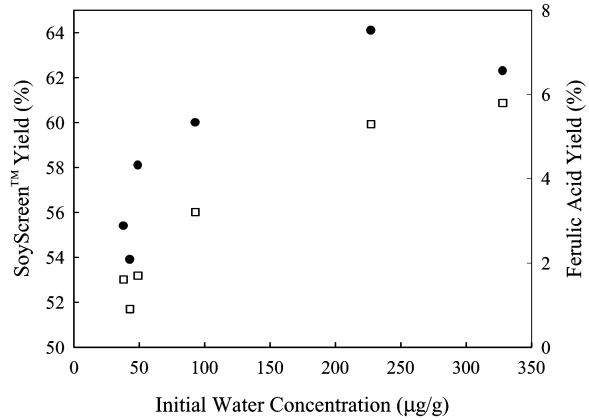

Fig. 3 Relationship between initial reactor water content and yield of SoyScreen™ (●; left axis) and ferulic acid (□; right axis) after 144 h. Initial water content was adjusted by drying the SBO with molecular sieves or by adding water to the EF–SBO mixture at the beginning of the reaction.

The large volumes of reactants employed and the high ratio of enzyme support to fluid phase in the present work made controlling water activity by conventional means such as hydrated salt complexes not feasible. Therefore, to study the influence of water on the reaction, only the initial water content of the fluid phase was adjusted. Increasing water concentration raised enzyme activity, raising product yield, but escalating as well the rate of EF hydrolysis (Fig. 3). This indicates that optimization of the reaction will require consideration of the concurrent trends of increasing SoyScreen™ yield (to a limit) and increasing ferulic acid by-product production with greater water activity.

Evaluation of EF adsorption to support

The concentration of total ferulates in the recirculated eluate from the reactor varied in a consistent manner of being slightly lower initially than the applied EF concentration, but then slowly rising over the 144 h reaction period to 10% above the applied EF concentration (Fig. 1). The variation in total ferulates with time can be attributed to the adsorption/desorption of EF to the enzyme's acrylic support. The adsorption properties of Novozym 435 were investigated using heat-inactivated material. There was substantial adsorption of EF to the enzyme support with SBO as the solvent. Over the EF concentration range relevant to this study, 0.2 to 0.9 M, the extent of EF adsorption increased linearly from 70 to 270 mg EF g $support^{-1}$ (data not shown). To minimize the effects of EF adsorption on the transesterification reaction kinetics, the resin was pre-equilibrated with a volume of EF in SBO (*i.e.*, a volume, equal to that which was recirculated, was passed through the column and discarded). The reaction products, FMG and FDG, showed little affinity for the enzyme support (data not shown). Therefore, only EF adsorption and desorption from the enzyme support contributed to the total ferulate concentration fluctuations during the course of the transesterification reaction.

Dossat and colleagues[12] found that glycerol generated during the transesterification of sunflower oil with 1-butanol in a packed-bed bioreactor of Lipozyme accumulated on the enzyme support and diminished enzyme activity. The amount of glycerol generated in the SoyScreen™ reaction was not

evaluated. However, adsorption of EF to the support may have a similar impact on the reactivity of Novozym 435, acting as a physical barrier to diglyceride and triglyceride reactants reaching the enzyme.

Post-reactor processing

Unreacted EF could be separated from SoyScreen™ at the end of the bioreactor stage. Liquid CO_2 (25 °C, 8.6 MPa) percolated through SoyScreen™ extracted EF, FAEE and FA. The FA formed a white precipitate in the extract. Passage of 3000 L (STP) of CO_2 lowered EF concentrations in the product to trace levels. No SoyScreen™ products or triglycerides were removed by liquid CO_2. Attempts to separate EF from the FAEE fraction using liquid and supercritical CO_2 were unsuccessful.

As with liquid CO_2 extraction, EF, FA and FAEE were readily separated from the SoyScreen™ products by low temperature molecular distillation (120 °C). FA crystallized from the distillate on cooling below room temperature. Complete removal of EF from the residue (SoyScreen™) fraction would require a second pass through the apparatus. This is a limitation of the bench-scale unit employed and would not be expected to be necessary at higher production volumes.

FAEE and EF recovered from either liquid CO_2 extraction or high vacuum distillation were converted to SoyScreen™ by adding glycerol or diacetin (glycerol diacetate) and Novozym 435 in a batch reactor. With the glycerol or diacetin concentration approximately equimolar to the EF, conversion to SoyScreen™ proceeded to about 50% after 144 h. Greater conversion would be expected if the competing transesterification products, either ethanol or ethyl acetate, were driven off under reduced pressure during the reaction, although this was not attempted.

How green is SoyScreen™?

Both the product and the processes to produce SoyScreen™ adhere closely to the principles of green chemistry.[23] SoyScreen™ is likely to be biodegradable and to have negligible toxicity, although this has yet to be verified. The raw materials for SoyScreen™, FA and SBO, are from annually renewable resources. A preliminary assessment indicates that FA can be isolated from phytosterol fractions (these sterols have commercial value as well) more economically than by *de novo* chemical synthesis.[24,25] Esterification of FA in ethanol to make EF can be accomplished using recyclable solid acid catalysts. Ethanol is the only reaction component that may not be practically conserved in the process, so SoyScreen™ synthesis has a high degree of atom economy. No solvents, separating agents (other than CO_2 perhaps), or intermediary protecting groups are needed. Processing substrates and products with liquid CO_2 is particularly advantageous because solutes are readily recovered by partial depressurization, which also lessens the energy costs associated with its use. The distillation steps for EF synthesis and SoyScreen™ fractionation are the most energy intensive steps, yet their requirements are quite modest. The biocatalyst shows long term stability in a packed-bed reactor. Future work will focus on improving catalyst turnover rates to shorten synthesis times.

Experimental

Reagents

Novozym 435 was obtained from Novo Nordisk BioChem North America (now Novozymes North America, Franklinton, NC). EF (ethyl 4-hydroxy-3-methoxycinnamate) was purchased from Senn Chemicals USA (San Diego, CA). Colored contaminants were removed from the EF by either passage through alumina (60–325 mesh, Acid Brockman Activity I) with the EF dissolved in acetone, or by liquid CO_2 extraction (see below). SBO was obtained from a local grocery store. Other reagents were from Sigma-Aldrich and Fisher Scientific. Glycerol was spectroscopic grade (< 0.1% w/w water). Diacetin was technical grade.

Packed-bed bioreactor

Novozym 435 (34 g) was solvated in SBO under reduced pressure for 30 min, then transferred to a jacketed chromatography column (2.5 × 30 cm, 147 mL nominal internal volume). Using β-carotene as a marker, the bed included volume was estimated to be 85 mL. The enzyme bed was conditioned overnight by recirculating about 340 mL of SBO at 2 mL min^{-1}. The reactor was maintained at 60 °C using a circulating bath. Reactants (EF and SBO) were fed into the top of the reactor using a peristaltic pump at 2 mL min^{-1}. Reactor effluent was collected in a small reservoir (30 mL), which was kept under a slow stream of N_2 with the contents magnetically stirred, and recirculated back into the packed-bed bioreactor. The reaction mixture was prepared by combining 40 g of EF with 160 g of SBO at 60 °C. While retaining 25 mL of this solution for the reservoir, the reaction mixture was passed onto the column, discarding the displaced SBO to waste, then directing the reactants back to the reservoir once the reactor was entirely loaded. (See the supplemental materials for a schematic of the apparatus†). A drying bed of 3A molecular sieves (8 g), when used, was placed between the pump and the reactor column.

Samples (0.5 mL) were collected daily from the column effluent for analysis by HPLC and UV spectroscopy (325 nm). Sample water content was determined using coulometric Karl Fischer analysis with 70 : 30 (v/v) Hydranal AG–H/chloroform as the analyte.

HPLC analysis

Samples from the bioreactor were analyzed by HPLC largely following previously published procedures.[9] A Thermo Separation Products (San Jose, CA) HPLC was equipped with a UVB-visible detector and a Prodigy C8 column (Phenomenex, Torrance, CA). For the separation of various feruloyled lipids, the column was developed isocratically at 1.5 mL min^{-1} with 40 : 60 (v/v) acetone (containing 1% glacial acetic acid)–acetonitrile. Samples were prepared by 200-fold dilution into acetone. The eluate was monitored at 360 nm. For the quantitation of FA, FG, and EF, a water–methanol gradient elution regime was employed, with detection at 325 nm and with the acetone-diluted samples further diluted 20-fold with methanol.[9] (See supplemental materials for example chromatograms†). Detector response (325 nm) was calibrated with FA and EF, using low concentrations of EF to establish a calibration curve for FG. Responses were linear for all three species in the range employed in this study (100 to 250 μM for EF, 2 to 20 μM for FA and FG). The sample injection volume was 10 μL for both modes of analysis.

Measurement of EF adsorption

For the study of EF adsorption to the support resin, Novozym 435 was autoclaved to inactivate the enzyme. SBO (1 mL) containing 0.25 to 1.0 M EF was equilibrated with 150 mg of autoclaved Novozym 435 in stirred vials at 60 °C for 24 h. The equilibrated concentration of EF was determined by UV spectroscopy (325 nm). The amount of adsorbed EF was taken

as the difference between the initial and final EF concentrations.

Carbon dioxide extraction

Liquid CO_2 fractionations were performed in a column packed with protruded stainless-steel packing (0.41 cm Pro-Pak, Scientific Development Co., State College, PA), which provided a 94% void volume. The column included a precooling section and four separate zones, each having an internal diameter of 1.43 cm and a height of 63.3 cm (see supplemental materials for a schematic diagram of the CO_2 fractionation system†). The column had a total height of 253.2 cm and an internal volume of 412 mL.

For liquid CO_2 extraction, all zones were cooled to 25 °C by silicone tubing attached to a refrigerated circulating bath. Heating mantles enclosed each zone and were independently controlled to heat the column to the desired temperature during the post-extraction cleanup. The temperature was recorded by Type-J thermocouples attached to the column wall. Two thermocouples were inserted into the top and bottom of the column to monitor the internal column temperature.

Sample (120 mL of unextracted SoyScreen™) was introduced into the column above the first zone by a liquid metering pump (Model MS-188, Haskel Inc., Burbank, CA) connected to a stroke counter controller. Welding-grade carbon dioxide (Airgas Inc., Radnor, PA) was introduced from a commercial cylinder through a filter containing alumina C to a booster pump (Model AG-30, Haskel Inc., Burbank, CA). The column was pressurized to 8.6 MPa and equilibrated for 0.5 h before the outlet valve was opened to begin the extraction. CO_2 was passed upward through the column and sample. Solute-loaded liquid CO_2 exited the column as expanded gas at a flow rate of 3–5 L min^{-1} (STP) across a micrometering valve allowing the extract (EF, FA and FAEE) to be collected in a flask. Finally, the gas stream passed through a dry test meter (Singer Model DTM-115, American Metering Division, Philadelphia, PA) to measure the total gas volume and was then vented to the atmosphere. Purified SoyScreen™ was then collected from the bottom of the second zone through a micrometering valve as the column was depressurized.

After each extraction, the column was cleaned to prevent contaminants from being carried over to subsequent runs. The refrigerated circulating bath was turned off and the column was heated to 80 °C and pressurized to 58.6 MPa with supercritical CO_2. One-thousand L (STP) of CO_2 were run through the column at 5 L min^{-1} for cleanup.

Molecular distillation

SoyScreen™ fractionation also was performed using high vacuum (short-path) distillation (Myers Vacuum, Inc., Ittanning, PA). The centrifugal rotor temperature was 120 °C and the condensing surface was held at 40 °C with the chamber operating at 16 mTorr.

Acknowledgements

The authors thank Leslie Smith for her excellent technical assistance with this study.

References

1 M. S. Reisch, *Chem. Eng. News*, 2001, **79**(Dec. 3), 25–29.
2 M. E. Griffin, T. D. Bourget and N. J. Lowe, *Sunscreens. Development, Evaluation, and Regulatory Aspects*, ed. N. J. Lowe, N. A. Shaath and M. A. Pathak, Marcel Dekker, New York, 1997, pp. 499–512.
3 J. J. P. Morton, *J. Toxicol. Cutaneous Ocul. Toxicol.*, 1992, **11**, 239–247.
4 M. Schlumpf, B. Cotton, M. Conscience, V. Haller, B. Steinmann and W. Lichtensteiger, *Environ. Health Perspect.*, 2001, **109**, 239–244.
5 G. J. Nohynek and H. Schaefer, *Regul. Toxicol. Pharmacol.*, 2001, **33**, 285–299.
6 M. S. Reisch, *Chem. Eng. News*, 2001, **79**(Apr. 16), 23–28.
7 C. G. Daughton and T. A. Ternes, *Environ. Health Perspect.*, 1999, **107**(suppl. 6), 907–938.
8 D. L. Compton and J. A. Laszlo, *US Pat.*, 6346236, 2002.
9 D. L. Compton, J. A. Laszlo and M. A. Berhow, *J. Am. Oil Chem. Soc.*, 2000, **77**, 513–519.
10 F. X. Malcata, H. R. Reyes, H. G. Garcia and C. G. Hill Jr., *J. Am. Oil Chem. Soc.*, 1990, **67**, 890–910.
11 Y. Watanabe, Y. Shimada, A. Sugihara and Y. Tominaga, *J. Am. Oil Chem. Soc.*, 2001, **78**, 703–707.
12 V. Dossat, D. Combes and A. Marty, *J. Biotechnol.*, 2002, **97**, 117–124.
13 L. B. Fomuso and C. C. Akoh, *Food Res. Int.*, 2002, **35**, 15–21.
14 K.-H. Huang and C. C. Akoh, *J. Am. Oil Chem. Soc.*, 1996, **73**, 245–250.
15 S. Colombié, R. J. Tweddell, J.-S. Condoret and A. Marty, *Biotechnol. Bioeng.*, 1998, **60**, 362–368.
16 L. Kvittingen, *Tetrahedron*, 1994, **50**, 8253–8274.
17 G. Koller, M. J. Aris, Z. Ujang and A. M. Vaidya, *Biocatal. Biotransform.*, 2001, **19**, 37–49.
18 S. Barreiros, N. Fontes, M. Conceicão Almeida, R. Ruivo and T. Corrêa de Sampaio, *4th International Symposium on Supercritical Fluids*, May 11–14, Sendai, Japan, 1997, pp. 111–113.
19 M.-P. Bousquet-Dubouch, M. Graber, N. Sousa, S. Lamare and M.-D. Legoy, *Biochim. Biophys. Acta*, 2001, **1550**, 90–99.
20 F. Chamouleau, D. Coulon, M. Girardin and M. Ghoul, *J. Mol. Catal. B: Enzym.*, 2001, **11**, 949–954.
21 J.-H. Xu, Y. Kato and Y. Asano, *Biotechnol. Bioeng.*, 2001, **73**, 493–499.
22 Y. Li and D. G. Rethwisch, *Biotechnol. Bioeng.*, 2002, **79**, 15–22.
23 P. T. Anastas and M. M. Kirchhoff, *Acc. Chem. Res.*, 2002, **35**, 686–694.
24 H. Taniguchi, A. Hosoda, T. Tsuno, Y. Maruta and E. Nomura, *Anticancer Res.*, 1999, **19**, 3757–3762.
25 H. Taniguchi, E. Nomura, T. Tsuno and S. Minami, *US Pat.*, 5908615, 1999.

Pressurized water extraction of naphtodianthrones in St. John's wort (*Hypericum perforatum* L.)

Mari Mannila† and Chien M. Wai*

Department of Chemistry, University of Idaho, Moscow 83844, Idaho, USA

Received 12th December 2002
First published as an Advance Article on the web 20th June 2003

A high pressure water extraction (PWE) method was developed for separation of naphtodianthrones (hypericin, protohypericin, pseudohypericin, and protopseudohypericin) in St. John's wort. The effects of extraction temperature, pressure, pH, particle size, and modifier were studied, and the PWE method was compared to a conventional solvent extraction method. The most important factors affecting the extraction efficiency were found to be temperature, pH and particle size. The highest extraction efficiency of naphtodianthrones was achieved when the extraction was performed using a fine sample powder (≤80 mesh), a low temperature (ambient), and 100 bar pressure at pH ≥ 7. Using these conditions the PWE efficiency to extract naphtodianthrones (the summed amount of hypericin, pseudohypericin and their protoforms) compared to methanol extraction (with ultrasound) was about 80% (90% pseudohypericin and 60% hypericin). PWE extraction efficiency was further improved when ethanol was added to the sample as a modifier before the extraction. Using ethanol modified PWE at pH 7 the summed amount of naphtodianthrones was 90% (95% pseudohypericin and over 80% hypericin) compared to the methanol extraction with ultrasound. Reproducibility of the optimized PWE method was comparatively good; the relative standard deviation of both hypericin and pseudohypericin was 8%.

Introduction

St. John's wort has been used as a remedy for wounds, kidney troubles, and nervous disorders for thousands of years.[1,2] Today the extract of St. John's wort is one of the most widely used herbal supplements for treatment of mild depression and various psychological and neurologic disorders.[2–4] The extract of St. John's wort has been reported to have antidepressant[5–7] and antiviral[8] activity. The antiviral activity of this plant is related to its constituents, napthodianthrones, including hypericin and its hydroxy derivative pseudohypericin (Fig. 1A). These compounds efficiently deactivate a broad range of viruses.[9–12] Furthermore, recent studies suggest that hypericin can (1) modify the levels of neurotransmitter in the brain involved in depression[13] and (2) inhibit the growth of human ovarian carcinoma cells.[14] The pathway of hypericin's antiviral activity is believed to be based on its light-induced biological activity described in a review article by Lavie *et al.*[15] In addition to hypericin and pseudohypericin, St. John's wort also contains the protonated forms of these compounds (Fig. 1B). Protoforms of hypericin and pseudohypericin are easily converted to the hypericin and pseudohypericin, respectively, by exposure to light.[16,17]

Although St. John's wort is a widely used herbal supplement, the analysis and processing of this plant are mostly based on organic solvent extractions. Separation of hypericin from St. John's wort has been performed most often using methanol[17–20]

Green Context

St John's wort is a natural renewable source of a number of medicinally useful compounds. In particular antiviral activity of the plant is related to naphtodianthrones including hypericin. The extraction of such compounds from this plant is traditionally based on traditional organic solvents which detracts from the green chemistry credentials. The use of more environmentally acceptable supercritical CO_2 has had limited success. Here the use of pressurized water is tested for the extraction of the valuable naphtodianthrones from St John's wort. High total extracted amounts are obtained and the extraction efficiency is shown to be improved by the additional presence of ethanol in the solvent system. ***JHC***

† Current address: National Public Health Institute, Department of Environmental Health, P.O. Box 95, FIN-70701 Kuopio, Finland.

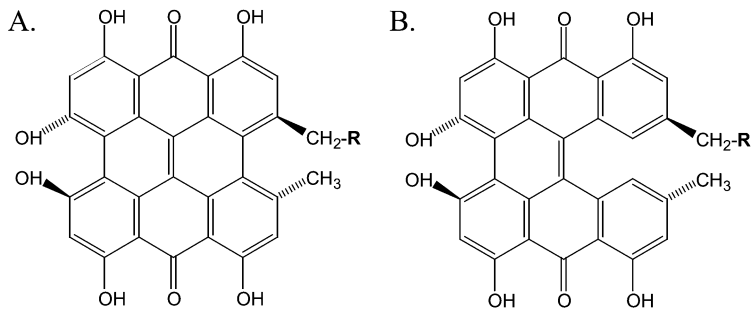

Fig. 1 Structures of (A) hypericin (R=H), pseudohypericin (R=OH), and (B) protohypericin (R=H) and protopseudohypericin (R=OH).

or with a mixture of methanol and acetone.[21] The solubility of free hypericin is very poor in most organic solvents, but as a monobasic salt it is generally soluble in polar solvents. In the plant material hypericin occurs as a potassium salt,[15] which explains its solubility in organic solvents. In organic solvents the salt form of hypericin is red and has a strong UV adsorption at 590 nm.

Supercritical carbon dioxide has been used in several herbal separations during the past few years.[22] However, the polarity of CO_2 (even when modified with methanol) is too low to obtain efficient extraction of hypericin from St. John's wort.[23] Boiling water has been used widely in herbal extractions for thousands of years. At elevated temperatures, the dielectric constant of H_2O decreases due to weakening of hydrogen bonds. Thus, a temperature increase improves the solubility of less polar compounds in water. Subcritical water extraction (extraction at elevated temperature and pressure) has gained a lot of interest in the environmental analysis of persistent organic pollutants[24–27] and it has also been applied to the extraction of essential oils in plant material[25] and to foodstuff extractions.[26,27] The drawbacks with hot water extraction are the decomposition of thermally-labile compounds and undesirable reactions such as oxidation and rearrangement of molecules at elevated temperature.[28,29] Water under high pressure at room temperature is suitable for extraction of thermally labile compounds. Lang and Wai used this pressurized water extraction (PWE) method for the extraction of active compounds terpene trilactones from leaves of *Ginkgo biloba*.[30] As a nontoxic, safe, cheap, and easily available solvent, pressurized water offers an attractive alternative to organic solvent-based methods for analysis and processing of herbal products.

The goal of this study was to investigate the suitability of using pressurized water for extraction of naphtodianthrones in St. John's wort. The effects of extraction temperature, pressure, pH, extraction time, particle size, and modifier addition were studied.

Results

Temperature and pressure

Pressurized water at low temperature (ambient/25 °C) appears beneficial for the extraction of hypericin and pseudohypericin in St. John's wort. Increasing the temperature (from 25 up to 100 °C) lowered the extraction of hypericin significantly (Fig. 2). At

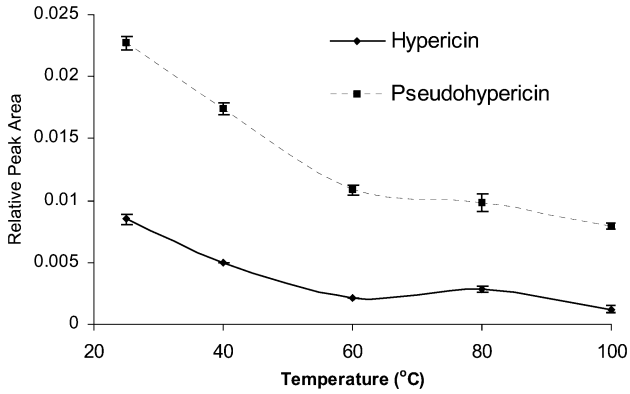

Fig. 2 Effect of temperature on the PWE efficiency to extract hypericin and pseudohypericin from St. John's wort (sample A, $n = 2$) at constant pressure (100 bar).

elevated temperature the dielectric constant of water is decreased due to the weakened hydrogen bonding. This may result in lower extraction efficiency towards polar molecules such as hypericin. Decomposition of hypericin is another possible reason causing reduced extraction efficiency of hypericin at elevated temperature. However, Poutaraud *et al.*[31] obtained the highest extraction efficiency of hypericin and pseudohypericin at 80 °C in a mixture of water : ethanol (40 : 60 v/v). This suggests that hypericin and pseudohypericin are thermally stable compounds, and lowered extraction in PWE was caused by weakened solvation properties of water at elevated temperature.

Increasing pressure above 100 bar did not have any significant effect on the extraction efficiency of hypericin and pseudohypericin. However, using 50 bar pressure the extraction efficiency was poor, because water was not able to penetrate the sample matrix during the dynamic step and the extraction could not be completed. Based on this, 100 bar pressure was needed to obtain a good flow during the dynamic step.

Extraction rate

In the PWE process, the volume of water should be optimized so that the concentration of the solute in the extract solution is high enough for direct analysis. In the extraction of 1 g plant, 20 ml water was needed to obtain over 90% recovery (of the total extracted amount) of HY and PHY during the dynamic step. After 20 ml, the amount of these compounds increased only slightly and slowly. The concentration of HY and PHY in 20 ml of water was adequate for direct analysis by HPLC.

To evaluate the extraction rate of naphtodianthrones in St. John's wort, the extraction was performed using different static times (5, 15, and 30 min). Even 5 min static extraction (before dynamic mode) resulted in the same efficiency as extractions with 15 or 30 min static modes. This suggests that PWE of hypericin and pseudohypericin most probably depends on the volume of fresh water carrying these analytes out from the vessel. Probably water is rapidly saturated (< 5 min) by the extracted compounds. If contact time between water and hypericin was the limiting factor, with extended static time the naphtodianthrones should have been carried out faster from the vessel during the dynamic extraction.

Particle size

Sample A was pulverized by the manufacturer to very fine powder (less than 325 mesh or particle diameter less than 0.045 mm) so it could not be used in particle size studies. To study the effect of particle size, sample B was powderized and sieved through four different sieves. Particle size showed a significant effect on the PWE efficiency; the extracted amount of hypericin and pseudohypericin increased as the particle size was decreased (Fig. 3). PWE with 20 mesh particles resulted in only 17% pseudohypericin and 25% hypericin of that obtained with 325 mesh particles. Extraction was improved as the particle size was reduced so that with 80 mesh particles 78% pseudohypericin and 91% hypericin were extracted compared to that with 325 mesh particles. Thus, a very small particle size is needed to obtain efficient extraction of HY and PHY in St. John's wort by PWE. It seems that pressurized water can not penetrate effectively inside this plant matrix if particle size is greater than 80 mesh.

pH

Neutral to basic conditions were found beneficial in the PWE (at 25 °C and 100 bar) of hypericin and pseudohypericin from St. John's wort (Fig. 4). HY is an acidic compound and it forms monobasic salts with inorganic bases at a pH range of 4–11.[15] Free HY and PHY are insoluble in water, whereas the salt forms are generally soluble in polar solvents. In the plant, HY occurs

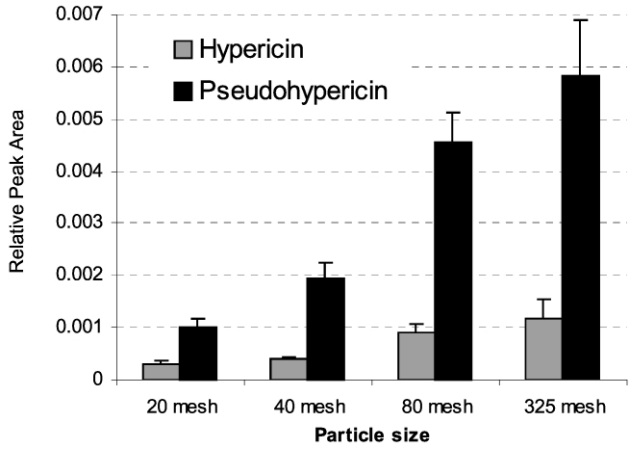

Fig. 3 Effect of particle size on the PWE efficiency (at 25 °C, 100 bar) to extract hypericin and pseudohypericin in St. John's wort (sample B, n = 2).

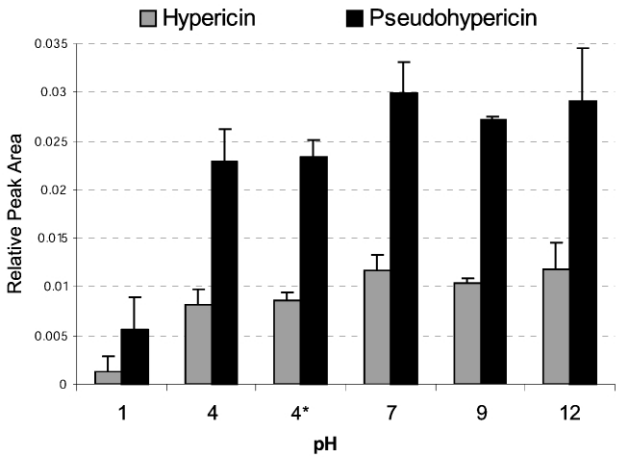

Fig. 4 Effect of pH on the PWE efficiency (at 25 °C, 100 bar) to extract hypericin and pseudohypericin in St. John's wort (sample A, n = 2). 4* = without pH controlling reagent.

mainly as a potassium salt,[15] which explains its extractability in organic solvents such as methanol.

Using strongly acidic conditions (pH 1), very poor extraction of hypericin and pseudohypericin was obtained by PWE; less than 20% of both hypericins was extracted using acidic conditions than when using pH 7 (Fig. 4). This is probably due to the fact that these compounds can be converted from salt form to the insoluble free forms of HY and PHY in acidic solutions. When the extraction was performed without any pH modifications (natural conditions), hypericin and pseudohypericin were extracted at a level comparable to that achieved with weak acidic conditions at pH 4. The natural pH of unmodified PWE extract was also found to be pH 4. The best PWE efficiency was obtained at neutral to basic conditions. Increasing the pH above 7 did not further improve the extraction of hypericin and pseudohypericin. This probably means that the salt formation was already achieved at pH 7 and thus basic conditions could not improve the extraction. This conclusion is supported by the result of Piperopoulos *et al.*[21] who examined the yield of [M–H] quasi molecular ions of hypericin obtained in different pHs: using pH 7 high intensities of the deprotonated (*i.e.* salt) form of hypericin were detected by electrospray ionization mass spectrometry. Basic conditions have been found to increase significantly the extraction of impurities from the plant matrix, which might deteriorate the quality of the extract and could cause difficulties in analysis.[32] Therefore, pH 7 was concluded to be the optimal extraction pH for the extraction of naphtodianthrones from St. John's wort.

PWE with pure water with sample A yielded 80% hypericin and pseudohypericin compared to those of PWE at pH 7. However, PWE efficiency to separate naphtodianthrones from sample B with pure water was only 65% of that obtained with PWE at pH 7 (325 mesh). Thus, adjusting the extraction conditions to pH 7 had a greater effect on the PWE efficiency from sample B than sample A. The higher extraction efficiency from sample A was probably related to the smaller particle size compared to sample B (325 mesh). Interestingly, using the PWE at pH 7, the same result was obtained with 80 mesh and 325 mesh particles of sample B. This indicates that adjusting the pH to 7 decreases the need for very fine sample powder. Because 80 mesh particles were easier to prepare (using a mortar and pestle), and the risk of blocking the filter of the extraction vessel was lower, we chose to use the 80 mesh particles in our further studies of sample B.

Modifier

To further enhance the extraction efficiency of the naphtodianthrones, ethanol was added to the PWE extraction. Ethanol was chosen due to its low toxicity compared to the other organic solvents. Modified PWE extractions (at pH 7) were performed by (1) water containing varying amounts of ethanol (5, 20, and 40%), and (2) by direct spiking of ethanol (1, 2, and 3 ml) to the sample matrix before PWE. Even when an extraction solution contained 40% ethanol, the PWE extraction efficiency for hypericin and pseudohypericin was not increased compared to the PWE with water (at pH 7). However, when the sample was spiked with ethanol before the extraction, the PWE efficiency to extract naphtodianthrones increased (Fig. 5.). However, a rather

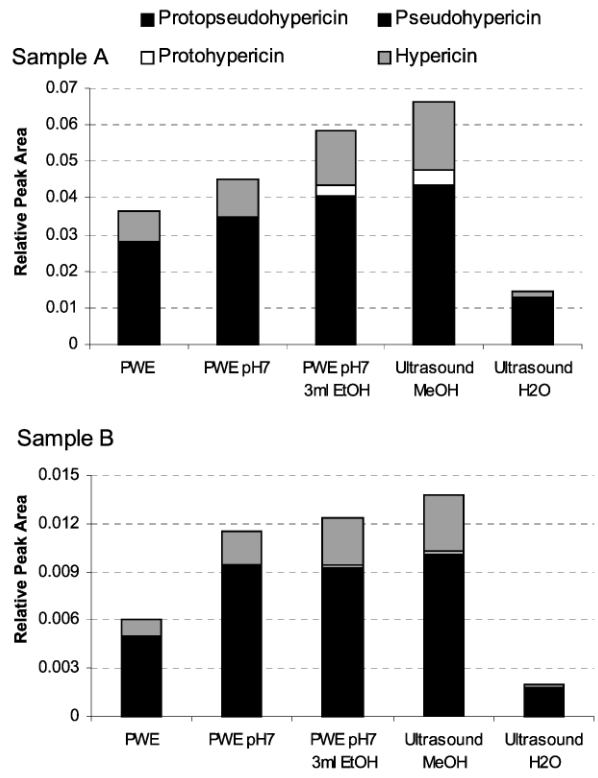

Fig. 5 Pressurized water extraction (at 25 °C and 100 bar) using different conditions (uncontrolled pH, pH 7, and addition of ethanol) compared to the ultrasound extraction using methanol and water as an extraction solvent.

high amount of ethanol was needed to obtain improved extraction (3 ml/300 mg dry sample powder). Furthermore, the color of spiked ethanol extract was dark brownish indicating that the amount of co-extracted impurities was increased as well.

Comparison to the solvent extraction method

Methanol extraction was used for comparison with the PWE method, because methanol is the most widely used solvent in the extraction of hypericin from St. John's wort. In addition to methanol, ultrasound extraction was performed with pure water to compare the efficiency of water under atmospheric pressure to extraction with high-pressure water. It should be noted that the pH of the methanol extract was neutral or slightly basic (7–8), which seemed to be a suitable condition for the salt formation of naphtodianthrones.

The comparison between ultrasound extractions and PWE for samples A and B are presented in Fig. 5. Ultrasonic extraction with water showed very poor efficiency for the extraction of naphtodianthrones. This is interesting since both ultrasonic and PWE extractions were performed at room temperature and the pH was same in both extracts (pH 4). Thus, it is obvious that pressure plays an important role in obtaining efficient extraction of naphtodianthrones by water.

PWE efficiency using pure water (without any added reagents or solvents) in extraction of all naphtodianthrones was about half (55% for sample A and 45% for sample B) of the efficiency obtained by methanol extraction (with ultrasound). When extraction pH was increased to 7 (from uncontrolled pH 4) the extraction efficiency of naphtodianthrones, especially from sample B, was improved significantly and the results were closer to those of methanol extraction (70% for sample A and 83% for sample B) (Fig. 5). Pseudohypericin was easily extracted by PWE compared with the other analysed naphtodianthrones, whereas protohypericin was the most difficult to extract by PWE. Using pH 7 the extracted amounts of pseudohypericin in samples A and B were 90 and 96% respectively, whereas only about 10% of protohypericin was extracted at these conditions. Addition of ethanol (3 ml spiking in the 300 mg sample) to the PWE (at pH 7) resulted in nearly 100% extraction of pseudohypericin, at least 80% extraction of hypericin, and over 70% extraction of protohypericin from both samples compared to the methanol extraction. The PWE extraction efficiency of the summed amount of all naphtodianthrones was about 90% for both samples when ethanol was used as a modifier in PWE. Unfortunately, ethanol addition also increased the extraction of impurities from the plant matrix.

Pseudohypericin is the major naphtodianthrone type compound in St. John's wort and PWE efficiency to separate this compound was comparatively good under all the studied conditions. Therefore, the total extracted amount of naphtodianthrones was comparatively high (70–80%) even without ethanol addition at pH 7 (Fig. 5). Because the antiviral activity of hypericin and pseudohypericin are believed to be equal, this result is a promising indication of the capability of PWE to extract the naphtodianthrones in St. John's wort.

The reproducibility of the developed PWE method (at room temperature, 100 bar, pH 7) was comparatively good showing relative standard deviation of 8% (n = 4) for both hypericin and pseudohypericin. As a long term control of the analysis, sample A was extracted (at room temperature and 100 bar, pH not controlled) a total of 11 times during a five month period and these results showed comparatively high reproducibility as well: the relative standard deviations were 11% for hypericin and 8% for pseudohypericin. However, the developed PWE method is not suitable for quantitative analysis, since the extracted amounts of naphtodianthrones were lower than those obtained by methanol extraction. Anyhow, the PWE method can be applied to manufacturing processes for the rapid and environmentally benign isolation of naphtodianthrones from St. John's wort. The synthesis of hypericin is expensive and involves a long procedure[33] therefore isolation from the plant would be a beneficial technique for obtaining pure hypericin for further studies of this compound. However, an efficient purification method would be needed (whether the extraction was performed by methanol or pressurized water) because of the unselective extraction and low concentration of hypericins compared to other polar compounds in St. John's wort. PWE is most probably suitable also for extraction of other bioactive polar compounds, flavonoids, in St. John's wort, which are extractable by methanol and modified supercritical CO_2.[23] Overall, this study gives valuable information about optimization of a PWE method that can be applied to other herbal extractions.

Experimental

Samples

Two different commercially available St. John's wort samples were used in this study. Most of the extractions were performed with St. John's wort powder (particle size less than 325 mesh) purchased from the Frontier Natural Products Co. (USA). This plant material (sample A) originated from Chile. Another sample (B) was purchased from an Internet company (Bullseye Services, Pahrump, NV). No further information on the plant materials was available. Sample B was reduced to a powder using a mortar and pestle and sieved through 20, 40, 80, and 325 mesh sieves (U.S. Standard Sieve series, Dual MFG. Co., Chicago, USA).

Standard

Hypericin standard for identification was provided by Dr. Hakwon Kim (Department of Chemistry & GNRL, Kyung Hee University, Korea). Pseudohypericin and protoforms of HY and PHY were verified based on comparison of HPLC retention times.[16,21] Furthermore, the identity of protoforms and corresponding HY and PHY was confirmed by HPLC analysis after photoconversion (sample subjected to light for 3 days) as described by Sirvent and Gibson.[16]

PWE procedure

Pressurized water extractions were performed with an Isco Supercritical Fluid Extractor (SFX 2–10, ISCO, Lincoln, NB), which was connected to the pressure control unit (Spe-ed SFE, Applied Separations) and compressor (5.5 HP 30 GAL, Craftzman, Hoffman Estates, IL). The flow rate of the water during dynamic extraction was controlled by a manual valve. A stainless steel capillary tubing was connected to the outlet of the extractor and inserted into a collection vial.

On the bottom of the extraction vessel was placed a filter paper (1.6 µm, GF/A, glass microfiber filters, Whatman) to prevent blocking of the outlet connection of the vessel during the extraction. Samples (1 g dry plant powder A) were extracted at different temperatures (25 to 100 °C) and pressures (50 to 300 atm), varying one parameter at a time. The effect of pH (1, 4, 7, 8, and 12) was studied at 25 °C and 100 atm adding 1 ml of a pH controlling reagent on the top of the sample before the extraction. The solutions prepared to control pH were as follows: acetic acid (pH = 1); 5% NaH_2PO_4 (pH = 4); 5% NH_4HCO_3 (pH = 7), $Na_2HPO_4{\cdot}12H_2O$ (pH = 8); and aqueous NaOH (pH = 12). The static extraction time was 15 min followed by dynamic flushing (about 30 min) until the volume of the extract was 20 ml when the eluting extract was colorless. The crude extract (20 ml) was filtered through a PVDF syringe filter (0.45 µm, Alltech) for the HPLC analysis. All extractions of sample B, and comparison studies with sample A were performed using 300 mg sample with 200 µl pH controlling reagent, and a total collection of 7–10 ml extract during the

dynamic step. All extractions were performed with at least two replicates.

Solvent extraction procedure

The extraction efficiency of methanol and water were investigated with ultrasonication (at ambient temperature). Ultrasound-aided extraction was performed by extracting a dry plant (300 mg) in 10 ml of the solvent for 90 min. After extraction, the crude sample extract was centrifuged and the extract was filtered through a PVDF syringe filter (0.45 µm, Alltech) for the HPLC analysis.

HPLC analysis

Samples were analyzed by a HPLC (Waters 1525 pump) connected to a UV detector (Waters 2487 dual absorbance detector). The injections (10 µl) were performed by autosampler (Waters 717). Compounds were separated by a Supelcosil LC-18-DB column (25 cm x 4.6 mm, 5 µm, Supelco, US). HPLC analysis was performed with two solvents: (A) water–85% phosphoric acid (99.9 : 0.1 v/v), and (B) acetonitrile. The solvent gradient program was the following: initial 70% A; at 25 min 15% A, which was retained until 30 min. The flow rate of the mobile phase was 1.0 ml min^{-1} and the peaks were detected at 590 nm.

Because the exact concentration of the used hypericin standard was not known the extracted amounts of each compound are presented using relative peak areas, which were obtained from the HPLC of the sample (corrected with the volume of the collected extraction solvent and weighted mass of the original sample). Unfortunately, a suitable internal standard that could be detected at 590 nm as naphtodianthrones was not available. Therefore, one sample (A) was extracted at the same conditions (25 °C, 100 bar) in the beginning of each sample set as an external control for the analysis. The variance in the HPLC/UV peak responses between different days was controlled by analysis of hypericin standard. Furthermore, all experiments considering the same parameter (such as temperature) were performed during the same day and detected in the same HPLC sample set to make results more reliable.

Acknowledgements

We wish to thank Dr. Hakwon Kim for valuable discussions and for providing the hypericin standard. We also wish to thank Dr. Armando McDonald for providing the HPLC instrument for our analyses.

References

1 C. Hobbs, *Herbal Gram*, 1989, **18/19**, 24.
2 A. R. Bilia, S. Gallori and F. F. Vincieri, *Life Sci.*, 2002, **70**, 3077.
3 B. Gaster and J. Holroyd, *Arch. Intern. Med*, 2000, **160**, 152.
4 K. Linde, G. Ramirez, C. D. Mulrow, A. Pauls, W. Weidenhammer and D. Melchart, *Br. Med. J.*, 1996, **313**, 253.
5 G. Laakmann, A. Dienel and M. Kieser, *Phytomedicine*, 1998, **5**(6), 435.
6 A. Singer, M. Wonnemann and W. E. Muller, *J. Pharmacol. Exp. Ther.*, 1999, **290**(3), 1363.
7 S. S. Chatterjee, S. K. Bhattacharya, M. Wonnemann, A. Singer and W. E. Muller, *Life Sci.*, 1998, **63**(6), 499.
8 J. Park, D. S. English, Y. Wannemuehler, S. Carpenter and J. W. Petrich, *Photochem. Photobiol.*, 1998, **68**(4), 593.
9 G. Lavie, Y. Mazur, D. Lavie, A. M. Prince, D. Pascual, L. Liebes, B. Levin and D. Meruelo, *Transfusion*, 1995, **35**, 392.
10 N. D. Weber, B. K. Murray, J. A. North and S. G. Wood, *Antiviral Chem. Chemother.*, 1994, **5**, 83.
11 D. Meruelo, G. Lavie and D. Lavie, *Proc. Natl. Acad. Sci. USA*, 1988, **85**, 5230.
12 G. Lavie, F. Valentine, B. Levin, Y. Mazur, G. Gallo, G. Lavie, D. Weiner and D. Meluero, *Proc. Natl. Acad. Sci. USA*, 1989, **86**, 5963.
13 V. Butterweck, T. Bockers, B. Korte, W. Wittkowski and H. Winterhoff, *Brain Res.*, 2002, **930**(1–2), 21.
14 M.-S. Hwang, Y.-N. Yum, J.-H. Joo, S. Kim, K.-K. Lee, S.-W. Gee, H.-I. Kang and O.-H. Kim, *Anticancer Res.*, 2001, **21**, 2649.
15 G. Lavie, Y. Mazur, D. Lavie and D. Meruelo, *Med. Res. Rev.*, 1995, **15**, 111.
16 T. Sirvent and D. M. Gibson, *J. Liq. Chromatogr. Related Technol.*, 2000, **23**(2), 251.
17 A. G. Jensen, C. Cornett, L. Gudiksen and S. H. Hansen, *Phytochem. Analysis*, 2000, **11**, 387.
18 P. Mauri and P. Pietta, *Rapid Commun. Mass Spectrom.*, 2000, **14**, 95.
19 D. G. Gray, G. E. Rottinghaus, H. E. G. Garrett and S. G. Pallardy, *J. AOAC Int.*, 2000, **83**(4), 944.
20 M. Brolis, B. Gabetta, R. Fuzzatti, R. Pace, F. Panzeri and F. Peterlongo, *J. Chromatogr., A*, 1998, **825**, 9.
21 G. Piperopoulos, R. Lotz, A. Wixforth, T. Schmierer and K.-P. Zeller, *J. Chromatogr., B*, 1997, **695**, 309.
22 Q. Lang and C. M. Wai, *Talanta*, 2001, **53**, 771–782.
23 M. Mannila, H. Kim, Caarlson and C. M. Wai, *Green Chem.*, 2002, **4**, 331.
24 B. van Bavel, K. Hartonen, C. Rappe and M-L. Riekkola, *Analyst*, 1999, **124**, 1351.
25 A. Kubátová, B. Jansen, J-F. Vaudoisot and S. B. Hawthorne, *J. Chromatogr., A*, 2002, **975**, 175.
26 R. M. Smith, *J. Chromatogr., A*, 2002, **975**, 31.
27 L. Ramos, E. M. Kristenson and U. A. Th. Brinkman, *J. Chromatogr., A*, 2002, **975**, 3.
28 W. K. Modey, D. A. Mulholland, H. Mahomed and M. W. Raynor, *J. Microcolumn Sep.*, 1996, **8**, 67.
29 T. D. Thornton, D. E. LaDue III and P. E. Savage, *Environ. Sci. Technol.*, 1991, **25**, 1507.
30 Q. Lang and C. M. Wai, Pressurized Water Extraction, US patent #6,524,628, February 25th, 2003.
31 A. Poutaraud, A. Lobstein, P. Girardin and B. Weniger, *Phytochem. Anal.*, 2001, **12**, 355.
32 Q. Lang, PhD Dissertation, ch. 5, University of Idaho, Idaho, USA, 1999.
33 E. Gruszecka-Kowalik and L. H. Zalkow, *Org. Prep. Proced. Int.*, 2000, **32**, 57.

Potential impacts of deep-sea injection of CO_2 on marine organic chemistry

Ji Hu, Nino Malic, Janet L. Scott and Christopher R. Strauss*

Centre for Green Chemistry, Building 23, Monash University, Victoria 3800, Australia.
E-mail: c.strauss@sci.monash.edu.au; Fax: +61 3 99054597; Tel: +61 3 99059630

Received 13th May 2003
First published as an Advance Article on the web 21st July 2003

The extent of reaction of epoxides in saltwater changed markedly through introduction of gaseous or liquid CO_2. Higher levels of β-chlorohydrins in carbonated saltwater compared with those in saltwater alone were attributed to greater acidity of the aqueous phase. This suggests that regimes for sequestration of CO_2 by deep sea injection should take account of potential effects on marine organic chemistry. No evidence was obtained for enhanced nucleophilicity of the chloride ion through potential desolvation at the CO_2–water interface.

Introduction

Owing to increased energy consumption and the burning of fossil fuels, since the beginning of the industrial revolution the atmospheric concentration of CO_2 has risen from 280 ppm to about 370 ppm currently[1] and without remedial action, it has been projected to exceed 500 ppm during this century.[2] The potential consequences of CO_2 accumulation include global warming and climate change.[3] A significant natural means for sequestration of CO_2 is by slow diffusion into seawater followed by formation of calcium and magnesium carbonate salts that fall to the ocean floor.[4–6] The increasing levels of atmospheric CO_2 indicate that at present rates of power generation, the ecosystem cannot process the gas quickly enough for the concentration to attain a steady state.[1,2] In 1977, Marchetti proposed that the rate of increase in atmospheric concentrations could be slowed by collection and compression of CO_2 at power plants, followed by deep sea injection and sequestration as liquid.[7] In contrast with natural sequestration, pockets of liquid CO_2 or clathrates would be produced.[2] Only in exceptional circumstances would such systems occur naturally. The potential effects of direct disposal of liquefied CO_2 include localized lowering of seawater pH and other geochemical, physical and inorganic chemical interactions.[2,8–10]

Proposals based upon Marchetti's concept have garnered support[11–14] and been the subject of international collaborative oceanological studies.[15] Although implementation may be imminent, the possibility of impacts on mobile deep-sea animals, on marine biodiversity and on food webs has received relatively scant attention.[16–19] The potential effects on marine organic chemistry do not appear to have been explored at all. This may be because CO_2 occurs naturally in abundance, is relatively inert and has established, fundamental roles in microbiology and in biology. Also, marine organic chemicals tend to occur in complex, ill-defined mixtures and in high dilution. Since their concentration also decreases with ocean depth,[20] definitive studies into the influence of CO_2 on organic compounds in seawater would be difficult to conduct. Nonetheless, implementation of the above proposals could create opportunities for gaseous, liquid, or clathrated CO_2 to influence the chemistry of organic and bio-organic compounds in seawater,[2,17] particularly near injection points. Some of these aspects have been subjected to preliminary investigations.

Experimental

General methods

All reagents were obtained from commercial sources and used without further purification. Saltwater used in experiments was composed of 3.5 wt% NaCl and 0.012 wt% NaBr. Saltwater saturated with CO_2 was made by bubbling the gas through the solution until a constant pH (of 3.8) was obtained. A slow stream of CO_2 was maintained above the solution during reaction. Reactions involving liquid CO_2 were performed in stainless steel pressure vessels which consisted of a length of 316 stainless steel tubing (20 mm OD, 3 mm wall and 75 mm length) capped with Swagelock fittings, one of which having a reducing union connecting it to a length of 0.65 mm tubing running to a valve and high pressure gauge. The total volume of the reactor and extension tubing was 12 mL. Reaction products were identified using gas chromatography (GC) and gas chromatography-mass spectroscopy (GC-MS) and verified using authentic samples. Quantitative analysis of reactants and products was obtained by analysing response factors of known quantities. All GC analyses were performed in triplicate for reproducibility.

General method for reactions in saltwater, saltwater saturated with CO_2 and acidified saltwater

The epoxide (50 mg) added to saltwater (6 mL), saltwater saturated with CO_2 or saltwater acidified with HCl or acetic acid, was stirred for designated periods at ambient temperature. Parallel experiments with epoxide–saltwater mixtures containing various minerals (50 mg) were also performed. Upon

Green Context

Deep-sea injection has been proposed as a "sink" for the rising levels of CO_2. While these proposals are being taken seriously, the effects of this on the marine environment have not been so well studied. This article suggests that the process could have profound implications for the chemistry occurring in sea water. ***DJM***

 DOI: 10.1039/b305401m

reaction completion the aqueous solutions were filtered (when minerals used) and extracted with ether, the organic phase dried ($MgSO_4$) prior to analysis.

General method for reactions in seawater–liquid CO_2 mixtures

To the pressure vessel was added the epoxide (50 mg), saltwater (6 mL), a stir bar and mineral (50 mg, where applicable). Liquid CO_2 was introduced at the required pressure, the quantity of which was determined by the mass difference of the apparatus. Larger introduced quantities of CO_2 were achieved by prior cooling of the apparatus and its contents in an ice bath. After reaction completion, depressurization of the reactor was achieved by slowly venting through a series of cold traps. The aqueous contents were extracted with diethyl ether together with the material trapped upon depressurization.

Results and discussion

Studies involving authentic systems or close models would require ranges of low and varied levels of CO_2 in seawater along with highly dilute, defined mixtures of marine organic natural products.[21] These resources, the huge body of work required and the associated timeframes (many years rather than days and months) were beyond the present scope. Instead, this feasibility study employed 1,2-epoxides with CO_2–saltwater mixtures. Epoxides have biological roles and can undergo chemical transformations such as ring opening by substitution or addition, insertion, including by CO_2, and rearrangement.[22] They are susceptible to attack under a range of conditions including at ambient temperature and they react largely by established mechanisms along competing pathways.[22] Epoxides have been employed previously in a loosely analogous manner, to probe effects of sub-surface sediments on organics in contaminated groundwater.[23] In contrast with marine ecosystems, they were used here at ambient temperature, in saltwater instead of seawater and in high (*i.e.* g L^{-1}) concentrations to facilitate analysis.

The epoxides examined, in approximately decreasing order of polarity based on their water solubilities, were 7-oxabicyclo[4.1.0]heptan-2-one (**1a**), cyclohexene oxide (**2a**) phenyloxirane (styrene oxide; **3a**) and 1,2-epoxy-3-phenoxypropane (**4a**) (Scheme 1). For experiments shown in Table 1, each epoxide (*ca.* 50 mg) in saltwater (6 mL) was stirred for designated periods at ambient temperature, alone, saturated with gaseous CO_2 or with CO_2 (1.8 g) under *ca.* 5 MPa pressure.

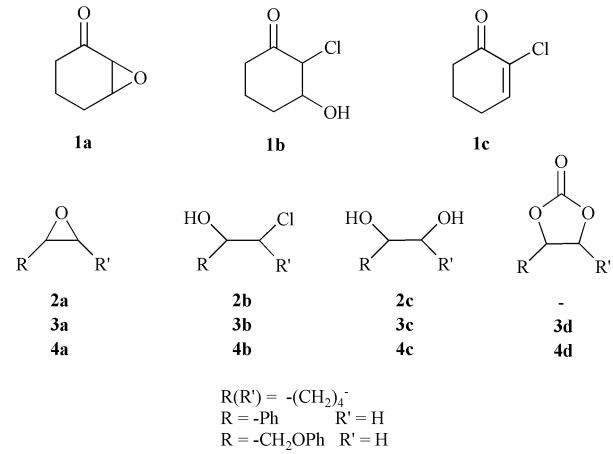

Scheme 1 Epoxides and products.

Phase diagrams indicated that under the last conditions, a liquid phase for CO_2 would have existed.[2]

Only 7-oxabicyclo[4.1.0]heptan-2-one (**1a**) reacted similarly under all test conditions (data not presented in Table 1). After 7 days at ambient temperature, approximately 30% of it remained, the major products being isomers of 2-chloro-3-hydroxycyclohexanone (**1b**; 60%) along with 2-chlorocyclohex-2-enone (**1c**; 10%). In recent studies of epoxides with metal halides supported individually on silica gel in dry media, Kotsuki *et al.* found that traces of water associated with the silica gel were necessary for reaction to occur and that lithium ions were far more effective than sodium ions in promoting the process.[24,25] Within the lithium halide series, the order of reactivity was determined to be LiI > LiBr ≫ LiCl, with typical major products being β-halohydrins and 1,2-diols. Consistent with conclusions from that work, epoxides **2a–4a** were relatively unreactive in saltwater (Table 1). In stark contrast, however, **2a** and **3a** degraded within hours in the CO_2-saturated saltwater and biphasic CO_2-saturated saltwater–liquid CO_2 systems. The regioselectivity of attack by chloride ion was almost exclusively at the less hindered position, indicative of "normal" nucleophilic opening of epoxides and seemingly militating against mechanisms involving acid catalysis.[22] With cyclohexene oxide (**2a**), in the presence of CO_2 the *trans*-β-chlorohydrin (**2b**) was the exclusive product after 24 h (Table 1). Diol **2c** gradually accumulated over several days until the ratio of **2b** : **2c** was approximately 1 : 1. Styrene oxide (**3a**) was so reactive under the CO_2–saltwater conditions that the β-chlorohydrin **3b** was observed only in early samples and even then, diol **3c** predominated (Table 1). 1,2-Epoxy-3-phenoxypropane (**4a**) although more stable than **2a** and **3a**, suffered

Table 1 Distribution of products from epoxides **2a**, **3a** and **4a** in saltwater alone, in saltwater saturated with gaseous CO_2 and in a mixture of saltwater and liquid CO_2 at ambient temperature

Starting epoxide/Time at ambient temperature	Reaction medium	Product distribution		
		Starting epoxide (%)	Chlorohydrin (%)	Diol (%)
2a/24 h	3.6% aq. NaCl	**2a** (100)	—	—
	3.6% aq. NaCl saturated with CO_2	**2a** (56)	**2b** (44)	—
	3.6% aq. NaCl and liquid CO_2	**2a** (4)	**2b** (96)	—
	Std. error[a]	3%	4%	3%
3a/4 h	3.6% aq. NaCl	**3a** (100)	—	—
	3.6% aq. NaCl saturated with CO_2	**3a** (68)	**3b** (5)	**3c** (26)
	3.6% aq. NaCl and liquid CO_2	**3a** (43)	**3b** (13)	**3c** (44)
	Std. error[a]	1%	2%	4%
4a/7 d	3.6% aq. NaCl	**4a** (93)	**4b** (1)	**4c** (3)
	3.6% aq. NaCl saturated with CO_2	**4a** (82)	**4b** (11)	**4c** (4)
	3.6% aq. NaCl and liquid CO_2	**4a** (68)	**4b** (26)	**4c** (3)
	Std. error[a]	6%	5%	1%

[a] The standard error was obtained at the 95% confidence level for replicate experiments analysed in triplicate.

approximately 30% degradation after 7 days in the presence of liquid CO_2, but remained largely intact in saltwater alone after the same time (Table 1).

The enhanced reactivity of epoxides **2a–4a** in saltwater containing CO_2 rather than in saltwater alone, was investigated. Saltwater in equilibrium with CO_2 at 5 MPa and ambient temperature, has a pH of about 3.[26] In the absence of added CO_2, styrene oxide (**3a**) was allowed to react in saltwater containing either HOAc or HCl at ambient temperature, but under pH conditions within the range 3–4. With dilute HOAc, after 6.5 h, only 3% of **3a** remained and the major products were diol **3c** (73%) and the chlorohydrin **3b** (22%). Similarly, with dilute HCl, after 5 h, only 4% of **3a** remained and **3c** (69%) and **3b** (25%) were the major products. Somewhat surprisingly, the "abnormal" product, 2-chloro-2-phenylethanol, was not detected in either of these experiments. These results strongly suggested that increased acidity of the saltwater through the introduction of CO_2 had a role in the enhanced reactivity of the epoxides and the products formed, as shown in Table 1.

Apart from pH effects, recent theoretical studies indicate that the CO_2–water interface is narrow (in the order of 10–80 Å) and adsorbs anions.[27] This raises questions as to whether in the present media, chloride ions could become desolvated, thereby increasing their nucleophilicity and facilitating reactions at the CO_2–water interface. This possibility was investigated by treatment of epoxide **4a** for 7 days with equimolar ratios of NaBr and NaCl (a) in water alone (b) in water acidified to pH 3 with HOAc and (c) in water containing liquid CO_2. Epoxide **4a** was relatively stable under conditions (a) affording traces of diol **4c**. However, it underwent approximately 55% conversion under conditions (b) and (c) with the β-bromohydrin predominating in both cases. Had desolvation of chloride or bromide occurred under conditions (c), the former anion, with a higher charge density, would have been expected to have become a more powerful nucleophile than the latter, larger anion and β-chlorohydrin formation should have been favoured.

Although no evidence was obtained to indicate the presence of desolvated choride ions in the saltwater–CO_2 mixtures, polar chlorohydrins in such mixtures could be expected to dissolve preferentially in the aqueous phase and an equilibrium with their corresponding 1,2-diols could become established. Products of such behaviour were observed with **2a** and **3a**, but to a much lesser extent with **4a**, where the chlorohydrin **4b** may have been taken up preferentially in the liquid CO_2 phase, somewhat removed from the hydrolytic environment. Data in Table 1 show that the concentration of **4b** relative to that of **4c** increased with the level of CO_2 present.

Consistent with that conclusion, when styrene oxide (**3a**) was stirred in saltwater (6 mL) containing 3.6 g of liquid CO_2 the extent of reaction was lower than that with 1.8 g of CO_2 (as in Table 1) even though the pH of the saltwater would have remained at about 3. In contrast with the data in Table 1 (4 h reaction time), after 5 h, 62% of **3a** was recovered and only 14% of **3b** and 24% of **3c** were formed. Presumably, enhanced dissolution of **3a** in the higher volume of CO_2 slowed its rate of degradation and the conversion of chlorohydrin **3b** to diol **3c**.

Notably, authentic carbonates **3d** and **4d** prepared from styrene oxide (**3a**) and 1,2-epoxy-3-phenoxypropane (**4a**) were unreactive in saltwater alone or in CO_2–saltwater mixtures. The carbonates were not detected in product mixtures either, suggesting that CO_2 did not have a direct role in the ring opening of **3a** and **4a**. Addition of minerals including $CaCO_3$, montmorillonite K10 and kaolin to styrene oxide (**3a**) and phenoxymethyloxirane (**4a**) afforded little change in the extents of degradation or the product distributions shown in Table 1. An exception occurred in the reaction of styrene oxide (**3a**) with saltwater in the presence of CO_2 and $CaCO_3$. The cyclic carbonate **3d** was formed in modest amounts, confirming the capability of CO_2 to participate in reactions in saltwater solutions under appropriate conditions.

In a survey of naturally occurring organohalogen compounds, Gribble presented several examples of β-halohydrins from terrestrial and aquatic sources.[28–30] The origins of organohalogens were ascribed to combustion of organics in the presence of halides or halogens or, alternatively, through biosynthesis involving haloperoxidase enzymes. This work suggests that addition of the elements of HBr, HCl and HI (derived from the corresponding sodium salts in water) to epoxides in the presence of CO_2 now could be considered as well, particularly for metabolites of corals and coralline microalgae[31] that inhabit seawaters containing high levels of CO_2.

Before the reports of Kotsuki *et al.*,[24,25] lithium halides had been employed in the presence of acetic acid[32] or the acid resin Amberlyst 15[33] to form vicinal halohydrins from epoxides *via* acid catalysis. Under those conditions, however, styrene oxide produced mixtures of both possible regioisomers with the secondary chloride predominating. This regioselectivity occurs through stabilisation of an intermediate benzylic carbocation and has been observed in many other reported procedures,[34] but surprisingly, it was not obtained here, suggesting that the formal carbocation was not formed under the conditions. In addition to acid catalysis, lithium halides in combination with nickel, copper and titanium halides, can form complexes of the type Li_2MX_4, which also have been reported to be effective reagents for the synthesis of vicinal halohydrins from monosubstituted epoxides.[35–37] Other metal halide systems that perform similarly are $SnCl_2{\cdot}2H_2O$–Mg[38] and iodides of Na, Li, Mg and Zn together with Bu_3SnH/AIBN, which can produce iodohydrin intermediates in the synthesis of secondary alcohols from epoxides.[39–40] The present study not only presents cautionary results with regard to CO_2 disposal in seawater, but it also suggests that saltwater–liquid CO_2 systems could have useful synthetic applications at least with regard to the opening of epoxides. Undoubtedly, saltwater–CO_2 represents a greener alternative to several of the reaction systems mentioned above.

To summarise, this feasibility study with simple systems suggests that disposal of CO_2 by compression and deep sea dispersal has the potential to affect the nature and distribution of organics in seawater by mechanisms including sequestration, chemical reactions involving CO_2 itself and by localized increased acidity of seawater. No evidence was obtained to suggest a role for desolvation of chloride ions at the CO_2–water interface. Although it appears that ring opening of epoxides occurred in the aqueous phase, CO_2 as a supercritical fluid or as a liquid is widely used for extraction of organic compounds. In that regard, deep sea disposal of CO_2 could facilitate extraction and concentration of natural products from seawater into the organic phase and promote processes that would not normally occur, *e.g.* the reaction of CO_2 with amine groups to produce carbamates. Alternatively, organic compounds that otherwise would be hydrolyzed in seawater, could be sequestered and stabilized in the CO_2 phase instead. The potential ramifications could extend to lengthening of the half-lives of compounds that are naturally degraded hydrolytically in seawater.

Acknowledgements

The authors gratefully acknowledge CSIRO Molecular Science for seconding C. R. S., the Australian Research Grants Commission (ARC) for funding of the Monash University ARC Special Research Centre for Green Chemistry, the Victorian State Government also for financial assistance toward this work and Dr Peter Nichols and Dr Bronte Tilbrook both of CSIRO Marine Laboratories, Hobart, for helpful suggestions and comment.

References

1 F. Smalberg, J. Moulijn and H. van Bekkum, *Green Chem.*, 2000, **2**, G97.
2 C. S. Wong and S. Hirai, *Ocean Storage of Carbon Dioxide. A Review of Oceanic Carbonate and CO_2 Hydrate Chemistry*, IEA Greenhouse Gas R&D Programme, Cheltenham, UK, 1997.
3 Editorial (joint statement by 16 national academies and the Royal Society, UK), *Science*, 2001, **292**, p. 126.
4 T.-H. Peng, R. Wanninkhof, J. L. Bullister, R. A. Feeley and T. Takahashi, *Nature*, 1998, **396**, 560.
5 P. G. Brewer and F. M. Orr Jr., *Chem. Ind.*, 2000, 567.
6 A. Poisson, *Nature*, 1998, **396**, 521.
7 C. Marchetti, *Clim. Change*, 1977, **1**, 59.
8 W. J. Harrison, R. F. Wendlandt and E. D. Sloan, *Appl. Geochem.*, 1995, **10**, 461.
9 K. Caldeira and G. H. Rau, *Geophys. Res. Lett.*, 2000, **27**, 225.
10 P. G. Brewer, E. T. Peltzer, G. Friederich, I. Aya and K. Yamane, *Mar. Chem.*, 2000, **72**, 83.
11 C. N. Murray, L. Visintini, G. Bidoglio and B. Henry, *Energy Convers. Manage.*, 1996, **37**, 1067.
12 K. A. Hunter, *Mar. Freshwater Res.*, 1999, **50**, 755.
13 P. G. Brewer, G. Friederich, E. T. Peltzer and F. M. Orr, Jr., *Science*, 1999, **284**, 943.
14 L. Ametistova, J. Twidell and J. Briden, *Sci. Total Environ.*, 2002, **289**, 213.
15 H. Audus, *Energy*, 1997, **22**, 212.
16 P. M. Haugan, *Waste Manage.*, 1997, **17**, 323.
17 M. H. Huesemann, A. D. Skillman and E. A. Crecelius, *Mar. Pollut. Bull.*, 2002, **44**, 142.
18 M. N. Tamburri, E. T. Peltzer, G. E. Friederich, I. Aya, K. Yamane and P. G. Brewer, *Mar. Chem.*, 2000, **72**, 95.
19 B. A. Seibel and P. J. Walsh, *Science*, 2001, **294**, 319.
20 J. I. Hedges, J. A. Baldock, Y. Gelinas, C. Lee, M. Peterson and S. G. Wakeham, *Nature*, 2001, **409**, 801.
21 S. Emerson, P. Quay, D. Karl, C. Winn, L. Tupas and M. Landry, *Nature*, 1997, **389**, 951.
22 R. E. Parker and N. S. Isaacs, *Chem. Rev.*, 1959, **59**, 737.
23 W. R. Haag and T. Mill, *Environ. Sci. Technol.*, 1988, **22**, 658.
24 H. Kotsuki and T. Shimanouchi, *Tetrahedron Lett.*, 1996, **37**, 1845.
25 H. Kotsuki, T. Shimanouchi, R. Ohshima and S. Fujiwara, *Tetrahedron*, 1998, **54**, 2709.
26 K. L. Toews, R. M. Shroll, C. M. Wai and N. G. Smart, *Anal. Chem.*, 1995, **67**, 4040.
27 R. Schurhammer, F. Berny and G. Wipff, *Phys. Chem. Chem. Phys.*, 2001, **3**, 647.
28 G. W. Gribble, *J. Nat. Prod.*, 1992, **55**, 1353.
29 G. W. Gribble, *J. Chem. Educ.*, 1994, **71**, 907.
30 G. W. Gribble, *Acc. Chem. Res.*, 1998, **31**, 141.
31 U. Riebesell, I. Zondervan, B. Rost, P. D. Tortell, R. E. Zeebe and F. M. M. Morel, *Nature*, 2000, **407**, 364.
32 J. S. Bajwa and R. C. Anderson, *Tetrahedron Lett.*, 1991, **32**, 3021.
33 C. Bonini, C. Giuliano, G. Righi and L. Rossi, *Synth. Commun.*, 1992, **22**, 1863.
34 C. Bonini and G. Righi, *Synthesis*, 1994, 225 and references therein.
35 R. D. Dawe, T. F. Molinaki and J. V. Turner, *Tetrahedron Lett.*, 1984, **25**, 2061.
36 J. A. Ciaccio, K. J. Addess and T. W. Bell, *Tetrahedron Lett.*, 1986, **27**, 3697.
37 J. A. Ciaccio, E. Heller and A. Talbot, *Synlett*, 1991, 248.
38 C. Sarangi, N. B. Das, B. Nanda, A. Nayak and R. P. Sharma, *J. Chem. Res. (S)*, 1997, 180.
39 C. Bonini and R. Di Fabio, *Tetrahedron Lett.*, 1988, **29**, 819.
40 C. Bonini, R. Di Fabio, G. Sotgiu and S. Cavagnero, *Tetrahedron*, 1989, **45**, 2895.

TBD-catalysed solventless synthesis of symmetrically *N,N′*-substituted ureas from primary amines and diethyl carbonate

Roberto Ballini,[a] Dennis Fiorini,[a] Raimondo Maggi,*[b] Paolo Righi,*[c] Giovanni Sartori[b] and Raffaella Sartorio[b]

[a] *Dipartimento di Scienze Chimiche dell'Università, Via S. Agostino 1, I-62032 Camerino (MC), Italy*
[b] *Dipartimento di Chimica Organica e Industriale dell'Università, Parco Area delle Scienze 17A, I-43100 Parma, Italy*
[c] *Dipartimento di Chimica Organica "A. Mangini " dell'Università, Viale del Risorgimento 4, I-40136 Bologna, Italy*

Received 18th February 2003
First published as an Advance Article on the web 30th May 2003

Symmetrically *N,N′*-substituted ureas were obtained from primary amines in very good yields under solvent-less conditions using diethyl carbonate (DEC) as the carbonylation reagent and 1,5,7-triazabicyclo[4.4.0]dec-5-ene (TBD) as the base catalyst. The products are precipitated directly from the reaction mixture after a volatile organic compound (VOC) free aqueous work-up. The catalyst can be recovered and reused.

Introduction

Ureas have found a wide variety of large scale applications such as dyes for cellulose fibre, antioxidants in gasoline, corrosion inhibitors, and intermediates for production of carbamates, which represent raw materials for agrochemicals. Their biological activities as plant growth regulators, agroprotectives as well as tranquillising and anticonvulsant agents are also important.[1] Moreover, ureas substituted with aminoacid groups have been shown to be potent HIV-1 protease inhibitors.[2]

Ureas are commonly prepared by methodologies mainly based on the use of dangerous reagents such as phosgene and isocyanates. Over the last few years, the pressure of a growing environmental awareness and the demand for cleaner synthetic methodologies has produced a number of alternatives to these toxic reagents.[3,4]

In this regard, carbonic acid dialkyl esters have emerged as possible safe, cheap and environmentally acceptable alternatives to phosgene or other toxic carbonylating agents, and to alkyl halides or other dangerous alkylating agents such as dimethyl sulfate. They are produced by a clean process[5] and are biodegradable, and their use avoids the formation of saline by-products. All these features make them true *green reagents*, allowing prevention of pollution at the source.[6]

TBD is a strong guanidine base (pK_b = 25)[7] widely utilised as an acid scavenger and base catalyst. In our continuing effort to devise environmentally benign methodologies based on the use of this base as the homogeneous and heterogeneous catalyst,[8,9] we decided to investigate the possibility of using TBD as the catalyst in a homogenous fashion in a solvent-less synthesis of symmetrical *N,N′*-substituted ureas[10] using diethyl carbonate as the carbonylating agent, according to Scheme 1.

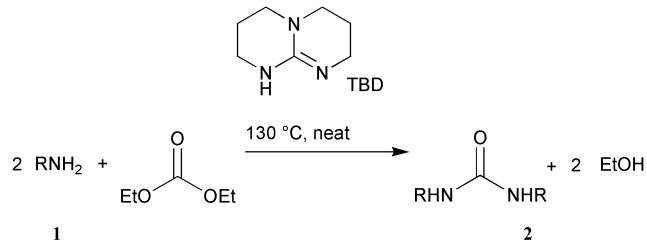

Scheme 1

Results and discussion

As was already known, by tuning the temperature carbonic acid alkyl diesters can function either as alkylating agents or as carbonylating agents.[6] In this case we found that the best results in terms of yield and selectivity were achieved by performing the reaction at 130 °C.

A number of different amines were chosen to assess the scope of the reaction. The reactions were performed under solvent-less conditions, by mixing at room temperature stoichiometric amounts of diethyl carbonate (DEC) and of the corresponding amine, along with a catalytic amount (5% mol mol^{-1} of DEC) of the guanidine base TBD and by heating the mixture at 130 °C for 10 h.

The synthetic results of the reactions performed on several different amines are presented in Table 1. Generally speaking this reaction gives very good yields with primary aliphatic amines allowing us to obtain the corresponding ureas as the only product. No product arising from the alkylation of the amine was ever observed under these reaction conditions.

Green Context

The combination of solvent free processes and the use of recoverable catalysts is one of the more powerful green chemical technology procedures. Here this is applied to the synthesis of *N,N′*-substituted ureas from primary amines and diethyl carbonate as the carbonylation reagent. The catalyst found to be very effective in this chemistry is a strong guanidine base. Product yields are very good and no salt is produced in the reaction, the only by-product being ethanol. The work-up is also VOC free. ***JHC***

 DOI: 10.1039/b301951a

Entry	Amine (**1**)	Product (**2**)	Yield (%)
a	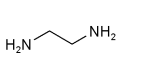		95
b	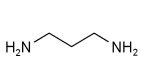		95
c[a]	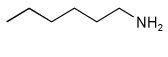	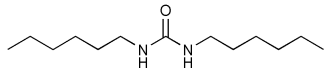	78
d	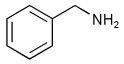	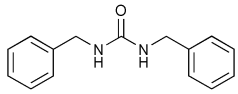	93
e	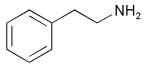	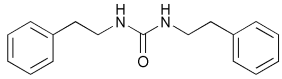	97
f	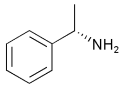	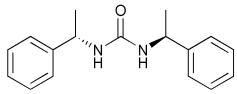	92
g		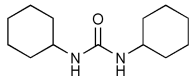	90
h	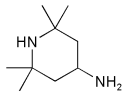	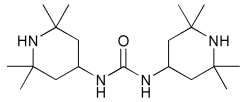	82
i		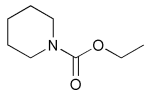	89
j	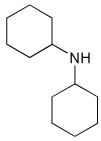	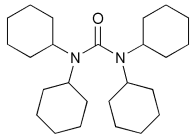	no reaction
k[b]		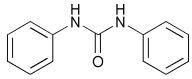	68
l[b]	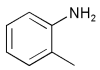	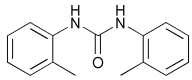	53

[a] Aqueous work-up performed at room temperature. [b] Reaction stopped after 48 h.

Five- and six-membered cyclic ureas (**2a** and **2b**) can be obtained with this methodology, while when longer diamines are employed as the starting materials, the reaction gives mainly polymeric products.

It is also worthy of note that in the case of (*S*)-1-phenylethyl amine (**1f**) the corresponding urea (**2f**) is obtained with no detectable loss of optical purity.[11]

The reaction seems to be very sensitive to steric effects. For example, when a secondary amine, such as piperazine (entry i), was used only one amino group was introduced and after 24 h the reaction selectively afforded in very good yield the corresponding ethyl carbamate **2i**. When even more encumbered amines were used, such as dicyclohexyl amine (**1j**), no product at all was obtained and the starting materials were recovered unchanged. Thus, the scope of this reaction seems to be limited to primary amines.

The reaction also works on anilines (entries k and l) affording the corresponding diphenylureas. However, as was anticipated, in this case the reaction is slower and affords slightly lower yields of the products. Diphenylurea[13] (BPU) and its derivatives have found many useful applications as drugs, antioxidants in gasoline, and herbicides.[1]

Concerning the mechanism, presumably, as we recently proposed,[8] TBD initially attacks the carbonate to give an active guanidium salt that can undergo nucleophilic attack by the amine more easily.[14] The use of other bases such as 4-dimethylaminopyridine (DMAP) and *N*-propyl-1,1,1′-carboxyimidoyl bispiperidine gave only low yields (10–15%) of the urea after prolonged reaction times. As expected, running the reaction with no base catalyst (amine autocatalysis) gave only moderate yields of the carbamate.

Isolation of the products posed some questions, especially regarding the use of organic solvents. Most of the time, ureas are sparingly soluble in common organic solvents such as diethyl ether. So a quick way to isolate the products, was to cool the reaction mixture and take up the residue three times with two volumes of diethyl ether decanting the solids. In this way, traces of unreacted reagents and TBD are dissolved, while the urea is not, which is obtained in a more than acceptable purity.

However, to avoid the use of VOCs during the work-up, we devised and optimized an aqueous treatment of the reaction mixture. In this case, after cooling the reaction mixture to 80 °C, hot water was added and the mixture was stirred at this temperature for an additional 30 min. The mixture was then filtered while still hot. We observed that the aqueous filtrate contains most of the traces of unreacted reagents and TBD. The solid product can be further purified by crystallization from an appropriate solvent. Evaporation of the aqueous phase allows us to recover the base catalyst which can be reused at least three times without detrimental effects on both reaction times and yields (*i.e.* for the synthesis of *N*,*N*′-dibenzyl urea: first cycle 93% yield; second cycle 89% yield; third cycle 84% yield).

Conclusions

In conclusion, we have reported a new, effective and environmentally friendly methodology for the preparation of symmetric *N*,*N*′-substituted ureas that makes use of diethyl carbonate as the carbonylating agent and of TBD as the base catalyst. This methodology works under solvent-less conditions and affords in very good yields the corresponding ureas. No salt is formed during the reaction, the only by-product being ethanol. A VOC free aqueous work-up was devised that allows the precipitation of the product directly from the reaction media and recovery of the base catalyst, which can be reused. The reaction works very well for primary aliphatic amines, while the use of diamines is limited to 1,2-ethanediamine and 1,3-propanediamine. Anilines, as well, react under these conditions to afford the corresponding ureas, albeit in lower yields. Secondary amines and sterically hindered amines in general cannot be used.

Experimental

Typical procedure

A mixture of the selected amine (10 mmol), DEC (5 mmol) and TBD (0.25 mmol) was heated with an oil bath at 130 °C for 10 h, under magnetic stirring. The flask was equipped with an air condenser and left open throughout the course of the reaction. After cooling to 80 °C, hot water (20 ml) was added and vigorous stirring was continued for an additional 30 min. The solid product was then filtered off and purified by crystallisation from methanol. The aqueous phase containing TBD (and a little DEC and amine) was evaporated to dryness and reused for additional cycles. Satisfactory IR, MS, ^{1}H and ^{13}C NMR, and mp data were obtained for all the ureas **2** and were consistent with those found in the literature.

Acknowledgements

We wish to thank the Ministero dell'Istruzione, dell'Università e della Ricerca (MIUR), Italy and the Universities of Bologna, Parma and Camerino (National Projects "Stereoselezione in Sintesi Organica. Metodologie ed Applicazioni" and "Processi puliti per la Chimica Fine") for financial support.

References

1 T. P. Vishnyakova, I. A. Golubeva and E. V. Glebova, *Russ. Chem. Rev. (Engl. Transl.)*, 1985, **54**, 249.
2 K. Matsuda, *Med. Res. Rev.*, 1994, **14**, 271; D. P. Getman, G. A. DeCrescenzo, R. M. Heintz, K. L. Reed, J. J. Talley, M. L. Bryant, M. Clare, K. A. Houseman, J. J. Marr, R. A. Mueller, M. L. Vazquez, H. S. Shieh, W. C. Stallings and R. A. Stegeman, *J. Med. Chem.*, 1993, **36**, 288.
3 For a review on the synthesis of ureas using phosgene substitutes, see: F. Bigi, R. Maggi and G. Sartori, *Green Chem.*, 2000, **2**, 140.
4 I. Vauthey, F. Valot, C. Gozzi, F. Fache and M. Lemaire, *Tetrahedron Lett.*, 2000, **41**, 6347.
5 Y. Ono, *Appl. Catal. A: Gen.*, 1997, **155**, 133.
6 For a recent account, see: P. Tundo and M. Selva, *Acc. Chem. Res.*, 2002, **35**, 706.
7 R. Schwesinger, J. Willaredt, H. Schlemper, M. Keller, D. Schmitt and M. Fritz, *Chem. Ber.*, 1994, **127**, 2435.
8 S. Carloni, D. E. De Vos, P. A. Jacobs, R. Maggi, G. Sartori and R. Sartorio, *J. Catal.*, 2002, **205**, 199.
9 R. Ballini, G. Bosica, D. Fiorini, R. Maggi, P. Righi, G. Sartori and R. Sartorio, *Tetrahedron Lett.*, 2002, **43**, 8445.
10 For an alternative preparation see: F. Bigi, B. Frullanti, R. Maggi, G. Sartori and E. Zambonin, *J. Org. Chem.*, 1999, **64**, 1004.
11 $[\alpha]_D^{20}$ −65.0 (*c* 1.012, EtOH). Lit.[12] $[\alpha]_D^{20}$ −64.4 (*c* 0.4, EtOH).
12 A. Tillack, M. Michalik, D. Fenske and H. Goesmann, *J. Organomet. Chem.*, 1994, **482**, 85.
13 For a recent *green* preparation of BPU see: N. Nagaraju and G. Kuriakose, *Green Chem.*, 2002, **4**, 269.
14 The ability of guanidines and other bases to react with CO_2 or carbonates has been recently reported: (*a*) E. R. Pérez, M. Odnicki da Silva, V. C. Costa, U. P. Rodrigues-Filho and D. W. Franco, *Tetrahedron Lett.*, 2002, **43**, 4091; (*b*) M. George and R. G. Weiss, *J. Am. Chem. Soc.*, 2001, **123**, 10393; (*c*) M. Abla, J.-C. Choi and T. Sakakura, *Chem. Commun.*, 2001, 2238.

Catalyst performance in reforming of tar derived from biomass over noble metal catalysts

Keiichi Tomishige,* Tomohisa Miyazawa, Mohammad Asadullah, Shin-ichi Ito and Kimio Kunimori

Institute of Materials Science, University of Tsukuba 1-1-1, Tennodai, Tsukuba, Ibaraki 305-8573, Japan. E-mail: tomi@tulip.sannet.ne.jp; Fax: +81-29-853-5030; Tel: +81-29-853-5030

Received 25th March 2003
First published as an Advance Article on the web 30th May 2003

An activity test in the reforming of tar derived from cedar biomass over M–CeO_2–SiO_2 (M = Rh, Pt, Pd, Ru, Ni) was carried out in a secondary fluidized catalyst bed at lower temperature range (823–923 K) than the conventional methods. We have measured the formation rate of CO, CO_2, CH_4, H_2, and the yield of coke deposited on the catalyst surface and the yield of char accumulated in the primary bed. It was found that Rh–CeO_2–SiO_2 exhibited much higher performance than other metal catalysts in terms of the activity of tar reforming, and the yield of gas and coke.

Introduction

The use of biomass as an energy resource would lead to a decrease in the emission of CO_2, NO_x, SO_x, and particulate matter into the atmosphere.[1] This is because plants, the source of biomass, naturally recycle CO_2 from the atmosphere during their growth and the biomass derived fuels in various forms are super clean. Biomass is gasified to synthesis gas at around 1073–1223 K, and the produced gas can be used either as a gaseous fuel for power generation or as a feedstock for the synthesis of clean transportation fuels such as methanol, dimethyl ether, and Fischer–Tropsch oils, or many other chemicals. The formation of tar (a complex mixture of organic liquid constituents) and char (solid carbonaceous materials) during the gasification process is the most severe problem.[2–13]

The removal of tar from the product gas stream by catalytic cracking and reforming is one of the most promising methods and has been investigated for more than two decades.[14–23] The studies on the catalytic gasification of biomass include the use of a catalyst either in the gasifier itself or in separate reactors downstream from the gasifier.[24] Some nickel based catalysts,[25–32] dolomite[33] and olivine[34] catalysts have been found to be active catalysts for tar cracking in the primary reactor within a temperature range of 1073–1173 K for dolomite and olivine, and 973–1073 K for nickel based catalysts. The Ni-based catalysts were deactivated significantly by coke deposition on the catalyst surface.[25,26,29,35,36]

Recently we have carried out catalyst development for the catalytic gasification of biomass and cellulose. A CeO_2 supported Rh catalyst efficiently converted the total carbon in the cellulose to gas products even at 823 K.[37] However, the sintering of CeO_2 and, as a result, the decreasing of the surface area of the catalyst under the reaction conditions, caused the deactivation of the catalyst.[38] The loading of CeO_2 on other supports seems to prevent the sintering of CeO_2. And this phenomenon was actually observed in our Rh–CeO_2–SiO_2 catalyst with 35 mass% CeO_2 content for the gasification of cellulose.[39–43] Furthermore, we have demonstrated that the Rh–CeO_2–SiO_2 catalyst is applicable to the gasification of the biomass (wood powder).[44] In these studies, biomass is directly supplied to the catalyst bed. In this case, all components of the biomass can contact catalyst particles. In terms of the practical view, biomass can contain various kinds of impurities such as ash which can cause catalyst deactivation. Therefore, we have investigated the catalyst performance in the reforming of tar using the dual-bed (primary and secondary) reactor where only the tar can contact catalyst particles.

Experimental

Biomass

The gasification of cedar wood was carried out. The moisture content of the wood was about 10%. This wood was ground with a ball mill to about 0.1–0.3 mm size. The composition of the wood granules was C 45.99, H_2O 10, H 5.31, O 38.25, N 0.11, Cl 0.01, S 0.02, and ash 0.3 mass%.

Catalyst

The catalysts we have used in this investigation are M–CeO_2–SiO_2 (M = Rh, Pd, Pt, Ru, Ni) with 1.2×10^{-4} mol g-cat.$^{-1}$ The CeO_2–SiO_2 was prepared by the incipient wetness method using an aqueous solution of $Ce(NH_4)_2(NO_3)_6$ and SiO_2 (Aerosil, 380 m^2 g^{-1}). The loading of CeO_2 on SiO_2 was 60 mass%. After loading the Ce salt on SiO_2, it was dried at 383 K for 12 h followed by calcination at 773 K for 3 h under an air atmosphere. Then the M (Rh, Pd, Pt, Ru) was loaded on CeO_2–SiO_2 by impregnation of the support with an acetone solution of

Green Context

The conversion of biomass to syngas represents an attractive alternative source to this important product. As such it has been investigated in great detail. One of the unresolved difficulties is the production of very heavy byproducts – tar and coke. Efforts to convert these to useful products have been made, and this paper deals with a novel catalyst system which can carry out this process under milder conditions than previously possible, thereby making a valuable contribution to this aspect of biomass utilisation. ***DJM***

$Rh(C_5H_7O_2)_3$, $Pd(C_5H_7O_2)_2$, $Pt(C_5H_7O_2)_2$, $Ru(C_5H_7O_2)_3$, respectively. The acetone solvent was then evaporated at around 333 K with constant stirring. The catalyst thus produced was then dried at 383 K for 12 h. The final catalyst was pressed, crushed and sieved to 45–150 μm particle size. In the case of $Ni–CeO_2–SiO_2$, $Ni(NO_3)_2·6H_2O$ aqueous solution was used. Calcination at 773 K for 3 h was carried out after drying at 383 K for 12 h. In each run of the activity test, 3 g of catalyst was used and pretreated by a hydrogen flow at 773 K for 0.5 h.

The fresh (after H_2 treatment) and used catalysts were characterized by a Brunauer–Emmett–Teller (BET) analysis. Chemisorption experiments were carried out in a high-vacuum system by volumetric methods. Research grade gas (H_2: 99.99%, Takachiho Trading Co. Ltd.) was used without further purification. Before H_2 adsorption measurement, the catalysts were treated in H_2 at 773 K for 0.5 h. H_2 adsorption was performed at room temperature. Gas pressure at adsorption equilibrium was about 1.1 kPa. The sample weight was about 0.2 g. The dead volume of the apparatus was about 60 ml.

Apparatus for reforming of tar derived from biomass

The gasification of biomass was carried out in a laboratory scale continuous feeding and fluidized bed gasifier as shown in Fig. 1. This reactor contained a primary bed for pyrolysis of biomass

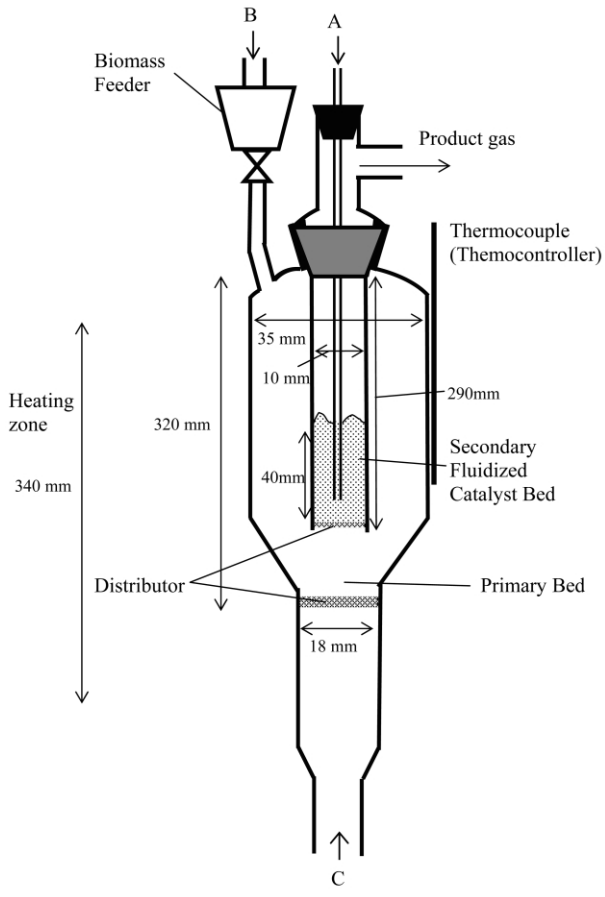

Fig. 1 Schematic diagram of the reactor. Activity test of reforming of tar from biomass A: O_2, B: N_2 + biomass, C: N_2; Coke estimation A: O_2, B: N_2, C: N_2; Char estimation A: N_2, B: O_2, C: O_2.

and accumulation of char and ash, and a secondary fluidized catalyst bed for tar reforming. The dimensions of the gasifier, which is made of quartz glass, with the fluidized catalyst bed, which is just located at the middle of the reactor, are also shown in Fig. 1. The biomass feeder consisted of a conical glass vessel with a screw valve at the bottom, allowing continuous feeding of biomass particles by vibrating the vessel with an electric vibrator. The opening size of the valve can be controlled by the screw so as to control the feeding rate of biomass particles. The vibration rate of the vibrator can also control the feeding rate. Nitrogen gas flow of 50 ml min^{-1} was usually used for transporting the biomass particles to the catalyst bed through the side tube of the outer reactor. This reaction system had three ports for gas introduction and one port for the effluent gas. We chose gases from each port for the catalyst evaluation (activity test and measurement of coke and char yield). In the activity test for tar reforming, oxygen was introduced into the catalyst bed through the thin tube in the inner reactor for the contact between oxygen and catalyst particles. If oxygen is supplied from the bottom of the reactor, a considerable amount of oxygen is consumed by combustion of char before contact with the catalyst particles. The biomass with N_2 carrier gas was introduced to the primary bed through the side tube of the outer reactor, and N_2 was fed from the bottom of the outer reactor through a quartz distributor. In the case of estimation of the yield of coke deposited on the catalyst surface, after the feeding of biomass was stopped, oxygen was introduced from the same port, and N_2 gas was fed from two other ports. This procedure corresponds to the combustion of coke. Furthermore in the case of estimation of the char yield, the carrier gas for biomass feeding was changed to oxygen, and N_2 was introduced from the catalyst bed. This corresponds to the combustion of char accumulated in the primary bed.

The temperature of the fluidized catalyst bed is controlled through the thermocouple at the outside wall of the reactor as shown in Fig. 1. In addition, we have carried out temperature measurements in the catalyst bed during the reaction at various points by using other thermocouples. The temperature difference in the catalyst bed was very small because of the catalyst fluidization, and the temperature was about 15 K lower than the outside thermocouple. The process was carried out under atmospheric pressure by adding 3 g of a catalyst to the fluidized bed. Before the activity test, the catalyst was pretreated under an H_2 stream of 40 ml min^{-1} at 773 K for 30 minutes. The product gas was successively entered through a filter (sintered metal, pore size 7 μm) and trap cooled with iced water so as to remove any solid or liquid materials from the product gas stream. The clean sample of the product gas was collected from the sampling port by micro syringe and analyzed by gas chromatograph (GC). CO, CO_2, CH_4, H_2, and H_2O were formed as the products. The gas product did not contain higher hydrocarbons and light aromatics such as benzene, and this was checked by GC analysis. The concentration of CO, CO_2 and CH_4 was determined by FID-GC equipped with a methanator using a stainless steel column packed with Gasukuropack 54 and the concentration of hydrogen was determined by TCD-GC using a stainless steel column packed with a molecular sieve 13X. The flow rate of the gas flowing out of the reactor was measured by a soap membrane meter. The formation rate of the gas products was calculated from GC analysis of the gas flowing out of the reactor in the unit of μmol min^{-1}. The carbon-based conversion to gas (C-conv) was calculated by "A/B × 100", where A represents the forming rate of $CO + CO_2 + CH_4$ and B represents the total carbon supplying rate of biomass. The yield of coke and char was determined by the amount of the gas (mainly CO_2) formed from the combustion after each activity test. After the reaction, the reactor was purged with N_2, O_2 was introduced from port A and N_2 was introduced from ports B and C. In this case, O_2 can not reach the primary bed, and only the carbonaceous materials deposited on the catalyst bed can react with oxygen. By this procedure, the coke yield can be determined. After the formation of CO_2 stopped, the feeding condition was changed. The introduction of oxygen was carried out from ports B and C and that of nitrogen from port A. In this case, the materials accumulated in the primary bed can interact with oxygen. The feeding of oxygen is continued until the

formation of CO_2 is not observed. This procedure corresponds to the determination of char yield. There is no interference between coke and char estimation. The yield of coke and char is calculated by (total CO_2 + CO)/(total carbon amount in fed biomass) × 100. The amount of tar is defined as (100 − C-conv (%) − coke yield (%) − char yield (%)). The feeding rate of biomass, N_2, and oxygen are described in each result. The equivalence ratio can be calculated by (oxygen weight/dry biomass weight)/(stoichiometric oxygen/biomass ratio for complete combustion).

Results and discussion

Fig. 2 shows the reaction time dependence on formation rate and C-conversion in the reforming of tar from biomass over Rh–CeO_2–SiO_2 and Ni–CeO_2–SiO_2 catalysts. The catalyst stability with respect to the C-conversion and product distribution is one of the most important factors to make the process efficient. The formation rate of CO, H_2, CO, and CH_4 was almost constant over Rh–CeO_2–SiO_2. Furthermore the C-conversion was 77% throughout the reaction. On the other hand, over Ni–CeO_2–SiO_2, the C-conversion decreased with time on stream from 70 to 58%, and the formation rate of CO, H_2, and CH_4 also decreased with time on stream, whereas on the other hand, that of CO_2 increased. The details of the results of the activity test over M–CeO_2–SiO_2 are listed in Table 1. The formation rate and C-conversion are averages in a 15-min reaction test. In order to compare the performance, the formation rate of CO + H_2 + CH_4 and C-conversion over various catalysts are shown in Fig. 3. The order of the activity at 823 K in the reforming of tar to synthesis gas is as follows: Rh > Pt > Pd > Ni = Ru. In the case of Ru, the activity at 923 K is also the lowest. On the other hand, the activity of Ni at 923 K becomes higher than that over Pd (Rh > Ni > Pd > Pt > Ru). This indicates that the Ni–CeO_2–SiO_2 catalyst can give high performance at high temperature. In contrast, Rh–CeO_2–SiO_2 exhibited excellent performance in the range of 823–923 K. The order of the catalyst performance, except the Ru catalyst at 923 K, is similar to that in methane reforming as reported previously.[45] The activity in the reforming of tar from biomass is suggested to be related to that in reforming of methane and hydrocarbons. In addition, the low activity over the Ru catalyst can be due to the loss of Ru metal from the catalyst surface, which is caused by the oxidation of Ru to volatile Ru oxide.

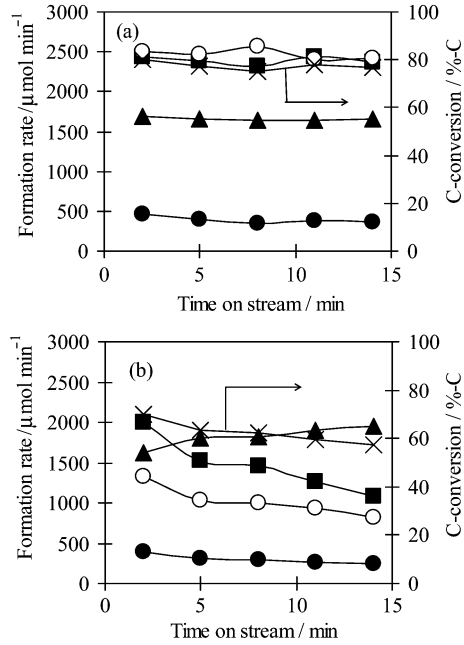

Fig. 2 Effect of time on stream on the C-conversion and product distribution over (a) Rh–CeO_2–SiO_2 and (b) Ni–CeO_2–SiO_2 in reforming of tar from biomass. ×: C-conversion, ○ H_2, ■ CO, ▲ CO_2, ● CH_4. Reaction conditions: catalyst 3 g, biomass 150 mg min^{-1} (H_2O 10%, C, 5748 μmol min^{-1}; total H_2, 4815 μmol min^{-1}; total O_2, 2208 μmol min^{-1}), supplied O_2 35 ml min^{-1} (1432 μmol min^{-1}), ER = 0.25, total N_2 150 ml min^{-1} (6138 μmol min^{-1}), and temperature 873 K.

Yield of char which is accumulated in the primary bed, yield of coke which is deposited on the catalyst surface, and yield of tar which is not reformed are also listed in Table 1. The char yield was about 23% even at high reaction temperature. This corresponds to the amount of fixed carbon in the biomass, which is mainly due to lignin content. This is supported by thermogravimetric analysis as shown below. The coke yield over the Rh catalyst was lower than that over the other catalysts. Furthermore, it is very interesting that the yield of tar was much lower than the other catalysts, especially at low reaction temperature 823 K. This also indicates that the Rh catalyst has much higher activity in tar reforming.

Table 1 Catalyst properties and performance in the reforming of tar from biomass over M–CeO_2–SiO_2

		Formation rate/μmol min^{-1}								Characterization	
Metal	*T*/K	CO	H_2	CH_4	CO_2	C-conv/ %-C	Char yield/ %-C	Coke yield/ %-C	Tar yield/ %-C	H_2 adsorption H/M (mol/mol)	BET/ m^2 g^{-1}
Rh	823	1486	2248	385	1779	64	35	1	0	0.16	135
	873	2389	2466	387	1655	77	22	1	0		
	923	2682	3526	158	1545	77	22	1	0		
Pt	823	890	1217	193	1647	48	31	5	16	0.21	128
	873	1475	2211	268	2023	66	27	2	5		
	923	2234	3171	85	2018	76	23	1	0		
Pd	823	1488	1049	258	1437	55	30	5	10	0.14	127
	873	1830	2347	226	1944	69	24	2	5		
	923	2287	2834	82	1802	73	23	2	2		
Ru	823	841	579	159	1604	45	32	6	17	—	—
	873	1139	1111	263	2079	61	30	3	6		
	923	1433	764	388	1459	57	30	3	10		
Ni	823	827	579	154	1907	50	36	3	11	0.05	136
	873	1454	993	299	1821	64	27	2	7		
	923	2096	2542	339	1726	73	24	2	1		

M–CeO_2–SiO_2: loading of M = 1.2 × 10^{-4} mol g-cat^{-1}, loading of CeO_2 = 60 mass%. Reaction conditions: catalyst 3.0 g, biomass 150 mg min^{-1} (H_2O 10 mass%, C 5748 μmol min^{-1}, total H_2 4815 μmol min^{-1}, total O_2 2208 μmol min^{-1}), supplied O_2 35 ml min^{-1}(1432 μmol min^{-1}), ER = 0.25, total N_2 150 ml min^{-1} (6138 μmol min^{-1}).

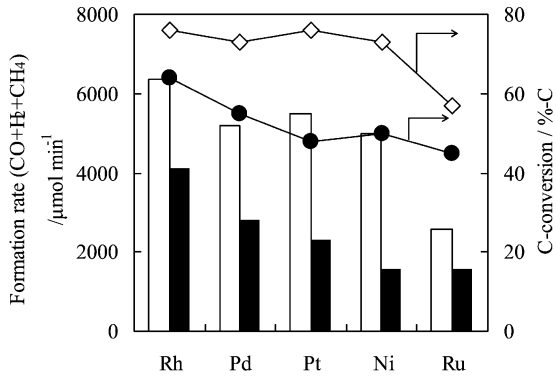

Fig. 3 Comparison of M–CeO_2–SiO_2 catalysts (M = Rh, Pd, Pt, Ru, Ni) in reforming of tar from biomass in terms of productivity and C-conversion. C-conversion: ◊ 923 K, ● 823 K. Formation rate of CO + H_2 + CH_4: open bar 923 K, filled bar 823 K. Reaction conditions: catalyst 3 g, biomass 150 mg min^{-1} (H_2O 10%, C, 5748 μmol min^{-1}; total H_2, 4815 μmol min^{-1}; total O_2, 2208 μmol min^{-1}), supplied O_2 35 ml min^{-1} (1432 μmol min^{-1}), ER = 0.25, total N_2 150 ml min^{-1} (6138 μmol min^{-1}).

The results of H_2 chemisorption are also shown in Table 1. It was found that the H/M molar ratio on the Rh catalyst was not so outstanding as that of the other catalysts. Therefore the high activity is not explained by high metal dispersion, but the properties of the metal. In addition, the BET surface area was almost the same on various catalysts.

In the primary bed, the biomass was first thermally decomposed to tar, char, steam, and a small fraction of product gas. Although solid char and ash was accumulated on the distributor of the primary bed, the volatile tar contacted with the catalyst particles in the secondary catalyst bed. Almost all the tar was introduced to the catalyst bed. This is supported by the results of the activity test. When the tar yield is zero in Table 1, the carbon-based amount was balanced before and after the reaction; in other words, all the carbon in the supplied biomass was converted to gas, coke, and char products, whose amount is determined by the analysis. It is possible that part of the tar can come in contact with the external walls of the reactor and can be converted to char, however this amount is very small because of the results of char yield. The char yield was in the range of 22–36%-C, which is much dependent on the reaction temperature, and indicates that the amount of char formed from tar is very small. Since oxygen is introduced to the catalyst bed through the thin tube near the bottom of the bed, the lower part of the catalyst bed where oxygen is present and a part of the tar can take part in the combustion reaction to form CO_2 and H_2O. Then the catalyst interacted with tar quickly moves up by the fluidization and is reduced at the upper part where oxygen is absent under these reaction conditions. The reforming of tar with steam and/or CO_2 on the catalyst surface can proceed to form CO and H_2. In this case, the catalyst is in the cycle of reduction–oxidation. In this system, both reforming and combustion reactions are very important for high product yield and C-conversion.

To evaluate the catalytic activity of the different catalysts in the combustion, thermogravimetric analysis (TGA) of the 1 : 1 mixture of biomass and catalyst was carried out. Wood usually contains approximately 30 mass% of lignin. In the TGA experiment about 68 mass% decrease was observed in the biomass in the non-catalyst system up to 600 K and then the rest of the carbon slowly decreased with increasing temperature. In the case of Ni–CeO_2–SiO_2, the temperature becomes a little lower, and the loss becomes a little larger than those in the non-catalyst system. In contrast, on Rh, Pt, and Pd catalysts, the reaction temperature range drastically decreased and the loss is larger than those on Ni and non-catalyst systems. This indicates that even heavy tar can burn on Rh, Pt, and Pd catalyst. This property is related to the combustion of coke derived from tar on the catalyst surface. Since Rh–CeO_2–SiO_2 exhibited high performance in the reforming and combustion reaction, the catalyst is totally suitable for this reaction system for the gasification of biomass. The high performance of the Rh–CeO_2–SiO_2 catalyst is thought to be due to the smooth redox properties in the combination of Rh and CeO_2.[46]

Conclusions

We have carried out an activity test in the reforming of tar derived from cedar biomass using M–CeO_2–SiO_2 (M = Rh, Pt, Pd, Ru, Ni) at a lower temperature range (823–923 K) than the conventional methods. In the case of Rh–CeO_2–SiO_2, even at 823 K, almost all the tar can be converted to gas products, and the amount of coke deposited on the catalyst surface derived from tar decomposition was very small. From the comparison, Rh–CeO_2–SiO_2 exhibited much higher performance than other metal catalysts in terms of the activity of tar reforming, and the yield of gas and coke. The effective catalyst can give highly efficient conversion of biomass to synthesis gas at low temperature.

Acknowledgement

This research was supported by the Future Program of Japan Society for the Promotion of Sciences under the Project "Synthesis of Ecological High Quality of Transportation Fuels" (JSPS-RFTF98P01001) and the 21st Century COE program under the Ministry of Education, Culture, Sports, Science and Technology.

References

1 J. M. Ogden, *Annu. Rev. Energy Environ.*, 1999, **24**, 227.
2 M. A. Caballero, J. Corella, M. P. Aznar and J. Gil, *Ind. Eng. Chem. Res.*, 2000, **39**, 1143.
3 F. Miccio, O. Moersch, H. Spliethoff and K. R. G. Hein, *Fuel*, 1999, **78**, 1473.
4 C. Brage, Q. Yu, G. Chen and K. Sjostrom, *Biomass Bioenergy*, 2000, **18**, 87.
5 I. Narváez, A. Orío, M. P. Aznar and J. Corella, *Ind. Eng. Chem. Res.*, 1996, **35**, 2110.
6 P. Vriesman, E. Heginuz and K. Sjöström, *Fuel*, 2000, **79**, 1371.
7 C. D. Blasi, G. Signorelli and G. Portoricco, *Ind. Eng. Chem. Res.*, 1999, **38**, 2571.
8 J. Gil, M. P. Aznar, M. A. Caballero, E. Francés and J. Corella, *Energy Fuels*, 1997, **11**, 1109.
9 A. A. C. M. Beenackers, *Renewable Energy*, 1999, **16**, 1180.
10 F. Miccio, O. Moersch, H. Spliethoff and K. R. G. Hein, *Fuel*, 1999, **78**, 1473.
11 K. Maniatis and A. A. C. M. Beenackers, *Biomass Bioenergy*, 2000, **18**, 1.
12 N. Abatzoglou, N. Barker, P. Hasler and H. Knoef, *Biomass Bioenergy*, 2000, **18**, 5.
13 H. A. M. Knoef and H. J. Koele, *Biomass Bioenergy*, 2000, **18**, 55.
14 L. Mudge, E. G. Baker and D. G. Mitchell, *Investigations on Catalyzed Steam Gasification of Biomass*, PNL-3695, Pacific Northwest National Laboratory, Richland, WA, 1981.
15 C. Ekstrom, N. Lindman and R. Petterson, *Proceedings of the Fundamentals of Thermochemical Conversion of Biomass Conference*, ed. R. P. Overend, T. A. Milne and L. K. Mudge, Elsevier Applied Press, London, 1982, p. 601.
16 A. A. C. M. Beenackers and K. Maniatis, *Gas Cleaning in Electricity Production via Gasification of Biomass*, in Conclusions of the Workshop, *Advances in Thermochemical Biomass Conversion*, ed. A. V. Bridgewater, Blackie Academic Press, London, 1994, p. 540.
17 A. V. Bridgwater, *Appl. Catal.*, 1994, **116**, 5.
18 P. Simell, E. Kurkela and P. Ståhlberg, *Formation and Catalytic Decomposition of Tars from Fluidized Bed Gasification*, in *Advances*

in Thermochemical Biomass Conversion, ed. A. V. Bridgwater, Blackie Academic Press, London, 1994, p. 265.
19 N. Abatzoglou, P. Legast, P. Delvaux, D. Bangala and E. Chornet, *Gas Conditioning Technologies for Biomass and Waste Gasification*, in *Proc. Third Biomass Conf. Americas*, ed. R. P. Overend, and E. Chornet, Elsevier Science Ltd., Oxford, 1997, p. 599.
20 M. P. Aznar, J. Corella, J. Gil, A. Martin, M. A. Caballero, A. Olivares and P. Perez, *Biomass Gasification with Steam and Oxygen Mixtures at Pilot Plant Scale and Catalytic Gas Upgrading, Part I*, in *Developments in Thermochemical Biomass Conversion*, A. V. Bridgwater and D. G. B. Boocock, Blackie Academic and Professional, London, 1997, p. 1194.
21 T. A. Milne, N. Abatzoglou and R. J. Evans, *Biomass Gasifier "Tars": Their Nature, Formation, and Conversion*, NREL/TP-570-25357, National Renewable Energy Laboratory, Golden, CO, 1998.
22 M. A. Caballlero, M. P. Aznar, J. Corella, J. Gil and J. A. Martin, *Proc. Fourth Biomass Conf. Americas*, R. P. Overend, and E. Chornet, Pergamon, Oxford, 1999, p. 979.
23 J. Corella, M. A. Caballero, M. P. Aznar and J. Gil, *Proc. Fourth Biomass Conf. Americas*, R. P. Overend and E. Chornet, Pergamon, Oxford, 1999, p. 933.
24 D. Sutton, B. Kelleher and J. R. H. Ross, *Fuel Proc. Technol.*, 2001, **73**, 155.
25 L. García, M. L. Salvador, J. Arauzo and R. Bilbao, *Energy Fuels*, 1999, **13**, 851.
26 L. García, M. L. Salvador, J. Arauzo and R. Bilbao, *Fuel Proc. Technol.*, 2001, **69**, 157.
27 L. García, R. French, S. Czernik and E. Chornet, *Appl. Catal. A: Gen.*, 2000, **201**, 225.
28 L. García, M. L. Salvador, J. Arauzo and R. Bilbao, *Ind. Eng. Chem. Res.*, 1998, **37**, 3812.
29 J. Arauzo, D. Radlein, J. Piskorz and D. S. Scott, *Ind. Eng. Chem. Res.*, 1997, **36**, 67.
30 J. Arauzo, D. Radlein, J. Piskorz and D. S. Scott, *Energy Fuels*, 1994, **8**, 1192.
31 C. Courson, E. Makaga, C. Petit and A. Kiennemann, *Catal. Today*, 2000, **63**, 427.
32 Y. Tanaka, T. Yamaguchi, K. Yamasaki, A. Ueno and Y. Kotera, *Ind. Eng. Chem. Res.*, 1984, **23**, 225.
33 J. Gil, M. A. Caballero, J. A. Martin, M.-P. Aznar and J. Corella, *Ind. Eng. Chem. Res.*, 1999, **38**, 4226.
34 S. Rapagna, N. Jand, A. Kiennemann and P. U. Foscolo, *Biomass Bioenergy*, 2000, **19**, 187.
35 E. G. Baker, L. K. Mudge and M. D. Brown, *Ind. Eng. Chem. Res.*, 1987, **26**, 1335.
36 E. G. Baker, L. K. Mudge and W. A. Wilcox, *Catalysis of gas phase reactions in steam gasification of biomass*, in *Fundamentals of Thermochemical Biomass Conversion*, R. P. Overend, T. A. Milne and L. Mudge, Elsevier Applied Science, London, 1985, p. 863.
37 M. Asadullah, K. Tomishige and K. Fujimoto, *Catal. Commun.*, 2001, **2**, 63.
38 M. Asadullah, K. Tomishige and K. Fujimoto, *Ind. Eng. Chem. Res.*, 2001, **25**, 5894.
39 M. Asadullah, S. Ito, K. Kunimori, M. Yamada and K. Tomishige, *J. Catal.*, 2002, **208**, 255.
40 M. Asadullah, S. Ito, K. Kunimori and K. Tomishige, *Ind. Eng. Chem. Res.*, 2002, **41**, 4567.
41 M. Asadullah, S. Ito, K. Kunimori, M. Yamada and K. Tomishige, *Environ. Sci. Technol.*, 2002, **36**, 4476.
42 K. Tomishige, M. Asadullah, S. Ito and K. Kunimori, *Kagaku Kogaku Ronbunshu*, 2002, **28**, 666.
43 K. Tomishige, T. Miyazawa, M. Asadullah, S. Ito and K. Kunimori, *J. Jpn. Petrol. Inst.*, 2003, **46**, 69.
44 M. Asadullah, T. Miyazawa, S. Ito, K. Kunimori, M. Yamada and K. Tomishige, *Green Chem.*, 2002, **4**, 385.
45 S. Wang and G. Q. Lu, *Energy Fuels*, 1996, **10**, 896.
46 A. Trovarelli, *Catal. Rev.*, 1996, **38**, 439.

Development of a green LAB process: alkylation of benzene with 1-dodecene over mordenite

Tseng-Chang Tsai,*[a] Ikai Wang,*[b] Shu-Ju Li[b] and Jun-Yao Liu[b]

[a] *Department of Applied Chemistry, National University of Kaohsiung, Kaohsiung, Taiwan 811, R.O.C. E-mail: tctsai@nuk.edu.tw; Fax: +886-7-591-9348; Tel: +886-7-591-9351*
[b] *Department of Chemical Engineering, National Tsing Hua University, Hsinchu, Taiwan, 300, R.O.C*

Received 6th December 2002
First published as an Advance Article on the web 4th June 2003

This work examines the linear alkylbenzene (LAB) production reaction by alkylation of benzene with 1-dodecene over a commercial mordenite, containing 30% Al_2O_3 as a binder, in a fixed bed reactor. The effects of various steam pretreatments on the properties of mordenite were studied in the LAB reaction and characterized by means of temperature programming desorption of ammonia. It was found that with steam pretreatment at 10.7 kPa partial pressure, the mordenite catalyst has a maximum acidity and activity, selectivity of 98% LAB product with 67% 2-phenyl isomer and stability beyond 600 hours operation. In the proposed reaction pathway, the isomer selectivity and catalytic stability were attributed to the result of product shape selectivity from zeolite pore structures and the comparative reaction rate of isomerization and alkylation of 1-dodecene, in which alkylation was catalyzed by strong acid sites. The extent to which external (liquid–solid) and internal (pore diffusion) mass transfer affects the main reaction was also carefully examined. Furthermore, in benzene enriched feeds, the LAB reaction was found to be first order with respective to 1-dodecene, with an apparent activation energy of 17 kcal mol^{-1}.

Introduction

The increasing use of detergents by households discharges large quantities of alkylbenzene and its sulfonated derivatives into rivers. Rapid biodegradation of the disposed organic compounds is important to keep the pollution levels as low as possible. Among the isomers of linear alkylbenzene (LAB), 2-phenyl LAB is the most biodegradable, making it an environmentally favorable isomer.

LAB is produced industrially from benzene alkylation by using an alkylation reagent, such as α-olefin particularly dodecene, or chloroalkanes, over HF or $AlCl_3$ homogenous catalyst. However, those processes have serious disadvantages such as environmental pollution, equipment corrosion, and separation difficulty. To ensure environmental protection, the detergent industry must develop a clean LAB production process capable of not only replacing the conventional homogeneous catalysts but also having a high selectivity for the 2-phenyl LAB isomer. In response to this need, Universal Oil Products (UOP) in 1995 commercialized a new process in Canada, using solid acid catalyst in a cyclic operation.[1,2]

Kocal *et al.* summarized the historical development and research trends of the LAB process.[3] As they noted, using solid acid catalysts has been one of the major approaches for the development of environmental friendly LAB processes, such as pillared clay,[4,5] zeolite (Y, mordenite, Beta),[6–16] amorphorous silica–alumina, silicotungstic acid $[SiO_4(W_3O_9)_4]$,[17] sulfated zirconia super acid,[18] and hetereogenized $AlCl_3$ system on MCM-41.[19] However, it was also noted that most of those solid catalysts suffer a serious deactivation problem, which is a major problem for industrial applications. Liang *et al.* proposed an extraction procedure of coke by benzene, through which activity of aged faujasite can be regenerated.[11] On the other hand, Sivasanker and Thangaraj reported that mordenite has very high selectivity of up to 64%, compared to 26 ~ 33% selectivity for most other catalysts[8,9] and low selectivity of 14 ~ 20% over HF and Re-Y zeolite. Cao *et al.* reported that product selectivity over zeolite increases as its structure becomes more restricted.[14] Furthermore, Almedia *et al.* found that only having mesoporous pores generated by dealumination, mordenite can exhibit activity and 2-phenyl LAB selectivity.[10]

This work evaluates the applicability of a commercial mordenite sample in an environmentally friendly LAB production process. Also reported are the reaction kinetics in diffusion-free conditions, together with the effects of steam pretreatment modification and reaction conditions on the catalytic stability of mordenite.

Experimental

A commercial mordenite sample was supplied by the Sud Chemie Corporation (Germany), having an Si : Al ratio of 90 : 1, containing 30% Al_2O_3 binder in 1.6 and 3.2 mm extrudate. A high porosity extrudate sample prepared by adjusting the pellet

Green Context

The alkylation of aromatic substrates is an important reaction in many industrial sectors. One of the largest users of the chemistry is the detergency industry which continues to use linear alkylbenzene sulfonates (LABS) on an enormous scale. The existing LABS manufacturing technology still utilizes traditional acid catalysts such as HF, which has environmental concerns with calls for new replacement technology, such as the use of solid acid catalysts. Solid catalysts are safer to handle and use and can give enhanced selectivities including the more biodegradable 2-isomer. Here we see described studies on the use of mordenite catalysis for the alkylation process. With an appropriate steam pre-treatment the catalyst has excellent activity, selectivity and stability under controlled conditions. ***JHC***

 DOI: 10.1039/b212156p

pressure was also supplied. Benzene (LC grade), 1-dodecene (LC grade) and n-decane (LC grade) were used without further purification. In addition, n-decane was used as an internal standard for measuring conversion of 1-dodecene.

Reactions were conducted in a continuous flow, fixed-bed reactor (316 stainless, 19 mm o.d.). The sliced or crushed mordenite samples (8–12, 12–20, 20–30 mesh) mixed with quartz sand (*ca.* 10–20 mesh) were packed into the reactor. Prior to the reaction, mordenite was calcined in air at 813 K for 8 hours. The reactor was then cooled down to the desired reaction temperature in a flowing N_2 atmosphere. Next, after the reaction conditions were regulated appropriately, a reaction product at specified intervals was taken for analysis using a gas chromatography equipped with a flame ionization detector and an OV101 packed column. Linear alkylbenzene isomers were identified using a mass spectrometer coupled to a gas chromatograph (GC/MS) equipped with a HP DB-1 capillary column.

The acidity of various mordenite samples were measured by means of temperature programming desorption (TPD) of ammonia. Subject to TPD measurement, the mordenite sample was first calcined at 673 K for 8 hours and then cooled down to 423 K under a helium stream. The sample was then exposed in a flowing ammonia vapor for saturation adsorption of ammonia. After the flowing gas was switched to helium for desorption measurement, the sample was first kept at 423 K for 8 hours for removal of physisorbed ammonia, then heated up to 923 K at 5 °C min^{-1}. Weight loss from ammonia desorption at various temperatures was measured with a thermal gravimetric analyzer (TGA).

Results and discussion

The conversion and selectivity of mordenite in the LAB production reaction were measured in various operating conditions within the temperature range of 398 to 433 K; pressure between 0.1 and 3.0 MPa; WHSV between 1.48 and 48 hr^{-1}; H_2/hydrocarbon molar ratio between 0.6 and 2.0; and feed compositions with a benzene : 1-dodecene : 1-decane ratio between 9 : 2 : 1 to 9 : 1 : 1. The stoichiometric coefficient of benzene to 1-dodecene in LAB production is in equimolar proportions. Since benzene was in excess with respect to 1-dodecene at the specified reaction feed compositions, conversion was therefore accounted for in terms of 1-dodecene and selectivity of dodecylbenzene yield was calculated on molar base using the following equations:

$$Selectivity = \frac{\text{Dodecylbenzene isomer wt\%}}{\text{Dodecene wt\% reacted}} \times \frac{154}{232}$$

Notably, n-decane did not react in the specified operating conditions range, so it was used as an internal standard to ensure the measurement accuracy.

Fig. 1 shows the catalytic performance and temperature trajectory, while maintaining at a constant conversion level of the parent commercial mordenite in LAB reaction. Severe deactivation of mordenite activity was observed, and activity was still not adequate at temperatures up to 483 K. The deactivation phenomenon was always observed in benzene alkylation over zeolites.[11,14,16] Interestingly, it was noted that catalytic activity becomes more stable at reaction temperatures greater than 450 K. In contrast, Cao *et al*. reported that in a batch reactor, faujasite exhibits a faster deactivation rate at high reaction temperatures in benzene alkylation.[14] Significantly, it can be observed in Fig. 2 that a steam pretreatment at a steam

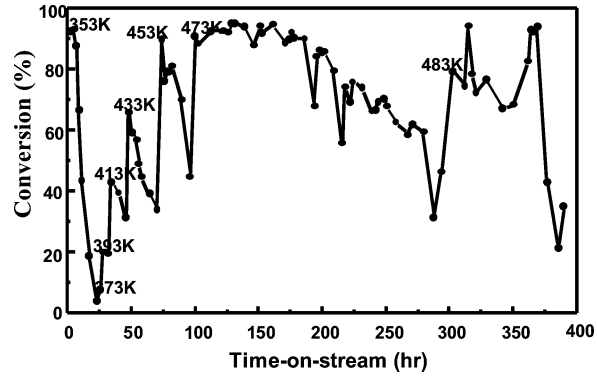

Fig. 1 Performance of parent mordenite (pressure: 2.0 MPa; temperature: 353–483 K; WHSV: 1.94 hr^{-1}; H_2/HC: 0.63 mol mol^{-1}).

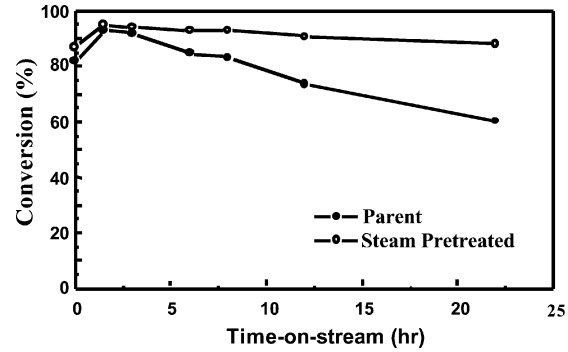

Fig. 2 Effect of mild steam pretreatment (steam partial pressure: 4 kPa, 813 K, 2 hours; reaction condition: temperature: 398 K; pressure: 0.8 MPa; WHSV: 4 hr^{-1}, H_2/HC: 2 mol mol^{-1}).

partial pressure of 4 kPa at 813 K for 2 hours, can greatly improve the catalyst stability of the parent mordenite. Therefore, steamed mordenite was used for the rest of the present study.

External mass resistance was examined by conducting experiments at a constant WHSV by varying the feed rate in accordance with the amount of catalyst sample. The conversion over both 3.2 mm and 1.6 mm sliced mordenite, increased as the catalyst weight increased from 1.5 to 6.0 g, corresponding to the L/D ratio (catalyst bed length to reactor diameter) of 0.9 and 3.6 respectively, as presented in Fig. 3. This effect clearly indicated the presence of external mass transfer resistance on reaction rate, as there was a concentration gradient between bulk fluid and outside surface. This result suggests the use of a minimum L/D ratio of 3 to eliminate the disguise of reaction data from external mass transfer resistance.

Internal mass transfer resistance was studied by changing the catalyst particle size. The skin effect of catalyst particles

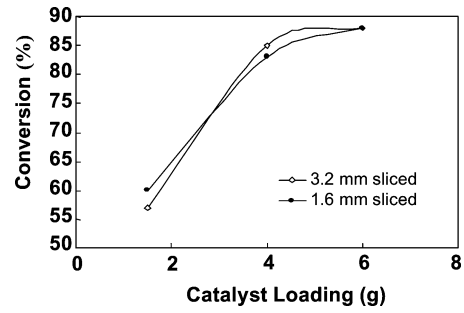

Fig. 3 Plot of 1-dodecene conversion *versus* catalyst loadings for various sizes of sliced catalyst at a constant WHSV of 4 hr^{-1} (pressure: 2.0 MPa, temperature: 413 K, H_2/HC: 0.70 mol mol^{-1})

$$Conversion = \frac{\text{Dodecene wt\% in reactor feed} - \text{Dodecene wt\% in reactor effluent}}{\text{Dodecene wt\% in reactor feed}}$$

prepared by slicing or crushing was also studied. It is clearly shown in Table 1 that the conversion of the 8–12 mesh crushed

Table 1 Effects of intraparticle diffusion on dodecene conversion (pressure: 3.0 MPa; temperature: 433 K; WHSV: 16 hr^{-1}; H_2/HC: 0.7 mol mol^{-1}; Time-on-stream: 20 hours).

Extrudate	3.2 mm				1.6 mm	1.6 mm
Method	Crush	Crush	Crush	Sliced	Sliced	Sliced (high porosity)
Mesh	20–30	12–20	8–12			
Conversion	96%	96%	89%	62%	52%	96%

sample is lower than that of other smaller crushed samples, namely the 12–20 mesh and 20–30 mesh samples, implying the existence of internal mass transfer resistance. In addition, the conversion of the sliced catalyst sample at either 3.2 mm or 1.6 mm was significantly lower than that of the crushed samples. Furthermore, it can be noted in Fig. 4 that the 3.2 mm sliced

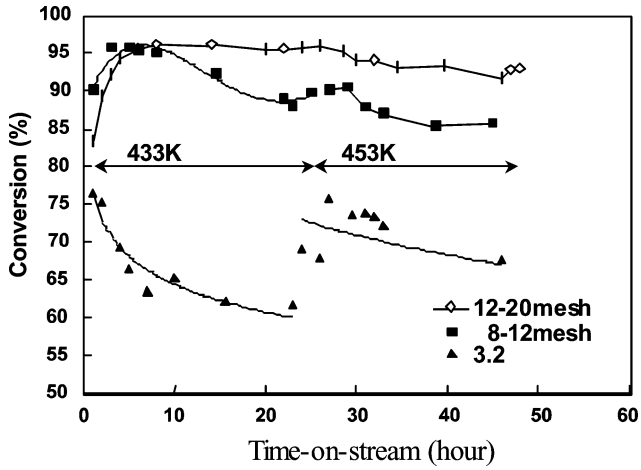

Fig. 4 Plot of 1-dodecene conversion *versus* time-on-stream using different sizes of mordenite (pressure: 3.0 MPa; temperature: 433–453 K; WHSV: 16 hr^{-1}, H_2/HC: 0.70 mol mol^{-1}).

sample had a much higher deactivation rate than those crushed samples either in 8–12 mesh or 12–20 mesh. The effects of using slicing against crushing can be attributed to the volume of mesopores on the skin of the extrudates, which is less for the slicing sample than the crushing sample. As for the cut samples, the 8–12 mesh particles exhibited a slight faster deactivation than the 12–20 mesh particles, in which the deactivation at reaction temperatures of 453 K and of 433 K resembled each other.

Ercan *et al.* concluded that at larger molecular size, the mass transfer effect of pore diffusion in cumene reaction is much more pronounced than ethylbenzene reaction.[20] It has also been observed that mesoporosity in mordenite as a result of dealumination can contribute to catalytic activity and 2-phenyl LAB selectivity.[10,12] An attempt was made in the present study to reduce the mass transfer resistance of skin effect by preparing a high porosity extrudate in 1.6 mm with high pore volumes on the skin. It was found that the high porosity sample improves significantly both 1-dodecence conversion (Table 1) and catalytic stability.

Table 2 summarizes the catalytic results collected from a time-on-stream of 6 hours at a temperature in the range between 373 K and 473 K under constant pressure, WHSV and feed ratio. Catalyst particles at 12–20 mesh size were used for intraparticle diffusion-free operation. As expected, conversion increases with reaction temperature. From the thermodynamics calculation, LAB production is an exothermic reaction, in which

Table 2 Dodecene conversion and product selectivity under various temperatures over 12–20 mesh mordenite (pressure: 2.0 MPa; WHSV: 4 hr^{-1}; H_2/HC: 0.7 mol mol^{-1}; time-on-stream: 6 hours)

Temperature/K	373	403	473
Conversion (%)	70.3	98.5	98.6
Product distribution (wt%)			
Lights	< 1	< 1	37
Propylbenzene	< 1	< 1	12
Dodecylbenzenes	75	99	51
Dodecene dimers	22	< 1	< 1
Heaviers	2	< 1	< 1

thermodynamic equilibrium is favorable at low temperature, approaching 100% conversion at 500 K.[21] At a reaction temperature of 403 K, conversion was 98.5% and dodecylbenzene selectivity reached a maximum of 99%. At a lower reaction temperature of 373 K, dodecylbenzene selectivity was 75% with dodecene dimers as the main by-product. At a higher reaction temperature of 473 K, dodecylbenzene selectivity dropped to 51% with light hydrocarbons including propylbenzene as the main by-product.

Cao *et al.* proposed that in a LAB production reaction,[14] dodecene forms a carbenium ion over acid catalyst, then undergoes a rapid double bond migration, and finally alkylates benzene. The relative rate ratio of alkylation reaction to double bond migration determines isomer selectivity of phenyl substitution, 2-phenyl isomer increases as the ratio increases. Taking those earlier results into consideration, here we propose a reaction pathway in Fig. 5 to account for the high selectivity

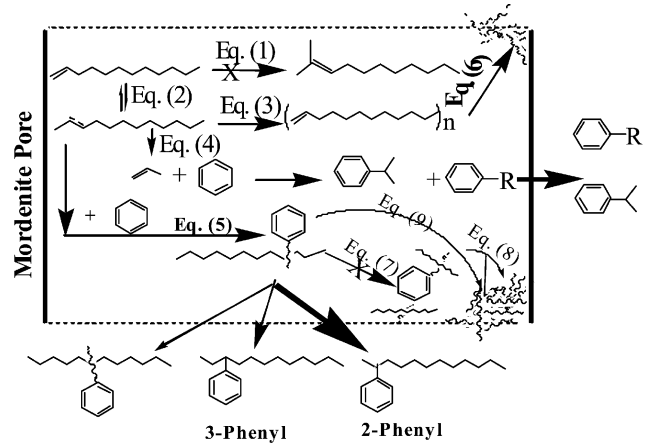

Fig. 5 Schematic reaction pathway.

of 2-phenyl substituted isomer over mordenite. As skeleton isomerization of 1-dodecene, eqn. (1) in Fig. 5, does not proceed over mordenite, 1-dodecene proceeds fast double bond migration, eqn. (2), forming 2- and 3-dodecyl carbenium ions to alkylate benzene into corresponding LAB isomers. It has been reported that over various zeolites, the 2-phenyl isomer selectivity decreases in the order of mordenite, beta, EMT and faujasite.[8,13,14,16] In addition, Da *et al.* reported that diffusion of 5-phenyl isomer is slower than 2-phenyl isomer, and the relative diffusion resistance of 5-phenyl isomer to 2-phenyl isomer over zeolite beta is 1.5 times larger than that over faujasite.[15] Therefore, the isomer selectivity can be attributed to the "product shape selectivity", which is controlled by the diffusion resistances imposed by the pore size of zeolite.[11,14,15] The greater 2-phenyl LAB isomer selectivity of mordenite is a result of its narrow pore opening.

This shape selectivity does not only control LAB isomer selectivity, it also affects coke formation. Two coking schemes are shown in Fig. 5, an alkylation route: eqn. (3) + (6) and a transalkylation route: eqn. (7) + (8). By taking the alkylation route, the coke constituents are mono-alkyl benzene and dimers

of olefins; whereas by taking the transalkylation route, the coke is polyalkylbenzene in nature. The coking route alternates with the pore structure of zeolite. It was observed that over zeolite beta,[15] 2-phenyl and 3-phenyl LAB isomers appear as the reaction product and other LAB isomers form coke being trapped inside the zeolite pore. As discussed in Table 2 above, over mordenite, at a low reaction temperature, *i.e.*, 373 K, dodecene dimer is the main by-product (eqn. (3)), whereas at higher reaction temperature such as 473 K, dodecene cracks into small molecules, followed by the formation of propylbenzene as the major by-product, eqn. (4). As a result of slow desorption, those molecules are trapped inside the zeolite pore following the formation of coke and deactivation of zeolite activity (eqn. (6)). For those zeolites in which the occurrence of transalkylation is inhibited by their pores, such as mordenite and zeolite beta, the alkylation route is supposed to be the main coking mechanism. In contrast, the pore voidage space of fajusite is large enough for the occurrence of transalkylation as well as polyalkylbenzene formation, as shown in eqns. (7) and (8). Therefore, polyalkylbenzenes appeared as coke constituents, which can be up to a content of 31 wt% C, equilibrating with the compositions of LAB product isomers, namely 2-, 3-, 4-, 5- and 6-phenyl isomers.[16]

Fig. 6 plots the conversion of 1-dodecene against operating pressures. The effect of reaction pressure on conversion and

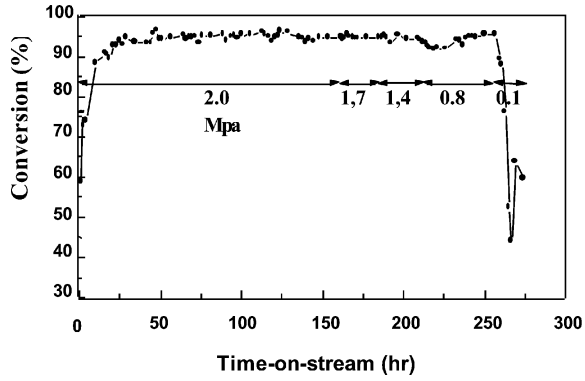

Fig. 6 1-Dodecene conversion *versus* the reaction time under various pressures with 3.2 mm 12–20 mesh mordenite (temperature: 433 K; WHSV: 1.92 hr^{-1}; H_2/HC: 0.71 mol mol^{-1}).

catalyst stability was insignificant in the pressure range between 0.1 and 2.0 MPa. The conversion reached 95% when reaction pressures exceeded 0.8 MPa. As the reaction conditions raised above 0.8 MPa, both benzene and 1-dodecene were in the liquid phase, *e.g.*, the boiling point of 99% pure benzene at 101.3 and 517 kPa partial pressure are 353.1 and 443 K, respectively. Notably, the catalyst deactivated quickly as the reaction pressure dropped to 0.1 MPa, at which point benzene was in the vapor phase.

Earlier investigations on the ratio of benzene to 1-dodecence[9,11,17] showed that a high ratio can reduce the by-products of 1-dodecene oligomerization and the formation of polyalkylbenzene, under the stipulation of recycling a large amount of benzene. Fig. 7 presents the effects of feed ratio, indicating that feed ratios only slightly affect the conversion and selectivity (not shown in the figure) because the ratio is greater than 5.

In selecting an appropriate range of reaction temperature by considering the faster aging rate at lower reaction temperatures, such as at 373 K (Fig. 1), it can be observed in Fig. 8 that catalyst stability is significantly improved at 433 K. At the reaction temperature, the catalyst can maintain a high selectivity of LAB, up to 98%, and a conversion level of 96% beyond 600 hours. Among the LAB isomer products observed in the present study, the 2- and 3-phenyl isomer were around 63–67 and 35–31%, respectively and other isomers were negligible, as identified with GC/MS spectroscopy. In addition, no iso-dodecylbenzene isomer appeared. The 2-phenyl substituted

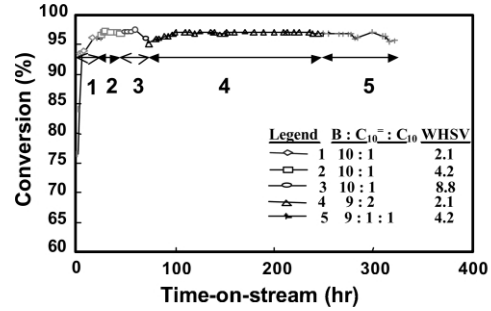

Fig. 7 1-Dodecene conversion *versus* the reaction time under various space velocity and ratio of feed (benzene to 1-dodecene or benzene to n-decane and 1-dodecene) with 3.2 mm 12–20 mesh mordenite (pressure: 2.0 MPa; temperature: 413 K; WHSV: 2.1–8.8 hr^{-1}; H_2/HC: 0.60 mol mol^{-1}).

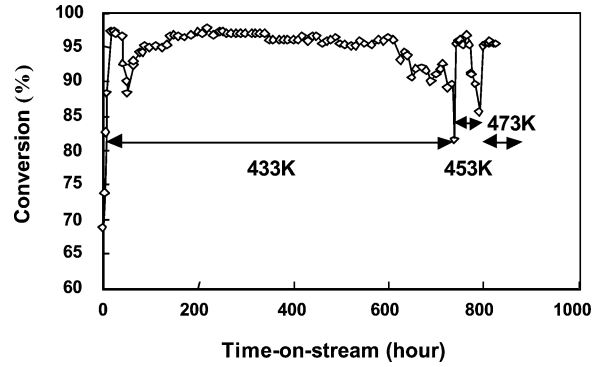

Fig. 8 1-Dodecene conversion *versus* the reaction time using 12–20 mesh mordenite (temperature: 433–473 K, pressure: 2.0 MPa, WHSV: 1.92 hr^{-1}, H_2/HC: 0.70 mol mol^{-1}).

isomer selectivity, consistent with the results of Sivasanker and Thangaraj,[8] exceeded the thermodynamic equilibrium composition, which was substantially higher than other catalyst systems such as faujasite and $AlCl_3$. The catalytic stability and selectivity demonstrate the potential of steam-pretreated mordenite for industrial applications.

Herein, reaction kinetics were also studied at reaction conditions in the range of pressure: 1.4 MPa, temperature: 393–413 K, WHSV: 10–50 hr^{-1}, H_2/HC: 0.5 mol mol^{-1}. A linear correlation between $\ln(1-X)$ and space time (1/WHSV) was obtained, as shown in Fig. 9, indicating that the reaction

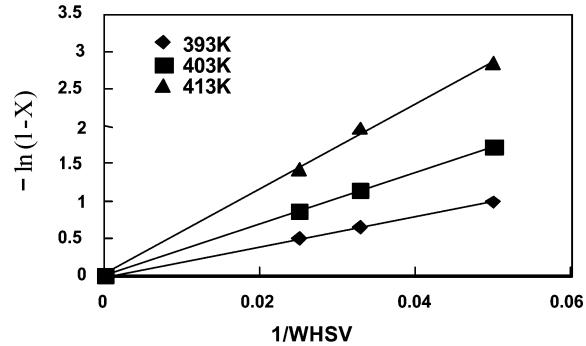

Fig. 9 Plot of $-\ln(1-X)$ against 1/WHSV (12–20 mesh 1/16″ extrudate; pressure: 1.4 MPa, temperature: 393–413 K, WHSV: 10–50 hr^{-1}, H_2/HC: 0.5 mol mol^{-1}).

follows a first order rate expression. Fig. 10 plotted the first order rate constant (k_1) against reaction temperature in the temperature range of 393–413 K, yielding an activation energy of 17.0 kcal mol^{-1}. Comparing to a previous study, Cao *et al.* reported the first order rate expression with activation energy of

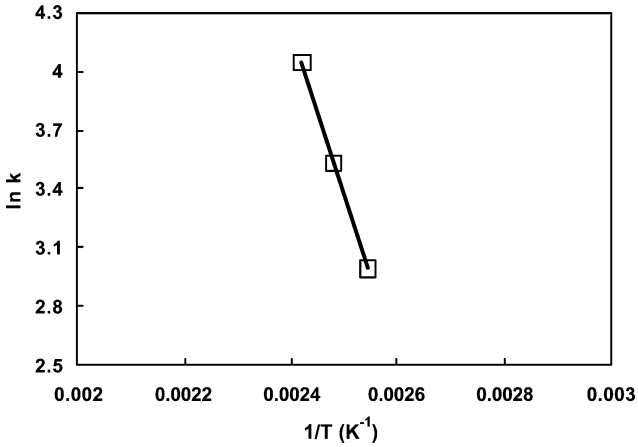

Fig. 10 Apparent activation energy of the alkylation reaction over mordenite (12–20 mesh 1/16″ extrudate; pressure: 1.4 MPa, temperature: 393–413 K, WHSV: 10–50 hr^{-1}, H_2/HC: 0.5 mol mol^{-1}).

12 ± 3 kcal mol^{-1} for faujasite, 10 ± 3 kcal mol^{-1} for EMT, and 9 ± 3 kcal mol^{-1} for zeolite beta.[14]

Earlier reports on the effects of steam were non-conclusive. Liang *et al.* observed a detrimental effect of water on the conversion of LAB reaction in a batch reactor.[11] On the other hand, Haag observed earlier an enhancement of ZSM-5 activity in hexane cracking after mild steam pretreatment.[22] This current work examines how steam pretreatment affects the performance of the commercial mordenite sample. According to Fig. 11, the

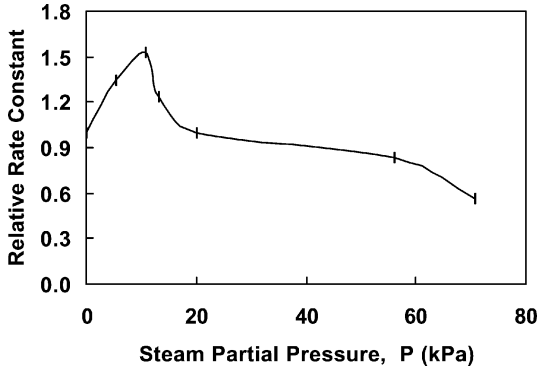

Fig. 11 Plot of relative first order rate constant *versus* partial pressure of pretreatment steam (treatment: 2 hours at 813 K).

relative first order rate constant initially increased with increasing the partial pressure of steam, and then reached a maximum at a partial pressure of 10.7 kPa. However, deeper steam pretreatment reduced the activity, for example, the rate constant of sample pretreated at 70.6 kPa was lower than that of parent mordenite.

Brønsted acid sites are normally responsible for catalytic activity. The acidities of the parent mordenite and steam treated samples were measured with ammonia TPD (temperature programming desorption) (Fig. 12). There were two major ammonia desorption peaks over the parent mordenite at 663 and 718 K, which represented M (medium) and S (strong) acid sites, respectively. Interestingly, after steam pretreatment at 10.7 kPa, the S acid site number remained, although the M acid site decreased. Furthermore, the desorption temperature of the S site shifted to a temperature higher by around 10 °C, indicating enhanced acid strength upon the steam pretreatment, and that of M site shifted to be around 10 °C lower. Deeper steam pretreatment at higher steam partial pressures, such as upon 26.7 kPa pretreatment shown in Fig. 12, further shifted the desorption temperature of the S acid site by another 8 °C, but the total amounts of acid sites and S acid sites both dropped. As shown in both the TPD data (Fig. 12) and the catalytic test data

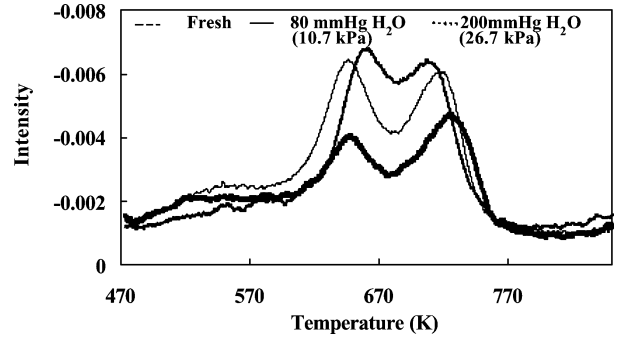

Fig. 12 TPD spectrum of parent mordenite and steam pretreated mordenite (treatment: 2 hours at 813 K; H_2O partial pressure: 0–26.7 kPa).

(Fig. 11), the acid strength reaches a maximum at the optimum treatment of 10.7 kPa steam partial pressure, suggesting that alkylation is catalyzed by strong acid sites. Cao *et al*. attributed the activity of a zeolite to its acidity, in accordance with the Si/Al ratio, diffusion rate and early deactivation.[14] On the other hand, it was observed that mesoporosity contributes to the activity and 2-phenyl LAB selectivity of dealuminated mordenite.[10,12] In the present study, the enhancement of acid strength by mild steam pretreatment at an optimum partial pressure was accounted for by the existence of maximum activity.

Conclusion

This work studied alkylation of benzene with 1-dodecene over a commercial mordenite which contains 30% Al_2O_3 as the binder. Similar to earlier investigations over various catalysts, the parent mordenite sample displayed serious deactivation. The steam pretreatment procedure was studied in the present study in an attempt to solve the deactivation problem. The effects of various steam pretreatments on the properties of mordenite were studied in the LAB reaction and characterized by TPD. Subject to steam pretreatment at 10.7 kPa, the catalyst can maintain a conversion up to 96% and selectivity of 98% linear alkylbenzene for 600 hours under proper operating conditions: pressure > 1.0 MPa, temperature: 393–433 K, benzene/1-dodecene > 5 mol mol^{-1} and H_2/hydrocarbon > 0.6 mol mol^{-1}. In addition, selectivity of the 2-phenyl substituted isomer was around 67%, which is the highest value among all the reported catalysts.

External mass transfer can be prevented by properly selecting the catalyst bed length to diameter ratio at a minimum of 3. Sliced samples performed differently from crushed ones, showing a substantially lower activity and faster deactivation. This indicated the importance of the skin property of the extrudate catalyst, which controls the liquid–solid volumetric mass transfer coefficient.

This work has also proposed a reaction pathway. Herein, the reaction selectivity of mordenite can be attributed to its shape selectivity of product isomers and high alkylation rate *versus* double bond migration rate. This was supported by ammonia TPD data indicating that alkylation is catalyzed by strong acid sites. This hypothesis can interpret well the differences in reaction selectivity at various reaction conditions and over various zeolites.

The kinetics were also studied in a large excess of benzene. Here, the reaction was first order with respect to 1-dodecene and the apparent activation energy for this reaction was 17 kcal mol^{-1}.

Acknowledgments

The authors would like to thank Professor S. F. Cheng for ammonia TPD measurement. We also thank the Taiwan Styrene

Monomer Company (TSMC) for financial support of this research, and Sud Chem Inc. of Germany and its Taiwan agent, Jansco, for kindly supplying the catalyst.

References

1 T. Imai, J. A. Kocal and B. V. Vora, *Stud. Surf. Sci. Catal.*, 1995, **92**, 339.
2 K. Tanabe and W. A. Hölderich, *Appl. Catal. A: Gen.*, 1999, **181**, 399.
3 J. A. Kocal, B. V. Vora and T. Imai, *Appl. Catal. A: Gen.*, 2001, **221**, 295.
4 M. Y. He, Z. H. Li and E. Min, *Catal. Today*, 1988, **2**, 321.
5 R. Mokaya and W. Jones, *J. Chem. Soc., Chem. Commun.*, 1994, **8**, 929.
6 P. B. Venuto, L. A. Hamilton, P. S. Landis and J. J. Wise, *J. Catal.*, 1966, **4**, 81.
7 L. B. Young, U.S. Patent 4,301,316, 1981.
8 S. Sivasanker and A. Thangaraj, *J. Catal.*, 1992, **138**, 386.
9 S. Sivasanker, A. Thangaraj, R. A. Abulla and P. Ratnasamy, *Stud. Surf. Sci. Catal.*, 1993, **75**, 397.
10 J. L. G. de Almedia, M. Dufaux, Y. B. Taarit and C. Naccache, *Appl. Catal. A: Gen.*, 1994, **114**, 141.
11 W. Liang, Y. Jin, Z. Yu, Z. Wang, B. Han, M. Y. He and E. Min, *Zeolites*, 1996, **17**, 297.
12 P. Magnoux, A. Mourran, S. Bernard and M. Guisnet, *Stud. Surf. Sci. Catal.*, 1997, **108**, 107.
13 P. Mériaudeau, Y. B. Taarit, A. Thangaraj, J. L. G. Almeida and C. Naccache, *Catal. Today*, 1997, **38**, 243.
14 Y. Cao, R. Kessas, C. Naccache and Y. B. Taarit, *Appl. Catal. A: Gen.*, 1999, **184**, 231.
15 Z. Da, Z. Han, P. Magnoux and M. Guisnet, *Appl. Catal. A: Gen.*, 2001, **219**, 45.
16 Z. Da, P. Magnoux and M. Guisnet, *Appl. Catal. A: Gen.*, 1999, **182**, 407.
17 R. T. Sebulsky and A. M. Henke, *Ind. Eng. Chem. Proc. Des. Dev.*, 1971, **10**, 272.
18 J. H. Clark, G. L. Monks, D. J. Nightingale, P. M. Price and J. F. White, *J. Catal.*, 2000, **193**, 348.
19 X. Hu, M. L. Foo, G. K. Chuah and S. Jaenicke, *J. Catal.*, 2000, **195**, 412.
20 C. Ercan, F. M. Dautzenberg, C. Y. Yeh and H. E. Barner, *Ind. Eng. Chem. Res.*, 1998, **37**(5), 1724.
21 D. R. Stull, E. F. Westrum and G. C. Sinke, *The Chemical Thermodynamics of Organic Compounds*, John Wiley & Sons, Inc., New York, 1967.
22 W. O. Haag, U.S. Patent 4,418,235, 1983.

Studies on biodegradable chelating ligands: complexation of iminodisuccinic acid (ISA) with Cu(II), Zn(II), Mn(II) and Fe(III) ions in aqueous solution

Helena Hyvönen,[a] Marjatta Orama,[a] Heikki Saarinen*[a] and Reijo Aksela[b]

[a] *Department of Chemistry, Laboratory of Inorganic Chemistry, University of Helsinki, P.O. Box 55, FIN-00014 University of Helsinki, Finland*
[b] *Kemira Oyj, Espoo Research Centre, P.O. Box 44, 02271 Espoo, Finland*

Received 25th March 2003
First published as an Advance Article on the web 5th June 2003

In a search for biodegradable chelating ligands for industrial applications, study was made of the protonation and complex formation equilibria of iminodisuccinic acid (ISA) as a mixture of two of its stereoisomers (50% [*S*,*S*] and 50% [*R*,*S*]) with Cu(II), Zn(II), Mn(II) and Fe(III) ions in aqueous 0.1 M NaCl solution by potentiometric titration at 25 °C. The model of the complexation and the stability constants of the different complexes were determined for each metal ion using the computer program SUPERQUAD. With all metals the complex formation was dominated by stable ML^{n-4} complexes. Biodegradable and of low nitrogen content, ISA was found to be a good chelating agent in pulp bleaching.

Introduction

Aminopolycarboxylates such as ethylenediaminetetraacetic acid (EDTA) and diethylenetriaminepentaacetic acid (DTPA) have been used for over 60 years as effective chelating agents in a variety of large-scale industrial applications from detergents to agrochemicals. During the past few years, the non-biodegradability of most of these ligands and their accumulation in the environment have been the cause of a great deal of concern.[1]

Both EDTA and DTPA are common chelating agents in pulp bleaching. Both are virtually nonbiodegradable in waste water treatment plant conditions[2] and they are difficult to remove from bleaching effluents. As an extra environmental concern they have the capability to remobilize toxic heavy metal ions from soil.[3] Thus replacement of these ligands by more environmentally friendly chelating agents would be highly desirable.

In general, alternative chelating agents for pulp bleaching should meet three main criteria. Their complex forming properties should be equal to or better than those of EDTA and DTPA. Their nitrogen content should be as low as possible to keep the nitrogen in effluents low. And last but not least, they should degrade in nature at least partially.[4]

One candidate ligand to replace EDTA is ethylenedisuccinic acid (EDDS), the complexation of which with Fe(III), Cu(II), Zn(II) and Mn(II) ions was described in our earlier paper.[5] In continuation of our studies on biodegradable chelating agents, we now report the complexation of iminodisuccinic acid (ISA) with the same metal ions in aqueous solution.

Iminodisuccinic acid readily acts as a pentadentate N,O donor ligand in its coordination to metal ions. The location of the five donor atoms in the molecule is such that the formation of mono complexes is likely to prevail in the solutions.

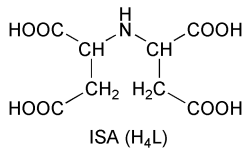

ISA (H_4L)

As is well-known, the stereoisomeric form of a compound may have a pronounced effect on its biodegradability. Owing to its two chiral carbon atoms, iminodisuccinic acid may occur in the form of three stereoisomers: chiral [*S*,*S*] and [*R*,*R*] and achiral [*R*,*S*] form. All three stereoisomers of ISA are biodegradable in some degree. For the preliminary tests of this study, two different mixtures of ISA isomers were synthesised: one containing 50% [*S*,*S*] and 50% [*R*,*S*] forms and the other containing 25% [*S*,*S*], 25% [*R*,*R*] and 50% [*R*,*S*] forms. The former was found to be more biodegradable (ISO9439-test)[6] and more efficient in extracting Cu(II) ions from pulp.[7] On this basis, this mixture was elected for further pulp bleaching tests[4] and subjected to aqueous metal complexation studies.

Experimental

Preparation of iminodisuccinic acid

The mixture of isomers of consisting of 50% [*S*,*S*] and 50% [*R*,*S*] forms of iminodisuccinic acid (ISA), used here as the starting material, was synthesised *via* a Michael addition of L-aspartic acid and maleic acid.[8–10] The preparation, in alkaline solution, was checked for purity by NMR method and found to contain small amounts of disodium aspartate, disodium fumarate and disodium maleate as by-products.

Green Context

Common chelating agents such as EDTA and DTPA have been used for over 60 years. Their scale of application in areas such as pulp bleaching can be very large. There are now concerns over the non-biodegradability of these compounds and their ability to remobilize heavy metal ions from soil. Here we can read about studies on the alternative biodegradable chelating ligand iminodisuccinic acid (ISA). Complex formation is demonstrated for several important metal ions. Overall ISA is shown to be a very promising environmentally benign metal chelating agent. ***JHC***

 DOI: 10.1039/b303372b

Stock solutions of metal ions

Aqueous Cu(II) and Mn(II) chloride solutions were prepared by dissolving $CuCl_2$ and $MnCl_2$ hydrates in distilled water. Zinc(II) chloride solution was prepared by dissolving zinc oxide in aqueous hydrochloric acid. Fe(III) chloride solution was prepared from a Fixanal ampoule (Riedel-de Haën). The metal contents of the stock solutions were standardized by EDTA titration. The copper(II) concentration was also determined electrogravimetrically. The acid contents of the metal solutions were determined by titration with 0.1 M NaOH solution after liberation of the H^+ ions by cation exchange.

Potentiometric measurements

The protonation and complex formation equilibria were studied in aqueous 0.1 M NaCl at 25 °C through a series of potentiometric EMF titrations carried out with a Schott–Geräte GmbH titrator TPC2000 and utilizing titration software TR600 version 5.00. The cell arrangement for the measurement of the hydrogen ion concentration $[H^+]$ was the following:

$$-\text{RE} \mid \text{equilibrium solution} \mid \text{GE}+ \qquad (1)$$

where GE denotes a glass electrode, Schott N2680, and RE is Hg, $Hg_2Cl_2 \parallel$ 0.1 M NaCl.

On the assumption that the activity coefficients are constant, the following expression is valid

$$E = E_0 + 59.157\log[H^+] + j_H[H^+] + j_{OH}[OH^-] \qquad (2)$$

The cell parameter E_0 and the liquid junction coefficient j_H, valid in acidic solution, were determined for each titration by addition of a known amount of HCl to the background electrolyte. The value of the coefficient j_{OH} was assumed to be constant (230 mV M^{-1}). Only stable emf readings (0.2 mV/2–3 min) were used in the calculations.

During the measurements of the metal complex equilibria aqueous NaOH or HCl was added to the solution. The ratio of the total concentrations of metal, C_M, to ligand, C_L, was usually held constant. The initial concentrations were varied within the limits $0.0007 \leq C_M \leq 0.0029$ M and $0.0010 \leq C_L \leq 0.0031$ M, covering the metal-to-ligand ratios 1 : 1, 1 : 2 and 1 : 4. In some runs aqueous metal chloride was used as the titrant. Four to seven independent titrations were carried out for each system. The number of data points used in the calculation of the stability constants varied between 226 and 345 in the pH (= $-\log[H^+]$) ranges 2.2–9.0 (Fe), 2.1–10.5 (Cu), 2.2–10.5 (Zn) and 3.8–9.2 (Mn). In some titrations the upper pH values were limited by the appearance of a precipitate or too slow attainment of equilibrium. The reproducibility and reversibility of the equilibria were tested by performing forward (increasing pH) and backward (decreasing pH) titrations.

Data treatment

When an alkaline ligand solution was titrated with aqueous HCl, there was an easily detected inflection point at pH 7. The data were analysed using this base content as the zero level of C_L.

Protonation/deprotonation of the ligand was controlled with HCl/NaOH additions. To visualize the experimental data sets, curves of Z_H *versus* pH were drawn. Z_H describes the average number of protons added or liberated per mole of ligand.

$$Z_H = (C_H - [H^+] + k_w[H^+]^{-1})/C_L \qquad (3)$$

where C_H denotes the total concentration of protons calculated over the zero level HL^{3-}, H_2O and M^{n+}.

In evaluating the equilibrium constants the following two-component equilibria were considered

$$n\text{H}^+ + \text{HL}^{3-} \rightleftharpoons \text{H}_{n+1}\text{L}^{n-3},\ n = 1\text{–}4;\ \beta_{n01} \qquad (4)$$

$$\text{HL}^{3-} \rightleftharpoons \text{L}^{4-} + \text{H}^+;\ \text{p}K_{a4} \qquad (5)$$

In evaluation of H^+–M^{n+}–HL^{3-} systems, the complexation can be characterized by the general three-component equilibrium:

$$p\text{H}^+ + q\text{M}^{n+} + r\text{HL}^{3-} \rightleftharpoons (\text{H}^+)_p(\text{M}^{n+})_q(\text{HL}^{3-})_r;\ \beta_{pqr} \qquad (6)$$

The hydrolysis of metal ions can be written

$$p\text{H}^+ + q\text{M}^{n+} \rightleftharpoons (\text{H}^+)_p(\text{M}^{n+})_q;\ \beta_{pq0} \qquad (7)$$

The protonation constants of the ligand and the hydrolysis constants of the metal ions[11] were considered as known parameters in the evaluation of the three-component system (6).

The mathematical analysis of the systems involves a search for the complex models (*pqr*-triplets) and the equilibrium constants of the complexes that best describe the experimental data. The calculations were carried out with the computer program SUPERQUAD.[12] The sample standard deviation *s* and the χ^2-statistics used as criteria in selection of the complex models were those given by the program.[12]

Results and discussion

Protolytic properties of ISA

The curve Z_H *versus* pH for ISA presented in Fig. 1 shows the increase of Z_H from 0 to 3 as the pH decreases from 7 to 2. A decrease of Z_H from 0 to −1 occurs when the pH increases from 7 to 11. It is clear that at around pH 7 the ligand is in the form of HL^{3-}, and it is protonated or deprotonated with decreasing or increasing pH.

In evaluation of the acidity constants, the amounts of the known protolytic impurities in the starting material were taken into account in the calculations. The relevant protonation constants, taken from ref. 13, were considered as known parameters in the refinement. It can be assumed that uncertainty in the values of the protonation constants for ISA caused by the presence of the impurities is relatively small and meaningless for the purpose of this study. The acidity constants of ISA, together with the corresponding values given previously for EDTA and DTPA, are shown in Tables 1 and 2.

Complex formation of ISA with Cu(II), Zn(II), Mn(II) and Fe(III)

The analysis of the data was started by drawing curves of Z_H *versus* pH, (Fig. 1).

In all systems the Z_H reaches the value −1 when pH is increased, indicating the coordination of ISA to the metal ions in the form of L^{4-}. The formation of species ML^{n-4} is dominant in all systems. Z_H values lower than −1 are also obtained, which indicates the presence of hydroxo complex species in all systems. For Cu(II), Zn(II) and Fe(III), the formation of species MHL^{n-3} is evident, and for Cu(II) also the species MH_2L^{n-2}.

The aqueous complexation of the polydentate ligand ISA is characterized by the formation of a stable mononuclear 1 : 1 metal to ligand complex as the major species. No bis or binuclear species were found. Because of the relatively strong complexation of aspartic acid, present as an impurity in the starting solutions, with the metal ions, the stability constants of the metal complexes of aspartic acid were included as known parameters in the calculations.

There are some earlier reports on the metal complex formation of ISA. However, these investigations were carried out in different background electrolytes, the stereoisomers of ISA used were not stated, and calculation procedures were often

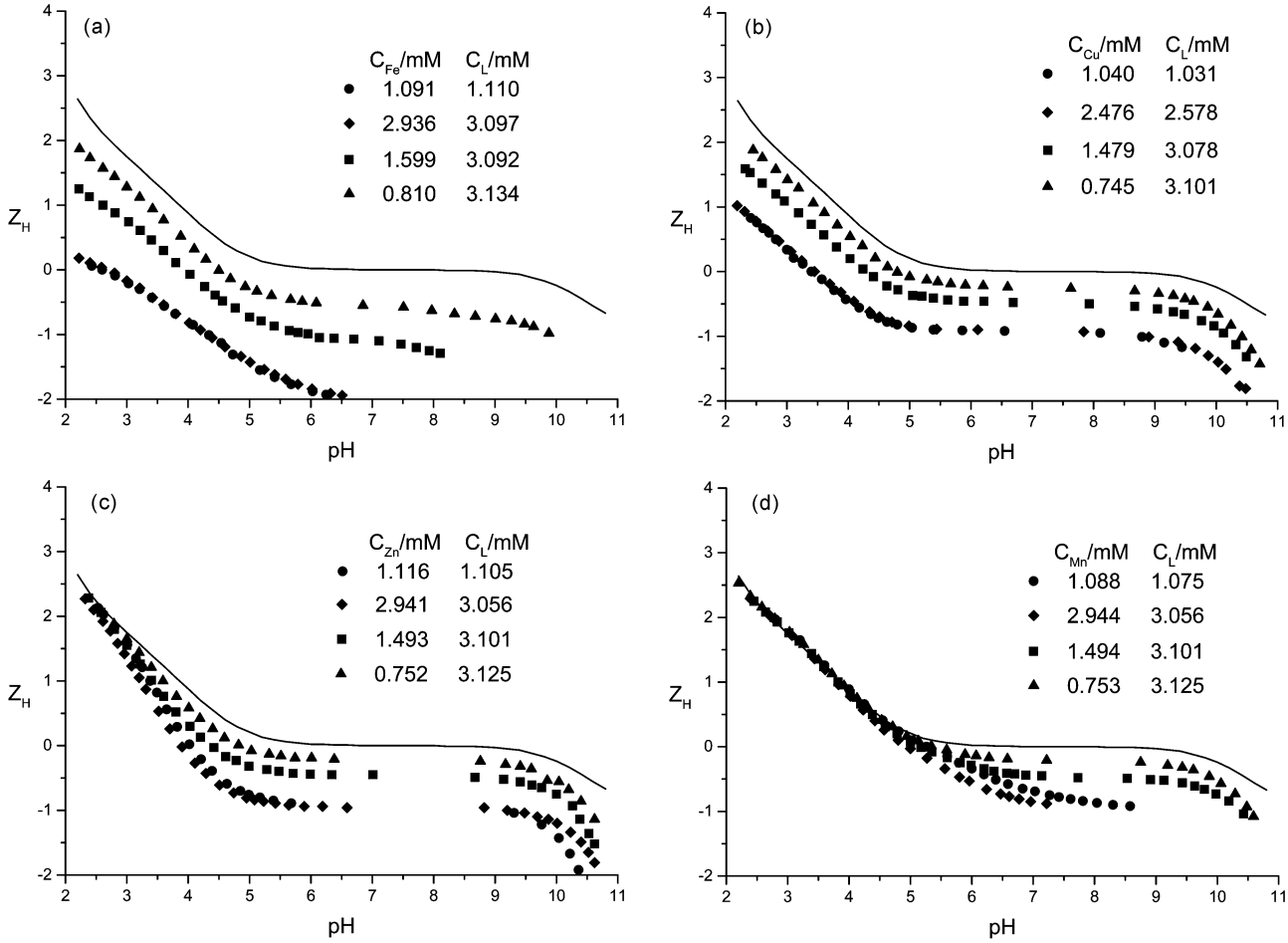

Fig. 1 (a) Z_H *versus* pH for complexation of Fe(III) with ISA (solid line: Z_H *versus* pH for ISA). (b) Z_H *versus* pH for complexation of Cu(II) with ISA (solid line: Z_H *versus* pH for ISA). (c) Z_H *versus* pH for complexation of Zn(II) with ISA (solid line: Z_H *versus* pH for ISA). (d) Z_H *versus* pH for complexation of Mn(II) with ISA (solid line: Z_H *versus* pH for ISA).

Table 1 The protonation and stability constants of ISA with Cu(II), Zn(II), Mn(II) and Fe(III)

	pqr eqn. (6)		log (β_{pqr} ± 3σ)
H^+	101	H_2L^{2-}	4.55 ± 0.02
	201	H_3L^-	8.08 ± 0.02
	301	H_4L	10.51 ± 0.04
	401	H_5L^+	12.02 ± 0.15
	−101	L^{4-}	−10.52 ± 0.03
χ^2/s	142.53/1.41		
Titrations/points	4/286		
Cu^{2+}	111	CuH_2L	9.88 ± 0.10
	011	$CuHL^-$	6.75 ± 0.07
	−111	CuL^{2-}	2.36 ± 0.10
	−211	$CuOHL^{3-}$	−8.04 ± 0.12
χ^2/s	73.25/2.98		
Titrations/points	4/266		
Zn^{2+}	011	$ZnHL^-$	4.04 ± 0.03
	−111	ZnL^{2-}	−0.37 ± 0.03
	−211	$ZnOHL^{3-}$	−11.63 ± 0.18
χ^2/s	82.20/1.45		
Titrations/points	7/345		
Mn^{2+}	−111	MnL^{2-}	−3.26 ± 0.04
	−211	$MnOHL^{3-}$	−14.52 ± 0.34
χ^2/s	53.50/1.46		
Titrations/points	6/226		
Fe^{3+}	011	FeHL	7.23 ± 0.11
	−111	FeL^-	3.34 ± 0.11
	−211	$FeOHL^{2-}$	−1.96 ± 0.14
χ^2/s	70.55/2.28		
Titrations/points	7/255		

Table 2 The protonation and complexation of ISA compared to corresponding values of EDTA and DTPA

Reaction	ISA (H_4L)	EDTA[13] (H_4L)	DTPA[13] (H_5L)
H^+			
$L^{x-} + H^+ \rightleftharpoons HL^{1-x}$	10.52	9.52–10.37	9.9–10.79
$HL^{1-x} + H^+ \rightleftharpoons H_2L^{2-x}$	4.55	6.13	8.40–8.60
$H_2L^{2-x} + H^+ \rightleftharpoons H_3L^{3-x}$	3.53	2.69	4.28
$H_3L^{3-x} + H^+ \rightleftharpoons H_4L^{4-x}$	2.43	2.00	2.7
$H_4L^{4-x} + H^+ \rightleftharpoons H_5L^{5-x}$	1.52	(1.5)	2.0
Cu^{2+}			
$Cu^{2+} + L^{x-} \rightleftharpoons CuL^{2-x}$	12.88	18.78	21.2
$CuL^{2-x} + H^+ \rightleftharpoons CuHL^{3-x}$	4.39	3.1	4.80
$CuHL^{3-x} + H^+ \rightleftharpoons CuH_2L^{4-x}$	3.13	2.0	2.96
$CuOHL^{1-x} + H^+ \rightleftharpoons CuL^{2-x}$	10.40	(11.4)	
Zn^{2+}			
$Zn^{2+} + L^{x-} \rightleftharpoons ZnL^{2-x}$	10.15	16.5	18.2
$ZnL^{2-x} + H^+ \rightleftharpoons ZnHL^{3-x}$	4.41	3.0	5.60
$ZnOHL^{1-x} + H^+ \rightleftharpoons ZnL^{2-x}$	11.26	(11.6)	
Mn^{2+}			
$Mn^{2+} + L^{x-} \rightleftharpoons MnL^{2-x}$	7.26	13.89	15.2
$MnOHL^{1-x} + H^+ \rightleftharpoons MnL^{2-x}$	11.26		
Fe^{3+}			
$Fe^{3+} + L^{x-} \rightleftharpoons FeL^{3-x}$	13.86	25.1	28.0
$FeL^{3-x} + H^+ \rightleftharpoons FeHL^{4-x}$	3.89	(1.3)	3.56
$FeOHL^{2-x} + H^+ \rightleftharpoons FeL^{3-x}$	5.30	7.37	9.66

inadequate. In these earlier studies ISA was found to form weak complexes with alkaline earth metals[13] and to form the moderately stable transition metal mono complexes NiL^{2-}, CdL^{2-} and CoL^{2-}.[14–16]

The complex models found in the present study are somewhat different from those given in the literature. The species $M(OH)L^{3-}$ found here for Cu(II) and Zn(II) has not been

reported in earlier papers.[16,17] We also did not find the species FeH_2L^+, FeL_2^{5-} and $Fe(OH)_2L^{3-}$ proposed in ref. 18. In our study, data collected from conditions where the formation of such species was proposed could well be explained merely by the binary hydrolysis of Fe(III).

The formulas of the species with the corresponding formation constants found in the equilibrium analysis of the different H^+–M^{n+}–HL^{3-} systems are shown in Table 1. To facilitate comparison with the findings of earlier studies carried out with EDTA and DTPA, the equilibrium constants of the stepwise complexation reactions for all three ligands are given in Table 2.

ISA forms moderately stable ML^{n-4} complexes with all four metal ions. The stability of the complexes follows the Irving–Williams order: $\log K_{MnL}$ (7.26) < $\log K_{Fe(II)L}$ (9.00) < $\log K_{CoL}$ (9.96) < $\log K_{NiL}$ (11.68) < $\log K_{CuL}$ (12.88) > $\log K_{ZnL}$ (10.15).[14,16,19]

The percentage distribution of the metals among the different complex species is visualized in Fig. 2 as a function of pH in the millimolar concentration area. It may be assumed that in dilute solution ISA is an effective chelating agent (more than 80% of metal is bound) over a wide pH range: for Cu(II) 3–12, Zn(II) 5–11 and Mn(II) 7–11. For Fe(III) the conditions are limited to acidic region 3–6. The competitive hydrolysis of Fe(III) overcomes the complex formation between Fe(III) and ISA in the micromolar concentration area. For the other metal ions the dilution of the solution increases the lower pH limit of the effective chelating region to the more basic direction.

In industrial applications it is usually more practical to consider conditional stability constants rather than conventional stability constants. The conditional constant, $\log K'_{ML}$ for the major complex species ML^{n-4} is given by the relation

$$K'_{ML} = \frac{\alpha_{ML}}{\alpha_M \alpha_L} K_{ML} \quad (8)$$

where the side reaction coefficients α_M, α_L and α_{ML} are defined as

$$\alpha_M = \frac{\Sigma(H^+)_p(M^{n+})_q}{[M^{n+}]} \quad (9)$$

$$\alpha_L = \frac{\Sigma(H^+)_p(L^{4-})}{[L^{4-}]} \quad (10)$$

$$\alpha_{ML} = \frac{\Sigma(H^+)_p(M^{n+})_q(L^{4-})_r}{[ML^{n-4}]} \quad (11)$$

$$K_{ML} = K(M^{n+} + L^{4-} \rightleftharpoons ML^{n-4}) \quad (12)$$

The values of the conditional stability constants of ISA complexes, as calculated with the aid of the equilibrium constants determined in this study and the binary hydrolysis constants of the metal ions given in the literature,[11] vary as a function of pH as shown in Fig. 3a. For comparison, the same plots for the DTPA complexes are given in Fig. 3b. The plots for EDDS and EDTA have been presented earlier.[5]

The values $\log K'_{ML} \geq 6$ are often considered as a criterion for an efficient complexation. On this assumption, the approximate pH ranges suitable for use of ISA as a chelating agent in the metal transition are the following: Cu(II) 4–12, Zn(II) 6–11 and Mn(II) 9–12. Except for Fe(III), the results are virtually the same as obtained for EDDS,[5] the useful chelating range being slightly narrower than for EDTA[5] and DTPA. The stabilities of the

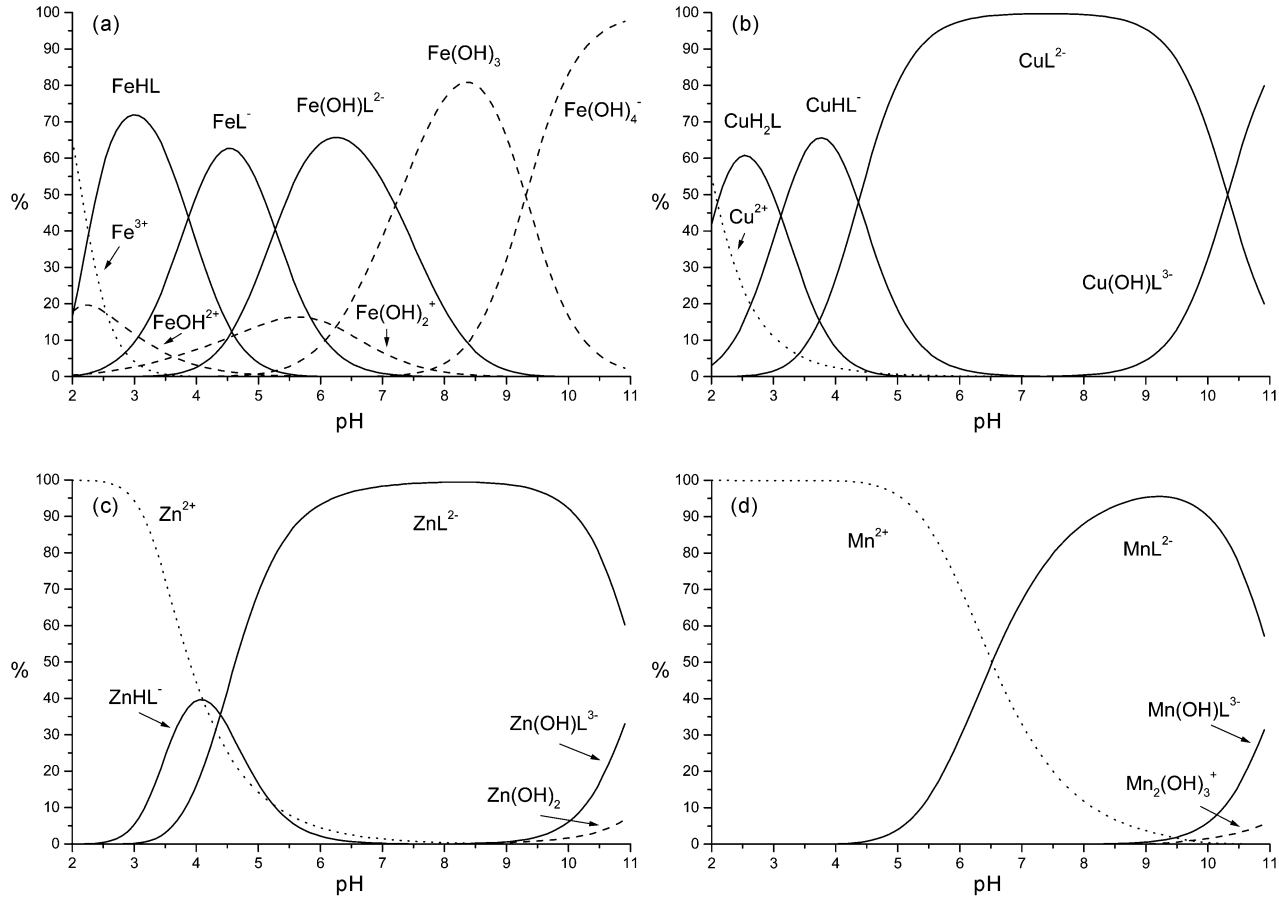

Fig. 2 (a) Percentage distribution of the different Fe(III) complexes *versus* pH (C_M = C_L = 1 mM). (b) Percentage distribution of the different Cu(II) complexes *versus* pH (C_M = C_L = 1 mM). (c) Percentage distribution of the different Zn(II) complexes *versus* pH (C_M = C_L = 1 mM). (d) Percentage distribution of the different Mn(II) complexes *versus* pH (C_M = C_L = 1 mM).

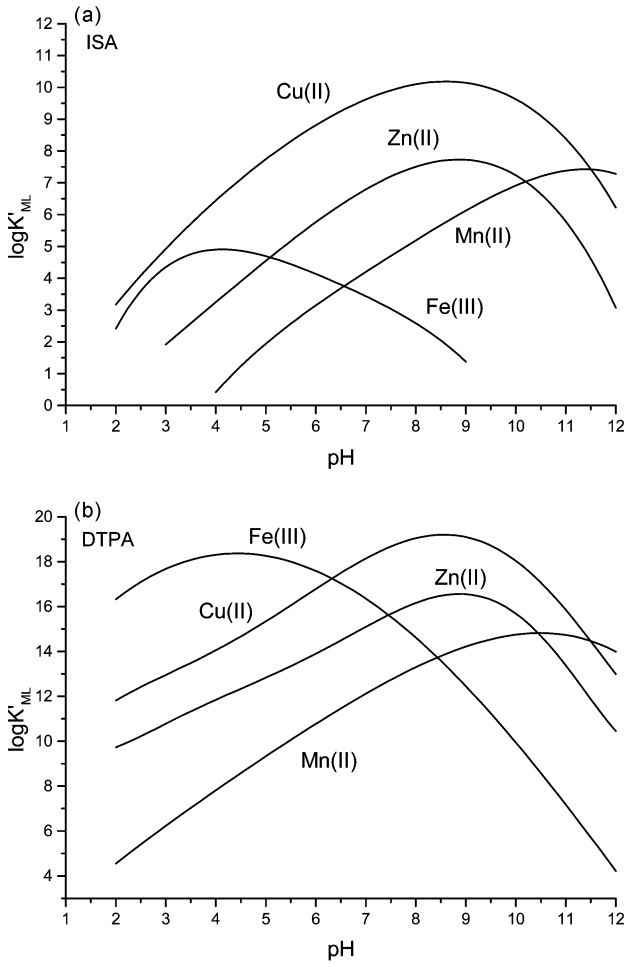

Fig. 3 (a) Conditional stability constants for ML complexes of ISA *versus* pH. (b) Conditional stability constants for ML complexes of DTPA *versus* pH.

complexes are great enough for many practical applications, however.

Results obtained in pulp bleaching tests with the stereoisomeric ISA mixture (50% [*S*,*S*], 50% [*R*,*S*]) showed ISA to be equally effective to DTPA as a chelating agent.[4] ISA can be used as a biodegradable chelating agent in mechanical pulp bleaching. The nitrogen content of ISA is lower than that of EDTA or DTPA, and can be lowered further by a combination of ISA with, for example, citrate ion as chelating agent. Thus, ISA has been shown to be a competitive biodegradable alternative to EDTA and DTPA in the bleaching of high yield pulp. A successful full-scale mill trial has also been carried out with use of ISA as chelating agent for thermomechanical pulp (TMP).[4]

References

1 D. Williams, *Chem. Br.*, 1998, **34**, 48.
2 J. L. Means, T. Kucak and D. A. Crerar, *Environ. Pollut., Ser. B*, 1980, **1**, 45.
3 V. Hornburg and G. W. Brümmer, *Z. Pflanzenernähr. Bodenk.*, 1993, **156**, 467.
4 R. Aksela, A. Parén, J. Jäkärä and I. Renvall, *Application of Ethylenediamine Disuccinic Acid and Iminodisuccinic acid as Biodegradable Chelating Agents in Pulp Bleaching*, 4th International Conference on Environmental Impacts of the Pulp and Paper Industry, June 12–15, 2000, Helsinki, Finland, Proceedings of the Conference, pp. 340–344.
5 M. Orama, H. Hyvönen, H. Saarinen and R. Aksela, *J. Chem. Soc., Dalton Trans.*, 2002, 4644.
6 M. Itävaara and M. Vikman, Technical Research Centre of Finland, 1997, Research Report no. BEL 235/97.
7 Unpublished results, Kemira Chemicals Oy.
8 F. Pavelik and J. Majer, *Chem. Zvesti*, 1978, **32**, 37.
9 I. Renvall, R. Aksela and A. Parén, Patent application, WO 9700106, Kemira Chemicals Oy.
10 I. Renvall, R. Aksela and A. Parén, Patent application, WO 9700107, Kemira Chemicals Oy.
11 C. F. Baes and R. E. Mesmer, *The Hydrolysis of Cations*, Wiley, New York 1976.
12 P. Gans, A. Sabatini and A. Vacca, *J. Chem. Soc., Dalton Trans.*, 1985, 1195.
13 A. E. Martell and R. M. Smith, Critical Stability Constants Database, NIST, Gaithersburg, MD, USA, Dec. 1997.
14 V. P. Vasilev, A. V. Katrovtseva, I. P. Gorelov and N. V. Tukumova, *Zh. Neorg. Khim.*, 1996, **41**(8), 1320.
15 V. P. Vasilev, G. A. Zaitseva and N. V. Tukumova, *Zh. Fiz. Khim.*, 1996, **70**(5), 815.
16 V. P. Vasilev, A. V. Katrovtseva, S. A. Bychkova and N. V. Tukumova, *Zh. Neorg. Khim.*, 1998, **43**(5), 808.
17 V. P. Vasilev, G. A. Zaitseva, N. V. Tukumova and G. B. Bukushina, *Zh. Neorg. Khim.*, 1999, **44**(7), 1165.
18 V. M. Nikolskii, N. E. Knyazeva, V. G. Alekseev and I. P. Gorelov, *Zh. Neorg. Khim.*, 2002, **47**(7), 1184.
19 N. E. Knyazeva, V. M. Nikolskii, V. G. Alekseev, S. S. Ryasenskii and I. P. Gorelov, *Zh. Neorg. Khim.*, 2002, **47**(2), 262.

Pressurized water extraction (PWE) of terpene trilactones from *Ginkgo biloba* leaves

Qingyong Lang and Chien M. Wai*

Department of Chemistry, University of Idaho, Moscow, ID 83844-2343, USA

Received 13th January 2003
First published as an Advance Article on the web 5th June 2003

As a simple and green chemistry procedure, pressurized water extraction (PWE) was developed for removing the terpene trilactones, ginkgolides and bilobalide, from leaves of *Ginkgo biloba* L. Compared with conventional boiling-solvent extraction methods, PWE is a more effective, selective, economical and environmentally benign technique for the extraction of intermediate to polar compounds from herbal plants. In contrast to high temperature extraction, PWE at low temperature can minimize undesirable reactions such as thermal decomposition or degradation and remove much smaller amounts of impurities from the herbal materials. The other important advantage of PWE is that the extraction efficiency can be quantitatively assessed using a kinetic extraction model. Experimental results were proven to be closely consistent with the predicted values. After PWE, the terpene trilactones could be easily enriched by a liquid–liquid extraction and the extracts readily determined with a GC-FID method.

Introduction

The demand for ginkgo extract has been estimated to increase by 26% each year, and every year more than 4,000 tons of dried ginkgo leaves are processed to obtain *Ginkgo biloba* extracts (GBE).[1] The major pharmaceutical uses of standardized GBE include (1) to improve circulation in the body, particularly the brain and peripheral vascular system; (2) to help relieve vertigo, tinnitus, headache, short-term memory loss, and (3) to provide a potent antioxidant.[2] Commercial GBE products have very complex compositions and show significant variation in the concentration and composition of the most important active ingredient – ginkgo terpene trilactones (Fig. 1).[3–4] This kind of

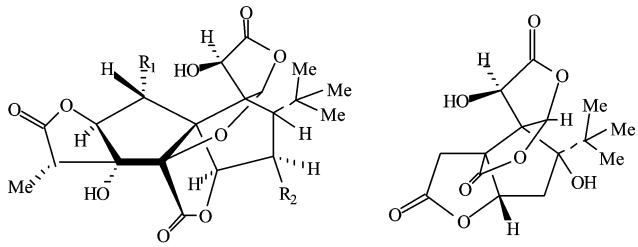

G-A: $R_1 = R_2 = H$
G-B: $R_1 = OH$, $R_2 = H$
G-C: $R_1 = R_2 = OH$
G-J: $R_1 = H$, $R_2 = OH$

B-B

Fig. 1 Molecular structures of the ginkgo terpene trilactones. Ginkgolides A (G-A), B (G-B), C (G-C), J (G-J) and bilobalide (B-B).

variation could be due to differences in the raw ginkgo leaves[5] but more likely resulted from the different extraction, purification and concentration techniques used by different manufacturers,[6] because the quality of a GBE product is highly dependent on the manufacturing process.

Solvent boiling methods have been used for thousands of years in China to prepare herbal remedies. Using mixtures of water–ethanol or water–acetone as the extraction solvents, these conventional methods are still widely used today in herbal remedy production.[5] For ginkgo studies, different solvents such as boiling water,[7] acetone[8] and mixtures of methanol and water[5,9] have been used for removing ginkgolides and bilobalide from leaves. The major disadvantages of solvent boiling methods are low selectivity and loss of thermally labile or volatile components in the heating process.

Through multi-step reactions, Corey, the Nobel Prize winner in 1990, and his co-workers have successfully synthesized one of the most important terpene trilactones, the ginkgolide B,[10] which was believed to be a milestone in the breathtaking development of organic synthesis over the last thirty years.[11] However, the major source of such complex natural compounds is still the plant. Therefore, for pharmacological studies it is desirable to maximally recover this group of compounds from the raw leaves.

In recent years, subcritical or super-heated water extraction has drawn some attention in a variety of research areas such as in environmental, food and herbal studies.[12–15] Water has several distinguishing properties that make it one of the most ideal solvents in herbal studies. First, water is the greenest, cheapest and most easily available solvent. Secondly, by adjusting pH or adding certain salts water can provide very selective extraction.[4] Finally, the polarity of water can vary significantly with temperature changes so that water may be used to extract a variety of compounds with different polarities.[16]

Green Context

While there is an increasing amount of interest in the use of plants as sources of useful organic chemicals, it is vital that we develop environmentally acceptable procedures for extracting, and, where appropriate, modifying, plant extracts. The extraction of a product from a renewable resource using a toxic solvent is hardly a good example of green chemistry! Here we see an excellent example of combining the green chemical technologies of renewable resources feedstocks and environmentally benign solvents. Pressurised water is used to remove the terpene trilactones from *Ginkgo biloba* leaves. As well as the obvious environmental and health advantages of water, it also proves to be more selective and effective as an extraction medium and side reactions that can be induced by hot solvents are minimised. ***JHC***

However, high temperature is not always desirable for herbal studies because unwanted reactions such as oxidation, decomposition, degradation or rearrangement reactions may occur at elevated temperatures.[17–18] For instance, bilobalide, one of the important terpene trilactones, can be lost if extracted at high temperature (≥100 °C). On the other hand, ginkgolides and bilobalide are moderately soluble in weakly acidic aqueous solution (at least 300 μg mL^{-1}); therefore, it should be possible to extract them at a mild temperature with good selectivity.

In this paper, we report the PWE procedure used in ginkgo terpene trilactone extraction studies. The PWE results were compared with those obtained with several commonly used boiling methods. Of all the methods tested, PWE gave the best yield with the highest selectivity. This technique is particularly effective in recovering bilobalide, the least stable terpene trilactone in ginkgo leaves.

After PWE, the terpene trilactones could be further enriched using a liquid–liquid extraction procedure with ethyl acetate–tetrahydrofuran (EOA–THF, 7 : 3). For analytical purposes, the terpene trilactones can be easily determined either with a GC-FID method as we described in another article,[4] or using a HPLC equipped with an evaporative light scattering detector (ELSD)[19,20] or refractive index detector (RID).[9,21] Recently a comprehensive review paper on chemical analysis of *Ginkgo biloba* was published in the *Journal of Chromatography A*, interested readers may refer to it.[22] In this study, GC-FID was used for the quantification.

Results and discussion

In order to achieve maximal extraction of terpene trilactones, all factors possibly affecting the extraction efficiency were investigated. These factors included temperature, pressure, pH of the solvent (water), flow rate and sample particle sizes. Of all factors, temperature and pH were found to have the most significant influences on the extraction results.

Temperature

Setting pressure at 100 atm and the flow rate at about 1 mL min^{-1}, the temperature effect was first tested. Since it has been known that lower pH could enhance the solubility of the terpene trilactones, water used for the extraction was always adjusted with acetic acid to a pH ~5 prior to use.[5] Adjusting the pH to approximately 5 was also desirable for the following liquid–liquid extraction separation.[4] Following a 15 min static extraction, a dynamic extraction was started. When 20 mL of extract solution were collected, the extraction was terminated.

In Fig. 2 the analytical results of terpene trilactones *versus* temperatures are plotted. Based on duplicate measurements, the different profiles in Fig. 2 as well as in Fig. 4, 5, and 6 are clearly separated. Due to lack of the standard reference and the low concentration, ginkgolide J (G-J) was not quantified in this study although the G-J peak did show up in the chromatograms. As the temperature was raised from room temperature (21 ± 2 °C) to above 60 °C, it was found that the recoveries of terpene trilactones started to decrease; particularly, bilobalide showed strong temperature dependence. Compared with extraction results at room temperature, about 25% of the bilobalide was lost at 80 °C, only about 15% was left at 100 °C, and no detectable bilobalide was observed as the temperature was raised to 140 °C. This temperature effect can be clearly seen in Fig. 3, where the bilobalide peak heights or areas (peak No. 1) varied dramatically with temperature. At room temperature, it was the most abundant peak (bottom); at 100 °C, it became a tiny peak (middle); and at 140 °C, it completely disappeared (top). For ginkgolides, compared with their recoveries at ≤ 60 °C, at least one-fourth was lost at 100 °C and only about two-thirds remained at 140 °C.

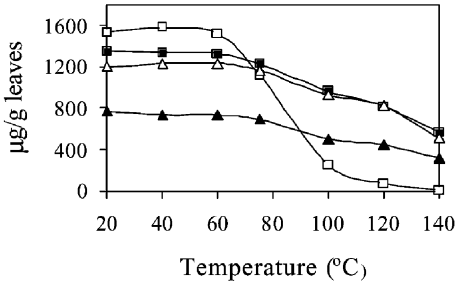

Fig. 2 Temperature effects on extraction results of terpene trilactones. B-B (□), G-A (■), G-B (▲), G-C (Δ).

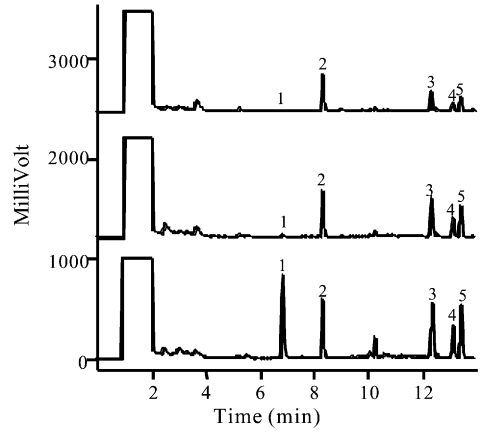

Fig. 3 Chromatograms of a leaf sample extracted at 140 °C (top), 100 °C (middle), and room temperature (bottom). Peak markings (1) B-B, (2) IS (internal standard, squalane); (3–5) Ginkgolide A–C, respectively.

Another disadvantage of PWE at high temperature (≥100 °C) was the extraction of large quantities of impurities. When the extraction was conducted at 140 °C, the extract became thick and almost black due to impurities co-extracted. Increased amounts of impurities in the extract would not only cause clogging problems, but also could deteriorate the quality of the extracts. Furthermore, too much organic material in the extracts could also cause analytical difficulties.

Based on our observations, a low temperature such as room temperature was preferred for PWE of the terpene trilactones. Under this temperature condition, PWE could enable maximal recovery of terpene trilactones and provide a more economical extraction technique since no heating energy was required.

Pressure

Once temperature was decided, pressure effects were tested. It was found that a "threshold" pressure seemed present for the extraction of terpene trilactones from leaf samples. Below the threshold pressure, either the solvent could not flow through the sample bed due to the low porosity of the packed leaf powder, or a slow extraction rate was observed that probably was due to the slow diffusion of the solvent through the sample matrices. According to our experiments, such a threshold pressure was approximately 50 atm under our experimental conditions. However, above this threshold pressure, further increases of pressure would have little effect on the extraction results. This threshold pressure is apparently required for the solvent molecules to overcome the surface barrier (*e.g.*, leaf surface wax layer) and penetrate inside the leaf particles. The leaf surface wax layer, a hydrophobic material on the leaves, protects the leaves from losing moisture under natural conditions.

The extraction efficiencies against pressures are plotted in Fig. 4. In all the experiments hereafter we used 100 atm pressure for all the extractions.

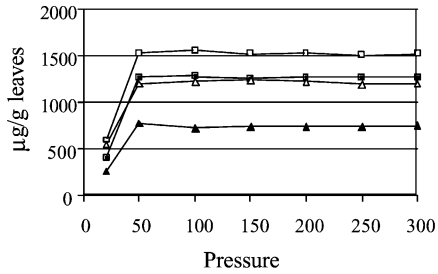

Fig. 4 Pressure effects on the extraction of B-B (□), G-A (■), G-B (▲) and G-C (Δ) at room temperature with flow rates 1–2 mL min^{-1}. The extraction volume was 20 mL.

Acidity

If the extraction was conducted with pure water, poor reproducibility was always observed even under optimized temperature and pressure. Since the acidic condition was known to have profound effects on the solubility of the terpene trilactones in water,[5] the pH effects were further tested. Acids or salts used for adjusting pH included HCl, HCOOH, CH_3COOH, citric acid, H_3PO_4, sodium acetate, sodium citrate, KH_2PO_4, Na_2HPO_4 and Na_2CO_3. The best results, in terms of reproducibility, efficiency and selectivity, were obtained by using dilute (0.2% v/v) acetic acid or 5% KH_2PO_4. Because acetic acid is the edible acid in vinegar and is more acceptable for herbal studies, it was chosen for all the experiments.

The solubility of ginkgolides could also be enhanced under basic conditions, and ginkgolide B was found to undergo reversible ionization and re-lactonization reactions.[23] The recovery of bilobalide, however, was decreased with the increased pH (Fig. 5). At pH 8, more than half of the bilobalide

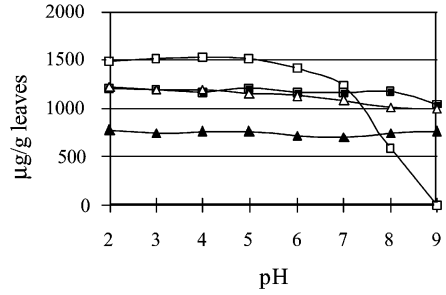

Fig. 5 pH effects on extraction results of B-B (□), G-A (■), G-B (▲) and G-C (Δ) by PWE.

would be lost, while at pH ≥ 9 no detectable bilobalide was observed. The strong pH dependence of bilobalide was due to its irreversible hydrolysis reactions; therefore, acidic conditions were preferable for the PWE experiments.

Another disadvantage for extraction at high pH (≥8) was the co-extraction of a large amount of impurities. As mentioned above, large quantities of impurities would not only reduce the quality of the extract, but would also cause difficulties in the separation and analysis steps.

Particle sizes

Sample particle sizes can affect both the diffusion rates and the porosity of the sample bed in the extraction cell. Diffusion rates include the diffusion of (1) the solvent molecules into the leaf particles and (2) the dissolved solutes from the sample particles into the bulk solvent. Four particle size ranges were examined, which included 20 > *d* > 42, 42 > *d* > 60, 60 > *d* > 80 and *d* < 80-mesh.

The extractions were performed under identical optimized conditions, and the extraction results *versus* the particle sizes are shown in Fig. 6. Instead of the finest particles (< 80-mesh), particles of 42–60-mesh were found to give the maximal extraction results. Further tests indicated that as samples passed a 42-mesh sieve, extraction results were good and reproducible.

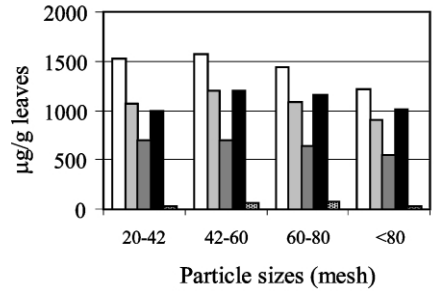

Fig. 6 Effects of sample particle sizes on the extraction results of (columns from left to right) bilobalide, ginkgolides A, B, C and J, respectively.

When the particle sizes were too small, *e.g.*, ≤80-mesh, the porosity or the permeability of the sample bed would be reduced so that not all the sample particles could effectively interact with the solvent molecules. When the sample particle sizes were too coarse, *e.g.*, > 20-mesh, a lower extraction rate could result due to the longer diffusion time required.

From the particle size tests we can conclude that in order to achieve maximal extraction of the active compounds from plants, the raw herbal materials must be pulverized into a suitable size range. Both too coarse and too fine leaf powders might result in a low yield. Based on our tests, 42-mesh is a suitable upper limit when PWE is used for the extractions.

Other factors

Before dynamic extraction, a static extraction was found necessary to achieve a satisfactory result. That is, it was necessary to pump solvent into the extraction vessel but keep the outlet valve closed. After some preliminary tests, it was found that at least 10 min static time were required for effective extraction. In all the experiments, a 15 min static extraction was therefore conducted. A static extraction of more than 15 min did not result in any further improvement in extraction.

The flow rate did not show obvious effects on the extraction results as long as it was controlled below 3 mL min^{-1}. A flow rate of 1.0 to 2 mL min^{-1} was suitable.

After all the variables were investigated and decided, quantitative extraction of the terpene trilactones from leaf samples was easily achieved. At room temperature, under 100 atm pressure, and with 20 mL of water containing 0.2% acetic acid, reproducible extraction results from 1 g of leaf sample were obtained.

Comparison of extraction methods

Table 1 shows the extraction results of a ginkgo leaf sample using solvent boiling methods and PWE. Obviously, the PWE method gave the best results of all. Reasons for the lower extraction efficiencies of the boiling methods may include the following: (1) thermal decomposition or other undesirable

Table 1 Comparison of PWE and solvent boiling extraction results (μg g^{-1} leaves). The numbers in the parentheses show RSD obtained from triplicate measurements (n = 3)

Method[a]	B-B	G-A	G-B	G-C	Total	RR (%)[b]
Acetone	1074 (3.1)	864 (8.9)	361 (8.2)	514 (10.0)	2813 (3.9)	54
Ethanol	1594 (11.4)	1326 (12.1)	625 (13.1)	771 (11.2)	4316 (11.8)	83
Methanol	1399 (5.3)	1204 (5.1)	617 (5.3)	769 (3.5)	3989 (1.3)	77
Water	1576 (1.3)	1344 (11.9)	629 (4.0)	745 (7.9)	4294 (4.0)	83
Methanol–water	1008 (3.7)	926 (9.9)	482 (2.2)	686 (4.0)	3102 (1.0)	60
PWE	1857 (0.9)	1360 (2.9)	771 (2.5)	1197 (2.3)	5185 (0.2)	100

[a] Except for PWE, all others were boiling solvent extraction. [b] RR: Relative Recoveries to that of PWE.

reactions happened during the extraction process, (2) part of the samples was lost during the repeated transfer, and (3) for samples prepared with methanol–water (3 : 7), possible losses were due to the difficulty of the filtration. In addition to lower efficiency, lower selectivity and higher energy consumption due to the heating requirement, other major disadvantages of the solvent boiling method are its time-consuming operations, which include repeated sample boiling, filtration, and transfer, as well as dish washing.

The good efficiency and selectivity of the PWE method can be attributed to its several unique characteristics. (1) PWE is performed in a closed system so that when pressure is applied, the solvent molecules can effectively penetrate through the surfaces of the leaf particles to replace and then remove the targeted solutes from the matrix sites. (2) During the entire extraction process, fresh solvent is continuously forced through the sample bed so that maximal dissolution and removal of the terpene trilactones are possible. (3) At room temperature, many undesired reactions such as decomposition or degradation do not take place. (4) Most of the impurities, particularly the lipophilic compounds, would not dissolve in water, so that a better selectivity is obtained. Because of these advantages, PWE is not only a useful technique for analytical purposes, but could also be a promising technique for the manufacturing process. For instance, after PWE an enriched terpene trilactone extract (>70%) could be readily obtained using a liquid–liquid extraction with EOA–THF. In fact, we have patented this technique for herbal medicine studies and production.

Kinetic extraction studies

Exactly like supercritical fluid extraction (SFE), PWE can also be used for kinetic extraction studies. The first 5 mL of extract would remove the majority of the terpene trilactones (>80%), while in the first 10 mL more than 94% of the trilactones were extracted. Obviously, in a real industrial process it is not economically worthwhile to try to recover 100% of the terpene trilactones with extra extraction time and solvent.

Using a kinetic extraction model, the extraction efficiency can be easily estimated so that the optimal extraction volume can be decided – this optimal extraction volume can be extremely important for a manufacturer! If the total mass of a terpene trilactone originally in the ginkgo leaves was assumed to be M_0, the masses of this trilactone extracted in the first, second and third extractions, or in the first, second and the third 5 mL of extract as in this case, are M_1, M_2, and M_3. As in the model used by Walker *et al.* in their supercritical fluid extraction study,[24] the following equation will apply:

$$M_0 = M_1 + M_2^2/(M_2 - M_3)$$

Table 2 shows the calculated or predicted values of M_0 for the terpene trilactones and the duplicate experimental results obtained by exhaustive extraction (M_E). The good consistency between the two groups of values indicates that the kinetic extraction model is applicable in PWE. This kinetic model can provide a simple way to design an optimal extraction procedure,

Table 2 Predicted and exhausted extraction results (μg g^{-1} leaves) of terpene trilactones from ginkgo leaves

Compounds	Predicted	Extracted	% of predicted
B-B	1839	1857	101.0
G-A	1360	1355	99.6
G-B	771	783	101.6
G-C	1197	1227	102.5

and this is extremely important for production. On the other hand, it is hard, if not impossible, to assess the extraction efficiency for a solvent boiling method.

Experimental

Samples

One local leaf sample was collected in late October, 1997, from a young ginkgo tree on the University of Idaho campus. The leaf sample was air dried in our laboratory at room temperature. Caution must be taken to prevent the fresh leaves from going moldy, otherwise the terpene trilactones, particularly bilobalide, would be lost dramatically. The dried leaves were pulverized in a coffee blender and passed through a 42-mesh sieve. The leave powder was kept in a dry glass bottle and kept in a refrigerator at ≤4 °C.

Chemicals and instruments

Ginkgolides A (*ca.* 90%), B (*ca.* 90%) and bilobalide (*ca.* 95%) were purchased from Sigma (HPLC grade, Sigma); Ginkgolide C was from AmPharm Research (≥95%, HPLC grade, AmPharm, Salt Lake City, UT). A mixture of pure ginkgolides (crystal) and a raw ginkgo extract (powder) used as references were purchased from Lubao Biochemical Corp. (Xiuzhou, China). The mixture of ginkgolides contains G-A 46.6, G-B 19.1, G-C 31.7, G-J 1.6% and total terpene trilactones 98.9%. Other reagents included N,O-Bis(trimethylsilyl)trifluoroacetamide–trimethylchlorosilane (BSTFA–TMCS, 99 : 1) (derivatization grade, Aldrich); dimethylformamide (DMF, certified A.C.S., Fisher); ethanol (200 proof, McCormick Distilling Co.); acetone (certified A.C.S., Fisher); methanol (HPLC grade, Fisher); methylene chloride (HPLC-GC/MS grade, Fisher); ethyl acetate (certified A.C.S., Fisher); fine sand (80-mesh, lab prepared); tetrahydrofuran (THF) (certified A.C.S., Fisher); acetic acid (certified A.C.S., Fisher); KH_2PO_4 (J. T. Baker Chemical Co.); squalane (99%, Aldrich) and nitrogen (99.999%, Oxarc).

The standards were so prepared that the final concentrations were equal to 400 μg mL^{-1} (400 ppm). The concentrations of the standard solutions were corrected with the reference samples and then kept in a freezer (≤20 °C). The stock solutions were stable at least for several weeks.

A Hewlett Packard 5890 gas chromatograph installed with a DB-5 column (30 m × 0.32 mm × 0.25 μm) was used for the

quantitative analyses. A flame ionization detector (FID) was used for the detection. An ISCO supercritical fluid extractor, SFX™ 2–10, equipped with an ISCO syringe pump (model 260 D) and a pump controller of series D was used for the PWE.

Extraction of terpene trilactones

PWE

A 10 mL stainless steel sample cell was packed first with 1 g of fine sand at bottom, then 1 g of a leaf sample mixed with about 1 g of sea sand, 0.5 g NaCl on top of the sample, and finally filled to full with sea sand. Water containing 0.2% acetic acid was used as the solvent. At room temperature (from here on, unless otherwise indicated, all PWE was conducted at room temperature) and 100 atm of pressure, a 15 min static extraction was first conducted. Then, with the outlet valve slowly opened, dynamic extraction began. The flow rate was controlled between 1.5 and 2.0 mL min^{-1}. The extraction was accomplished when 20 mL of extract were collected. The sample solution was adjusted to pH ~ 5 with dilute NaOH, and the final volume was brought to 50 mL in a volumetric flask.

Solvent boiling methods

Five different solvents including ethanol, methanol, acetone, water, and a mixture solvent of methanol and water (3 : 7 v/v), were used for sample preparation, and all the results were based on duplicate extractions. In 20 mL of each solvent, 1 g of ginkgo leaf powder was boiled gently on a hot plate twice. The first time was for approximately 2 min and then, after filtrating with a piece of No. 4 Whatman filter paper, the residue was boiled again for about 5 min. The solid residue was washed with a few mL of the corresponding solvent and the final volume was brought to 50 mL. One mL of each sample solution corresponded to 20 mg leaves.

Liquid–liquid extraction of aqueous solutions

For aqueous samples, either from PWE or from solvent boiling methods, 5 mL of each solution were directly used for separation and analysis. For samples prepared with organic solvents or mixed solvents, 5 mL of solution from each of the samples were transferred into a beaker and evaporated on a hot plate at ≤60 °C to remove the organic solvents. The solid residue was dissolved in 5 mL of water which was previously adjusted to pH ~ 5 with KH_2PO_4. Ultrasonic agitation could be used to speed up the dissolution.

We have reported a simple separation method in a previous article,[4] which we describe here briefly. Five mL of each aqueous solution were filtered through a 0.45 μm syringe filter into a 15 mL sample vial, 1 g of NaCl was added and dissolved in the capped vial under ultrasonic agitation. Finally 5 mL of EOA–THF (7 : 3 v/v) and 25 μg of squalane in hexane were added, and the tightly capped vials were shaken for 1 minute either with a mechanical shaker or manually (one can easily handle at least 10 vials by hand simultaneously). After extraction, about 4 mL of the organic phase were transferred with a disposable pipet to a dry and clean 4 mL sample vial. The solvent was blown down to dryness with a gentle stream of nitrogen gas in a hood.

Determination of terpene trilactones

After the solvent was completely evaporated, 300 μL of DMF and 300 μL of BSTFA–TMSC (99 : 1) were added to each vial, and the capped vials were placed in a GC oven at 120 °C for 45 minutes for derivatization. The standard references were also prepared and derivatized accordingly and simultaneously. After cooling down to room temperature, 1 μL of the sample was injected into the GC for quantification.

Nitrogen was used as the carrier gas. Column head pressure was set at 1.23 atm (18 psi), which corresponded to a column flow rate of approximately 3.0 mL min^{-1}. The injector was set at 280 °C and the detector at 300 °C. The GC temperature program was started from the initial temperature of 200 °C. After 1 min, the temperature was increased to 280 °C at a rate of 10 °C min^{-1}. The final time was 6 min. For each sample, the total GC analysis time was 15 min.

As described previously,[4] the concentrations of ginkgolides and bilobalide in the samples were calculated based on the peak areas of the analytes and the internal standard (IS). For comparison purposes, a series of standard solutions (10 to 200 ppm of each compound with 25 μg of squalane) was also prepared simultaneously with the leaf samples. Over this concentration range and based on repeated injection results, the FID response ratios for the analytes and IS were stable.

Conclusions

Pressurized water extraction (PWE) at room temperature is a very effective and selective method to remove terpene trilactones from ginkgo leaves, particularly for the extraction of the thermally unstable bilobalide. Compared to conventional solvent boiling methods, the recovery and precision values of PWE would be good. Furthermore, PWE method is a more time-, solvent- and energy-saving technique for herb studies. By using the kinetic extraction model, one can easily estimate the efficiency of an extraction procedure and determine the experimental design for maximal yield with minimal time or cost. This technique was useful for extraction of water-soluble, even slightly water-soluble, compounds from plant samples. For instance, it has been successfully used in extraction of hypericin from St. John's Wort and sweetener compounds from Stevia in our laboratory.

Other observations include the following. For maximal recovery of the trilactone compounds, it is important to prevent leaves from molding during sample drying and storage processes. If the PWE method is used, leaf powders with the particle sizes ≤42-mesh are fine enough for quantitative extraction, further grinding the leaves could result in lower recovery due to the lower porosity or the permeability of the sample bed.

References

1 M. L. Chavez and P. I. Chavez, *Hosp. Pharm.*, 1998, **33**, 658.
2 J. Glison, R. Crawford and S. Street, *The Nurse Practitioner*, 1999, **24**, 28–47.
3 Consumers Union, *Consum. Rep.*, 1999, **64**, 44.
4 Q. Lang, H. K. Yak and C. M. Wai, *Talanta*, 2001, **54**, 673.
5 J. T. B. Strode III, L. T. Taylor and T. A. van Beek, *J. Chromatogr. A*, 1996, **738**, 115.
6 H. J. Woerdenbag and T. A. van Beek, *Adverse Effects of Herbal Drugs*, **Vol. 3**, Springer-Verlag, New York 1997 51.
7 K. Okabe, K. Yamada and S. Takada, *J. Chem. Soc. C*, 1967, **21**, 2201.
8 N. Chauret, J. Carrier, M. Mancini, R. Neufeld, M. Weber and J. Archambault, *J. Chromatogr.*, 1991, **588**, 281.
9 T. A. van Beek, H. A. Scheeren, T. Rantio and W. C. Melger, *J. Chromatogr.*, 1991, **543**, 375.
10 E. J. Corey and W. G. Su, *J. Am. Chem. Soc.*, 1987, **109**, 7534.
11 E. J. Corey, *Angew. Chem.*, 1991, **30**, 455.
12 A. Basile and A. A. A. Clifford, *Proc. 5th Meet. Supercrit. Fluids*, Nice, France, 1998, 635.

13 M. Das, J. R. Vedasiromoni and D. K. Ganguly, *Planta Med.*, 1994, **60**, 470.
14 S. B. Hawthorne, Y. Yang and D. J. Miller, *Anal. Chem.*, 1994, **66**, 2912.
15 Y. Yang, S. Bowadt, S. B. Hawthorne and D. J. Miller, *Anal. Chem.*, 1995, **67**, 4571.
16 Y. Yang, S. B. Hawthorne and D. J. Miller, *Environ. Sci. Technol.*, 1997, **31**, 430.
17 W. K. Modey, D. A. Mulholland, H. Mahomed and M. W. Raynor, *J. Microcolumn Sep.*, 1996, **8**, 67.
18 J. P. Bartley and P. Foley, *J. Sci. Food Agric.*, 1994, **66**, 365.
19 Y. Yuzhen and X. Peishan, *Yaowu Fenxi Zazhi (Chin. J. Pharm. Anal.)*, 2001, **21**, 173.
20 M. Ganzera, J. Zhao and I. A. Khan, *Chem. Pharm. Bull.*, 2001, **49**, 1170.
21 J. Zhang, J. Pan, H. Xie, Z. Yang, X. Hu and K. Yang, *Fenxi Huaxue (Chin. J. Anal. Chem.)*, 2000, **28**, 53.
22 T. A. van Beek, *J. Chromatogr. A*, 2002, **967**, 21.
23 O. Zekri, P. Boudeville, P. Braquet, P. Jouenne and J. L. Burgot, *Anal. Chem.*, 1996, **68**, 2598.
24 D. F. Walker, K. D. Bartle, D. G. Breen, A. A. Clifford and S. Costiou, *Analyst*, 1994, **119**, 2789.

Heterogeneous catalytic epoxidation of fatty acid methyl esters on titanium-grafted silicas

M. Guidotti,[a] N. Ravasio,*[a] R. Psaro,[a] E. Gianotti,[b] L. Marchese[c] and S. Coluccia[b]

[a] *CNR – ISTM and Dip. Chimica Inorganica, Metallorganica e Analitica, via G. Venezian 21, Milano, Italy. E-mail: n.ravasio@istm.cnr.it; Fax: +39-02-50314405*
[b] *Dip. di Chimica IFM, Università di Torino, via P. Giuria 7, Torino, Italy*
[c] *Dip. di Scienze e Tecnologie Avanzate, Università del Piemonte Orientale, c.so Borsalino 54, Alessandria, Italy*

Received 20th March 2003
First published as an Advance Article on the web 6th June 2003

Three different titanium-grafted silicates, with different morphological features were compared in the epoxidation, using *tert*-butylhydroperoxide as oxidant, of methyl oleate, methyl elaidate and of a mixture of methyl esters, obtained from high-oleic sunflower oil. Ti-MCM-41, a well-ordered mesoporous catalyst, showed very high conversions and excellent selectivity on all the substrates. The fatty acid methyl esters derived from renewable raw material were epoxidised selectively with very high yields in a reaction medium completely free from organic acidic compounds. The influence of the pore order of the catalysts on the catalytic performance was also examined. The interactions between the organic substrate and the ordered array of mesopores in Ti-MCM-41 were evidenced.

Introduction

In recent decades much emphasis has been placed on the utilisation of renewable resources as an alternative to fossil and mineral raw materials. In this context, vegetable oils and fats are promising feedstocks. Moreover, thanks to the advancement of oleochemistry technology, a wide range of competitive products, which are both consumer- and environment-friendly, are now available.[1–3] Among these, epoxidised fatty acids and their derivatives have been used for many commercial applications, *e.g.*, as plasticisers and stabilisers in chlorine-containing resins,[4–5] as additives in lubricants,[6] as components in thermosetting plastics,[7] in urethane foams[8] and as wood impregnants.[9]

Epoxy fatty acid compounds are obtained on industrial scale mainly by the Prileshajev peracid process.[2] However, there are several drawbacks to be improved in such a procedure: (i) selectivity to epoxidised products is relatively low due to the acid-catalysed oxirane ring opening; (ii) the separation of acidic by-products, whose presence may be detrimental for further applications, is not easy; (iii) the handling of highly-concentrated hydrogen peroxide and strong acids is dangerous and causes corrosion problems. Thus, several papers in recent years dealt with the setting up of catalytic processes, which could overstep such disadvantages using more sustainable compounds and technologies.[10–13]

With this aim, some heterogeneous titanium-grafted catalytic systems, already extensively tested in the epoxidation of terpenic substrates,[14–15] have been applied to the selective epoxidation of C-18 unsaturated fatty acid methyl esters (FAMEs) using a very stable organic peroxide, *tert*-butylhydroperoxide (TBHP).

Results and discussion

Three titanium-containing silicate materials, namely, Ti-MCM-41 (**A**), Ti–SiO_2 (**B**) and Ti–SiO_2 (**C**), were used as heterogeneous catalysts. In all of them, titanium species were grafted onto the silica surface by the technique proposed by Maschmeyer *et al.*[16] By this grafting procedure, a high surface concentration of accessible, well-spaced and structurally well defined Ti(IV) sites can be obtained on MCM-41. Nevertheless, the catalysts have different structural features: **A** is a titanosilicate with an ordered array of mesopores; **B** is a porous titanosilicate without an ordered network of mesopores; **C** is a non-porous titanosilicate, obtained from pyrogenic silica.

First, the three solids were tested in the epoxidation of two pure unsaturated fatty methyl esters: methyl (*Z*)-9-octadecenoate (methyl oleate; Scheme 1, structure **1**) and methyl (*E*)-9-octadecenoate (methyl elaidate; Scheme 1, structure **2**), the most remarkable difference between them being the steric features. Indeed, in (*Z*)-unsaturated fatty acids (and their derivatives) the configuration of the double bond causes a bend in the carbon chain, which prevents the molecule from having a straight rod-like conformation. On the contrary, in (*E*)-fatty acids the carbon chain is able to be in a straight conformation and their properties resemble those of the corresponding saturated fatty acids. Although elaidic acid derivatives are very rarely found in renewable raw materials (almost all of the

Green Context

Epoxidised fatty acids and their derivatives derived from renewable feedstocks are useful in many commercial applications including lubricant additives, components in plasticisers and wood impregnants. The traditional peracid method of epoxidising the natural compounds takes a lot away from the green chemistry credentials of the final products. The reagents are dangerous to handle and the process leaves acid waste. Here the excellent titanium-based epoxidation procedure developed for simple alkenes is extended to fatty acids for more environmentally benign routes to the useful epoxide products. ***JHC***

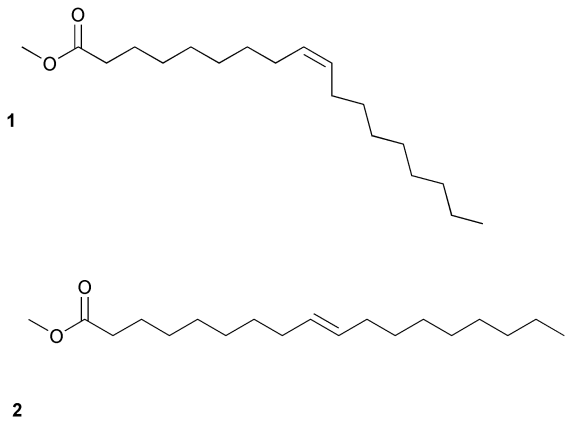

Scheme 1

natural unsaturated fatty acids are in (*Z*)-configuration), they have been here considered because they are often obtained by non-selective partial hydrogenation of polyunsaturated fatty compounds. Ethyl acetate was the solvent of choice, because it is considered an environmentally sustainable medium more than other nitrogen- or chlorine-containing solvents.[12,17] The conversion profiles *vs.* reaction time of **1** and **2** on **A**, **B** and **C** are reported in Fig. 1–3. The selectivity to epoxy-stearate was very high (> 95%) in all cases and no products other than the epoxidised derivatives were identified in the GC-analysis. In fact, the use of TBHP as oxidant remarkably reduces the formation of acid-catalysed by-products and increases the epoxide selectivity.[12] The selectivity towards TBHP was also excellent in all tests and in none of the runs has the organic hydroperoxide been the limiting agent of the reaction. Moreover, the epoxidation reaction ran stereospecifically: only *cis*-epoxy-stearate was selectively obtained from the (*Z*)-isomer and *trans*-epoxy-stearate from the (*E*)-isomer, respectively. This is a significant feature and confirms that epoxidation with

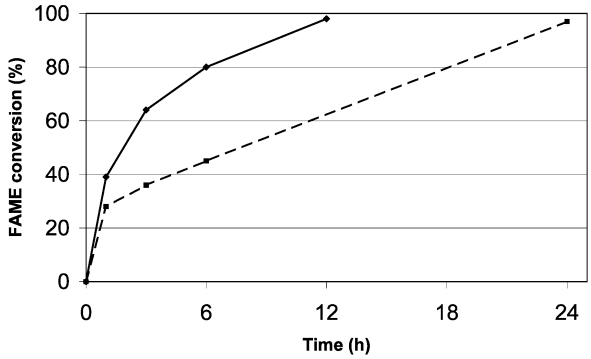

Fig. 1 Conversion of methyl oleate **1** (◆) and methyl elaidate **2** (■) *vs.* reaction time on Ti-MCM-41 (**A**).

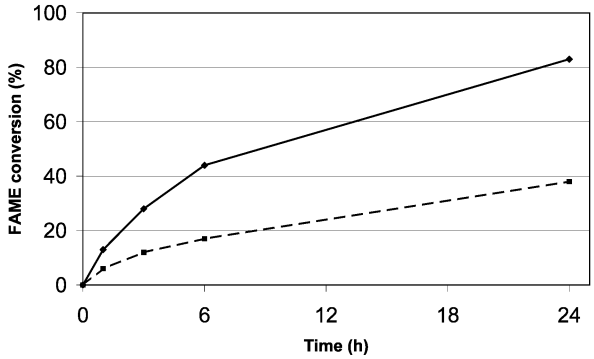

Fig. 2 Conversion of methyl oleate **1** (◆) and methyl elaidate **2** (■) *vs.* reaction time on Ti–SiO_2 (**B**).

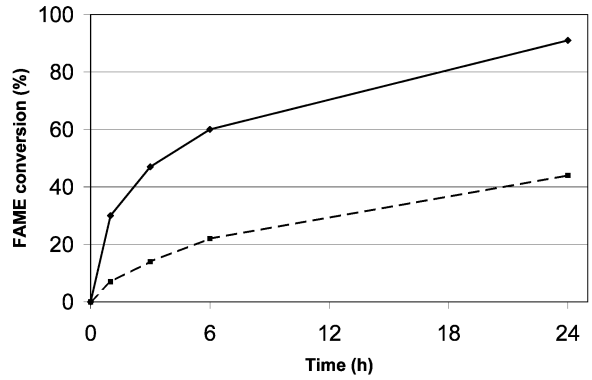

Fig. 3 Conversion of methyl oleate **1** (◆) and methyl elaidate **2** (■) *vs.* reaction time on Ti–SiO_2 (**C**).

TBHP on titanium-based silicate catalysts proceeds *via* a non-radical mechanism with retention of the configuration of the C=C double bond.[18]

Ti-MCM-41 (**A**) is the most active catalyst among the three solids (Fig. 1): **1** was epoxidised almost completely after 12 h and **2** was completely and selectively converted to *trans*-epoxystearate after 24 h. Conversely, neither on **B** nor on **C** the two FAMEs reached complete conversion even after 24 h reaction (Fig. 2 and 3). It is proposed that the excellent performances obtained on Ti-MCM-41 are due to the presence of a high concentration and high dispersion of Ti(IV) tetrahedral active centres,[19–20] which were monitored by DR UV-Vis spectroscopy.† In fact, Ti-MCM-41 (**A**) shows a narrow absorption at *ca.* 210 nm, which indicates the presence of isolated Ti(IV) sites in tetrahedral coordination. On the contrary, both catalysts **B** and **C** exhibit band maxima at $\lambda \geq 240$ nm, which are consistent with a decrease of the tetrahedral character of the titanium environment and with an incipient oligomerisation of Ti(IV) species.[15,19,20]

On all catalysts, methyl oleate **1** was more readily epoxidised than methyl elaidate **2**. The higher activity of **1** is commonly attributed to steric effects: the approach of the double bond in (*Z*)-configuration is, in fact, less hindered than in (*E*)-configuration.[10,11] A comparable behaviour has also been observed in the epoxidation of *cis*- and *trans*-stilbene on a similar Ti-MCM-41 catalyst: *cis*-stilbene was easily epoxidised, whereas only negligible amounts of the *trans*-isomer were converted.[18]

Table 1 Turnover frequencies in the epoxidation of **1** and **2**

Catalyst[a]	TOF on substrate/h^{-1}		TOF **1** : TOF **2** ratio
	1[b]	**2**[c]	
A	56	40	1.4
B	20	9	2.2
C	47	11	4.3

[a] Reaction conditions: AcOEt solvent; 363 K; TBHP : FAME molar ratio = 1.33; FAME : catalyst molar ratio = 160. [b] Turnover frequency ([mol converted **1**] [mol Ti]$^{-1}$ h^{-1}) after 1 h. [c] Turnover frequency ([mol converted **2**] [mol Ti]$^{-1}$ h^{-1}) after 1 h.

It is noteworthy that, after 1 h reaction (Table 1), the maximum gap between the epoxidation rate of **1** and **2** was recorded on the Ti–SiO_2 (**C**), that does not show any micro- or meso-porosity: indeed, the (*Z*)-isomer **1** reacted four times faster than the (*E*)-isomer **2**. On porous non-ordered catalyst **B** the gap decreased and **1** was epoxidised two times faster than **2**.

† DR UV-Vis spectra were obtained on a Perkin Elmer (Lambda 900) spectrometer equipped with an integrating sphere attachment. The measurements were conducted at room temperature under strict exclusion of air.

These values resemble those reported in previous works on completely different catalytic systems: the oleic ester was epoxidised 2 and 2.5 times faster than the elaidic ester on molybdenum–tin on charcoal[10] and on molybdenum on alumina,[11] respectively. Nevertheless, whenever epoxidation was carried out on solid **A**, which has an ordered array of parallel pores, the difference in activity between **1** and **2** became the smallest (Table 1) and methyl elaidate **2** was completely converted after 24 h. To our knowledge, this is the first time in which such a small difference has been recorded in the epoxidation of these two substrates.

The results obtained on catalyst **A** suggest that the straight aliphatic chains of the (*E*)-isomer **2** could fit inside the cylindrical-shape pores of Ti-MCM-41 more easily than the bent chains of the (*Z*)-isomer **1**. In fact, the location of the C=C double bond in the middle of the carbon chain ($\Delta^{9,10}$), as in **1** and **2**, amplifies the difference in steric hindrance between the (*Z*)- and the (*E*)-isomer. So, when the double bond is in (*Z*)-configuration, the oxygen-transfer during the epoxidation reaction is favoured, whilst the fitting into the straight mesopores is not. When the double bond is in (*E*)-configuration, the opposite is true: the fitting is easier, whilst the epoxidation is more difficult. Such a counterbalance reduced the gap in the reactivity of **1** *vs.* **2**. However, since the pore dimensions of the catalyst are large enough to allow good diffusion of both **1** and **2**, the interactions between Ti-MCM-41 and the substrates are likely to be not only of steric nature. In fact, also the hydrophobic–hydrophilic properties of the molecular sieves may play a key role in the epoxidation of fatty esters[12] and, therefore, the polar interactions between the FAME molecules and the hydrophilic silicate walls may be considerably influenced by the position of the two hydrophobic aliphatic moieties with respect to the C=C bond.

In summary, on catalyst **A** both **1** and **2** displayed very good activity values because of the high intrinsic reactivity of the titanium sites; concurrently, the balance of the different steric and/or polar interactions cut down the gap in the rate of epoxidation of **1** and **2** on catalyst **A**.

The titanosilicate systems were also tested in the epoxidation of a mixture of methyl esters, whose major constituent is methyl oleate and which was obtained from a natural renewable source, high-oleic sunflower oil. The results are summarised in Table 2.

Table 2 Catalytic performances in the epoxidation of a mixture of high-oleic sunflower oil methyl esters

Catalyst[a]	*C*[b] (%)	*S*[c] (%)	TOF[d]/h^{-1}
A	98	85	71
B	76	94	44
C	95	96	47

[a] Reaction conditions: AcOEt solvent; 363 K; TBHP : FAME molar ratio = 1.33; FAME : catalyst molar ratio = 160. [b] Conversion of unsaturated FAMEs after 24 h. [c] Selectivity to mono-epoxy compounds after 24 h. [d] Turnover frequency ([mol converted FAME] [mol Ti]$^{-1}$ h^{-1}) after 1 h reaction.

Ti-MCM-41 (**A**) showed excellent activity with such a mixture of FAMEs as well. The trend of the TOF values on this mixture (**A** > **C** ≥ **B**) parallels the order observed in the epoxidation of **1** and **2**. Nevertheless, solid **A** displayed the lowest selectivity to mono-epoxides. These data are mainly explained by the excellent activity of **A** itself, which leads to the double epoxidation of the diene fraction in sunflower methyl ester (here 9.7 wt%) and therefore to the transformation of the already formed mono-epoxides into di-epoxides. On the contrary, the epoxidation reaction on **B** and **C** stopped before the doubly-epoxidised derivatives were formed. The low mono-epoxy selectivity could be also explained, to a lesser extent, by the higher intrinsic acidic character of **A** with respect to the other two titanosilicates, as showed elsewhere.[15] The acidic properties of titanium centres in **A** may account for the formation of tiny amounts of acid-catalysed by-products (mostly methyl oxostearate) during the 24 h reaction. It is worth noting that, using catalysts **A** and **C**, virtually all the unsaturated FAMEs were converted at the end of the 24 h time. On the contrary, catalyst **B** showed, after a short reaction time (1 h), a behaviour similar to **C**, whereas, after longer times (24 h), a sort of deactivation of the catalytic site took place and the reaction did not reach completion after 24 h. With regard to the productivity after 24 h, the use of an ordered mesoporous material, such as Ti-MCM-41 (**A**), in the epoxidation of the sunflower methyl esters is not strictly essential, under the conditions adopted in this work.

Conclusions

Titanium-grafted silicates were shown to be efficient heterogeneous catalysts in the epoxidation of unsaturated fatty acid methyl esters in a reaction medium completely free from organic acidic compounds. In particular, Ti-MCM-41 (**A**) displayed very high activity and selectivity in the epoxidation of methyl oleate and elaidate, due to the presence of isolated tetrahedral Ti(IV) active sites. Interesting performances were also observed on non-ordered catalysts obtained by means of easy and cheap synthesis methodologies. However, the structural features of an ordered solid, such as Ti-MCM-41 catalyst, are necessary whenever methyl elaidate has to be converted completely and selectively to *trans*-epoxystearate. Fatty methyl esters derived directly from renewable raw materials were also epoxidised selectively, and with very high yields, on titanosilicates catalysts.

Experimental

Catalysts

The siliceous MCM-41 was synthesised according to literature methods.[21] The as-synthesised MCM-41 was calcined at 823 K in flowing oxygen (80 mL min^{-1}) for 10 h to remove the templating surfactant before anchoring the titanium.

Ti-MCM-41 (**A**), Ti–SiO_2 (**B**) and Ti–SiO_2 (**C**) were obtained respectively from siliceous MCM-41, from SiO_2 Davison 62 (Grace) and from SiO_2 Aerosil 380 (Degussa) by grafting titanium sites, using a solution of titanocene dichloride ($TiCp_2Cl_2$; Fluka) in chloroform (Carlo Erba, RPE) and triethylamine (Aldrich).[16,22] All catalysts were calcined at 823 K in flowing oxygen (80 mL min^{-1}) for 6 h before use.

BET specific surface area and pore diameters were determined by N_2-adsorption at 77 K using a Micromeritics ASAP 2010 apparatus. Table 3 reports the BET surface area, the mean pore sizes and the titanium loading, determined by ICP-AES,[14] of the three catalysts. Pyrogenic material **C** showed neither micro- nor meso-porosity.

Table 3 Specific surface area (S_{BET}), mean pore diameter (D_p) and titanium loadings of the solid samples after calcination

	Catalyst	S_{BET}/m^2 g^{-1}	D_p/nm	Ti content (wt.%)
A	Ti-MCM-41	955	2.5	1.88
B	Ti–SiO_2 Davison	303	12.7	1.75
C	Ti–SiO_2 Aerosil	268	n.d.[a]	1.78

[a] Not determined.

Catalytic tests

Methyl oleate **1** and methyl elaidate **2** were used as received from Aldrich and Fluka, respectively. The fatty acid methyl ester mixture was obtained from high-oleic sunflower oil, kindly supplied by Tampieri S.p.A., Faenza (Italy), by esterification with $NaOCH_3$ and following distillation. The composition of the FAME mixture is (wt.%): oleate (84.0), linoleate (9.7), stearate (3.5), palmitate (1.7), erucate (0.5), others (0.6).

The epoxidation tests were carried out under inert atmosphere in a glass batch reactor at 363 K using ethyl acetate as solvent (solvent/substrate volume ratio = 8), anhydrous *tert*-butylhydroperoxide as oxidant (oxidant/substrate molar ratio = 1.33) and substrate/catalyst molar ratio = 160. Samples were taken after a reaction time of 1, 3, 6, 12 and 24 h and the products analysed by GC-MS (methyl palmitate as internal standard) and ^{1}H-NMR spectroscopy.

The need for titanium as an effective active site on which epoxidation takes place was first checked. Neither significant auto-oxidation nor support-catalysed contributions to epoxidation were recorded in epoxidation tests with titanium-free siliceous supports.

The presence of the oxidant at the end of each reaction was systematically checked by means of either GC analysis or iodometric titration and a sensible amount of unreacted TBHP was always found after every catalytic run.

Acknowledgements

The authors express their gratitude to Dr. Paola Tampieri for the supply of a sample of high-oleic sunflower oil. Mr. Pasquale Illiano is also gratefully acknowledged for the recording of the NMR spectra.

References

1 K. Hill, *Pure Appl. Chem.*, 2000, **72**, 1255.
2 U. Biermann, W. Friedt, S. Lang, W. Lühs, G. Machmüller, J. O. Metzger, M. Rüsch gen. Klaas, H. J. Schäfer and M. Schneider, *Angew. Chem., Int. Ed.*, 2000, **39**, 2206.
3 *Recent developments in the synthesis of fatty acid derivatives*, ed. G. Knothe, J. T. P. Derksen, AOCS press, Champaign, IL, 1999.
4 F. P. Greenspan and R. J. Gall, *Ind. Eng. Chem.*, 1953, **45**, 2722.
5 H. Naito and H. Naito, *Int. Appl. Pat.*, WO 99 27,009, 1999.
6 G. Bert, *DE Pat.*, 4,201,343, 1993.
7 M. Skwiercz, C. Priebe and K. Boege, *DE Pat.*, 19,834,048, 2000.
8 H. Kluth, P. Daute, J. Klein, R. Gruetzmacher and W. Klauck, *DE Pat.*, 4,202,758, 1993.
9 M. Niki and K. Otani, *JP Pat.*, 02,206,613, 1989.
10 Y. Itoi, M. Inoue and S. Enomoto, *Bull. Chem. Soc. Jpn.*, 1986, **59**, 3941.
11 A. Debal, G. Rafaralahitsimba and E. Ucciani, *Fat Sci. Technol.*, 1993, **95**(6), 236.
12 M. A. Camblor, A. Corma, P. Esteve, A. Martìnez and S. Valencia, *Chem. Commun.*, 1997, 795.
13 I. V. Kozhevnikov, G. P. Mulder, M. C. Steverink-de Zoete and M. G. Oostwal, *J. Mol. Catal. A: Chem.*, 1998, **134**, 223.
14 C. Berlini, M. Guidotti, G. Moretti, R. Psaro and N. Ravasio, *Catal. Today*, 2000, **60**, 219.
15 M. Guidotti, N. Ravasio, R. Psaro, G. Ferraris and G. Moretti, *J. Catal.*, 2003, **214**(2), 247.
16 T. Maschmeyer, F. Rey, G. Sankar and J. M. Thomas, *Nature*, 1995, **378**, 159.
17 W. H. Cheung, W. Y. Yu, W. P. Yip, N. Y. Zhu and C. M. Che, *J. Org. Chem.*, 2002, **67**, 7716.
18 R. D. Oldroyd, J. M. Thomas, T. Maschmeyer, P. A. MacFaul, D. W. Snelgrove, K. U. Ingold and D. D. M. Wayner, *Angew. Chem., Int. Ed.*, 1996, **35**, 2787.
19 L. Marchese, T. Maschmeyer, E. Gianotti, S. Coluccia and J. M. Thomas, *J. Phys. Chem. B*, 1997, **101**, 8836.
20 L. Marchese, E. Gianotti, V. Dellarocca, T. Maschmeyer, F. Rey, S. Coluccia and J. M. Thomas, *Phys. Chem. Chem. Phys.*, 1999, **1**, 585.
21 A. T. Kresge, M. E. Leonowicz, W. J. Roth, J. C. Vartuli and J. S. Beck, *Nature*, 1992, **359**, 710.
22 M. Guidotti, L. Conti, A. Fusi, N. Ravasio and R. Psaro, *J. Mol. Catal. A*, 2002, **182–183C**, 131.

Epoxidation of α,β-unsaturated ketones in water. An environmentally benign protocol

G. Fioroni, F. Fringuelli,* F. Pizzo* and L. Vaccaro

Department of Chemistry, University of Perugia – Perugia, Italy. E-mail: frifra@unipg.it; pizzo@unipg.it; Fax: +39 075 5855560; Tel: +39 075 5855546

Received 7th April 2003
First published as an Advance Article on the web 9th June 2003

An easy, cheap procedure is proposed for the epoxidation of α,β-unsaturated ketones in water as the sole reaction medium and using bases such as NaOH and CTAOH as promoting agents and hydrogen peroxide as oxidant. By using solely water, the reaction medium can be recycled which is important for reducing wastes. An example of an α-functionalization of α,β-unsaturated ketones by a *one-pot* procedure in water is reported.

Introduction

Waste minimization[1] is a very important aspect of an environmentally benign protocol. Practically, this means performing reactions with high conversions, using green reagents and a green reaction medium followed by an efficient recycling program. Examples of reusing the aqueous reaction medium are rare.[2] The recycling of organic solvents requires that they be purified by distillation, while the recycling of ionic liquids is difficult because immiscible organic solvents are required to separate the products. The use of water alone (without co-solvents) as reaction medium overcomes these problems and makes recycling very easy and cheap. In addition, the aqueous medium allows one-pot multi-step processes to be performed.

For several years we have been interested in performing organic reactions in water alone and have investigated chemoselective oxidations,[3] epoxidations of olefins and allylic alcohols,[4] aldol-like condensations,[5,2b] Diels–Alder cycloadditions,[6] nucleophilic ring opening of oxiranes,[7] and reduction of azides.[8] Recently we showed that even Lewis acids, such as $AlCl_3$, $TiCl_4$ and $SnCl_4$, for which anhydrous conditions are recommended, can be used as catalysts in water, if the pH of the aqueous medium is controlled.[2a,9]

As a continuation of these studies and in an effort to develop a clean chemistry, we are interested in the α-functionalization of α,β-unsaturated ketones by a one-pot procedure in water as sole reaction medium. The epoxidation of α,β-unsaturated ketones is the first step of this strategy.

α,β-Epoxyketones are used as constituents in perfume formulations, as intermediates in the production of flavouring substances[10] and are important building blocks in organic synthesis because they allow a regioselective functionalization of α,β-unsaturated ketones by nucleophilic ring-opening of the oxirane ring.

Homogeneous epoxidations of α,β-unsaturated ketones using hydrogen peroxide under alkaline conditions (NaOH, KOH, LiOH, Na_2CO_3, K_2CO_3) in aqueous methanol or in solely methanol is the most common procedure.[10a,b,11] Under these conditions a large amount of methanol is used to solubilize the ketone, and when H_2O_2 is used in large excess, oxidation by-products and a competing aldol-type condensation are observed.[12] Recently heterogeneous epoxidations of α,β-unsaturated ketones were developed using H_2O_2 in various reaction media (H_2O, PhMe, MeOH, H_2O–PhMe, dioxane, PhMe–CH_2Cl_2) and promoted by basic hydrotalcites[13] and amberlyst A-26 supported hydroperoxide,[14] polymer-bound quaternary ammonium salts[15] and short solid phase-bound peptides[16] in the presence of bases (NaOH, LiOH, Na_2CO_3), or carried out in phase-transfer (H_2O(NaOH)–PhMe, H_2O(LiOH)–Bu_2O) promoted by micellar aggregates[12c,13b] and quaternary ammonium salts.[17] Ionic liquids (1-butyl-3-methylimidazolium tetrafluoroborate [bmim][BF_6], H_2O_2, NaOH)[18] and titanium-containing zeolites under liquid-phase conditions were recently used.[19]

To our knowledge only one[13c] investigation of the epoxidation of α,β-unsaturated ketones carried out in water alone has been reported. Here we report an efficient procedure for the epoxidation of α,β-enones in water as sole reaction medium. The protocol is a combination of three green techniques that effectively improve the environmental performance of the reaction: (i) the oxidation with H_2O_2 (one of the safest and least wasteful oxidants[20]), (ii) the use of water as sole reaction medium (the least environmentally threatening solvent), and (iii) the recycling of the reaction medium (an important way to reduce wastes). An example of α-functionalization of α,β-unsaturated ketones by a *one-pot* procedure in water is also reported.

Results and discussion

3-Hepten-2-one (**1**), isophorone (**2**), 2-methyl-1,4-naphthoquinone (**3**) and *trans*-chalcone (**4**) were chosen as representative compounds because of their markedly different reactivities and solubilities in water. Ketone **1** was totally soluble, **2** was partially soluble and poorly reactive, **3** and **4** were practically insoluble but **3** was very reactive. Epoxidation in water at 0–2 °C with H_2O_2 (1.5–2.0 molar equiv.) and using NaOH as base (0.1–1.7 molar equiv.) [procedure A] allowed the epoxyketone to be isolated quickly and in excellent yields only when the starting materials were sufficiently soluble in water (Table 1,

Green Context

Epoxidation is one of the most important synthetic methods since it can easily add considerable value to a simple substrate. Apart from oxygen, hydrogen peroxide is the most environmentally and economically attractive oxidant. Here we see how this oxidant can be applied to the epoxidation of α,β-unsaturated ketones in a methodology that has the added attraction of being water-based and involving only a single step. ***JHC***

entries, 1, 4, and 7). Discouraging results were obtained in the case of very low solubility (Table 1, entry 10). Interestingly the epoxidation of **1** occurred in less than 30 minutes under these very mild conditions; it had been expected to be poorly reactive.[13b,c]

To evaluate the importance of the solubilization of the reagents and the role of water, epoxidations were also carried out in aqueous methanol, under the same above-mentioned reaction conditions of temperature and concentration. Excellent results were obtained for poorly water-soluble **3** and **4**, while ketones **1** and **2**, present in large amounts in the aqueous medium, gave low reaction conversions. This shows that water, as reaction medium, plays a specific role that is still not understood.[6b] Consequently the results sometimes seem to be conflicting. The methanol increases the solubility of organic substrates but destroys the liquid water structure.[6b]

To generalize this procedure, the commercial cetyltrimethylammonium hydroxide (CTAOH, 0.1–1.7 molar equiv.) in water was used at 0–2 °C [procedure B]. CTAOH had a great beneficial effect on all the ketones (Table 1, entries 3, 6, 9, and 12) because it favours the solubility of ketone in aqueous medium, assures the necessary basic environment, and sometimes accelerates the reaction (Table 1, entries 6 and 9). A catalytic amount or a light stoichiometric excess of CTAOH greatly enhanced the epoxidation rate of isophorone (**2**), 2-methyl-1,4-naphtoquinone (**3**) and chalcone (**4**) (Table 1, entries 6, 9, and 12) that usually give very little of the corresponding 1,2-epoxides.[13b,c] The CTAOH- protocol was applied to other α,β-unsaturated ketones. The results are illustrated in Table 2. Quantitative conversions were always observed and the epoxyketones were obtained in high yields.

The recycling of aqueous medium was investigated using the same representative compounds **1–4** and following either protocol A or B. When the reaction was carried out on a small scale the resulting epoxyketone was separated by extraction with diethyl ether. When large quantities of enone were used the liquid product was separated by using a separatory funnel without adding organic solvent. Solid α,β-epoxyketones were separated by büchner filtration. Table 3 illustrates the results obtained using 50 mmol of substrate. The final basic aqueous phase (mother liquor) was reused in subsequent runs. If the pH of the mother liquor was 13 only the necessary amount of hydrogen peroxide was added. Otherwise, it was necessary to first adjust the pH value to 13 by adding some drops of NaOH

Table 2 Epoxidation of α,β-unsaturated ketones in water with CTAOH at 0–2 °C

Ketone	H_2O_2 (CTAOH)/ molar equiv.	Time/ h	1,2-Epoxide	*C*[a] (%)	Yield (%)
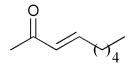	1.5 (0.25)	0.5	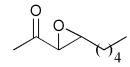	99	82
	1.5 (0.5)	0.25		98	75[b]
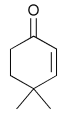	1.5 (0.5)	4	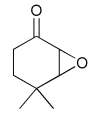	95	80[c]
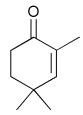	1.5 (1.5)	3	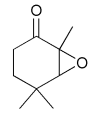	95	80
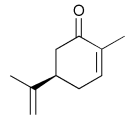	2 (0.5)	1	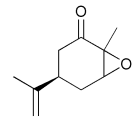	95	90
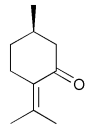	4 (1.5)	4	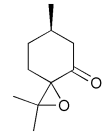	98	75[d]
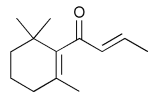	4 (0.2)	2	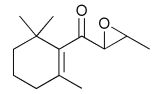	99	85
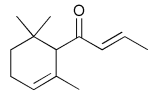	4 (0.2)	1.5	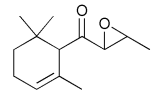 (51 : 49)	95	82[e]

[a] Reaction conversion. [b] Using procedure A, *C* (%) and yield (%) were 99 and 80, respectively. [c] Using procedure A, *C* (%) and yield (%) were 95 and 90, respectively. [d] 54 : 46 *cis*/*trans* diastereoisomeric mixture. [e] 46 : 54 *syn*/*anti* diasteroisomeric mixture.

Table 1 Epoxidation of α,β-unsaturated ketones in aqueous medium at 0–2 °C

Entry	Ketone	Protocol	Reaction medium	H_2O_2/ molar equiv.	Base/ molar equiv.	Time/h	1,2-Epoxide	*C* (%)[b]	Yield (%)[c]
1	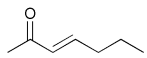 1	A	H_2O	1.5	NaOH (0.5)	0.5	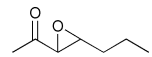	99	90
2			H_2O/MeOH[a]	1.5	NaOH (0.5)	0.5		25	
3		B	H_2O	1.5	CTAOH (0.1)	0.5		97	89
4	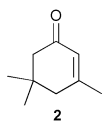 2	A	H_2O	1.5	NaOH (0.5)	8	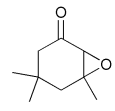	98	90
5			H_2O/MeOH[a]	1.5	NaOH (0.5)	6		70	50
6		B	H_2O	1.5	CTAOH (0.1)	6		96	90
7	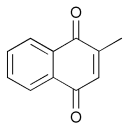 3	A	H_2O	1.5	NaOH (0.5)	3	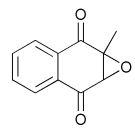	95	84
8			H_2O/MeOH[a]	1.5	NaOH (0.5)	3		95	90
9		B	H_2O	1.5	CTAOH (0.1)	1		95	90
10	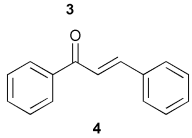 4	A	H_2O	2	NaOH (1.7)	2	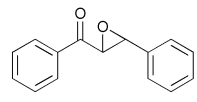	5	
11			H_2O/MeOH[a]	2	NaOH (1.7)	2		98	90
12		B	H_2O	2	CTAOH (1.7)	2		98	85

[a] H_2O/MeOH, 1:4 v/v [b] reaction conversion [c] yield of isolated product.

Table 3 Recycling of aqueous mother liquor in the epoxidation of α,β-unsaturated ketones[a]

Ketone	Protocol	Base/molar equiv.	Time/h	Yield (%)[b]
1	A	NaOH (0.5)	0.5	90
	A	2nd run	0.5	92
	A	3rd run	0.5	92
2	A	NaOH (0.5)	8	90
	A	2nd run	8	90
3	B	CTAOH (0.1)	1	90
	B	2nd run	1	95
	B	3rd run	1	95
	B	4th run	1	98
4	B	CTAOH (1.7)	2	80
	B	2nd run	2	79
	B	3rd run	2	84

[a] Reactions carried out starting from 50 mmol of ketones. [b] Yield of isolated product.

aqueous solution. In all runs, the reaction conversions and yields of the isolated products were excellent and the reaction times did not vary. In the second and third runs, higher yields were sometimes found. If the α,β-epoxyketone product was highly hydrophilic and procedure B was used, it was difficult to completely extract it from the aqueous medium using the customary laboratory techniques. Therefore the aqueous medium used for the second run already contained the equilibrium amount of α,β-epoxyketone. The low concentration of H_2O_2 and the basic medium used favour recycling because under these reaction conditions H_2O_2 decomposes very little[12] which greatly reduces the production of secondary oxidation products.

These results allowed α,β-unsaturated ketones to be functionalized in the α-position by a *one-pot* procedure carried out exclusively in aqueous medium. An example is the synthesis of 2-phenylthio-2-cyclohexene-1-one (**6**). 2-cyclohexene-1-one (**5**) which was reacted with H_2O_2 (1.5 molar equiv.) in aqueous NaOH at 0–2 °C to give the α,β-epoxycyclohexanone that *in situ* was treated with thiophenol at 30 °C. Thiol nucleophilic attack and water-elimination occurred in 30 min and 2-thiophenyl-2-cyclohexen-1-one (**6**) was isolated in 90% overall yield[22]

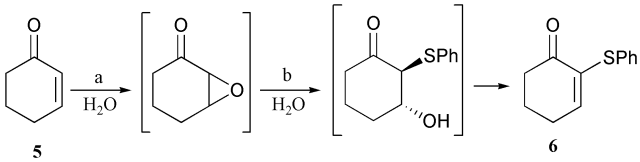

5 6

Scheme 1 *One-pot* synthesis of 2-thiophenyl-2-cyclohexene-1-one.

(Scheme 1). This procedure was faster and easier than that most recently reported in the literature, *i.e.* the phenylsulfenylation of cyclohexanone with phenylsulfenyl chloride in dry CH_2Cl_2–MeCN at r.t. for 24 h.

This α-substitution reaction is now being extended to different α,β-unsaturated ketones and to various functional groups.

Conclusions

An easy epoxidation of α,β-unsaturated ketones was carried out in water at 0–2 °C using a low concentration of H_2O_2 and generally catalytic amounts of NaOH or CTAOH. The re-use of the basic aqueous medium, makes this protocol clean, inexpensive and environmentally safe.

Experimental

General

All chemicals were purchased and used without any further purification. ^{1}H NMR spectra (200 MHz) were recorded in ppm (δ) downfield from Me_4Si (δ = 0.00) in $CDCl_3$ as solvent. The nature and purity of the products were determined by GC, IR and GC–MS analyses and ^{1}H NMR spectroscopy.

The 1,2-epoxides are all known in the literature[10c,13b,c,21] except the epoxide arising from the epoxidation of 2,4,4-trimethyl-cyclohex-2-en-1-one. The structure of **6** was consistent with that reported in the literature.[22]

Procedure A

In a standard procedure, 0.112 g (1.0 mmol) of 3-hepten-2-one (**1**) and 0.25 mL (0.5 molar equiv.) of 2 M NaOH aqueous solution were dissolved in 1.62 mL of water at 0–2 °C. After stirring at this temperature for 10 minutes, 0.13 mL of 35 wt% aqueous hydrogen peroxide (1.5 molar equiv.) was added. After 0.5 h, the product was extracted with three 10 mL portions of diethyl ether. The organic phase was dried over Na_2SO_4 and evaporated under reduced pressure to give 0.116 g of 3,4-epoxy-2-heptanone with 99% purity.

Procedure B

In a standard procedure, 0.172 g (1.0 mmol) of 2-methyl-1,4-naphtoquinone (**3**) and 0.3 mL (0.1 molar equiv.) of 10 wt% CTAOH were dissolved in 4.57 mL of water at 0–2 °C. After stirring at this temperature for 10 minutes, 0.13 mL of 35 wt% aqueous hydrogen peroxide (1.5 molar equiv.) was added. After 1 h, the reaction was complete and the product was separated by filtration, to give 0.170 g of epoxide with 95% purity.

Recycling of the aqueous medium

According to procedure B, the mother liquor derived from the epoxidation of **3** (on 50.0 mmol scale) was prepared for re-use by first adjusting the pH to 13 and then adding 1.5 molar equiv. of H_2O_2 35 wt% and 2-methyl-1,4-naphthoquinone (50 mmol). The results are reported in Table 3.

The mother liquor derived from the epoxidation procedure A was recovered and prepared for re-use in the same way.

One-pot synthesis of 2-phenylthio-2-cyclohexen-1-one (6)

0.196 g (2.0 mmol) of 2-cyclohexenone (**5**) and 0.25 mL (0.5 molar equiv.) of 2 M NaOH aqueous solution were dissolved in 1.62 mL of water at 0–2 °C. After stirring at this temperature for 10 minutes, 0.13 mL (1.5 molar equiv.) of 35 wt.% aqueous hydrogen peroxide was added. After 0.5 h, 0.215 mL (1.05 molar equiv.) of thiophenol were added at 30 °C and the stirring was continued for 30 min. The reaction mixture was then extracted with three 5 mL portions of diethyl ether. The organic phase was dried over Na_2SO_4 and evaporated under reduced pressure to give the title product in 90% overall yield.

2,4,4-trimethyl-2,3-epoxycyclohexan-1-one

Oil; IR (CCl_4) ν = 910 (s), 1380 (m), 1715 (s), 2900 (w); H^1 NMR ($CDCl_3$) δ = 1.07 (s, 3H, Me-4); 1.19 (s, 3H, Me-4); 1.39 (s, 3H, Me-2); 1.66–2.74 (m, 4H); 3.01 (s, H-3); GC/MS: (154) *m*/*z* (%): 154 (4, M^+), 111 (32), 97 (19), 83 (49), 69 (100), 55

(54). Anal. calc. for $C_9H_{14}O_2$ (154): C, 70.10; H, 9.15. Found: C, 70.12; H, 9.10%.

Acknowledgements

The Ministero dell'Università e della Ricerca Scientifica e Tecnologica (MURST) and the Consiglio Nazionale delle Ricerche (CNR) are thanked for financial support.

References

1 (*a*) P. T. Anastas and J. C. Warner, *Green Chemistry: Theory and Practice*, Oxford University Press., Oxford, 1998; (*b*) P. Tundo and P. T. Anastas, *Green Chemistry: Challenging Perspectives*, Oxford University Press, Oxford, 1999.

2 (*a*) F. Fringuelli, F. Pizzo and L. Vaccaro, *Tetrahedron Lett.*, 2001, **42**, 1131–1133; (*b*) D. Amantini, F. Fringuelli, O. Piermatti, F. Pizzo and L. Vaccaro, *Green Chem.*, 2001, **3**, 229–232; (*c*) F. Fringuelli, F. Pizzo and L. Vaccaro, *J. Org. Chem.*, 2001, **66**, 3554–3558.

3 (*a*) F. Fringuelli, R. Germani, F. Pizzo and G. Savelli, *Gazz. Chim. Ital.*, 1989, **119**, 249; (*b*) F. Fringuelli, R. Pellegrino and F. Pizzo, *Synth. Commun.*, 1993, **23**, 3157–3163; (*c*) F. Fringuelli, R. Pellegrino, O. Piermatti and F. Pizzo, *Synth. Commun.*, 1994, **24**, 2665–2673; (*d*) F. Fringuelli, O. Piermatti and F. Pizzo, in *Organic Synthesis in Water*, ed. P. A. Grieco, Blackie Academic and Professional, London, 1998, 223–247.

4 (*a*) F. Fringuelli, R. Germani, F. Pizzo and G. Savelli, *Tetrahedron Lett.*, 1989, **30**, 1427–1428; (*b*) F. Fringuelli, R. Germani, F. Pizzo and G. Savelli, *Org. Prep. Proced. Int.*, 1989, **21**, 757–761; (*c*) F. Fringuelli, R. Germani and F. Pizzo, *Synlett*, 1991, 475–476; (*d*) F. Fringuelli, R. Germani, F. Pizzo, F. Santinelli and G. Savelli, *J. Org. Chem.*, 1992, **57**, 1198–1202; (*e*) D. Ye, F. Fringuelli, O. Piermatti and F. Pizzo, *J. Org. Chem.*, 1997, **62**, 3748–3750; (*f*) F. Fringuelli, O. Piermatti and F. Pizzo, *Trends Org. Chem.*, Pb. Research Trends T. C., 1997, **6**, 181–197.

5 (*a*) F. Fringuelli, G. Pani, O. Piermatti and F. Pizzo, *Tetrahedron*, 1994, **50**, 11499–11508; (*b*) F. Fringuelli, G. Pani, O. Piermatti and F. Pizzo, *Life Chem. Rep.*, 1995, **13**, 133–140; (*c*) G. Brufola, F. Fringuelli, O. Piermatti and F. Pizzo, *Heterocycles*, 1996, **43**, 1257–1266; (*d*) G. Brufola, F. Fringuelli, O. Piermatti and F. Pizzo, *Heterocycles*, 1997, **45**, 1715–1721; (*e*) F. Fringuelli, O. Piermatti and F. Pizzo, in *Organic Synthesis in Water*, ed. P. A. Grieco, Blackie Academic and Professional, London, 1998, 250–261.

6 (*a*) F. Fringuelli, O. Piermatti and F. Pizzo, *Targets in Heterocyclic Systems, Chemistry and Properties*, 1997, **1**, 57–73; (*b*) F. Fringuelli, O. Piermatti, F. Pizzo and L. Vaccaro, *Eur. J. Org. Chem.*, 2001, **3**, 439–455; (*c*) O. Attanasi, L. De Crescentini, P. Filippone, F. Fringuelli, F. Mantellini, M. Matteucci, O. Piermatti and F. Pizzo, *Helv. Chim. Acta*, 2001, **84**, 513–525; (*d*) F. Fringuelli, M. Matteucci, O. Piermatti, F. Pizzo and M. C. Burla, *J. Org. Chem.*, 2001, **66**, 4661–4666; (*e*) D. Amantini, F. Fringuelli and F. Pizzo, *J. Org. Chem.*, 2002, **67**, 7238–7243.

7 (*a*) F. Fringuelli, O. Piermatti, F. Pizzo and L. Vaccaro, *J. Org. Chem.*, 1999, **64**, 6094–6096; (*b*) F. Fringuelli, F. Pizzo and L. Vaccaro, *Synlett*, 2000, 311–314; (*c*) D. Amantini, F. Fringuelli, F. Pizzo and L. Vaccaro, *J. Org. Chem.*, 2001, **66**, 4463–4467; (*d*) F. Fringuelli, F. Pizzo, S. Tortoioli and L. Vaccaro, *Adv. Synth. Catal.*, 2002, **344**, 379–384.

8 (*a*) F. Fringuelli, F. Pizzo and L. Vaccaro, *Synthesis*, 2000, **5**, 646–650; (*b*) D. Amantini, F. Fringuelli, F. Pizzo and L. Vaccaro, *Org. Prep. Proced. Int.*, 2002, **34**, 111–147.

9 F. Fringuelli, F. Pizzo and L. Vaccaro, *J. Org. Chem.*, 2001, **66**, 4719–4722.

10 (*a*) T.-L. Ho and S. H. Liu, *Synth. Commun.*, 1983, **13**, 685–690; (*b*) T.-L. Ho and S. H. Liu, SCM Glidco Organics Corp., US, 1981, 4359586; (*c*) K. H. Schulte-Elte and D. Kastner, Firmenich SA, EP, 1985, 181475.

11 (*a*) H. O. House and R. L. Wasson, *J. Am. Chem. Soc.*, 1957, **79**, 1488–1492; (*b*) D. Felix, C. Wintner and A. Eschenmoser, *Org. Synth.*, 1976, **55**, 52–56; (*c*) M. E. Kuehne and J. A. Nelson, *J. Org. Chem.*, 1970, **35**, 161–170; (*d*) H. H. Westen, *Helv. Chim. Acta*, 1964, **47**, 575–590; (*e*) N. Lindquist, M. A. Battiste, W. M. Whitten, N. H. Williams and L. Strekowski, *Phytochemistry*, 1985, **24**, 863–865; (*f*) P. Dowd, R. Hershline, S. W. Ham and S. Naganathan, *Nat. Prod. Rep.*, 1994, **11**, 251–264; (*g*) A. L. Smith, S. F. Williams and A. B. Holmes, *J. Am. Chem. Soc.*, 1988, **110**, 8696–8698; (*h*) B. Boyer, A. Hambardzoumian, G. Lamaty, A. Leydet, J. -P. Roque and G. Bouchet, *New J. Chem.*, 1996, **20**, 985–988; (*i*) S. Arai, H. Tsuge and T. Shioiri, *Tetrahedron Lett.*, 1998, **39**, 7563–7566.

12 (*a*) R. D. Temple, *J. Org. Chem.*, 1970, **35**, 1275–1280; (*b*) M. G. Evans and N. Uri, *Trans. Faraday Soc.*, 1949, **45**, 224–230; (*c*) B. Boyer, A. Hambardzoumian and J. -P. Roque, *Tetrahedron*, 1999, **55**, 6147–6152.

13 (*a*) B. M. Choudary, M. L. Kantam, B. Bharathi and C. V. Reddy, *Synlett*, 1998, **11**, 1203–1204; (*b*) K. Yamaguchi, K. Mori, T. Mizugaki, K. Ebitani and K. Kaneda, *J. Org. Chem.*, 2000, **65**, 6897–6903; (*c*) T. Hanma, M. Nakajo, T. Mizugaki, K. Ebitani and K. Kaneda, *Tetrahedron Lett.*, 2002, **43**, 6229–6232.

14 M. M. Lakouraj, B. Movassagh and K. Bahrami, *Synth. Commun.*, 2001, **31**, 1237–1242.

15 R. V. Anand and V. K. Singh, *Synlett*, 2000, 807–808.

16 A. Berkessel, N. Gasch, K. Glaubitz and C. Koch, *Org. Lett.*, 2001, **3**, 3839–3842.

17 (*a*) Y. H. Kim, J. P. Hwang and S. G. Yang, *Tetrahedron Lett.*, 1997, **38**, 3009–3012; (*b*) S. Arai, H. Tsuge, M. Oku, M. Miura and T. Shioiri, *Tetrahedron*, 2002, **58**, 1623–1630.

18 O. Bortolini, V. Conte, C. Chiappe, G. Fantin, M. Fogagnolo and S. Maietti, *Green Chem.*, 2002, **4**, 94–96.

19 M. Sasidharan, P. Wu and T. Tatsumi, *J. Catal.*, 2002, **205**, 332–338.

20 G. Grigoropoulou, J. H. Clark and J. A. Elings, *Green Chem.*, 2003, **5**, 1–7.

21 (*a*) W. Reusch and C. K. Johnson, *J. Org. Chem.*, 1963, **28**, 2557–2560; (*b*) H. Pluim and H. Wynberg, *J. Org. Chem.*, 1980, **45**, 2498–2502; (*c*) K. L. Reed, J. T. Gupton and T. L. Solarz, *Synth. Commun.*, 1989, **19**, 3579–3587; (*d*) M. R. Roberts, W. H. Parsons and R. H. Schlessinger, *J. Org. Chem.*, 1978, **43**, 3970–3972.

22 T. Yechezkel, E. Ghera, D. Ostercamp and A. Hassner, *J. Org. Chem.*, 1995, **60**, 5135–5142.

Transesterification of urea and ethylene glycol to ethylene carbonate as an important step for urea based dimethyl carbonate synthesis

Bhalchandra M. Bhanage,[ac] Shin-ichiro Fujita,[a] Yutaka Ikushima[bc] and Masahiko Arai*[ac]

[a] *Division of Materials Science and Engineering, Graduate School of Engineering, Hokkaido University, Sapporo 060-8628, Japan. E-mail: marai@eng.hokudai.ac.jp*
[b] *Supercritical Fluid Research Center, National Institute of Advanced Industrial Science and Technology, Sendai 983-8551, Japan*
[c] *CREST, Japan Science and Technology Corporation (JST), Japan*

Received 16th April 2003
First published as an Advance Article on the web 9th June 2003

Two-step synthesis of dimethyl carbonate (DMC) from urea has been investigated with various solid catalysts. The first step involves reaction of urea with ethylene glycol (EG) to form ethylene carbonate (EC) and the second step transesterification of EC formed with methanol to give DMC and EG. It has been found that ZnO is highly active and selective for the two steps, of which the former should be conducted under reduced pressure. At around ambient pressure, 2-oxazolidone and ethyleneurea are formed in the first step. Similar to EG, other glycols such as 1,2- and 1,3-propanediols can also be transformed to corresponding cyclic carbonates.

Introduction

Dimethyl carbonate (DMC) is an important chemical, which finds extensive applications such as a solvent, an octane booster in gasoline to meet oxygenate specifications, and as a starting material for organic synthesis *via* carbonylation and methylation replacing the use of poisonous phosgene and dimethyl sulfate.[1] It is also used as a precursor for polycarbonate resins, for which phosgene is used.[1] DMC is synthesized by oxidative carbonylation of methanol (non-phosgene route, ENICHEM process) or by phosgenation of methanol. Both of these routes involve the use of poisonous and/or corrosive gases such as chlorine, phosgene, and carbon monoxide, and there is also a possibility of explosion hazards in the case of methanol carbonylation. Many researchers attempted direct synthesis of DMC from carbon dioxide and methanol in the presence of organometallic complexes, inorganic bases or zirconium oxide.[2] However, most of these systems suffer from several drawbacks such as low yields, high cost of the starting materials and problems associated with catalyst–product separation due to the homogeneous nature of the catalysts. The urea alcoholysis route has also been reported by many researchers and, in this case, urea and methanol are reacted together to form DMC and ammonia.[3] Formation of several side products, which results in poor selectivity, is one of the major drawbacks of using this reaction. Use of homogeneous catalysts also poses catalyst product separation and deactivation problems in some cases.[1e,3]

DMC can be synthesized *via* the transesterification of ethylene carbonate (EC) and methanol (reaction 1 of Scheme 1). There are several reports concerning this reaction.[4] The present authors have also reported that basic metal oxide[4e] and smectite catalysts[4f,g] are active and selective for this reaction. Although DMC can be obtained at high yield *via* this reaction, ethylene glycol (EG) produced along with DMC could be a disadvantage of the reaction,[1f] since the demands for these two products are usually different from each other. Note, however, that EG can be converted to EC *via* transesterification with urea, in which ammonia is co-produced (reaction 2). Ammonia formed can be

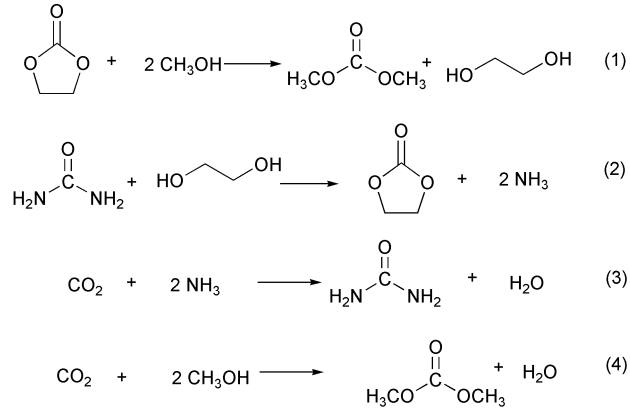

Scheme 1 Dimethyl carbonate (DMC) synthesis from carbon dioxide and methanol (reaction 4) involving three reactions such as (1) transesterification of ethylene carbonate and methanol producing DMC and ethylene glycol following (2) production of ethylene carbonate from urea and ethylene glycol, and (3) production of urea by recycling of ammonia.

Green Context

The importance of dimethylcarbonate in many application areas, its simple structure and the traditional use of toxic phosgene in its manufacture have combined to attract a lot of research directed at new, efficient and environmentally friendly synthetic processes. The new Enichem commercial route avoids phosgene but still employs a toxic chemical. Here we see good progress made in what is probably the ideal green chemistry route to this important chemical – the reaction of CO_2 with methanol. This is effectively achieved in a two-step process by first forming ethylene carbonate from urea and then carrying out a transesterification. The simple and inexpensive catalyst ZnO is highly active and selective for the two steps. ***JHC***

easily converted to urea, since the urea synthesis from ammonia and carbon dioxide has been established (reaction 3). Thus, DMC synthesis from CO_2 and methanol (reaction 4) can be achieved by combining these three reactions. This has merit in that EG and ammonia are recyclable for reactions 2 and 3, respectively. The transesterification of urea with EG is first revealed in a patent of Mitsubishi Gas Chemicals.[5] However, there is no available study on this reaction in the open literature. Since reaction 1 has been well studied as described above, the major aim of the present work is to establish suitable catalysts and reaction conditions for reaction 2, in which high EG conversion and high EC selectivity are important issues for achieving the urea based DMC synthesis (Scheme 1).

Results and discussion

When the transesterification of EG and urea was carried out at 150 °C for 4 h at a reduced pressure of 3 kPa (by dynamic evacuation), the main product was EC. Table 1 lists the reaction

Table 1 Results of reaction (2) of urea and EG under reduced pressure

Entry	Catalyst	BET area/ $m^2\ g^{-1}$	Urea conversion (%)	Selectivity (%)[a]		
				1	**2**	**3**
1	ZnO(1)	17	97	98	1.3	0.5
2	ZnO(2)	40	100	98	1.7	0.5
3	MgO	14	67	80	5.2	15
4	CeO_2	40	47	45	47	6.6
5	La_2O_3	5	55	71	12	16
6	CaO	173	16	trace	0	53[b]
7	ZrO_2	49	26	54	42	1.8
8	$Zn(AcO)_2$	—	84	88	11	0.7
9	Hydrozincite	—	54	83	3.0	14

Urea, 200 mmol; EG, 270 mmol; catalyst, 1.2 g; pressure, 3 kPa; temperature, 150 °C; time, 3 h.[a] Selectivity = moles of **1**, **2** or **3** formed/mole of urea reacted. For **1**, **2** and **3**, see Scheme 2. [b] 2-Hydroxyethyl oxazolidone and ethylene urea were also formed with selectivities of 44 and 3%, respectively.

results obtained with various catalysts. ZnO(1) and ZnO(2) give high conversions of urea and selectivities for EC **1**. By-products formed with these catalysts are 2-hydroxyethyl carbamate **2** and 2-oxazolidone **3**. The other catalysts show lower urea conversions and EC selectivities as compared with the ZnO catalysts. With CaO, *N*-(2-hydroxyethyl)-2-oxazolidone **4** and ethyleneurea **5** were also formed in selectivities of 44 and 3.4%, respectively. These products were also formed in small quantities with La_2O_3. The lower urea conversions obtained with MgO, CeO_2, La_2O_3, CaO and ZrO_2, compared with ZnO(1) and ZnO(2), cannot be explained by their BET surface areas. Previously, the present authors measured the basic properties of the present oxide catalysts by temperature programmed desorption (TPD) of adsorbed carbon dioxide.[4e] It was shown that ZnO and MgO have weakly and moderately basic sites, while the other oxide catalysts have strongly basic sites. Furthermore, it was also found that the strength of the moderately basic sites of ZnO is weaker than that of MgO. On the basis of these results, it was concluded that the high activity and selectivity of ZnO for reaction 2 result from its basic properties.

The reaction of EG and urea was carried out with ZnO(1) and ZnO(2) for various reaction times. When the reaction time was 30 min, the urea conversions were 29 and 49% for ZnO(1) and ZnO(2), respectively. There was also a difference in the selectivity for EC, being 63% with ZnO(1) and 70% with ZnO(2). Fig. 1 plots the selectivities for EC and **2** against the total urea conversion. It is seen that the EC selectivity depends

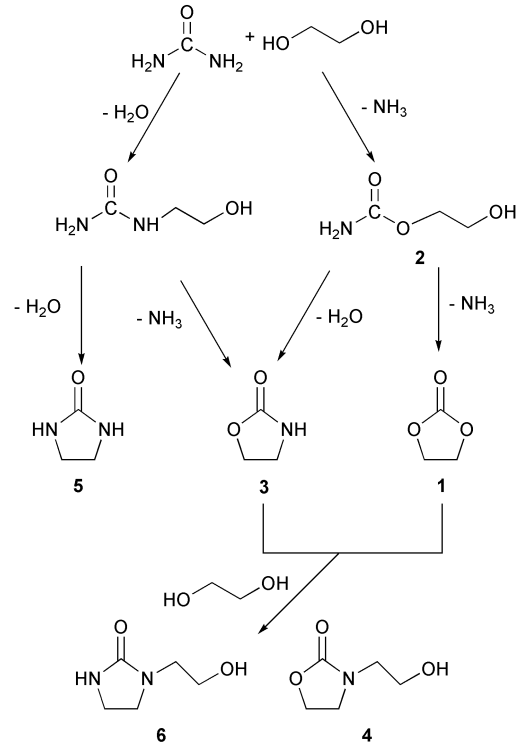

Scheme 2 Possible reaction pathways for the reaction (2) of urea and ethylene glycol.

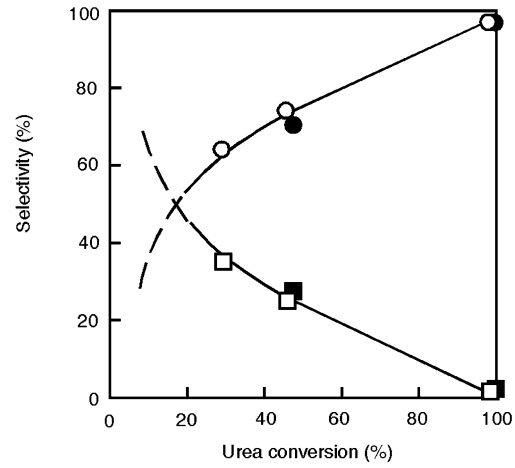

Fig. 1 Selectivities for EC (○, ●) and 2-hydroxyethyl carbamate (□, ■) *versus* urea conversion in reaction (2). Open and closed symbols represent the data obtained with ZnO(1) and ZnO(2), respectively. Reaction conditions: urea, 200 mmol; glycol, 270 mmol; catalyst, 1.2 g; pressure, 3 kPa; temperature, 150 °C.

on the conversion but not on the catalysts used when compared at the same conversion levels. Hence, the difference in the BET surface area between the catalysts (Table 1) would be responsible for the difference in the conversion observed, resulting in the different EC selectivities. Fig. 1 also shows that, at higher conversion levels, the selectivity for EC increases, while that for **2** decreases. These results lead us to the conclusion that **2** is the intermediate for the EC production from urea.

The effect of reaction pressure is shown in Fig. 2. The minimum urea conversion appears at around 100 kPa. The EC selectivity rapidly decreases with increasing the pressure. The selectivities for **3** and **4** show maxima at around 100 kPa and those for **5** and *N*-(2-hydroxyethyl)-2-imidazolidone **6** increase in a higher pressure region. Most plausible reaction pathways for the formation of all those products are illustrated in Scheme

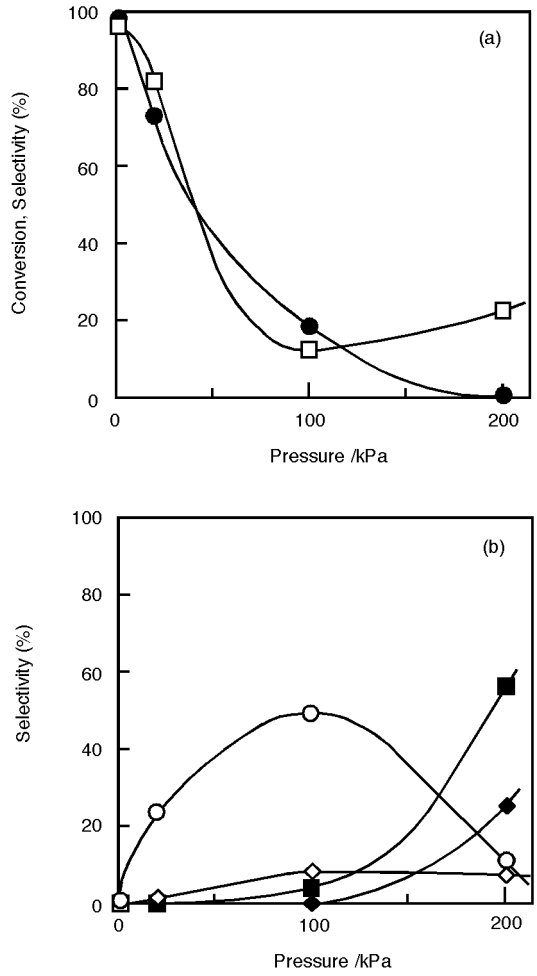

Fig. 2 Influence of reaction pressure on reaction (2), the transesterification of EG and urea. (a) Urea conversion (□) and selectivity for EC (●). (b) Selectivities for 2-oxazolidone (○), ethyleneurea (■), *N*-(2-hydroxyethyl)-2-oxazolidone (◇) and *N*-(2-hydroxyethyl)-2-imidazolidone (◆). Reaction conditions: urea, 200 mmol; glycol, 270 mmol; catalyst, 1.2 g; temperature, 150 °C; time 3 h.

2. EG and urea are condensed to **2** by releasing ammonia. Compound **2** is converted to EC or **3** *via* intramolecular deammonization or dehydration, respectively. In a similar manner, if the intermolecular dehydration reaction of EG and urea occurs, *N*-(2-hydroxyethyl)urea is formed as an intermediate and then converted to **5**. This intermediate can be also transformed to **3** by deammonization. Thus, only deammonization is required for the selective formation of EC and, on the other hand, only dehydration is required for the selective formation of **5**. The formation of **3** is possible by both reactions, dehydration and deammonization. Hence, the results of Fig. 2 mean that the deammonization is dominating over the dehydration at reduced pressures.

The formation of **4** and **6** is complicated. In separate runs, it was found that **4** and **6** were not produced from a mixture of EG and **3** nor from that of EG and **5** at 150 °C for 4 h in the autoclave in the presence of CaO catalyst. When a mixture of EG, EC and **3** was used, both **4** and **6** were formed, while a mixture of EG, EC and **5** gave no product under the same conditions. Thus, the presence of the three compounds EG, EC and **3** is required for the formation of **4** and **6**, although the reaction mechanisms are not clear at present.

The ability to recycle the catalyst is important for mass production. Therefore, attempts were made to reuse the ZnO(1) catalyst 3 times by filtration, washing with ethanol and water, and drying after each run. The results obtained are given in Table 2, indicating that the catalyst can retain its activity and selectivity performance during the recycles.

Table 2 Results of catalyst recycling of ZnO(1) for reaction (2)

Run	Urea conversion (%)	Selectivity for EC (%)
1	97	98
2	97	96
3	100	97
4	99	97

Urea, 200 mmol; EG, 270 mmol; ZnO(1), 1.2 g; pressure, 3 kPa; temperature, 150 °C; time, 3 h.

The influence of the structure of glycol on the reaction was also investigated. 1,2-Propanediol and 1,3-propanediol were used for the transesterification with urea (Scheme 3). The

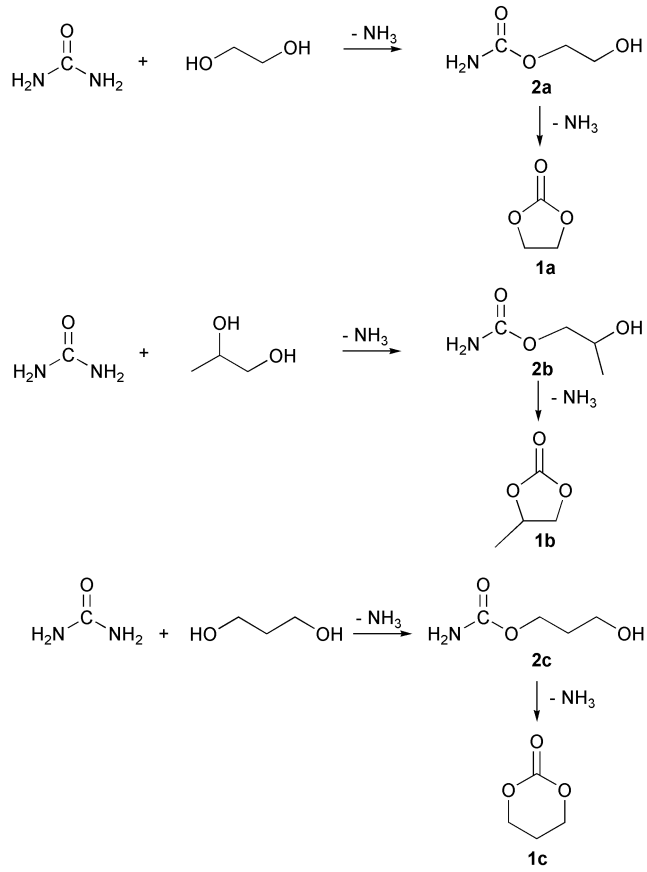

Scheme 3 Formation of cyclic carbonates *via* reaction (2) of urea and different glycols.

results are presented in Table 3. 1,2-Propanediol gives 77% conversion with 91% selectivity towards propylene carbonate **1b**. A very small quantity of a by-product of 1-methyl-1-hydroxyethyl carbamate **2b** was also formed. On the basis of

Table 3 Influence of the structure of glycols for reaction (2)

Entry	Glycol	Urea conversion (%)	Selectivity (%)	
			1	**2**
1	Ethylene glycol	97	98	1.3
2	1,2-Propanediol	77	91	9.0
3	1,3-Propanediol	59	72	27

Urea, 200 mmol; glycol, 270 mmol; ZnO(1), 1.2 g; pressure, 3 kPa; temperature, 150 °C; time, 3 h.

Scheme 2, this compound should be the intermediate for the production of **1b**. The conversion is lower than that obtained with EG. This may be attributed to the steric hindrance caused

by the bulky methyl group present in 1,2-propanediol as compared with EG. The reaction of 1,3-propanediol and urea produces 1,3-dioxan-2-one **1c** and 3-hydroxypropyl carbamate **2c**. The urea conversion and the cyclic carbonate selectivity decrease further by changing the glycol from EG to 1,3-propanediol. Probably, the 6-membered ring formation from this substrate should be more difficult than the other two glycols.

The transesterification of EC and methanol to form DMC and EG, reaction (1) of Scheme 1, was also investigated. After the reaction of EG and urea was carried out with ZnO(1), the reaction mixture was further subjected to the reaction with methanol at 150 °C for 4 h. EC was converted to DMC and EG with a conversion of 60%. The molar ratio of DMC/EG formed was 0.92, which was slightly lower than the expected value of unity from reaction 1, probably due to the decomposition of EC with water to EG and carbon dioxide and/or the decomposition of DMC with water to methanol and carbon dioxide.[4e,6] As shown previously,[4g] the reaction of EC and methanol to form DMC and EG is a reversible reaction and higher EC conversions can be obtained with higher initial ratios of methanol/EC. Hence, more DMC can be produced using an increased amount of methanol.

Conclusion

In conclusion, DMC can be synthesized with very high atom efficiency from urea as a starting material by using a ZnO catalyst. In the first step (reaction 2 of Scheme 1), the urea reacts with EG to form EC. This reaction needs to be conducted under reduced pressure to obtain high selectivity for EC. The catalyst is very stable and recyclable without any loss of the activity and selectivity performance. Besides EG, other glycols such as 1,2- and 1,3-propanediols can also be transformed to the corresponding cyclic carbonates but with smaller selectivities. In the second step (reaction 1), EC is transesterified with methanol to give DMC and EG in the presence of the same catalyst at high yield and selectivity. Thus, urea based two-step DMC synthesis will be one of the possible alternatives in the quest for an environmentally benign route to DMC synthesis.

Experimental

Catalysts

Two types of ZnO (ZnO(1), ZnO(2)), MgO, CeO_2, La_2O_3, CaO, ZrO_2, zinc acetate and hydroxy zinc carbonate (hydrozincite) were used. ZnO(2), CeO_2 and ZrO_2 were prepared by decomposition of hydroxy zinc carbonate at 350 °C for 4 h, cerium carbonate octahydrate at 500 °C for 3 h, and zirconium oxynitrate at 500 °C for 3 h, respectively. The other catalysts were commercially available reagents. BET surface areas of those catalysts are given in Table 1.

Reaction (2) of urea and ethylene glycol (EG)

The reactions were performed in a 100 cm^3 glass reactor with a mechanical agitator attached and water-cooled condenser with a water aspirator attached above the condenser for creating suitable reduced pressure for removal of ammonia. After urea (200 mmol) and EG (270 mmol) along with 1.2 g of the catalyst were charged into the reactor, the reactor was agitated under a reduced pressure of about 3 kPa. Then the reactor was heated to 150 °C and kept at this temperature for 3 h. After the reaction, the reactor was cooled to room temperature. The reaction mixture was diluted with ethanol to 100 cm^3 and then analyzed on a gas chromatograph equipped with a flame ionization detector. The quantities of EG consumed and products formed were determined from the results obtained from authentic standards. The structures of the compounds were confirmed by mass spectrometry. A few runs were conducted in a 100 cm^3 autoclave under auto-generated pressure.

Reaction of (1) of ethylene carbonate (EC) and methanol

After the reaction (2) of urea and EG, the reaction mixture including the catalyst was transferred to a 100 cm^3 autoclave and 50 cm^3 of methanol was added. Then, the reactor was purged with carbon dioxide, heated to 150 °C and kept at the same temperature for 4 h. After the reaction, the reaction mixture was analyzed using similar procedures as described above.

Reaction of EG, EC and 2-oxazolidone

EG (270 mmol), EC (25 mmol) and 2-oxazolidone (25 mmol) along with 1.2 g of CaO were charged into a 100 cm^3 autoclave. Then, the reactor was heated to 170 °C and kept at the same temperature for 3 h. After the reaction, the reaction mixture was analyzed using similar procedures as described above.

Acknowledgements

The authors wish to express their thanks for financial support obtained from Japan Science and Technology (JST) under CREST program.

References

1 (*a*) P. Tundo and M. Selva, *CHEMTECH*, 1995, 31; (*b*) A. A. Shaikh and S. Sivaram, *Chem. Rev.*, 1996, **96**, 951; (*c*) Y. Ono, *CATTECH*, 1997, **1**, 31; (*d*) M. Aresta and E. Quaranta, *CHEMTECH*, 1997, 32; (*e*) M. A. Pacheco and C. L. Marshall, *Energy Fuels*, 1997, **11**, 2; (*f*) D. Delledonne, F. Rivetti and U. Romano, *Appl. Catal. A: Gen.*, 2002, **221**, 241.

2 (*a*) J. Kizlink, *Collect. Czech. Chem. Commun.*, 1993, **58**, 1399; (*b*) J. Kizlink and I. Pastucha, *Collect. Czech. Chem. Commun.*, 1994, **59**, 2116; (*c*) J. Kizlink and I. Pastucha, *Collect. Czech. Chem. Commun.*, 1995, **60**, 687; (*d*) T. Zhao, Y. Han and Y. Sun, *Fuel Proc. Technol.*, 2000, **62**, 187; (*e*) N. S. Isaacs, B. O. Sullivan and C. Verhaelen, *Tetrahedron*, 1999, **55**, 11949; (*f*) S. Fang and K. Fujimoto, *Appl. Catal. A*, 1996, **142**, L1; (*g*) K. Tomishige, T. Sakaihori, Y. Ikeda and K. Fujimoto, *Catal. Lett.*, 2000, **58**, 225; (*h*) Y. Ikeda, T. Sakaihori, K. Tomishighe and K. Fujimoto, *Catal. Lett.*, 2000, **66**, 5; (*i*) T. Sakakura, Y. Saito, M. Okano, J. C. Choi and T. Sako, *J. Org. Chem.*, 1998, **63**, 7095; (*j*) T. Sakakura, J. C. Choi, Y. Saito, T. Masuda, T. Sako and T. Oriyama, *J. Org. Chem.*, 1999, **64**, 4506; (*k*) T. Sakakura, J. C. Choi, Y. Saito and T. Sako, *Polyhedron*, 2000, **19**, 573; (*l*) S. Fujita, B. M. Bhanage, Y. Ikushima and M. Arai, *Green Chem.*, 2001, **3**, 87.

3 E. N. Suciu, B. Kuhlmann, G. A. Knudsen and R. C. Michaelson, *J. Organomet. Chem.*, 1998, **556**, 41 and references therein.

4 (*a*) J. F. Knifton and R. G. Duranleau, *J. Mol. Catal.*, 1991, **67**, 389; (*b*) T. Tatsumi, Y. Watanabe and K. A. Koyano, *Chem. Commun.*, 1996, 2281; (*c*) M. Kirishiki, Y. Onda and H. Tsuneki, *Shokubai (Catalysts and Catalysis)*, 1996, **38**, 92; (*d*) Y. Watanabe and T. Tatsumi, *Microporous Mesoporous Mater.*, 1998, **22**, 399; (*e*) B. M. Bhanage, S. Fujita, Y. Ikushima and M. Arai, *Appl. Catal. A*, 2001, **219**, 259; (*f*) B. M. Bhanage, S. Fujita, Y.-F. He, Y. Ikushima, M. Shirai, K. Torri and M. Arai, *Catal. Lett.*, 2002, **83**, 137; (*g*) B. M. Bhanage, S. Fujita, Y. Ikushima, K. Torri and M. Arai, *Green Chem.*, 2003, **5**, 71.

5 M. Doya, K. Kimizuka and Y. Kanbara, Assigned Mitsubishi Gas Chemical Company, Tokyo, Japan, 1996, *US Patent 5489 702*.

6 T. Baba, A. Kobayashi, T. Yamauchi, H. Tanaka, S. Aso, M. Inamoto and Y. Kawanami, *Catal. Lett.*, 2002, **82**, 193.

Reductive coupling of aromatic aldehydes and ketones in sunlight

Ji-Tai Li,* Jin-Hui Yang, Jun-Fen Han and Tong-Shuang Li

College of Chemistry and Environmental Science, Hebei University, Key Laboratory of Analytical Science and Technology, Hebei Province, Baoding 071002, P. R. China

Received 6th January 2003
First published as an Advance Article on the web 10th June 2003

Sunlight is a cheap, efficient and environmentally friendly natural resource. Reductive coupling of aromatic aldehydes and ketones leading to 1,2-diols has been achieved with high yield in isopropanol in sunlight. The notable advantage of the present method seems to be the negligible formation of side products arising mainly due to reduction of the carbonyls to the corresponding alcohols, Cannizzaro reaction and the formation of olefins.

Introduction

1,2-Diols are very useful synthons for a variety of organic syntheses,[1] which have been used as intermediates for the construction of biologically important natural product skeletons.[2–4] 1,2-Diols have been synthesized by reductive coupling of aromatic ketones and aldehydes with active metals or metallic complexes, such as Al,[5] Mg,[6] Te,[7] Mn,[8] $TiBr_2$–Cu and TiI_4–Cu,[9] and rare earth metals.[10] In spite of their potential utility, some of these methods, unfortunately, were associated with the use of toxic reagents and heavy metals, which would lead to economical and environmental concerns. In order to improve environmental performance it is, therefore, very significant to develop a new methodology for this important carbon–carbon bond formation reaction by identifying alternative reaction conditions and by utilization of less toxic reagents and solvents. Many modifications of this reaction, such as pinacol coupling in aqueous media under ultrasound irradiation[11] or using metal reagents in the presence of aqueous sodium hydroxide,[12,13] have been reported recently.

The photochemical reactions of organic compounds attracted great interest in the 1960's. As a result, many useful and fascinating reactions were uncovered, and photochemistry became an important synthetic tool in organic chemistry. The coupling of aromatic ketones to give pinacols has been demonstrated photochemically. The classic example is the photolysis of benzophenone in isopropanol to give a good yield of benzopinacol in sunlight.[14] In 1961, Moore *et al.* studied the photochemical reduction of benzophenone by benzohydrol,[15] toluene and cumene respectively.[16] In benzohydrol, the reduction coupling product was only benzopinacol, the conversion was 56.1%. In toluene, photochemical reduction of benzophenone gave benzopinacol (51% yield) and benzyldiphenylcarbinol (38–46%) after four weeks in sunlight. The products formed in cumene were benzopinacol (24%), tertiary carbinol (48–60%) and 1,2-diphenyl-1,2-dimethyl butane (24%). In 1968, Cohen and Chao[17] reported that the photoreduction of benzophenone by secondary and tertiary amines was accompanied by formation of light-absorbing transients and by-products. Recently, Ji *et al.*[18] have investigated the self-coupling reaction of cyclic ketones in MeOH, EtOH, i-PrOH, hexane, hexane–H_2O or cyclohexane–H_2O under a high-pressure mercury lamp. Adam and Walther[19] have also reported the photoreduction of benzophenone leading to cross-coupling pinacols in alcohol (MeOH, EtOH or i-PrOH) solvent during Laser-Jet photolysis. Earlier investigations on the conventional photochemistry of benzophenone in various hydrogen-donating reagents have shown that isopropanol possessed special attributes; in the previous works stated above, the influence of different hydrogen-donating agents on the photopinacolization of ketones and the corresponding mechanism has mainly been investigated.[15,16,20]

Sunlight is a cheap, efficient and environmentally friendly natural resource. To the best of our knowledge, there are no literature examples of pinacol coupling of aromatic aldehydes to synthesize 1,2-diols by the utilization of solar energy. All these stated above prompted us to study the possibility of the pinacol coupling using sunlight. Herein we report a simple and clean procedure for preparation of pinacols *via* coupling of aromatic aldehydes and ketones in isopropanol in sunlight (Scheme 1).

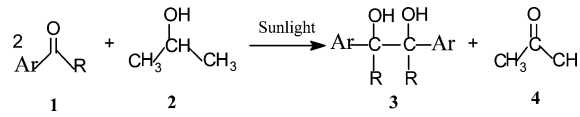

1 2 3 4

Scheme 1

Results and discussion

As shown in Table 1, several structurally different aromatic aldehydes and ketones underwent photoreductive coupling to corresponding 1,2-diols in good yields. The data in Table 1 show that sunlight irradiation is a highly chemoselective method. For example, benzaldehyde (**1a**), *p*-methylbenzaldehyde (**1d**) and acetophenone (**1g**) were irradiated at r.t. for 7–10 days in isopropanol in sunlight, the corresponding pinacol product was obtained in 96 (**3a**), 94 (**3d**) and 98% (**3g**) yield

Green Context

Sunlight is a cheap, environmentally friendly and often efficient natural resource. While there has been research on photochemically initiated organic reactions, many important reactions have not been properly studied in this context. This article describes, for the first time, the use of solar energy in the synthesis of 1,2-diols from pinacol coupling of aldehydes. Advantages compared to more traditional methods include high yield, operational simplicity and fewer by-products. ***JHC***

Table 1 Photopinacolization of aromatic aldehydes and ketones in isopropanol in sunlight

Entry	Ar	R	Irradiation time/d	Conversion of **1** (%)[a]	Isolated Yield of **3** (%)	*dl*/*meso*
a	C_6H_5	H	10	96	96	34/66
	C_6H_5	H	10	94	94[b]	—
	C_6H_5	H	10	91	91[c]	—
	C_6H_5	H	10	88	88[d]	—
	C_6H_5	H	10	68	68[e]	—
b	4-ClC_6H_4	CH_3	10	95	84	40/60
	4-ClC_6H_4	CH_3	7	93	78	—
c	C_6H_5	C_6H_5	10	100	94	—
d	4-$CH_3C_6H_4$	H	7	94	94	46/54
e	3-ClC_6H_4	H	10	82	79	60/40
f	4-ClC_6H_4	H	10	97	78	94/6
g	C_6H_5	CH_3	10	100	98	54/46
h	C_6H_5	CH_2Cl	10	60	60	56/44
i	C_6H_5	CH_2Br	10	45	45	52/48
j	2,4-$Cl_2C_6H_3$	H	10	92	55	38/62
k	4-$CH_3OC_6H_4$	CH_3	10	6.5	6.2	23/77
l	3,4-$(OCH_2O)C_6H_3$	H	8	3	3	65/35

[a] Conversion = (reacted substrate/starting substrate) × 100%. [b] Using recycled mixture of isopropanol and acetone, the first time. [c] Using recycled mixture of isopropanol and acetone, the second time. [d] Using recycled mixture of isopropanol and acetone, the third time. [e] Using 13 mL isopropanol and 7 mL acetone.

respectively. The competing Cannizzaro reaction, giving alcohol and carboxylic acid, was not observed. The *dl*/*meso* ratio of products **3** is nearly 1/1, except that 1,2-bis(4-dichlorophenyl-)ethane-1,2-diol (**3f**) is 94/6. In the present procedure, benzopinacol was obtained in 94% yield compared to that (51%) in toluene by prolonged exposure to sunlight for four weeks.[16] It was also found that prolonged irradiation time could increase the product yield, for example, 4-chloroacetophenone (**1b**) results in **3b** in 84% yield under irradiation within 10 d, while the yield of **3b** is 78% within 7 d.

A common reaction of photoexcited carbonyl groups is hydrogen atom abstraction from solvent or another hydrogen donor to give alpha-hydroxybenzyl radicals. Most aromatic aldehydes and ketones react by hydrogen atom abstraction and the stable products are diols formed by coupling of the resulting alpha-hydroxybenzyl radicals.[21] The following sequence of reactions appears to afford a satisfactory explanation of the mode of formation of products of the photoreduction of aromatic aldehydes and ketones in isopropanol in sunlight (Scheme 2).[22]

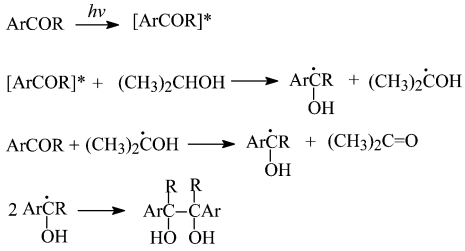

Scheme 2

We also tried to use recovered solution (mixture of isopropanol and acetone). When the substrate was benzaldehyde, the solution could be recycled for up to three times (Table 1[b–d]), the yield was 94, 91 and 88% respectively. In order to study the effect of the amount of isopropanol on the reaction, we combined isopropanol (13 mL) with acetone (7 mL) as reaction solution. After 10 days irradiation, the yield of the pinacol was only 68% (Table 1[e]). This indicated that a low concentration of isopropanol in the reaction solution would reduce the yield of pinacol.

When vanillin, 3- or 4-nitrobenzaldehyde, 2- or 4-hydroxybenzaldehyde, 4-methoxybenzaldehyde, 4-aminobenzaldehyde, furfural, cinnamic aldehyde and cyclohexanone were used as the substrates, in the same way as **3k** and **3l** in Table 1, no or less pinacol products were obtained. These results show that this method has some limitation with respect to some aromatic aldehydes and ketones.

Conclusions

In conclusion, the present photochemical procedure in isopropanol in sunlight provides a very useful, economically and environmentally friendly method for the pinacol coupling of some aromatic aldehydes and ketones. The important advantages offered by this procedure include: higher yield, operational simplicity, low cost, minority of by-product and no pollution.

Experimental

Liquid aldehydes were distilled before use. IR spectra were recorded on a Bio-Rad FTS-40 spectrometer (KBr). MS were determined on a VG-7070E spectrometer (EI, 70 eV). ^{1}H NMR and ^{13}C NMR spectra were measured on a Bruker AVANCE 400 (400 MHz) spectrometer using TMS as internal reference and $CDCl_3$ as solvent. The *dl* : *meso* of **3** was determined by ^{1}H NMR.

General coupling procedure

A mixture of benzaldehyde (**1**, 1 mmol) and one drop of glacial acetic acid was added to a 20 mL ground-glass test tube, which was afterwards filled with isopropanol (**2**) (if the substrate does not dissolve at r.t., it should be warmed). The ground-glass test tube was closed with a ground-glass plug, and was supported in an inverted position in a beaker and exposed to direct sunlight. After ten days of exposure, isopropanol and acetone were removed under reduced pressure. The residue was separated by column chromatography on silica (200–300 mesh), eluted with petroleum ether or a mixture of petroleum ether and diethyl ether. All the products were confirmed by comparing their R_f value with that of the authentic samples, and IR, MS, ^{1}H NMR, ^{13}C NMR spectral data.

3a. ^{1}H NMR: δ2.20 (2H, s, OH, *meso*), 2.83 (2H, s, OH, *dl*), 4.72 (2H, s, CH, *dl*), 4.84 (2H, s, CH, *meso*), 7.14–7.32 (20H, m, Ph–H). Assignments were made by comparing the relative areas of proton signals at δ4.72 and 4.84, respectively; ^{13}C NMR: 78.45, 79.50, 127.39, 127.53, 128.30, 128.46, 140.16, 140.29; *m*/*z* (%)**:** 214 (1), 180 (7.6), 167 (12.5), 149 (6.0), 107 (93.8), 79 (100), 77 (73.8).

3b. ^{1}H NMR: δ 1.47 (6H, s, CH_3, *dl*), 1.54 (6H, s, CH_3, *meso*), 2.28 (2H, s, OH, *meso*), 2.57 (2H, s, OH, *dl*), 7.08–7.30 (16H, m, Ph–H). Assignments were made by comparing the relative areas of proton signals at δ 1.47 and 1.54, respectively; ^{13}C NMR: 25.11, 25.41, 78.69, 78.94, 127.73, 127.77, 128.92, 129.27,133.38, 133.58, 142.16, 142.61; *m*/*z* (%): 276 (14), 249 (32), 155 (100), 111 (8).

3c. ^{1}H NMR: δ3.04 (2H, s, OH,), 7.17–7.19 (20H, m, Ph–H); ^{13}C NMR: 83.48, 127.41, 127.75, 129.07, 144.62; *m*/*z* (%): 184 (16), 183 (99), 165 (7), 106 (8), 105 (100), 78 (6), 77 (72), 51 (11), 43 (2).

3d. ^{1}H NMR: δ 2.06(2H, s, OH, *meso*), 2.75 (2H, s, OH, *dl*), 4.68 (2H, s, CH, *dl*), 4.75 (2H, s, CH, *meso*) 7.04–7.26 (16H, m, Ph–H). Assignments were made by comparing the relative areas of proton signals at δ 4.68 and 4.75, respectively; ^{13}C NMR: 21.59, 21.62, 78.38, 79.18, 127.33, 127.49, 129.20, 129.35, 137.38, 137.43, 137.82. 138.11; *m*/*z* (%): 242 (1.2), 195 (6), 121 (100), 107 (12), 77 (13).

3e. ^{1}H NMR: δ 3.29 (4H, b, OH), 4.56 (2H, s, CH, *dl*), 4.74 (2H, s, CH, *meso*), 6.87–7.36 (16H, m, Ph–H). Assignments were made by comparing the relative areas of proton signals at δ 4.56 and 4.74, respectively; ^{13}C NMR: 78.68, 125.62, 127.34, 128.72, 129.85, 134.64, 141.94; *m*/*z* (%): 263 (1.2), 251 (1.6), 178 (4.6), 165 (4.6), 141 (100), 113 (23.8), 77 (71.0).

3f. ^{1}H NMR: δ 2.87 (4H, s, OH), 4.63 (2H, s, CH, *dl*), 4.84 (2H, s, CH, *meso*) 7.02–7.26 (16H, m, Ph–H). Assignments were made by comparing the relative areas of proton signals at δ 4.633 and 4.84, respectively; ^{13}C NMR: 78.82, 128.75, 129.00, 134.14, 134.20, 138.16, 138.37; *m*/*z* (%): 282 (10), 235 (12), 165 (5.5), 141 (100), 107 (19), 77 (10).

3g. ^{1}H NMR: δ1.46 (6H, s, CH_3, *dl*), 1.53 (6H, s, CH_3, *meso*), 2.52 (2H, s, OH, *meso*), 2.68 (2H, s, OH, *dl*), 7.03–7.36 (20H, m, Ph–H). Assignments were made by comparing the relative areas of proton signals at δ 1.46 and 1.53, respectively; ^{13}C NMR: 25.36, 25.52, 79.01, 79.27, 127.31, 127.34, 127.56, 127.79, 143.83, 144.20; *m*/*z* (%): 225 (4), 206 (4), 181 (32), 165 (9), 121 (100), 105 (12), 77 (11), 43 (80).

3h. ^{1}H NMR: δ 1.51 (4H, s, CH_2, *dl*), 1.58 (4H, s, CH_2, *meso*), 2.27 (2H, s, OH, *meso*), 2.57 (2H, s, OH, *dl*), 7.20–7.24 (20H, m, Ph–H). Assignments were made by comparing the relative areas of proton signals at δ1.51 and 1.58, respectively; ^{13}C NMR: 25.35, 25.52, 79.02, 79.27, 127.31, 127.35, 127.46, 127.56, 127.69, 127.80, 143.84, 144.21; *m*/*z* (%): 155 (3), 121 (13), 105 (100), 77 (13), 51 (2), 43 (18).

3i. ^{1}H NMR: δ1.51 (4H, s, CH_2, *dl*), 1.59 (4H, s, CH_2, *meso*), 2.27 (2H, b, OH, *meso*), 2.58 (2H, s, OH, *dl*), 7.21–7.25 (20H, m, Ph–H). Assignments were made by comparing the relative areas of proton signals at δ 1.51 and 1.59, respectively; ^{13}C NMR: 25.36, 25.53, 79.01, 79.27, 127.31, 127.34, 127.47, 127.56, 127.69, 127.80, 143.83, 144.20; *m*/*z* (%): 303 (11), 301 (12), 240 (4), 239 (23), 201 (2), 199 (2), 123 (8), 121 (23), 105 (100), 81 (26), 43 (2).

3j. ^{1}H NMR: δ 3.46 (4H, s, OH), 5.15 (2H, s, CH, *dl*), 5.47 (2H, s, CH, *meso*), 7.10–7.26 (12H, m, Ph–H). Assignments were made by comparing the relative areas of proton signals at δ 5.15 and 5.47, respectively; ^{13}C NMR: 71.71, 73.02, 127.26, 127.64, 128.74, 129.58, 130.12, 130.51, 133.53, 134.20, 134.53, 134.85, 135.05, 136.00; *m*/*z* (%): 352 (1), 305 (1.4), 233 (10), 175 (100), 145 (10), 111 (25), 77 (15).

3k. ^{1}H NMR: δ 1.26 (6H, s, CH_3, *dl*), 1.46 (6H, s, CH_3, *meso*), 2.36 (4H, b, OH), 3.80 (12H, s, CH_3O), 6.77–7.30 (20H, m, Ph–H). Assignments were made by comparing the relative areas of proton signals at δ 1.26 and 1.46, respectively; ^{13}C NMR: 25.42, 25.57, 55.60, 78.90, 79.13, 112.81, 112.96, 127.57, 128.51, 128.94, 129.78, 136.42, 136.42; *m*/*z* (%): 302 (1), 151 (100), 135 (5), 109 (4), 77 (3), 43 (60).

3l. ^{1}H NMR (DMSO as solvent): δ 4.44 (4H, s, OH), 5.14 (2H, s, CH, *dl*), 5.27 (2H, s, CH, *meso*), 5.96 (8H, s, CH_2), 6.52–6.82 (12H, m, Ph–H). Assignments were made by comparing the relative areas of proton signals at δ5.14 and 5.27, respectively; ^{13}C NMR: 40.28, 40.49, 77.57, 78.15, 101.38, 108.02, 108.09, 108.34, 108.52, 121.31, 121.45, 137.18, 138.04, 146.64, 147.28; *m*/*z* (%): 302 (1), 284 (2.5), 268 (5.0), 255 (11.8), 151 (100), 123 (32), 93 (77.1), 65 (39.0).

Acknowledgements

This project was supported by Educational Ministry of China, Educational Department of Hebei Province (2001104) and Natural Science Foundation of Hebei Province, China (203107).

References

1 A. Ghribi, A. Alexakis and J. F. Normant, *Tetrahedron Lett.*, 1984, **40**, 3083.
2 G. M. Robertson, in *Comprehensive Organic Synthesis*, ed. B. M. Trost and I. Fleming, Pergamon, New York, 1991, vol. 3, 563.
3 T. Wirth, *Angew. Chem., Int. Ed. Engl.*, 1996, **35**, 61.
4 M. Avalos, R. Babano, P. Cintas, J. L. Jimenez and J. C. Palacios, *Recent Res. Dev. Org. Chem.*, 1997, **1**, 159.
5 J. M. Khurana and A. Sehgal, *J. Chem. Soc., Chem. Commun.*, 1994, 571.
6 W. C. Zhang and C. J. Li, *J. Org. Chem.*, 1999, **64**, 3230.
7 R. H. Khan, R. K. Mathur and A. C. Ghosh, *Synth. Commun.*, 1997, **27**, 2193.
8 R. D. Rieke and S. H. Kim, *J. Org. Chem.*, 1998, **63**, 5235.
9 T. Mukaiyama, N. Yoshimura, K. Igarashi and A. Kagayama, *Tetrahedron*, 2001, **57**, 2499.
10 A. Ogawa, H. Takeuchi and T. Hirao, *Tetrahedron Lett.*, 1999, **40**, 7113.
11 (*a*) M. Mečarová and S. Toma, *Green Chem.*, 1999, 257; (*b*) J. T. Li, Y. J. Bian, H. J. Zang and T. S. Li, *Synth. Commun.*, 2002, **32**, 547; (*c*) H. J. Lim, G. Keum, S. B. Kang, B. Y. Chung and Y. Kim, *Tetrahedron Lett.*, 1998, **39**, 4367.
12 S. M. Liu, J. T. Li, Y. J. Bian, J. H. Yang and T. S. Li, *Chin. J. Org. Chem.*, 2002, **22**, 675.
13 S. Bhar and C. Panja, *Green Chem.*, 1999, 253.
14 W. E. Bachmann, *Organic Syntheses*, **Col. Vol. II**, John Wiley and Sons, Inc., New York, 1948, p. 71.
15 W. M. Moore, G. S. Hammond and R. P. Foss, *J. Am. Chem. Soc.*, 1961, **83**, 2789.
16 G. S. Hammond, W. P. Baker and W. M. Moore, *J. Am. Chem. Soc.*, 1961, **83**, 2795.
17 S. G. Cohen and H. M. Chao, *J. Am. Chem. Soc.*, 1968, **90**, 165.
18 S. J. Ji, M. Matsushita, T. T. Takahashi and C. A. Horiuchi, *Tetrahedron Lett.*, 1999, **40**, 6791.
19 W. Adam and B. Walther, *Tetrahedron*, 1996, **52**, 10399.
20 A. Schőnberg and A. Mustafa, *Chem. Rev.*, 1947, **40**, 181.
21 F. A. Carey and R. J. Sundberg, *Advanced Organic Chemistry*, Part A, Plenum Press, New York, 1990, p. 741.
22 J. N. Pitts, R. L. Letsinger, R. P. Taylor, J. M. Patterson, G. Recktenwald and R. B. Martin, *J. Am. Chem. Soc.*, 1959, **81**, 1068.

Easy and environmentally friendly uncatalyzed synthesis of β-hydroxy arylsulfides by thiolysis of 1,2-epoxides in water

F. Fringuelli, F. Pizzo,* S. Tortoioli and L. Vaccaro

Department of Chemistry, University of Perugia – Perugia, Italy. E-mail: pizzo@unipg.it; Fax: +39 075 5855560; Tel: +39 075 5855546

Received 14th March 2003
First published as an Advance Article on the web 13th June 2003

The title compounds were prepared *via* thiolysis of alkyloxiranes by arylthiols in basic aqueous medium at 30 °C. The nucleophilic addition is *anti* diastereoselective and occurs on the less substituted carbon of the oxirane ring. The aqueous medium was reused and crystalline sulfides were isolated by filtration carrying out a solventless process. The protocol was used for a *one-pot* synthesis of hexahydrodibenzo[1,4]oxathiepinone **9**.

Introduction

Water as a reaction medium has become increasingly important in organic synthesis for the preparation of building block and target molecules with chemical advantages in terms of reactivity and selectivity of process, as well as from an economical and ecological point of view.[1] Within the problems related to chemical pollution prevention and waste minimization, a great advantage[2] of using an aqueous medium is the possibility of recycling the reaction medium and isolating insoluble products by filtration and decantation, carrying out in this way a solventless process. The aqueous medium also allows *one-pot* consecutive and multicomponent reactions to be carried out.

The combination of this strategy with the solventless protocol provides an excellent tool for achieving an environmentally friendly, economical organic synthesis.

As a part of our program designed to investigate organic processes in water,[3] we are now interested in a *one-pot* consecutive synthesis of the oxathiepine ring, a promising heterocyclic system which has been scarcely investigated.[4] A key step in a possible synthetic strategy is the ring-opening of 1,2-epoxides by *o*-carboxy-thiols, followed by intramolecular esterification. Oxirane ring-opening by thiols and thiolates has been widely investigated because of its importance in the field of pharmaceutical[5] and natural products[6] and has been performed (i) using various promoters and catalysts in organic solvents (THF, CH_2Cl_2, MeOH, MeCN),[7] (ii) under basic conditions in anhydrous media,[8] and (iii) catalyzing the deprotonation of thiols by onium salts.[9]

Recently we reported the first cleavage of 1,2-epoxides with thiophenol in acidic water, catalyzed by $InCl_3$, showing that the regioselectivity of thiolysis was markedly influenced by the pH of the aqueous medium.[3i]

This paper describes the uncatalyzed preparation of β-hydroxy-arylsulfides in alkaline aqueous medium by nucleophilic addition of thiolates to 1,2-epoxides and the *one-pot* synthesis of the hexahydro[1,4]oxathiepinone ring using an environmentally friendly protocol following Green Chemistry principles and *Click Chemistry* standards.[1,10]

Results and discussion

The thiolysis of 1-methyl-1,2-cyclohexene oxide (**1**) in water at 30 °C occurred under heterogeneous conditions. In acidic medium, Brønsted catalysis makes the nucleophilic addition of water the highly predominant reaction (Table 1, entry 1). Under basic conditions, the thiolate is the prevalent nucleophile (pK_a of *o*-$NH_2C_6H_4SH$ = 6.54[11]) and the crystalline sulfide **1f** was the main reaction product (Table 1, entries 3 and 4) that was isolated in 90% yield by simple filtration because of the high solubility of diol **8** in aqueous medium. The reaction was totally *anti* diastereoselective and occurred exclusively on the less substituted β-carbon of the oxirane ring.

Table 1 Thiolysis of 1-methyl-1,2-cyclohexene oxide (**1**) with *o*-aminothiophenol (**7f**) at different pH values

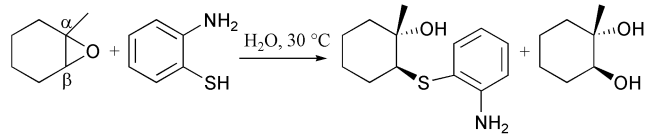

1 **7f** **1f** **8**

Entry	pH	*t*/h[a]	Sulfide **1f**/Diol **8**
1	4.0	1.5	9/91
2	7.0	8	30/70
3	9.0	4	94/6
4	11.0	3	95/5

[a] Conversion > 99%.

No improvement, in terms of reactivity and selectivity was observed at pH values higher than 9.0.[12]

The protocol was applied to a variety of alkyloxiranes (**1–6**) by using a number of arylthiophenols (**7a–h**) which allowed β-hydroxy arylsulfides (**1–6**, **a–h**) to be isolated with excellent yields (Table 2).[13] The arylsulfides **1b–h**, **2c**, **3e–6e** are new compounds and their structures, proven by spectroscopic measurements, are described in the experimental section. All the reactions proceeded quickly (from 5 min to 5 h) with the exception of thiolyses of **1** and **6** with **7h** and **7e**, respectively,

Green Context

Water has many attractions as an environmentally benign solvent and as a replacement for toxic or environmentally damaging volatile organic solvents. Here the uncatalysed preparation of hydroxyarylsulfides in aqueous solution is described. The reaction described occurs at moderate temperatures and is *anti* diastereoselective. Crystalline products can easily be obtained by filtration. This simple and clean synthetic process is successfully applied to the one-pot synthesis of hexahydrodibenzo[1,4]oxathiepinone. *JHC*

 DOI: 10.1039/b303011c

Table 2 Thiolysis of oxiranes **1–6** in water under basic conditions

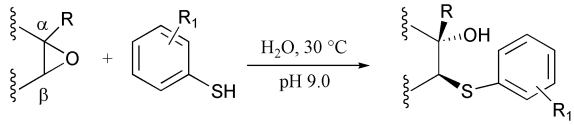

7 **1-6 (a-h)**

Entry	Oxirane		R_1	*t*/h	Sulfide	Yield (%)[a]
1		**a**	H	2	**1a**	90[b]
2		**b**	*p*-COOH	0.08	**1b**	85[c]
3		**c**	*o*-COOH	0.20	**1c**	90[c]
4		**d**	*o*-COOMe	1.5	**1d**	85
5	**1**	**e**	*p*-NH_2	2.0	**1e**	85
6		**f**	*o*-NH_2	4.0	**1f**	90[d]
7		**g**	*p*-NHCOMe	1.0	**1g**	90
8		**h**	*o*-Me	10	**1h**	90
9		**a**	H	3	**2a**	95
10	**2**	**c**	*o*-COOH	0.5	**2c**	95[c]
11		**a**	H	0.3	**3a**	95
12	**3**	**e**	*p*-NH_2	0.5	**3e**	90
13	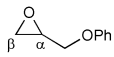 **4**	**e**	*p*-NH_2	3	**4e**	94
14	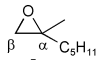	**a**	H	2	**5a**	88[e]
15	**5**	**e**	*p*-NH_2	3.5	**5e**	95
16	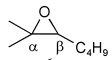	**a**	H	4.8	**6a**	80
17	**6**	**e**	*p*-NH_2	22	**6e**	95[f]

[a] Yield of isolated product. [b] Regioselectivity of the reaction α/β = 3/97. [c] Product isolated after acidification of the final reaction mixture. [d] Chemoselectivity of the reaction: sulfide/diol = 96/4. [e] Regioselectivity of the reaction α/β = 5/95. [f] At 50 °C.

that required longer reaction times. (Table 2, entries 8 and 17). The high reactivity of *para*- and *ortho*-carboxythiophenols **7b**, **7c** (Table 2, entries 3, 4, and 10) with respect to that of the aminoderivatives analogues **7e**, and **7f**, cannot be ascribed to electronic effects but rather to a higher concentration of the nucleophile in the basic medium when the carboxy group is the substituent. The nucleophilic attack of thiolates occurred almost exclusively on the less substituted β-carbon of the oxirane ring with *anti* mode. Very little α-addition (3–5%) was observed only in the thiolyses of **1** and **5** with **7a** (Table 2, entries 1 and 14). The higher nucleophilicity of ArS^-, with respect to N_3^-,[14] makes the thiolysis of alkyl oxiranes in basic aqueous medium much more β-regioselective than the azidolysis one.[15] This also influences the well-known reversed regioselectivity of nucleophilic ring-opening of aryloxiranes.[7–9] Thus, while the azidolysis of styrene oxide with NaN_3 in aqueous medium (pH 9.5, 30 °C) gave a regioselectivity α/β = 32, the thiolysis of the same compound with thiophenol (pH 9.0, 30 °C) gave a lower α-regioselectivity (α/β = 3).[3i]

Competition of nucleophilic oxygen species (OH^-, H_2O) with ArS^- was rarely observed[14,16] (Table 2, entry 6) and the by-product diol was never an obstacle to the purification of sulfide because the latter is poorly soluble in aqueous medium and, if it is a crystalline solid, it can be separated easily from the former by filtration.

The aqueous reaction medium (mother liquors from filtration) can be reused for further thiolyses.[17] An example is the thiolysis of 2,3-epoxypropyl-phenylether (**4**) with *p*-aminothiophenol (**7e**). The same aqueous medium was used for three runs without significant variation in the reaction time and yield (Table 3). No further amount of sodium hydroxide was added after the first time and sulfide **4e** was isolated in pure form by simple filtration.

Table 3 Re-use of the aqueous medium

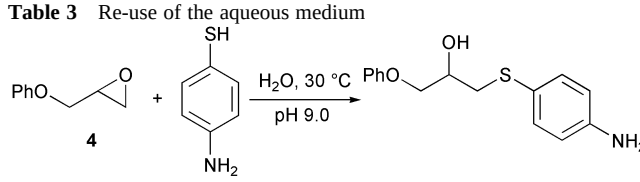

4 **7e** **4e**

Run	*t*/h	Yield (%)
I	3	94
II	4	95
III	4	95

The protocol of thiolysis in basic aqueous medium was used for the *one-pot* synthesis of 1,4-benzoxathiepinone **9**[18] (eqn. 1).

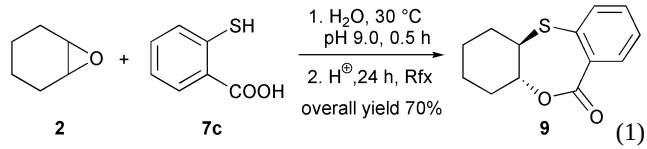

2 **7c** **9** (1)

Reaction of cyclohexene oxide (**2**) with thiosalicylic acid (**7c**) in water at 30 °C and pH 9.0 gave the sodium 2-[(2′-hydroxycyclohexyl)thio]benzoate which underwent lactonization reaction *in situ* under acidic conditions (H^+, 100 °C, 24 h) to give **9** in 70% overall yield.

Conclusions

In conclusion we report an environmentally benign procedure for preparing β-hydroxy arylsulfides *via* ring-opening of unsymmetrical alkyloxiranes in basic aqueous medium at 30 °C. The addition occurred on the less substituted carbon and was *anti* diastereoselective. Crystalline sulfides were isolated by filtration and the aqueous medium can be reused. The protocol was used for a *one-pot* synthesis of hexahydrodibenzo[1,4]oxathiepinone **9**.

Experimental

General

All chemicals were purchased and used without any further purification. GC analyses were performed with an SPB-5 fused silica capillary column (30 m, 0.25 mm diameter), an "on column" injector system, an FID detector, and hydrogen as the carrier gas. GC-MS analyses were carried out with 70 eV electron energy. ^1H and ^{13}C NMR spectra (200 and 50.3 MHz respectively) were recorded in ppm (δ) downfield from Me_4Si (δ = 0.00) in $CDCl_3$ and CD_3COCD_3 as solvents. All the thiols, cyclohexene oxide (**2**) and 2,3-epoxypropyl-phenylether (**4**) are commercially available; the 1,2-epoxides **1**, **3**, **5** and **6** were prepared by oxidation of the corresponding alkene as reported in the literature.[19] Compounds **1a**, **2a**, **3a**, **5a**, and **6a** are known.[3i] Compound **1c** was isolated as methyl ester after treatment with an ethereal solution of diazomethane.

Preparation of β-hydroxy arylsulfides. Typical procedure

An aqueous solution of NaOH 5 M (4.0–4.25 mmol, 0.80–0.85 mL) was added to a stirred solution of thiophenol **7** (4.5 mmol) in water (5.2 mL) at 30 °C until the pH value was 9.0. The 1,2-epoxide (3.0 mmol) was added and the mixture stirred for the time reported in Table 2.

The β-hydroxy arylsulfides precipitated as solid crystalline structures, were isolated by filtration after cooling the reaction mixture to 4 °C; oils were extracted with diethyl ether and worked up as usual.

4-[(2′-Hydroxy-2′-methylcyclohexyl)thio]benzoic acid (1b)

Solid, mp = 170–172 °C (1,4-dioxane). IR (CsI): ν = 3431 (m); 2945 (s); 2864 (m); 1690 (s); 1594 (m); 1235 (m); 1126 (s); 852 (s); 697 (m). ^{1}H NMR (CD_3COCD_3) δ = 1.28 (*s*, 3H, Me), 1.34–1.78 (*m*, 8H, H-3′,-4′,-5′,-6′), 3.44 (*dd*, 1H, *J* = 3.9, 9.6 Hz, H-1′), 7.49 (*d*, 2H, *J* = 8.5 Hz, H-3,-5), 7.92 (*d*, 2H, *J* = 8.4 Hz, H-2,-6). ^{13}C NMR (CD_3COCD_3) δ = 23.3, 24.1, 25.1, 31.5, 40.4, 57.5, 72.8, 127.9, 128.8, 130.6, 145.0, 167.1. GC/MS on derivative methyl ester (280) *m*/*z* (%): 280 (100, M^+), 248 (13), 220 (49), 168 (62), 137 (45), 43 (40). Anal. calc. for $C_{14}H_{18}O_3S$ (266): C, 63.13; H, 6.81. Found: C, 63.45; H, 6.80%.

Methyl 2-[(2′-hydroxy-2′-methylcyclohexyl)thio]benzoate (1d)

Oil, IR ($CHCl_3$): ν = 3531 (m); 3442 (m); 3009 (s); 2941 (s); 2861 (m); 1716 (s); 1436 (s); 1293 (s); 1113 (s); 954 (m). ^{1}H NMR ($CDCl_3$) δ = 1.38 (*s*, 3H, Me), 1.16–1.92 (*m*, 8H, H-3′,-4′,-5′,-6′), 2.12 (*m*, 1H, OH), 3.22 (*dd*, 1H, *J* = 4.0, 11.9 Hz, H-1′), 3.93 (*s*, 3H, OMe), 7.22 (*t*, 1H, *J* = 7.5 Hz, H-5), 7.43 (*t*, 1H, *J* = 7.6 Hz, H-4), 7.58 (*d*, 1H, *J* = 8.0 Hz, H-3), 7.81 (*d*, 1H, *J* = 7.7 Hz, H-6). ^{13}C NMR ($CDCl_3$) δ = 22.3, 22.6, 25.2, 31.2, 39.5, 51.7, 58.4, 71.9, 124.8, 129.6, 129.9, 130.6, 131.4, 138.3, 166.9. GC/MS *m*/*z* (%): 280 (11, M^+), 262 (60), 168 (32), 136 (100), 108 (14), 95 (26), 43 (36). Anal. calc. for $C_{15}H_{20}O_3S$ (280): C, 64.26; H, 7.19. Found: C, 64.20; H, 6.73%.

2-[(4′-Aminophenyl)thio]-1-methylcyclohexanol (1e)

Solid, mp = 109–111 °C (85 : 15 Et_2O–petroleum ether). IR ($CHCl_3$): ν = 3493 (w); 3406 (w); 3006 (m); 2941 (s); 1622 (s); 1600 (s); 1496 (s); 1283 (m); 1131 (m); 920 (w). ^{1}H NMR ($CDCl_3$) δ = 1.26 (*s*, 3H, Me), 1.21–2.06 (*m*, 8H, H-3,-4,-5,-6), 2.84 (*dd*, 1H, *J* = 4.2, 11.9 Hz, H-2), 3.70 (*br s*, 2H, NH_2), 6.61 (*d*, 2H, *J* = 8.7 Hz, H-3′,-5′), 7.30 (*d*, 2H, *J* = 8.6 Hz, H-2′,-6′). ^{13}C NMR ($CDCl_3$) δ = 22.4, 23.1, 25.9, 31.8, 39.6, 63.1, 72.5, 115.4, 122.3, 135.3, 146.4. GC/MS *m*/*z* (%): 237 (63, M^+), 150 (2), 125 (100), 93 (7), 80 (6), 43 (6). Anal. calc. for $C_{13}H_{19}NOS$ (237): C, 65.78; H, 8.07; N, 5.90. Found: C, 65.82; H, 8.04; N, 5.93%.

2-[(2′-Aminophenyl)thio]-1-methylcyclohexanol (1f)

Solid, mp = 102–104 °C (7 : 3 Et_2O–petroleum ether). IR ($CHCl_3$): ν = 3481 (w); 3356 (w); 3007 (m); 2939 (s); 2860 (m); 1607 (s); 1470 (s); 1309 (m); 1132 (m); 919 (w). ^{1}H NMR ($CDCl_3$) δ = 1.21–1.81 (*m*, 8H, H-3,-4,-5,-6), 1.33 (*s*, 3H, Me), 1.99–2.17 (*m*, 1H, OH), 2.85 (*dd*, 1H, *J* = 4.2, 12 Hz, H-2), 3.84 (*br s*, 2H, NH_2), 6.73 (*d*, 1H, *J* = 8.1Hz, H-3′), 6.69 (*t*, 1H, *J* = 7.4 Hz, H-5′), 7.14 (*t*, 1H, *J* = 7.6 Hz, H-4′), 7.41 (*d*, 1H, *J* = 7.6 Hz, H-6′). ^{13}C NMR ($CDCl_3$) δ = 22.0, 23.3, 25.9, 32.3, 40.2, 61.3, 72.7, 115.1, 117.8, 118.6, 129.9, 137.0, 148.4. GC/MS *m*/*z* (%): 237 (61, M^+), 162 (8), 125 (100), 93 (12), 80 (14), 43 (13). Anal. calc. for $C_{13}H_{19}NOS$ (237): C, 65.78; H, 8.07; N, 5.90. Found: C, 65.76; H, 7.99; N, 5.86%.

N-{4-[(2′-Hydroxy-2′-methylcyclohexyl)thio]phenyl}-acetamide (1g)

Foam. IR ($CHCl_3$): ν = 3186 (w); 3016 (s); 2940 (m); 2861 (m); 1691 (m); 1508(s); 1115(w); 833 (w). ^{1}H NMR ($CDCl_3$) δ = 1.28 (*s*, 3H, Me), 1.43–2.02 (*m*, 9H, H-3′,-4′,-5′,-6′,OH), 2.17 (*s*, 3H, $COCH_3$), 2.72 (*br s*, 1H, NH), 2.99 (*dd*, 1H, *J* = 4.2, 11.8 Hz, H-1′), 7.24–7.68 (*m*, 4H, H-aromatic). ^{13}C NMR ($CDCl_3$) δ = 22.6, 23.2, 24.5, 25.9, 32.2, 39.7, 62.3, 72.7, 120.5, 133.3, 137.2, 142.6, 168.6. GC/MS *m*/*z* (%): 279 (100, M^+), 246 (6), 167 (65), 125 (82), 95 (13), 69 (6). Anal. calc. for $C_{15}H_{21}NO_2S$ (279): C, 64.48; H, 7.58; N, 5.01. Found: C, 64.37; H, 7.50; N, 4.97%.

1-Methyl-2-[(2′-methylphenyl)thio]cyclohexanol (1h)

Oil. IR ($CHCl_3$): ν = 3543 (m); 3490 (m); 3010 (s); 2939 (s); 1468 (s); 1378 (m); 1131 (m); 929 (m). ^{1}H NMR ($CDCl_3$) δ = 1.33 (*s*, 3H, Me), 1.01–1.99 (*m*, 8H, H-3,-4,-5,-6), 2.44 (*s*, 3H, *o*-Me), 2.63 (*s*, 1H, OH); 3.07 (*dd*, 1H, *J* = 4.1, 11.7 Hz, H-2), 7.12–7.26 (*m*, 3H, H-4′,-5′,-6′), 7.42–7.49 (*m*, 1H, H-3′). ^{13}C NMR ($CDCl_3$) δ = 20.8, 22.8, 23.1, 25.7, 31.8, 39.6, 60.0, 72.4, 126.4, 126.7, 130.2, 131.6, 134.7, 139.4. GC/MS *m*/*z* (%): 236 (90, M^+), 178 (4), 137 (22), 124 (100), 91 (34), 43 (49). Anal. calc. for $C_{14}H_{20}OS$ (236): C, 71.14, H, 8.53. Found: C, 71.08; H, 8.49%.

2-[(2′-Hydroxycyclohexyl)thio]benzoic acid (2c)

Solid, mp = 103–105 °C (6 : 4 petroleum ether–$CHCl_3$). IR ($CHCl_3$): ν = 3023 (w); 3012 (w); 2935 (m); 2860 (w); 1709 (s); 1588 (w), 1448 (w); 1247 (m); 1116 (w); 1040 (m). ^{1}H NMR ($CDCl_3$) δ = 1.21–2.24 (*m*, 8H, H-3′,-4′,-5′,-6′), 3.07 (*ddd*, 1H, *J* = 3.9, 9.8, 11.6 Hz, H-1′), 3.53 (*dt* (apparent), 1H, *J* = 4.3, 9.8, H-2′), 7.27 (*t*, 1H, *J* = 7.5 Hz, H-5), 7.47 (*t*, 1H, *J* = 7.6 Hz, H-4), 7.57 (*d*, 1H, *J* = 7.9 Hz, H-3), 7.98 (*d*, 1H, *J* = 7.8 Hz, H-6), 8.48 (*br s*, 2H, OH). ^{13}C NMR ($CDCl_3$) δ = 24.1, 25.8, 32.6, 33.9, 54.9, 73.2, 125.8, 130.4, 130.8, 131.6, 132.5, 138.0, 171.3. GC/MS on derivative methyl ester (266) *m*/*z* (%): 266 (3, M^+), 248 (42), 136 (100), 81 (27), 69 (9), 55 (8). Anal. calc. for $C_{13}H_{16}O_3S$ (252): C, 61.88; H, 6.39. Found: C, 62.02; H, 6.50%.

1-{[(4′-Aminophenyl)thio]methyl}cyclohexanol (3e)

Solid, mp = 71–72 °C (ethyl acetate). IR ($CHCl_3$): ν = 3670 (w); 3489 (m); 3403 (m); 3011 (s); 2936 (s); 2858 (m); 1620 (s); 1599 (m); 1496 (s); 1279 (m); 1177 (m). ^{1}H NMR ($CDCl_3$) δ = 1.17–1.64 (*m*, 10H, H-2,-3,-4,-5,-6), 2.30 (*br s*, 1H, OH), 2.98 (*s*, 2H, C*H2*S), 3.73 (*br s*, 2H, NH_2), 6.59 (*d*, 2H, *J* = 6.5 Hz, H-3′,-5′), 7.27 (*d*, 2H, *J* = 6.5 Hz, H-2′,-6′). ^{13}C NMR ($CDCl_3$) δ = 21.9, 25.4, 34.1, 50.1, 71.1, 115.5, 124.0, 133.3, 145.7. GC/MS *m*/*z* (%): 237 (61, M^+), 139 (100), 124 (60), 94 (14), 81 (23), 55 (7). Anal. calc. for $C_{13}H_{19}NOS$ (237): C, 65.78; H, 8.07; N, 5.90. Found: C, 65.79; H, 8.11; N, 6.01%.

1-[(4′-Aminophenyl)thio]-3-phenoxypropan-2-ol (4e)

Solid, mp = 77–79 °C (CH_3OH) IR (neat): ν = 3481 (m); 3445 (m); 3355 (s); 2927 (w); 1636 (m); 1597 (s); 1496 (s); 1246 (s); 825 (m); 759 (m). ^{1}H NMR ($CDCl_3$) δ = 2.89 (*br s*, 1H, OH), 2.90 (*dd*, 1H, *J* = 3.6, 6.8 Hz, H-1a), 2.99 (*dd*, 1H, *J* = 2.6, 6.8 Hz, H-1b), 3.73 (*br s*, 2H, NH_2), 3.89–3.91 (*m*, 1H, H-2), 3.94–3.96 (*m*, 2H, H-3), 6.45–6.49 (*m*, 2H, H-aromatic), 6.62–7.00 (*m*, 3H, H-aromatic), 7.18–7.40 (*m*, 4H, H-aromatic). ^{13}C NMR ($CDCl_3$) δ = 39.8, 68.1, 69.9, 114.3, 115.5, 120.8, 121.4, 129.2, 133.8, 146.2, 158.1. GC/MS *m*/*z* (%): 275 (100, M^+), 138 (38), 124 (53), 94 (38), 77 (18), 51 (5). Anal. calc. for $C_{15}H_{17}NO_2S$ (275): C, 65.43; H, 6.22; N, 5.09. Found: C, 65.34; H, 6.31; N, 5.03%.

1-[(4′-Aminophenyl)thio]-2-methylheptan-2-ol (5e)

Oil, IR (neat): ν = 3446 (s); 3420 (s); 3358 (s); 3230 (m); 2954 (s); 1620 (s); 1595 (m); 1494 (s); 1283 (s); 823 (m). ^{1}H NMR ($CDCl_3$) δ = 0.87 (*t*, 3H, *J* = 6.6 Hz, H-7), 1.19 (*s*, 3H, Me), 1.16–1.28 (*m*, 6H, H-4,-5,-6), 1.43–1.51 (*m*, 2H, H-3), 2.30 (*br s*, 1H, OH), 2.94 (*d*, 1H, *J* = 13.2 Hz, H-1a), 3.02 (*d*, 1H, *J* = 13.2 Hz, H-1b), 3.74 (*br s*, 2H, NH_2), 6.59 (*d*, 2H, *J* = 8.6 Hz, H-3′,-5′), 7.26 (*d*, 2H, *J* = 8.6 Hz, H-2′,-6′). ^{13}C NMR ($CDCl_3$) δ = 13.8, 22.4, 23.5, 26.0, 32.0, 41.0, 49.4, 72.4, 115.4, 123.7, 133.3, 145.8. GC/MS *m*/*z* (%): 253 (38, M^+), 139 (100), 124 (68), 94 (13), 55 (12), 43 (9). Anal. calc. for $C_{14}H_{23}NOS$ (253): C, 66.36; H, 9.15; N, 5.53. Found: C, 66.45; H, 8.99; N, 5.34%.

3-[(4′-Aminophenyl)thio]-2-methylheptan-2-ol (6e)

Oil; IR ($CHCl_3$): ν = 3669 (w); 3481 (s); 3400 (s); 3212 (m); 2928 (s); 2860 (s); 1882 (w); 1618 (m); 1495 (m); 1278 (m); 1120 (m). ^{1}H NMR ($CDCl_3$) δ = 0.88 (*t*, 3H, *J* = 7.1 Hz, H-7); 1.18 (*s*, 3H, Me), 1.28 (*s*, 3H, H-1), 1.32–1.54 (*m*, 4H, H-5,-6), 1.68–1.78 (*m*, 2H, H-4), 2.76 (*d*, 1H, *J* = 8.9 Hz, H-3), 3.49 (*br s*, 2H, NH_2), 6.56 (*d*, 2H, *J* = 6.5 Hz, H-3′,-5′), 7.28 (*d*, 2H, *J* = 6.5 Hz, H-2′,-6′). ^{13}C NMR ($CDCl_3$) δ = 13.8, 22.2, 25.8, 26.9, 30.3, 31.9, 66.9, 72.9, 115.4, 124.1, 134.1, 145.9. GC/MS *m*/*z* (%): 253 (59, M^+), 195 (76), 124 (100), 93 (26), 80 (19), 59 (15). Anal. calc. for $C_{14}H_{23}NOS$ (253): C, 66.36; H, 9.15; N, 5.53. Found: C, 66.27; H, 9.22; N, 5.60%.

Re-use of the aqueous media

By using the typical procedure, the 2,3-epoxypropyl-phenyl-ether (**4**) (0.410 mL, 3.0 mmol) was added at 30 °C and under stirring to a basic aqueous solution (5.2 mL of water and 0.85 mL of 5 M NaOH) of *p*-aminothiophenol (**7e**) (0.593 g, 4.5 mmol). The mixture was stirred for 3 h and then cooled to 4 °C and the β-hydroxy arylsulfide **4e** was filtered (purity 98% and yield 94%).

The mother liquors were reused at 30 °C adding **7e** and **4**.

After stirring for 4 h at 30 °C the sulfide **4e** was filtered (purity 98% and yield 95%) and the aqueous medium reused again.

***One-pot* synthesis of *trans*-5a,6,7,8,9,9a-hexahydro-11*H*-dibenzo[*b*,*e*][1,4]oxathiepin-11-one (9)**

Cyclohexene oxide (**2**) (0.31 mL, 3 mmol) was added at 30 °C to a basic aqueous solution (5.2 mL of water and 0.8 mL of 5 M NaOH) of thiosalicylic acid (**7c**) (0.477 g, 3.03 mmol). The mixture was stirred for 0.5 h, then acidified with 12 M HCl (1.4 mL) and refluxed for 24 h. After cooling, the resulting mixture was extracted with diethyl ether and worked up as usual. Purification of crude product by column chromatography on silica gel eluting with 1 : 1 petroleum ether–diethyl ether afforded pure dibenzoxathiepinone **9** (0.491 g 70% overall yield) as a white crystalline solid.

mp = 113–114 °C (6 : 4 ethyl acetate–petroleum ether). IR ($CHCl_3$): ν = 3026 (w); 3013 (w); 2946 (m); 2862 (w); 1721 (s); 1588 (w); 1438 (m); 1290 (s); 1239 (w); 1106 (m); 1062 (w); 966 (w). ^{1}H NMR ($CDCl_3$) δ = 1.15–1.85 (*m*, 6H, H-6,-7,-8), 2.08–2.26 (*m*, 2H, H-9), 3.19 (*ddd*, 1H, *J* = 3.8, 10.4, 12.1 Hz, H-5a), 3.87 (*dt* (apparent), 1H, *J* = 4.1, 10.6 Hz, H-9a), 7.36–7.49 (*m*, 3H, H-aromatic), 7.66–7.71 (*m*, 1H, H-aromatic). ^{13}C NMR ($CDCl_3$) δ = 24.1, 25.6, 32.3, 35.2, 51.1, 79.5, 128.7, 128.9, 130.5, 132.3, 133.9, 136.9, 170.0. GC/MS *m*/*z* (%): 234 (97, M^+), 216 (12), 163 (100), 136 (53), 108 (18), 69 (8). Anal. calc. for $C_{13}H_{14}O_2S$ (234): C, 66.64; H, 6.02. Found: C, 66.77; H, 6.20%.

Acknowledgements

The Ministero dell'Istruzione dell'Università e della Ricerca (MIUR) and the Università degli studi di Perugia are thanked for financial support.

References

1 (*a*) P. T. Anastas, *Green Chemistry: Theory and Practice*, Oxford University Press, Oxford, 1998; (*b*) P. Tundo and P. T. Ananstas, *Green Chemistry: Challenging Perspectives*, Oxford University Press, Oxford, 1999; (*c*) *Organic Synthesis in Water*, ed. P. A. Grieco, Blackie Academic and Professional, London, 1998; (*d*) C. J. Li and T. H. Chang, *Organic Reactions in Aqueous Media*, Wiley, New York, 1997.

2 For a list of advantages and disadvantages of water as reaction medium see F. Fringuelli, O. Piermatti, F. Pizzo and L. Vaccaro, *Eur. J. Org. Chem.*, 2001, 439.

3 For recent works: (*a*) F. Fringuelli, F. Pizzo and L. Vaccaro, *Tetrahedron Lett.*, 2001, **42**, 1131; (*b*) D. Amantini, F. Fringuelli, F. Pizzo and L. Vaccaro, *Green Chem.*, 2001, **3**, 229; (*c*) O. Attanasi, L. De Crescentini, P. Filippone, F. Fringuelli, F. Mantellini, M. Matteucci, O. Piermatti and F. Pizzo, *Helv. Chim. Acta*, 2001, **84**, 513; (*d*) F. Fringuelli, M. Matteucci, O. Piermatti, F. Pizzo and M. C. Burla, *J. Org. Chem.*, 2001, **66**, 4661; (*e*) F. Fringuelli, F. Pizzo and L. Vaccaro, *J. Org. Chem.*, 2001, **66**, 3554; (*f*) F. Fringuelli, F. Pizzo and L. Vaccaro, *J. Org. Chem.*, 2001, **66**, 4719; (*g*) D. Amantini, F. Fringuelli, F. Pizzo and L. Vaccaro, *J. Org. Chem.*, 2001, **66**, 6734; (*h*) D. Amantini F. Fringuelli, F. Pizzo and L. Vaccaro, *J. Org. Chem.*, 2002, **67**, 7238; (*i*) F. Fringuelli, F. Pizzo, S. Tortoioli and L. Vaccaro, *Adv. Synth. Catal.*, 2002, **344**, 379.

4 (*a*) H. Sugihara, H. Mabuchi, M. Hirata, T. Iamamoto and Y. Kawamatsu, *Chem. Pharm. Bull.*, 1987, **35**, 1930; (*b*) C. G. Aifheli and P. T. Kaye, *Synth. Commun.*, 1996, **26**, 4459.

5 J. R. Luly, N. Yi, J. Soderquist, H. Stein, J. Choen, T. J. Perun and J. J. Plattner, *J. Med. Chem.*, 1987, **30**, 1609.

6 (*a*) E. J. Corey, D. A. Clark, G. Goto, A. Marfat, C. Mioskowski, B. Samuelsson and S. Hammarstroem, *J. Am. Chem. Soc.*, 1980, **102**, 1436; (*b*) E. J. Corey, D. A. Clark and G. Goto, *Tetrahedron Lett.*, 1980, **21**, 3143; (*c*) P. Meffre, L. Vo Quang, Y. Vo Quang and F. Le Goffic, *Tetrahedron Lett.*, 1990, **31**, 2291; (*d*) S. Apparao and R. R. Schmidt, *Synthesis*, 1987, 896.

7 (*a*) P. N. Guivisdalsky and R. Bittman, *J. Am. Chem. Soc.*, 1989, **111**, 3077 [BF_3–Et_2O] (*b*) O. Bortolini, F. Di Furia, G. Licini and G. Modena, *Phosphorus Sulfur Silicon Relat. Elem.*, 1988, **37**, 171 [$LnCl_3$] (*c*) M. Chini, P. Crotti, E. Giovani, F. Macchia and M. Pineschi, *Synlett*, 1992, 303 [$LiClO_4$] (*d*) J. Iqbal, A. Pandey, A. Shukla, R. R. Srivastava and S. Tripathi, *Tetrahedron*, 1990, **46**, 6423 [$CoCl_3$] (*e*) G. H. Posner and D. Z. Rogers, *J. Am. Chem. Soc.*, 1977, **79**, 8208 [Al_2O_3] (*f*) P. Raubo and J. Wicha, *Pol. J. Chem.*, 1995, **69**, 78 [SiO_2] (*g*) J. M. Chong and K. B. Sharpless, *J. Org. Chem.*, 1985, **50**, 1560 [Ti(O–*i*-Pr)$_4$] (*h*) G. Lin, Z. Shi and C. Zeng, *Tetrahedron: Asymmetry*, 1993, **4**, 1533 [Ti(O-*i*-Pr)$_4$] (*i*) I. W. J. Still and L. P. J. Martin, *Synth. Commun.*, 1998, **28**, 913 [SmI_2] (*j*) J. S. Yadav, B. V. S. Reddy and G. Baisha, *Chem. Lett.*, 2002, 906 [$InCl_3$] (*k*) S. Chanrasekar, Ch. R. Reddy, B. N. Babu and G. Chandrashekar, *Tetrahedron Lett.*, 2002, **43**, 3801[$B(C_6F_5)_3$] (*l*) D. Albanese, D. Landini and M. Penso, *Synthesis*, 1994, 34[Bu_4NF] (*m*) A. K. Maiti, G. K. Biswas and P. Bhattacharyya, *J. Chem. Res.: Synop.*, 1993, 325 [Montmorillonite] (*n*) A. K. Maiti and P. Bhattacharyya, *Tetrahedron*, 1994, **50**, 10483 [polyethylene glycol] (*o*) J. Choi and N. M. Yoon, *Synthesis*, 1995, 373 [hydrosulfide exchange resin] (*p*) M. R. Younes, M. M. Chaabouni and A. Baklouti, *Tetrahedron Lett.*, 2001, **42**, 3167 [Triton-B] (*q*) J. C. J. de Pomar and J. A. Soderquist, *Tetrahedron Lett.*, 1998, **39**, 4409 [DBU] (*r*) M. H. Wu and E. N. Jacobsen, *J. Org. Chem.*, 1998, **63**, 5252 [(salen) chromium complex] (*s*) J. Wu, X.-L. Hou, L.-X. Dai, L.-J. Xia and M.-H. Tang, *Tetrahedron: Asymmetry*, 1998, **9**, 3431 [titanium complex] (*t*) S.

Fukuzawa, H. Kato, M. Ohtaguchi, Y. Hayashi and H. Yamazaki, *J. Chem. Soc., Perkin Trans. 1*, 1997, **20**, 3059 [carbonyl chromium complex] (*u*) T. Iida, N. Yamamoto, H. Sasai and M. Shibasaki, *J. Am. Chem. Soc.*, 1997, **119**, 4783 [gallium complex] (*v*) H. Yamashita, *Bull. Chem. Soc. Jpn.*, 1998, **61**, 1213 [zinc tartrates].

8 (*a*) O. Yamada and K. Ogasawara, *Synlett*, 1995, 427; (*b*) C. H. Behrens and K. B. Sharpless, *J. Org. Chem.*, 1985, **50**, 5696.

9 (*a*) T. Nishikubo, T. Iizawa, M. Shimojo, T. Kato and A. Shiina, *J. Org. Chem.*, 1990, **55**, 2536; (*b*) T. Iizawa, A. Goto and T. Nishikubo, *Bull. Chem. Soc. Jpn.*, 1989, **62**, 597.

10 H. C. Kolb, M. G. Finn and K. B. Sharpless, *Angew. Chem., Int. Ed.*, 2001, **40**, 2004.

11 G. Chuchani and A. Frohlich, *J. Chem. Soc. B*, 1971, **7**, 1417.

12 9.0 is the pH value of the aqueous medium at t_0. In the course of the reaction, the pH gradually increases to *ca.* 12.5 due to the difference between the pK_a of ArSH (*ca.* 6–8) and the pK_a of ROH (*ca.* 17–18)[14a].

13 The reaction of non-aromatic thiols with 1,2-epoxide in water at pH 9.0 is possible even if their pK_a values (*ca.* 11)[14a] are higher than those of aromatic ones and longer reaction times could be required. As an example butanethiol reacted at pH 9.0 at 30 °C in solely water with cyclohexene oxide (**2**) to give after 12 h the corresponding 2-butylthio-cyclohexanol in 90% yield.

14 (*a*) M. B. Smith and J. March, *March's Advanced Organic Chemistry*, Wiley-Interscience Publication, New York, 5th edn., 2001; (*b*) A. Streitwieser, *Chem. Rev.*, 1956, **56**, 571 cfr. p. 582.

15 F. Fringuelli, F. Pizzo and L. Vaccaro, *J. Org. Chem.*, 1999, **64**, 6094.

16 This result was expected considering that the nucleophilic ability of phenylthiolate is *ca.* 50000 times that of water, while under our reaction conditions there are *ca.* 75 mmol of water per 1 mmol of phenylthiolate.[14] Hydroxide ion and phenylthiolate have comparable nucleophilic ability[14] but under our reaction conditions (pH 9.0) the concentration of OH^- is *ca.* 7.5×10^{-6} smaller than that of the thiolate.

17 When, *p*- and, *o*-carboxythiophenols **7b** and **7c** were used, the aqueous medium could not be reused exactly as it was because it had to be acidified to isolate the sulfide.

18 R. Krishnamurti, S. Nagy and T. F. Smolka, US patent No. 5621153, 1997.

19 F. Fringuelli, R. Germani, F. Pizzo and S. Savelli, *Tetrahedron Lett.*, 1989, **30**, 1427.

Clean synthesis of an array of N-benzoyl–N′-aryl ureas using polymer-supported reagents

Guichun Yang, Zuxing Chen and Haiqing Zhang

Faculty of Chemistry and Material Science, Hubei University, Wuhan, Hubei 430062, China

Received 23rd April 2003
First published as an Advance Article on the web 19th June 2003

An efficient clean synthesis of an array of N-benzoyl–N′-aryl ureas using polymer-supported isothiocyanate and iodate as reagents and strong acidic ion-exchange resin as scavenger is described. Representative ureas were obtained with moderate to high yield and excellent purity. The process of the reaction and purity of the isolation were easily monitored by TLC or HPLC.

1 Introduction

Solid-phase organic synthesis has become an especially attractive technology for the preparation of combinatorial libraries of low molecular weight organic molecules.[1] Recently polymer-supported scavengers have been developed to remove an excess of reactants or side products from reaction solutions and thus give the required product in high yield, purity and in a single operation.[2,3] Ley and co-workers have reported orchestrated multi-step syntheses using polymer-supported reagents and sequestrants.[4–6] This approach combines the advantages of polymer-supported reactions as well as allowing the progressing reactions to be monitored by standard TLC and HPLC methods. The reactions proceeded in a clean and efficient fashion rather than spending time on the purification of large libraries.

The substituted ureas have drawn considerable attention in a number of investigations due to their biological activity and wide variety of applications.[7] Most syntheses of ureas have been reported using conventional solution methods and solid-phase synthesis.[8–13] Recently we have reported the synthesis of thioureas by reaction of poly(ethyl glycol) bound benzoyl chloride with amines.[14–16] In this article, we report a simple, fast and flexible method for synthesis of ureas using polymer-supported reagents. The synthesis of ureas is outlined in Scheme 1.

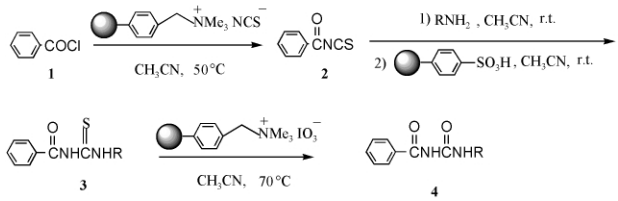

Scheme 1

2 Experiment

2.1 Synthesis

Melting points were determined on an Electrothermal melting point apparatus and were uncorrected. HPLC purities were determined with a Shimzdu equipped with an ODS Eclipse XDB-C18 3.5 mm 30 × 2.1 mm C18 column, eluting with 75 : 25 MeOH–H_2O at 1 mL min^{-1}, and detected by UV at 254 nm. Element analyses were obtained on a PE 2400 CHN analyzer, IR spectra were recorded on an IR-Spectrum One (PE), ^{1}HNMR spectra were recorded on a JNM-FX 90Q(JEOL) using TMS as an internal standard. Amberlyst 201 (Cl type resin, ion-exchange capacity: 3.2 mmol g^{-1}) and Amberlyst 732 (strong acidic ion-exchange resin, capacity: 4.2 mmol g^{-1}) were purchased from Chemical Company of Nankai University (Tianjin, China).

2.1.1 Preparation of polymer-supported reagents. Polymer-supported isothiocyanate was prepared according to a literature procedure[17] starting from Amberlyst 201 and its capacity was approximately 2.2 mmol isothiocyanate per gram of resin. Polymer-supported iodate was prepared according to a literature procedure[18] and its capacity was approximately 2.0 mmol iodate per gram of resin.

2.1.2 General procedure for the preparation of N-benzoyl–N′-aryl ureas. A mixture of benzoyl chloride (0.44 mL, 1.0 mmol), polymer-supported isothiocyanate (1.8 g, 4 mmol) and anhydrous acetonitrile (30 mL) was stirred at 50 °C for 6 h. As TLC analysis (SiO_2 plates, elution with petroleum ether–ether 6 : 1) revealed the absence of benzoyl chloride, the resin was filtered off and thoroughly washed with acetonitrile. The combined filtrates were concentrated to approximately 30 mL to give a solution of **2**, to which amines (2.0 mmol) were added and the solution was stirred at r.t. for 1 h after stirring, Amberlyst 732 (1.5 g) was added and the suspension was stirred at r.t. for an additional 2 h. The resin was filtered off and washed with acetonitrile to give a solution of **3**. Then, to the solution of **3** was added polymer-supported iodate (2.0 g) and the

Green Context

Solid-phase organic synthesis has become an important technique for the preparation of combinatorial libraries of organic species. Here a relatively straightforward and clean synthesis based on this approach is described for ureas. Representative ureas are prepared in high yield and excellent purity by this attractively simple methodology.

JHC

suspension was shaken at 70 °C for 3 h. The resin was filtered off and washed thoroughly with acetonitrile. The combined filtrates were concentrated and the residues were recrystallised from a solution of ethanol, filtered and dried under high vacuum to yield N-benzoyl–N′-aryl ureas.

3 Results and discussion

The procedure shown in Scheme 1 was used to synthesize a representative urea derivative library. The reaction of commercially available benzoyl chloride **1** with polymer-supported isothiocyanate in anhydrous acetonitrile at 50 °C for 6 h afforded **2** in 90% yield and 92% purity simply by filtration of the mixture to remove the spent polymer-supported reagent followed by evaporation of the solution. **2** reacted efficiently with various excess representative amines at r.t. for 1 h. The excessive amines were used to drive the reaction to completion. Upon completion of the reaction, the excessive amine was removed by addition of commercially available Amberlyst 732 strong acidic ion-exchange resin as sequestering agent at r.t. for an additional 2 h. **3** was obtained in 90–95% yield and 95–97% purity simply by filtration of the mixture to remove the spent resin and evaporation of the solvent. Next, compounds **3** were treated with polymer-supported iodate as oxidising agent in acetonitrile at 70 °C for 3 h to give **4** N-benzoyl–N′-aryl ureas, which were obtained simply by filtration of the mixture to remove the spent polymer-supported reagent and the combined filtrates were concentrated and the residues were recrystallized from a solution of ethanol to remove iodine, filtered and dried under high vacuum, giving 90–94% yield and a purity of 92–96%. A representative selection of the compounds synthesized is shown in Table 1.

Table 1 Yield, mp and purities of ureas

Product[a]	Substrate (RNH_2)	mp/°C[b]	Yield[c] (%)	Purity[d](%)
VIIa	$C_6H_5NH_2$	205–206	76.5	93
VIIb	o-$CH_3C_6H_4NH_2$	167–168	74.2	94
VIIc	p-$CH_3C_6H_4NH_2$	221–223	75.0	96
VIId	m-$CH_3COC_6H_4NH_2$	166–168	74.5	93
VIIe	p-$ClC_6H_4NH_2$	234.5–235.5	75.0	92
VIIf	p-$BrC_6H_4NH_2$	230–232	76.5	94
VIIg	o-$BrC_6H_4NH_2$	216–218	73.0	90
VIIh	β-$C_{12}H_7$ NH_2	217–218	75.5	95
VIIi	α-$C_{12}H_7$ NH_2	241–242	74.6	94
VIIj	p-$CH_3OC_6H_4NH_2$	215–217	76.5	96
VIIk	m-$NO_2C_6H_4NH_2$	230–231	75.0	92
VIIl	p-$NO_2C_6H_4NHNH_2$	225–227	74.0	95
VIIm	2,4-$(NO_2)_2C_6H_3NHNH_2$	209–213	73.5	95

[a] Products were characterized by IR, ^{1}HNMR and elemental analysis. [b] mp corresponding with reference 19. [c] Based on benzoyl chloride. [d] Analyzed by HPLC.

4 Conclusion

We have demonstrated a high-yielding, three-step library synthesis of ureas that relies on polymer-assisted solution-phase (PASP) synthesis techniques as the sole method of purification to give products in high purity.

Acknowledgement

We gratefully acknowledge financial support from the Education Department of Hubei Province and Hubei University.

References

1 A. Kirschning, H. Monenschein and R. Wittenberg, *Angew. Chem., Int. Ed.*, 2001, **40**, 650–679.
2 J. Eames and M. Watkinson, *Eur. J. Org. Chem.*, 2001, 1213–1224.
3 S. Bhattacharyya, *Indian J. Chem., Sect. B: Org. Chem. Incl. Med. Chem.*, 2001, **40**, 878–890.
4 S. V. Ley and A. Massi, *J. Chem. Soc., Perkin Trans. 1*, 2000, 3645–3654.
5 J. Habermann, S. V. Ley and R. Smits, *J. Chem. Soc., Perkin Trans. 1*, 1999, 2421–2423.
6 J. Habermann, S. V. Ley and J. J. Scicinski, *J. Chem. Soc., Perkin Trans. 1*, 1999, 2425–2427.
7 D. P. Getman, G. A. DeCrescenzo and R. M. Heintz, *J. Med. Chem.*, 1993, **36**, 288–291.
8 S. Kotachi, Y. Tsuji, T. Kondo and Y. Watanabe, *J. Chem. Soc., Chem. Commun.*, 1990, 549–550.
9 A. Basha, *Tetrahedron Lett.*, 1988, **29**, 2525–2526.
10 X. C. Wang, Z. Li and Y. X. Da, *Synth. Commun.*, 2000, **30**, 4543–4553.
11 M. K. Leung, J. L. Lai and K. H. Lau, *J. Org. Chem.*, 1996, **61**, 4175–4179.
12 J. Fournier, C. Bruneau, P. H. Dixneuf and S. Lecolier, *J. Org. Chem.*, 1991, **56**, 4456–4458.
13 N. Adel, A. O. Nhi and A. H. Richard, *Tetrahedron Lett.*, 2000, **41**, 5441–5446.
14 G. C. Yang, Z. X. Chen and Z. J. Zhang, *React. Funct. Polym.*, 2002, **31**, 1–6.
15 Z. X. Chen, G. C. Yang and Z. J. Zhang, *Synthesis*, 2001, 1483–1486.
16 G. C. Yang, Z. X. Chen and Z. J. Zhang, *Chin. J. Chem.*, 2002, **20**, 178–181.
17 K. Saito and K. Harada, *Bull. Chem. Soc. Jpn.*, 1989, **62**, 2562–2566.
18 C. R. Harrison and P. Hodge, *J. Chem. Soc., Perkin Trans. 1*, 1982, 509–511.
19 F. K. Beilstein, *Handbuch der Organischen Chemie*, Hauptwerk, 12, Spring-Verlay Press, Berlin, Germany, 1956.

Ionic liquid salt-induced inactivation and unfolding of cellulase from *Trichoderma reesei*

Megan B. Turner, Scott K. Spear, Jonathan G. Huddleston, John D. Holbrey and Robin D. Rogers*

Center for Green Manufacturing and Department of Chemistry, The University of Alabama, Tuscaloosa, AL 35487

Received 6th March 2003
First published as an Advance Article on the web 30th June 2003

The potential for performing cellulase-catalyzed reactions on cellulose dissolved in 1-butyl-3-methylimidazolium chloride ([bmim]Cl) has been investigated. We have carried out a systematic study on the irreversible solvent and ionic strength-induced inactivation and unfolding of cellulase from *Trichoderma reesei* (E.C. #3.2.1.4). Experiments, varying both cellulase and IL solvent concentrations, have indicated that [bmim]Cl, and several other ILs, as well as dimethylacetamide–LiCl (a well-known solvent system for cellulose), inactivate cellulase under these conditions. Despite cellulase inactivity, results obtained from this study led to valuable insights into the requirements necessary for enzyme activity in IL systems. Enzyme stability was determined during urea, NaCl, and [bmim]Cl-induced denaturation observed through fluorescence spectroscopy. Protein stability of a PEG-supported cellulase in [bmim]Cl solution was investigated and increased stability/activity of the PEG-supported cellulase in both the [bmim]Cl and citrate buffer solutions were detected.

Introduction

The use of ionic liquids (ILs) as solvents, or co-solvents, for enzyme-catalyzed reactions has been a field of increasing interest and importance in recent years.[1] Interest can be attributed to several unique aspects of ILs including: implications of green chemistry, previously unexplored solvent properties that can lead to new chemistry, mild enzyme-friendly environments, higher rates of conversion, increased enantioselectivity, and increased stability of the enzyme in ILs compared to organics.[1–3]

To date, the most thoroughly studied enzyme in ILs is *Candida antarctica* lipase B (E.C. # 3.1.1.3). The robustness of the enzyme in organic solvents is a desirable, and important, aspect of lipases that make them an exemplary model for study in ILs.[4] The use of ILs in lipase-catalyzed reactions has led to increased reaction rates, higher enantioselectivity and increased stability of the enzyme.[5–9] Recycling of the enzyme is also enabled allowing for continuous processing.[10–11] Additional applications of biocatalysis in IL solvent systems include, whole cell-catalyzed biotransformations and liquid–liquid extraction of antibodies,[12] thermolysin-induced formation of *Z*-aspartame,[6] α-chymotrypsin transesterification of *N*-acetyl-L-phenylalanine ethyl ester,[13] exploration of the peroxidase activity of hemin, cytochrome c, and microperoxidase-11,[14] and transglycosylation reactions catalyzed by β-galactosidase.[15]

Although the major focus of current research has been on lipase-catalyzed reactions, the need to explore an array of enzymes to gain an accurate and precise picture of biocatalysis in ILs is essential. In addition, most studies have been carried out with some other solvent, often water, present when using 'ionic liquids'. It is thus necessary to also study the effect of concentration of added ionic liquid salt solution on enzymatic activity.

Previous studies by Swatloski, *et al.* have determined that 1-butyl-3-methylimidazolium chloride, [bmim]Cl, dissolves unmodified cellulose, making subsequent reactions, or modifications, of cellulose in this solvent an attractive possibility.[16] Increased rate of cellulose hydrolysis *via* cellulase in [bmim]Cl solutions could lead to increased production of fermentable sugars that can be converted into fuels such as ethanol or lactic acid for use in polymers. These exciting and commercially profitable possibilities led us to explore cellulase activity in [bmim]Cl solutions.

Our studies of cellulose azure hydrolysis, conducted in [bmim]Cl solutions, resulted in loss of enzymatic activity and led us to also investigate possible IL-related denaturation. Possible adverse enzyme IL interactions have been alluded to in previous studies involving biocatalysis and these known IL properties have prompted researchers to exploit enzymes possessing broad stability and activity. The result has been almost exclusive use of lipases for enzymatic studies in ILs. As is evident from this study, the durability of an enzyme does play a significant role in its subsequent activity in an IL.

Here we report the activity of cellulase from *Trichoderma reesei* in a solution containing ILs, as a function of concentration, including [bmim]Cl, 1-butyl-3-methylimidazolium tetrafluoroborate ([bmim][BF_4]), and a solution of 5% lithium chloride–95% dimethylacetamide. Cellulase was observed to become deactivated by the presence of the halide ionic liquid, and we provide experimental evidence that supports a probable deactivation induced by enzyme unfolding and denaturation.

Green Context

The use of enzymes in ionic liquids is established. However, the scope of this utility is less well understood. This paper details investigations on cellulase enzymes, which are shown to be irreversibly denatured in ionic liquids. While a definitive mechanism for denaturation is not detailed, some potential routes are eliminated, and light is shed on the complexities of the subject. This paper is valuable since it begins to broaden the understanding of enzyme–ionic liquid systems. ***DJM***

Experimental

General

Cellulase (E.C. # 3.2.1.4) from *Trichoderma reesei* was purchased in its lyophilized (K_2HPO_4 complexed) form from Sigma (St. Louis, MO) and used in a solution of citrate buffer unless otherwise noted. Cellulose azure was purchased from Sigma (St. Louis, MO) and used without further processing. Citric acid monohydrate, also purchased from Sigma (St. Louis, MO), was processed for use as 0.05 M citrate buffer, pH 4.8, adjusted with 1 M NaOH. Cellulase was characterized and purity assessed using SDS-PAGE gel electrophoresis (Fisher Scientific, Pittsburgh, PA). All water was purified using a Barnstead (Dubuque, IA) commercial deionization and polishing system. Dimethylacetamide (DMAc) and LiCl were purchased from Aldrich (Milwaukee, WI) and used as received. Sodium dodecylsulfate (SDS), urea, PEG–1000, sodium chloride, sodium hydroxide, and potassium phosphate were all from Sigma (St. Louis, MO).

Ionic liquids ([bmim]Cl and [bmim][BF_4]) were prepared according to methods developed in house and used without further purification.[17] Purity of the ILs was determined using NMR spectroscopy. Residual water content of the ILs was not quantified due to subsequent water equilibration with the aqueous enzymatic solution introduced into the IL media.

Determination of cellulase activity

Activity of the soluble enzyme and PEG-supported cellulase was determined using cellulose azure as the substrate.[18] Absorbance of liberated azure dye molecules at a predetermined wavelength, 572 nm, and given time intervals (10, 20, 30, and 60 min) was measured on a Milton Roy Spectronic 21D Spectrophotometer (Ivyland, PA). (UV/Vis scans of the liberated cellulose azure were taken prior to activity determination in each solvent to assure measurement at optimal wavelength using a Cary 3C spectrophotometer (Palo Alto, CA)). Reactions contained varied concentrations of both substrate (cellulose azure) and enzyme (cellulase) in 2.0 mL solvent (0.05 M citrate buffer, [bmim]Cl, [bmim][BF_4], and 5% LiCl–95% DMAc) to explore concentration effects on the observed activity of cellulase. All reactions were run at a temperature of 50 °C and continuously stirred (60 rpm) in a New Brunswick Scientific C25 Incubator Shaker (Edison, NJ). At the previously specified time intervals, 20 μL of the reaction solution was diluted to 3.00 mL in 0.05 M citrate buffer and vortexed for 30 sec and the subsequent solution was centrifuged for 5 min at 4000 rpm. Absorbance was measured following centrifugation.

Fluorescence measurements of unfolded/refolded enzyme

Unfolding and refolding of cellulase was measured on a Horiba Jobin Yvon Fluoromax-3 Spectrometer (Edison, NJ). For unfolding experiments, vessels containing a total volume of 2.00 mL of varying concentrations, from 10%–95% [bmim]Cl or NaCl, in 0.05 M citrate buffer were prepared at room temperature. To each solution, 0.10 mL of 2.13 mg mL^{-1} cellulase was added and allowed to sit for one hour before measurement. Emission scans were then taken from 300–500 nm (λ_{ex} = 284 nm) with a slit width of 5.0 nm. (The cellulose-binding domain of the enzyme contains 1 tryptophan and 4 tyrosine moieties; in the catalytic domain there are 6 tryptophan and 15 tyrosine moieties, all of which contribute to the overall fluorescence of the enzyme within this emission range.) Measurements for refolding enzyme were taken according to a similar procedure as follows. Eight solutions of varying concentration of denaturant were prepared, 100%–0% [bmim]Cl–NaCl, and 0.10 mL unfolded cellulase (which had previously been unfolded in 22.44% wt/wt [bmim]Cl–22.50% wt/wt NaCl) were added and allowed to "stabilize" in solution for one hour. Emission scans of the refolded enzyme were taken from 300–500 nm (λ_{ex} = 284 nm) with a slit width of 2.5 nm. Integration and increment times for both experiments were set at 1.00 s nm^{-1}.

Preparation of PEG-stabilized cellulase

A solution of 106.4 mg K_2HPO_4, 111 mg 1,000 MW poly(ethylene glycol) (PEG), and 102 mg cellulase in 10 mL distilled water was prepared, flash frozen in liquid nitrogen, and lyophilized for 96 h according to the method of Laszlo and Compton.[13] The resulting solid enzyme was redissolved in 0.05 M citrate buffer for activity determination experiments. Enzymatic activity was determined in the manner previously described using 4.10 mg mL^{-1} PEG-stabilized enzyme and 4.00 mg mL^{-1} of native, or "free" enzyme.

Results and discussion

In the present study, cellulose azure was used as a substrate in a cellulose degradation assay aimed at measuring the activity of cellulase in ILs. Cellulose azure was added to the ILs 1-butyl-3-methylimidazolium-based [bmim]Cl and [bmim][BF_4], and LiCl–DMAc, a known cellulose solvent, into which aqueous cellulase solution was introduced. After allowing the enzyme to interact with the cellulose azure, aliquots were taken from the original mixtures, diluted to normalized concentrations, and absorbance measured (Fig. 1). As cellulase hydrolyzes the

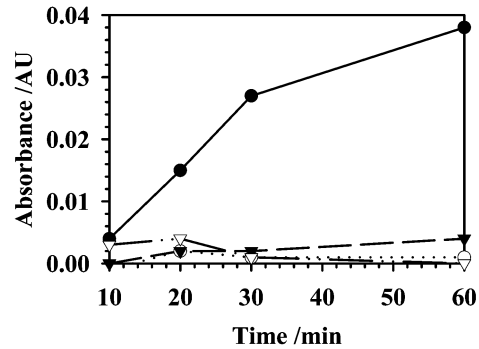

Fig. 1 Cellulase activity in [bmim]Cl, [bmim][BF_4], and 5% LiCl–95% DMAc compared to aqueous solution (● – cellulase (0.70 mg mL^{-1}) in 0.05 M citrate buffer solution; ▽ – cellulase in 5% LiCl–95% DMAc; ▼ – cellulase in [bmim][BF_4]; ○ – cellulase in [bmim]Cl).

repeating β, (1–4) linkages in cellulose, glucose subunits with covalently attached azure dye molecules are liberated.[18] Escalated liberation of these dye molecules is proportional to the activity intensity and accessibility measured through absorbance of the reaction solution.[18]

Factors contributing to the overall hydrolysis of cellulosic bonds include enzyme, substrate, and IL concentrations (Fig. 2). Increasing concentrations of either cellulose azure or cellulase result in increased activity. In contrast, the concentration of IL in solution is inversely proportional to the activity of the cellulase (Fig. 3a). Reactions with as little as 22 mM [bmim]Cl show diminished activities due to the possible denaturing effect of the Cl^- in the IL.

To explore the nature of the Cl^- ion concentration on the activity and stability of cellulase, NaCl was used in experiments analogous to those described above for [bmim]Cl and other IL solvents (Fig. 3b). Similar results obtained for both the

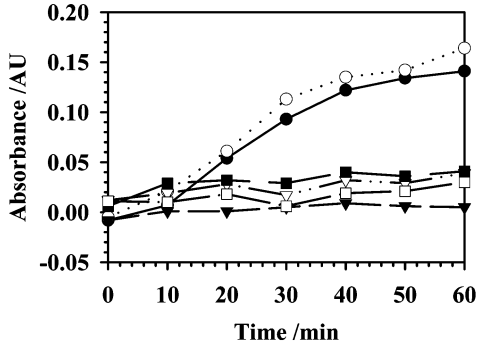

Fig. 2 Cellulase activity in [bmim]Cl solution *vs.* aqueous solution – varied enzyme and substrate concentrations (○ – 1.80 mg mL^{-1} cellulase in 0.05 M citrate buffer; ● – 1.00 mg mL^{-1} cellulase in 0.05 M citrate buffer; ■ – 1.80 mg mL^{-1} cellulase in [bmim]Cl; ▽ – 1.00 mg mL^{-1} cellulase in [bmim]Cl; □ – experimental control in [bmim]Cl; ▼ – experimental control in 0.05 M citrate buffer).

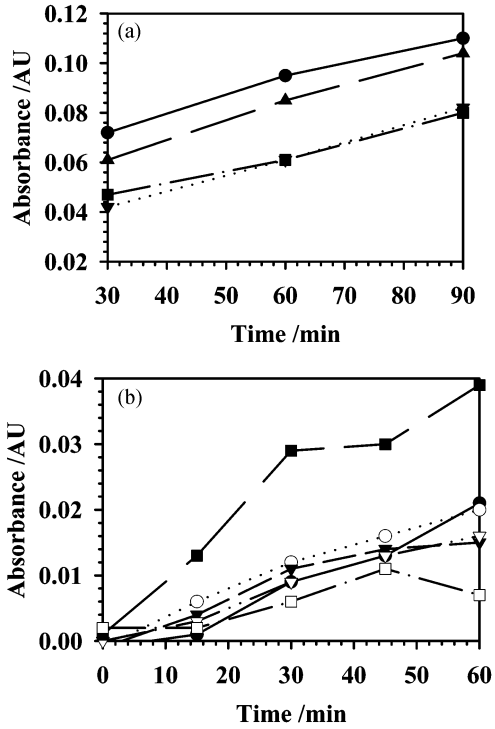

Fig. 3 (a) Cellulase (0.34 mg mL^{-1}) activity in low concentrations of [bmim]Cl (● – experimental control (0 mM [bmim]Cl solution); ▲ – 21.80 mM [bmim]Cl solution; ▼ – 39.70 mM [bmim]Cl solution; ■ – 59.80 mM [bmim]Cl solution). (b) Cellulase (0.35 mg mL^{-1}) activity in low concentrations of NaCl (■ – experimental control (0 M NaCl solution and 0.35 mg mL^{-1} cellulase); ○ – cellulase in 0.35 M NaCl solution; ● – cellulase in 0.60 M NaCl solution; ▼ – cellulase in 0.82 M NaCl solution; ▽ – cellulase in 1.23 M NaCl solution; □ – experimental control (0 M NaCl and 0 mg mL^{-1} cellulase)).

[bmim]Cl and NaCl solutions led us to conclude that the Cl^- ion was, in part, responsible for the inactivation of the cellulase as previously observed by Woodward *et al.*[19] Because the high Cl^- ion concentration in [bmim]Cl is similar to concentrated brine, denaturation of the enzyme is a predictable result. The strongly basic, 'salt-like', IL produces a dehydrating, and thus denaturing, environment that is not advantageous for most enzymes. However, interesting possibilities lay in the exploration of activities of microbial enzymes (which commonly thrive in high salt–high temperature environments) in ILs.

Previous literature has noted that enzymes dissolved in ILs become inactive, but do not proceed with experimental evidence supporting the inactivation.[2] Using spectrofluorometric techniques based on tryptophan fluorescence,[19] we were able to account for the observed inactivity through the denaturation of the cellulase (Fig. 4). The enzyme was first

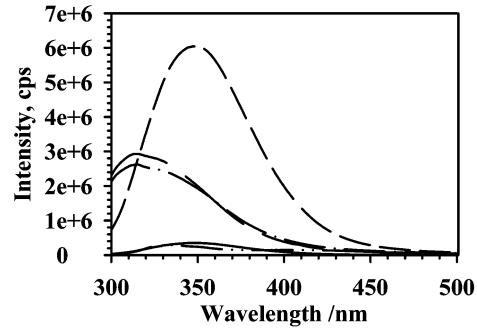

Fig. 4 Cellulase denaturation in solutions of SDS, SDS–8 M urea, [bmim]Cl, and NaCl (--- native cellulase (0.34 mg mL^{-1}) in 0.05 M citrate buffer; – – – cellulase (0.34 mg mL^{-1}) in a solution of 10% SDS–0.05 M citrate buffer; ·-·-·- cellulase (0.34 mg mL^{-1}) in a solution of 10% SDS and 8 M urea–0.05 M citrate buffer; — cellulase (0.97 mg mL^{-1}) in a solution of 80% [bmim]Cl; –··–··–cellulase (0.96 mg mL^{-1}) in a solution of 80% NaCl).

introduced into solutions containing known denaturants (SDS and 8 M Urea) to observe their effect on protein conformation enabling comparisons to be drawn between the effects of the known denaturants and [bmim]Cl. Evidence of protein denaturation is observed as the enzyme's fluorescence intensity associated with the protein's aromatic amino acid residues, namely tryptophan, is reduced upon addition of both [bmim]Cl and NaCl (Fig. 5a–b). Increasing concentrations of [bmim]Cl

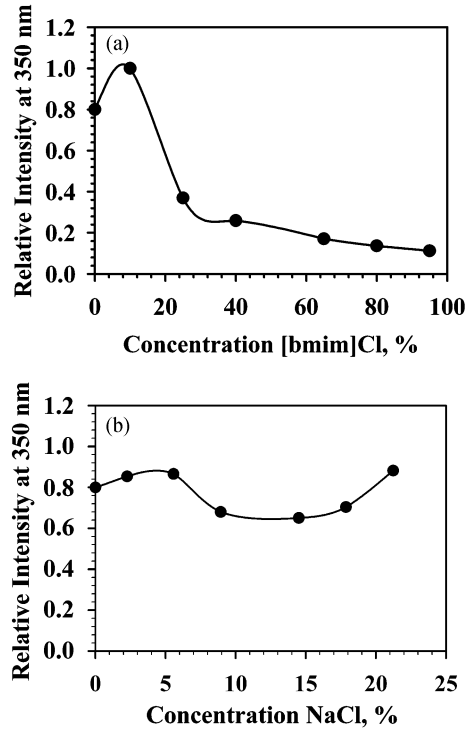

Fig. 5 Relative fluorescence intensities of cellulase refolding in (a) [bmim]Cl solutions (b) NaCl solutions.

progressively denature the cellulase, illustrated by the relative intensity of the enzyme through the range of IL concentrations. Denaturation of cellulase was also studied in NaCl solutions,

but the mechanism of unfolding differs. Addition of NaCl in increasing concentrations indicates denaturation in steps, creating intermediate conformations of the cellulase similar to previous results obtained for cellulase in guanidinium chloride solutions.[19]

Refolding of denatured cellulase into varying concentrations of [bmim]Cl solutions resulted in refolding of the enzyme contacting only the most dilute solutions (0–5% [bmim]Cl) as detected by fluorescence spectroscopy. Again, studies were conducted using NaCl solutions to determine if similarities exist between the refolding processes of the cellulase in [bmim]Cl *vs.* NaCl. However, as was observed in the unfolding of the enzyme, cellulase tends to refold inversely proportional to [bmim]Cl concentration and refolding in NaCl solutions takes place stepwise with conformational intermediates.

Although the protein's fluorescence spectra indicate refolding of the cellulase in the dilute [bmim]Cl solutions, the intrinsic activity may be compromised. A loss in activity in the enzyme can be attributed to a negatively induced conformational change within the enzyme upon refolding. The notion that solvent, in which the enzyme is dissolved, forces protein aggregation during refolding has previously been observed by Flowers and Summers.[20] These aggregations serve to 'lock' proteins in inactive conformations and may be the cause of the lack of activity of the refolded cellulase in [bmim]Cl solutions.[20] Proteins become inactivated when exposed regions of hydrophobicity interact with these similar exposed regions on other proteins.[20] Because the [bmim]Cl is a hydrophilic IL the formation of the aggregates appears to be entropically driven.

Prior studies involving biocatalysis in IL have noted that PEG-stabilized enzymes not only remain active, but demonstrate increased activity compared to traditional reaction media due to increased stability provided by the support.[1] To test the effect of a support on cellulase, the enzyme was attached to a PEG support according to the method of Laszlo and Compton.[13] Experiments were run as previously described in both aqueous solution, as well as in [bmim]Cl (Fig. 6). The PEG-stabilized

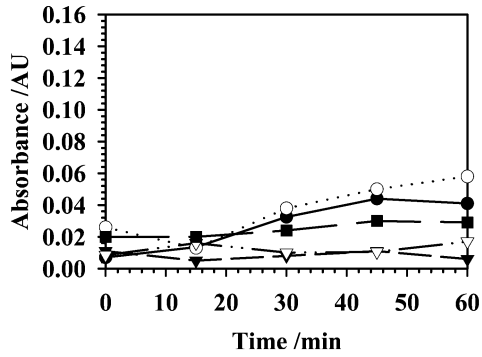

Fig. 6 Activity of PEG-stabilized cellulase in aqueous solution *vs.* [bmim]Cl (● – free cellulase (0.67 mg mL^{-1}) in buffer solution; ○ – PEG-stabilized cellulase (0.68 mg mL^{-1}) in 0.05 M citrate buffer; ■ – PEG-stabilized cellulase (0.68 mg mL^{-1}) in [bmim]Cl; ▽ – free cellulase (0.67 mg mL^{-1}) in [bmim]Cl; ▼ – experimental control (cellulose azure in buffer solution with no enzyme present)).

enzyme performed better than the native enzyme in both the aqueous solution and the [bmim]Cl solution. The stabilization provided by the PEG moiety seems to allow the enzyme to remain in an active conformation in the [bmim]Cl solutions notwithstanding the previously noted adverse effects the IL has on the native enzyme.

The potential activity of cellulase in these solutions is dependent upon both the IL anion–enzyme interactions and the environment of the enzyme while in solution. Introduction of an enzyme into an IL that possesses the same hydrogen bond donor ability and/or acceptor ability as a protic organic solvent, or into a hydrophobic IL that isolates the enzyme into aqueous microdomains, would pose the least threat, in terms of denaturing environment, to the enzyme.

The use of [bmim]Cl in these reactions poses several unique, and possibly troublesome, aspects. First, [bmim]Cl is a hydrophilic IL and thus, readily soluble in water, the major component of the enzyme solution. It has been determined, however, that increased amounts of water, as an impurity in the IL, led to diminished effective cellulose dissolution. Because cellulase produces water as a byproduct, the need for a system that can readily tolerate water is of major importance and, as noted above, the [bmim]Cl–cellulose mixture is sensitive to added water. Secondly, ILs are salts and cellulase, and a vast majority of all proteins, become denatured in environments with high salt concentrations.

Conclusions

Although [bmim]Cl has previously been shown to dissolve cellulose, its use in a solvent system to aide in increased cellulase activity cannot be supported with our experimental findings. The inhibition of cellulase by the ionic strength of [bmim]Cl in solution appears not to be solely linked to high Cl^- ion concentration that leads to unfolded, and inactive, enzyme. Experiments have shown that once cellulase becomes denatured by the [bmim]Cl solution, and other IL solutions, its subsequent refolding/reactivation cannot be achieved by methods explored here. It is evident that further research is needed to explore biocatalysts in ionic liquids, not just as novel solvents but also as working systems with broad applications.

Acknowledgements

This research has been supported by the U.S. Environmental Protection Agency's STAR program through grant number R-82825701–0. (Although the research described in this article has been funded in part by EPA, it has not been subjected to the Agency's required peer and policy review and therefore does not necessarily reflect the views of the Agency and no official endorsement should be inferred.) Additional support was provided to the Center for Green Manufacturing from the National Science Foundation Grant EPS-9977239.

References

1 R. A. Sheldon, R. M. Lau, M. J. Sorgedrager, F. van Ranywijk and K. R. Seddon, *Green Chem.*, 2002, **4**, 147–151.
2 P. Lozano, T. de Diego, D. Carrie, M. Vaultier and J. L. Iborra, *Chem. Commun.*, 2002, 692–693.
3 M. T. Reetz, W. Wiesenhofer, G. Francio and W. Leitner, *Chem. Commun.*, 2002, 992–993.
4 R. M. Lau, F. van Ranywijk, K. R. Seddon and R. A. Sheldon, *Org. Lett.*, 2000, **2**, 4189–4191.
5 M. Eckstein, P. Wasserscheid and U. Kragl, *Biotechnol. Lett.*, 2002, **24**, 763–767.
6 M. Erbeldinger, A. J. Mesiano and A. J. Russell, *Biotechnol. Prog.*, 2000, **16**, 1129–1131.
7 P. Kielbasinski, M. Albrycht, J. Luczak and M. Mikolajczyk, *Tetrahedron: Asymmetry*, 2002, **13**, 735–738.
8 K.-W. Kim, B. Song, M.-Y. Choi and M.-J. Kim, *Org. Lett.*, 2001, **3**, 1507–1509.
9 S. Panke and M. G. Wubbolts, *Curr. Opin. Biotechnol.*, 2002, **13**, 111–116.
10 T. Itoh, E. Akasaki, K. Kudo and S. Shirakami, *Chem. Lett.*, 2001, 262–263.

11 S. Park and R. J. Kazlauskas, *J. Org. Chem.*, 2001, **66**, 8395–8401.
12 S. G. Cull, J. D. Holbrey, V. Vargas-Mora, K. R. Seddon and G. J. Lye, *Biotechnol. Bioeng.*, 2000, **69**, 227–233.
13 J. A. Laszlo and D. L. Compton, *Biotechnol. Bioeng.*, 2001, **75**, 181–186.
14 J. A. Laszlo and D. L. Compton, *J. Mol. Catal. B: Enzym.*, 2002, **18**, 109–120.
15 N. Kaftzik, P. Wasserscheid and U. Kragl, *Org. Process Res. Dev.*, 2002, **6**, 553–557.
16 R. P. Swatloski, S. K. Spear, J. D. Holbrey and R. D. Rogers, *J. Am. Chem. Soc.*, 2002, **124**, 4974–4975.
17 J. G. Huddleston, A. E. Visser, W. M. Reichert, H. D. Willauer, G. A. Broker and R. D. Rogers, *Green Chem.*, 2001, **3**, 156–164.
18 H. N. Fernley, *J. Biochem.*, 1962, **87**, 90–95.
19 J. Woodward, N. E. Lee, J. S. Carmichael, S. L. McNair and J. M. Wichert, *Biochim. Biophys. Acta*, 1990, **1037**, 81–85.
20 C. A. Summers and R. A. Flowers, *Protein Sci.*, 2000, **9**, 2001–2008.

Heterogeneously catalysed selective hydrogenation reactions in ionic liquids

Kris Anderson,[ab] Peter Goodrich,[a] Christopher Hardacre*[ac] and David W. Rooney[ab]

[a] *The QUILL Centre, Queen's University Belfast, Belfast, Northern Ireland BT9 5AG. E-mail: c.hardacre@qub.ac.uk; Fax: +44 28 9038 2117; Tel: +44 28 9027 4592*
[b] *School of Chemical Engineering, Queen's University Belfast, Belfast, Northern Ireland BT9 5AG*
[c] *School of Chemistry, Queen's University Belfast, Belfast, Northern Ireland BT9 5AG*

Received 19th May 2003
First published as an Advance Article on the web 2nd July 2003

The selective hydrogenation of α,β unsaturated aldehydes has been performed in a range of room temperature ionic liquids. The reaction data reported show that it is possible to enhance the selectivity of supported palladium catalysts for the reduction of the conjugated C=C bond by using ionic liquids as solvents compared with conventional molecular organic solvents. The catalyst system is easily recycled without the need to isolate or filter the catalyst and may be used without further treatment.

Introduction

Ionic liquids have been studied extensively as clean solvents for a wide range of chemistry. The interest is a direct result of the diverse physical properties which these liquids have and the way in which they may be systematically varied, for example the density, viscosity and water miscibility. Since they also have effectively zero vapour pressure this makes them ideal engineering solvents for reactive chemistry allowing direct distillation from the solvent and simple solvent recycle without the production of VOC's.[1] A wide range of reactions have been performed in ionic liquids to date including alkylations,[2] C–C bond coupling reactions,[3–5] polymerisations,[6–8] hydrogenations,[9,10] hydroformylation,[11] and alkoxycarbonylation.[12] These reactions have been extensively reviewed recently.[13]

Many of the reactions reported in ionic liquids are catalytic; however, the vast majority have only been performed using homogeneous catalysts. Other catalytic systems have been reported, for example colloidal metal has been found to be active for Heck coupling,[14,15] oxidation reactions,[16] and hydrogenations,[17] but in each case the colloids were formed *in situ.* Only one study has been performed using heterogeneous catalysts suspended in the ionic liquid. Hagiwara *et al.* investigated the Heck reaction using carbon supported palladium in [bmim][PF_6] and found good recyclability and activity.[18] Carlin and Fuller also immobilised palladium on carbon in an ionic liquid co-polymer membrane for gas phase (propene) hydrogenation.[19] In this paper we report on the selective hydrogenation of α,β unsaturated aldehydes using a supported palladium catalyst in a range of ionic liquids and compare their reactivity and selectivity with conventionally used organic solvents. Two systems have been investigated, cinnamaldehyde to form hydrocinnamaldehyde and citral to form citronellal. The two reaction schemes with the range of products expected are shown in Fig. 1.

The selective reduction of α,β unsaturated aldehydes has been studied in detail and has been the subject of a number of reviews.[20] Reduction of either the C=C or C=O double bonds without further reduction is desirable for the manufacture of fragrances and other fine chemicals. Conventionally palladium is used to reduce the C=C double bond forming the saturated aldehyde and platinum the C=O double bond forming the

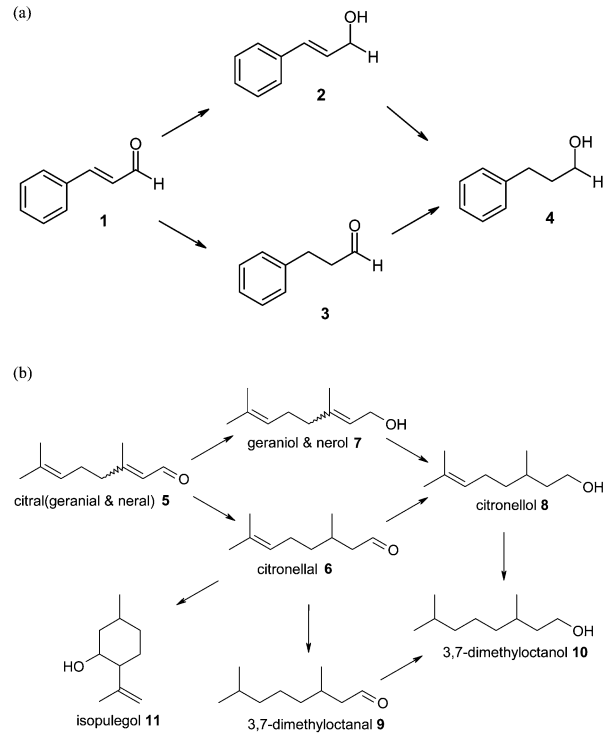

Fig. 1 Schematic of (a) cinnamaldehyde and (b) citral reduction pathways.

Green Context

Highly selective reductions can be difficult to achieve in many cases. Here, an effective method is developed using an ionic liquid as solvent and Pd–C catalysts. It is clear that the correct choice of conditions and of the anion are important, but that selectivities can be excellent with the correct system. Isolation of product and reuse of the catalyst are also readily achieved. ***DJM***

 DOI: 10.1039/b305633c

unsaturated alcohol; however, it is often difficult to prevent formation of the fully saturated alcohol as well.

By using promoters, modifying the catalyst preparation and using different supports a wide range of selectivities are possible. Many studies have been performed using Lewis acid additives, such as $FeCl_2$, which promote the reduction of the carbonyl group. Recent work, by Zhang *et al.*,[21] found that ferrous chloride promotes the formation of the fully saturated product 3-phenyl propanol over Pd/C following the reduction of cinnamaldehyde. Aramendia *et al*[22] showed that the effect of $FeCl_2$ on citral reduction over palladium was dependent on the $FeCl_2$: Pd ratio but again found it increased the reduction of the C=O double bond. Similar effects were observed using platinum catalysts forming the unsaturated alcohol in those cases.[23]

The catalyst support can also have a significant effect on the selectivity.[24] Recently, Pham-Huu *et al* have shown that changing the palladium support from high surface area charcoal to carbon nanofibres, selectivities of cinnamaldehyde to hydrocinnamaldehyde were increased.[25] Using graphite as the support for platinum catalysts has been reported to also increase the selectivity towards cinnamylalcohol.[26]

In both homogeneous and heterogeneously catalysed processes,[27] the choice of solvent can strongly influence both the catalytic activity and selectivity; however, few systematic studies have examined this for the selective reduction of α,β unsaturated aldehydes. Aramendia *et al*[22] studied a range of solvent polarities and found that the dielectric constant changed both the selectivity and activity of palladium catalysts for citral reduction. Alkaline-aqueous organic biphasic systems have also been shown by a number of groups to enhance the selectivity for C=C double bond over palladium and C=O double bond over platinum.[28] Supercritical CO_2 has been studied as a solvent for selective reduction of cinnamaldehyde over platinum and although it can promote the selectivity towards cinnamylalcohol, the selectivity achieved is highly dependent on the reaction conditions.[29] In the present study, the use of heterogeneous carbon catalysts in ionic liquids is illustrated. Herein the effects of temperature, pressure and ionic liquid composition are discussed as well as the recyclability of the catalyst–ionic liquid system.

Experimental

Trans-cinnamaldehyde (Aldrich, 99%) and citral (Lancaster, 99%; 1 : 1 E:Z isomer) were used as received. HPLC grade organic solvents were also used as received. The ionic liquids tested were prepared in house following standard preparative procedures, the details may be found elsewhere.[30,31] In each case the ionic liquid was washed extensively to ensure that halide contamination from the preparation process was < 10 ppm and then treated under vacuum at 60 °C to minimise water content. Viscosity measurements were carried out using a Brookfield cone and plate viscometer (LVDV-II). The procedure used has been described previously.[32]

10% Pd on activated carbon was obtained from Aldrich (BET surface area: 1144 $m^2\ g^{-1}$; metal dispersion: 21%). The gases used were all research grade and were supplied by BOC.

All reactions were carried out in a Baskerville mini autoclave under hydrogen pressure. In a typical reaction ionic liquid or organic solvent (2 cm^3), catalyst (5.5 mg) and substrate (4 mmol) were introduced to the autoclave and degassed with argon for one hour. Hydrogen at the required pressure was introduced to the autoclave and heated to the reaction temperature. Samples were taken periodically and analysed using a Hewlett Packard 6890 GC fitted with an RTX-5 column (30 m, 0.25 μm diameter). The retention time of the peaks were compared against authentic samples. In the case of organic solvents samples were analysed directly. When ionic liquids were used, the samples were extracted using diethyl ether in a volume ratio 1 : 10 (IL : ether), repeated four times, then the extract phase samples combined and analysed. For the recycle tests, the organics were extracted from the ionic liquids with diethyl ether following reaction, upon which fresh substrate was added to the catalyst solution and hydrogenation repeated as detailed above. Where recycle with pre-treatment with hydrogen was performed, the extracted ionic liquid–catalyst system was degassed with argon and then stirred under hydrogen at the pressure of the subsequent reaction for one hour. On release of the hydrogen, the substrate was injected into the reaction vessel and hydrogen at the required pressure was introduced to the autoclave and heated to the reaction temperature. The extraction procedure was found to result in a mass balance $> 99.5\%$ for the extracted material. For all results reported, the selectivity is defined as follows:

$$\%\text{selectivity } n = \frac{\%n}{\sum \%\text{products formed}} \times 100$$

where $\%n$ is the percentage yield of the compound n. Throughout the text, the selectivity refers to the conversion of cinnamaldehyde to hydrocinnamaldehyde or citral to citronellal.

Results

Cinnamaldehyde reduction

Table 1 summarises the results of the reduction of cinnamaldehyde in a range of ionic liquids giving the selectivity and conversion at various pressures and temperatures. Within the table, the highest selectivity and the conditions used for the hydrogenation in a range of molecular organic solvent systems is also given. The reactions in all the ionic liquids proceed slowly when compared with organic solvents. For example, at 5 bar and 30 °C in toluene, dioxane and cyclohexane, 100% conversion of cinnamaldehyde is obtained in 45 minutes compared with 240 minutes in the best ionic liquid used, [emim][NTf_2]. However, the selectivity towards hydrocinnamaldehyde is constantly above 97%, even at 100% conversion in these ionic liquids compared with a maximum of 85% (toluene), 89% (dioxane) and 79% (cyclohexane) over a range of temperatures (20–120 °C) and pressures (3–43 bar). In both ionic liquids and molecular organic solvents, the only products observed were hydrocinnamaldehyde and 3-phenylpropanol. From Table 1, it can be seen that all the ionic liquids tested were active for the hydrogenation and that although the choice of ionic liquid anion can affect the selectivity of the reduction; the selectivity observed is also strongly dependent on the reaction conditions, as described below.

Fig. 2 and 3 summarise the results on recycling the [bmim][BF_4] catalyst system. From Fig. 2, it is clear that there is a significant reduction in catalyst activity after the first reaction, from 100% conversion after four hours, to 50% conversion after four hours for each successive recycle. However, although the rate of reaction is reduced, this deactivation is not totally irreversible. If the catalyst–ionic liquid system is treated under the reaction conditions in the absence of substrate for 1 hour, the activity can be increased on recycle, as shown in Fig. 3. For all recycles, the selectivity of the system remains $> 97\%$ at all conversions. Increasing the residence time also enabled the reaction to proceed to completion, indicating that the catalyst does not deactivate further during the reaction. Similar recycle results were found for both [C_8Py][BF_4] and [emim][NTf_2]. In the former, the activity dropped from 58 to 50% conversion after 4 hours at 40

Table 1 Percentage distribution with solvent type for cinnamaldehyde(**1**), hydrocinnamaldehyde (**3**) and 3-phenylpropanol (**4**) and selectivity towards *hydrocinnamaldehyde* following reduction of cinnamaldehyde using 10%Pd/C for 4 hours unless otherwise stated. Under *all* reaction conditions studied, cinnamyl alcohol (**2**) was not observed

Solvent[a]	Temp/°C	Press./bar	% **1**	% **3**	% **4**	%sel **3**	Viscosity/cP
[bmim][PF_6]	60	40	0	100	0	100	48.9
[bmim][OTf]	60	40	0	91	9	91	39.0
[bmim][OAc]	60	40	0	78	22	78	23.1
[bmim][BF_4]	60	40	0	100	0	100	15.4
	60	5	51	49	0	100	
[C_6Py][BF_4]	60	40	23	77	0	100	38.1
	60	20	34	66	0	100	
[C_8Py][BF_4]	60	40	29	71	0	100	56.3
[$N_{8,8,8,1}$][BF_4]	60	40	90	9	1	90	405.5
[bmim][NTf_2]	60	40	0	88	12	88	16.7
[emim][NTf_2]	60	40	0	84	16	84	12.0
	30	40	18	81	< 1	99	30.6
	30	5	37	63	0	100	
	30	5 (16 h)	29	71	0	100	
[$N_{6,2,2,2}$][NTf_2]	60	40	59	41	0	100	54.0
[$N_{8,8,8,1}$][NTf_2]	60	40	20	69	11	86	61.9
[C_8Py][NTf_2]	60	40	30	58	12	83	27.9
Toluene	30	3 (1 h)	0	85	15	85	0.6
Cyclohexane	30	3 (1 h)	0	79	21	79	1.1
Dioxane	30	3 (1 h)	0	89	11	89	1.4

[a] Abbreviations used: *e.g.* [C_6Py] is *N*-hexylpyridinium, [C_8Py] is *N*-octylpyridinium, [emim] is 1-ethyl-3-methylimidazolium, [bmim] is 1-butyl-3-methylimidazolium, [$N_{6,2,2,2}$] is hexyltriethylammonium, [$N_{8,8,8,1}$] methyltrioctylammonium, [NTf_2] is *bis*(trifluoromethylsulfonyl)amide, [OTf] is triflate, and [OAc] is acetate.

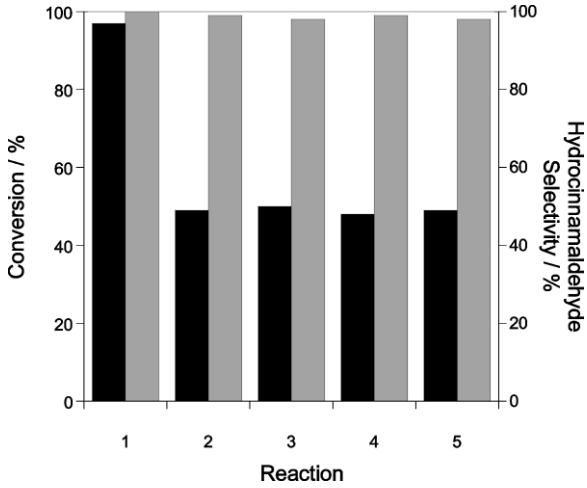

Fig. 2 Variation of cinnamaldehyde conversion (black) and selectivity (grey) on five successive reactions in [bmim][BF_4] at 60 °C and 40 bar after 4 hours.

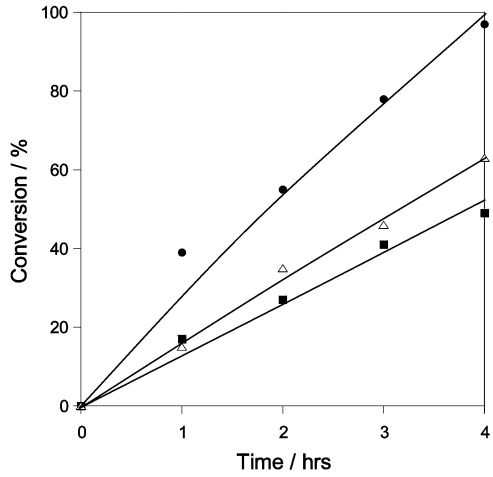

Fig. 3 Time variation of cinnamaldehyde conversion in [bmim][BF_4] (circles), on recycle without hydrogen pre-treatment (squares) and on recycle with hydrogen pre-treatment (triangles) at 60 °C and 40 bar. At all conversions, the selectivity towards hydrocinnamaldehyde was > 97%.

bar and 60 °C but this was maintained for five recycles whilst in the latter the conversion dropped from 63 to 41% (at 5 bar and 30 °C for 4 hours).

Fig. 4 shows how both the conversion and selectivity vary with temperature in [bmim][BF_4], [C_8Py][BF_4] and [emim][NTf_2]. As expected, conversion increased with increasing temperature; however, the selectivity was also affected. In the ionic liquids, the selectivity towards hydrocinnamaldehyde dropped from 99% at 90 °C to 94% at 120 °C in [C_8Py][BF_4] whereas in [bmim][BF_4] and [emim][NTf_2] the selectivity changes at much lower temperatures, *i.e.* above 60 °C. In comparison, from Table 1, it can be seen that the selectivity is not changed with pressure. This is in agreement with the temperature and pressure effects reported for the selective hydrogenation of cinnamaldehyde over Pd/SiO_2 in toluene.[33] Under all conditions where high selectivity is found in the ionic liquids, extending the time for the reaction has little effect on the selectivity, as shown in Table 1.

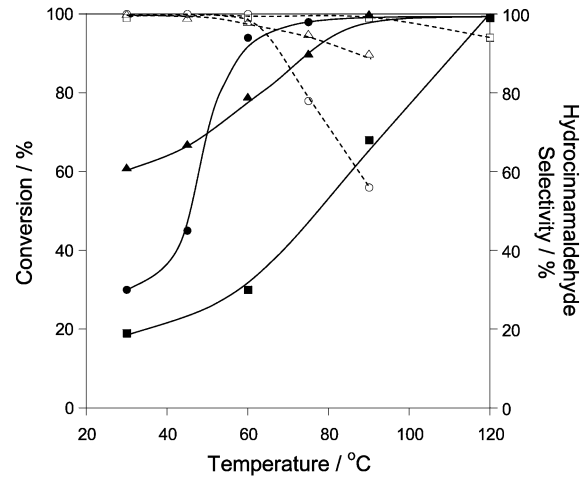

Fig. 4 Temperature variation of cinnamaldehyde conversion (closed symbols) and selectivity (open symbols) towards hydrocinnamaldehyde in [bmim][BF_4] (circles) and [C_8Py][BF_4] (squares) at 40 bar and in [emim][NTf_2] (triangles) at 5 bar after 4 hours.

Citral reduction

Table 2 summarises the results from citral reduction in a range of ionic liquids and organic solvents. As with cinnamaldehyde, described above, the ionic liquids provide a medium where high selectivity to C=C bond reduction can be achieved but again the selectivity is strongly dependent on the conditions employed, in particular the temperature. Whilst the selectivity in the ionic liquids exceeded that in the organic solvents studied, the rates were again found to be lower. It should be noted that, although high selectivities could be achieved with organic solvents, these only occur at low conversions, for example the highest selectivity observed with the organic solvents tested was in toluene at 90% but this was only achieved at 22% conversion at 3 bar and 20 °C after 30 min.

Fig. 5 shows the variation in products with temperature in [bmim][BF_4] and [emim][NTf_2] at 40 bar and 5 bar, respectively. As found for cinnamaldehyde, increasing temperature leads to greater conversion but a decrease in selectivity. Below 75 °C this system maintained high selectivity; however, above this temperature, the formation of citronellol leads to a decrease in selectivity. A similar trend is observed in [emim][NTf_2] where a decrease in selectivity occurs above 30 °C. The citral used for the experiment contains 1 : 1, *E* : *Z*, isomer ratio and it is interesting to note that the ratio of *E*/*Z* isomers of the unreacted citral in these experiments remained constant throughout the reductions in the ionic liquids. This may be compared with the organic solvents where, depending on the conditions and solvent used, between 5 and 10% of *E* citral was preferentially reduced during the hydrogenation in agreement with Aramendia *et al.*[22] In the ionic liquids, even at high temperatures (*i.e.* where the selectivity was reduced) and high pressures there was no evidence for the formation of the completely hydrogenated product 3,7-dimethyl octan-1-ol or geraniol/nerol. In all ionic liquid systems only trace quantities of isopulegol were observed compared with the organic solvents where up to 8% was formed.

Fig. 6 shows that, on recycle, the activity dropped significantly. For example, in [emim][NTf_2], the conversion dropped from 100 to 63%, after 4 hours. This level of activity remained for subsequent recycles, as before no change to the selectivity was observed on each recycle. Once again, however, pre-treatment of the ionic liquid–catalyst system with hydrogen did reactivate the system as illustrated in Fig. 6.

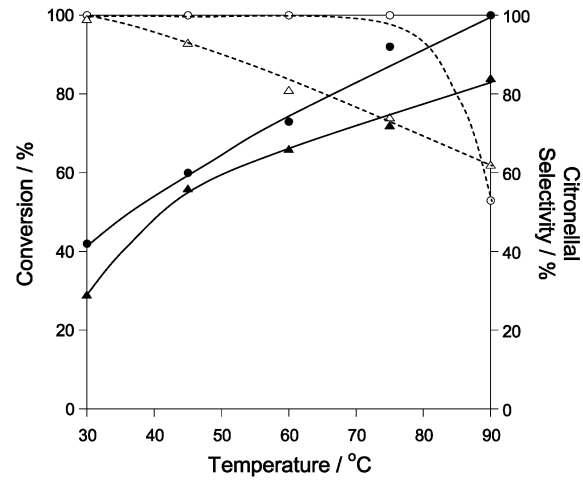

Fig. 5 Temperature variation of citral conversion (closed symbols) and selectivity (open symbols) towards citronellal in [bmim][BF_4] (circles) after 4 hours at 40 bar and [emim][NTf_2] (triangles) after 1 hour at 5 bar.

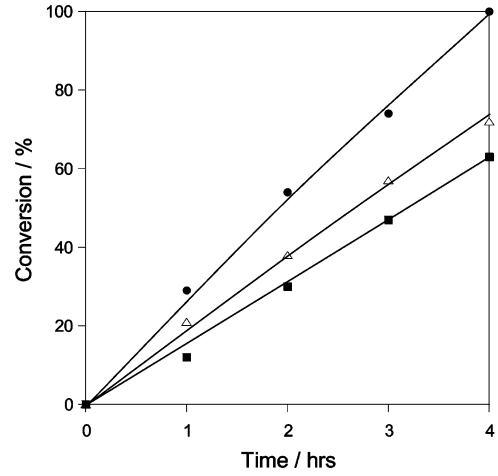

Fig. 6 Time variation of citral conversion in [emim][NTf_2] (circles), on recycle without hydrogen pre-treatment (squares) and on recycle with hydrogen pre-treatment (triangles) at 30 °C and 5 bar. At all conversions, the selectivity towards citronellal was > 98%.

Discussion

For both citral and cinnamaldehyde substrates the trends in reactivity and selectivity of the ionic liquid solvents with regard to temperature and pressure are similar, although in general, the conversion of citral was found to be higher than for cinnamaldehyde under the same conditions. For example in [bmim][BF_4] at 60 °C and 40 bar, the initial rate of citral reduction is 0.55 mol dm^{-3} s^{-1} compared with 0.13 mol dm^{-3} s^{-1} for cinnamalde-

Table 2 Percentage distribution with solvent type for citral (**5**), citronellal (**6**), geraniol/nerol (**7**), citronellol (**8**), 3,7-dimethyloctanal (**9**), 3,7 dimethyloctanol (**10**), isopulegol (**11**) and selectivity towards *citronellal* at various temperatures and pressures using 10% Pd/C, for 4 hours unless otherwise stated

Solvent	Temp/°C	Pres./bar	%**5**	%**6**	%**7**	%**8**	%**9**	%**10**	%**11**	%sel **6**
[bmim][PF_6]	60	40	28	69	—	3	—	—	—	96
[bmim][BF_4]	60	40	—	99	—	—	—	—	< 1	99
	30	10	48	52	—	—	—	—	—	100
[C_8Py][BF_4]	60	40	15	84	—	1	—	—	—	100
	30	10	68	32	—	—	—	—	—	100
[C_6mim][NTf_2]	60	40	7	75	—	16	—	< 1	< 1	81
[emim][NTf_2]	60	40	—	81	—	17	—	< 1	< 1	81
	30	5	—	99	—	< 1	—	—	< 1	99
	30	5 (16 h)	—	99	—	< 1	—	—	< 1	99
Cyclohexane	30	3 (1 h)	—	62	—	—	5	27	6	62
Toluene	30	3 (1 h)	31	53	3	< 1	1	5	6	77
	30	3 (2 h)	11	61	5	< 1	3	10	7	68
Dioxane	30	3 (1 h)	44	43	< 1	2	< 1	4	5	77
	30	3 (2 h)	—	69	< 1	< 1	3	18	8	69

hyde. The reactivity/selectivity is changed by the nature of the anion; bis(trifluoromethylsulfonyl)amide salts enabling reduction of both the C=C and C=O double bonds at much lower temperatures resulting in poor selectivity compared with the tetrafluoroborate salts under the same conditions, in general.

As described above, the rôle of solvents in many catalytic processes is unclear; however, in selective hydrogenations the polarity of the solvent is thought to be influential. High polarity solvents, such as methanol, were found to favour the formation of citronellal and hydrocinnamaldehyde in the selective reduction of citral and cinnamaldehyde, respectively, over palladium whereas in lower polarity solvents, such as cyclohexane and toluene, the selectivity was reduced.[21,22] Although the polarity of ionic liquids is difficult to measure, the hydrogen bonding accepting/donating properties which determine their interaction with other molecules has been determined using solvatochromatic dyes.[34] In general these studies indicate that the ionic liquids have similar hydrogen bonding characteristics to methanol. This is consistent with the previous findings that high selectivities can be obtained in media of this polarity. However, it should be noted that significant conversion of the aldehydes to the corresponding acetals has been observed in methanol which cannot occur in ionic liquids, and therefore any comparison of these two solvent systems could be misleading.

The mechanism by which the ionic liquid works may be associated with the strong interaction of the carbonyl groups with the ionic liquid.[35] Blanchard and Brennecke[36] have shown that ketones are difficult to extract from ionic liquids and work performed in our own laboratory shows a significant boiling point elevation for the distillation of ketones from a range of ionic liquids when the ketone is at submolar ratios. Delbecq and Sautet rationalised the relative selectivities of palladium and platinum by examining the adsorption geometry of α,β-unsaturated aldehydes using Hückel calculations.[37] They showed that on palladium, an η_4 adsorption geometry, *i.e.* a surface interaction with both the C=O and C=C double bonds, was most favoured and this lead to the reduction of both groups. The ionic liquid–carbonyl interaction may adjust the adsorption geometry of the aldehyde by weakening the interaction of the carbonyl with the surface of the catalyst thus favouring the π_{CC} or di-σ_{CC} interactions as opposed to the η_4 adsorption.

The change in selectivity with temperature and the observation that the conditions under which it occurs are dependent on the ionic liquid can be explained by a weakening of this interaction. Both the hydrogen bond donor ability, which is governed by the cation, and nucleophilicity, governed by the anion, will contribute to any interaction with the carbonyl.[38] It is therefore unsurprising that changing the ionic liquid should significantly alter how the reaction selectivity varies with respect to temperature.

In general, homogeneously catalysed reactions in ionic liquids show enhanced reaction rates when compared against organic solvents; however, in the case of the heterogeneously catalysed reactions studied here, lower rates have been observed. Normally, the higher rates found in homogeneous catalyst–ionic liquid systems are associated with increased stabilisation of transition states. Although stabilisation of the surface transition state may also be affected by solvents, any effect will be much smaller than that found for dissolved catalysts due to the lack of solvation. Mass transfer effects are likely to be the main reason for the reduced rates over heterogeneous catalysts. As shown in Table 1, in general, the viscosity of ionic liquids is higher than for many organic solvents and this subsequently reduces rate of diffusion of the aldehyde to the surface of the catalyst. A preliminary estimate using the Wilke and Chang correlation[39] to compare predicted diffusivities of the substrate in the ionic liquids with that of organic solvents, indicates that the diffusion coefficient in [bmim][BF_4] would be approximately twenty times lower than when using toluene as a solvent. Such significant differences in the diffusion of substrate would lead to decreased catalyst effectiveness and reduced reaction rates; however, the catalyst particle diameter was small ($\approx$ 54 μm), indicating that internal diffusion resistances would be negligible. Furthermore the hydrogen solubility in the ionic liquids has also been shown to be very small which will also limit the reaction rate.[40] It is also likely that film diffusion effects will limit the transfer of substrate and hydrogen onto the surface of the catalyst. The differential (or slip) velocity between the catalyst particle and the solvent is much smaller in ionic liquids than in conventional solvents due to both the higher viscosity and higher density leading to increased buoyancy. This effect is easily observed by noting the extended settling times required to separate the catalyst from the ionic liquid through gravity settling. This indicates that even when subjected to rapid shear during mixing the slip velocity between the catalyst particle and the ionic liquid would be low, hence lower mass transfer rates to the catalyst surface. These limitations are overcome by solvation in the case of homogeneous catalysed processes.

Other possible reasons for the lower rates may be associated with contaminants present in the ionic liquid, for example water or chloride.[30,31] Comparison of electrolysed ionic liquid samples, where the Cl^- < 1 ppm, produced similar results to the original ionic liquid and therefore the effect of halide contamination is unlikely to be the cause, in this study. It should be noted however, that halide contamination can affect the reaction. For example, the addition of increasing concentrations of [bmim]Cl to [bmim][BF_4], in order to mimic the effect of chloride, gradually decreased both the selectivity towards hydrocinnamaldehyde, and cinnamaldehyde conversion. On addition of above 50 ppm [bmim]Cl, no significant reaction was observed after 4 hours. In comparison, although the presence of water strongly affects the viscosity,[32] neither the rate or selectivity were significantly affected by low levels of water (< 1 wt%) in [bmim][BF_4], for example.[41]

Although the high viscosity of the ionic liquids may explain the lower rates it cannot account for the reduction in rate on recycle. Of significant consequence, in this regard, is the size of the ionic liquid compared with the micro/meso-pore structure of the carbon used in this study. Since much of the metal surface is inside these pores this may not be as accessible compared with conventional organic solvents, *i.e.* the diffusion of the ionic liquids into the pores will be limited and ultimately pore blockage can occur. This is indicated by the BET surface areas of the catalyst before and after interaction with the ionic liquid shown in Table 3. Clearly the pore volume and total surface area has been reduced significantly in all cases. In these cases the catalysts were washed extensively with acetonitrile to ensure that as much of the free ionic liquid was removed as possible. It should be noted that ICP analysis of the ionic liquid following reaction showed that no palladium leaching was detected and that the filtered ionic liquid had negligible hydrogenation activity.

Table 3 Variation of BET surface area and pore volume for 10%Pd/C following contact with various ionic liquids

Ionic liquid	Specific surface area/m^2 g^{-1}	Pore specific volume/cm^3 g^{-1}
Fresh catalyst	1144.67	1.1185
[bmim][PF_6]	309.16	0.3434
[bmim][BF_4]	460.25	0.5845
[C_8Py][BF_4]	561.61	0.6228
[emim][NTf_2]	533.62	0.4495
[C_6Py][NTf_2]	461.91	0.5125

The extraction with diethyl ether to enable the recycle is made facile by the fact that the catalyst remains in the ionic liquid phase during extraction thus enabling the catalyst and ionic liquid solvent to be reused without any filtering (a

hazardous process when carried out industrially due to the flammable nature of the solvent/hydrogen/catalyst filter sludge) and or laborious product and solvent separation procedures[42] It should be stressed that the recycle of the ionic liquid is facile in comparison to organic solvents and that the option of vacuum distillation is possible thus avoiding the use of extraction solvents. Combined with the results from the recycle experiments which show that after an initial deactivation all subsequent recycles have the same activity, there is significant potential for a "green" industrial process based on this overall system. Although there are significant process advantages concerning ionic liquids, it is clear that, since the exact reaction conditions affect both the rate and selectivity of the reductions, a full evaluation of the reaction space is required before significant conclusions regarding the comparison between organic solvents and ionic liquids may be drawn.

Conclusions

Ionic liquids have been shown to be highly selective solvents for the C=C double bond hydrogenation of cinnamaldehyde and citral forming hydrocinnamaldehyde and citronellal, respectively. By changing the anion of the ionic liquid or the temperature at which the reaction is performed, it is possible to vary the selectivity and selectivities close to 100% are possible when using a Pd/C catalyst although the rate is slower than in conventional organic media. The ionic liquid system also facilitates facile organic solvent extraction or vacuum distillation of the product phase without the removal of the catalyst and the system shows good recyclability.

Acknowledgements

The authors would like to thank the Department of Education in Northern Ireland (K. A.), the Queen's University Ionic Liquids Laboratory (K. A.), the Institute of Applied Catalysis (K. A.) and the EPSRC (P. G.) for financial support under grant GR/L58156.

References

1 M. Freemantle, *Chem. Eng. News*, 1998, **76**(March 30), 32; J. D. Holbrey and K. R. Seddon, *Clean products and processes*, 1999, **1**, 223.
2 C. E. Song, W. H. Shim, E. J. Roh and J. H. Chio, *Chem. Commun.*, 2000, 1695.
3 C. J. Mathews, P. J. Smith and T. Welton, *Chem. Commun.*, 2000, 1249.
4 A. J. Carmichael, M. J. Earle, J. D. Holbrey, P. B. McCormac and K. R. Seddon, *Org. Lett.*, 1999, **1**, 997.
5 C. deBellefon, E. Pollet and P. Grenouillet, *J. Mol. Catal.*, 1999, **145**, 121.
6 A. J. Carmichael, D. M. Haddleton, S. A. F. Bon and K. R. Seddon, *Chem. Commun.*, 2000, 1237.
7 M. F. Pinheiro, R. S. Mauler and R. F. deSouza, *Macromol. Rapid Commun.*, 2001, **22**, 425.
8 C. Hardacre, J. D. Holbrey, S. P. Katdare and K. R. Seddon, *Green Chem.*, 2002, **4**, 143.
9 Y. Chauvin, L. Mussman and H. Olivier, *Angew. Chem., Int. Ed. Engl.*, 1995, **34**, 2698.
10 P. J. Dyson, D. J. Ellis and T. Welton, *Can. J. Chem.*, 2001, **79**, 705; P. J. Dyson, D. J. Ellis, D. G. Parker and T. Welton, *Chem. Commun.*, 1999, 25.
11 P. W. N. M. vanLeeuwen, P. C. J. Kamer, J. N. H. Reek and P. Dierkes, *Chem. Rev.*, 2000, 100.
12 D. Zim, R. F. deSouza, J. Dupont and A. L. Monteiro, *Tetrahedron Lett.*, 1998, **39**, 7071.
13 For example T. Welton, *Chem. Rev.*, 1999, **99**, 2071; C. M. Gordon, *Appl. Catal., A*, 2002, **222**, 101; P. Wasserscheid and W. Keim, *Angew. Chem., Int. Ed.*, 2000, **39**, 3772; D. Zhao, M. Wu, Y. Kou and E. Min, *Catal. Today*, 2002, **1**, 2654; R. Sheldon, *Chem. Commun.*, 2001, 2399; J. Dupont, R. F. de Souza and P. A. Z. Suarez, *Chem. Rev.*, 2002, **102**, 3667.
14 R. R. Deshmukh, R. Rajagopal and K. V. Srinivasan, *Chem. Commun.*, 2001, 1544.
15 N. A. Hamill, C. Hardacre and S. E. J. McMath, *Green Chem.*, 2002, **4**, 139.
16 K. R. Seddon and A. Stark, *Green Chem.*, 2002, **4**, 119.
17 J. Dupont, G. S. Fonseca, A. P. Umpierre, P. F. P. Fichtner and S. R. Teixeira, *J. Am. Chem. Soc.*, 2002, **124**, 4228.
18 H. Hagiwara, Y. Shimizu, T. Hoshi, T. Suzuki, M. Ando, K. Ohkuboc and C. Yokoyamac, *Tetrahedron Lett.*, 2001, **42**, 4349.
19 R. T. Carlin and J. Fuller, *Chem. Commun.*, 1997, 1345.
20 P. Gallezot and D. Richard, *Catal. Rev.*, 1998, **40**, 81; U. K. Singh and M. A. Vannice, *Appl. Catal., A*, 2001, **213**, 1.
21 L. Q. Zhang, J. M. Winterbottom, A. P. Boyes and S. Raymahasay, *J. Chem. Technol. Biotechnol.*, 1998, **72**, 264.
22 M. A. Aramendia, V. Borau, C. Jiménez, J. M. Marinas, A. Porras and F. J. Urbano, *J. Catal.*, 1997, **172**, 46.
23 D. Richard, J. Ockelford, A. Giroir-Fendler and P. Gallezot, *Catal. Lett.*, 1989, **3**, 53.
24 U. K. Singh and M. A. Vannice, *J. Mol. Catal. A: Chem.*, 2000, **163**, 233.
25 C. Pham-Huu, N. Keller, L. J. Charbonniere, R. Ziessle and M. J. Ledoux, *Chem. Commun.*, 2000, 1871.
26 A. Giroir-Fendler, D. Richard and P. Gallezot, *Stud. Surf. Sci. Catal.*, 1988, **41**, 171.
27 J. T. Wehrli, A. Baiker, D. M. Monti, H. U. Blaser and H. P. Jalett, *J. Mol. Catal.*, 1989, **57**, 245; H. U. Blaser, H. P. Jalett and J. Wiehl, *J. Mol. Catal.*, 1991, **68**, 215; L. Gilbert and C. Mercier, *Stud. Surf. Sci. Catal.*, 1993, **78**, 51; J. C. Van der Waal and H. van Bekkum, *J. Mol. Catal. A: Chem.*, 1997, **124**, 137.
28 V. Satagopan and S. B. Chandalia, *J. Chem. Technol. Biotechnol.*, 1994, **60**, 17; V. Satagopan and S. B. Chandalia, *J. Chem. Technol. Biotechnol.*, 1994, **59**, 57; H. Yamada, H. Urano and S. Goto, *Chem. Eng. Sci.*, 1999, **54**, 5231.
29 B. M. Bhanage, Y. Ikushima, M. Shirai and M. Arai, *Catal. Lett.*, 1999, **62**, 175; F. Y. Zhao, Y. Ikushima, M. Shirai, T. Ebina and M. Arai, *J. Mol. Catal. A: Chem.*, 2002, **180**, 259.
30 J. D. Holbrey and K. R. Seddon, *J. Chem. Soc., Dalton Trans.*, 1999, 2133; C. M. Gordon, J. D. Holbrey, A. R. Kennedy and K. R. Seddon, *J. Mater. Chem.*, 1998, **8**, 2627.
31 P. Bônhote, A. P. Dias, N. Papageorgiou, K. Kalyanasundaram and M. Grätzel, *Inorg. Chem.*, 1996, **35**, 1168.
32 K. R. Seddon, A. Stark and M. J. Torres, *Pure Appl. Chem.*, 2000, **72**, 2275.
33 S. Mahmoud, A. Hammoudeh, S. Gharaibeh and J. Melsheimer, *J. Mol. Catal. A: Chem.*, 2002, **178**, 161.
34 For example S. N. V. K. Aki, J. F. Brennecke and A. Samanta, *Chem. Commun.*, 2000, 413; A. J. Carmichael and K. R. Seddon, *J. Phys. Org. Chem.*, 2000, **13**, 591.
35 R. M. Lynden-Bell, N. A. Atamas, A. Vasilyuk and C. G. Hanke, *Mol. Phys.*, 2002, **100**, 3225.
36 L. A. Blanchard and J. F. Brennecke, *Ind. Eng. Chem. Res.*, 2001, **40**, 287.
37 F. Delbecq and P. Sautet, *J. Catal.*, 1995, **152**, 217.
38 M. J. Muldoon, C. M. Gordon and I. R. Dunkin, *J. Chem. Soc., Perkin Trans. 2*, 2001, 433.
39 C. R. Wilke and P. Chang, *AIChE J.*, 1955, **1**, 264. The estimation is based on the assumption that the association factor of the ionic liquids = 1.9, *i.e.*, close to that for methanol.
40 J. L. Anthony, E. J. Maginn and J. F. Brennecke, *J. Phys. Chem. B*, 2002, **106**, 7315.
41 K. Anderson, C. Hardacre, P. Goodrich and D. Rooney, *paper in preparation*.
42 P. K. W. Lau and A. Koenig, *Chemosphere*, 2001, **44**, 9.

Cross-flow ultrafiltration of micellar solutions containing selected phenols

M. Bielska, K. Materna and J. Szymanowski*

Institute of Chemical Technology and Engineering, Poznan University of Technology, Pl. M. Sklodowskiej-Curie 2, 60-965 Poznan, Poland. E-mail: jan.szymanowski@put.poznan.pl

Received 2nd April 2003
First published as an Advance Article on the web 15th July 2003

Cross-flow ultrafiltration of micellar solutions containing phenols (phenol, 4-methylphenol, 4-chlorophenol, 2,4-dichlorophenol and 4-methoxyphenol) was studied. Oxyethylated coconut fatty acid methyl esters of an average oxyethylation degree of 10 and hexadecyltrimethylammonium bromide were used as surfactants. It was found that the hydrophilic membranes made of cellulose and polyethersulfone were useful for repeated separation of phenols from micellar solutions containing oxyethylated fatty acid methyl esters and hexadecyltrimethylammonium bromide. The membranes could be used several times because of the reversible blocking with surfactants. The rejection of phenols could be modelled by the Abraham linear solvation energy relationship. The pollutant hydrophobicity and basicity were the most important parameters affecting the rejection. Mixed micelles containing non-ionic and cationic surfactants improved solubilization of phenols and their rejection in membrane ultrafiltration.

Introduction

Phenols are toxic pollutants, frequently found in waste streams, but also in surface and tap waters. They are listed in the US Environmental Protection Agency priority list of pollutants and in the 76/464/EEC Directive of the European Union, related to hazardous substances discharged into the aquatic environment. Solvent extraction is the most often used technique to recover phenols from various aqueous effluents. Previously, aromatic and aliphatic hydrocarbons were used. Now, low molecular ketones and ethers are used. The position of *tert*-butyl methyl ether, a solvent produced in many countries and used as a gasoline additive, is special.

Classical extraction exhibits important drawbacks, connected with discharge of wastes containing dissolved solvents, or even dispersion or emulsion of solvents in water. These problems can be eliminated using membrane processes, which seem to be natural successors of the traditional extraction processes. There is no previous history of using such membrane processes for the extraction. However, reverse osmosis and ultrafiltration are commercially used in water treatment and in the food industry.

Direct removal of phenols by ultrafiltration of aqueous solutions is not possible. Such separation can be achieved using surfactant solutions in which organic pollutants are solubilized in surfactant micelles.[1–4] The average molecular mass of the spherical micelles is in the range of 20–30 kDa. Hence, the micelles along with the solubilized pollutants can be separated using membranes of appropriate pore diameter or cut-off. Due to the membrane fouling, the separation is also possible on membranes with a relatively large cut-off.[5,6]

The main drawback of micellar enhanced ultrafiltration is the transfer of surfactant monomers through the membrane being in equilibrium with the micelles and the membrane fouling caused by several factors, including surfactant gelation and adsorption.[1,7–10] The choice of surfactant type is crucial for potential applications.

Oxyethylated fatty acid methyl esters are new surfactants[11–14] which fulfil the requirements of green chemistry. Being esters, they are easily hydrolysed in sewage systems. They fulfil the requirements given in the Directives of the European Union (73/404/EEC, 82/242/EEC). Cationic surfactants are environmentally less friendly but they are easily precipitated in the sewage after neutralization with anionic surfactants used in a great excess.

Ultrafiltration of phenols was studied by several authors.[1,4,15–19] The works carried out in batch ultrafiltration cells with perpendicular flows proved that such separation is possible. However, such studies cannot be transferred to the continuous processes with cross-flow filtration.

The aim of the work was to study continuous cross-flow ultrafiltration of surfactant solutions containing different phenols. A binary mixture of oxyethylated fatty acid methyl esters and hexadecyltrimethylammonium bromide was selected as the most advantageous surfactant in agreement with our previous work[19] in which dead-end ultrafiltration was carried out in a batch cell.

Experimental

Chemicals

Oxyethylated coconut fatty acid methyl esters of an average oxyethylation degree equal to 10 (OCM-10) from the Institute of Heavy Organic Synthesis (ICSO), Kedzierzyn Kozle, Poland and hexadecyltrimethylammonium bromide (CTAB) (purum) from Merck, Germany were used as surfactants. OMC-10 was synthesized in a direct reaction of fatty acid methyl esters with

Green Context

The removal of phenols from waste streams is an important process, and one which must work efficiently and continuously. This paper deals with the development of cross-flow ultrafiltration as a technique for the selective removal of phenols from solutions containing newer green surfactants. The correct choice of membrane material allowed an efficient removal of the phenols from the system. ***DJM***

 DOI: 10.1039/b303666a

ethylene oxide according to the method described previously.[13,14] Commercial methyl esters, PK-12-18F Cognis, Germany were used. Their composition (in %) was as follows: C_8, 6.64; C_{10}, 5.59; C_{12}, 47.73; C_{14}, 19.01; C_{16}, 9.7; C_{18}, 8.65; C_{20}. 0.55; unidentified. 1.03; glycerides, 1.1; water below 0.18; iodine value, 10–15 g J_2 per 100 g; saponification number, 235–245 mg KOH g^{-1}; and acid number below 1 mg KOH g^{-1}.

Sodium chloride was used as a salting-out electrolyte. Phenol (pure), POCh, Poland, 4-methylphenol (pure) from Merck, Germany, 4-chlorophenol (pure) from Aldrich, Germany, 2,4-dichlorophenol (pure) from Aldrich, Germany and 4-methoxyphenol (pure) from Aldrich, Germany were used as pollutants. Deionized water from reverse osmosis was used as a solvent.

Membrane cell and membranes

Cross–flow membrane filtration was carried out in SEPA CF Membrane Cells, Osmonics, USA equipped with three types of polymeric flat-sheet membranes made of cellulose, polyethersulfone and polyvinylidene fluoride (Table 1). Effective membrane surface area was 0.0155 m^2. The membranes were used repeatedly. Prior to ultrafiltration, the membranes were conditioned in deionizated water for 24 h and then the deionized water was filtered for 5 h.

Table 1 Membrane parameters

Material	Symbol	Cut off	Max. ΔP/ bar	Possible pH	Max. ΔT/ °C
Cellulose	CQ	15 000–30 000	3.5	2–8	30
Polyethersulfone	PES	15 000–0 000	3.5	2–11	90
Polyvinylidene fluoride	PVDF	15 000–25 000	3.5	2–11	90

Ultrafiltration process

Ultrafiltration was carried out at room temperature in a continuous way under adjusted overpressure. Two ultrafilration options were considered: with retentate recirculation to the aqueous feed vessel and collection of permeate, and with recycling of both the permeate and the retentate to the feed vessel.

The first version was used in experiments in which the separation of phenols was studied. The second version was used to study the blocking of membrane pores. After each ultrafiltration of the surfactant solution, the membranes were washed by filtration with deionized water for 0.5 h.

The concentration of phenols in the aqueous feed (initial volume equal to 1 L) was changed from 0.005 to 0.05 g L^{-1}. The pH of the aqueous solutions was near 6. The concentration of surfactants used individually and in a binary mixture was always equal to 5 CMC or 10 CMC each in deionized water. The critical micelle concentration (CMC) in deionized water was equal to 9.2×10^{-4} mol L^{-1} and 5.4×10^{-4} mol L^{-1} for CTAB and OCM-10, respectively.

Concentrations of phenols were determined in the aqueous feed, permeate and retentate by UV using a Secomam S.750 Spectrofotometer, France. Blank samples contained appropriate surfactant concentration (1 CMC, 5 CMC and 9 CMC for permeate, aqueous feed and retentate, respectively). The neutral forms were analyzed at 270 nm, 278 nm, 283 nm, 288 nm and 287 nm for phenol, 4-methylphenol, 4-chlorophenol, 2,4-dichlorophenol and 4-methoxyphenol, respectively. The concentration of OMC-10 in the permeate was determined from the surface tension measurement. A Tracker tensiometer, I. T. Concept, France was used. Prior to the measurement, the retentate was diluted with water to reduce the surfactant concentration below its CMC.

Results and discussion

Membranes blocking

Fig. 1 demonstrates the effect of time upon the volume of the permeate in three successive ultrafiltration experiments: of deionized water on the new membrane, of surfactant solution, and then of deionized water again after the membrane washing. Significant blocking of the membrane with the surfactant was observed. The phenomenon depended on the membrane type, surfactant and electrolyte presence. The blocking was partially reversible for cellulose and polyethersulfone membranes. This indicated that the initial membrane permeability was not obtained after working with water. The irreversible blocking was observed for polyvinylidene fluoride membrane. In this case, the membrane pores were blocked even stronger after washing.

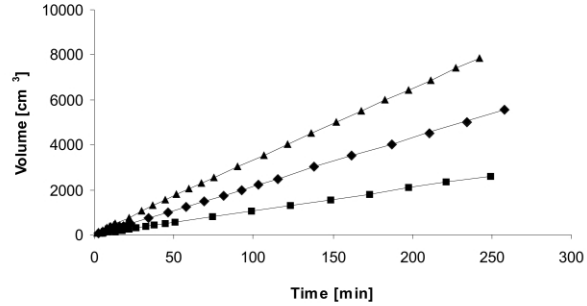

Fig. 1 Volume of permeate *versus* time for the polyethersulfone membrane: water through a new membrane (▲), ultrafiltration of OMC-10 solution (■), water ultrafiltration after membrane washing (◆), (ΔP = 0.1 MPa, [OMC-10] = 10CMC).

The function, where $V = at^n$, V stands for the permeate volume and t is the ultrafiltration time, well approximated the experimental data (Table 2). Thus, the flux could be easily estimated:

$$J = \frac{\mathrm{d}V}{s\,\mathrm{d}t} = \frac{a\,n\,t^{n-1}}{s}\ [\mathrm{m^3 m^{-2} s^{-1}}] \qquad (1)$$

where s is the effective membrane surface area.

Table 2 Statistical characteristics of the approximation $V = at^n$ (OMC-10 (10 CMC) as surfactant, ΔP = 0.1 MPa)

Membrane	Feed	a	n	Correlation coefficient
Cellulose	Water	0.944	0.945	0.987
	Surfactant	0.417	0.983	0.992
	Water	0.714	0.962	0.996
Polyethersulfone	Water	0.762	0.964	0.998
	Surfactant	0.215	0.978	0.995
	Water	0.387	0.992	0.997
Polyvinylidene fluoride	Water	3.09	0.936	0.999
	Surfactant	13.4	0.675	0.989
	Water	0.522	0.953	0.998

As it is shown in Figs. 2 and 3, the flux of the permeate decreased in the initial period and quickly achieved approximately constant values for hydrophilic membranes of cellulose and polyethersulfone. A relatively small decrease of this

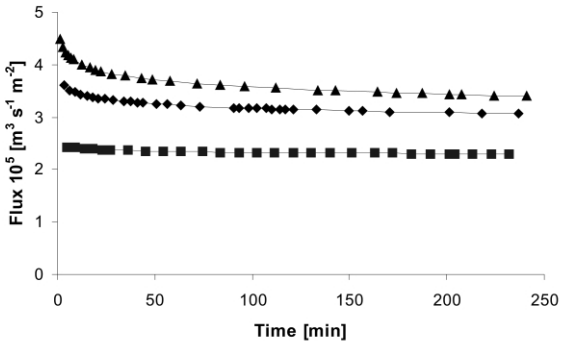

Fig. 2 Permeate fluxes for the cellulose membrane: water through a new membrane (▲), ultrafiltration of OMC-10 solution (■), water ultrafiltration after membrane washing (◆), (ΔP = 0.1 MPa, [OMC-10] = 10CMC).

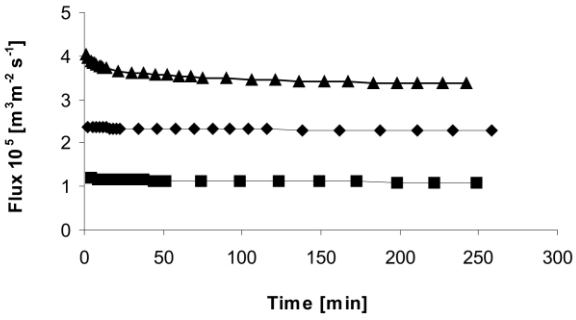

Fig. 3 Permeate fluxes for the polyethersulfone membrane: water through a new membrane (▲), ultrafiltration of OMC-10 solution (■), water ultrafiltration after membrane washing (◆), (ΔP = 0.1 MPa, [OMC-10] = 10CMC).

asymptotic flux for the membrane used again for water after the experiment with the surfactant solution, compared to the new membrane, was observed only for the cellulose membrane. They were equal to 3.4 × 10^{-5} and 3.7 × 10^{-5} $m^3m^{-2}s^{-1}$, respectively. Thus, the membrane could be used several times. A stronger decrease of the flux was obtained for the polyethersulfone membrane. The hydrophobic polyvinylidene fluoride membrane was irreversibly blocked (Fig. 4) but after the

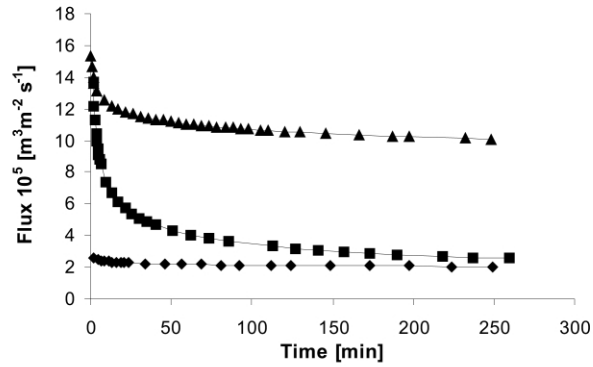

Fig. 4 Permeate fluxes for the polyvinylidene fluoride membrane: water through a new membrane (▲), ultrafiltration of OMC-10 solution (■), water ultrafiltration after membrane washing (◆), (ΔP = 0.1 MPa, [OMC-10] = 10CMC).

blocking the flux was comparable to that observed for the cellulose membrane. The initial and the final fluxes (in percents) of the surfactant solutions and water after washing in comparison with the initial and the final fluxes of deionized water ultrafiltrated through a new membrane for different ultrafiltration conditions are given in Table 3. The results were in agreement with those published by Kim[6] who demonstrated the advantageous properties of the hydrophilic membrane made of cellulose acetate.

Efficiency of separation

Efficiency of separation is usually characterized by rejection (R) defined as:

$$R = \left(1 - \frac{C_P}{C_R}\right)100\% \quad (2)$$

Table 3 Relative fluxes of surfactant solutions and deionized water in comparison to the initial and the final flux of deionized water ultrafiltrated through a new membrane

Membrane	Surfactant	NaCl concentration/ M	Ultrafiltration mode	Flux (%)	
				Initial	Final
Cellulose	OMC-10	0.0	Surfactant	54.2	67.0
			Water	80.3	90.0
	CTAB	0.0	Surfactant	75.6	67.6
			Water	85.4	76.5
	OMC-10	0.5	Surfactant	76.1	67.2
			Water	85.8	92.4
	OMC-10 + CTAB	0.5	Surfactant	76.0	64.4
			Water	58.0	71.1
Polyethersulfone	OMC-10	0.0	Surfactant	29.4	32.7
			Water	58.8	68.1
	CTAB	0.0	Surfactant	26.4	35.4
			Water	52.0	54.4
	OMC-10	0.5	Surfactant	9.8	17.7
			Water	53.4	60.3
	OMC-10 + CTAB	0.5	Surfactant	10.0	20.7
			Water	57.0	54.0
Polyvinylidene fluoride	OMC-10	0.0	Surfactant	89.0	25.1
			Water	16.5	20.2
	CTAB	0.0	Surfactant	41.3	71.0
			Water	37.5	58.1
	OMC-10	0.5	Surfactant	74.6	62.0
			Water	32.4	60.5
	OMC-10 + CTAB	0.5	Surfactant	88.7	86.0
			Water	32.0	38.8

where C_P and C_R denote concentration of the solute in the permeate and the retentate, respectively. The concentration of phenols in the permeate did not change with time. The concentration of phenols in the range from 0.005 to 0.05 g L^{-1} caused relatively small changes of the rejection calculated for ultrafiltration experiments in which half of the feed was taken as a permeate. As a result, the average rejections could be calculated from 6 independent measurements (Table 4).

The obtained results indicated that rejection depended on the type of phenol and the surfactant. Addition of the hydrophilic non-ionic surfactant to CTAB enhanced rejection of phenols, irrespective of the type of the membrane. However, the effect was not so well defined for 4-methylphenol and 4-methoxyphenol. Depending upon the membrane, an increase or a decrease of rejection was observed.

Rejection depended significantly on the hydrophobicity of the membranes, especially when CTAB only was used as the surfactant. The effect of membrane hydrophobicity decreased or was even negligible for the mixture of CTAB and OMC-10. Similar values of rejection were obtained for both the hydrophilic membranes (cellulose and polyethersulfone).

The effect of the surfactant could be partly connected with their ability to form mixed micelles. Fig. 5 shows the surface tension isotherms for OMC-10, CTAB and their binary mixture (1:1.7 mol mol^{-1} as equivalent to the ratio in CMC scale equal to 1:1). A high synergism in the surface tension reduction was observed for the binary mixture. It could be explained by solubilisation of some hydrophobic components present in the surfactants, *i.e.* polyoxyethylene homologues have a low number of oxyethylene units and polyoxyethylene glycol diesters of fatty acids. The mixed micelles were formed at lower surfactant concentration, *i.e.* at 9.2×10^{-4}, 5.4×10^{-4} and 1.58×10^{-4} mol L^{-1} for CTAB, OMC-10 and their binary mixture, respectively. Moreover, the mixed micelles had usually a higher degree of aggregation and a larger statistical diameter than the micelles of ionic surfactants because the repulsion forces between positively charged molecules of the ionic surfactant were decreased by the presence of nonionic surfactant molecules.[19] Thus, a decrease of CMC and an increase of the aggregation number and micelle diameter had a positive effect on solubilization of phenols and then their rejection in ultrafiltration.

Cationic surfactants, including CTAB, adsorb strongly upon the surfaces of solids, including membranes.[9,10,20,21] The phenomenon could cause a higher rejection by a decrease of pore diameter if the pores were not small enough, or a decrease of rejection when the pore diameter was small, and strong adsorption caused a decrease of the surfactant effective concentration. Moreover, the layers of the surfactant adsorbed on the pore walls could also act like a stratified material of liquid crystalline nature, and flow over the inner pore walls as they were dragged along by the viscous liquid passing through as was postulated by Frens *et al.*[9,10] Addition of a nonionic surfactant decreased the undesired adsorption of CTAB. The explanation agreed well with the experimental data given in Table 4 for the hydrophobic polyvinylidene fluoride membrane.

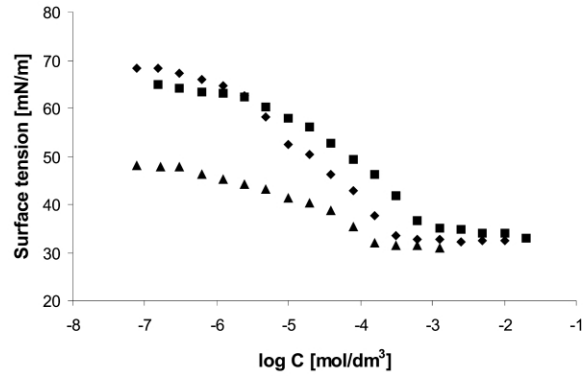

Fig. 5 Surface tension isotherms (CTAB (■), OMC-10 (◆), binary mixture of CTAB and OMC-10 1.7 : 1 (mol mol^{-1}) (▲)).

A strong increase of rejection was observed when the mixture of CTAB and OMC-10 was used.

To understand the physicochemical phenomena involved in the ultrafiltration of phenols, the results can be discussed on the basis of the general linear solvation energy relationship introduced by Abraham:[22–24]

$$\%R = c + a\sum\alpha_2^H + b\sum\beta_2^H + s\pi_2^H + rR_2 + vV_x/100 \qquad (3)$$

where $\Sigma\alpha_2^H$ is the solute hydrogen-bond acidity, $\Sigma\beta_2^H$ is the solute hydrogen-bond basicity, π_2 is the solute dipolarity/polarizability, R_2 is the solute excess molar refraction and V_x is the molar volume. The coefficients *a*, *b*, *s*, *r* and *v* denote relative contributions of each parameter. The values of the Abraham parameters were collected in Table 5, and the regression coefficients of the model after elimination of the least important parameters together with determination coefficient in Table 6. Rejection for the same molar concentration (3.7×10^{-4} M) of phenols were taken into consideration. Both, individual systems, *i.e.* for one type of membrane and surfactant, and the collective system for hydrophilic membranes (CQ and PES) were taken into consideration. Thus, the number of experimental data increased from 5 to 20 and enabled the computing. It was observed that the estimated and experimental values of rejection were in satisfactory agreement (Fig. 6). The most important thing was that the effect of the considered

Table 5 Values of pK_a and Abraham parameters for studied phenols[24]

Pollutant	pK_a	Σa_2^H	$\Sigma\beta_2^H$	π_2	R_2	V_x/100
Phenol	9.9	0.60	0.31	0.89	0.805	0.755
4-Methylphenol	10.3	0.57	0.32	0.87	0.820	0.916
4-Chlorophenol	9.4	0.67	0.21	1.08	0.915	0.898
2,4-Dichlorophenol	7.9	0.53	0.19	0.84	0.960	1.020
4-Methoxyphenol	9.5	0.57	0.48	1.17	0.900	0.975

Table 4 Average rejections (*R*) of phenols at different experimental conditions (for 6 independent measurements at significance level of 0.05 CL – confidence limit, concentration of surfactant equal to 5 CMC in deionized water)

		Phenol		4-Methylphenol		4-Chlorophenol		2,4-Dichlorophenol		4-Methoxyphenol	
Membrane	Surfactant	R	CL	R	CL	R	CL	R	CL	R	CL
Cellulose	CTAB	48.31	4.95	73.68	2.43	80.88	1.12	88.18	4.88	60.19	1.47
	CTAB + OMC-10	52.61	4.59	69.39	1.90	96.17	0.97	93.24	3.44	51.31	2.67
Polyethersulfone	CTAB	45.19	3.78	74.99	3.53	81.89	1.19	90.01	7.65	50.95	7.16
	CTAB + OMC-10	54.44	6.11	63.55	5.45	97.16	2.22	90.84	7.42	59.06	0.83
Polyvinylidene fluoride	CTAB	33.27	3.93	51.54	3.51	69.60	2.27	73.47	8.56	45.84	6.38
	CTAB + OMC-10	53.25	1.91	68.95	1.71	92.91	1.45	78.76	7.14	57.87	7.94

Table 6 Regression coefficients of the Abraham model (R^2 – determination coefficient, n – number of experimental data, c – constant, phenol concentration equal to 3.7×10^{-4} M)

Membrane	Ultrafiltration mode	n	a	b	s	r	v	c	R^2
CQ	CTAB	5	—	−112,14	—	—	114.03	—	0.997
	OMC-10 + CTAB	5	—	−151.23	—	133.57	—	—	0.992
PES	CTAB	5	—	−163.35	—	—	129.62	—	0.995
	OMC-10 + CTAB	5	—	−125.17	—	126.86	—	—	0.993
PVDF	CTAB	5	—	−75.92	—	—	87.72	—	0.993
	OMC-10 + CTAB	5	—	–	—	83.09	—	—	0.971
CQ + PES	CTAB	10	—	−137.78	—	—	121.84	—	0.995
	CTAB	10	—	−133.82	—	—	136.86	−14.95	0.906
	OMC-10 + CTAB	10	—	−138.20	—	130.21	75.80	—	0.998
	OMC-10 + CTAB	10	—	−127.33	—	168.14	—	−36.78	0.851
	CTAB, OMC-10 + CTAB	20	—	−164.17	24.21	—	106.51	—	0,994
	CTAB, OMC-10 + CTAB	20	78.49	−139.26	—	—	135.66	−56.83	0.917

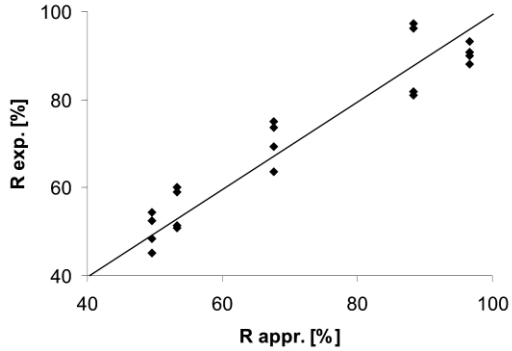

Fig. 6 Comparison of experimental and calculated values of %R for phenols.

parameters was well defined, *i.e.*, v, r, s and a coefficients were positive, and b and c were negative. The solute basicity showed a strong negative effect because both the non-ionic surfactant and CTAB had no hydrogens able to form hydrogen-bonding with solute molecules. The rejection was improved by the solute hydrophobicity and in some cases by the solute excess molar refraction, solute dipolarity/polarizability and solute hydrogen-bond acidity. The change of parameters present in the derived equation suggested their mutual correlation. The rejection increased with the phenol molecular volume. The effect was very important for mixed micelles containing OMC-10 and CTAB. The pseudo-micellar phase was less hydrophilic than the pseudo-aqueous phase and showed higher affinity to the more hydrophobic phenols.

The surfactant micelles presented in the micellar pseudo-phase exhibited higher basicity than the aqueous pseudo-phase. The effect could be explained by the presence of positively charged nitrogen in CTAB and oxygen atoms in polyoxy-ethylene chains of OMC-10 which were able to interact with the hydrogen atoms of the phenols' hydroxy groups.

The ultrafiltration experiments permitted the estimatation of the loading of micelles with solutes defined by the following equation:

$$L_M = \frac{[PhOH]_R - [PhOH]_P}{[S]_R - CMC}\left[\frac{mol}{mol}\right] \quad (4)$$

In the considered case, $V_R = V_P = \frac{1}{2}V_F$, the subscripts R, P and F denote the retentate, the permeate and the feed, respectively.

The loading depended upon the concentration of the solutes in the feed $[PhOH]_F$, approximately linearly in the considered concentration range (Fig. 7). The linearity suggested that the

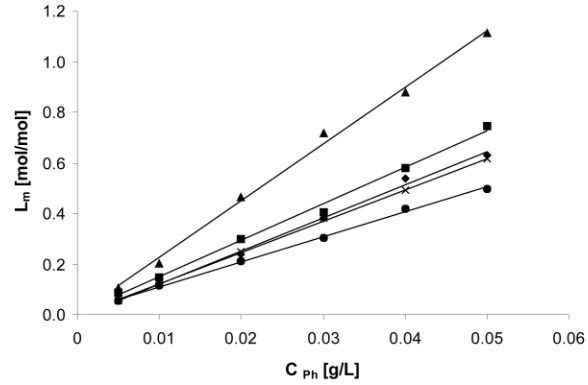

Fig. 7 Loading of mixed micelles ([CTAB] = [OMC-10] = 5 CMC) from ultrafiltration experiments through cellulose membrane (phenol (◆), 4-methylphenol (■), 4-chlorophenol (▲), 2,4-dichlorophenol (×), 4-methoxyphenol (●)).

micelles were still able to solubilize more pollutants. The type of membrane did not affect the loading, which proved that both the ultrafiltration experiments and the analytical procedure were correct. The use of surfactant mixture caused a sharp increase of loading which could be explained by an increase of micelle diameter.

The loading estimated for the same molar concentration given in Table 7 showed that the CTAB micelles contained approximately 1 phenol molecule per 10 CTAB molecules.

Table 7 Micelle loading with phenols (3.7×10^{-4} mol L^{-1} of phenols, concentration of each surfactant equal to 5 CMC)

	CQ		PES		PVDF		Average	
Pollutant	CTAB	CTAB + OMC-10	CTAB	CTAB + OMC-10	CTAB	CTAB + OMC-10	CTAB	CTAB + OMC-10
Phenol	0.063	0.380	0.087	0.435	0.063	0.405	0.071	0.406
4-methylphenol	0.086	0.407	0.084	0.437	0.072	0.471	0.081	0.438
4-chlorophenol	0.121	0.880	0.131	0.845	0.104	0.790	0.118	0.838
2,4-dichlorophenol	0.104	0.614	0.124	0.643	0.108	0.597	0.112	0.618
4-methoxyphenol	0.079	0.416	0.067	0.470	0.071	0.520	0.072	0.468

However, as a result of solubilization, the number of phenol molecules in the mixed micelles increased to 5–10.

Conclusions

Cross-flow ultrafiltration experiments showed the usefulness of hydrophilic membranes made of cellulose and polyethersulfone for repeated separation of phenols from micellar solutions containing oxyethylated fatty acid methyl esters and hexadecyltrimethylammonium bromide. The membranes could be used several times because of the reversible blocking with surfactants.

The rejection of phenols could be modelled by the Abraham linear solvation energy relationship. The pollutant hydrophobicity and basicity were the most important parameters affecting the rejection.

Mixed micelles containing non-ionic and cationic surfactants improved solubilization of phenols and their rejection in membrane ultrafiltration.

Acknowledgements

The work was supported by the DS grant No. 32/044/2003.

References

1 R. O. Dunn, Jr., J. F. Scamehorn and S. D. Christian, *Sep. Sci. Technol.*, 1985, **20**, 257–284.
2 R. O. Dunn, Jr., J. F. Scamehorn and S. D. Christian, *Sep. Sci. Technol.*, 1987, **22**, 763–789.
3 R. O. Dunn, Jr., J. F. Scamehorn and S. D. Christian, *Colloids Surf.*, 1989, **35**, 49–56.
4 S. D. Christian and J. F. Scamehorn, in *Surfactant-Based Separation Processes*, ed. J. F. Scamehorn and J. H. Harwell, Marcel Dekker, New York, pp. 3–28.
5 J. J. Hong, S. M. Yang and C. H. Lee, *J. Chem. Eng. Japan*, 1994, **27**, 314–320.
6 C. K. Kim, S. S. Kim, D. W. Kim, J. C. Lim and J. J. Kim, *J. Membr. Sci.*, 1998, **147**, 13–22.
7 S. N. Bhat, G. A. Smith, E. E. Turker, S. D. Christian, J. F. Scamenhorn and W. Smith, *Ind. Eng. Chem. Res.*, 1987, **26**, 1217–1222.
8 M. Syamal, De. Sirshendu and P. K. Bhattacharya, *J. Membr. Sci.*, 1997, **137**, 99–107.
9 A. Bakx, A. Timmerman and G. Frens, *Colloid Polym. Sci.*, 2000, **278**, 418–424.
10 A. Bakx, A. Timmerman and G. Frens, *Colloids Surf., A. Phys. Eng. Asp.*, 2001, **183–185**, 149–157.
11 I. Hama, T. Okamoto and H. Nakamura, *J. Am. Oil Chem. Soc.*, 1995, **72**, 781–784.
12 I. Hama, T. Okamoto, E. Hidai and K. Yamada, *J. Am. Oil Chem. Soc.*, 1997, **74**, 19–24.
13 W. Hreczuch, *J. Surf. Deterg.*, 1999, **2**, 287–292.
14 D. Makowska, J. Zimoch, M. Bogacki and J. Szymanowski, *J. Surf. Deterg.*, 2001, **4**, 121–126.
15 H. Adamczak, K. Materna, R. Urbański and J. Szymanowski, *J. Colloid Interface Sci.*, 1999, **218**, 743–750.
16 J. Sabate, M. Pujola, E. Centelles, M. Galan and J. Llorens, *Colloids Surf. A. Phys. Eng. Asp.*, 1999, **150**, 229–245.
17 H. Adamczak, F. Talens and J. Szymanowski, *J. Membr. Sci.*, 2001, **192**, 155–163.
18 Ch.-Ch. Tung, Y.-M. Yang, Ch.-H. Chang and J.-R. Maa, *Waste Manage.*, 2002, **22**, 695–701.
19 B. Korzystka, H. Adamczak, A. Sobczyńska and J. Szymanowski, *Colloids Surf., A*, 2003, **212**, 175–183.
20 Z. Lukaszewski and A. Szymański, *Anal. Chim. Acta.*, 1990, **231**, 77–84.
21 R. Urbanski, E. Góralska, H. J. Bart and J. Szymanowski, *J. Colloid Interface Sci.*, 2002, **253**, 419–426.
22 M. H. Abraham, *Chem. Soc. Rev.*, 1993, **22**, 73–83.
23 M. H. Abraham, *J. Phys. Org. Chem.*, 1993, **6**, 660–684.
24 M. H. Abraham, H. S. Chadha, J. P. Dixon, C. Rafols and C. Treiner, *J. Chem. Soc., Perkin Trans. 2*, 1997, **1**, 19–24.

Production of lactic acid esters catalyzed by heteropoly acid supported over ion-exchange resins

Ayturk Engin,[a] Hamamci Haluk[b] and Karakas Gurkan*[a]

[a] *Middle East Technical University, Chemical Engineering Department, 06531, Ankara, Turkey*
[b] *Middle East Technical University, Food Engineering Department, 06531, Ankara, Turkey*

Received 24th March 2003
First published as an Advance Article on the web 16th July 2003

The heterogeneous liquid-phase esterification reaction of lactic acid with ethyl alcohol accompanied with lactoyllactic acid hydrolysis over heteropoly acid supported on ion exchange resin catalysts was investigated at 343 K with ethanol to lactic acid molar ratio of 1:1. The catalysts with 5–20% of tungstophosphoric ($H_3PW_{12}O_{40}{\cdot}xH_2O$) and molybdophosphoric ($H_3PMo_{12}O_{40}{\cdot}xH_2O$) acid type of heteropoly acids over Lewatit® S100 showed higher activities than the resin itself. DRIFTS and XRD analysis indicated the formation of amorphous heteropoly acid layer, which is strongly bonded to the resin surface with hydrate structure. Reaction experiments showed molybdophosphoric acid has slightly higher activity than the tungstophosphoric acid, which yields slower deactivation. The reaction model was established by considering the hydrolysis reaction of lactoyllactic acid under the reaction conditions and the esterification step. Reaction rate constants for homogeneous self catalyzed, ion exchange resin catalyzed, and kinetic contribution of heteropoly acid loading were calculated. Kinetic analysis of the reaction data revealed that the active proton sites do not increase proportionally with the amount of heteropoly acids over the resin surface and proton efficiency of the catalysts decreases with increasing loading. It was observed that molybdophosphoric acid loaded S100 catalysts have higher proton efficiency than the tungstophosphoric acid loaded counterpart.

Introduction

A growing interest has been developed for the synthesis and production of environmentally benign solvents and green chemicals. The significance of lactic acid arises from its utility as a monomer for biodegradable solvents and polymers in which the hydroxyl and the carboxyl functional groups permit it to participate in a wide variety of chemical reactions.[1] Lactic acid, whose occurrence in nature is widespread, can be produced in large quantities by fermentation at low cost and esterification is an important step for both lactic acid purification and for the production of the environmentally benign solvents. Lactic acid esters are nontoxic and biodegradable materials having excellent solvent properties and could potentially replace toxic and halogenated solvents for a wide range of industrial and consumer uses, corresponding to up to 80% of worldwide solvent consumption. Developing low-cost production technologies for lactate esters could make them viable for use in various formulations. One of the major hurdles from which current production processes for lactate esters suffer is low conversion and purity, which make production technically and economically uncompetitive. Therefore, efficient catalysts and separation processes are essential for the development of ecologically sound technologies for lactate esters. The use of membrane reactors for separation of a reaction product or pervaporation assisted esterification type hybrid processes, especially for esterification type reversible reactions, are attractive in terms of increasing conversion by shifting the equilibrium and resulting in a considerable reduction in the reaction time and in the amounts of reactants required.[2–3] To achieve these goals, a better understanding of the esterification reaction of lactic acid is crucial where the hydrolysis/dehydrolysis reaction of lactic acid is the limiting step for both lactic acid purification and also for the esterification reaction.

$$C_3H_6O_3 + C_2H_5OH \Leftrightarrow C_5H_{10}O_3 + H_2O \quad (1)$$

$$C_6H_{10}C_5 + H_2O \Leftrightarrow 2C_3H_6O_3 \quad (2)$$

The reaction of lactic acid is traditionally catalyzed by acids such as anhydrous hydrogen chloride, sulfuric acid or many other conventional acid catalysts, which cause many problems such as corrosion, side reactions, difficulty in purification, and other environmental issues. The incentive for environmentally benign, safe and selective green processes leads to more extensive adoption of heterogeneous composite catalysts for the production of a variety of specialty and bulk chemicals aiming to replace traditional homogeneous catalysts. However, only a few studies were to be found in the literature describing lactic acid esterification with heterogeneous catalysts.[4–7] An accumulating knowledge and a growing interest have been developed over the past years leading to the increased number of applications of these compounds as highly active solid acid catalysts in liquid-phase reactions.[8–12] Heteropoly acids (HPAs), and their salts are known to be active solid acid catalysts for many homogeneous and heterogeneous acid catalyzed reactions with inherent advantages like ease of handling and removal, reusability, fewer side reactions, strong Brønsted acidity approaching to superacid region, high proton mobility, stability, and catalytic activity.[13–15] Also the unique pseudo-liquid phase behavior of the solid heteropolyacids possesses extremely high proton mobility and polar molecules within the reaction mixture undergo catalytic reactions not only over the surface of the catalyst, but also within the bulk of the crystallites.[16] However the heteropoly acids are soluble in many

Green Context

Lactate esters show promise as green solvents, but the esterification of lactic acid can be difficult. This contribution investigates the process, and proposes a resin-supported heteropolyacid as a suitable strongly acidic catalyst for the synthesis of these products in very good yield. ***DJM***

 DOI: 10.1039/b303327a

liquid phase reactions, especially in the presence of water, while their Cs, Ba, and Ce salts yield fine, high surface area water/solvent insoluble particles with lower catalytic activity per unit weight.[17–19] Insoluble salts of heteropoly acids have significant activity in the presence of excess water such as in hydrolysis reactions.[19] Therefore, further improvements on the synthesis of active, stable and insoluble HPA-supported systems will play an important role in the applications of green chemistry for future processes.

In the present study, reversible liquid-phase esterification of lactic acid with ethyl alcohol over the ion-exchange resin supported tungstophosphoric $H_3PW_{12}O_{40}{\cdot}xH_2O$, (HPW) and molybdophosphoric $H_3PMo_{12}O_{40}{\cdot}xH_2O$, (HPMo) acids was investigated.

Experimental

Reaction experiments and product analysis

The effects of variables such as resin type as support, catalyst concentration, initial reactant molar ratio and temperature on the reaction rate were studied with the catalysts Lewatit® S100 and Amberlite® IR-120, in H^+ form, having strongly cationic gel type structure. The reaction temperature was selected as 343 K (±1 K) in order to avoid inefficient sampling due to ethanol vaporization occurring at higher temperatures, and to prevent thermal decomposition of lactic acid species. Also the ethanol to lactic acid molar ratio was kept at 1:1 in order to observe the effect of catalyst on the reaction rate under the minimized inhibition effect of ethyl alcohol.[4,5] Experiments were carried out in 30 ml sealed vials placed in a constant temperature bath with an inside orbital shaker tray operating at 300 rpm at 1 atm. L(+)-Lactic acid (92 wt%, Merck) and ethyl alcohol (99.5 wt% Aldrich) were used as the reagents for all experiments. The concentration of lactic acid in aqueous solutions could be quantitatively determined by an acid–base titration.[1] However, since lactic acid has a tendency to form polymeric lactic esters by self-polymerization, a hydrolysis step is needed in order to determine the total acid content. Therefore, examination of the lactic acid and the amount of lactoyllactic acid present in the sample, were done by means of two sequential acid–base titrations with accuracies of 0.05 ml 0.1N KOH and 0.05 ml 0.1N HCl corresponding to ±0.05 mol l^{-1} of lactic acid and lactoyllactic acid. Lactate ester, ethanol and water in the reaction mixture were analyzed by a Hewlett-Packard 5890A gas chromatograph (GC) equipped with a 10% packed FFAP/Chromosorb AW (60/80) column and a TCD detector by using He as the carrier gas with 0.5 μL injections. The GC analyses were carried out by using calibration standards and the relative response factors with respect to the ethanol, and the total areas under the chromatograms were corrected with respect to the lactic acid and lactoyllactic acid contents of the sample – neither acids are volatile species. Total molar conversion and the product distribution throughout the reaction time were determined by coupling the GC and the titration analysis and resulted in at least 99% accuracy in the carbon balance. The reproducibility of the experiments was checked by carrying out all reactions in triplicate; the results were combined.

Catalyst preparation and characterization

A typical regeneration procedure was employed to obtain proper ionic forms of strongly acidic, gel type ion-exchange resins IR-120 and S100. Lewatit® S-100 has a mono-disperse particle size (0.6 ± 0.05 mm) and Amberlite® IR-120 has a particle size range of 0.3–1.19 mm. The ion exchange resins were washed, regenerated to the H^+ or Na^+ forms, dried, and conditioned at 340 K under vacuum for 24 hours and finally sieved and the 24–28 mesh (0.71–0.59 mm) fraction collected and kept in a dessicator for further use. Tungstophosphoric ($H_3PW_{12}O_{40}{\cdot}xH_2O$) and molybdophosphoric ($H_3PMo_{12}O_{40}{\cdot}xH_2O$) acids were analytical grade products from Acros Chemicals and their water contents were determined by thermal gravimetric analysis (951-Dupont TGA) and found to be 22 and 27 mol per mol respectively. HPA loaded composite resin catalysts were prepared by an aqueous impregnation technique in the loading range of 2–20 wt% followed by aging and vacuum drying procedures as described elsewhere.[20] The catalyst samples were conditioned in a dessicator for further use. The catalyst samples were characterized by using XRD equipped with nickel filtered CuK_α radiation (Phillips PW1840). The FTIR spectra of the samples were obtained by using a Bruker Equinox 55 FTIR spectrophotometer and a Harrick diffuse reflectance (DRIFTS) cell. For the FTIR sampling, KBr spectrum was used as the background for bulk HPAs and conditioned ion-exchange resin spectra were used as background for loaded catalyst samples. The BET surface areas of the catalyst samples were measured by using N_2 in a Micromeritics ASAP-2000 apparatus.

Results and discussions

Catalyst characterization studies

In order to determine the interaction of HPAs with the support resin, diffuse reflectance spectra of the loaded catalysts at various loadings were investigated. The DRIFTS spectra of the bulk HPW and HPMo were obtained with respect to the background spectra of the KBr and HPA loaded S100-H^+ catalysts were examined with respect to the background spectra of the bare S100-H^+ in order to reveal HPA-support interactions. Characteristic vibration bands related to the intact Keggin structure of HPW and HPMo loaded catalysts appear as, for edge sharing oxygen connecting metal atoms (M–O_e–M) at 811 and 790 cm^{-1}, for corner sharing oxygen connecting M_3O_{13} units (M–O_c–M) at 889 and 869 cm^{-1}, for terminal oxygen bonding to one metal atom (M=O_t) at 978 and 962 cm^{-1}, and for internal oxygen bond connecting P and one metal atom (P–O_i) at 1077 and 1055 cm^{-1}, respectively (Figs 1 and 2).

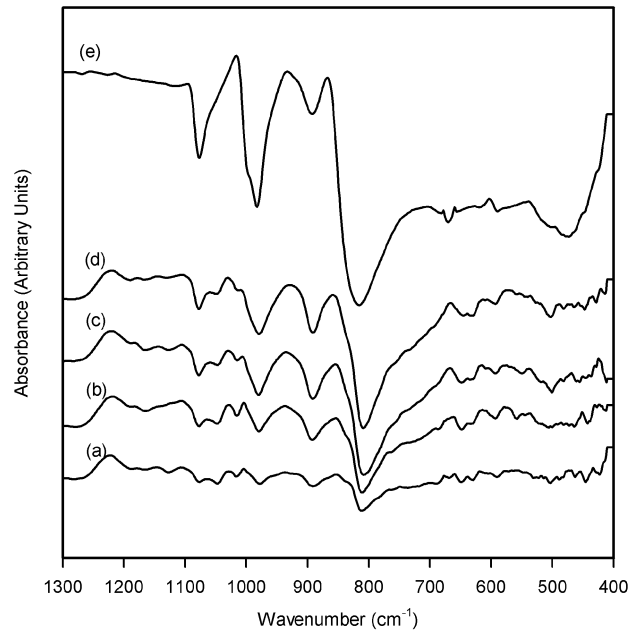

Fig. 1 DRIFTS-Spectra for HPW loadings over S100-H^+ resin (background S100-H^+). (a) 2 wt%; (b) 5 wt%; (c) 10 wt%; (d) 20 wt%; (e) bulk HPW (background KBr).

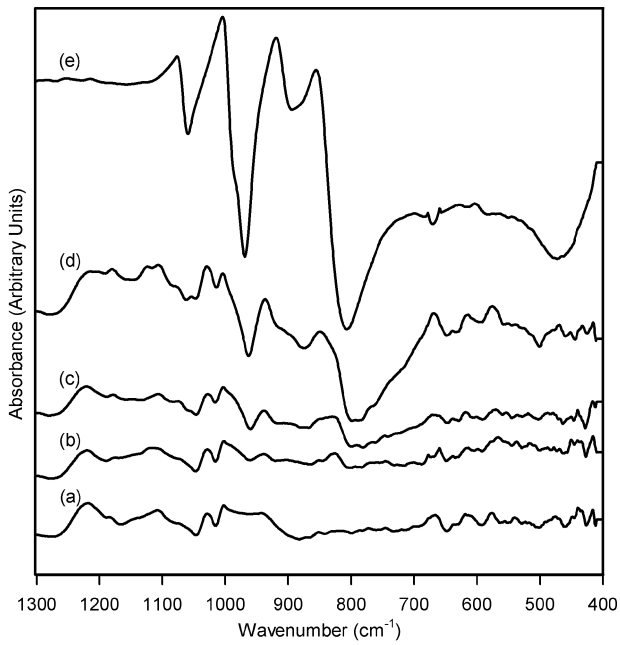

Fig. 2 DRIFTS-Spectra for HPMo loadings over S100-H^+ resin (background S100-H^+). (a) 2 wt%; (b) 5 wt%; (c) 10 wt%; (d) 20 wt% (e); bulk HPMo (background KBr).

The edge-and-corner bridging oxygen atoms with higher electron density than the terminal oxygen atoms are the main protonation sites for the HPAs in solution. However, in solid HPAs, protons take part in the formation of HPA crystals and more accessible terminal oxygens are protonated.[13,16] The obtained spectra coincide with those of bulk acids since the resulting M–O_e–M, M–O_c–M and M–O_t bands become more significant with increased loadings. For HPW and HPMo loaded catalysts, bands at 1046 and 1055 cm^{-1} split into doublets originating from the P–O_i bonding. Since some shifts in the wave numbers occur due to the loss of hydrogen bonding of terminal oxygen atoms and the bound and free water molecules for the conditioned catalysts, the stable bands at 1009 and 1011 cm^{-1} indicate the formation of hydrate structure relating the strong interaction of the HPA and resin surface with respect to the increasing loading. For both type of catalysts, shoulders appearing around 910 cm^{-1} were identified as M–O(P) stretch which are more significant for the HPMo loaded catalysts, and bands between 400–600 cm^{-1} were assigned as the symmetric/anti-symmetric stretching modes of terminal and bridging metal–oxygen groups and their bending vibrations, which are in good agreement with the literature values.[21] In addition, a shoulder between 720–680 cm^{-1} and peaks between 1285–1110 cm^{-1} suggest heteropoly anion interaction ($PW_{12}O_{40}^{3-}$) with the support.

For the HPA loaded resin catalysts prepared by the aqueous impregnation technique, it was seen that the resulting BET surface area values were slightly higher with the HPA loading compared to the support resin (S100-H^+) itself. The BET surface areas of the conditioned S100-H^+ resin (gel type) and bulk HPA were measured at less than 0.5 $m^2\ g^{-1}$ and 5 $m^2\ g^{-1}$, respectively. However, the surface area of HPA loaded S100-H^+ samples were determined as 2 $m^2\ g^{-1}$ and the % loading of the HPA had almost no effect on the surface area. So, it was confirmed that HPAs were not only captured by the pores of the resin at small loadings, but also attached to the support surface. X-Ray powder diffraction patterns obtained using nickel filtered CuK_α radiation for the composite catalysts indicate that with the increasing HPA loading, the intensity of the peaks between 2θ = 5–40 shifts or disappears, suggesting the change of the original Keggin structure. The original HPA structure was not observed over the apparent amorphous polymer phase of the S100-H^+ surface, indicating a finely dispersed amorphous monolayer structure below 10 wt% loading for both HPW and HPMo loaded catalysts. On the other hand, the appearance of signals characteristic of HPMo obtained at excessive loadings above 10 wt% represented the original Keggin structure (Fig. 3), which resembles the formation of small crystallites over the

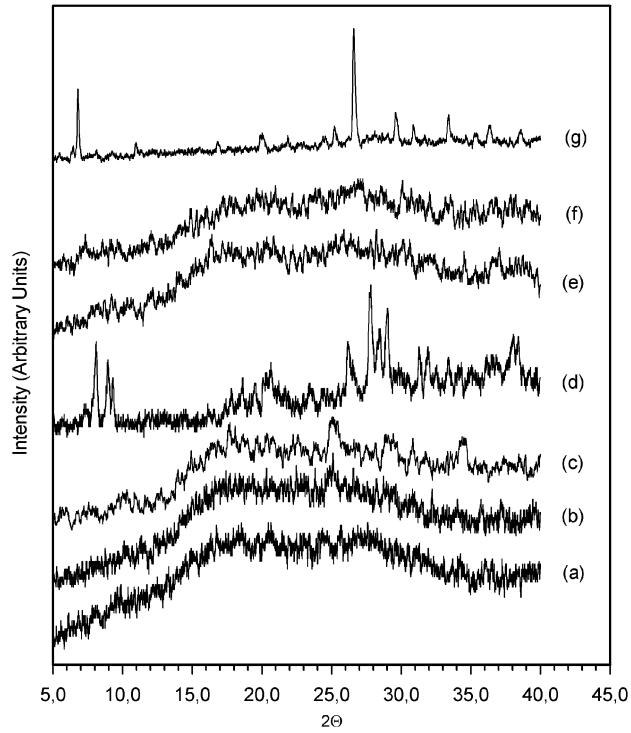

Fig. 3 XRD patterns for HPA loadings over S100-H^+ resin: (a) bulk S100-H^+; (b) 10 wt% HPW/S100; (c) 20 wt% HPW/S100; (d) bulk HPW; (e) 10 wt% HPMo/S100; (f) 20 wt% HPW/S100; (g) bulk HPMo.

surface. However, for HPW loadings above 10 wt%, a different crystalline phase which does not represent the original Keggin structure was observed around 2θ = 25, 28, 34, and 40. Similar results were reported in literature[22,23] for activated carbon and silica, which emphasize the formation of a finely dispersed amorphous phase under certain loadings.

Catalytic activity of bulk and supported heteropoly acid catalysts

Preliminary reaction tests with bare IR-120-H^+ indicated that the activity of IR-120-H^+ was not more different than the homogeneous reaction, which is catalyzed by lactic acid itself in the absence of ion exchanger catalyst at 343 K. It was also observed that, strongly cationic S100-H^+ resin catalyzed the lactic acid esterification effectively at various catalyst concentration series. In Figs 4 and 5, the conversion of lactic acid with respect to time under the identical reaction conditions in the absence of catalyst, bare S100-H^+ and different loadings of HPW and HPMo are given. The figures depict that, the catalytic activity of 2–20% HPA loaded S100-H^+ resin catalysts showed remarkably higher catalytic activities compared with that of the bare resin. Higher reaction rates were achieved for both HPW and HPMo types of supported catalysts with the increasing HPA loadings, resulting in higher reaction rates with respect to bare resin and the homogeneous reaction without catalyst. When the results of reaction experiments were compared, slightly higher reaction rates were observed on HPMo/S100 catalysts especially at 10 wt% and higher loadings, which indicate higher catalytic activity or more stable catalyst over the resin surface. The interaction between heteropoly anion, $PW_{12}O_{40}^{3-}$, and the protonated substrate is very important for reactions catalyzed by

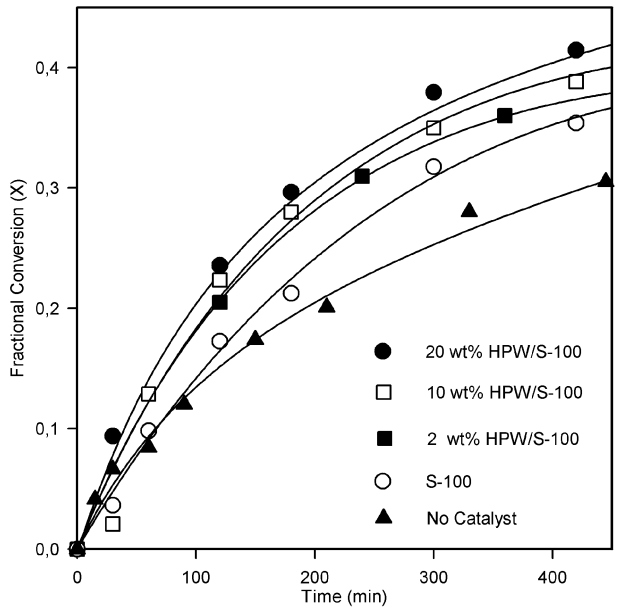

Fig. 4 Conversion *vs.* time data for $H_3PW_{12}O_{40}$ loadings over S100-H^+ catalyst, at 343 K, 1:1 reactant molar ratio and 1 wt% catalyst concentration with respect to bare resin and the homogeneous reaction.

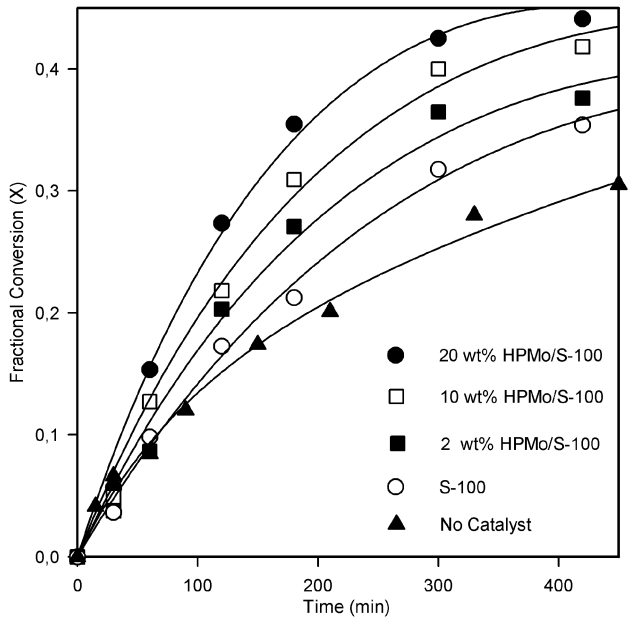

Fig. 5 Conversion *vs.* time data for $H_3PMo_{12}O_{40}$ loadings over S100-H^+ catalyst, at 343 K, 1:1 reactant molar ratio and 1 wt% catalyst concentration with respect to bare resin and the homogeneous reaction.

HPA loaded heterogeneous catalysts. HPA solutions in liquid phase have the same molecular structure with the solid phase, which have extremely high proton mobility. As was reported in literature,[20,24] for a HPA/ion-exchanger catalyst system, higher activities compared to those of the resin without supported anions were explained by the created synergy between the protons originating from the ion-exchanger and the interacting heteropoly anions.

Besides using strong cation-exchange resin S100 with H^+ form, different ionic forms were also tested in order to understand the possible HPA binding mechanisms over the resin surface such as the attachment of the active proton sites of the HPAs or by W or Mo sites. No catalytic activity was observed for the 10 wt% HPW and HPMo loaded over S100-Na^+ catalysts, indicating no active proton sites available over the catalyst surface – heteropoly anions require hydrogen as the active site in order to function over the surface of the cationic ion-exchange resins.

The stabilities and the deactivation rates of 5 wt% HPW and HPMo over S100-H^+ catalysts were tested with a series of deactivation experiments. Five consecutive runs under the same conditions were performed with the same catalyst sample and each catalyst sample was tested for more than 50 hours (Figs. 6 and 7). Although, the observed activities of the HPA supported

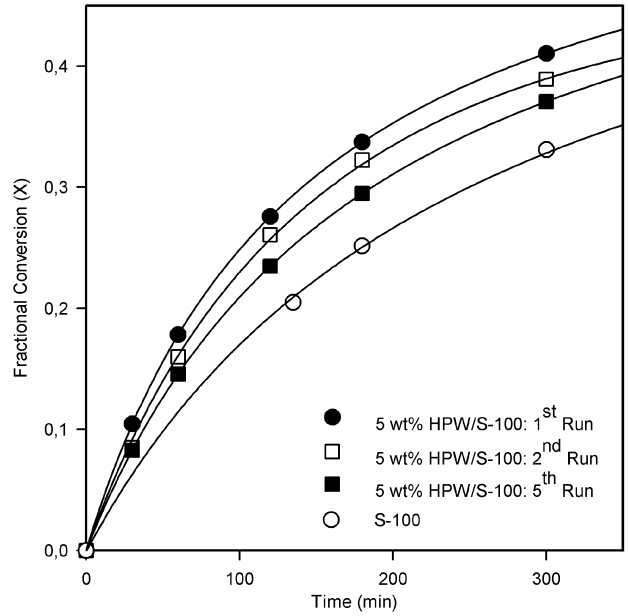

Fig. 6 Catalyst deactivation data for 5 wt% $H_3PW_{12}O_{40}$ loaded S100-H^+ catalyst at 343K, 1:1 reactant molar ratio and 1 wt% catalyst concentration.

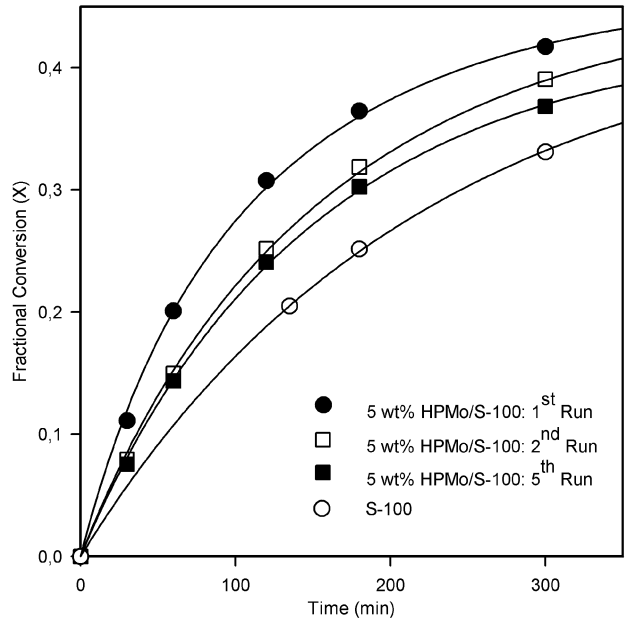

Fig. 7 Catalyst deactivation data for 5 wt% $H_3PMo_{12}O_{40}$ loaded S100-H^+ catalyst at 343K, 1:1 reactant molar ratio and 1 wt% catalyst concentration.

catalysts were still higher than the bare S100-H^+ after the 5th run, both HPW and HPMo catalysts reach almost the same catalytic activity after the 5th run. It is also clear that the deactivation rate of HPW catalyst was much slower than the HPMo catalyst. The deactivation mechanism of the catalysts might be attributed to the solubility or the washdown of structurally different HPAs from the support surface[17] and thermal aging and dissolution of sulfonic acid groups from ion exchange resins and their subsequent deactivation.[25,26]

Lactoyllactic acid hydrolysis

Lactoyllactic acid, which is a polymeric ester of aqueous lactic acid, exists in different amounts in all forms of lactic acid solutions, depending on the amount of water. In order to examine the kinetic parameters of the lactic acid esterification reaction, lactoyllactic acid hydrolysis kinetics was also investigated. The hydrolysis reaction of lactoyllactic acid was studied at the reaction conditions, both in the presence and in the absence of 5 wt% HPW and 5 wt% HPMo loaded over S100-H^+ catalysts. For this purpose, relaxation experiments were carried out by using samples of 90 wt% lactic acid solution conditioned at 293 K for more than six months. After this period the solution was assumed at equilibrium. The lactic acid samples were tested against increase in the temperature from 293 K to 343 K with or without catalyst and lactic acid. The measurements of lactoyllactic acid concentration with respect to time revealed that neither temperature change nor catalyst addition altered the dynamic equilibrium between lactic acid, lactoyllactic acid, and water and the initial concentrations of lactic and lactoyllactic acid remained constant for more than 40 hours. Moreover, the proposed hydrolysis reaction was studied separately at different initial water concentrations. It was observed that dilution with water enables the hydrolysis of lactoyllactic acid to lactic acid and that higher hydrolysis rates are achieved with higher increasing dilution of the initial solution. Equilibrium experiments performed to reveal the dilution effect in the absence of catalyst showed that lactoyllactic acid hydrolysis is a very slow reaction and may be a rate-limiting step in ethyl lactate formation, especially at higher conversions (Fig. 8).

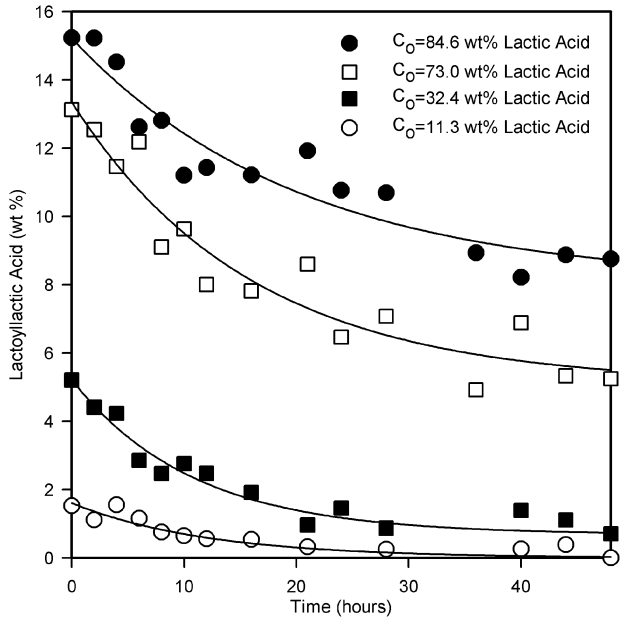

Fig. 8 Lactoyllactic acid hydrolysis data for various initial concentrations of lactic acid solution at 343 K in the absence of catalyst.

One important point is that esterification reactions suffer from low conversions because of their equilibrium limited nature. To overcome this difficulty, there exist several methods in which equilibrium is shifted by the removal of one of the reaction products to increase the product yield and conversion. As the reaction proceeds, lactic acid and ethyl alcohol consumption produces ethyl lactate and water (eqn. (1)). Water formed as a result of esterification increases the lactoyllactic acid hydrolysis, and additional lactic acid formation (eqn. (2)) also favors the formation of ethyl lactate. For this case, the water concentration is relatively small and remains almost constant with respect to time and conversion when compared with that of the produced ester, which shifts the equilibrium (Fig. 9) further to the ester side.

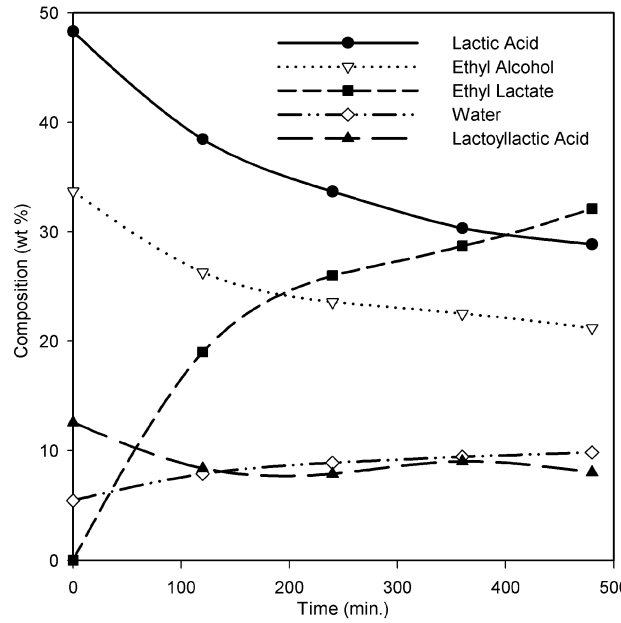

Fig. 9 Species concentrations *vs.* time data for 10 wt% $H_3PMo_{12}O_{40}$ loaded on S100-H^+ catalyst at 343 K, 1:1 reactant molar ratio and 1 wt% catalyst concentration.

Reaction kinetics

The kinetics of the esterification reaction of lactic acid and ethyl alcohol, accompanied with lactoyllactic acid hydrolysis was investigated by using a perfectly mixed constant-volume batch reactor approach. From reactions (1) and (2), the disappearance rate of lactic acid (LA) and the lactoyllactic acid (LLA), can be expressed in the following form.†

$$-\frac{dC_{LA}}{dt} = k_1 C_{LA} C_{EtOH} - k_2 C_{Ester} C_{Water} - k_3 C_{LLA} C_{Water} + k_4 C_{LA}^2 \quad (3)$$

$$-\frac{dC_{LLA}}{dt} = k_3 C_{LLA} C_{Water} - k_4 C_{LA}^2 \quad (4)$$

It should be noted that, in considering gel-type resins within the well-agitated reaction system, internal and external mass transfer resistance were neglected and discussion regarding the reaction kinetics was carried out in terms of observed reaction rate constants. Analysis of reaction rate data in order to estimate the heterogeneous reaction rate constants was performed using computational non-linear regression analysis with numerical differentiation by fitting rate eqns. (3) and (4), which are functions of species concentrations. Since the catalyst and the temperature did not affect the lactoyllactic acid hydrolysis (eqn. (2)), data obtained from performed experiments at the reaction temperature of 343K for different molar ratios were used to estimate overall forward and backward reaction rate constants

† **Notations**

k_1, k_2	Observed forward and backward rate constants of reaction (1), $l.mol^{-1}.min^{-1}$
k_3, k_4	Homogeneous forward and backward rate constants of reaction (2), $l.mol^{-1}.min^{-1}$
$k_1^{hom.}$, $k_2^{hom.}$	Homogeneous forward and backward rate constants of reaction (1), $l.mol^{-1}.min^{-1}$
$k_2^{het.}$, $k_2^{het.}$	Heterogeneous forward and backward rates constants, $l.mol^{-1}.min^{-1}$
k_1^{HPA}, k_2^{HPA}	Forward and backward rate contributions by HPAs, $l^2.(g\ HPA)^{-1}.mol^{-1}.min^{-1}$
$k_1^{Supp.}$, $k_2^{Supp.}$	Forward and backward rate contributions by Support, $l^2.(g\ Support)^{-1}.mol^{-1}.min^{-1}$
β^{HPA}, $\beta^{Supp.}$	Catalyst concentration, $(g\ HPA).(l\ Soln.)^{-1}$
X	Conversion in terms of lactic acid weight fraction

(k_3 and k_4) of lactoyllactic acid hydrolysis at homogeneous conditions. However, the homogeneous lactic acid esterification (eqn. (1)), under the reaction conditions was quite significant relative to the heterogeneous reaction rate. So, the overall forward and backward observed reaction rate constants k_1 and k_2 were discretized separately, as homogeneous and heterogeneous reaction rate constants by assuming that catalyst had no effect on homogeneous reaction rate constant. This approach can be considered reasonable because of high proton mobility of HPAs, which leads to a high catalytic efficiency for liquid-phase reactions, favoring the reaction kinetics and the participation of all structural protons in the reaction.†

$$k_i = k_i^{\text{hom.}} + k_i^{\text{HPA}}.\beta^{\text{HPA}} + k_i^{\text{Supp.}}.\beta^{\text{Supp.}} \quad (5)$$

Using the results of the lactoyllactic acid hydrolysis, forward and backward homogeneous reaction rate constants $k_1^{\text{hom.}}$, $k_2^{\text{hom.}}$ and the corresponding heterogeneous reaction rate constants $k_1^{\text{het.}}$ and $k_2^{\text{het.}}$ were estimated within a variance range of 94.6% and 99.4% by using the Statistica® software with Quasi-Newton method, suggesting good agreement between the predicted *versus* observed values of the proposed model (eqn. (3)). The equilibrium constant of reaction (1) was evaluated as 1.9 at 343 K with 1:1 molar ratio of ethanol to lactic acid. The reaction rate constants evaluated from the kinetic analysis were further analyzed for catalytic activity and kinetic contributions of support and HPAs in terms of $k_i^{\text{Supp.}}$ and k_i^{HPA} (eqn. (5)). The net effects of HPA loading on the kinetic contribution of HPAs are plotted in Fig. 10. The figure depicts that the kinetic

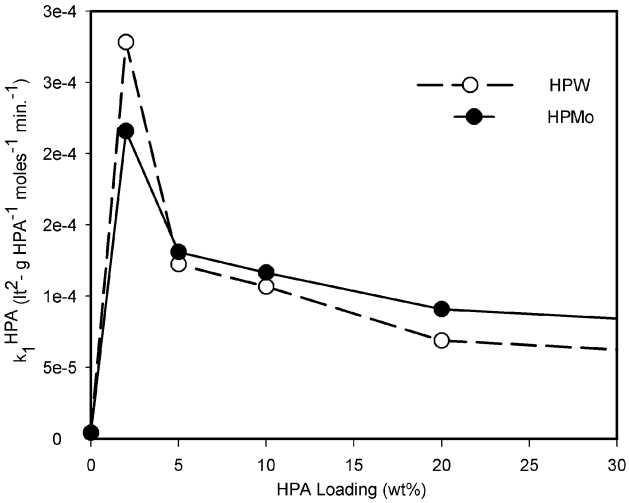

Fig. 10 Kinetic contributions of HPW and HPMo supported on S100 catalysts with respect to wt% HPA loadings.

contribution of HPA loading decreases drastically with increasing HPA loadings for both HPW and HPMo. Comparing the contribution of 2 wt% HPW and HPMo on the forward reaction rate constant with the zero loading case (bare S100-H^+) synergistic effect of HPA's over the catalytic activity is apparent. However the synergistic effect diminishes at the higher loadings of HPAs. In other words, the presence of 2 wt% HPA over the S100-H^+ surface shows maximum net increase ($k_1^{\text{Supp.}} = 4.1 \times 10^{-6}$ and $k_1^{\text{HPA}} = 2.7 \times 10^{-4}$ l^2.g mol^{-1}.min^{-1}) on the overall reaction rate k_i, while excessive loadings have a positive effect on the reaction rate, but not in the same order of magnitude. One of the possible explanations for the decrease in the kinetic contribution of the HPA loadings is that the number of available active sites (protons) over the catalyst surface does not increase at the same proportion with loading. For this purpose, the proton content of the bare S100-H^+ and HPW and HPMo loaded S100-H^+ catalyst samples were determined by titration. For bare S100-H^+, the proton concentration was measured as 3.3 mmol H^+ g^{-1} S100, while the HPA loaded S100-H^+ samples had between 4.5 and 4.7 mmol H^+ g^{-1} catalyst for 2wt% HPW, and HPMo respectively. The change in the ratio of overall forward and backward heterogeneous reaction rate constants ($k_i^{\text{Supp}}.\beta^{\text{Supp}} + k_i^{\text{HPA}}.\beta^{\text{HPA}}$) to proton concentration with HPA loading is shown in Fig. 11. The

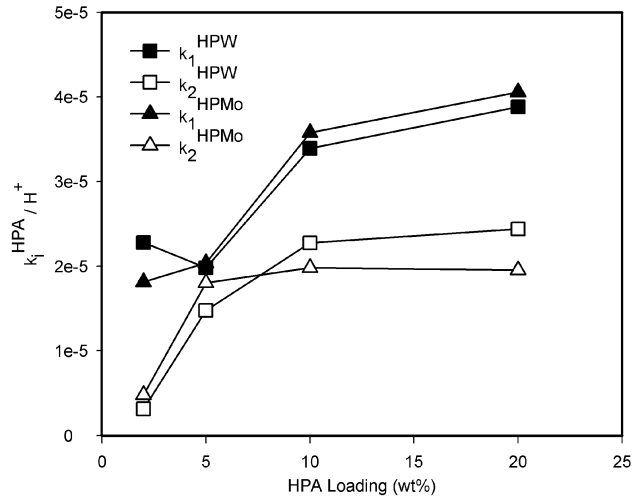

Fig. 11 Benchmark data of HPA supported on S100-H^+ catalyst for forward and backward rate per available proton sites with respect to increasing HPA loadings.

reaction rate constant per active site is not a linear function of HPA loading and HPMo loaded catalyst samples have higher proton efficiency than HPW loaded catalysts. However the proton efficiency decreases with increasing catalyst loading for all of the HPA loaded catalysts. These results are in good agreement with reaction experiments where higher reaction rates were observed with HPMo catalysts.

The experimental evidence such as observing a different phase with the HPW loaded S100-H^+ catalyst by XRD and determining smaller number of protons reveal that catalyst surface of HPW loaded S100-H^+ catalysts have less accessible protonated terminal oxygen species than HPMo catalysts. In other words, the formation of different crystalline phase in addition to the Keggin structure over the catalyst surface causes loss of HPW activity on the esterification kinetics and its deactivation rate is slower than HPMo because of lower solubility in the liquid phase. Unlike the macroreticular (macroporous) resins, gel-type resins have a non-porous structure in the dry state. In the presence of solvents, swelling enables accessibility of the reactant(s) to the functional groups. The accessibility depends on the degree of swelling, which can be described as the increase of inter-chain molecular distance of the polymer chains as a result of solvation. Since the S100 has a non-porous structure, higher loadings of HPA's can not cause any increase on the intra-particular mass transfer resistance. Therefore the decrease in proton efficiency might be explained as the formation of a different phase structure of HPA's having restricted accessibility over the surface or the decrease in the swelling ability of the catalyst as a result of the interaction of surface HPA species with gel-matrix.[27]

Conclusions

Application of HPA supported on ion-exchange resins as heterogeneous catalysts contributes high reaction rates for the esterification reaction of lactic acid and ethyl alcohol. As evidenced by the catalyst characterization studies, there is a strong interaction between the heteropoly anions and the ion-exchange resin, explaining the observed high reaction rates. Besides strongly catalyzing the proposed reaction as efficient

heterogeneous catalysts and being advantageous in terms of ease of handling and producing no side reactions, kinetic contributions of the HPW and HPMo type HPAs on the reaction rate differ slightly. The number of available protons on the catalyst surface does not follow a linear trend with respect to increasing HPA loadings. In this respect, the net kinetic contribution effect of the % loading of HPAs on the reaction rate decreases, and is less for HPMo loaded catalysts compared with that of the HPW loadings. On the other hand, the lactoyllactic acid hydrolysis reaction gives a broad insight in terms of both favoring ethyl lactate formation and estimating the kinetic parameters of the heterogeneous reaction. Deactivation is one of the main drawbacks of heteropoly acid supported heterogeneous catalysts. Further stability improvements are necessary to achieve lower deactivation rates.

References

1 C. H. Holten, *Lactic Acid; Properties and Chemistry of Lactic Acid and Derivatives*, 1971, Verlag Chemie, Weinheim.
2 J. J. Jafar, P. M. Budd and R. Hughes, *J. Membr. Sci.*, 2002, **199**, 117–1213.
3 K. Tanaka, R. Yoshikawa, C. Ying, H. Kita and K. Okamato, *Chem. Eng. Sci.*, 2002, **57**, 1577–1584.
4 S. Dassy, H. Wiame and F. C. Thyrion, *J. Chem. Tech. Biotechnol.*, 1994, **59**, 146–156.
5 J. I. Choi, W. H. Hong and H. N. Chang, *Int. J. Chem. Kinet.*, 1996, **28**, 37–41.
6 G. D. Yadav and H. B. Kulkarni, *React. Funct. Polym.*, 2000, **44**, 153–165.
7 M. T. Sanz, R. Murga, S. Beltran, J. L. Cabezas and J. Coca, *Ind. Eng. Chem. Res.*, 2002, **41**, 512–517.
8 Y. Izumi, R. Hasebe and K. Urabe, *J. Catal.*, 1983, **84**, 402–409.
9 T. Okuhara, T. Nishimura, H. Watanabe and M. Misono, *J. Mol. Catal.*, 1992, **74**, 247–256.
10 F. Lefebre and P. Dupont, *J. Mol. Catal. A: Chem.*, 1996, **114**, 299–307.
11 H. Van Bekkum, M. J. Verhoef, P. J. Kooyman and J. A. Peters, *Microporous Mesoporous Mater.*, 1999, **27**, 365–371.
12 T. Okuhara, X. Chen and Z. Xu, *Appl. Cat. A: Gen.*, 1999, **180**, 261–269.
13 I. V. Kozhevnikov, *Chem. Rev.*, 1998, **98**, 171–198.
14 N. Mizuno and M. Misono, *Chem. Rev.*, 1998, **98**, 199–217.
15 F. Cavani, *Catal. Today*, 1998, **41**, 73–86.
16 M. Misono, *Catal. Rev. Sci. Eng.*, 1987, **29**(2&3), 269–321.
17 G. Koayano, K. Ueno and M. Misono, *Appl. Catal. A: Gen.*, 1999, **181**(2), 267–275.
18 I. V. Kozhevnikov, M. N. Timofeeva, R. I. Maksimovskaya and E. A. Paukshtis, *J. Mol. Cat. A: Chemical*, 1995, **102**(2), 73–77.
19 M. Kimura, T. Nakato and T. Okuhara, *Appl. Catal. A: Gen.*, 1997, **165**(1–2), 227–240.
20 T. Baba, Y. Ono, T. Ishimoto, S. Moritaka and S. Tanooka, *Bull. Chem. Soc. Jpn.*, 1985, **58**, 2155–2156.
21 G. Mestl, T. Ilkenhans, D. Spielbauer, M. Dieterle, O. Timpe, J. Kröhnert, F. Jenhoft, H. Knözinger and R. Schlögl, *Appl. Catal. A: Gen.*, 2001, **210**, 13–34.
22 M. A. Schwegler, P. Vinke, M. VanDer Eijk and H. VanBekkum, *Appl. Catal. A: Gen.*, 1992, **80**, 41–57.
23 I. V. Kozhevnikov, *Catal. Rev. Sci. Eng.*, 1995, **37**(2), 311–352.
24 T. Baba and Y. Ono, *Appl. Catal.*, 1986, **22**, 321–324.
25 V. C. Malshe and E. S. Sujatha, *React. Funct. Polym.*, 1997, **35**, 159–168.
26 S. M. Mahajani, M. M. Sharma and T. Sridhar, *Chem. Eng. Sci.*, 2001, **56**(19), 5625–5633.
27 B. Corain, M. Zecca and K. Jerabek, *J. Mol. Catal. A: Chem.*, 2001, **177**, 3–20.

Optimisation of solvent free parallel synthesis under microwave irradiation: synthesis of new arylacrylonitriles

Didier Villemin,* Arnaud Jullien and Nathalie Bar

Ecole Nationale Supérieure d'Ingénieurs de Caen (ENSICAEN), Université de Caen, ISMRA, UMR CNRS 6507, 6 Boulevard du Maréchal Juin, F-14050 Caen cedex, France.
E-mail: didier.villemin@ismra.fr; Fax: 33 2 31 45 28 97; Tel: 33 2 31 45 28 40

Received 15th May 2003
First published as an Advance Article on the web 18th July 2003

Nitriles were condensed with benzaldehyde and piperonal under microwave irradiation in dry conditions. Fifty reactions were effected on five different catalyst supports in Eppendorf microtubes, coupled with TLC analysis. This parallel synthesis allows the choice of the catalyst support. Arylacrylonitriles were prepared with the best catalyst found.

Introduction

The solvent-free reactions by adsorption of a mixture of organic reactives on inorganic solids is well established.[1] Microwave irradiation is the best method for accelerating such reactions[2] in which the use of large volumes of solvent is avoided, reducing solvent emissions and redistillation:

– Work up is considerably simplified because in many cases the pure product can be obtained directly from the crude reaction mixture by simple extraction, distillation or sublimation.[3]

– Recyclable solid supports can be used as acid–base catalysts, replacing highly polluting mineral acids or organometallic bases.

– Safety is increased by reducing the risk of overpressure and explosions.

Nevertheless finding good reaction conditions is not easy and it is necessary to search by trial and error. We report herein a new method for fast optimisation of reaction conditions. The choice of catalyst, stoichiometry of reaction and irradiation conditions (time, power) can be determined by performing parallel synthesis on small samples using a commercially available microwave oven. The method illustrated is the condensation of phenylacetonitriles with aldehydes. To our knowledge no dry reaction of phenylacetonitriles with aldehydes has been reported.

Discussion

This reaction has been chosen because condensation products are generally coloured (because of their strong conjugation). It thus becomes thus possible to envisage a parallel synthesis where the appearance of a colour signals a reaction, and products are immediately identified by thin layer chromatography.[4]

The condensation of phenylacetonitriles with aldehydes works using either an acidic or basic solid catalyst (support). Five supports, with various acidities were used: montmorillonite K10 known for its high acidity; silica: a weak acid; neutral alumina: an amphoteric compound;[5] potassium carbonate: a weak base and potassium fluoride on alumina: a strong base.[6] Fifty reactions were conducted at the same time. We chose to use inexpensive Eppendorf vials (1.5 ml) from polypropylene, a plastic transparent to microwaves which is unaffected by heat up to 110 °C. For our purposes this choice was adequate. (For reactions performed at higher temperature glass vials will be more adapted). Reagents can be added using Eppendorf micropipettes or multipipettes.

Reactions

Products formed were extracted with acetonitrile and analysed by TLC. TLC plates were photographed with digital camera for analysis.

The parameters obtained were the R_f (dependent on the nature of the product), the color of the product in visible light and under UV (indication of nature of the product, conjugate nitrile), the surface of spots (indication of yield). Once conditions were optimised the reaction was performed on a larger scale using the best catalyst. The resulting arylacrylonitrile was isolated and characterised. Arylacrylonitriles (**1a–5b**, Scheme 1) have been known since around 1900 but are not

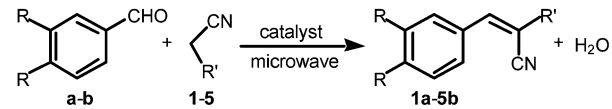

R = **a**: R=H; **b**: R=CH_2OCH_2
R' = **1**: C_6H_5; **2**: *p*-ClC_6H_4; **3**: *p*-CH_3O-C_6H_4; **4**: *p*-$NO_2C_6H_4$; **5**: CO-*p*-C_6H_4Cl

Scheme 1

described much in the literature; they were studied again in the 1950s as estrogens.

With the analyses so far we observed that using alumina or potassium fluoride on alumina as support allowed us to obtain

Green Context

Solvent free processes utilising microwaves and solid acids are the subject of this paper. Parallel screening is utilised (with colour as the screening analysis) in order to discover the most active catalysts. This rapid method uncovered the active catalysts, which were then used to prepare a series of arylacrylonitriles. Extension to continuous reactors would help to make solvent-free the isolation of the products, which were formed in excellent yields. ***DJM***

a better yield of Knoevenagel products. These supports were thus used to synthesise 10 products **1a** to **5b**, under microwave irradiation and without solvent (Table 1). In all cases the products were isolated and characterised. After a few minutes of irradiation, conversion was total for majority of reactions (as shown by TLC and NMR).

Table 1 Synthesis of arylacrylonitriles under microwave irradiation

Phenylacetonitrile	Aldehyde	Support	*t*/min	Yield (%)[a]	Mp/°C (lit.)	Ref.
1	**a**	Al_2O_3–KF	4	90	86–87 (87)	8
2	**a**	Al_2O_3–KF	3	77	116–117 (116)	9
3	**a**	Al_2O_3–KF	0.75	95	90–91 (94)	10
4	**a**	Al_2O_3	2	99	176–177 (177)	11
5	**a**	Al_2O_3	15	83	133–134	12
1	**b**	Al_2O_3–KF	5	99	120–122 (122)	9
2	**b**	Al_2O_3	15	97	166–168 (165)	13
3	**b**	Al_2O_3–KF	2	74	138–139 (143)	13
4	**b**	Al_2O_3	2	82	183–184 (187)	9
5	**b**	Al_2O_3	15	59	159–160	

[a] Crystallised from absolute ethanol

Products were recovered by elution with dichloromethane followed by filtration. Recrystallisation in ethanol allowed traces of aldehyde and possible secondary products to be removed, to thus obtain the pure condensation compound.

Conclusions

In conclusion, we have described a new approach for fast screening of solvent free parallel reactions under microwave irradiation using commercially available plastic vials and micropipettes. The method is fast and inexpensive. This approach can not only be used to optimise reaction conditions as described above (choice of catalyst, stoichiometry, irradiation conditions) but also for the preparation of homologous compouds for screening properties.

In the future, we envisage coupling TLC studies with IR reflectance, UV fluorescence spectra or thermal desorption of the spots coupled with an ion trap mass spectrometer (MS/MS).

Experimental

^{1}H and ^{13}C NMR spectra were recorded on a Bruker DPX 250 instrument, at 250 MHz and 62.9 MHz respectively. Chemical shifts δ are given in ppm downfield from TMS.

Coupling constants J are given in Hz. Infrared absorption spectra were recorded on a Perkin-Elmer 16 PC FT-IR spectrophotometer. Frequencies of absorption bands ν are given in cm^{-1}.

GC/MS analyses were done on a Varian instrument equipped with CP 3800 (GC) and Saturn 2000 (MS/MS) modules. The column was a CPSIL8 CB low bleed MS (30 m × 0.25 mm).

Thin layer chromatography was carried out on Merck 60 F254 silica gel sheets.

Melting points were determined with a Köfler bank without correction and are given in °C.

Microwave irradiation was made either in a monomode cavity Prolabo Synthewave 402 (max power 300 W), controlled by computer, or in a Brandt Navis domestic oven (maximum power, 750 W).

Photography of tube and TLC plates was taken with an Epson PC Photo 600 digital camera.

KF-Alumina was prepared according to the literature.[7]

Substrates/supports chosen

We chose five nitriles and two aromatic aldehydes, not previously studied under these conditions, as substrates and the following catalysts:

clay K10, very acidic
silica (SiO_2) slightly acidic, almost neutral
alumina (Al_2O_3) slightly basic
potassium carbonate K_2CO_3, weakly basic
KF–alumina, strongly basic

This meant five supports of different acidity/basicity which made a total of 50 different reactions (5 × 2 × 5) to study, with the substrates and support catalysts as variables.

Protocol for parallel synthesis under microwave irradiation

Stoichiometric amounts of reagent were added using an Eppendorf micropipette. All reagents (aldehyde or nitrile) were dissolved in dichloromethane or acetonitrile. The solutions of reagent were mixed and the solid support was added to a polypropylene Eppendorf tube (1.5 mL). The one gram of support was added with a spoon of known volume. Solvents (dichloromethane or acetonitrile) were evaporated off by a flow of nitrogen. All tubes containing support were agitated on a vibration table. The tubes were irradiated (750 W) in a multimode commercial microwave on a rotating plate. After irradiation (power, time), the tubes were opened and photographed with a digital camera. An aliquot of the same volume (of solid) (using a special spoon) was taken from each vial and added to acetonitrile. Using a microsyringe the same quantities of solution were taken from a sample and spotted on to a TLC plate (SiO_2, polyester, 20 × 10). TLC plates after elution were photographed with a digital camera. The R_f, the colour (in visible light and under UV) and the surface intensity were all recorded.

Preparative reactions

The aldehyde (2 mmol) and acidic methylene compound (2 mmol) were dissolved in dichloromethane, and a small quantity of ether. The support was added (1.0–1.2 g support) and the solvent removed by rotary evaporation. The solid obtained was irradiated in a multimode microwave oven, for 1 to 2 minutes, taking care to mix the solid well between the two successive irradiations. In the reaction there is a release of water, which condenses on the walls of the vial. Irradiation is stopped as soon as the solid turns a brownish color or when condensation is no longer observed. After cooling, the solid is extracted with dichloromethane (3 × 10 ml). The solvent is then eliminated using a rotary evaporator. Products are finally purified by recrystallisation in absolute ethanol.

Z-2,3-Diphenylacrylonitrile (1a)

Obtained from benzaldehyde **a** and phenylacetonitrile **1** on Al_2O_3–KF; irradiation 4 min; white crystals; yield 90%; mp 86–87 °C (lit.[8] 87–88 °C); $C_{15}H_{11}N$; RN 2510–95–4; $\delta_H(CDCl_3)$: 7.36–7.52 (m, 6H), 7.55 (s, 1H), 7.66–7.71 (m, 2H), 7.87–7.92 (m, 2H); $\delta_C(CDCl_3)$: 111.73, 117.97, 126.00, 128.95, 129.06, 129.20, 129.26, 130.52, 133.73, 134.49, 142.25; ν(KBr)/cm^{-1}: 1446, 1492 (C=C arom.), 1654 (C=C), 2218 (CN), 3030 (H–C=).

Z-2-(4-Chlorophenyl)-3-phenylacrylonitrile (2a)

Obtained from benzaldehyde **a** and (4-chlorophenyl)acetonitrile **2** on Al_2O_3–KF; irradiation 3 min; white crystals; yield 77%;

mp 116–117 °C (lit.[9] 115–116 °C); $C_{15}H_{10}ClN$; RN 3695–93–0; $\delta_H(CDCl_3)$: 7.39–7.50 (m, 5H), 7.52 (s, 1H), 7.58–7.65 (m, 2H), 7.85–7.91 (m, 2H); $\delta_C(CDCl_3)$: 110.55, 117.65, 127.23, 129.01, 129.27, 129.30, 130.79, 132.98, 133.44, 135.25, 142.54; ν(KBr)/cm^{-1}: 684 (C–Cl), 1492, 1596 (C=C arom.), 2216 (CN), 3054 (H–C=).

Z-2-(4-Methoxyphényl)-3-phenylacrylonitrile (3a)

Obtained from benzaldehyde **a** and (4-methoxyphenyl)acetonitrile **3** on Al_2O_3–KF; irradiation 45 s; yellow crystals; yield 95%; mp 90–91 °C (lit.[10] 94 °C); $C_{16}H_{13}NO$; RN 5840–59–5; $\delta_H(CDCl_3)$: 3.85 (s, 3H), 6.94–6.98 (m, 2H), 7.40–7.50 (m, 4H), 7.59–7.64 (m, 2H), 7.83–7.88 (m, 2H); $\delta_C(CDCl_3)$: 55.42, 111.29, 114.42, 118.11, 126.97, 127.31, 128.88, 129.03, 130.11, 133.96, 140.12, 160.44; ν(KBr)/cm^{-1}: 1030, 1254 (CAr–O), 2212 (CN), 3056 (H–C=).

Z-2-(4-Nitrophenyl)-3-phenylacrylonitrile (4a)

Obtained from benzaldehyde **a** and (4-nitrophenyl)acetonitrile **4** on Al_2O_3; irradiation 2 min; yellow orange crystals; yield 99%; mp 176–177 °C (lit.[11] 177–179 °C); $C_{15}H_{10}N_2O_2$; RN 3695–95–2; $\delta_H(CDCl_3)$: 7.49–7.54 (m, 3H), 7.69 (s, 1H), 7.83–7.89 (m, 2H), 7.92–7.97 (m, 2H), 8.29–8.35 (m, 2H); $\delta_C(CDCl_3)$: 109.54, 117.13, 124.35, 126.74, 128.93, 129.19, 129.72, 131.69, 132.88, 140.56, 147.91; ν(KBr)/cm^{-1}: 1342 (NO_2 s), 1514 (NO_2 as), 2218 (CN), 3054 (H–C=).

Z-2-(4-Chlorobenzoyl)-3-phenylacrylonitrile (5a)

Obtained from benzaldehyde **a** and (4-chlorobenzoyl)acetonitrile **5** on Al_2O_3; irradiation 15 min; brown crystals; yield 83%; mp 133–134 °C (lit.[12] 125 °C); $C_{16}H_{10}ClNO$; RN 64646–26–0; $\delta_H(CDCl_3)$: 7.46–7.64 (m, 5H), 7.84–7.91 (m, 2H), 8.01–8.06 (m, 2H), 8.08 (s, 1H); $\delta_C(CDCl_3)$: 109.57, 116.85, 129.06, 129.38, 130.71, 131.20, 131.7, 133.60, 134.07, 140.04, 155.82, 187.52; ν(KBr)/cm^{-1}: 680 (C–Cl), 1652 (C=O), 2224 (CN), 3040 (H–C=).

Z-3-Benzo[1,3]dioxol-5-yl-2-phenylacrylonitrile (1b)

Obtained from piperonal **b** and phenylacetonitrile **1** on Al_2O_3–KF; irradiation 5 min; pale yellow crystals; yield 99%; mp 120–122 °C (lit.[9] 122 °C); $C_{16}H_{11}NO_2$; RN 6948–55–6; $\delta_H(CDCl_3)$: 6.05 (s, 2H), 6.89 (d, 1H, $^3J_{HH}$ = 8.2), 7.31 (ddd, 1H, $^3J_{HH}$ = 8.2, $^4J_{HH}$ = 1.8, $^4J_{HH}$ = 0.4), 7.60 (d, 1H, $^4J_{HH}$ = 1.8), 7.62–7.67 (m, 2H), 7.36–7.48 (m, 4H); $\delta_C(CDCl_3)$: 101.74, 108.13, 108.63, 109.18, 118.27, 125.81, 128.08, 128.86, 129.01, 134.70, 141.84, 148.31, 149.67; ν(KBr)/cm^{-1}: 1114 (CH_2–O), 1040, 1266 (C_{Ar}–O), 1450, 1498 (C=C arom.), 1618 (C=C conj.), 2210 (CN), 2902 (HC–H), 3058 (H–C=).

Z-3-Benzo[1,3]dioxol-5-yl-2-(4-chlorophenyl)acrylonitrile (2b)

Obtained from piperonal **b** and (4-chlorophenyl)aetonitrile **2** on Al_2O_3–KF; irradiation 15 min; yellow crystals; yield 97%; mp 166–168 °C (lit.[13] 165 °C); $C_{16}H_{10}ClNO_2$; RN 104089–74–9; $\delta_H(CDCl_3)$: 6.06 (s, 2H), 6.89 (d, 1H, $^3J_{HH}$ = 8.2), 7.30 (ddd, 1H, $^3J_{HH}$ = 8.2, $^4J_{HH}$ = 1.8, $^4J_{HH}$ = 0.4), 7.37–7.44 (m, 3H), 7.54–7.61 (m, 3H); $\delta_C(CDCl_3)$: 101.81, 107.89, 108.05, 108.66, 117.95, 126.03, 127.01, 129.19, 133.20, 134.83, 142.11, 148.35, 149.90; ν(KBr)/cm^{-1}: 1042, 1260 (C_{Ar}–O), 1108 (CH_2–O ether), 1450, 1504 (C=C arom.), 2214 (CN conj.), 2900 (HC–H).

Z-3-Benzo[1,3]dioxol-5-yl-2-(4-methoxyphenyl)-acrylonitrile (3b)

Obtained from piperonal **b** and (4-methoxyphenyl)acetonitrile **3** on Al_2O_3–KF; irradiation 2 min; brown crystals; yield 74%; mp 138–139 °C (lit.[12] 143 °C); $C_{17}H_{13}NO_3$; RN 98841–67–9; $\delta_H(CDCl_3)$: 3.85 (s, 3H), 6.04 (s, 2H), 6.87 (d, 1H, $^3J_{HH}$ = 8.1), 6.91–6.98 (m, 2H), 7.25–7.31 (m, 2H), 7.55–7.60 (m, 3H); $\delta_C(CDCl_3)$: 55.42, 101.67, 108.01, 108.59, 108.88, 114.40, 118.40, 125.34, 127.12, 127.20, 128.33, 139.83, 148.24, 149.32, 160.21; ν(KBr)/cm^{-1}: 1028, 1258 (C_{Ar}–O), 2208 (CN).

Z-3-Benzo[1,3]dioxol-5-yl-2-(4-nitrophenyl)acrylonitrile (4b)

Obtained from piperonal **b** and (4-nitrophenyl)acetonitrile **4** on Al_2O_3; irradiation 2 min; yellow orange crystals; yield 82%; mp 183–184 °C (lit.[13] 187 °C); $C_{16}H_{10}N_2O_4$; RN 42172–83–8; $\delta_H(CDCl_3)$: 6.09 (s, 2H), 6.92 (d, 1H, $^3J_{HH}$ = 8.2), 7.36 (dd, 1H, $^3J_{HH}$ = 8.2, $^4J_{HH}$ = 1.8), 7.56 (s, 1H), 7.67 (d, 1H, $^4J_{HH}$ = 1.8), 7.79–7.84 (m, 2H), 8.28–8.32 (m, 2H); $\delta_C(CDCl_3)$: 102.07, 106.71, 108.20, 108.85, 117.49, 124.33, 126.43, 127.19, 127.30, 130.09, 140.93, 147.63, 148.59, 150.80; ν(KBr)/cm^{-1}: 1344 (NO_2 s), 1512 (NO_2 as), 2210 (CN), 3074 (H–C=).

E-3-Benzo[1,3]dioxol-5-yl-2-(4-chlorobenzoyl)acrylonitrile (5b)

Obtained from piperonal **b** and (4-chlorobenzoyl)acetonitrile **5** on Al_2O_3; irradiation 15 min; yellow crystals; yield 59%; mp 159–160 °C; $C_{17}H_{10}ClNO_3$; $\delta_H(CDCl_3)$: 6.12 (s, 2H), 6.93 (d, 1H, 3JHH = 8.3), 7.45 (dd, 1H, $^3J_{HH}$ = 8.3, $^4J_{HH}$ = 1.8), 7.46–7.53 (m, 2H), 7.78 (d, 1H, $^4J_{HH}$ = 1.8), 7.82–7.87 (m, 2H), 8.00 (s, 1H); $\delta_C(CDCl_3)$: 102.39, 106.37, 109.00, 117.44, 126.22, 128.94, 130.30, 130.56, 134.45, 139.68, 148.77, 152.68, 155.45, 187.77; $\delta_C(CDCl_3)$ undecoupled: 117.86 (d, $^3J_{CHtrans}$ = 13.8), 188.32 (dd, $^3J_{CHcis}$ = 9.2, 3JCH = 3.9); ν(KBr)/cm^{-1}: 1656 (C=O), 2215 (CN), 2924 (HC–H), 3448 (H–C=); MS *m*/*z* (%):313 (26), 311 (80), 276 (22), 139 (46), 111 (37), 44 (100).

References

1 R. S. Varma, *Green Chem.*, 1999, **1**, 43; R. S. Varma in *Microwaves in Organic Synthesis*, ed. A. Loupy, Wiley-VCH, Weinheim, 2002, pp. 181–218.
2 A. Ben Alloum, B. Labiad and D. Villemin, *J. Chem. Soc., Chem. Commun.*, 1989, 386; B. L. Hayes, *Microwave Synthesis–Chemistry at the Speed of Light*, CEM Publishing, Matthews, 2002.
3 D. Fildes, V. Caignaert, D. Villemin and P. A. Jaffrès, *Green Chem.*, 2001, **3**, 52.
4 W. Lorenzo, *Chem. Commun.*, 2000, 435.
5 G. W. Kabalka and R. M. Pagni, *Tetrahedron*, 1997, **53**, 7999.
6 B. E. Blase, *Tetrahedron*, 2002, **58**, 9301.
7 D. Villemin and A. Ben Alloum, *Synthesis*, 1991, 301.
8 L. Chalanay and E. Knoevenagel, *Chem. Ber.*, 1892, **25**, 297.
9 R. von Walther and A. Wetzlich, *J. Prakt. Chem.*, 1900, **61**, 183.
10 R. A. Caldwell, N. T. Ghali, C.-K. Chien, D. DeMarco and L. Smith, *J. Am. Chem. Soc.*, 1978, **100**, 2857.
11 R. B. Davis and R. C. Boguslaski, *J. Chem. Eng. Data*, 1970, **15**, 38.
12 A. von Meyer, *J. Prakt. Chem.*, 1915, **92**, 184.
13 N. P. Buu-Hoï and N. D. Xuong, *Bull. Soc. Chim. Fr.*, 1957, 650.

Carbon tetrachloride free benzylic brominations of methyl aryl halides

Catelijne H. M. Amijs, Gerard P. M. van Klink and Gerard van Koten*

Department of Metal-Mediated Synthesis, Debye Institute, Utrecht University, Padualaan 8, 3584 CH Utrecht, The Netherlands. E-mail: g.vankoten@chem.uu.nl; Fax: +31 30 2523615; Tel: +31 30 2533120

Received 29th April 2003
First published as an Advance Article on the web 21st July 2003

A series of mono- and dimethyl aryl halides was α-brominated with NBS using either light-induction or microwave-assistance. Instead of the commonly used CCl_4 or other chlorinated solvents, MeOAc was used as an environmentally more benign solvent for these side-chain bromination reactions. Moreover, in MeOAc the use of initiator was not required, while the product yields were comparable. With microwave-assistance various benzylic bromides became accessible in short reaction times *via* direct α-bromination of the corresponding arenes. Finally, aryl halides that were unreactive in CCl_4 could be brominated in moderate to good yields in MeOAc under microwave conditions.

Introduction

For six decades carbon tetrachloride has been the preferred solvent for the *N*-bromosuccinimide (NBS) side-chain bromination reaction of alkyl arenes, with the first report dating back to 1942.[1] These brominations are radical reactions, which are either photo-initiated or promoted by addition of azobisisobutyronitrile (AIBN) or dibenzoyl peroxide (Bz_2O_2). Carbon tetrachloride has proven to be a very useful solvent for the bromination of a wide range of compounds, and reports on its use still appear frequently.[2–4] A major drawback of carbon tetrachloride, however, is that it is both toxic and carcinogenic and that it exhibits ozone-layer damaging properties.[5] The effects on the global environment, in particular, have led to international agreements restricting the use of carbon tetrachloride.[6] Consequently, there is a quest for alternative, environmentally friendlier solvents or solvent systems.

In 1977, Vögtle and co-workers reported benzylic brominations of several arenes with NBS in non-chlorinated solvents, *e.g.*, methyl acetate or methyl formate.[7] In a later study, the list of solvents for this reaction was extended to tBuCO$_2$Me, CH_2Cl_2, $CHCl_3$, C_6H_6 and CS_2.[8] Since then, only a few other reports on the use of non-chlorinated solvents for benzylic bromination reactions have appeared in the literature. Shaw *et al.* reported ring- and side-chain brominations of simple hydrocarbons with bromine in water under irradiation of a mercury lamp.[9] Ishii and co-workers used the brominating reagent system $NaBrO_3$–$NaHSO_3$ in combination with EtOAc–H_2O as solvent for the benzylic bromination of alkyl benzenes.[10] Mestres and Palenzuela recently reported the benzylic bromination of 4-benzoyloxytoluene using a combined bromine–hydrogen peroxide system in non-chlorinated solvents such as EtOAc, *i*PrOAc, methyl isobutyrate and methyl pivalate.[3]

It must be noted, however, that these bromination reactions in non-chlorinated solvents were restricted to non-halogenated arenes only. For the benzylic bromination of halide-substituted arenes, the use of different solvents is relatively unexplored. Carbon tetrachloride remains the generally used solvent (see references in Table 1). The first benzylic bromination of a halogeno arene in a non-halogenated solvent was reported by our group in 1996.[11] Since then, only a few reports on the use of other solvents have appeared, *viz*. methyl and ethyl acetate and acetonitrile.[10,12–14]

In this paper, we report the synthesis of a series of bromomethyl mono- and dihalogeno arene compounds. The standard protocol comprises the use of methyl acetate as solvent, NBS as the bromide source, and light as initiator (see Scheme 1). Furthermore, microwave-assisted heating of the reaction mixture as an alternative way to carry out benzylic brominations was also investigated. The latter, new procedure extends the range of compounds that can be prepared in methyl acetate, a solvent less toxic and more environmental-friendly than carbon tetrachloride. To our knowledge no radical bromination reactions under microwave conditions have been reported so far.

Results and discussion

Light-induced bromination reactions

A variety of substituted methyl aryl halides was brominated using a standard protocol; *i.e.* a solution of equimolar amounts of the arene and NBS in MeOAc was heated to reflux by illumination with an 80 W IR light bulb. No additional initiators were used. In general these reactions were complete in 16 hours. No attempts were made to improve the conversion and yield of

Green Context

Bromination is an important chemical process especially when it is used to selectively activate functional groups in organic molecules. Traditional bromination processes are often made environmentally unacceptable through the use of hazardous solvents and auxiliaries. Here efficient benzylic brominations are achieved in a much more environmentally benign medium than usual and in the absence of initiation. The use of microwave irradiation further adds to the green chemistry credentials by reducing reaction times. ***JHC***

 DOI: 10.1039/b304673g

the reactions. The results are summarised in Table 1. For comparison the results of known reactions are also provided.

The use of MeOAc, instead of CCl_4 in the synthesis of compounds **2a–2c** and **2e–2g** had no effect on either the selectivity of the reaction or the yields (entry 1–12, 16–29). In some cases the yields were even higher (**2c**, **2f** and **2g**). The product distribution was unaffected by the absence of additional initiators like AIBN and Bz_2O_2.

During the reactions with the iodine substituted compounds **1a–1d**, **1i** and **1k** some formation of I_2 took place as was observed by the colour of the reaction mixture turning gradually dark-purple. This is most likely a result of iodine–bromine exchange *via* a radical substitution reaction. In most cases, the loss of iodine occurred in such low amounts (below 5%) that the side products could not be observed by ^1H NMR analysis. Only in the case of the bromination of **1d** (entry 14) did the iodine–bromine exchange take place extensively, to the effect that formation of a byproduct, *i.e.* 1-bromo-2,6-bis(bromomethyl)benzene (**2g**) was observed. This has also been noted by Vögtle and co-workers when performing this reaction in CH_2Cl_2.[19]

The use of the standard protocol was not always successful. During the benzylic bromination of **1h** the formation of a mixture of compounds (**2h**, 1,4-dibromo-2-bromomethyl-5-methylbenzene (**2h′**) and 1,4-dibromo-2-bromomethyl-5-dibromomethylbenzene (**2h″**)) was observed, and it was not possible to isolate **2h** *via* either extraction or precipitation (entry 32). When CCl_4 instead of MeOAc was used as solvent, less side products were formed, and consequently isolation of **2h** was possible (entry 30, 31).[25,26]

Whereas compound **1i** (entry 34) could easily be brominated, much to our surprise isomer **1j** turned out to be unreactive (entry 38). Prolonged reaction times, up to 36 hours, did not change this result. Changing the solvent to CCl_4 also did not result in

Table 1 Light-induced and microwave-assisted benzylic brominations of halide substituted arenes using various solvents and initiators[a]

Entry	Compound	1	2	*hν* or *μν*	Solvent	Initiator[b]	Conversion (mol%)[c]	Yield (mol%)	Ref.
1[d]	**a**		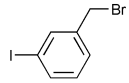	*hν*	—	—			15
2[d]				*hν*	CCl_4	I_2			16
3				*hν*	CCl_4	AIBN	67[e]		17
4				*hν*	MeOAc		84	40	*f*
5				*μν*	MeOAc	AIBN	68	n.d.	*f*
6	**b**	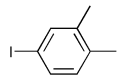	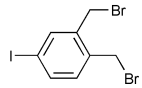	*hν*	MeOAc	—	82	44	*f*
7				*μν*	MeOAc	AIBN	82	n.d.	*f*
8	**c**	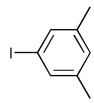	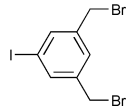	*hν*	CCl_4	AIBN		33	18
9				*hν*	HCOOMe	AIBN		55	12
10				*hν*	MeOAc	AIBN		47	13
11				*hν*	MeOAc	—	83	49	*f*
12				*μν*	MeOAc	AIBN	78	n.d.	*f*
13	**d**	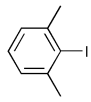	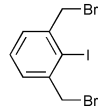	*hν*	CH_2Cl_2	—		11	19
14				*hν*	MeOAc	—	86	mix[g]	*f*
15				*μν*	MeOAc	AIBN	64	mix[g]	*f*
16	**e**	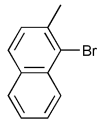	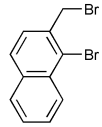	*hν*	CCl_4	Bz_2O_2		60, 85	4,20
17				*hν*	MeOAc	—	86	75	*f*
18				*μν*	MeOAc	AIBN	88	n.d.	*f*
19	**f**	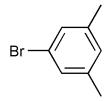	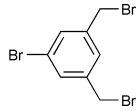	*hν*	CCl_4	Bz_2O_2		20	21
20				*hν*	HCOOMe	AIBN		51	11
21				*hν*	MeCN	AIBN		48	12
22				*hν*	MeOAc	—	79	56	*f*
23				*μν*	MeOAc	AIBN	75	49	*f*
24				*μν*	MeOAc[h]	AIBN	18	n.d.	*f*
25				*μν*	—	AIBN	64	n.d.	*f*
26	**g**	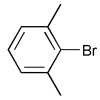	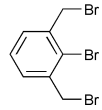	*hν*	CCl_4	Bz_2O_2		55	22
27				*hν*	CCl_4	—		75	23,24
28				*hν*	MeOAc	—	89	74	*f*
29				*μν*	MeOAc	AIBN	89	n.d.	*f*
30	**h**	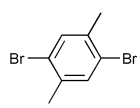	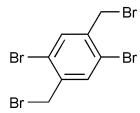	*hν*	CCl_4	AIBN		38	25
31				*hν*	CCl_4	—		34	26
32				*hν*	MeOAc	—	69	mix[i]	*f*
33				*μν*	MeOAc	AIBN	72	39	*f*

Continued

Table 1 *Continued*

Entry	Compound	1	2	*hν* or *μν*	Solvent	Initiator[b]	Conversion (mol%)[c]	Yield (mol%)	Ref.
34	**i**	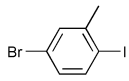	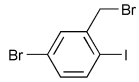	*hν*	MeOAc	—	79	52	*f*
35				*μν*	MeOAc	AIBN	85	n.d.	*f*
36	**j**	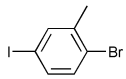	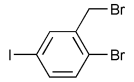	*hν*	—	Bz_2O_2		62[j]	27
37				*hν*	CCl_4	AIBN	—	—	*f*
38				*hν*	MeOAc	AIBN	—	—	*f*
39				*μν*	MeOAc	AIBN[k]	81	48	*f*
40	**k**	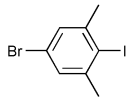	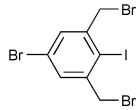	*hν*	MeOAc	—	75	mix[l]	*f*
41				*μν*	MeOAc	AIBN	79	mix[l]	*f*
42	**l**	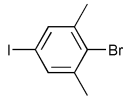	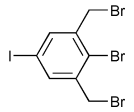	*hν*	CCl_4	AIBN	—	—	*f*
43				*hν*	MeOAc	AIBN	—	—	*f*
44				*μν*	MeOAc	AIBN[m]	83	63	*f*

[a] See experimental section for details. [b] Microwave-assisted reactions: 1 mol% used per Me-group. [c] Determined by ^{1}H NMR, calculated per Me-group. [d] Br_2 was used as bromide source. [e] Calculated theoretical conversion. [f] This work. [g] A mixture of **2d** and **2g** was obtained. [h] 10 mL of MeOAc per vessel was used. [i] A mixture of tri-, tetra- and pentabromides was obtained. [j] Low reproducibility as a consequence of poor stirring of the reaction mixture. [k] 4.5 mol% of initiator was used. [l] A mixture of **2k** and 1,4-dibromo-3,5-bis(bromomethyl)benzene (**2k′**) was obtained. [m] 15 mol% of initiator was added in three equal portions, before each run.

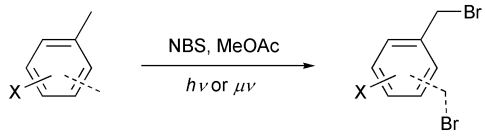

1 **2** X = Br, I

Scheme 1 New protocols for benzylic bromination reactions in a non-chlorinated solvent, either photo- (*hν*) initiated or microwave- (*μν*) promoted.

the formation of **2j** (entry 37). However, **2j** was accessible using a solvent-free system in which NBS, **1j**, and Bz_2O_2 were heated at 80 °C for 24 hours (entry 36).[27] Unfortunately, this is a very sluggish reaction, which is difficult to stir thereby lowering the reproducibility of this reaction. A similar lack of reactivity also applies to the bromination of xylene derivative **1l** (entry 42–43). Bromination of the regio isomer **1k** to give **2k**, was however possible by using our standard protocol. Again, during this reaction the earlier mentioned iodine–bromine exchange reaction played a significant role and a second product, 1,4-dibromo-3,5-bis(bromomethyl)benzene (**2k′**) was also obtained in a 5 : 4 ratio (**2k** : **2k′**) (entry 40). It was not possible to separate these compounds by crystallization or column chromatography.

It must be noted, however, that application of microwave-assistance solved the problems encountered for the bromination of **1h**, **1j** and **1l**, *vide infra*.

A blank reaction was carried out to determine the reactivity of MeOAc towards NBS. This reaction was performed without the addition of an aryl halide and in the presence of *tert*-butylbenzene as an internal standard.[28] During the reaction a small amount of MeOAc was converted to methyl bromoacetate (0.80 mmol, 0.064% based on MeOAc, 1.8% based on NBS).

Microwave-assisted reactions

The microwave-assisted reactions were all performed using MeOAc as solvent. Since no light source is present in the microwave oven, AIBN had to be added to initiate the reaction. No reaction was observed without the addition of initiator. The results are listed in Table 1.

The bromoxylene compound **1f** was converted to **2f** in 75% in 10 minutes when heated in the microwave at 112 °C (5 bar, entry 23). Prolonged reaction times (30 min) or higher temperature and pressure (127 °C, 7 bar) did not result in significantly higher conversions. We have also investigated whether the use of the microwave-assisted heating could open the way to (nearly) solvent-free benzylic brominations. When performing the reaction in a higher concentration, *i.e.* 10 mL MeOAc instead of 40 mL per vessel, the conversion decreased to 18% (entry 24). The reaction was also performed without the addition of solvent (entry 25). This resulted in a conversion of 64%, probably caused by poor mixing of the reagents. During the reaction the NBS decomposed to HBr and an insoluble tar-like material.

We applied the best procedure, *i.e.* MeOAc as solvent, 10 minutes at 112 °C, 5 bar, 1 mol% of AIBN per methyl group, as a standard protocol for the microwave-assisted benzylic bromination reaction of all previously mentioned compounds. The bromination reactions resulted in the formation of α-brominated arenes without affecting the conversion and product distributions (compounds **a–g**, **i**, and **k**). A few compounds were isolated as described in the experimental section. The yields were also comparable to earlier obtained results (compounds **f**, **h**, **j**, and **l**). Since both conversion and yield were not influenced by performing the reactions in the microwave, for most compounds only the conversion was determined.

Applying the microwave-assisted reaction method for **1h**, it was possible to synthesise **2h** without the use of CCl_4 (entry 33). This result contrasts with the poor results of the light-induced benzylic bromination of **1h** in MeOAc, which resulted in the formation of large amounts of side products (entry 32).

When the standard protocol was used for **1j**, which was unreactive under the standard bromination reactions, a conversion of 56% in 10 minutes was observed. Lengthening of the reaction time to 30 minutes again did not result in a higher conversion. However, an almost complete conversion to the benzylic bromide **2j** was obtained within 5 minutes when 4.5

mol% of initiator was used (entry 39). The reaction appeared to be instantaneous when AIBN initiates the reaction. Unfortunately, the lifetime of the initiator is short, probably due to the harsh reaction conditions. The bromination of the xylene derivative **1l** could not be completed in one run. When 5 mol% of initiator was added, the conversion to **2l** was only 38%. The use of 10 mol% of initiator only led to a conversion of 40%. When a fresh portion of AIBN (5 mol%) was added to the reaction mixture after 10 minutes, the conversion increased to 73% in a second reaction run. A further conversion to 83% was obtained when a third portion of AIBN (5 mol%) was added to the reaction mixture (entry 44).

A blank reaction was also performed as previously described.[29] In the microwave a small amount of methyl bromoacetate was formed too (0.28 mmol, 0.056% based on MeOAc, 1.6% based on NBS).

In conclusion, we have shown that benzylic bromination of a wide range of mono- and bishalide substituted aryl compounds in traditional side-chain bromination reactions is possible by using methyl acetate as solvent. MeOAc is an environmentally more benign solvent and is, therefore, an excellent replacement for chlorinated solvents like CCl_4. We found that it is not necessary to use initiators like AIBN and Bz_2O_2 in most of these reactions. The use of a microwave reactor enabled us to perform benzylic bromination reactions in very short reaction times. Moreover, we were able to synthesise benzylic bromides from alkyl arenes, which were very unreactive in light-induced bromination reactions.

Experimental

General

3-Iodotoluene (**1a**),[13] 4-iodo-*o*-xylene (**1b**),[13] 5-iodo-*m*-xylene (**1c**),[13] 1-bromo-2-methyl-4-iodobenzene (**1j**),[27] 1-bromo-3,5-dimethyl-4-iodobenzene (**1k**),[30] and 1-bromo-2,6-dimethyl-4-iodobenzene (**1l**)[13] were synthesised according to (modified) literature procedures. All solvents and other reagents were obtained from commercial sources and were used without further purification. All NMR spectra were recorded on a Varian Inova 300 spectrometer at room temperature using $CDCl_3$ as solvent and TMS as an external standard. Chemical shifts are reported in ppm. Microwave-assisted reactions were performed in a Milestone ETHOS SEL microwave oven. The reaction mixtures were magnetically stirred in a pressurised vessel and the temperature was monitored continuously. Twelve reaction vessels could be used in one reaction run. **Caution**: benzylic bromides can be powerful lachrymators and should be used with adequate ventilation and precautions against skin contact or ingestion.

General procedure for light-induced bromination reactions

To a solution of the tolyl or xylyl starting compounds (120 mmol) in MeOAc (600 mL), was added NBS (1.1 equiv. per methyl group). The solution was refluxed by irradiation of the flask with an 80 W IR bulb for 16 h, after which the solvent was evaporated *in vacuo*. The solid residue was extracted with boiling hexanes (300 mL, 2×). The hexane solutions were cooled to −30 °C after which the precipitated compounds were isolated.

General procedure for microwave-assisted reactions

A solution of tolyl or xylyl starting compounds (8 mmol), NBS (1.1 equiv. per methyl group) and AIBN (1 mol% per methyl group) in MeOAc (20 or 40 mL, tolyl or xylyl derivative, respectively) was placed in a reaction vessel. The vessel was placed in the microwave and the reaction mixture was heated to 112 °C (5 bar) in 5 minutes, followed by heating at 112 °C for 10 minutes. After the reaction run, the reaction vessel was cooled in an ice-bath prior to opening. If necessary, fresh AIBN was added as a solution in MeOAc (0.5 mL) and the vessels were placed in the microwave for the next run. When the reaction was complete, the solvent was evaporated *in vacuo*. The solid residue was extracted with boiling hexanes (25 mL per vessel, 2×). The hexane solutions were cooled to −30 °C after which the precipitated compounds were isolated.

1,2-Bis(bromomethyl)-4-iodobenzene (2b)

^{1}H NMR (300 MHz): δ = 4.56 (s, 2H, CH_2Br), 4.58 (s, 2H, CH_2Br), 7.09 (d, 1H, $^3J_{H,H}$ = 8 Hz, ArH-6), 7.64 (d, 1H, $^3J_{H,H}$ = 8 Hz, ArH-5), 7.72 (s, 1H, ArH-3). ^{13}C{^{1}H} NMR (75.5 MHz): δ = 28.7 (CH_2Br), 29.2 (CH_2Br), 94.9 (ArC-4), 132.7 (ArC-6), 136.3, 138.6, 138.7 and 139.9 (ArC).

4-Bromo-2-bromomethyl-1-iodobenzene (2i)

^{1}H NMR (300 MHz): δ = 4.53 (s, 2H, CH_2Br), 7.12 (d, 1H, $^3J_{H,H}$ = 8 Hz, ArH-5), 7.60 (s, 1H, ArH-3), 7.69 (d, 1H, $^3J_{H,H}$ = 9 Hz, ArH-6). ^{13}C{^{1}H} NMR (75.5 MHz): δ = 37.7 (CH_2Br), 98.1 (ArC-1), 123.0 (ArC-6), 133.3, 133.4 and 141.5 (ArC), 142.4 (ArC-4).

1-Bromo-2,6-bis(bromomethyl)-4-iodobenzene (2l)

^{1}H NMR (300 MHz): δ = 4.54 (s, 4H, CH_2Br), 7.72 (s, 2H, ArH-3,5). ^{13}C{^{1}H} NMR (75.5 MHz): δ = 32.5 (CH_2Br), 92.5 (ArC-4), 126.6 (ArC-1), 139.9 (ArC-3,5), 140.4 (ArC-2,6).

References and notes

1 K. Ziegler, A. Späth, E. Schoof, W. Schuman and E. Winkelman, *Justus Liebigs Ann. Chem.*, 1942, **551**, 80.
2 S. Kotha, S. Halder and K. Lahiri, *Synthesis*, 2002, **3**, 339.
3 R. Mestres and J. Palenzuela, *Green Chem.*, 2002, **4**, 314.
4 J. Clayden, C. McCarthy, N. Westlund and C. S. Frampton, *J. Chem. Soc., Perkin Trans. 1*, 2000, 1363.
5 Material Safety Data Sheet.
6 Ozone Secretariat, United Nations Environment Programme, *The Montreal Protocol on Substances that Deplete the Ozone Layer*, UNON, Kenya, 2000, p. 12.
7 W. Offermann and F. Vögtle, *Synthesis*, 1977, **4**, 272.
8 W. Offermann and F. Vögtle, *Angew. Chem.*, 1980, **92**, 471.
9 H. Shaw, H. D. Perlmutter, C. Gu, S. D. Arco and T. O. Quibuyen, *J. Org. Chem.*, 1997, **62**, 236.
10 D. Kikuchi, S. Sakaguchi and Y. Ishii, *J. Org. Chem.*, 1998, **63**, 6023.
11 P. Steenwinkel, S. L. James, D. M. Grove, N. Veldman, A. L. Spek and G. van Koten, *Chem. Eur. J.*, 1996, **2**, 1440.
12 T. J. Ryan, G. Lecollinet, T. Velasco and A. P. Davis, *Proc. Natl. Acad. Sci. U.S.A.*, 2002, **99**, 4863.
13 H. P. Dijkstra, M. D. Meijer, J. Patel, R. Kreiter, G. P. M. van Klink, A. L. Spek, A. J. Canty and G. van Koten, *Organometallics*, 2001, **20**, 3159.
14 E. Díez-Barra, J. C. García-Martínez, S. Merino, R. Del Rey, J. Rodríguez-López, P. Sánchez-Verdú and J. Tejeda, *J. Org. Chem.*, 2001, **66**, 5664.
15 J. W. Baker and H. B. Hopkins, *J. Chem. Soc.*, 1949, 1089.
16 V. Zeller, G. Ramachander and E. A. Zeller, *J. Med. Chem.*, 1965, **8**, 440.
17 W. Offermann and F. Vögtle, *J. Org. Chem.*, 1979, **44**, 710.
18 K.-H. Duchêne and F. Vögtle, *Synthesis*, 1986, **13**, 659.
19 W. Wieder, R. Nätscher and F. Vögtle, *Liebigs Ann. Chem.*, 1976, 924.

20 M. Newman and A. I. Kosak, *J. Org. Chem.*, 1949, **14**, 375.
21 S. S. Moore, T. L. Tarnowski, M. Newcomb and D. J. Cram, *J. Am. Chem. Soc.*, 1977, **99**, 6398.
22 M. Newcomb, S. S. Moore and D. J. Cram, *J. Am. Chem. Soc.*, 1977, **99**, 6405.
23 H. Fujihara, J.-J. Chiu and N. Furukawa, *Chem. Lett.*, 1991, 141.
24 F. Vögtle, *Chem. Ber.*, 1969, **102**, 1784.
25 R. K. McCoy, F. E. Karasz, A. Sarker and P. M. Lathi, *Chem. Mater.*, 1991, **3**, 941.
26 T. Otsubo, T. Kohda and S. Misumi, *Bull. Chem. Soc. Jpn.*, 1980, **53**, 512.
27 Y.-H. Kiang, G. B. Gardner, S. Lee and Z. Xu, *J. Am. Chem. Soc.*, 2000, **122**, 6871.
28 A mixture of NBS (43.9 mmol) and *tert* -butylbenzene (5.1 mmol) in MeOAc (100 mL, 1258 mmol) was refluxed by irradiation for 16 h, after which the reaction mixture was analysed by ^{1}H NMR.
29 A mixture of NBS (17.6 mmol), AIBN (0.08 mmol) and *tert*-butylbenzene (2.1 mmol) in MeOAc (40 mL, 503 mmol) was irradiated for 10 min at 112 °C, 5 bar, after which the reaction mixture was analysed by ^{1}H NMR.
30 G. Rodríguez, M. Albrecht, J. Schoenmaker, A. Ford, M. Lutz, A. L. Spek and G. van Koten, *J. Am. Chem. Soc.*, 2002, **124**, 5127.

Michael addition of α-nitro ketones to conjugated enones under solventless conditions using silica†

Roberto Ballini,* Dennis Fiorini, Maria Victoria Gil and Alessandro Palmieri

Dipartimento di Scienze Chimiche dell'Università di Camerino, Via S. Agostino 1, I-62032 Camerino (MC), Italy. E-mail: roberto.ballini@unicam.it

Received 10th June 2003
First published as an Advance Article on the web 21st July 2003

Conjugate addition of both linear and cyclic α-nitro ketones to conjugated enones, can be efficiently performed under heterogeneous, solvent-free and mild acidic conditions, by silica. The procedure allows good yields of 2-nitro-1,5-diones and, it worthy of note that no products arising from the cleavage of α-nitro cycloalkanones were observed under these reaction conditions. Moreover, during the work up, the need of extraction with an organic solvent can be avoided since the crude mixture can be directly charged to a chromatography column for immediate purification.

Introduction

α-Nitro ketones are useful intermediates in organic synthesis.[1–7] This is mainly because the proton α to the nitro group is fairly acidic and can be easily removed under mild conditions, thus permitting C–C bond formation.[8–11] After C–C bond formation the nitro group can be reductively removed, leading to the formation of nitro-free compounds, on the other hand, the nitro group can either be converted into an amino functionality, to a carbonyl group or to many other functionalities.[12] In this context the Michael addition of an α-nitro ketone to α,β-unsaturated carbonyl compound is of great interest, and these reactions are typically run in homogeneous solutions of the reactants in an organic solvent using soluble bases.[2,13–17]

In recent years different heterogeneous catalysts have successfully been applied to carry out various chemical transformations. Environmental and economical considerations prompt an urgent need to redesign the important processes and, in this framework, heterogeneous catalysis plays a dramatic role.[18–20]

Results and discussion

In connection with our interest in the application of heterogeneous catalysts for fine chemicals preparation,[21,22] we planned the first heterogeneous catalyst able to promote the conjugate addition of α-nitro ketones **1** to α,β-unsaturated ketones **2**.

Although the Michael addition of **1** to **2**, in homogeneous solution, is normally performed under basic conditions,[2,13–17] based on our previous experience of the easy enolisation of the α-nitro ketones under acidic conditions,[10] we tested different heterogeneous acidic catalysts in order to find the best reaction conditions. As a model reaction we chose the reaction of benzoylnitromethane **1a** with methyl vinyl ketone **2a** and, as reported in Table 1, silica was found to be the most effective in the formation of the adduct **3aa**. A number of different α-nitro ketones **1** and conjugated enones **2** were chosen to assess the scope of the reaction (Scheme 1). The reactions were performed under solvent-free conditions, by mixing at room temperature stoichiometric amounts of **1** and **2** with silica (silica/substrate = 350 mg mmol^{-1}) and leaving the mixture at room temperature for the suitable reaction time (Table 2).

Table 1 Preparation of **3aa** by different heterogeneous catalysts

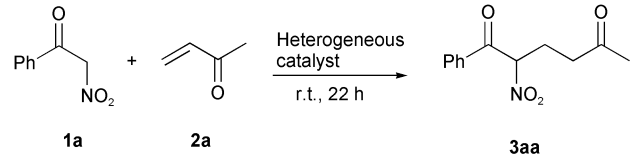

Heterogeneous catalyst	Yield % of **3aa** (Reaction time = 22h)
Silica Gel 60	87
Montmorillonite KSF	19
Montmorillonite K-10	27
Acidic Al_2O_3	61
Zeolite HSZ-330	74

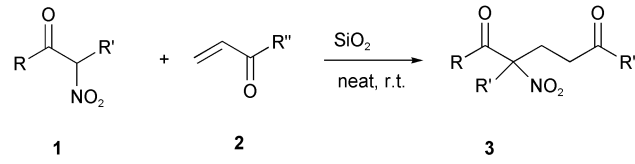

Scheme 1

The synthetic results of the reactions are presented in Table 2. This method gives good yields with both linear and cyclic α-nitro ketones. It also worthy of note that no products arising

Green Context

Michael additions are inherently atom economic and have therefore been the subject of considerable attention. This remarkably simple method, where silica is used as catalyst in a solvent-free, room temperature system, is a very attractive option amongst the many possible methods available for these reactions. ***DJM***

† Electronic supplementary information (ESI) available: IR, MS, ^{1}H and ^{13}C NMR data for all obtained 2-nitro-1,5-diones. See http://www.rsc.org/suppdata/gc/b3/b306359c/

Table 2 Conjugate addition of α-nitro ketones **1** to enones **2**

Entry	α-Nitro ketone **1**	Conjugate enone **2**	Yield[a] % of **3** (reaction time, h)
1	**1a** 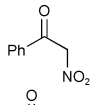	**2a** 	**3aa** 87 (22)
2	**1b** 	**2a** 	**3ba** 77 (48)
3	**1c** 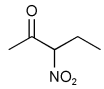	**2a** 	**3ca** 74 (100)
4	**1d** 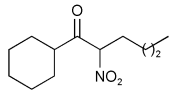	**2a** 	**3da** 86 (100)
5	**1e** 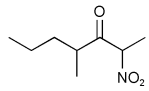	**2a** 	**3ea** 88 (35)
6	**1f** 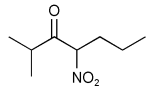	**2b** 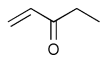	**3fb** 72 (120)
7	**1g** 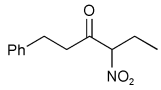	**2b** 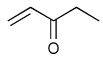	**3gb** 76 (120)
8	**1h** 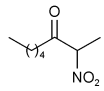	**2b** 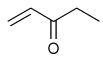	**3hb** 77 (50)
9	**1a** 	**2c** 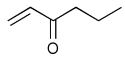	**3ac** 86 (23)
10	**1c** 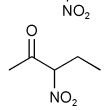	**2c** 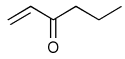	**3cc** 65 (100)
11	**1i** 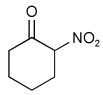	**2a** 	**3ia** 75 (44)
12	**1j** 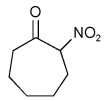	**2b** 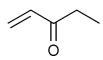	**3ja** 82 (90)
13	**1k** 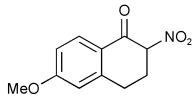	**2a** 	**3ka** 88 (70)

[a] Yield of pure, isolated product.

from the cleavage of α-nitro cycloalkanones[5] were observed under these reaction conditions.

Conclusions

In conclusion, we have reported the first, mild acidic, heterogeneous methodology for the Michael addition of both linear and cyclic α-nitro ketones to conjugated enones. This procedure works under solvent-free conditions and affords in good yields the corresponding 2-nitro-1,5-diones, without the need, during the work up, for extraction with any organic solvents, since the crude mixture can be directly charged to a chromatography column for immediate purification.

Experimental

Typical procedure

α-Nitro ketone **1** (1 mmol) was mixed with conjugated enone **2** (1 mmol), then, silica gel 60 (0.350 g, Merck 0.040–0.063 mm) was added. After mechanical stirring at room temperature for 30 min (until the starting materials are homogeneously adsorbed on silica), the mixture was left at room temperature for the appropriate time (established by TLC or GC, see Table 2), then charged to a flash chromatography column, the column was eluted (EtOAc/cyclohexane, 2 : 8), affording the pure adduct **3**. Satisfactory IR, MS, ^{1}H and ^{13}C NMR were obtained for all the 2-nitro-1,5-diones obtained (see supplementary material†).

Acknowledgements The work was carried out in the framework of the National Project "Il Mezzo Acquoso nelle Applicazioni Sintetiche dei Nitrocomposti Alifatici" supported by Ministero dell'Università e della Ricerca Scientifica e Tecnologica, Rome-Italy, by Fondazione della Cassa di Risparmio della Provincia di Macerata-Italy and by the University of Camerino-Italy. M. V. G. also thanks the Spanish Ministerio de Educacion, Cultura y Deporte for a postdoctoral fellowship.

References

1 R. H. Fisher and H. M. Weitz, *Synthesis*, 1980, 261.
2 H. Stach and M. Hesse, *Tetrahedron*, 1988, **44**, 1573.
3 G. Rosini and R. Ballini, *Synthesis*, 1988, 833.
4 G. Rosini, R. Ballini, M. Petrini, E. Marotta and P. Righi, *Org. Prep. Proc. Int.*, 1990, **22**, 707.
5 R. Ballini, *Synlett*, 1999, 1009.
6 R. Ballini, G. Bosica, E. Marcantoni, P. Vita and G. Bartoli, *J. Org. Chem.*, 2000, **65**, 5854.
7 M. Curini, F. Epifano, M. C. Marcotullio, O. Rosati, R. Ballini and G. Bosica, *Tetrahedron Lett.*, 2000, **41**, 8817.
8 H. Stach and M. Hesse, *Helv. Chim. Acta*, 1986, **69**, 1614.
9 N. Ono, I. Hamamoto and A. Kaji, *J. Org. Chem.*, 1986, **51**, 2832.
10 A. Fontana, P. De Maria, G. Siani, M. Pierini, S. Cerritelli and R. Ballini, *Eur. J. Org. Chem.*, 2000, 1641.
11 F. Gasparrini, M. Pierini, C. Villani, P. De Maria, A. Fontana and R. Ballini, *J. Org. Chem.*, 2003, **68**, 3173.
12 N. Ono, *The Nitro Group in Organic Synthesis*; Ed., H. Feuer, Wiley-VCH, New York, 2001.
13 C. J. Roxburgh, *Tetrahedron*, 1993, **49**, 10749.
14 N. Ono, H. Miyake and A. Kaji, *J. Chem. Soc., Chem. Commun.*, 1983, 875.
15 Y. Nakashita and M. Hesse, *Helv. Chim. Acta*, 1983, **66**, 845.
16 H. Stach and M. Hesse, *Helv. Chim. Acta*, 1987, **70**, 315.
17 Y. Nakashita and M. Hesse, *Angew. Chem. Ed. Engl.*, 1981, **20**, 1021.
18 P. Laszlo, *Acc. Chem. Res.*, 1986, **19**, 121.
19 S. V. Ley, I. R. Baxendale, R. N. Bream, P. S. Jackson, A. G. Leach, D. A. Longbottom, M. Nesi, J. S. Scott, R. J. Storter and S. J. Taylor, *J. Chem. Soc., Perkin Trans 1*, 2000, 3815; M. Chakrabarty, R. Bsak and N. Ghosh, *Tetrahedron Lett.*, 2001, **42**, 3913; A. de la Hoz, A. Díaz-Ortiz, M. V. Gómez, J. A. Mayoral, A. Moreno, A. M. Sánchez-Millagon and E. Vázquez, *Tetrahedron*, 2001, **57**, 5421; D. Michaud, F. Texier-Boullet and J. Hamelin, *Tetrahedron Lett.*, 1997, **38**, 7563.
20 R. Fricke, H. Hosslick, G. Lischke and M. Richter, *Chem. Rev.*, 2000, **100**, 2303.
21 M. Ballabeni, R. Ballini, F. Bigi, R. Maggi, M. Parrini, G. Predieri and G. Sartori, *J. Org. Chem.*, 1999, **64**, 1029; R. Ballini, F. Bigi, E. Gogni, R. Maggi and G. Sartori, *J. Catal.*, 2000, **191**, 348; R. Ballini, G. Bosica, R. Maggi, M. Ricciutelli, P. Righi, G. Sartori and R. Sartorio, *Green Chem.*, 2001, **3** , 178; R. Ballini, G. Bosica, D. Fiorini, R. Maggi, P. Righi, G. Sartori and R. Sartorio, *Tetrahedron Lett.*, 2002, **43**, 8445; R. Ballini, G. Bosica, D. Livi, A. Palmieri, R. Maggi and G. Sartori, *Tetrahedron Lett.*, 2003, **44**, 2271.
22 R. Ballini and G. Bosica, in *Recent Research Development in Organic Chemistry*, Transworld Research Network, Trivandrum, 1997, **vol. 1**, p. 11.

The Mannich reaction of hydrazones: improved reactivity under solvent-free conditions

L. El Kaïm,[a] L. Gautier,[a] L. Grimaud,[a] L. M. Harwood[b] and V. Michaut[a]

[a] *Laboratoire Chimie et Procédés, Ecole Nationale Supérieure de Techniques Avancées, 32 Bd Victor, 75015 Paris, France. E-mail: elkaim@ensta.fr; Fax: +33 1 45 52 83 22*
[b] *Department of Chemistry, University of Reading, PO BOX224, Whiteknights, Reading, UK RG6 6AD*

Received 3rd June 2003
First published as an Advance Article on the web 22nd July 2003

The Mannich reaction of hydrazones can be performed without solvent by simply mixing the hydrazone with two to three equivalents of a secondary amine and formaldehyde. Best yields and conditions are obtained with *p*-nitro substituted arylhydrazones. These conditions allow the efficient coupling of simple hydrazones that failed to react in toluene or ethanol solutions.

Introduction

The growing interest in environmentally friendly processes has focused the attention of organic chemists on definition of increasingly benign reaction conditions, one ultimate goal being to dispense with solvent.[1]

Pursuing our studies on the Mannich reaction of hydrazones,[2–4] we wished to explore new conditions to circumvent the reactivity problems encountered. This reaction, first described by Keil and Ried[5] and later extended to various aldehydes in our research group, allows efficient coupling between hydrazones **1**, aldehydes **2** and secondary amines **3** (Scheme 1). In all cases, the reaction remained limited to the

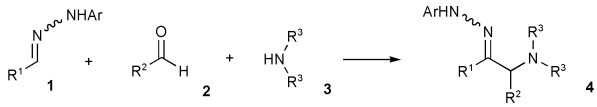

Scheme 1

coupling of hydrazones possessing electron-withdrawing groups on the hydrazone (R^1 = CO_2Et, COR′, CN…); simple hydrazones (R^1 = alkyl, aryl) did not react at all in ethanol, toluene or chlorobenzene, even after prolonged heating in the presence of several equivalents of amine and aldehyde.

Results and discussion

When the *N*-phenylhydrazone of benzaldehyde **1a** was heated with formaldehyde and *N*-benzylpiperazine **3** without solvent, we were pleased to observe the formation of novel hydrazone **4a** after a few hours. The best yield was obtained by heating hydrazone **1a** with two equivalents of *N*-benzylpiperazine and formaldehyde to 110 °C followed by addition of one more equivalent of each reagent after two hours. Hydrazone **4a** was then obtained in 82% isolated yield. A range of hydrazones derived from aromatic and heteroaromatic aldehydes behaved similarly, as shown in Table 1.

Furan, thiophene and indole substituted hydrazones were obtained in good to excellent yields. The results obtained with hydrazones derived from aliphatic aldehydes were however disappointing. Propionaldehyde phenylhydrazone **1f** gave only traces of the expected coupled product and these conditions

Table 1 Solvent-free Mannich reaction of hydrazones **1**

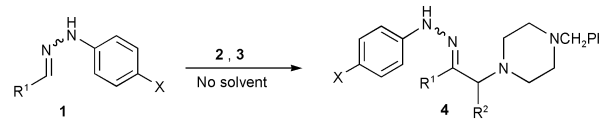

Starting **1**	Aldehyde **2**	Product	Conditions[b]	Yield (%)
1a	**2a**[a]	**4a**	A	82
1b	**2a**	**4b**	A	71
1c	**2a**	**4c**	A	94
1d	**2a**	**4d**	A	68
1e	**2a**	**4e**	A	73
1f	**2a**	**4f**	A	Traces
1g	**2a**	**4g**	B	97
1h	**2a**	**4h**	A	50
1g	**2b**	**4i**	B	86
1i	**2b**	**4j**	B	95

[a] Formaldehyde was used as a 40% solution in water. [b] A: To hydrazone **1** was added aldehyde **2** (2 eq) and amine **3** (2 eq) and the mixture heated at 110 °C under argon; after two hours, one more equivalent of **2** and **3** was added and the mixture further heated for two hours. Extraction with aqueous copper sulfate and chromatography affords hydrazone **4**. B: Same procedure, but two hours heating and two equivalents of each reagent are sufficient for completion.

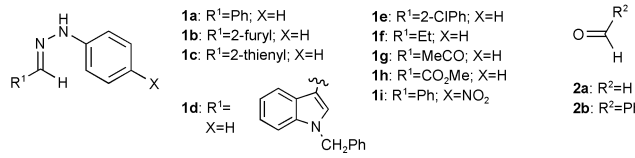

Green Context

Solvent free conditions have been developed for the three-component Mannich coupling, a reaction which provides richly functional products in a very atom economical fashion. Avoiding the solvent means that the three components are mixed and heated, leading directly to the product. An additional benefit is that products can be obtained in very good yield which do not form in the presence of solvent.

DJM

failed to give any Mannich adduct between more complex aldehydes and simple arylhydrazones. High pressure conditions (19 kbar with **1g, 1i** and **2b** without solvent and 9 kbar in toluene 2 M) were also tested without any success. From our previous reports, better results could be expected with starting hydrazones possessing electron-withdrawing groups. Although those hydrazones react with formaldehyde or aromatic aldehydes in solution, in the absence of solvent, the reactions are almost quantitative and only two equivalents of reactants are needed for completion of reaction (condition B, Table 1). Hydrazone **1g** for instance, benzaldehyde and *N*-benzylpiperazine afford the phenyl substituted hydrazone **4i** in 86% isolated yield.

The use of aryl substituted hydrazones does not alter the course of this reaction; a nitro substituent even seems to improve the conditions and yields of the coupling process: the nitro substituted hydrazone **1i** gave a Mannich adduct in a 95% isolated yield after two hours heating with only two equivalents of each reagent (Conditions B, Table 1).

These new conditions widen significantly the scope and interest of the Mannich reaction of hydrazones. Suitable starting hydrazones may be obtained through Japp–Klingemann coupling[6] of β-ketoesters with diazonium salts and the wide range of commercial aromatic and heteroaromatic aldehydes can now be involved in the Mannich reaction through their hydrazone derivatives. Improvement of reaction treatment by the selection of more volatile amines[7] and generation of azoalkenes from these new Mannich bases are under study in our research group and will be reported in due course.

Experimental

Proton and carbon nuclear magnetic resonance (^{1}H, ^{13}C NMR) were recorded on an Avance 400 (400 MHz) Bruker magnetic resonance spectrometer using chloroform-d as a solvent. Chemical shifts are reported as δ in units of parts per million downfield from tetramethylsilane (δ 0.0), used as an internal standard for ^{1}H NMR spectra. ^{13}C NMR spectra were calibrated to the 77 ppm signal of $CDCl_3$. IR spectra were recorded as neat samples or in CCl_4 solution on a Perkin-Elmer 299. Melting points were obtained on a Reichert apparatus and are uncorrected. Mass spectra were obtained on a MS 50 spectrometer. Chromatography was performed using Merck silica gel. Analytical TLC was performed using 0.25 mm Merck Kieselgel 60 P254 precoated silica gel plates. Visualization was accomplished with UV light, iodine vapor or by spraying a solution of vanillin in orthophosphoric acid–ethanol 1 : 1, followed by heating. The starting hydrazones were prepared from the corresponding ketones and arylhydrazines in ethanol as solvent.

N-[2-(4-Benzylpiperazin-1-yl)-1-phenylethylidene]-*N′*-phenylhydrazine 4a

To 1.57 g (8.00 mmol, 1.00 equiv) of *N*-benzylidene-*N′*-phenylhydrazine were added 1.24 mL (16.00 mmol, 2.00 equiv) of formaldehyde (in a 40% aqueous solution), and 2.78 mL (16.00 mmol, 2.00 equiv) of *N*-benzylpiperazine. The resulting mixture was heated at 110 °C and stirred for two hours. One more equivalent of aldehyde and amine were then added, and the whole was heated again for two hours. The mixture was diluted with CH_2Cl_2, and washed with 80 mL of a saturated aqueous solution of $CuSO_4$, so that the excess of amine precipitated. It was then filtered on celite, and the aqueous phase was extracted three times with CH_2Cl_2. The combined organic layers were washed with brine, dried over anhydrous $MgSO_4$, filtered and concentrated *in vacuo*. Purification by flash chromatography on silica gel with Et_2O–petroleum ether (20%) gave 2.52 g (82%) of Mannich adduct **4a** as an orange oil. R_f: 0.35 (Et_2O–petroleum ether, 40 : 60). ^{1}H NMR ($CDCl_3$, 400 MHz): δ 11.25 (s, 1H, NH), 7.83–7.80 (m, 2H), 7.44–7.30 (m, 10H), 7.24–7.22 (m, 2H), 6.94 (tt, J = 7.3, 1.1 Hz, 1H), 3.80 (s, 2H, N=C–CH_2–N), 3.59 (s, 2H, N–CH_2–Ph), 2.85–2.40 (m, 4 H_2, N–CH_2–CH_2–N). ^{13}C NMR ($CDCl_3$, 100.6 MHz): δ 146.1, 139.6, 139.4 (C_q, C=N, Ph_2), 138.4, 129.7, 129.6, 128.8, 128.7, 128.1, 127.6, 126.0, 120.2, 113.4, 63.3 (N–CH_2–Ph), 56.9 (N=C–CH_2–N), 53.8, 52.9 (N–CH_2–CH_2–N). IR/cm^{-1}: 3165, 3062, 3027, 2939, 2812, 2768, 1601, 1556, 1513, 1493, 1445, 1324, 1254, 1152, 1135, 1007. Mass (ID ICP NH3): *m*/*z* 384 (M+), 209, 177. Microanalysis for $C_{25}H_{28}N_4$: found: C 78.12, H 7.61, calculated: C 78.09, H 7.34%.

N-[2-(4-Benzylpiperazin-1-yl)-1-furan-2-ylethylidene]-*N′*-phenylhydrazine 4b

Two isomers (9 : 1) of this compound were obtained as orange oils similarly to **4a** in 71% overall yield.

Major isomer: R_f: 0.35 (Et_2O–petroleum ether, 40 : 60). ^{1}H NMR ($CDCl_3$, 400 MHz): δ 11.06 (s, 1H, NH), 7.48 (dd, J = 1.7, 0.6 Hz, 1H, H_c), 7.38–7.28 (m, 7H), 7.18 (dd, J = 8.6, 1.0 Hz, 2H), 6.92 (tt, J = 7.3 Hz, 1.0 Hz, 1H), 6.61 (dd, J = 3.3, 0.6 Hz, 1H), 6.46 (dd, J = 3.3, 1.7 Hz, 1H), 3.69 (s, 2H), 3.57 (s, 2H), 2.75–2.38 (m, 8H). ^{13}C NMR ($CDCl_3$, 100.6 MHz): δ 153.2, 145.7, 143.0, 138.4, 132.7, 129.7, 129.5, 128.7, 127.6, 120.3, 113.4, 111.9, 107.4, 63.3, 56.3, 53.8 (CH_2, N–CH_2–CH_2–N), 52.9 (CH_2, N–CH_2–CH_2–N). IR/cm^{-1}: 3163, 3027, 2939, 2812, 2768, 1602, 1559, 1514, 1494, 1456, 1316, 1258, 1166, 1154, 1135, 1072, 1008. Mass: (ID ICP NH_3) 375 (MH+), 292, 267, 199, 177. HRMS (CI, CH_4) for $C_{23}H_{27}N_4O$ (MH^+) *m*/*z* calculated: 375.2185; found: 375.2190.

Minor isomer: R_f: 0.20 (Et_2O–petroleum ether, 40 : 60).^{1}H NMR ($CDCl_3$, 400 MHz): δ 9.78 (s, 1H, NH), 7.61 (d, J = 1.6 Hz, 1H), 7.36–7.28 (m, 7H), 7.19 (d, J = 9.9 Hz, 2H), 6.92–6.88 (m, 2H), 6.45 (dd, J = 3.4, 1.6 Hz), 3.54 (s, 2H), 3.48 (s, 2H), 2.75–2.38 (m, 8H, N–CH_2–CH_2–N). ^{13}C NMR ($CDCl_3$, 100.6 MHz): δ 151.0, 145.3, 142.3, 138.6, 129.2 (C=N), 129.6, 129.5, 128.6, 127.4, 120.5, 113.3, 112.2, 111.8, 63.4, 63.0, 53.6, 53.4 (N–CH_2–CH_2–N).

N-[2-(4-Benzylpiperazin-1-yl)-1-thiophen-2-ylethylidene]-*N′*-phenylhydrazine 4c

This compound was obtained similarly to **4a** in 94% yield as an orange oil. R_f: 0.30 (Et_2O–petroleum ether, 60:40). ^{1}H NMR ($CDCl_3$, 400 MHz): δ 10.99 (s, 1H, NH), 7.37–7.28 (m, 7H), 7.23 (dd, J = 5.1, 0.9 Hz, 1H), 7.15 (d, J = 7.6 Hz, 2H), 7.11 (dd, J = 3.7, 1.0 Hz, 1H), 7.00 (dd, J = 5.1, 3.7 Hz, 1H), 6.91 (t, J = 7.3 Hz, 1H), 3.74 (s, 2H), 3.57 (s, 2H), 2.75–2.38 (m, CH_2, N–CH_2–CH_2–N). ^{13}C NMR ($CDCl_3$, 100.6 MHz): δ 145.3, 144.9, 135.8 (C=N), 137.8, 129.7, 129.0, 128.4, 127.3, 127.2, 126.0, 123.3, 119.9, 112.9, 62.9, 56.9, 53.3 (CH_2, N–CH_2–CH_2–N), 52.4 (CH_2, N–CH_2–CH_2–N). Mass (ID ICP NH_3): *m*/*z* 391 (MH+), 390, 215, 177. IR/cm^{-1}: 3170, 3064, 3027, 2938, 2812, 1601, 1564, 1495, 1456, 1314, 1255, 1153, 1134, 1008. HRMS(CI, CH_4) for $C_{23}H_{27}N_4S$ *m*/*z* calculated: 391.1956; found: 391.1955 (MH^+).

N-[1-(1-Benzyl-1*H*-indol-3-yl)-2-(4-benzylpiperazin-1-yl)ethylidene]-*N′*-phenylhydrazine 4d

Yellow solid obtained similarly to **4a** in 68% yield as a mixture of two inseparable isomers (9 : 1).

Major isomer: Mp: 165–166 °C (recrystallised in hot toluene–cyclohexane). R_f: 0.30 (EtOAc–petroleum ether, 25 : 75). ^{1}H NMR ($CDCl_3$, 400 MHz): δ 10.89 (s, 1H, NH), 8.71 (d, J = 7.6 Hz), 7.41–7.28 (m, 14H), 7.24 (d, J = 7.9 Hz, 2H), 7.16

(d, J = 7.1 Hz, 2H), 6.90 (t, J = 7.3 Hz, 1H), 5.34 (s, 2H), 3.71 (s, 2H), 3.57 (s, 2H), 2.75–2.51 (m, 8H, N–CH_2–CH_2–N). ^{13}C NMR ($CDCl_3$, 100.6 MHz): δ 146.8, 138.9 (C=N), 138.4, 138.0, 137.5, 129.7, 129.6, 129.3, 128.7, 128.2, 127.6, 127.2, 126.1, 124.1, 123.4, 121.4, 119.4, 116.8, 113.1, 110.0, 63.4, 58.1, 53.8 (N–CH_2–*CH_2*–N), 52.9 (N–*CH_2*–CH_2–N), 50.6. IR/cm^{-1}: 3162, 3065, 3011, 2942, 2816, 1600, 1540, 1496, 1465, 1455, 1386, 1311, 1258, 1167, 1130, 1008. Mass (ID ICP NH_3): 515 (MH_2+), 337, 177. Microanalysis for $C_{34}H_{35}N_5$: found: C 79.03, H 6.93, calculated: C 79.50, H 6.87%.

N-[2-(4-Benzylpiperazin-1-yl)-1-(2-chlorophenyl)-ethylidene]-*N′*-phenylhydrazine 4e

This compound was obtained similarly to **4a** in 73% yield as a yellow oil. R_f: 0.45 (Et_2O–petroleum ether, 40 : 60). ^{1}H NMR ($CDCl_3$, 400 MHz): δ 11.53 (s, 1H, NH), 7.46–7.44 (m, 1H), 7.42–7.39 (m, 1H), 7.36–7.35 (m, 4H), 7.33–7.25 (m, 5H), 7.11 (dd, J = 8.6, 1.0 Hz, 2H), 6.89 (tt, J = 7.3, 1.0 Hz, 1H), 3.76 (s, 2H, N=C–CH_2–N), 3.59 (s, 2H, N–CH_2–Ph), 2.85–2.40 (m, 8H, N–CH_2–CH_2–N). ^{13}C NMR ($CDCl_3$, 100.6 MHz): δ 145.8, 139.6 (C=N), 137.9, 132.7, 131.4, 130.3, 129.6, 129.4, 128.7, 128.7, 127.6, 127.2, 120.2, 113.4, 63.3 (N–CH_2–Ph), 60.2 (N=C–CH_2–N), 53.8, 52.8 (4 CH_2, N–CH_2–CH_2–N). IR/cm^{-1}: 3341, 3029, 2962, 2827, 2810, 1695, 2654, 1602, 1556, 1492, 1446, 1365, 1332, 1264, 1233, 1195, 1169, 1152, 1133, 1003. Mass (ID ICP NH3): *m*/*z* 419 (M + H$^+$), 258, 243, 205, 177. Microanalysis for $C_{25}H_{27}ClN_5$: found: C 71.84, H 6.97, calculated: C 71.67, H 6.50%.

4-(4-Benzylpiperazin-1-yl)-3-(phenylhydrazono)-butan-2-one 4g

This compound was obtained similarly to **4a** with only two equivalents of amine and aldehyde for completion giving hydrazone **4g** as a yellow solid in 97% yield. Mp: 92–94 °C. R_f: 0.70 (Et_2O). ^{1}H NMR ($CDCl_3$, 400 MHz): δ 12.21 (s, 1H, NH), 7.40–7.34 (m, 6H), 7.31–7.28 (m, 1H), 7.22 (dd, J = 8.4, 0.9 Hz, 2H), 7.04 (tt, J = 7.3, 0.9 Hz, 1H), 3.73 (s, 2H, N=C–CH_2–N), 3.56 (s, 2H, N–CH_2–Ph), 2.65–2.38 (m, 8H, N–CH_2–CH_2–N), 2.50 (s, 3H, CH_3). ^{13}C NMR ($CDCl_3$, 100.6 MHz): δ 197.3 (C=O), 146.1, 138.4, 138.3 (C=N), 129.8, 129.5, 128.7, 127.6, 122.6, 114.3, 63.3 (N–CH_2–Ph), 52.9 (N=C–CH_2–N), 53.7, 52.7 (N–CH_2–CH_2–N), 24.6 (CH_3). IR/cm^{-1}: 2944, 2829, 2803, 1660. Mass (ID ICP NH_3): 351 (MH+). FABHRMS calculated for $C_{21}H_{27}N_4O$ (MH+) 350.2185, found 350.2184.

3-(4-Benzylpiperazin-1-yl)-2-(phenylhydrazono)propionic acid methyl ester 4h

Yellow solid obtained similarly to **4a** in 50% yield as a mixture of two inseparable isomers (85–15). Mp: > 230 °C (dec).

Major isomer: R_f: 0.25 (Et_2O–petroleum ether, 40 : 60). ^{1}H NMR ($CDCl_3$, 400 MHz): δ 12.01 (s, 1H, NH), 7.36–7.25 (m, 7H), 7.22 (dd, J = 8.6, 1.0 Hz, 2H), 6.99 (t, J = 7.3 Hz, 1H), 3.84 (s, 3H, OMe), 3.74 (s, 2H, N=C–CH_2–N), 3.54 (s, 2H, N–CH_2–Ph), 2.65–2.38 (m, 8H, N–CH_2–CH_2–N). ^{13}C NMR ($CDCl_3$, 100.6 MHz): δ 165.9 (C=O), 144.0, 138.3 (C=N), 129.7, 129.5, 128.6, 127.5, 122.4, 114.3, 63.3 (N–CH_2–Ph), 55.4, 53.2, 52.6, 52.0 (CH_3, OMe). IR (neat)/cm^{-1}: 3025, 2938, 2806, 1699. Mass (ID ICP NH_3) 367 (MH+). FABHRMS calculated for $C_{21}H_{26}N_4O_2$ (M+) 366.2054, found 366.2062.

4-(4-Benzylpiperazin-1-yl)-4-phenyl-3-(phenylhydrazono)-butan-2-one 4i

This compound was obtained similarly to **4g** in 86% yield as a pale yellow solid. Mp 107–108 °C. R_f: 0.35 (Et_2O). ^{1}H NMR ($CDCl_3$, 400 MHz): δ 12.94 (s, 1H, NH), 7.46–7.44 (m, 2H), 7.40 (t, J = 7.7 Hz, 2H), 7.34–7.31 (m, 4H), 7.30–7.26 (m, 4H), 7.25 (d, J = 7.8 Hz, 2H), 7.06 (t, J = 7.4 Hz, 1H), 5.04 (s, 1H, N=C–CH–N), 3.57 (s, 2H, N–CH_2–Ph), 2.80–2.40 (m, 4H, N–CH_2–CH_2–N), 2.41 (s, 3H, CH_3). ^{13}C NMR ($CDCl_3$, 100.6 MHz): δ 197.1 (C=O), 143.8, 140.0, 138.0, 137.9 (C=N), 129.9, 129.5, 129.2, 128.7, 128.3, 127.6, 122.5, 114.1, 68.6 (N=C–CH–N), 63.2 (N–CH_2–Ph), 53.8, 51.9 (N–CH_2–CH_2–N), 25.0 (CH_3). IR (thin film)/cm^{-1}: 3056, 3036, 2815, 2760, 1671, 1601. Mass (ID ICP NH_3): 427 (MH+). FABHRMS calculated for $C_{27}H_{31}N_4O$ (MH+) 427.2498, found 427.2495.

N-[2-(4-Benzylpiperazin-1-yl)-1-phenylethylidene]-*N′*-(4-nitrophenyl)hydrazine 4j

This compound was obtained similarly to **4g** in 95% yield as a pale yellow solid. Mp 153–155 °C. R_f: 0.75 (EtOAc–petroleum ether, 60 : 40). ^{1}H NMR ($CDCl_3$, 400 MHz) δ 12.23 (s, 1H, NH), 8.20 (d, J = 8.6 Hz, 2H), 7.76 (d, J = 7.6 Hz, 2H), 7.41 (d, J = 7.7 Hz, 2H), 7.40–7.30 (m, 6H), 7.12 (d, J = 8.7 Hz, 2H), 3.83 (s, 2H), 3.59 (s, 2H), 2.85–2.40 (m, 4 H_2, N–CH_2–CH_2–N). ^{13}C NMR ($CDCl_3$, 100.6 MHz) δ 150.8, 143.8, 140.4, 138.2, 129.5, 129.2, 128.9, 128.7, 127.7, 126.6, 126.3, 112.2, 63.2, 57.5, 53.7 (N–CH_2–*CH_2*–N), 52.9 (N–*CH_2*–CH_2–N). IR (CCl_4, CaF_2)/cm^{-1}: 3619, 3025, 2974, 2941, 2820, 1600, 1503, 1325, 1274, 1206, 1132, 1110, 1005. Mass (ID ICP NH3) *m*/*z* 431 (MH_2^+), 254, 177. HRMS (CI, CH_4) for $C_{25}H_{28}N_5O_2$ (MH^+) calculated *m*/*z*: 430.2243; found: 430.2241.

References and notes

1 For some recent examples: (*a*) V. P. Balema, J. W. Wiench, M. Pruski and V. K. Pecharsky, *Chem. Commun.*, 2002, 724–725; (*b*) C. J. Li and C. Wei, *Chem. Commun.*, 2002, 268–269; (*c*) J. Long, J. Hu, X. Shen, B. Ji and K. Ding, *J. Am. Chem. Soc*, .2002, **124**, 10–11; (*d*) C. Cimarelli, A. Mazzanti, G. Palmieri and E. Volpini, *J. Org. Chem.*, 2001, **66**, 4759–4765; (*e*) A. Hoz, A. Diaz-Ortiz, T. Elguero, L. J. Martinez, A. Moreno and A. Sanchez-Migallon, *Tetrahedron*, 2001, **57**, 4397–4404; (*f*) J. M. Thomas, R. Raja, G. Sankar, B. F. G. Johnson and D. W. Lewis, *Chem. Eur. J.*, 2001, **7**, 2973–2978.

2 V. Atlan, H. Bienaymé, L. El Kaïm and A. Majee, *Chem. Commun.*, 2000, 1585–1586.

3 V. Atlan, L. El Kaïm, L. Grimaud, N. K. Jana and A. Majee, *Synlett*, 2002, 352–354.

4 J. E. Ancel, L. El Kaïm, A. Gadras, L. Grimaud and N. K. Jana, *Tetrahedron Lett.*, 2002, 8319–8322.

5 W. Ried and G. Keil, *Liebigs Ann. Chem.*, 1957, **605**, 167–179.

6 F. R. Japp and F. Klingemann, *Chem. Ber.*, 1887, **20**, 2492.

7 The elimination of *N*-benzylpiperazine in excess was performed by extraction using an organic solvent; this treatment could be suppressed by the use of more volatile amines (the use of morpholine instead of *N*-benzylpiperazine affords with hydrazone **1a** the corresponding hydrazone in a 57% isolated yield).

Utilization of waste biomass and replacement of stoichiometric reagents for the synthesis of nanocrystalline CeO_2, ZrO_2 and CeO_2–ZrO_2

Akinori Muto,[a] Thallada Bhaskar,[a] Yuki Kaneshiro,[a] Md. Azhar Uddin,[b] Yusaku Sakata,*[a] Yoshihiko Kusano[c] and Kazuyuki Murakami[d]

[a] *Department of Applied Chemistry, Faculty of Engineering, Okayama University, 3-1-1 Tsushima Naka, 700-8530 Okayama, Japan*
[b] *Process Safety and Environment Protection Group, School of Engineering, The University of Newcastle, Callaghan, NSW 2308, Australia*
[c] *College of the Arts, Kurashiki Univ. of Science and the Arts, Tsurajima-cho, Okayama 712-8505, Japan*
[d] *JFE Chemical Co., 1 Kawasaki-cho, Chuou-ku, Chiba-shi, 260-0835 Chiba, Japan*

Received 28th April 2003
First published as an Advance Article on the web 22nd July 2003

Nanocrystalline CeO_2, ZrO_2 and CeO_2–ZrO_2 with various Ce, Zr compositions (1:1, 1:2, and 2:1) have been prepared and characterized. The preparation method demonstrates the replacement of stoichiometric reagents and utilization of waste biomass for an important class of metal oxides useful for various applications. Physico-chemical characterization studies including HRTEM analysis for the representative samples showed the presence of CeO_2 with particle size 5–10 nm, ZrO_2 with particle size 5–10 nm and $Ce_{0.5}$ $Zr_{0.5}O_2$ particles in the range 5–10 nm. EDS analysis confirmed the particles to be in cubic phase.

Introduction

Green chemistry is coming of age with interest in it increasing in both academic and industrial laboratories.[1] The elimination of toxic and/or flammable organic solvents continues to be an area of intense interest.[2] Progress has been made in the search for processes that use fewer toxic chemicals and produce less waste while using less energy. However, many challenges remain in the shift to a sustainable future.[3] The use of sustainable resources is one of the concepts of green chemistry. The current generation of three-way catalysts for automotive exhaust gas treatment rely on ceria-zirconia as dynamic oxygen source. The ability of CeO_2 to store, transport and release oxygen is of great importance in a range of clean energy technologies from catalytic converters to solid-oxide fuel cells. Recent research literature reports that the addition of ZrO_2 into cubic CeO_2 resulted in increased thermal stability and also promoted the redox properties. The solid oxide CeO_2–ZrO_2 was also found to be active for the synthesis of dimethyl carbonate, steam reforming of ethanol and also catalytic oxidation of methane *etc*.[4–6] The design of materials for such purposes should weigh up the environmental impact against material functionality, as well as the costs and benefits of synthesizing and processing materials. There also needs to be shift in the materials community at large towards technology sustainability, specifically in terms of energy and environmental impacts.[7] In our earlier studies, we demonstrated the preparation of ultrafine W and Ni compounds by metal ion exchanged resin-carbo thermal reduction method (MIER-CTR)[8] and successfully applied these compounds to the catalytic hydrodechlorination of chlorobenzene.[9]

In the case of minimising waste there are two approaches. The traditional approach aims at reducing waste at the end of the pipeline by, for example, decreasing emissions through the catalytic incineration of exhaust fumes. The second approach is based on minimising waste at the source. In this case, innovative procedures have to be employed to change both the method and the technology used throughout the production. The conventional wet chemical mixed oxide preparation methods involves various steps such as precipitation, filtration, washing, drying and calcination and produces large amounts of waste. In the present investigation, we report for the first time the utilization of waste biomass (sawdust) and the replacement of stoichiometric chemical reagents for the synthesis of an important class of compounds, nanocrystalline CeO_2, ZrO_2, and CeO_2–ZrO_2, at low carbonization temperatures (700 °C) and their physico-chemical characterization by adsorption and spectroscopic techniques.

Results and discussion

A series of metal oxide materials consisting of CeO_2, ZrO_2 and their mixed oxide CeO_2–ZrO_2 with various Ce, Zr compositions (Zr:Ce = 1:1, 1:2 and 2:1) have been prepared. The surface area analysis and the particle size information from the powder X-ray diffraction and HRTEM analysis is shown in Table 1.

Green Context

A combination of a novel and simple reaction coupled with the use of waste biomass has been used for the production of various nanocrystalline oxides. Precursors were adsorbed onto sawdust and the resultant material calcined to give, in a direct and simple manner, the desired nanoparticles, avoiding the use of additional chemicals in the process.

DJM

 DOI: 10.1039/b304574a

Table 1 Textural properties of CeO_2, ZrO_2 and (Ce, Zr)O_2 oxides [carbonized at 700 °C in N_2 and calcined at 700 °C in air]

Sample Ce:Zr ratio	Metal content [M]	BET SA, $m^2\ g^{-1}$ Carbonized	BET SA, $m^2\ g^{-1}$ Calcined	Crystallite size from XRD, nm	Crystallite size from TEM, nm
CeO_2	0.03	370	33	10	10
ZrO2	0.03	250	43	9	5–10
1:1	0.015–0.015	320	43	5–10	5–10
1:2	0.01–0.02	321	24	—	—
2:1	0.02–0.01	424	37	—	—

Surface area analysis of carbonized (700 °C) samples shows their higher surface area than those carbonized and calcined at 700 °C. The surface area of carbonized Ce, Zr and Ce–Zr samples were 370, 250 and 320 $m^2\ g^{-1}$ respectively. However, after the calcination at 700 °C (carbon burn off), the Ce, Zr and Ce–Zr shows 33, 43, and 43 $m^2 g^{-1}$ respectively. Powder X-ray diffraction analysis of the carbonized samples shows that they are amorphous in nature and have no characteristic peaks due to CeO_2 or ZrO_2. This may possibly be due to the microcrystalline nature of the samples, or the particle size of metal oxide might be less than the detection limit of the X-ray diffraction technique. After calcination, the characteristic peaks due to CeO_2, ZrO_2 and (Ce, Zr)O_2 appeared (Fig. 1).

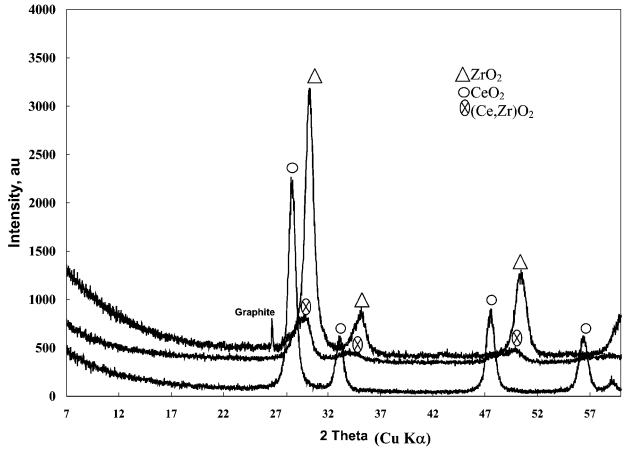

Fig. 1 Powder X-ray diffraction patterns for CeO_2, ZrO_2, (Ce, Zr)O_2 [Ce:Zr = 1:1] samples carbonized and calcined at 700 °C.

The calcination treatment was also performed at various temperatures such as 600 °C, 700 °C and 800 °C in air and the characteristic peaks due to the corresponding oxides were found. The ZrO_2 samples showed the graphite peak in addition to the ZrO_2 peaks, which is not present in either CeO_2 or CeO_2–ZrO_2 mixed oxide. From the width of the diffraction lines one can get a reasonable estimate of the average size of the particles. The particle sizes calculated by using the Scherrer equation showed that the CeO_2 has a particle size of 10 nm, ZrO_2 has 9 nm and that of CeO_2–ZrO_2 is within 5–10 nm. The deconvolution of CeO_2–ZrO_2 X-ray diffraction peaks shows that the particle size of CeO_2 is 9.5 nm and that of ZrO_2 is 6.8 nm. Increasing the calcination temperature from 600 °C to 800 °C increased the particle size from 5–10 nm to 15–20 nm . The presence of a higher surface area in the Ce-rich samples than the Zr-rich samples was observed (Table 1). Particle size analysis of the three representative samples was performed and is presented in Fig. 2 with the particle size on the *x*-axis and the fraction percentage on the *y*-axis. It clearly shows that the samples are in a uniformly wide distribution of the particle size with the maximum at 10 μm (fractional% 11).

The recent literature reports various preparative methods and analysis of $Ce_xZr_yO_2$ catalysts such as citrate[10] and the sol–gel

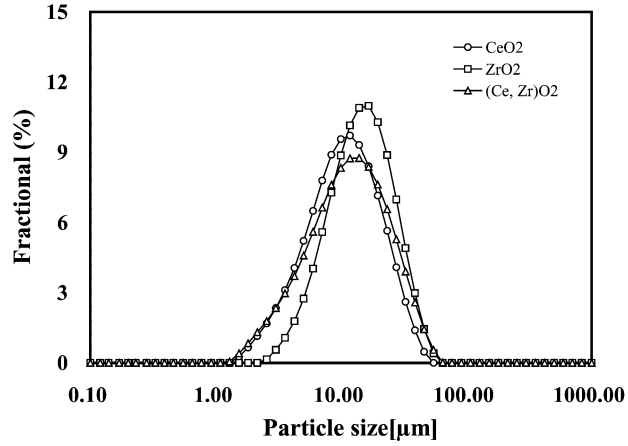

Fig. 2 Particle size analysis of CeO_2, ZrO_2, (Ce, Zr)O_2 [Ce:Zr = 1:1]samples carbonized and calcined at 700 °C.

preparation method,[11] and the microemulsion method.[12,13] The effects of redox treatments on the reducibility of supported ceria-zirconia[11] and microstructural analysis[14] were well reported. Due to the small differences in the diffraction lines of the CeO_2 and ZrO_2 and their mixed oxides, various researchers have used Rietveld refinement of the XRD patterns of these catalytic materials.[13] One of the most informative characterization techniques is transmission electron microscopy (TEM), because the electrons passing through the sample provide information not only about particle size and shape but also about the lattice structure and chemical composition of individual particles. Advances in controlled environment stages and electron optics now make it possible to examine catalysts at higher temperatures (1000 °C) and pressures up to 101 kPa.[15] High resolution transmission electron microscopy (HRTEM) analysis of CeO_2, ZrO_2 and CeO_2–ZrO_2 (Ce:Zr = 1:1) samples calcined at 700 °C are presented in Figs. 3(a)–3(c). Highly crystalline CeO_2 is shown in Fig. 3(a) and the particle size is around 10 nm.

The electron diffraction measurement for the CeO_2 is presented in Fig. 4(a). The left half is the measured electron diffraction pattern and right half is a simulation pattern and it clearly shows the cubic system with the value of a = 0.541 nm, in good agreement with the X-ray diffraction pattern (JCPDS: 34–0394). Highly crystalline ZrO_2 is shown in Fig. 3(b) and the particle size calculated from the HRTEM found to be 5–10 nm, which is smaller than for CeO_2. Electron diffraction studies for the ZrO_2 sample are presented in Fig. 4(b) and are in good agreement with the cubic system [JCPDS: 49–1642] having the value of a = 0.513 nm. In contrast to the CeO_2 sample the presence of spot without Debye ring was observed which might be due to the graphite (3R); the graphite was confirmed by the X-ray diffraction (Fig. 2). The particle size of mixed compound CeO_2–ZrO_2 [Ce:Zr = 1:1] is in the range of 5–10 nm (Fig. 3(c)). The formation of $Zr_{0.5}Ce_{0.5}O_2$ phase was in good agreement with the XRD data [JCPDS: 38–1436]. In addition, the energy dispersive X-ray spectroscopic (EDS) analysis also shows that even though the ratio of Ce:Zr is uniform, it might be possible that two other types of phases have been observed, due to rich in Ce (Fig. 4(c)) and rich in Zr phases (Fig. 4(d)), in addition to the equal in Ce and Zr content phase (Fig. 4(e)). We could not estimate the exact composition of each phase. However, the possible Zr-rich phase might be due to $Zr_{0.84}Ce_{0.16}O_2$ [JCPDS: 38–1437], and the Ce-rich phase might be due to $Zr_{0.4}Ce_{0.6}O_2$ [JCPDS: 38–1439]. Baiker *et al.*[16] reported the flame synthesis of nanocrystalline ceria-zirconia and concluded that the high temperature gas phase synthesis results in well-grown nanocrystals of ceria-zirconia with smooth surfaces and crystals that are not connected by sintering bridges. The Debye ring is broad due to the (Ce, Zr)O_2 solid

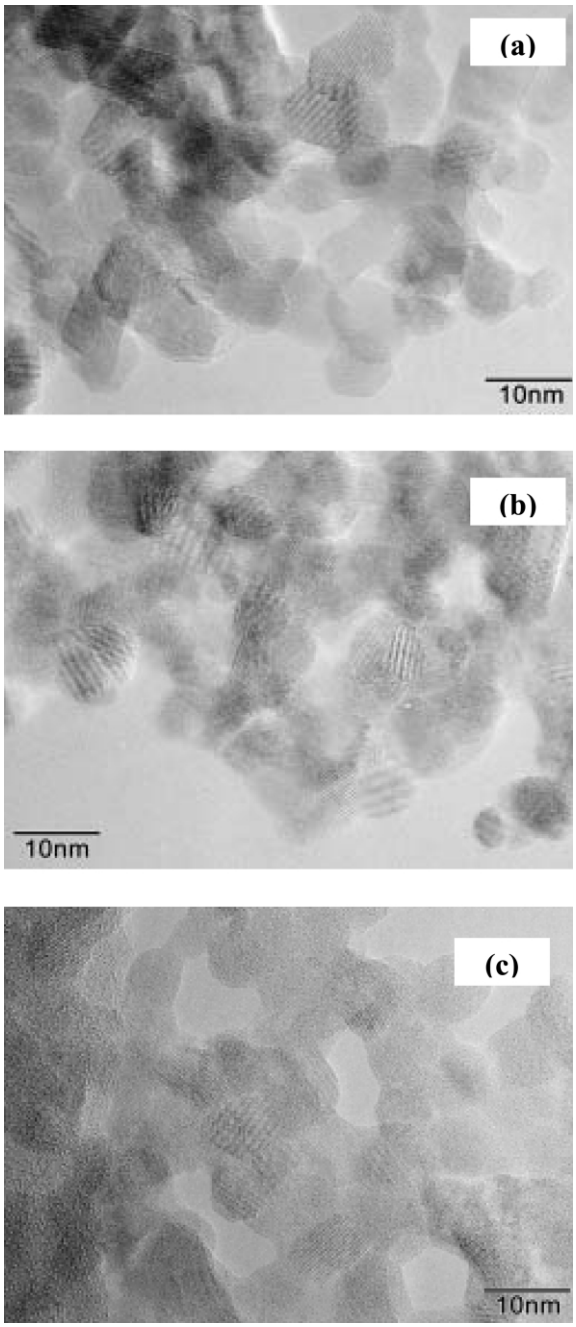

Fig. 3 HRTEM images of CeO_2, ZrO_2, (Ce, Zr)O_2 [Ce:Zr = 1:1]samples carbonized and calcined at 700 °C. (a) CeO_2 (b) CeO_2–ZrO_2 (c) ZrO_2.

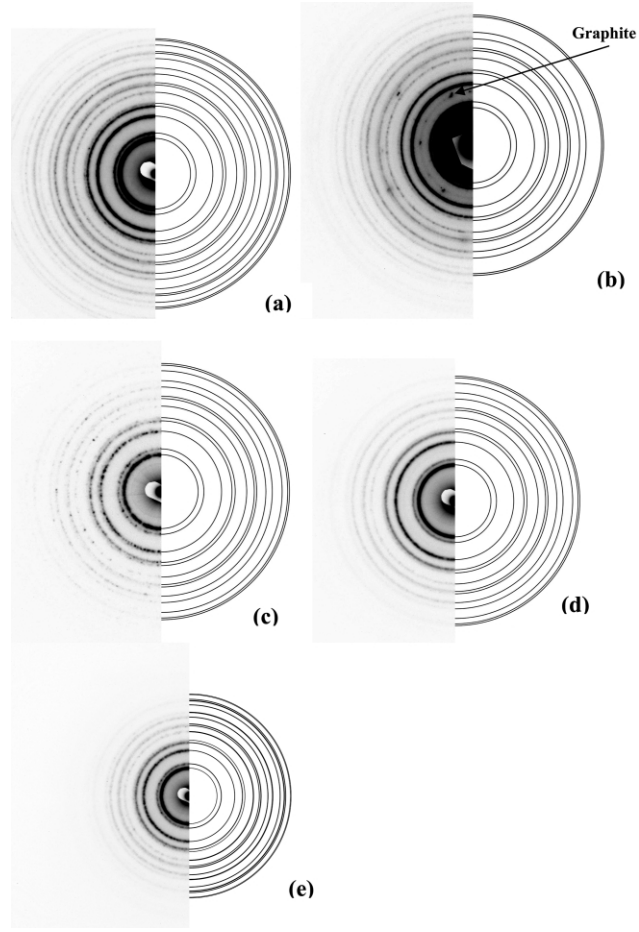

Fig. 4 Electron diffraction analysis of CeO_2, ZrO_2, and (Ce, Zr)O_2 [Ce:Zr = 1:1]samples carbonized and calcined at 700 °C. (a) CeO_2, (b) ZrO_2, (c) Ce-rich phase of (Ce, Zr)O_2, (d) Zr-rich phase of (Ce, Zr)O_2, (e) Ce and Zr equal phase of (Ce, Zr)O_2.

solution. Similar to CeO_2 and ZrO_2, (Ce, Zr)O_2 is also cubic with *a* values 0.536, 0.529 and 0.519. The three above samples show a polycrystalline phase with a narrow distribution of particle sizes. Electron diffraction patterns taken from selected areas of all samples show rings indexable according to a cubic fluorite structure. Lattice parameters are in good agreement with the XRD results. The CeO_2 and ZrO_2, the (Ce, Zr)O_2 crystals are loosely interconnected with the bridged crystallites, which contributes to the thermal stability and the TEM observations are in good agreement with the earlier findings.[16] The scanning electron microscopy (SEM) with the EDS analysis confirmed that the metal oxides are highly and homogeneously dispersed in the carbonized samples and this was confirmed by the elemental mapping. It is also possible to prepare the materials in bulk quantity using this method, unlike other high temperature gas phase methods. The temperature used for the carbonization and calcination process is a comparatively low 700 °C.

Experimental

Nanocrystalline metal oxides such as CeO_2, ZrO_2, and CeO_2–ZrO_2 mixed oxides with (Ce:Zr as 1:1. 2:1 and 1:2) were prepared using $ZrCl_4$ and $Ce(NO_3)_3{\cdot}6H_2O$ solutions, keeping the total metal concentration as 0.03 M. Briefly, about 130 g quantities of sawdust were mixed with 2 L metal solutions (0.015 M of Ce and Zr) and kept for 24 h for impregnation, the solution was removed and the impregnated sawdust was dried in air for 24 h. The dried sawdust was carbonized at 700 °C using a rotating pot type (specially made prototype) carbonization instrument (Nagato Electrical Machine Corporation, Osaka, Japan) in a N_2 atmosphere (300 ml min^{-1}). The rotating-pot type carbonization instrument is schematically shown in Fig. 5. The carbonized samples were calcined in air at 700 °C for 4 h. The BET surface area and pore volume of the materials were determined by using nitrogen physisorption at 77K taking 0.162 nm^2 as the cross sectional area of a N_2 molecule (BELSORP 28, NIHON BEL, Japan). Powder X-ray diffraction was carried out with a RINT2500/RIGAKU X-ray diffractometer. Thermogravimetric analysis was performed with a Shimadzu-TG51 instrument and particle size analysis with a Seishin-LMS-30 instrument. High resolution transmission electron microscopic (HRTEM) observations were performed by JEOL JEM-4000EX (400 kV) and Topcon EM-002B (200 kV) equipped with an energy dispersive X-ray spectroscope (EDS). Electron diffraction patterns were taken with the same system and could be analyzed in detail with digitization. The carbonization temperature 700 °C (2 h, 300 ml min^{-1}) was used for all the above samples and calcination (4 h, air 300 ml min^{-1}) temperatures of 600, 700 and 800 °C were used in the present

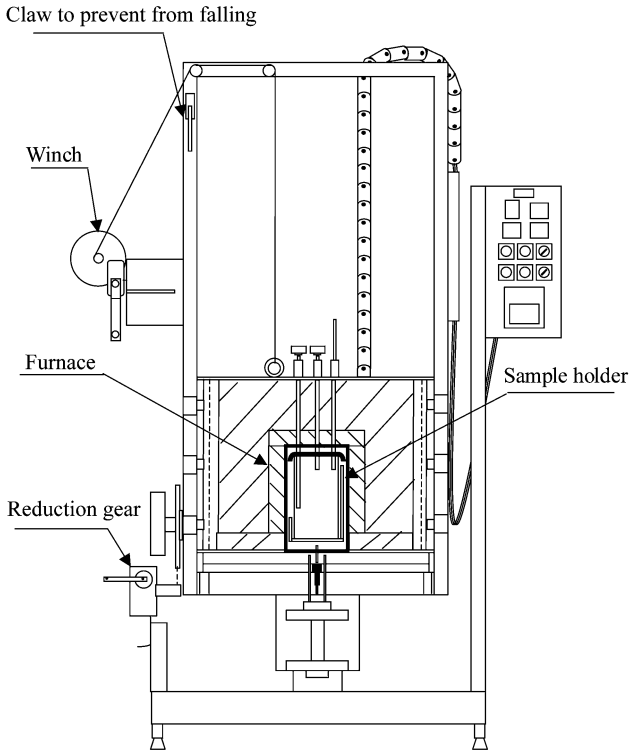

Fig. 5 Schematic experimental set-up for the carbonization procedure.

study. The waste biomass (sawdust) was obtained from Yonebayashi Milling Co., Ishikawa Prefecture, Japan.

Conclusions

A novel preparative method for the synthesis of nano crystalline and highly homogenous CeO_2, ZrO_2, and CeO_2–ZrO_2 metal oxides is reported for the first time. The utilization of waste biomass and replacement of stoichiometric reagents for the synthesis of this very important class of metal oxides were successfully performed. The X-ray diffraction and TEM analysis studies show that the metal oxides are in cubic system with a 5–10 nm range, which can be used for catalytic and various other applications. Catalysis studies and investigations into the effect of alkali metal ions present in the sawdust are in progress.

Acknowledgements

We thank Nagato Electrical Machine Corporation, Osaka, Japan for the preparation of the special instrument for the carbonization process.

References

1 P. T. Anastas and M. M. Kirchoff, *Acc. Chem. Res.*, 2002, **35**, 686(*a*) *Handbook of Green Chemistry and Technology*, eds. J. H. Clark and D. Macquarrie, Blackwell Science Publishers, Oxford, 2002; (*b*) P. T. Anastas and J. C. Warner, *Green Chemistry: Theory and Practice*, Oxford University Press, Oxford, 1998.
2 J. M. DeSimone, *Science*, 2002, **297**, 799.
3 J. Johnson, *Chem. Eng. News*, 7 October 2002, 6.
4 K. Tomishige and K. Kunimori, *Appl. Catal. A. Gen.*, 2002, **237**, 103.
5 S. Pengpanich, V. Meeyoo, T. Rirksomboon and K. Bunyakiat, *Appl. Catal. A.*, 2002, **234**, 221.
6 C. Diagne, H. Idriss and A. Kiennemann, *Catal. Commun.*, 2002, **3**, 565.
7 Materials for sustainability, News posted in *Nature*, **419**, 543, October 10, 2002.
8 Y. Sakata, A. Muto, Md. Azhar Uddin and K. Harino, *J. Mater. Chem.*, 1996, **6**, 1241.
9 N. Lingaiah, Md. Azhar Uddin, A. Muto and Y. Sakata, *J. Mol. Catal.*, 2000, **161**, 157.
10 M. Alifanti, B. Baps, N. Blangenois, J. Naud, P. Grange and B. Delmon, *Chem. Mater.*, 2003, **15**, 395.
11 A. I. Kozlov, D. H. Kim, A. Yezerets, P. Andersen, H. H. Kung and M. C. Kung, *J. Catal.*, 2002, **209**, 417.
12 A. Martinez Arias, M. Fernandez Garcia, Ana-Belen Hungria, J. C. Conesa and G. Munuera, *J. Phys. Chem. B*, 2003, **107**, 2667.
13 J. A. Rodriguez, J. C. Hanson, J. Y. Kim, G. Liu, A. Iglesias-Jeuz and M. Fernandex Garcia, *J. Phys. Chem. B*, 2003, **107**, 3535.
14 A. E. Nelson and K. H. Schulz, *Appl. Surf. Sci.*, 2003, **210**, 206.
15 A. T. Bell, *Science*, 2003, **299**, 1688.
16 W. J. Stark, L. Madler, M. Maciejewski, S. E. Pratsinis and A. Baiker, *Chem. Commun.*, 2003, 588.

In situ infrared study of oxidative carbonylation of aniline with methanol on Cu-based catalysts

Bei Chen and Steven S. C. Chuang*

Department of Chemical Engineering, The University of Akron, Akron, OH 44325-3906, USA.
E-mail: schuang@uakron.edu

Received 24th March 2003
First published as an Advance Article on the web 24th July 2003

Oxidative carbonylation of amines with alcohols provides an environmentally benign pathway to isocyanates and carbamates. Currently, the most active catalysts for the oxidative carbonylation of aniline with methanol are Pd-based catalysts. To further improve the economic feasibility of the carbamate synthesis process, we have investigated the activity of $CuCl_2$–NaI, $CuCl_2$–NaCl, and CuCl–NaI at 438 K and 0.41 MPa by *in situ* infrared spectroscopy. The activity of the catalysts for carbamate synthesis increased in the order: $CuCl_2$–NaCl < CuCl–NaI < $CuCl_2$–NaI. The presence of promoter (*i.e.*, NaI or NaCl) in the reactant–catalyst mixture is essential to promote carbamate synthesis. The formation of by-product, CO_2, can be suppressed by the sequential addition of NaI to CO/O_2/methanol/aniline/$CuCl_2$. Transient profiles of reactants/products obtained from *in situ* infrared spectroscopic studies revealed that CO_2 and carbamate were formed *via* two independent pathways. The infrared observation of a $Cu^0(CO)_2$ species and O_2 participation in carbamate synthesis suggest that the carbamate synthesis reaction involves a redox cycle of Cu^0/Cu^{II}.

Introduction

Isocyanates are important chemical feedstocks for the manufacture of fertilizers, pesticides, and various forms of polyurethane.[1] The value of isocyanate is reflected in not only its wide range of applications but also the polyurethane market of over a billion dollars in the automobile, construction, refrigeration, and biomaterial industries.[2] The current isocyanate synthesis process involves phosgenation of amines:

$$RNH_2 + COCl_2 \rightarrow RNCO + HCl \quad (1)$$

where R is an alkyl or aryl group.

The phosgenation process suffers from the difficulty of handling hazardous phosgene as well as the highly corrosive by-product HCl. To minimize the environmental impact of $COCl_2$, "green" routes without the phosgenation step have been extensively studied.[1,3–9] One notable environmentally benign synthesis pathway to isocyanate is the oxidative carbonylation of amines with alcohol followed by the thermal decomposition of carbamate to isocyanate.

Oxidative carbonylation:

$$RNH_2 + R'OH + CO + 1/2O_2 \rightarrow RNHCO_2R' + H_2O \quad (2)$$

Thermal decomposition of carbamate:

$$RNHCO_2R' \rightarrow RNCO + R'OH \quad (3)$$

where R and R′ are either alkyl or aryl groups.

This pathway offers a number of advantages: (i) the environmentally benign nature of the reactants, (ii) the high selectivity of the reaction processes, and (iii) the stability and low toxicity of carbamate products. Currently, the most active catalyst systems for the oxidative carbonylation of aniline with methanol are Pd-based catalysts, which produce high yields of carbamates in 2–6 hours at 433–453 K and pressures above 6.0 MPa.[10–13] The major drawbacks of these Pd-catalyzed carbonylation processes are the use of a costly noble metal as well as the requirement for high pressure and long reaction time to achieve high carbamate yields. To further improve the economic feasibility of the carbamate synthesis process, there is a need to develop a non-noble metal catalyst for catalyzing the reaction under mild conditions.

One rational approach for the development of a new catalyst for a specific reaction is to look into those catalysts which catalyze similar reaction processes. Examination of Pd- and Cu-based catalysts revealed that both catalysts exhibit activities for the oxidative carbonylation of methanol at 393–423 K and the oxidation of CO to CO_2 at 300–400 K.[14–20] The similarity in activity of Pd- and Cu-based catalysts for these two reactions led us to investigate the activity of Cu-based catalysts for the oxidative carbonylation of aniline with methanol.[9]

This paper reports the results of activity and mechanistic studies of carbamate synthesis from the oxidative carbonylation of aniline with methanol over $CuCl_2$–NaI, CuCl–NaI, and $CuCl_2$–NaCl catalysts. *In situ* infrared spectroscopic techniques were used to determine the dynamic behaviors of reactant conversion as well as intermediate and product formation during (i) batch reaction and (ii) the sequential addition of NaI promoter and O_2 into the reaction mixture. The transient profiles of reactants, intermediates, and products obtained allowed us to verify the activity of Cu-based catalysts, elucidate

Green Context

The preparation of useful isocyanates and carbamates can be achieved in a relatively environmentally acceptable way by the oxidative carbonylation of amines with alcohols. One drawback with this method is the need for palladium-based catalysts which are expensive and available from limited parts of the world. Here studies on less expensive and more widely available catalysts based on copper are reported. Efficient carbamate synthesis is shown to depend on inexpensive promoters. The article represents real progress in making this synthetic procedure a good example of green chemistry at work. ***JHC***

 DOI: 10.1039/b303283c

the sequence of reaction steps, and determine the role of NaI and O_2 in the catalyst cycle of carbamate synthesis.

Results and discussion

In situ study of oxidative carbonylation over $CuCl_2$–NaI

Fig. 1 shows the transmission IR spectra collected during the oxidative carbonylation of aniline with methanol over $CuCl_2$–NaI at 438 K and 0.41 MPa. The initial reactant–catalyst mixture gave amine bands at 1632 and 1605 cm^{-1}, gaseous CO bands at 2176 and 2115 cm^{-1}, and a band at 2046 cm^{-1}. The 2046 cm^{-1} band may be due to CO associated with Cu. It has been reported that CO adsorption on Cu/SiO_2 produced a band in the same region, which is considered as the asymmetric component of geminal complexes, $Cu^0(CO)_2$.[21] The symmetric component of the Cu complex would overlap with gaseous CO bands. Thus, the 2046 cm^{-1} band was tentatively assigned to $Cu^0(CO)_2$. The presence of $Cu^0(CO)_2$ suggested that the carbamate synthesis reaction involves a redox cycle of Cu^0/Cu^{II}. The absence of the 2070 and 2010 cm^{-1} bands[20,22] during the entire course of the reaction ruled out the possibility of CuCOCl serving as the reaction intermediate. As the reaction time increased, CO intensity decreased while CO_2 intensity (*i.e.*, 2360 and 2236 cm^{-1}) increased. After 15 min of reaction, the carbamate carbonyl stretching at 1722 cm^{-1} emerged.

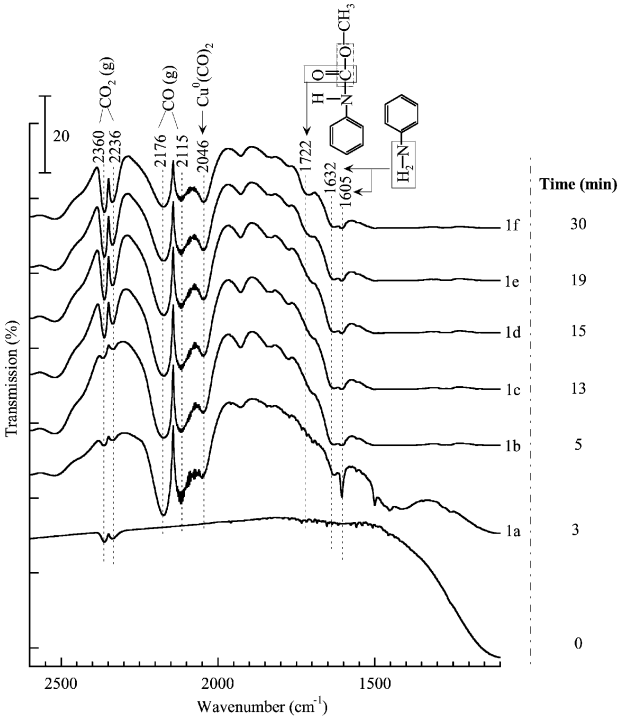

Fig. 1 Transmission IR spectra of the oxidative carbonylation over $CuCl_2$–NaI at 0.41 MPa and 438 K.

The conversions of reactants (*i.e.*, CO, methanol, and aniline) and the formation of products (*i.e.*, carbamate and CO_2) during the reaction can be clearly discerned from the difference spectra, shown in Fig. 2, which were obtained by subtraction of spectrum 1b in Fig. 1 from subsequent spectra. Spectrum 1b is used as a basis because it gave the highest aniline intensity and can serve as a reasonable representation of the initial reactant mixture. The negative bands of CO at 2115 and 2176 cm^{-1}, aniline at 1605 and 1632 cm^{-1}, and methanol at 1450, 1261, and 1174 cm^{-1} reflected the conversion of reactants while the positive bands of gaseous CO_2 at 2336 and 2360 cm^{-1} and carbamate at 1722 cm^{-1} reflected the formation of products.

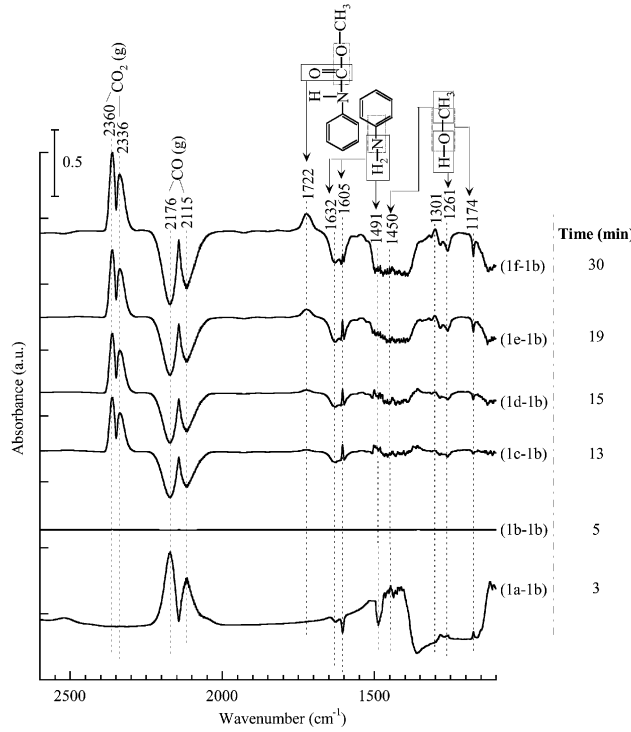

Fig. 2 Difference spectra of the oxidative carbonylation over $CuCl_2$–NaI obtained from subtraction of spectrum 1b from subsequent spectra in Fig. 1.

Fig. 3 shows the concentration profiles of reactants and products with respect to reaction time. Zero minutes (*i.e.*, $t = 0$) corresponds to the time when all the reactants were injected into the IR reactor at 438 K. Methanol and CO reached their initial designated concentration upon entering the reactor; the concentration of aniline showed a rapid increase to 0.08 mmol ml^{-1}, which corresponds to the initial concentration of aniline and the IR spectrum 1b in Fig. 1. The observed rise of aniline concentration is a result of its slow evaporation rate under reaction conditions. Prior to the complete vaporization of aniline, CO oxidation occurred, resulting in a gradual decline in CO concentration and an increase in CO_2 concentration. The formation of CO_2 led that of carbamate suggesting that CO_2 and carbamate were produced *via* two independent pathways. At the onset of CO oxidation, CO also interacted with Cu to produce $Cu^0(CO)_2$ at 2046 cm^{-1}. Following the complete vaporization at $t = 5$ min, the concentration of aniline and methanol began decreasing. The decrease in concentration of these reactants was accompanied by an increase in carbamate concentration. The reactant and product concentration profiles leveled off after 50 min of reaction, at which a 36% carbamate yield was achieved.

Comparison of Cu-based catalysts for the batch oxidative carbonylation reaction

In situ IR studies of the batch oxidative carbonylation reaction were also conducted over $CuCl_2$–NaCl and CuCl–NaI. Fig. 4 compares the concentration profiles of carbamate and CO_2 produced over $CuCl_2$–NaI, $CuCl_2$–NaCl, and CuCl–NaI at 438 K and 0.41 MPa. Carbamate formation decreased in the order of: $CuCl_2$–NaI > CuCl–NaI > $CuCl_2$–NaCl; CO_2 formation decreased in the order of: $CuCl_2$–NaI > $CuCl_2$–NaCl > CuCl–NaI. While these catalysts exhibited different activities for carbamate and CO_2 synthesis, the formation profiles of CO_2 consistently led that of carbamate. The results suggest that CO_2 and carbamate may be formed *via* two independent pathways. CuCl–NaI gave the highest selectivity for carbamate. The initial

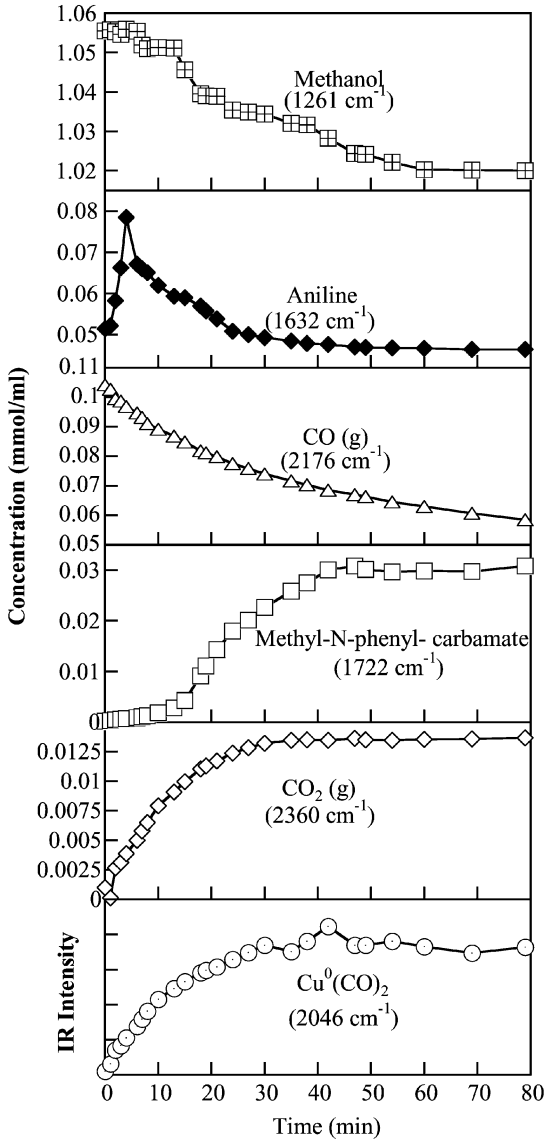

Fig. 3 Concentration profiles of reactants and products for the oxidative carbonylation over $CuCl_2$–NaI at 0.41 MPa and 438 K.

TOFs for carbamate and CO_2 formation over these three catalysts are listed in Table 1.

The effect of NaI and O_2 on the oxidative carbonylation over $CuCl_2$

Fig. 5(a) shows the transmission infrared spectra of CO_2, CO, and $Cu^0(CO)_2$ during the sequential addition of NaI and O_2 over $CuCl_2$ at 438 K; Fig. 5(b) shows the difference spectra by subtracting the first spectrum of each stage from the transmission spectra. The IR intensity of aniline and CO stayed constant prior to the addition of NaI. The addition of NaI to the existing CO/O_2/methanol/aniline/$CuCl_2$ mixture led to an initial increase followed by a decrease in $Cu^0(CO)_2$ intensity and emergence of carbamate at 1722 cm^{-1}; the addition of O_2 led to a further increase in carbamate intensity. The concentration profiles of reactants and products as well as the IR intensity of $Cu^0(CO)_2$ in Fig. 6 clearly show that the addition of NaI led to an initial increase in reactant concentrations followed by a decrease in reactant and $Cu^0(CO)_2$ concentrations as well as an increase in carbamate formation. In contrast to the variation in concentrations of these species, the concentration of CO_2 remained constant after NaI addition. The suppression of CO_2 formation during the reaction may be related to the change in chemical environment of the Cu species which could be brought about by the addition of NaI. The addition of excess halide, such as HCl, has been shown to suppress CO oxidation on the $PdCl_2$–$CuCl_2$/carbon catalyst through modification of the Cu environment.[23] Further addition of O_2 resulted in an increase in both $Cu^0(CO)_2$ species and carbamate. This observation revealed that O_2 is the limiting reactant under the present reaction conditions.

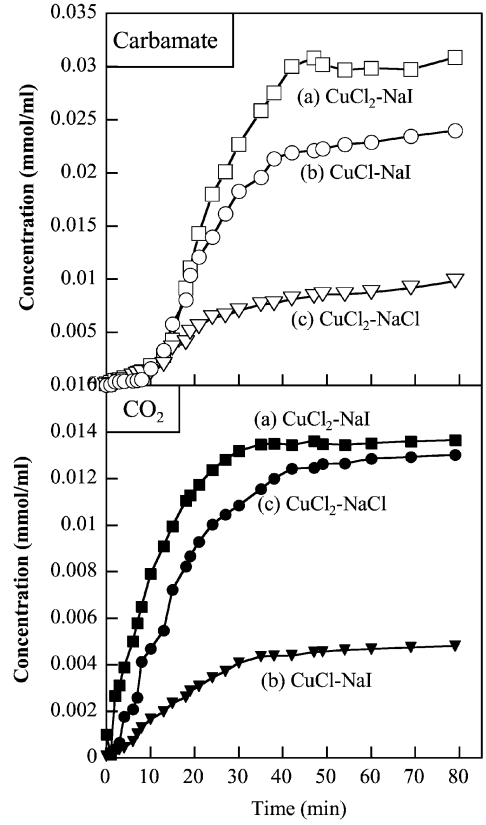

Fig. 4 Concentration profiles of carbamate and CO_2 over $CuCl_2$–NaI, $CuCl_2$–NaCl, and CuCl–NaI.

Table 1 Turnover frequency (TOF) of carbamate and CO_2 formation over copper catalysts

	Reaction conditions			TOF (h^{-1})[a]	
Catalyst	Temp/K	P/MPa	CO/O_2 (molar ratio)	Carbamate	CO_2
$CuCl_2$–NaI	438	0.41	10	1.37	0.42
$CuCl_2$–NaCl	438	0.41	10	0.91	0.30
CuCl–NaI	438	0.41	10	0.31	0.06

[a] Initial TOF for carbamate formation (the number of carbamate molecule formed per hour per metal atom) determined from the slope of the carbamate formation at $t = 0$ in Fig. 4.

The effect of O_2 on oxidative carbonylation over CuCl

Fig. 7 shows the concentration profiles of reactants and products for the oxidative carbonylation over CuCl–NaI at 0.41 MPa and 438 K. The profiles were obtained from the *in situ* infrared spectra taken during the reaction. The CuCl–NaI catalyst was first exposed to methanol/aniline/CO. Neither carbamate nor CO_2 was formed under this condition. Addition of O_2 resulted in the formation of carbamate and conversion of reactants (*i.e.*,

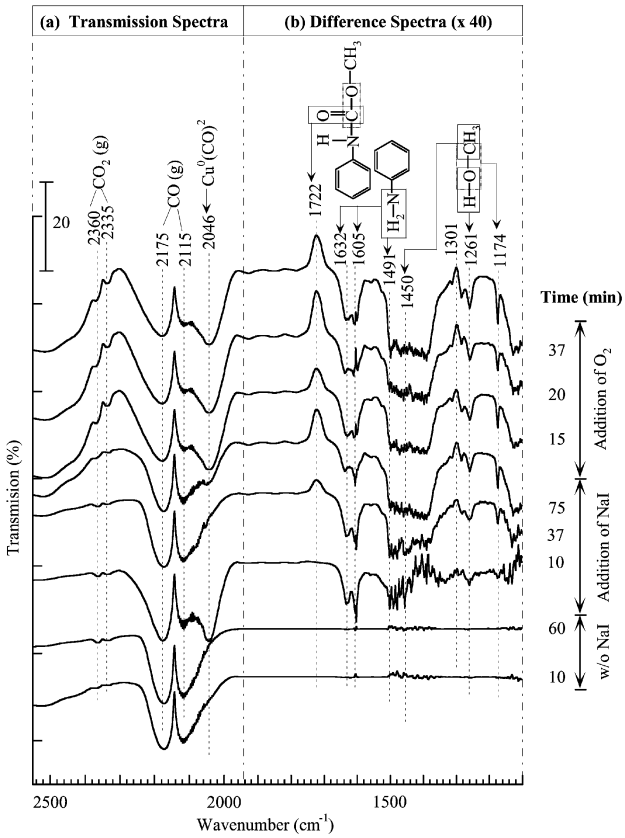

Fig. 5 (a) Transmission IR spectra collected during the study of the NaI effect in oxidative carbonylation of aniline over $CuCl_2$ at 438 K; (b) difference spectra collected during the study of the NaI effect in oxidative carbonylation of aniline over $CuCl_2$ at 438 K.

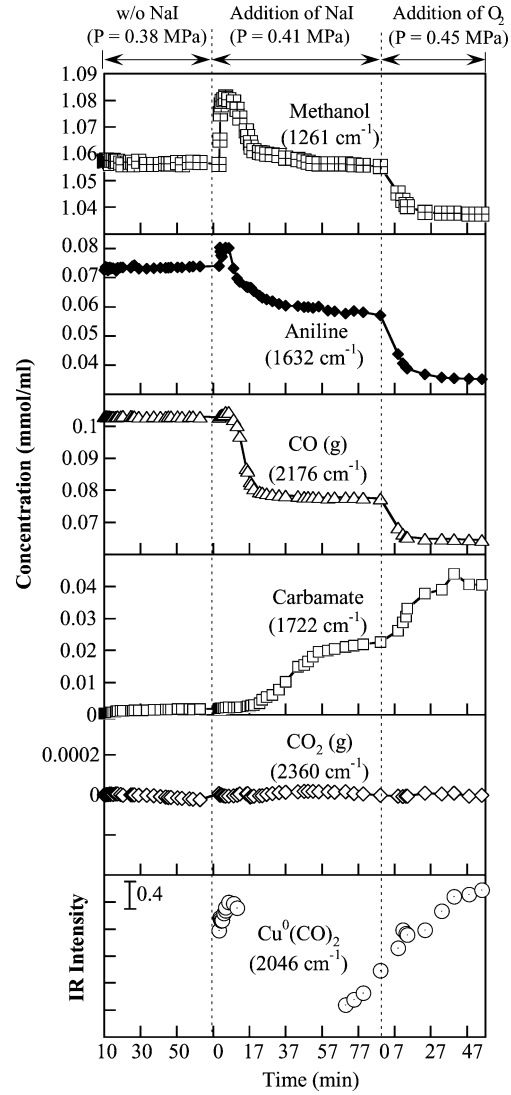

Fig. 6 Concentration profiles of reactants and products during the NaI effects study in oxidative carbonylation of aniline over $CuCl_2$ at 438 K.

aniline, methanol, and CO). The fact that O_2 is essential for the carbamate synthesis confirmed the presence of the redox cycle. Carbamate formation leveled off after 30 min of the reaction. Further addition of O_2 enhanced the formation of carbamate and CO_2. $Cu^0(CO)_2$ species may be overlapped by gaseous CO bands and was not observed throughout this study.

Proposed mechanism over Cu-based catalysts

Fig. 8 shows the proposed mechanism for the oxidative carbonylation of aniline with methanol over Cu-based catalysts. The proposed catalytic cycle involves: (i) the formation of $Cu^{II}(CO)_2IL$, where L may be CO, I^-, or Cl^-. (ii) the coordination of aniline onto a Cu complex *via* N atom, (iii) the insertion of CO into the Cu–N bond to form a carbamoyl species, (iv) the reductive elimination to produce *N*-iodobenzamide, (v) the reaction of *N*-iodobenzamide with methanol to produce carbamate, and (vi) the regeneration of the initial catalyst through the oxidative addition reaction.

The starting point of the catalytic cycle, *i.e.*, a $Cu^{II}(CO)_2IL$ species, was proposed on the basis of a Cu redox cycle (*i.e.*, $Cu^{II} \leftrightarrow Cu^0$) which includes two key steps: the reduction of Cu^{II} to Cu^0 through a reductive elimination [*i.e.*, step (iv)] and the oxidation of Cu^0 to be Cu^{II} *via* an oxidative addition [*i.e.*, step (vi)]. The required two electron transfer process ruled out Cu^I species as a starting point because its redox cycle would result in an unstable Cu^- species.[24] The redox cycle of Cu^{II}/Cu^0 proposed here is also supported by the fact that O_2 is essential to initiate the carbamate synthesis, as shown in Fig. 6 and 7.

Step (ii) has been proposed in the mechanism of the oxidative carbonylation of amine over Pd, Rh, Co, and Se catalysts and the CO insertion in step (iii) has been recognized as a key step for attaching a carbonyl group to a hydrocarbon molecule.[25–28] Halide, an essential promoter for carbamate synthesis over Pd/C and $PdCl_2$ catalysts, is also needed to promote Cu catalysts. In the absence of halide, neither CuCl nor $CuCl_2$ was active for the carbonylation reaction. The addition of NaI to the $CuCl_2$ resulted in the gradual formation of carbamate. It has been suggested that the major roles of halide are to stabilize the carbamoyl species and promote the CO insertion step by activating the CO ligand *via* electron donation.[10,11,25,29] Higher electron donating ability promoters would result in a higher rate of carbamate formation. Thus, the higher carbamate synthesis activity of $CuCl_2$–NaI compared with that of $CuCl_2$–NaCl can be attributed to the higher electron donating capability of I^-.

Reductive elimination in step (iv) produces *N*-iodobenzamide which resembles the acetyl iodide, an intermediate produced during methanol carbonylation over Rh in the presence of iodide as co-catalyst.[24] The *N*-iodobenzamide produced further reacted with methanol in step (v) to produce carbamate and I^-. Reductive elimination could also reduce Cu^{II} to Cu^0 which associates with CO as a $Cu^0(CO)_2$ species. These two proposed steps, step (iv) and (v), are consistent with the observed increase in $Cu^0(CO)_2$ and carbamate intensities upon addition of NaI and O_2 in Fig. 6. The last step of the catalytic cycle, step (vi), is the regeneration of $Cu^{II}(CO)_2IL$ from $Cu^0(CO)_2$ by oxygen-assisted oxidative addition of L and I. The O^{2-} produced then reacts with H^+ [step (ii) and (v)] to form H_2O.

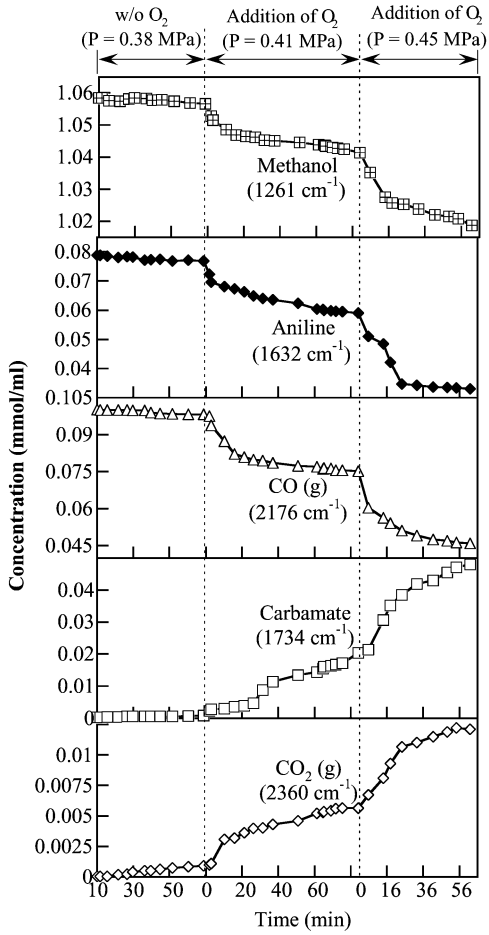

Fig. 7 Concentration profiles of reactants and products during the O_2 effects study in oxidative carbonylation of aniline over CuCl at 438 K.

While $Cu^0(CO)_2$ may be a key intermediate in the proposed catalytic cycle, it may also be produced from the direct interaction between CO and $CuCl_2$. The direct reduction of Cu^{II} to Cu^0/Cu^I has been observed during CO oxidation and adsorption.[20,21] The Cu^0 produced can further associate with CO to form $Cu^0(CO)_2$. This process appears to be relatively rapid compared with the catalytic cycle for carbamate formation as evidenced by the profile of $Cu^0(CO)_2$ leading that of carbamate in Fig. 3.

Experimental

Materials

Copper(II) chloride dihydrate (ACS grade), copper(I) chloride, and sodium iodide (metal basis, 99.9%) were purchased from Sigma Chemicals Co.; methanol (HPLC grade) and aniline (Certified ACS) from Fisher Scientific; oxygen (ultra high purity) and carbon monoxide (99.0%) from Praxair. All compounds were used without further treatment.

In situ infrared study of the batch oxidative carbonylation reaction

Fig. 9 shows the high pressure infrared (IR) cell for the reaction study. The IR cell consists of a stainless steel hollow cylinder and two flanges with Viton O-rings to from seals with CaF_2 windows. Two CaF_2 rods fill in the space between CaF_2 windows to provide a proper optical path length for the reactant–products mixture in the reactor.[30]

Oxidative carbonylation was carried out by (i) heating up the IR cell to 438 K with flowing He at 30 cm^3 min^{-1}, (ii) injecting 0.2 cm^3 reactants–catalyst–promoter mixture [the molar ratio of aniline : methanol : $CuCl_2$ or CuCl : NaI or NaCl = 38 : 518 : 1 : 0.69] into a CO/O_2 flow [CO/O_2 (v/v) = 10/1, total flow rate = 30 cm^3 min^{-1}] which entered the IR cell, and (iii) closing the outlet valve to bring the reaction pressure to 0.41 MPa to initiate the batch reaction. The initial reactant–catalyst mixture consists of 0.31 mmol of aniline, 4.23 mmol of methanol, 0.04 mmol of Cu catalyst, and 0.03 mmol of promoter (NaI or NaCl). The batch reaction was held for 80 min. The transmission IR spectra were collected during the reaction by a Nicolet MAGNA 550 Series II Fourier transform infrared spectrometer equipped with a DTGS (deuterated triglycine sulfate) detector at a resolution of 4 cm^{-1}. IR analysis showed that the product mixture gave characteristic carbonyl bands of carbamate at 1717–1737 cm^{-1}. The final reactant–product mixture was analyzed by a Gemini 300 ^{13}C nuclear magnetic resonance (NMR) spectrometer using $CDCl_3$ as a solvent. The ^{13}C NMR spectrum of the product sample gave a carbamate carbonyl peak at 154.5 ppm. Both IR and NMR results confirmed the formation of methyl *N*-phenylcarbamate.

The concentrations of reactants and products were determined by using the integrated IR absorbance of each species and

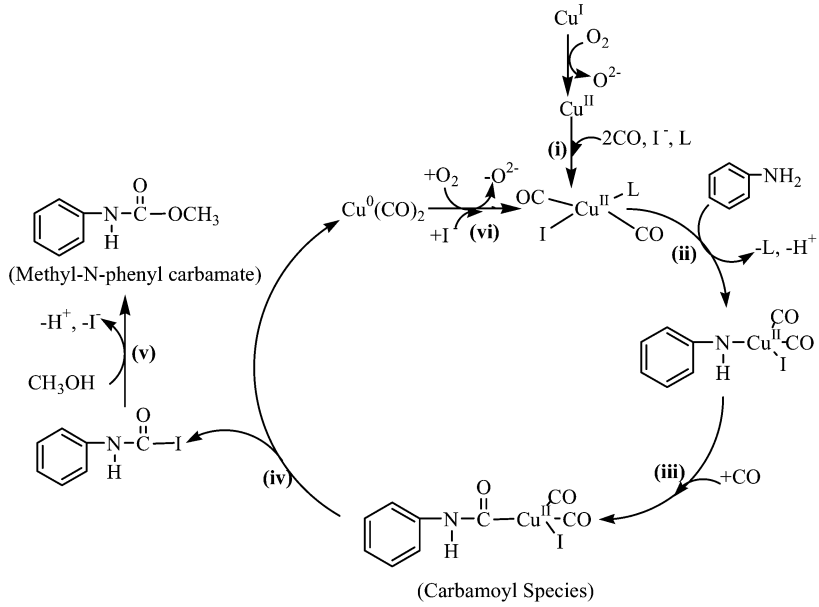

Fig. 8 Proposed mechanism for oxidative carbonylation of aniline over Cu-based catalysts.

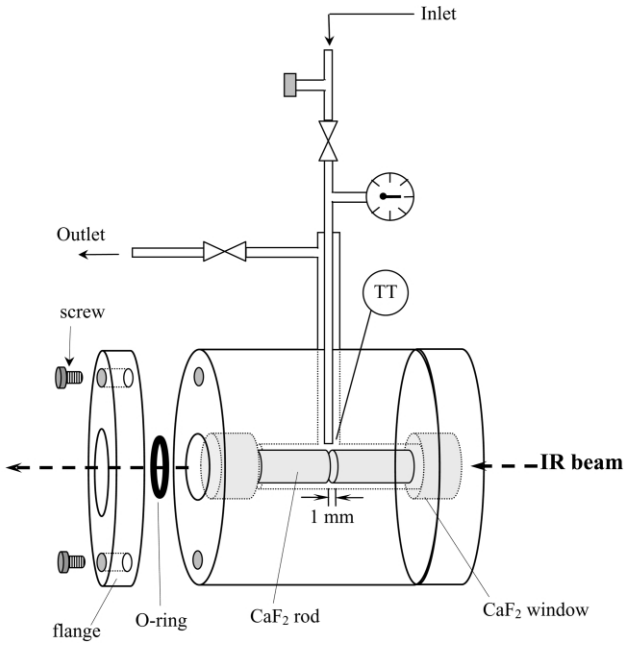

Fig. 9 High-pressure infrared cell.

its molar extinction coefficient. The molar extinction coefficient was determined from the slope of a calibration curve, which is a plot of the peak area *versus* the number of moles of the reagent in the IR cell. The carbamate yield is defined as the ratio of the moles of carbamate produced to the initial moles of aniline.

The effect of NaI and O_2 on $CuCl_2$

The effects of NaI on the oxidative carbonylation over $CuCl_2$–NaI at 438 K were studied by the addition of NaI (0.03 mmol NaI and 0.35 mmol CH_3OH) into the mixture of $CuCl_2$ (0.04 mmol), aniline (0.31 mmol), and methanol (4.23 mmol) at 0.41 MPa [CO/O_2 (v/v) = 10:1]. The effect of O_2 was determined by a further addition of O_2 to the above reactant mixture to 0.45 MPa.

The effect of O_2 on CuCl

The effect of O_2 on the reaction over CuCl–NaI was determined by the addition of O_2 to the reactants–catalyst mixture (*i.e.*, aniline/methanol/ CO/O_2/CuCl with a molar ratio of 38/518/1/0.69) at 0.41 MPa followed by a further injection of O_2 to bring the reaction pressure to 0.45 MPa.

Acknowledgements

This work has been supported by the NSF Grant CTS 9816954 and the Ohio Board of Regents Grant R5538. We greatly appreciate Dr Christopher Ziegler at The University of Akron for sharing his scientific insight on this research and the valuable discussions of the reaction mechanisms.

References

1 K. Weissermel and H. Arpe, *Industrial Organic Chemistry* 2nd edn., VCH, Weinheim, 1993.
2 R. H. Reinhard and R. D. Priester, Jr, in *Kirk-Othmer Encyclopedia of Chemical Technology*, John Wiley & Sons, Inc., New York, 1995.
3 Y. Ono, M. Shibata and T. Inui, *J. Mol. Catal. A*, 2000, **153**, 53.
4 S. Cenini, M. Pizzotti and C. Crotti, in *Aspects of Homogeneous Catalysis: A Series of Advances*, ed. R. Ugo, p. 97, D. Reidel Publishing, Holland, 1998.
5 W. L. Gladfelter and J. D. Garulak, in *Benign By Design: Alternative Synthetic Design for Pollution Prevention*, ed. P. Anastas and C. Farris, p. 46, American Chemical Society, Washington DC, 1994.
6 F. W. Hartstock, D. G. Herrington and L. B. McMahon, *Tetrahedron Lett.*, 1994, **35**(47), 8761.
7 K. V. Prasad and R. V. Chaudhari, *J. Catal.*, 1994, **145**(1), 204.
8 W. McGhee, D. Riley, K. Christ, Y. Pan and B. Parnas, *J. Org. Chem.*, 1995, **60**(9), 2820.
9 B. Chen and S. S. C. Chuang, *J. Mol. Catal.*, 2003, **195**, 37.
10 P. Xue, F. Zhang, W. Wang and Y. Pen, *Yingyong Huaxue*, 1997, **14**, 41.
11 A. A. Kelkar, D. S. Kolhe, S. Kanagasabapathy and R. V. Chaudhari, *Ind. Eng. Chem. Res.*, 1992, **31**, 172.
12 B. Wan, S. Liao and D. Yu, *Appl. Catal.*, 1999, **A 183**, 81.
13 S. Guan, M. Huang and Y. Jiang, *Chin. J. Polym. Sci.*, 1993, **11**, 97.
14 Y. Sato and Y. Souma, *Catal. Surv. Jpn.*, 2000, **4**(1), 65.
15 V. Raab, M. Merz and J. Sundermeyer, *J. Mol. Catal. A: Chem.*, 2001, **175**(1–2), 51.
16 M. S. Han, B. G. Lee, I. Suh, H. S. Kim, B. S. Ahn and S. I. Hong, *J. Mol. Catal. A: Chem*, 2001, **170**(1–2), 225.
17 G. E. Morris, D. Oakley, D. A. Pippard and D. J. H. Smith, *J. Chem. Soc., Chem. Commun.*, 1987, (6), 410.
18 R. J. Radel, J. M. Sullivan and J. D. Hatfield, *Ind. Eng. Chem. Prod. Res. Dev.*, 1982, **21**(4), 679.
19 P. Yang, Y. Cao, J.-C. Hu, W.-L. Dai and K.-N. Fan, *Appl. Catal., A*, 2003, **241**(1–2), 363.
20 K. I. Choi and A. M. Vannice, *J. Catal.*, 1991, **127**, 465.
21 K. Hadjiivanov, T. Vankov and H. Knözinger, *Catal. Lett.*, 2001, **75**, 55.
22 M. Hakansson and S. Jagner, *Inorg. Chem.*, 1990, **29**, 5241.
23 E. D. Park, S. H. Choi and J. S. Lee, *J. Phys. Chem. B*, 2000, **104**, 5586.
24 F. A. Cotton and G. Wilkinson, *Advanced Inorganic Chemistry*, John Wiley & Sons, New York, 1988.
25 V. Kenkatesh Prasad and R. V. Chaudhari, *J. Catal.*, 1994, **145**, 204.
26 S. A. R. Mulla, C. V. Rode, A. A. Kelkar and S. P. Gupte, *J. Mol. Catal.*, 1997, **122**, 103.
27 B. Chen and S. S. C. Chuang, in *Catalysis of Organic Reactions*, ed. D. G. Morrell, Marcel Dekker, Inc., New York, 2002.
28 S. S. C. Chuang and S. I. Pien, *J. Catal.*, 1992, **135**(2), 618.
29 H. S. Kim, Y. J. Kim, H. Lee, K. Y. Park and C. S. Chin, *J. Catal.*, 1998, **176**, 264.
30 S. S. C. Chuang, M. A. Brundage, M. Balakos and G. Srinivas, *Appl. Spectrosc.*, 1995, **49**, 1151.